ADVANCES IN MATHEMATICAL MODELLING OF MULTICOMPONENT FREE-RADICAL POLYMERIZATIONS IN BULK, SOLUTION AND EMULSION

by

Jun Gao

A thesis
presented to the University of Waterloo
in fulfillment of the
thesis requirement for the degree of
Doctor of Philosophy
in
Chemical Engineering

Waterloo, Ontario, Canada, 1999

The **University of Waterloo** requires the signatures of all persons using or photocopying this thesis. Please sign below, and give address and date.

Acknowledgements

First and foremost, I want to express my great appreciation to my supervisor, Professor Alexander Penlidis, who once said that fulfillment is a great bondage; it obliges one to achieve an even greater fulfillment. I have been fortunate to be able to develop myself to the utmost of my capabilities with his consistent encouragement. I am specially thankful for his guidance which made many of my achievement possible. I am also very grateful for all the knowledge he passed on me not only in this research project but also in almost any aspect of life in general.

My special thanks go to Prof. Marc Dube for his discussions in understanding and modelling emulsion polymerization and above all friendship. My appreciation also goes to Dr. Neil McManus for his assistance in conducting polymerization and characterizing polymers. My thanks go to Prof. J.M. Asua for helpful discussions on modelling of emulsion polymerization during his visit from Spain.

I also thank every member (graduate students and professors) in this research group for all the help I received during this project: Prof. Tom Duever, Dr. Raj Mutha, Dr. Annette Burke, Ken Tanaka, Luigi D'Agnillo, Louie Polic and many others that escape my memory at this point. I thank many undergraduate students in this department for generating experimental data that were valuable for the development of this simulation package in their design projects. Special thanks to Ms. Rosemary Anderson for her administrative work.

My everlasting appreciation goes to my parents for all the efforts and care they put into my life, which made all this possible.

Financial support from ICI/Glidden Worldwide is also gratefully acknowledged. Many thanks to the department of Chemical Engineering, University of Waterloo, and to NSERC, Canada.

ABSTRACT

A computer package has been developed to simulate free-radical multicomponent polymerization in bulk, solution and emulsion. The simulation package consists of two models, one for bulk and solution polymerization, and the other for emulsion polymerization. Great emphasis has been placed on making both models general and reliable. This has been achieved through in-depth kinetic studies, critical model evaluation and extensive model testing. Models have been gradually enhanced and extended from a homopolymerization case to two comprehensive multicomponent bulk/solution/emulsion models. Databases of physicochemical parameter values for both models have been developed in parallel. The bulk/solution model's database includes 12 monomers and the database for the emulsion model consists of 5 monomers. Both databases also have many initiators, solvents (in bulk/solution model's database only), chain transfer agents and emulsifiers (in emulsion model's database only). Such extensive databases allow the models to simulate multicomponent polymerizations for a wide range of reaction recipes.

In the first stage of model development, the bulk/solution model was developed and extensively tested with a total of 15 copolymer systems. Several important aspects in copolymerization kinetics were discussed. In most model testing cases, model predictions turned out to be very satisfactory and this confirms the reliability of the package. The literature review on copolymerizaiton kinetics and model testing presented in this thesis are believed to be the most extensive so far in the literature.

In the second stage of model development, terpolymerization kinetics in bulk/solution over the entire conversion range were investigated in detail. The bulk/solution copolymerization model was extended to simulate terpolymerization in bulk/solution and testing over the entire conversion range. This is the first time that a terpolymer system is modelled over the entire conversion range. Testing has been performed with the very challenging (and widely used commercially) system of butyl acrylate/methyl methacrylate/vinyl acetate in bulk and solution (toluene). Due to the scarcity of available experimental data in the literature, we were not able to test the model more

extensively with other terpolymerizations, however, the system in question was extremely challenging as a test case.

In the third stage of model development, a general and comprehensive emulsion model has been developed. This emulsion model is one of the very few that can simulate emulsion homopolymerization as well as copolymerization under a very wide range of reaction and operation conditions. The model can describe the most important physicochemical phenomena (micelle formation, particle nucleation, absorption and desorption of radicals, monomer partitioning, gel effect, etc.) occurring in emulsion polymerization. Difficult and challenging subjects in emulsion polymerization kinetics, such as monomer partitioning through thermodynamic equilibrium, particle nucleation, desorption, etc., have been solved satisfactorily in a general fashion. This model can predict important reaction characteristics (conversion profile and rate of polymerization) and polymer/latex properties (number of particles, particle size, molecular weight averages, copolymer composition and sequence, etc.).

The emulsion model has been tested with monomers of very different characteristics, like styrene (a "typical case 2" monomer with very low water solubility and no desorption), vinyl acetate (a typical "case 1" monomer with high water solubility and significant desorption) and methyl methacrylate (a typical "case 3" monomer that exhibits strong gel effect). The model has also been tested for the copolymer system of styrene/methyl methacrylate. In most cases, simulation results are satisfactory compared to experimental data collected either from the literature or from this laboratory.

After this systematic effort in refining and testing our multicomponent simulation model/package/database, we strongly believe that the package can provide a very flexible and useful tool that could guide academic and industrial research and development, as extensively demonstrated in Gao and Penlidis (1996, 1998) for homo- and copolymerizations, and in the present thesis for terpolymerizations and emulsion case.

La causa de lo que hacemos es lo que creemos y tambien lo que buscamos.

Table of Contents

Abstract v
List of Figures xv
List of Tables xxxii

Volume 1

Chapter 1. Introduction and Objectives 1
1.1 Objectives 3
1.2 Contributions of the Thesis 4
1.3 Organization of the Thesis 6

Chapter 2. Brief Theoretical Background on Bulk and Solution Copolymerization ... 9
2.1 Classical Theory 9
2.2 Recent Advances in Copolymerization Kinetics at High Conversion Levels 11
2.3 Penultimate Model and Model Discrimination 14

Chapter 3. Simulation Package Overview 17
3.1 Model Development and Implementation 18
3.2 Termination in Copolymerization 21
3.3 Modeling Considerations on Diffusion Controlled Kinetics. 23
3.4 Simulation of Copolymer Tg 24
3.4.1 Literature Review 25
3.4.2 Tg Model Implementation and Testing 29

Chapter 4. Package Database Overview 32

4.1 Database Structure and Items 36

Chapter 5. Model Testing Guidelines and Reactivity Ratio Estimation 38

5.1 Model Testing Guidelines 38

5.2 Brief Experimental Procedure Outline 39

5.3 Reactivity Ratio Estimation 40

Chapter 6. Simulation of Copolymerization of Styrene and Methyl Methacrylate . . 42

6.1 Literature Summary 42

6.2 Model Testing Results 44

Chapter 7. Simulation of Copolymerization of Styrene and Acrylonitrile 51

7.1 Literature Review 51

7.2 Model Testing 53

Chapter 8. Simulation of Copolymerization of Styrene and Acrylates 63

8.1 Simulation of Copolymerization of Styrene and Butyl Acrylate 63

8.1.1 Literature Summary 63

8.1.2 Model Testing 65

8.2 Simulation of Copolymerization of Styrene and Ethyl Acrylate 70

8.2.1 Literature Review 70

8.2.2 Model Testing 71

8.3 Simulation of Copolymerization of Styrene and 2-Hydroxyethyl Acrylate 84

8.3.1 Literature Review 84

8.3.2 Sty/2-HEA Copolymerization — A Problematic System 85

8.3.3 Full Conversion Range Experiments and Model Testing 85

8.3.4 Summary 87

Chapter 9. Simulation of Copolymerization of Methyl Methacrylate/Methyl Acrylate and Methyl Methacrylate/Ethyl Acrylate 88
9.1 Literature Review on MMA/EA Copolymerization 88
9.2 Model Testing on MMA/EA Copolymerization 88
9.3 Literature Review on MMA/MA Copolymerization 90
9.4 Model Testing on MMA/MA Copolymerization 91

Chapter 10. Simulation of Copolymerization of Methyl Methacrylate/Vinyl Acetate, Butyl Acrylate/Vinyl Acetate and Methyl Methacrylate/Butyl Acrylate 94
10.1 Simulation of Copolymerization of MMA/BA 94
10.1.1 Literature Summary 94
10.1.2 Model Testing 94
10.2 Simulation of Copolymerization of MMA/VAc 101
10.2.1 Model Testing 102
10.3 Simulation of Copolymerization of BA/VAc 105
10.3.1 Literature Summary 105
10.3.2 Model Testing 105

Chapter 11. Simulation of Copolymerization of Styrene and Carboxylic Acids .. 107
11.1 Monomer Characteristics 107
11.2 Copolymerization of Styrene/AA 107
11.3 Copolymerization of Sty/MAA 109
11.4 Remarks 110

Chapter 12. Simulation of Copolymerization of *p*-Methyl Styrene and Various Monomers. 111
12.1 Simulation of Copolymerization of Styrene and *p*-Methyl Styrene 112

12.1.1 Model Testing 113
12.2 Simulation of Copolymerization of Methyl Methacrylate and *p*-Methyl Styrene 119
12.3 Simulation of Copolymerization of Acrylonitrile and *p*-Methyl Styrene . 124

Chapter 13. Simulation of Terpolymerization in Bulk and Solution. 132
13.1 Brief Background on Terpolymerization. 133
13.2 Mathematical Modelling of Terpolymerization 136
13.3 Results and Discussion 139

References on Bulk/Solution (Volume 1) 152

Volume 2

14. Simulation of Emulsion Polymerization 175

14.1 Brief Overview of the Classical Smith-Ewart Theory 175

14.2 Recent Advances 180

15. Development of Emulsion Polymerization Simulation Package 184

15.1 Initiation 184

15.2 Particle Nucleation and Growth 186

15.2.1 Micellar Nucleation 187

15.2.2 Homogeneous Nucleation 189

15.2.3 Mass Balances of Radicals in the Water Phase 191

15.2.4 Recent Modelling Efforts on Particle Nucleation 199

15.2.5 Specific Modelling Considerations on Particle Nucleation 201

15.3 Monomer Partitioning in Emulsion Homopolymerization 203

15.3.1 Empirical Approach 205

15.3.2 Theoretical Approach: Thermodynamic Equilibrium 206

15.4 Desorption 215

15.5 Average Number of Radicals per Particle 219

15.6 Overall Mass Balances and Molecular Weight Development 221

15.7 Reaction Kinetics at High Conversion Levels 227

Chapter 16. Emulsion Simulation Package/Database Overview 229

16.1 General Description 229

16.2. Package Database Overview 232

16.2.1 Monomer Systems 232

16.2.2 Other Components 233

16.3 Description of Database Items 234

Chapter 17. Simulation of Styrene Emulsion Homopolymerization 237
17.1 Model Testing Results 240

Chapter 18. Simulation of Emulsion Homopolymerization of Vinyl Acetate 260
18.1 Model Testing Results 265

Chapter 19. Simulation of Homopolymerization of Acrylic Monomers: Methyl Methacrylate, Butyl Acrylate and Ethyl Acrylate 274
19.1 Simulation of Methyl Methacrylate Emulsion Homopolymerization 274
19.1.1 Model Testing Results 278
19.2 Simulation of Butyl Acrylate Emulsion Homopolymerization 295
19.2.1 Model Testing Results 298
19.3 Simulation of Ethyl Acrylate Emulsion Homopolymerization 305
19.3.1 Model Testing Results 306

Chapter 20. Extensions to Emulsion Copolymerization 309
20.1 Brief Literature Summary 309
20.2 Monomer Partitioning in Copolymerization 311
20.2.1 Literature Review 311
20.2.2 Model Implementation 315
20.3 Desorption in Copolymerization 321
20.4 Simulation of Copolymerization of Styrene/MMA in Emulsion 322

Chapter 21. Concluding Remarks and Future Work 332
21.1 Concluding Remarks 332
21.2 Future Work 333

Nomenclature 335

References on Emulsion (Volume 2) 342

Appendix 1. Seeded Emulsion Polymerization 359

Appendix 2. Impurity Effects on Emulsion Kinetics 361

List of Figures

Figure 1.1 Long-Term Model Development Goals 8

Figure 4.1 Reaction Formulation Screen 33

Figure 4.2 Computational Options Screen 33

Figure 4.3 Output Files Screen 35

Figure 4.4 Flow Options Screen 35

Figure 4.5 Database Structure of the Bulk/Solution Model. 37

Figure 6.1 Simulation of Methyl Methacrylate and Styrene Bulk Copolymerization at 60°C. BPO: 2 g/L. 45

Figure 6.2 Simulation of Methyl Methacrylate and Styrene Solution Copolymerization at 60°C.BPO as initiator: 4 g/L. 46

Figure 6.3 Simulation of methyl methacrylate and styrene copolymerization in bulk at 60°C.BPO as initiator: 2 g/L. 46

Figure 6.4 Composition Drift in Methyl Methacrylate and Styrene Bulk Copolymerization at 60°C. BPO: 2 g/L. 47

Figure 6.5 Simulation of methyl methacrylate and styrene bulk copolymerization at 60°C. BPO as initiator: 2 g/L, styrene in monomer feed: 60 mol% 49

Figure 6.6 Simulation of Methyl Methacrylate and Styrene Bulk Copolymerization at 60°C. BPO as initiator: 2 g/L, styrene in monomer feed: 60 mol% 49

Figure 6.7 Simulation of Methyl Methacrylate and Styrene Copolymerization in Bulk at 60°C.[AIBME]: 0.01 mol/L 50

Figure 6.8 Simulation of Composition Drift in Methyl Methacrylate and Styrenen in Bulk at 60°C. [AIBME]: 0.01 mol/L 50

Figure 7.1 Simulation of Styrene and Acrylonitrile Bulk Polymerization at 40°C. [AIBN]=0.05 mol/L. 54

Figure 7.2 Simulation of Monomer Feed Composition in Styrene and Acrylonitrile Bulk Polymerization at 40°C. [AIBN]=0.05 mol/L. 55

Figure 7.3 Simulation of Monomer Feed Composition in Styrene and Acrylonitrile Bulk

Polymerization at 40°C. [AIBN]=0.05 mol/L. 55
Figure 7.4 Simulation of Styrene and Acrylonitrile Bulk Polymerization at 60°C. [AIBN]=0.01 mol/L. 56
Figure 7.5 Simulation of Styrene and Acrylonitrile Bulk Polymerization at 60°C. [AIBN]=0.05 mol/L. 56
Figure 7.6 Simulation of Monomer Feed Composition in Styrene and Acrylonitrile Bulk Polymerization at 60°C. [AIBN]=0.01 mol/L. 57
Figure 7.7 Simulation of Monomer Feed Composition in Styrene and Acrylonitrile Bulk Polymerization at 60°C. [AIBN]=0.01 mol/L. 57
Figure 7.8 Simulation of Monomer Feed Composition in Styrene and Acrylonitrile Bulk Polymerization at 60°C. [AIBN]=0.05 mol/L. 58
Figure 7.9 Simulation of Monomer Feed Composition in Styrene and Acrylonitrile Bulk Polymerization at 60°C. [AIBN]=0.05 mol/L. 58
Figure 7.10 Simulation of Styrene and Acrylonitrile Bulk Copolymerization. [AIBN]=0.01 mol/L, 60% styrene. 59
Figure 7.11 Simulation of styrene and acrylonitrile copolymerization in toluene at 100°C. AN: 0.396 mol, Sty: 0.605 mol, toluene: 0.603 mol. 60
Figure 7.12 Simulation of Styrene and Acrylonitrile Copolymerization in Toluene. AN: 0.396 mol, Sty: 0.605 mol, toluene: 0.603 mol, BPO: 0.000289 mol. 61
Figure 7.13 Simulation of Styrene and Acrylonitrile Copolymerization in Toluene at 80°C. AN: 0.396 mol, Sty: 0.605 mol, toluene: 1.413 mol. 61
Figure 7.14 Simulation of Styrene and Acrylonitrile copolymerization in Toluene at 80°C. AN: 0.396 mol, Sty: 0.605 mol, BPO: 0.00045 mol. 62
Figure 8.1 Simulation of Styrene and Butyl Acrylate Copolymerization in Bulk at 50°C. [AIBN]: 0.05 mol/L. 67
Figure 8.2 Simulation of Composition Drift in Styrene and Butyl Acrylate Copolymerization in Bulk at 50°C. [AIBN]: 0.05 mol/L. 67
Figure 8.3 Simulation of Molecular Weight in Styrene and Butyl Acrylate

Copolymerization in bulk at 50°C. [AIBN]: 0.05 mol/L, f_{sty}: 0.942 68
Figure 8.4 Simulation of Styrene and Butyl Acrylate Copolymerization in Bulk at 50°C. [AIBN]: 0.1 mol/L. 68
Figure 8.5 Simulation of Composition Drift in Styrene and Butyl Acrylate Copolymerization in Bulk at 50°C. [AIBN]: 0.1 mol/L. 69
Figure 8.6 Simulation of Molecular Weight in Styrene and Butyl Acrylate Copolymerization in Bulk at 50°C. [AIBN]: 0.1 mol/L, f_{sty}: 0.942 69
Figure 8.7 Simulation of Styrene and Ethyl acrylate Copolymerization in Bulk at 50°C. [AIBN]: 0.05 mol/L. 74
Figure 8.8 Simulation of Composition Drift in Styrene and Ethyl Acrylate Copolymerization in bulk at 50°C. [AIBN]: 0.05 mol/L. 74
Figure 8.9 Simulation of Molecular Weight in Styrene and Ethyl Acrylate Copolymerization in Bulk at 50°C. [AIBN]: 0.05 mol/L, f_{sty}=0.762. 75
Figure 8.10 Simulation of Styrene and Ethyl Acrylate Copolymerization in Bulk at 50°C. [AIBN]: 0.1 mol/L. 75
Figure 8.11 Simulation of Composition Drift in Styrene and Ethyl Acrylate Copolymerization in Bulk at 50°C. [AIBN]: 0.1 mol/L. 76
Figure 8.12 Simulation of Molecular Weight in Styrene and Ethyl Acrylate Copolymerization in Bulk at 50°C. [AIBN]: 0.1 mol/L, f_{sty}=0.762. 76
Figure 8.13 Simulation of Styrene and Ethyl Acrylate Copolymerization in Bulk at 60°C. [AIBN]: 0.05 mol/L. 77
Figure 8.14 Simulation of Composition Drift in Styrene and Ethyl Acrylate Copolymerization in Bulk at 60°C. [AIBN]: 0.05 mol/L. 77
Figure 8.15 Simulation of Molecular Weight in Styrene and Ethyl Acrylate Copolymerization in Bulk at 60°C. [AIBN]: 0.05 mol/L. 78
Figure 8.16 Simulation of Styrene and Ethyl Acrylate Copolymerization in Bulk at 60°C. [AIBN]: 0.1 mol/L. 78
Figure 8.17 Simulation of Composition Drift in Styrene and Ethyl Acrylate Copolymerization in Bulk at 60°C. [AIBN]: 0.1 mol/L. 79

Figure 8.18 Simulation of Molecular Weight in Styrene and Ethyl Acrylate Copolymerization in Bulk at 60°C. [AIBN]: 0.1 mol/L. 79
Figure 8.19 Simulation of Styrene and Ethyl Acrylate Copolymerization with CTA in Bulk at 60°C. [AIBN]: 0.05 mol/L, f_{sty}=0.762. 80
Figure 8.20 Simulation of Styrene and Ethyl Acrylate Copolymerization with CTA in Bulk at 60°C. [AIBN]: 0.05 mol/L, f_{sty}=0.762. 80
Figure 8.21 Simulation of Styrene and Ethyl Acrylate Copolymerization with CTA in Bulk at 60°C. [AIBN]: 0.05 mol/L, f_{sty}=0.762. 81
Figure 8.22 Simulation of Styrene and Ethyl Acrylate Copolymerization with CTA in Bulk at 60°C. [AIBN]: 0.05 mol/L, f_{sty}=0.762. 81
Figure 8.23 Simulation of Copolymer Composition in Styrene and Ethyl Acrylate Copolymerization with CTA in Bulk at 60°C. [AIBN]: 0.05 mol/L, f_{sty}=0.762. 82
Figure 8.24 Simulation of Number Average Molecular Weight in Styrene and Ethyl Acrylate Copolymerization in Bulk at 60°C. [AIBN]: 0.05 mol/L, f_{sty}=0.762. 82
Figure 8.25 Simulation of Weight-Average Molecular Weight in Styrene and Ethyl Acrylate Copolymerization in Bulk at 60°C with [AIBN]=0.05 mol/L and f_{sty}=0.762. 83
Figure 8.26 Simulation of Sty/2-HEA Copolymerization in Bulk at 40°C. f_{sty}: 0.515 86
Figure 8.27 Simulation of Sty/2-HEA copolymerization in bulk at 50°C. f_{sty}: 0.515 87
Figure 9.1 Simulation of MMA/EA Copolymerization at 80°C. MMA:EA=100:15 in the Feed, n-Butyl Mercaptan as CTA, [CTA]: 0.4 v%. 89
Figure 9.2 Simulation of MMA/MA Copolymerization in Benzene at 50°C. [AIBN]=0.015 mol/L 92
Figure 9.3 Simulation of composition drift in MMA/MA copolymerization in benzene at 50°C. [AIBN]=0.015 mol/L 92

Figure 9.4 Simulation of MMA/MA Copolymerization in Bulk at 80°C. 93
Figure 9.5 Simulation of MMA/MA Copolymerization at Various Monomer Feed Ratio at 80°C. 93
Figure 10.1 Simulation of MMA/BA Copolymerization in Bulk at 80°C. MMA:BA=100:15 mol ratio, AIBN: 0.075 mol% of monomers 97
Figure 10.2 Simulation of MMA/BA Copolymerization in Bulk at 60°C. f_{BA}=0.439 97
Figure 10.3 Simulation of MMA/BA Copolymerization in Bulk at 60°C. f_{BA}=0.163 98
Figure 10.4 Composition Drift in MMA/BA Copolymerization in Bulk at 60°C. 98
Figure 10.5 Simulation of MMA/BA Copolymerization in Bulk at 60°C. f_{BA}=0.163, [AIBN]=0.005 mol/L 99
Figure 10.6 Simulation of MMA/BA Copolymerization in Bulk at 60°C. f_{BA}=0.163, [AIBN]=0.01 mol/L 99
Figure 10.7 Simulation of MMA/BA Copolymerization in Bulk at 60°C. f_{BA}=50 wt%, [AIBN]=0.005 mol/L 100
Figure 10.8 Simulation of MMA/BA copolymerization in bulk at 60°C. f_{BA}=50 wt%, [AIBN]=0.01 mol/L 100
Figure 10.9 Simulation of MMA/VAc Copolymerization in Bulk at 60°C. f_{MMA}=30 mol%, [AIBN]=0.01 mol/L 103
Figure 10.10 Simulation of MMA/VAc Copolymerization in Bulk at 60°C. f_{MMA}=30 mol%, [AIBN]=0.01 mol/L 104
Figure 10.11 Simulation of MMA/VAc copolymerization in Bulk at 60°C. f_{MMA}=30 mol%, [AIBN]=0.01 mol/L 104
Figure 10.12 Simulation of BA/VAc Copolymerization in Bulk at 60°C. f_{BA}=80 mol%, [AIBN]=0.00054 mol/L 106
Figure 10.13 Simulation of BA/VAc Copolymerization in Bulk at 60°C. f_{BA}=80 mol%, [AIBN]=0.00054 mol/L 106
Figure 12.1 Simulation of Sty/*p*-MSty Copolymerization in Bulk.

f_{Sty}=20 mol%. 114
Figure 12.2 Simulation of Sty/*p*-MSty Copolymerization in Bulk. f_{Sty}=75 mol%. 115
Figure 12.3 Simulation of Sty/*p*-MSty Copolymerization in Bulk. f_{Sty}=20 mol%. 115
Figure 12.4 Simulation of Sty/*p*-MSty Copolymerization in Bulk. f_{Sty}=75 mol%. 116
Figure 12.5 Simulation of Weight Average Molecular Weight in Sty/*p*-MSty Copolymerization in Bulk at 120°C.f_{Sty}=20 mol%. 116
Figure 12.6 Simulation of Weight Average Molecular Weight in Sty/*p*-MSty Copolymerization in bulk. f_{Sty}=20 mol%. 117
Figure 12.7 Simulation of Weight Average Molecular Weight in Sty/*p*-MSty Copolymerization in Bulk. f_{Sty}=75 mol% 117
Figure 12.8 Simulation of Number Average Molecular Weight in Sty/*p*-MSty Copolymerization in Bulk. f_{Sty}=20 mol%. 118
Figure 12.9 Simulation of Number Average Molecular Weight in Sty/*p*-MSty Copolymerization in Bulk. f_{Sty}=75 mol%. 118
Figure 12.10 Simulation of MMA/*p*-MSty copolymerization in bulk. f_{MMA}=54 mol%. 120
Figure 12.11 Simulation of MMA/*p*-MSty Copolymerization in Bulk. f_{MMA}=83 mol%, [AIBN]=0.0157 mol/L. 121
Figure 12.12 Simulation of MMA/*p*-MSty Copolymerization in Bulk at 80°C. f_{MMA}=21 mol%. 121
Figure 12.13 Simulation of MMA/*p*-MSty Copolymerization in Bulk at 60°C. f_{MMA}=21 mol%. 122
Figure 12.14 Simulation of Residual Monomer Composition in MMA/*p*-MSty Copolymerization in Bulk at 60°C. [AIBN]=0.0157 mol/L 122
Figure 12.15 Simulation of Residual Monomer Composition in MMA/*p*-MSty Copolymerization in Bulk at 80°C. [AIBN]=0.0157 mol/L 123

Figure 12.16 Simulation of Weight Average Molecular Weight in MMA/*p*-MSty Copolymerization in Bulk. [AIBN]=0.0157 mol/L 123
Figure 12.17 Simulation of Weight Average Molecular Weight in MMA/*p*-MSty Copolymerization in Bulk. [AIBN]=0.0157 mol/L 124
Figure 12.18 Simulation of AN/*p*-MSty Copolymerization in Bulk. [AIBN] as initiator, $f_{p\text{-MSty}}$=56 mol%. 126
Figure 12.19 Simulation of AN/*p*-MSty Copolymerization in Bulk at Different Temperatures. [AIBN]=0.01 mol/L, $f_{p\text{-MSty}}$=90 mol%. 126
Figure 12.20 Simulation of AN/*p*-MSty Copolymerization in Bulk at Different Temperatures. [AIBN]=0.05 mol/L, $f_{p\text{-MSty}}$=90 mol%. 127
Figure 12.21 Simulation of AN/*p*-MSty Copolymerization in Bulk at 60°C. $f_{p\text{-MSty}}$=80 mol%. 127
Figure 12.22 Simulation of AN/*p*-MSty Copolymerization in Bulk at 64°C. $f_{p\text{-MSty}}$=80 mol%. 128
Figure 12.23 Simulation of Composition in AN/*p*-MSty Copolymerization in Bulk at 40°C. [AIBN]=0.01 mol/L 128
Figure 12.24 Simulation of Composition in AN/*p*-MSty Copolymerization in Bulk at 60°C. [AIBN]=0.01 mol/L 129
Figure 12.25 Simulation of Composition in AN/*p*-MSty Copolymerization in Bulk at 80°C. [AIBN]=0.01 mol/L 129
Figure 12.26 Simulation of Molecular Weight in AN/*p*-MSty Copolymerization in Bulk at 60°C.[AIBN]=0.01 mol/L, $f_{p\text{-MSty}}$=56 mol%. 130
Figure 12.27 Simulation of Molecular Weight in AN/*p*-MSty Copolymerization in Bulk at 60°C.[AIBN]=0.05 mol/L, $f_{p\text{-MSty}}$=56 mol%. 130
Figure 12.28 Simulation of Molecular Weight in AN/*p*-MSty Copolymerization in Bulk at 80°C.[AIBN]=0.01 mol/L, $f_{p\text{-MSty}}$=56 mol%. 131
Figure13.1 Simulation of BA/MMA/VAc Terpolymerization in Bulk at 50°C. [AIBN]=0.01 mol/L 142
Figure 13.2 Simulation of Terpolymer Composition in BA/MMA/VAc Terpolymerization

in Bulk at 50°C. [AIBN]=0.01 mol/L 143
Figure 13.3 Simulation of Molecular Weight Average in BA/MMA/VAc Terpolymerization in Bulk at 50°C. [AIBN]=0.01 mol/L 143
Figure 13.4 Simulation BA/MMA/VAc Terpolymerization in Bulk at 50°C. ([AIBN]: 0.071 mol/L) 144
Figure 13.5 Simulation of Molecular Weight Average BA/MMA/VAc Terpolymerization at 50°C. ([AIBN]: 0.071 mol/L) 144
Figure 13.6 Simulation of Terpolymer Composition in BA/MMA/VAc Terpolymerization at 50°C. ([AIBN]: 0.071 mol/L) 145
Figure 13.7 Simulation of BA/MMA/VAc Terpolymerization in Bulk at 70°C. [AIBN]=0.01 mol/L 145
Figure 13.8 Simulation of BA/MMA/VAc Terpolymerization in Bulk at 70 °C. [AIBN]=0.01 mol/L 146
Figure 13.9 Simulation of Terpolymer Composition of BA/MMA/VAc Terpolymerization in Bulk at 70°C. [AIBN]= 0.01 mol/L 146
Figure 13.10 Simulation of Molecular Weight Averages of BA/MMA/VAc Terpolymerization in Bulk at 70°C. [AIBN]= 0.01 mol/L 147
Figure 13.11 Simulation of Molecular Weight Averages of BA/MMA/VAc Terpolymerization in Bulk at 70°C. [AIBN]= 0.071 mol/L 147
Figure 13.12 Simulation of Terpolymer Composition of BA/MMA/VAc Terpolymerization in Bulk at 70°C. ([AIBN]: 0.071 mol/L) 148
Figure 13.13 Simulation of Molecular Weight Averages of BA/MMA/VAc Terpolymerization in Bulk at 70°C. [AIBN]= 0.071 mol/L 148
Figure 13.14 Simulation of BA/MMA/VAc Terpolymerization in Toluene at 70°C. [AIBN]=0.071 mol/L 150
Figure 13.15 Simulation of Composition Drift in BA/MMA/VAc Terpolymerization in Toluene at 70°C. [AIBN]=0.071 mol/L 150
Figure 13.16 Simulation of BA/MMA/VAc Terpolymerization Rate in Toluene at 70°C. [AIBN]=0.071 mol/L 151

Figure 13.17 Simulation of Weight-Average Molecular Weight in BA/MMA/VAc Terpolymerization in Toluene at 70°C. [AIBN]=0.071 mol/L 151
Figure 14.1 Emulsion Polymerization Diagram (stages I and II) 176
Figure 14.2 Emulsion Polymerization Diagram 177
Figure 15.1 Particle formation in aqueous phase 194
Figure 15.2 Model testing on homogeneous particle nucleation 202
Figure 15.3 Gibbs Free Energy in Stages I and II in Styrene Homopolymerization in Emulsion 211
Figure 15.4 Gibbs Free Energy of Styrene in Stage III. 214
Figure 16.1 Reaction Formulation Screen 229
Figure 16.2 Computational Options Screen 230
Figure 16.3 Output Files Screen 231
Figure 16.4 Flow Options Screen 232
Figure 17.1 Simulation of Styrene Emulsion Homopolymerization at 60°C. (Runs #1 and #4) 242
Figure 17.2 Simulation of Styrene Emulsion Homopolymerization at 60°C. (Runs #2 and #5) 242
Figure 17.3 Simulation of Styrene Emulsion Homopolymerization at 60°C. (Run #3) 243
Figure 17.4 Simulation of Styrene Emulsion Homopolymerization at 60°C. (Model testing on particle generation) 243
Figure 17.5 Simulation of Styrene Emulsion Homopolymerization at 60°C. (Water: 700g, Styrene: 300g, SDS: 14.28g, KPS: 7.07g) 244
Figure 17.6 Simulation of Weight Average Molecular Weight in Styrene Emulsion Homopolymerization at 60°C. 244
Figure 17.7 Simulation of Emulsion Homopolymerization of Styrene at 50°C. (Monomer: 90g, water: 603g, KPS: 1.05 wt%, SDS 3.753 g) 245
Figure 17.8 Simulation of Styrene Emulsion Homopolymerization at 50°C.

(M: 196.53g, water: 393.06g, KPS: 0.0046 mol/L, SDS: 0.05 mol/L) . . 246
Figure 17.9 Simulation of Styrene Emulsion Homopolymerization at 50°C.
(M: 196.53g, water: 393.06g, KPS: 0.0046 mol/L, SDS: 0.06 mol/L) . . 247
Figure 17.10 Simulation of Styrene Emulsion Homopolymerization at 50°C.
(M: 196.53g, water: 393.06g, KPS: 0.0046 mol/L, SDS: 0.07 mol/L) . . 247
Figure 17.11 Heat of Reaction for Styrene Homopolymerization at 50°C.
(M: 196.53g, water:393.06g, KPS:0.0046 mol/L, SDS: 0.05 mol/L) . . . 249
Figure 17.12 Simulation of Styrene Emulsion Homopolymerization at 50 °C.
Prediction of Total Number of Particles. 250
Figure 17.13 Simulation of Styrene Emulsion Homopolymerization at 50 °C.
Prediction of Total Number of Particles 250
Figure 17.14 Simulation of Styrene Emulsion Homopolymerization at 50°C.
Prediction of Total Number of Particles. 251
Figure 17.15 Simulation of Styrene Emulsion Homopolymerization at 50 °C.
Prediction of Total Number of Particles. 251
Figure 17.16 Simulation of Styrene Emulsion Homopolymerization at 45°C.
(Sty: 100g, water: 200g, KPS: 0.5g, SDS: 5g) 252
Figure 17.17 Simulation of Styrene Emulsion Homopolymerization.
Styrene: 4 mol/L, KPS: 0.0075 mol/L, SDS: 0.132 mol/L. 253
Figure 17.18 Simulation of Styrene Emulsion Homopolymerization at 50°C.
Water: 1 L, monomer: 572 ml, [KPS]: 0.0046 mol/Lw 254
Figure 17.19 Simulation of Styrene Emulsion Homopolymerization at 70°C.
(Styrene: 130.7g, water: 515.6, KPS: 0.233g, SDS: 2.62g) 257
Figure 17.20 Simulation of Styrene Emulsion Homopolymerization at 70°C.
Unswollen Particle Diameter.
(Styrene: 130.7g, water: 515.6, KPS: 0.233g, SDS: 2.62g) 257
Figure 17.21 Simulation of Styrene Emulsion Homopolymerization at 70°C.
(Styrene: 130.7g, water: 515.6, KPS: 0.233g, SDS: 2.62g) 258
Figure 17.22 Simulation of Styrene Emulsion Homopolymerization at 70°C.

Unswollen Particle Diameter
(Styrene: 130.7g, water: 515.6, KPS: 0.233g, SDS: 2.62g) 258
Figure 17.23 Simulation of Number Average Molecular Weight in Styrene Emulsion Homopolymerization at 70°C.
(Styrene: 130.7g, water: 515.6, KPS: 0.233g, SDS: 2.62g) 259
Figure 17.24 Simulation of Weight Average Molecular Wegith in Styrene Emulsion Homopolymerization at 70°C.
(Styrene: 130.7g, water: 515.6, KPS: 0.233g, SDS: 2.62g) 259
Figure 18.1 Simulation of Vinyl Acetate Emulsion Polymerization at 50°C.
KPS: 1.25 g/Lw, M: 0.5 g/ml water. 265
Figure 18.2 Simulation of Vinyl Acetate Emulsion Polymerization at 50°C.
SDS: 6.25 g/Lw, M: 0.5 g/ml water. 266
Figure 18.3 Comparison of Model Predicted and Reported .
SDS: 6.25 g/Lw, KPS: 1.25 g/Lw, M: 0.5 g/ml water. 267
Figure 18.4 Monomer Partitioning in Vinyl Acetate Emulsion Homopolymerization at 50°C.
M: 0.5 g/ml water, SDS: 1.88 g/Lw, KPS: 1.25 g/Lw 267
Figure 18.5 Simulation of Vinyl Acetate Emulsion Homopolymerization at 50°C. (VAc: 1.1 L, Water: 3 L, SDS: 33.6 g, KPS: 2.5 g) 269
Figure 18.6 Simulation of Vinyl Acetate Emulsion Homopolymerization at 50°C. (VAc: 1.1 L, Water: 2.8 L, SDS: 33.6 g, KPS: 1.8 g) 269
Figure 18.7 Simulation of Vinyl Acetate Emulsion Homopolymerization at 50°C. (VAc: 1.15 L, Water: 2.86 L, SDS: 28.8 g, KPS: 3 g) 270
Figure 18.8 Simulation of Vinyl Acetate Emulsion Homopolymerization at Various Temperatures.
M: 1150 ml, water: 2860 ml, SDS: 28.8 g. 270
Figure 18.9 Average Unswollen Particle Diameter in Vinyl Acetate Emulsion Homopolymerization at 50°C. M: 1150 ml, water: 2860 ml, KPS: 3 g. .. 272
Figure 18.10 Weight Average Molecular Weight Data in Vinyl Acetate Emulsion Homopolymerization at 50°C.
M: 1150 ml, water: 2860 ml, KPS: 3g, SDS: 28.8 g 272

Figure 18.11 Weight Average Molecular Weight Data in Vinyl Acetate Emulsion Homopolymerization at 60°C.
M: 1150 ml, water: 2860 ml, KPS: 3 g, SDS: 28.8g. 273
Figure 18.12 Weight Average Molecular Weight Data in Vinyl Acetate Emulsion Homopolymerization at 40 and 70°C.
M: 1150 ml, water: 2860ml, SDS: 28.8 g 273
Figure 19.1 Simulation of Seeded Methyl Methacrylate Homopolymerization in Emulsion at 60C.
(0.294 gr polybutyl acrylate seed per ml latex, Np: 1.09E17 /L latex, initial seed diameter 170nm, final conversion in the seed: 95.6%, seed: 20 ml, MMA: 20 ml, water: 40 ml) 279
Figure 19.2 Simulation of Particle Size in Seeded Methyl Methacrylate Homopolymerization in Emulsion at 60C.
(0.294 gr polybutyl acrylate seed per ml latex, Np: 1.09E17 /L latex, initial seed diameter 170nm, final conversion in the seeds: 95.6%, seed: 20 ml, MMA: 20 ml, water: 40 ml) 280
Figure 19.3 Simulation of Methyl Methacrylate Emulsion Homopolymerization at 50 °C Using Calorimetry. 281
Figure 19.4 Simulation of Methyl Methacrylate Emulsion Homopolymerization at 60 °C.
(MMA: 1.5 kg, Water: 2.401 kg, APS: 1.0506g, AMA-80: 7.496g, AOT-75: 8.325g) 283
Figure 19.5 Simulation of Particle Size for Methyl Methacrylate Emulsion Homopolymerization at 60 °C.
(MMA: 1.5 kg, Water: 2.401 kg, APS: 1.0506g, AMA-80: 7.496g, AOT-75: 8.325g) 283
Figure 19.6 Simulation of Number of Particles in Methyl Methacrylate Emulsion Homopolymerization at 60°C.
(MMA: 1.5 kg, water:2.401 kg, APS: 1.0506 g, AMA-80: 7.496 g, AOT- 75: 8.325) 284

Figure 19.7 Simulation of Molecular Weight in Methyl Methacrylate Emulsion Homopolymerization at 60 °C. (MMA: 1.5 kg, Water: 2.401 kg, APS: 1.0506g, AMA-80: 7.496g, AOT-75: 8.325g) 285

Figure 19.8 Simulation of Conversion in Methyl Methacrylate Emulsion Homopolymerization at 50 °C. (MMA: 300 g, Water: 700 g, SDS: 0.02 mol/Lw) 287

Figure 19.9 Simulation of Conversion in Methyl Methacrylate Emulsion Homopolymerization at 50 °C. (MMA: 300 g, Water: 700 g, KPS: 0.005 mol/Lw) 287

Figure 19.10 Simulation of Conversion in Methyl Methacrylate Emulsion Homopolymerization at 50 °C. (MMA: 300 g, Water: 700 g, KPS: 0.005 mol/Lw) 288

Figure 19.11 Simulation of Conversion in Methyl Methacrylate Emulsion Homopolymerization at 50 °C. (MMA: 300 g, Water: 700 g, KPS: 0.005 mol/Lw) 288

Figure 19.12 Simulation of Conversion in Methyl Methacrylate Emulsion Homopolymerization at 50 °C. (MMA: 300 g, Water: 700 g, KPS: 0.005 mol/Lw) 289

Figure 19.13 Simulation of Particle Size in Methyl Methacrylate Emulsion Homopolymerization at 50 °C. (MMA: 300 g, Water: 700 g) 289

Figure 19.14 Simulation of Conversion in Methyl Methacrylate Emulsion Homopolymerization. (MMA: 300 g, Water: 700 g, KPS: 0.005 mol/Lw: SDS: 0.02 mol/Lw) . 290

Figure 19.15 Simulation of Conversion in Methyl Methacrylate Emulsion Homopolymerization at 50 °C. MMA: 220 g, water: 510 g, KPS: 0.005 mol/L. 291

Figure 19.16 Simulation of Conversion in Methyl Methacrylate Emulsion Homopolymerization at 50 °C. MMA: 220 g, water: 510 g, KPS: 0.005 mol/L. 292

Figure 19.17 Number of Particles in Methyl Methacrylate Emulsion Homopolymerization at 50 °C. MMA: 220 g, water: 510 g, KPS: 0.005 mol/L. 292
Figure 19.18 Simulation of Conversion in Methyl Methacrylate Emulsion Homopolymerization at 55 °C. M/W: 40/60, SDS: 0.244 wt%, KPS: 0.165 wt%. 293
Figure 19.19 Simulation of Conversion in Methyl Methacrylate Emulsion Homopolymerization Using Online Densitometry.
(M/W: 43%, [SDS]: 0.02 mol/Lw, [APS]: 0.01 mol/Lw) 294
Figure 19.20 Simulation of Conversion in Butyl Acrylate Homopolymerization in Emulsion at 60C. (Water: 100g, BA: 6.66g, SDS: 2g, APS: 0.2g) 298
Figure 19.21 Simulation of Conversion in Butyl Acrylate Homopolymerization in Emulsion at 60C. (BA: 100g, KPS: 4g, water: 600g, SDS: 0.1g) 299
Figure 19.22 Simulation of Conversion in Butyl Acrylate Emulsion Homopolymerization under Nonisothermal Conditions.
(initial temperature: 60°C, BA: 1436g, water: 2419 g, APS: 1.45 g AMA-80: 14.472 g, AOT-75: 14.325 g) 301
Figure 19.23 Simulation of Particle Size in Butyl Acrylate Emulsion Homopolymerization under Nonisothermal Conditions.
(Initial temperature: 60 °C, BA: 1436 g, water: 2419 g, APS:
145 g, AMA-80: 14.472g, AOT-75: 14.325) 301
Figure 19.24 Simulation of Number of Particles in Butyl Acrylate Emulsion Homopolymerization under Nonisothermal Conditions.
(initial temperature: 60°C, BA: 1436g, water: 2419 g, APS: 1.45 g AMA-80: 14.472 g, AOT-75: 14.325 g) 302
Figure 19.25 Simulation of Conversion in Butyl Acrylate Emulsion Homopolymerization at 60°C.
(BA: 1436g, water: 2419 g, APS: 1.45 g, AMA-80: 14.472 g, AOT-75: 14.325 g) 302
Figure 19.26 Simulation of Number of Particles in Butyl Acrylate Emulsion

Homopolymerization at 60°C.
(BA: 1436g, water: 2419 g, APS: 1.45 g, AMA-80: 14.472 g, AOT-75: 14.325 g) 303

Figure 19.27 Simulation of Particle Size in Butyl Acrylate Emulsion Homopolymerization at 60°C.
(BA: 1436g, water: 2419 g, APS: 1.45 g, AMA-80: 14.472 g, AOT-75: 14.325 g) 303

Figure 19.28 Simulation of Conversion in Butyl Acrylate Emulsion Homopolymerization at 60 °C. (water: 400 g, AOT: 3 g, AMA: 3 g, BA: 200 g, APS: 0.6 g) ... 304

Figure 19.29 Simulation of Conversion in Ethyl Acrylate Emulsion Homopolymerization at 60°C. (EA: 92.4g, water: 150 g, KPS: 0.1 g) 307

Figure 19.30 Simulation of Conversion in Ethyl Acrylate Emulsion Homopolymerization at 60°C. (EA: 92.4g, water: 150 g, KPS: 0.1 g) 307

Figure 19.31 Simulation of Conversion in Ethyl Acrylate Emulsion Homopolymerization at 60°C. (EA: 92.4g, water: 150 g, KPS: 0.1 g) 308

Figure 20.1 Calculation of Monomer Concentration in Polymer Particles in Styrene and Methyl Methacrylate Emulsion Copolymerization 319

Figure 20.2 Total Volume of All Three Phases in Styrene and Methyl Methacrylate Emulsion Copolymerization 319

Figure 20.3 Volume of Individual Monomers in Different Phases. 320

Figure 20.4 Comparison of Ratio of Volume of Styrene over Methyl Methacrylate in Monomer Droplets and Polymer Particles. 320

Figure 20.5 Simulation of Styrene/Methyl Methacrylate Emulsion Copolymerization at 50°C. Styrene: 100 g/Lw, MMA: 100 g/Lw, SDS: 6.25 g/Lw 325

Figure 20.6 Simulation of Styrene/Methyl Methacrylate Emulsion Copolymerization at 50°C. Styrene: 100 g/Lw, MMA: 100 g/Lw, KPS 1.25 g/Lw. 325

Figure 20.7 Prediction of Number of Particles in Styrene/Methyl Methacrylate Emulsion Copolymerization at 50°C.
Styrene: 100 g/Lw, MMA: 100 g/Lw, KPS 1.25 g/Lw. 326

Figure 20.8 Simulation of Styrene/Methyl Methacrylate Emulsion Copolymerization at Various Monomer Feeds.
Styrene: 100 g/Lw, MMA: 100 g/Lw, SDS 6.25 g/Lw, KPS: 1.25 g/Lw. 326
Figure 20.9 Calculation of Copolymer Composition in Styrene and Methyl Methacrylate Emulsion Copolymerization at 50°C. 327
Figure 20.10 Prediction of Styrene Concentration in Polymer Particles by Solving Thermodynamic Equilibrium Equations. 327
Figure 20.11 Prediction of Methyl Methacrylate Concentration in Polymer Particles by Solving Thermodynamic Equilibrium Equations. 328
Figure 20.12 Simulation of Styrene and Methyl Methacrylate Emulsion Copolymerization at 50 °C.
Sty+MMA: 90 g, KPS: 0.18 g, SDS: 2.25 g, water: 270 g. 329
Figure 20.13 Simulation of Styrene and Methyl Methacrylate Emulsion Copolymerization at 50 °C.
Sty+MMA: 90 g, KPS: 0.18 g, SDS: 2.25 g, water: 270 g. 330
Figure 20.14 Simulation of Styrene and Methyl Methacrylate Emulsion Copolymerization at 50°C.
Sty+MMA: 90 g, KPS: 0.18 g, SDS: 2.25 g, water: 270 g. 330
Figure 20.15 Simulation of Styrene and Methyl Methacrylate Emulsion Copolymerization at 50°C.
Sty+MMA: 90 g, KPS: 0.18 g, SDS: 2.25 g, water: 270 g. 331
Figure 20.16 Simulation of Styrene and Methyl Methacrylate Emulsion Copolymerization at 50°C.
Sty+MMA: 90 g, KPS: 0.18 g, SDS: 2.25 g, water: 270 g 331
Figure A2.1 Effect of Water Soluble Inhibitor in Styrene Homopolymerization at 60°C.
Styrene: 1053 g, water: 2L, SDS: 63.18g, KPS: 3.263g 362
Figure A2.2 Styrene Emulsion Homopolymerization without Impurities at 55°C.
Styrene: 100 g, water: 200 g, SDS: 6 g, KPS: 0.31 g. 363
Figure A2.3 Styrene Emulsion Homopolymerization with Monomer Soluble Impurities at 55°C.

Styrene: 100 g, water: 200 g, SDS: 6 g, KPS: 0.31 g. 363

Figure A2.4 Styrene Emulsion Homopolymerization with Monomer Soluble Impurities at 55°C.
Styrene: 100 g, water: 200 g, SDS: 6 g, KPS: 0.31 g. 364

Figure A2.5 Particle Size in Styrene Emulsion Homopolymerization with t-Butyl Catechol at 55°C.
Styrene: 100 g, water: 200 g, SDS: 6 g, KPS: 0.31 g. 364

Figure A2.6 Emulsion Homopolymerization of Vinyl Acetate without Monomer Soluble Inhibitor. (VAc: 1.15 L, water: 2.86 L) 365

Figure A2.7 Emulsion Homopolymerization of Vinyl Acetate with Monomer Soluble Inhibitor. (VAc: 1.15 L, water: 2.86 L) 366

Figure A2.8 Emulsion Homopolymerization of Vinyl Acetate with Monomer Soluble Inhibitor. (VAc: 1.15 L, water: 2.86 L) 366

Figure A2.9 Emulsion Homopolymerization of Vinyl Acetate without Monomer Soluble Inhibitor. (VAc: 1.15 L, water: 2.86 L) 367

Figure A2.10 Emulsion Homopolymerization of Vinyl Acetate with Monomer Soluble Inhibitor. (VAc: 1.15 L, water: 2.86 L) 367

Figure A2.11 Emulsion Homopolymerization of Vinyl Acetate with Monomer Soluble Inhibitor. (VAc: 1.15 L, water: 2.86 L) 368

List of Tables

Table 2.1 Useful Papers for Copolymerization Model Development and Testing ... 13
Table 3.1 Useful References on Modeling of Copolymer Tg ... 31
Table 6.1 Literature References on Methyl Methacrylate/Styrene Copolymer ... 42
Table 7.1 Literature references for Styrene/Acrylonitrile ... 51
Table 8.1 References on Styrene/Butyl Acrylate ... 64
Table 8.2 References on Sty/EA Copolymerization ... 71
Table 8.3 References on 2-hydroxyethyl acrylate polymerization ... 84
Table 9.1 Reactivity Ratios of MMA/EA ... 88
Table 9.2 Literature Listing for MMA/MA Copolymerization ... 90
Table 10.1 Literature Reference on MMA/BA Copolymerization ... 95
Table 10.2 References on MMA/VAc Copolymerization ... 101
Table 11.1 List of Reactivity Ratios for Sty/AA ... 108
Table 11.2 List of Reactivity Ratios for Sty/MAA ... 109
Table 12.1 Reference List for copolymerization of *p*-Methyl Styrene and Other Monomers ... 111
Table 14.1 Models of Emulsion Homo-/Copolymerization ... 181
Table 15.1 Water phase phenomena involving radicals ... 191
Table 15.2 Summary of Particle Nucleation Models ... 201
Table 15.3 Comparison of Methods for Monomer Partitioning in Emulsion Polymerization ... 204
Table 16.1 Monomer List ... 233
Table 16.2. Other Database Components ... 233
Table 16.3. Database Items for Potassium Sulphate ... 235
Table 16.4. Database Items for Sodium Dodecyl Sulphate ... 236
Table 17.1 Papers on Styrene Emulsion Polymerization Kinetics ... 239
Table 17.2 Reaction Recipes for Bataille et al.(1982) ... 240
Table 18.1 Selective Reference List for Vinyl Acetate Emulsion Polymerization ... 263

Table 19.1 Rate Constant for Termination and Propagation (MMA) 275
Table 19.2 Literature References on MMA Emulsion Polymerization 277
Table 19.3 Recipes of seeded emulsion polymerization of MMA 278
Table 19.4 Literature Review on Butyl Acrylate Emulsion Homopolymerization. .. 297
Table 19.5 Literature Summary on Ethyl Acrylate Emulsion Homopolymerization . 305

Chapter 1. Introduction and Objectives

Free-radical polymerization is of enormous importance to the polymer industry, however, models in the literature deal with only one or a limited number of monomer systems under rather restricted reaction conditions and hence are far from being general. This thesis presents a general approach to simulate free-radical multicomponent polymerizations in bulk, solution and emulsion. It gives an overview on kinetic studies and model development on multicomponent polymerization. The general approach consists of four steps: the first is an extensive literature search on both kinetic information as well as experimental data; the second is mathematical model development, the third is parameter estimation and database expansion and the final step is model testing. In this project, a flexible and powerful simulation package has been developed, which consists of two separate models, one for both bulk/solution and another for emulsion polymerization. Each model has its own database. The development of this simulation package marks the accomplishment of the long-term goals described in Figure 1.1 at the end of this chapter.

Most literature information on the modelling of polymerization in bulk and solution is restricted to the low conversion range. Studies on copolymerization or terpolymerization at high conversion range are very scarce. The first phase of this project is hence aimed at investigating this largely unstudied area. We started with the modelling of copolymerization in bulk and solution, the kinetics of which is relatively straightforward, and then we extended the work to terpolymerization.

The current bulk/solution model (an extension of previous work on bulk/solution homopolymerization, Gao and Penlidis, 1996) can describe the behaviour of co-/terpolymerization in bulk and solution over the entire conversion range. Information of physical/chemical properties of many polymerization components is stored in a comprehensive database. This bulk/solution model has been tested for many copolymer systems under a wide range of reaction conditions. The final step in building a general model to simulate multicomponent polymerization is to extend

the copolymerization model to terpolymerization. This has been accomplished and model testing results on terpolymerization are satisfactory.

The second phase of this project is the development of a model for emulsion polymerization. The kinetics of emulsion polymerization are much more complicated largely due to the heterogeneity of the reaction mixture. Emulsion polymerization is a chemical process which involves mass transfer of monomers, radical desorption, particle nucleation, etc. The same general approach used in the bulk/solution model development was adopted to build the emulsion model. The literature was first extensively searched, and other research groups' models on describing various important phenomena in emulsion were carefully studied, critically evaluated and selectively implemented. A mathematical model was then first built to simulate homopolymerization in emulsion. Great effort has been made to implement models that can describe most important physicochemical phenomena (micelle formation, particle nucleation, absorption and desorption of radicals, monomer partitioning, gel effect, etc.) occurring in emulsion polymerization and keep the model simple with a minimum number of parameters. The model can describe important reaction characteristics (conversion profile and rate of polymerization) and polymer properties (number of particles, particle size, molecular weight averages, copolymer composition and sequence, etc.). Monomer systems with very different kinetic characteristics ("case 2" monomers like styrene; "case 1" monomers like vinyl acetate; "case 3" monomers like methyl methacrylate, etc.) have been fully tested. Good simulation results have confirmed that the model can deliver reliable predictions over the entire conversion range. The emulsion model was then further extended to describe the kinetic behaviour of emulsion copolymerization. A database for this emulsion simulation package was also developed in parallel.

Three factors make the overall package distinct from other models available in the literature:

(1) many industrially important but not kinetically understood co-/terpolymer systems have been studied and simulated for the first time
(2) the simulator is user friendly and flexible

(3) the comprehensive database can describe the physical/chemical characteristics for many different polymerization ingredients

The last factor is most significant. The parallel development/enrichment of the database forces one to support a strong modelling effort with an equally strong experimental program. This is, indirectly, another factor that differentiates this package from other similar efforts.

1.1 Objectives

The overall objectives are described in detail below.

Model Development

The aim here is to first develop a comprehensive, user friendly, reliable and flexible simulation package for free-radical multicomponent polymerizations in bulk, solution and emulsion. Reactor configurations are batch, semibatch and continuously stirred tank reactors (CSTR). Temperature cases include isothermal, adiabatic, non-isothermal and user-defined temperature profiles. Initiation options include singular or multiple chemical initiators, thermal initiation or redox system. Both models can deliver predictions on reaction characteristics like conversion, rate of polymerization as well as polymer properties like molecular weight, composition and total number of particle and particle diameters in emulsion polymerization etc.

Database Establishment

The aim here is to establish, in a marked digression from common practice, a detailed, easy to update, comprehensive database for monomers, initiators, solvents, chain transfer agents, inhibitors, etc. The database of the emulsion package will certainly contain other components like emulsifiers. Each reaction species has its own database items by which its physical/chemical properties are defined.

Model Testing

The target here is to test the simulator's validity and reliability as widely as possible. No model can claim to be reliable until it is tested. Extensive literature search will be carried out to collect kinetic information and experimental data as much as possible for the testing phase. More importantly, all simulation results, regardless of reaction recipes, operation conditions and reactor configurations, will be generated based on the same database.

1.2 Contributions of the Thesis

Not too long ago, there were hardly any models presented in the literature. This was obviously due to two reasons: first, the lack of understanding on polymerization kinetics and second, the limitations of computational power. Recently, with great advances in computer science, the computation constraint can easily be overcome. This makes modelling of free-radical polymerization a feasible task, yet a large number of monomer systems of industrial importance are still unstudied. As a result, this lack of understanding limits most models represented in the literature to only a few monomers, mostly styrene or methyl methacrylate. This simulation package can be considered as an epitome of recent advances in kinetic understanding in free-radical polymerization in bulk, solution and emulsion up to high conversion levels. The overall project is very extensive, if not particularly ambitious, as commented by O'Neil and Torkelson (1997) "*...The result (*of this project*) is a simulator package containing a comprehensive database which appears to have the best chance of any current model to predict the course of a range of polymerization conditions for a range of monomers*".

The overall research effort was focused in two major areas: one was in the development of a model/database for bulk and solution, and the other for emulsion. Major contributions in each area are described below:

1) Bulk and solution model/database development

The current comprehensive bulk and solution model/database includes the 12 commercially most important monomer systems such as methyl methacrylate, styrene, vinyl acetate, *p*-methyl styrene, ethyl acrylate, methyl acrylate, butyl acrylate, acrylic acid, methacrylic acid, acrylonitrile, butyl

methacrylate, and hydroxy ethyl acrylate, as well as an extensive list of other reaction species (more than 50 initiators, many solvents, inhibitors and chain transfer agents). For the first time in the literature, full conversion range experiments and kinetic investigation and simulation of ethyl acrylate and methyl acrylate homopolymerization were carried out. Simulation results on these two monomers revealed the fact that reaction diffusion plays an important kinetic role. This model is also the only one known so far that is able to simulate homopolymerization of carboxylic acids over the entire pH range up to high conversion. It is known that the pH value of the reaction media significantly affects the rate of polymerization, its mechanism is very complicated and not well-understood, and to describe the pH effect on polymerization rate over the entire pH range is a very challenging task. Detailed simulation results can be found in Gao and Penlidis (1996).

Model testing results on copolymerization are summarized in the first volume in this thesis. Over 300 references are discussed and a total of 15 copolymer systems have been tested. This is the first time in the literature that simulation of glass transition temperature (Tg) of copolymers is reviewed. Additionally, for the first time, copolymerizations of styrene/ethyl acrylate, styrene/butyl acrylate, styrene/2-hydroxyethyl acrylate, butyl acrylate/vinyl acrylate, methyl methacrylate/vinyl acetate and methyl methacrylate/butyl acrylate were simulated over the entire conversion range. The 'double rate phenomenon' and severe composition drift first observed in the copolymerizations of butyl acrylate/vinyl acetate and methyl methacrylate/vinyl acetate are well described by the model. No other models so far are able to simulate such a large number of copolymers under such a wide range of reaction conditions.

Butyl acrylate, methyl methacrylate and vinyl acetate terpolymer is a typical example of a commercially important terpolymer system that has not been studied. This thesis discusses the kinetic scheme of terpolymerization over the entire conversion range. For the first time in the literature, terpolymerization in bulk and solution is simulated over the whole conversion range by this bulk/solution model.

Perhaps the most impressive feature of this simulation package is its extensive database. Based

on its rich collection of twelve monomers, fifty two initiators and dozens solvents, CTAs, etc., the database gives the simulation package great flexibility no other models have. It is believed that this model is the only one that is capable of simulating homopolymerization, copolymerization and terpolymerization in bulk, solution and suspension based on only ***one*** set of database characteristics.

2) Emulsion model/database development

Though there is a large number of papers published on emulsion polymerization, models that can describe important emulsion homo- and copolymerization characteristics up to high conversion are rare. Because of limited understanding of emulsion polymerization kinetics, models in the literature are usually developed under many assumptions and are restricted to specific monomers or reaction conditions. Obviously, there is a lack of a general model. By adopting a similar general approach, this emulsion model is perhaps the only one that can simulate emulsion homopolymerization as well as copolymerization under a very wide range of reaction and operation conditions (batch, semibatch, seeded or unseeded, soap-free, etc.) using the ***same*** set of database characteristics.

This emulsion model also has a comprehensive database that includes styrene (a typical "case 2" monomer with very low water solubility and no desorption), vinyl acetate (a typical "case 1" monomer with high water solubility and significant desorption), methyl methacrylate (a typical case 3 monomer that exhibits strong gel effect), butyl acrylate, ethyl acrylate and methyl acrylate, a number of initiators including redox systems, emulsifiers, inhibitors and CTAs. Similar to the bulk/solution model, the database gives the emulsion model great flexibility. The user can just simply select the ingredients from the database, set up reaction conditions and the model will deliver the desired predictions. Such a feature is not only user-friendly but it also avoids reevaluating parameters for each homopolymer or copolymer.

1.3 Organization of the Thesis

This thesis consists of two volumes. Volume 1 concentrates on simulation of bulk and solution

polymerization, whereas volume 2 focuses on emulsion polymerization. In volume 1, the thesis first gives a brief overview of the classical theory on bulk/solution copolymerization kinetics as well as recent advances in chapter 2. Description of the simulation package and its database is given in chapters 3 and 4. Chapter 5 discusses the general procedures for polymerization experiments and polymer characterization used in this laboratory. Guidelines used in model testing are also highlighted. Chapters 6 to 12 contain model testing results for 15 different copolymer systems. Chapter 13 summarizes the simulation of terpolymerization in bulk and solution. At the end of the volume, a bibliography is given for all the references cited on bulk/solution.

In volume 2, chapter 14 briefly introduces classical theories on emulsion polymerization. Chapter 15 discusses in great detail important aspects in emulsion polymerization and their modelling. Chapter 16 describes the database of the emulsion model. Chapters 17 to 19 present simulation results for emulsion homopolymerization of five different monomer systems (styrene, methyl methacrylate, vinyl acetate, butyl acrylate, ethyl acrylate). Chapter 20 shows the extension of model development to emulsion copolymerization as well as model testing results on styrene/methyl methacrylate emulsion copolymerizaiton. Finally, Chapter 21 makes concluding remarks and discusses immediate future steps. There are two appendices in volume 2. Appendix 1 presents model development for seeded emulsion polymerization. Appendix 2 discusses impurity effect on emulsion polymerization kinetics. The overall nomenclature for the entire thesis is given at the end of volume 2, along with references cited on the emulsion part.

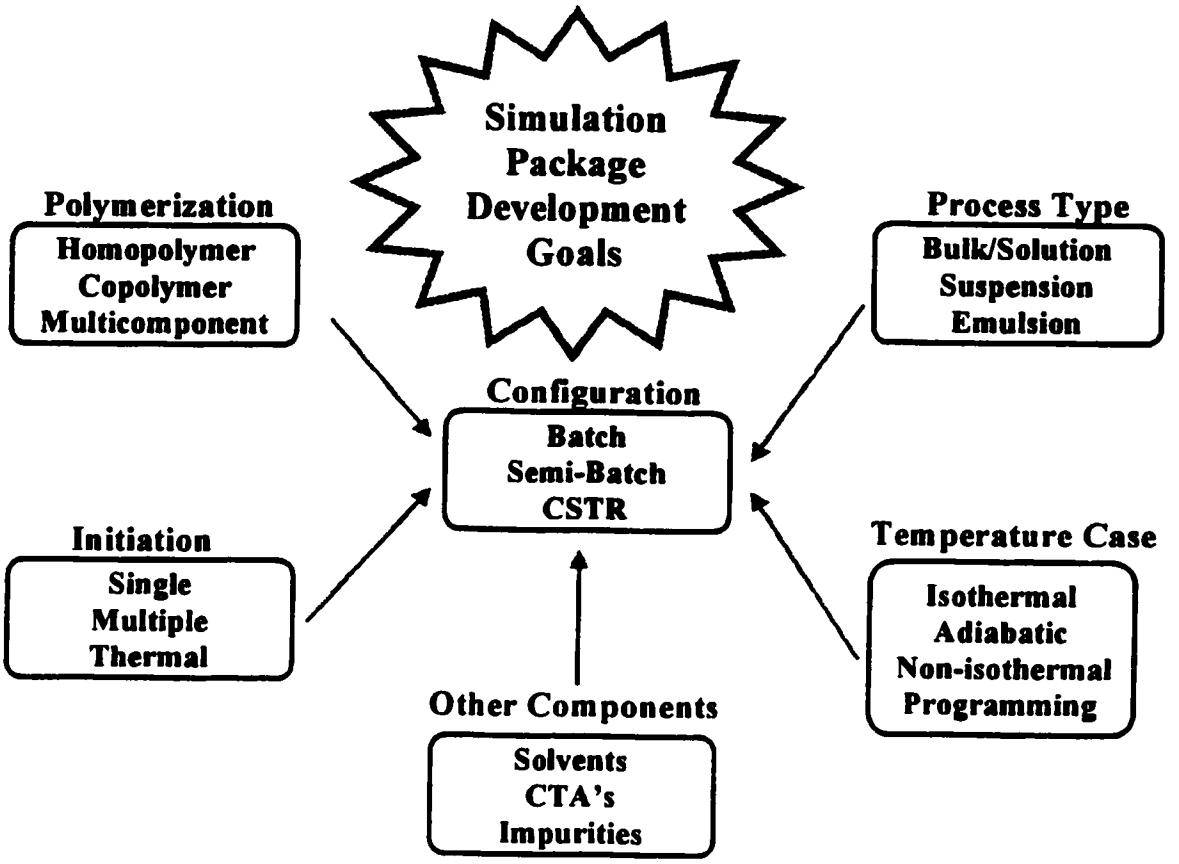

Figure 1.1 Long-Term Model Development Goals

Chapter 2. Brief Theoretical Background on Bulk and Solution Copolymerization

2.1 Classical Theory

Classical kinetics on copolymerization was first presented by Mayo and Lewis (1944) and Alfrey and Goldfinger (1944). The kinetics they presented is also known as the terminal model. Propagation is the most important step in copolymerization, because it influences both productivity (rate of polymerization) and quality (molecular weight, composition, sequence length) of the copolymer produced. In the terminal model, the reactivity of each radical is determined by the monomer unit at the active center of the chain end, hence the propagation reaction involves four steps as shown below.

$$R_{r,1}\cdot + M_1 \xrightarrow{kp_{11}} R_{r+1,1}\cdot \qquad (2.1)$$

$$R_{r,1}\cdot + M_2 \xrightarrow{kp_{12}} R_{r+1,2}\cdot \qquad (2.2)$$

$$R_{r,2}\cdot + M_1 \xrightarrow{kp_{21}} R_{r+1,1}\cdot \qquad (2.3)$$

$$R_{r,2}\cdot + M_2 \xrightarrow{kp_{22}} R_{r+1,2}\cdot \qquad (2.4)$$

where k_{p11}, k_{p12}, k_{p21}, k_{p22} are the propagation rate constants for reactions 2.1 to 2.4, respectively. Subscripts 1 and 2 used in the above reactions denote monomer/radical 1 and 2. Reactivity ratios are defined as $r_1 = k_{p11}/k_{p12}$, $r_2 = k_{p22}/k_{p21}$. Reactivity ratios indicate the preference of a radical reacting with two different types of monomers and hence directly reflect the reaction characteristics of a copolymer system. They are the most important parameters used in the modeling of copolymerization. $[R_1\cdot]$ and $[R_2\cdot]$ are defined as the concentrations (mol/L) of all radicals of type 1 and 2 with chain length from 1 to infinity, respectively.

According to the so-called long chain approximation of type II (LCA II),

$$kp_{12}[R_1\cdot][M_2] = kp_{21}[R_2\cdot][M_1] \qquad (2.5)$$

Xie and Hamielec (1993a, b) verified that equation 2.5 is valid for both linear and branched

copolymer systems as long as long chain polymer is produced. From equations 2.1 to 2.5, along with the steady-state hypothesis for radicals, the ratio of the instantaneous copolymer composition of monomer 1 over that of monomer 2 can be derived as:

$$\frac{F_1}{F_2} = \frac{r_1 f_1^2 + f_1 f_2}{f_1 f_2 + f_2^2} \tag{2.6}$$

where f_1 and f_2 are the composition of monomer 1 and 2 in the feed and F_1 and F_2 are the composition of monomer 1 and 2 in the copolymer chain. Equation 2.6 is commonly referred to as the Mayo-Lewis equation. Dead copolymer is produced through termination reactions as follows:

$$R_{r,1}\cdot + R_{s,1}\cdot \xrightarrow{kt_{11}} Dead\ \ Polymer \tag{2.7}$$

$$R_{r,1}\cdot + R_{s,2}\cdot \xrightarrow{kt_{12}} Dead\ \ Polymer \tag{2.8}$$

$$R_{r,2}\cdot + R_{s,2}\cdot \xrightarrow{kt_{22}} Dead\ \ Polymer \tag{2.9}$$

where k_{t11}, k_{t12} and k_{t22} are the rate constants of termination for reactions 2.7 to 2.9. k_{t12} is defined as the cross-termination rate constant, which received much literature attention in the early studies and will be discussed in more detail in section 3.2 below.

Reactions 2.1 to 2.4 and 2.7 to 2.9 describe the two most fundamental reactions in a copolymerization, i.e, chain growth (propagation) and chain termination. Most of the early studies done on copolymerization kinetics in the 50's and 60's were mainly concerned with the reactivity of different monomers and the derivation of an overall expression for the rate of polymerization, as well as for the rate of termination. Much emphasis was also put on composition drift and reactivity ratio determination. Mayo and Walling (1950) reviewed early studies on copolymerization kinetics and derived rate expressions for copolymerization. The determination of the cross-termination rate constant was specially addressed. Ham (1964) gave an extensive review on copolymerization theory and covered many aspects on copolymerization. The classical theory on copolymerization was consolidated in the 60's and 70's and can be found in many classical textbooks on polymerization kinetics such as Odian (1982), etc.

2.2 Recent Advances in Copolymerization Kinetics at High Conversion Levels

The classical theory clearly described the general copolymerization characteristics in propagation, termination and polymer composition, but only limited to very low conversion levels. This is mainly due to diffusion controlled phenomena and the composition drift at higher conversion levels for certain copolymer systems. Atherton and North (1962) stated that termination in the copolymerization of methyl methacrylate and vinyl acetate was diffusion controlled, and they attempted to use a new expression for the rate of termination, which is a function of each monomer feed composition. However, their work was still limited to low conversion. Progress in copolymerization kinetic studies was hampered by the occurrence of diffusional limitations. In the late 70's and early 80's, several research groups (Marten and Hamielec 1979, Soh and Sundberg 1982a-d, Chiu et al. 1983) successfully described the polymerization over the entire conversion range based on free volume theory. It is considered that termination in free radical polymerization is a process that involves three consecutive steps which are segmental diffusion, translational diffusion, and reaction diffusion. At very high conversion levels, reaction diffusion becomes an important means of termination. The segmental diffusion control model was proposed by Mahabadi and O'Driscoll (1997a-c). Allen and Patrick (1974), Stickler (1983) and Russell et al. (1988) all presented their model for reaction diffusion control. Marten and Hamielec (1979, 1982) proposed a semi-empirical method to describe the polymerization kinetics up to high conversion. Their method was adopted and implemented into the previously developed model for homopolymerization. In the simulation for copolymerization, the same approach was used, and since the detailed implementation of the approach was already discussed in Gao and Penlidis (1996), it is not presented here again.

In the recent literature, several other groups also reviewed copolymerization kinetics and some proposed their own mathematical model. Wittmer (1979) summarized studies on copolymerization kinetics and studied cross-termination kinetics in detail. He also compared and tested different expressions for the rate of termination for several copolymer systems. Russo (1987) gave an overview of various models in the literature and discussed the initiation, propagation and termination stages in a qualitative way. Like many other reviews, emphasis was

on comparing various expressions of the overall rate of termination. Russo (1987) questioned the analytical methods used to assess the validity of the terminal and penultimate models and commented on future directions of model discrimination. Maxwell and Russell (1993) extended equations for homopolymerization to copolymerization. They also discussed diffusional control mechanisms at high conversion levels. Overall rate expressions for propagation, termination, and transfer reactions in copolymerization were derived from their homopolymerization analogy. Their thesis is a starting point to simulate copolymerization up to high conversion, yet unfortunately they presented no simulation results. Achilias and Kiparissides (1992) compared three different methods for molecular weight development in copolymerization for both linear and branched systems. Christiansen (1990) presented a model for reversible copolymerization. Arriola (1989) developed a model for homopolymerization and extended the kinetic scheme to both linear and branched copolymerization systems. Simulated results for batch styrene-acrylonitrile and solution vinyl acetate-methyl methacrylate continuous stirred tank reactor (CSTR) operation were presented. Balaraman et al.(1986) used a mathematical model based on free volume theory to study multiplicity and stability in the copolymerization of styrene and methyl methacrylate in a CSTR. Fukuda's group (Fukuda et al. 1982, 1985a-b, 1987a-b, 1989) performed extensive studies on copolymerization kinetics, however all their work was limited to low conversion evaluation of alternative termination models. Hamielec et al.(1989) gave several examples and discussed some other alternative copolymerization kinetic models and model discrimination.

While only few research groups studied kinetics of copolymerization at high conversion, simulation and experimental results over the full conversion range are even more scarce. Hamielec et al. (1987) and Dube et al.(1997) proposed a model for multicomponent polymerization in bulk and emulsion using the pseudo-kinetic rate constant method. Their model can simulate multicomponent polymerizations under a wide range of conditions. Important aspects in multicomponent polymerization kinetics, like diffusion controlled initiation, propagation and termination, molecular weight for linear and branched systems, and composition drift control are discussed in detail. More importantly, they tested their model for several copolymer systems over the entire reaction course. Good agreement was achieved between their model predictions and

experimental results. There are also other groups that presented full conversion data for various copolymer systems. Table 2.1 below lists the most useful papers on modeling or experimental work from various groups in the literature.

Table 2.1 Useful Papers for Copolymerization Model Development and Testing

Reference	Data Type	Copolymer System
Johnson et al.(1978)	experimental data	Sty/MMA
Dionisio and O'Driscoll (1979)	experimental data	Sty/MMA
Sebastian and Biesenberger (1981)	experimental data	Sty/AN
Hamielec and MacGregor (1983)	modeling, simulation	
O'Driscoll et al. (1984)	experimental data	Sty/MMA
Lord (1984)	modeling, simulation, experimental data	Sty/AN
Garcia-Rubio et al.(1985)	modeling, simulation, experimental data	Sty/AN
Bhattacharya and Hamielec (1985, 1986)	modeling, simulation, experimental data, thermal initiation	p-MSty/Sty
Jones et al.(1986)	modeling, simulation, experimental data	p-MSty/MMA
Yaraskavitch et al.(1987)	modeling, simulation, experimental data	p-MSty/AN
Achilias and Kiparissides (1987)	modeling, simulation	p-MSty/Sty
Hamielec et al.(1987)	modeling, simulation, experimental data	Sty/AN, Sty/p-MSty, p-MSty/AN, p-MSty/MMA
Sharma and Soane (1988)	modeling, simulation	Sty/MMA
Tobita and Hamielec (1988)	modeling, simulation, network formation	
O'Driscoll and Huang(1989, 1990)	experimental data	Sty/MMA
Dube et al. (1990a, b)	modeling, simulation, experimental data	Sty/BA
Wang and Ruckenstein (1993)	experimental data	MMA/EA, MMA/MA, MMA/BA
Xie and Hamielec (1993a, b)	simulation results	

Kim (1994)	simulation, experimental data	Sty/2-HEA
Dube and Penlidis (1995a)	simulation, experimental data	MMA/BA, MMA/VAc BA/VAc
McManus and Penlidis (1996)	experimental data	Sty/EA

Abbreviations used in Table 2.1 above refer to different monomer systems, and are explained below.

AA:	acrylic acid	MA:	methyl acrylate
AN:	acrylonitrile	MMA:	methyl methacrylate
BA:	butyl acrylate	p-MSty:	p-methyl styrene
EA:	ethyl acrylate	Sty:	styrene
2-HEA	2-hydroxy ethyl acrylate	VAc:	vinyl acetate

2.3 Penultimate Model and Model Discrimination

The penultimate model is an alternative model for copolymerization. It takes account of the effect of the penultimate unit as well as of the terminal unit at the end of a growing chain on the radical activity, hence there will be four distinguishable radicals in a copolymerization. This leads to eight different propagation steps as shown below,

$$R_{r,11}\cdot + M_1 \xrightarrow{kp_{111}} R_{r+1,11}\cdot \tag{2.10}$$

$$R_{r,11}\cdot + M_2 \xrightarrow{kp_{112}} R_{r+1,12}\cdot \tag{2.11}$$

$$R_{r,12}\cdot + M_1 \xrightarrow{kp_{121}} R_{r+1,21}\cdot \tag{2.12}$$

$$R_{r,12}\cdot + M_2 \xrightarrow{kp_{122}} R_{r+1,22}\cdot \tag{2.13}$$

$$R_{r,21}\cdot + M_1 \xrightarrow{kp_{211}} R_{r+1,11}\cdot \tag{2.14}$$

$$R_{r,21}\cdot + M_2 \xrightarrow{kp_{212}} R_{r+1,12}\cdot \tag{2.15}$$

$$R_{r,22}\cdot + M_1 \xrightarrow{kp_{221}} R_{r+1,21}\cdot \tag{2.16}$$

$$R_{r,22}^{\cdot} + M_2 \xrightarrow{kp_{222}} R_{r+1,22}^{\cdot} \qquad (2.17)$$

Since it was first introduced by Merz et al.(1946), the penultimate model has received much attention in the literature, the main reason for this being that several researchers (Jones et al. 1985, Prementine and Tirrell, 1989, Klumperman and Kraeger, 1994) observed deviations from the Mayo-Lewis equation (equation 2.6) in some copolymer systems. Hill et al. (1982, 1989, 1991, 1992) studied styrene-acrylonitrile copolymerization in bulk and various solvents. They used sequence length to distinguish between the terminal and penultimate model and concluded that both models give an equally good fit to the composition data but the penultimate model is better in interpreting the sequence length distribution. Recently, Olaj et al.(1985) introduced the PLP method (pulsed laser polymerization) to measure the rate constant of propagation directly. Their results were then used by Fukuda's group in their research on various copolymer systems. Fukuda et al.(1982, 1985a-b, 1987a-b, 1989) and Ma et al.(1993) investigated penultimate effects in the copolymer systems of MMA/Sty, p-chlorostyrene/MA, etc. They found that the terminal model gave a good fit for composition data but failed to describe the overall rate constant of propagation. In contrast, the penultimate model gave a better fit for the propagation rate constant. Fukuda et al.(1992) reached similar conclusions that the penultimate model is better in interpreting the copolymer propagation rate constant and sequence length distribution.

Burke et al.(1994, 1997) gave an extensive review on model discrimination in the literature from a rigorous statistical viewpoint. They carefully examined discrimination methods and experimental data from both Fukuda's and Hill's groups and pointed out that all previous research shared some common characteristics with respect to experimental design, modeling assumptions and data analysis, and that no statistical model discrimination methods were employed. They also critically evaluated three different statistical model discrimination methods (the Buzzi-Ferraris method (Buzzi-Ferraris and Forzatti, 1983), the exact entropy method (Reilly, 1970) and the method of Hsiang and Reilly (Hsiang and Reilly, 1971)). Based on the work of Burke et al.(1994, 1997), it can be concluded that (1): systematic application of model discrimination methodology can reduce the number of experiments required to choose between the terminal and penultimate

models for copolymerization compared to designs in which experiments are spread over the entire range of feed compositions; (2): the Buzzi-Ferraris method which is shown to perform better than the other two previously mentioned statistical methods detects smaller penultimate effects than those found by Hill et al.(1982), and (3): using statistical model discrimination methods can improve the modeling of copolymer systems and that composition data may be more useful in discriminating between copolymer models than previously thought. From all the work done so far on model discrimination, it can be concluded that sound statistical methods must be used in order to discriminate between the terminal and penultimate models based on data collected from carefully designed experiments, otherwise, erroneous conclusions may be reached.

In this thesis, it is not intended to focus on model discrimination. As a matter of fact, the penultimate unit may or may not exhibit any effect on a copolymer system, with the magnitude of the effect varying from system to system. The penultimate model has also been implemented and set up as a user option. The penultimate model option can be invoked for systems that exhibit more significant penultimate effects or in cases when the simulation of copolymer microstructure is more important. This practical approach was also suggested by Hamielec et al.(1989).

Chapter 3. Simulation Package Overview

The general approach for simulation of co-/terpolymerization in bulk and solution in this thesis is very similar to what was described in Gao and Penlidis (1996). The literature was first extensively searched to collect all useful information on copolymerization kinetics and experimental data (over 300 literature papers were reviewed). The current model uses Hamielec's pseudo-kinetic rate constant method and elements from diffusion theory to describe the kinetic behaviour of co-/terpolymerization in bulk and solution up to high conversion. The model has been developed to be flexible and robust.

The database of the previous homopolymerization model has been further extended to include copolymerization characteristics of many important copolymer systems. It provides all the necessary information the model needs to simulate copolymerization under a variety of reaction recipes and conditions. The current database includes 12 different monomers which may possibly form as many as 66 copolymer pairs, although not every copolymer pair might be of research and/or industrial interest. Through an exhaustive literature search, kinetic and experimental information on 15 different copolymer systems has been collected. Chemical/physical properties and polymerization characteristics of these 15 copolymer systems are studied in detail. Simulation results for each system are compared with experimental results either collected from the literature or generated in this laboratory in order to test the model's reliability.

Comparatively, copolymerization kinetic equations are more complex than the analogous equations for homopolymerization. All rate expressions are derived using the pseudo-kinetic rate constant method. The pseudo-kinetic rate constant method was first used by Hamielec and MacGregor (1983) and later widely employed by many research groups (Kuo and Chen 1981, Broadhead et al. 1985, Lord 1984, Hamielec et al. 1987, etc.). It reduces a copolymerization kinetic scheme to that of a homopolymerization and it greatly simplifies the rate expressions for copolymerization. The validity of the pseudo-kinetic rate constant method was carefully examined by Tobita and Hamielec (1991) and Xie and Hamielec (1993a-b). As mentioned before, the

copolymerization model was extended based on a previously developed homopolymerization model. The mathematical model frame, i.e., mass balances for each reactant, energy balances and molecular weight development, is similar to that of the homopolymerization model. The section below only briefly outlines key model equations for copolymerization. For detailed model development, refer to Gao and Penlidis (1996).

3.1 Model Development and Implementation

All rate constants in this section are defined as chemically controlled, i.e., they are only a function of temperature.

Initiation

$$I \xrightarrow{kd} 2R_o\cdot \tag{3.1}$$

$$R_o\cdot + M_1 \xrightarrow{kp_{01}} R_1\cdot \tag{3.2}$$

$$R_o\cdot + M_2 \xrightarrow{kp_{02}} R_2\cdot \tag{3.3}$$

In the above reactions, I is the chemical initiator, $R_0\cdot$ is the primary radical from initiator decomposition, and $R_1\cdot$ and $R_2\cdot$ are radicals of chain length unity of monomer type 1 and 2, respectively. The rate of initiation in copolymerization is the same as that in homopolymerization, i.e.,

$$R_I = 2fk_d[I] \tag{3.4}$$

Propagation

Reactions 2.1 to 2.4 are the propagation steps. The rate of copolymerization is the rate of disappearance of both monomers,

$$R_p = -\frac{d([M_1]+[M_2])}{dt} = k_p[M][R\cdot] \tag{3.5}$$

[M] is the total concentration of monomers, while [R·] is the total concentration of radicals.

According to the terminal model kinetic scheme, the pseudo-k_p in the above equation can be expressed as

$$k_p = kp_{11}\phi_1 \cdot f_1 + kp_{12}\phi_1 \cdot f_2 + kp_{21}\phi_2 \cdot f_1 + kp_{22}\phi_2 \cdot f_2 \quad (3.6)$$

where k_{p11} and k_{p22} are the homopolymerization rate constants of propagation for monomer 1 and 2, respectively, k_{p12} and k_{p21} are the cross-propagation rate constants for reactions 2.2 and 2.3, and $\phi \cdot_1$ and $\phi \cdot_2$ are the mole fractions of radical type 1 and 2, respectively, which can be expressed as:

$$\phi_1 \cdot = \frac{kp_{21} f_1}{kp_{21} f_1 + kp_{12} f_2} \quad (3.7)$$

$$\phi_2 \cdot = \frac{kp_{12} f_2}{kp_{21} f_1 + kp_{12} f_2} \quad (3.8)$$

When the radical steady-state hypothesis is used, the total radical concentration can be calculated as:

$$[R \cdot] = \left(\frac{2 f k_d [I]}{k_t} \right)^{1/2} \quad (3.9)$$

Termination

Reactions 2.7 to 2.9 are the termination steps in the copolymerization. The rate of termination is then expressed as

$$R_t = kt[R \cdot]^2 = kt_{11}[R_1 \cdot]^2 + 2kt_{12}[R_1 \cdot][R_2 \cdot] + kt_{22}[R_2 \cdot]^2 \quad (3.10)$$

where k_{t11} and k_{t22} are the rate constants for homo-termination for monomer 1 and 2, respectively, and k_{t12} is the cross-termination rate constant. It is common in the literature to redefine the cross-termination rate constant k_{t12} as

$$kt_{12} = \phi (kt_{11} kt_{22})^{1/2} \quad (3.11)$$

ϕ in the equation above is called the cross-termination factor. From a simple statistical point of view, ϕ should be equal to unity, simply because unlike radicals are twice as likely to terminate than radicals of the same type, yet deviations of the ϕ factor from unity are reported by many research groups. A detailed discussion on the ϕ factor is given in section 3.2. The pseudo-overall

k_t in equation 3.10 can be written as:

$$kt = kt_{11}\phi_1^{\cdot 2} + 2\phi(kt_{11}kt_{22})\phi_1^{\cdot}\phi_2^{\cdot} + kt_{22}\phi_2^{\cdot 2} \tag{3.12}$$

Transfer to Monomer

$$R_{r,1}^{\cdot} + M_1 \xrightarrow{kfm_{11}} P_r + R_1^{\cdot} \tag{3.13}$$

$$R_{r,1}^{\cdot} + M_2 \xrightarrow{kfm_{12}} P_r + R_2^{\cdot} \tag{3.14}$$

$$R_{r,2}^{\cdot} + M_1 \xrightarrow{kfm_{21}} P_r + R_1^{\cdot} \tag{3.15}$$

$$R_{r,2}^{\cdot} + M_2 \xrightarrow{kfm_{22}} P_r + R_2^{\cdot} \tag{3.16}$$

The pseudo-rate constant for chain transfer to monomer is

$$kfm = kfm_{11}\phi_1^{\cdot}f_1 + kfm_{12}\phi_1^{\cdot}f_2 + kfm_{21}\phi_2^{\cdot}f_1 + kfm_{22}\phi_2^{\cdot}f_2 \tag{3.17}$$

k_{fm11} and k_{fm22} in the equation above are the rate constants for chain transfer to monomer 1 and 2, respectively, while k_{fm12} and k_{fm21} are the rate constants for cross-chain transfer to monomer. It is worth mentioning that there are reported values from different sources for the chain transfer to monomer rate constants, however there is very little information for the cross-chain transfer to monomer rate constants. Copolymerization models presented in the literature commonly use a value for the overall rate constant for chain transfer to monomer (k_{fm}). Although such practice makes modeling much easier, it is not accurate and may not properly reflect the chain transfer characteristics for the given copolymer system. Recently, Schoonbrood et al.(1996) examined the chain transfer reaction mechanism and used molecular weight distribution data at low conversion to estimate chain transfer rate constants for Sty/MMA and Sty/MA copolymer systems. For this method to be accurate, chain transfer must be the dominant chain termination mechanism. The cross-chain transfer to monomer rate constants were also deduced for Sty/MMA and Sty/MA. Though the validity of their estimation method needs to be verified further, they provide good starting values for the cross-chain transfer to monomer rate constants for Sty/MMA and Sty/MA. The estimation of the cross-chain transfer to monomer is still difficult and needs more systematic

investigations.

Other Chain Transfer Reactions

Transfer reactions to other small molecules (T) including solvent, chain transfer agent(CTA), initiator, etc. are all very similar and are generalized below

$$R_{r,1}\cdot + T \xrightarrow{kft_1} P_r + T\cdot \tag{3.18}$$

$$R_{r,2}\cdot + T \xrightarrow{kft_2} P_r + T\cdot \tag{3.19}$$

The pseudo-overall rate constant for transfer reactions is

$$k_{fl} = kft_1\phi_1\cdot + kft_2\phi_2\cdot \tag{3.20}$$

Chain Transfer to Inhibitor

$$R_{r,1}\cdot + Z \xrightarrow{kfz_1} P_r \tag{3.21}$$

$$R_{r,2}\cdot + Z \xrightarrow{kfz_2} P_r \tag{3.22}$$

The overall rate constant of transfer to inhibitor is,

$$kfz = kfz_1\phi_1\cdot + kfz_2\phi_2\cdot \tag{3.23}$$

Molecular Weight Development

Population balances for radicals and dead polymer molecules for both linear and branched homopolymerization systems can be used to calculate molecular weight averages and molecular weight distributions (where applicable) in copolymerization by substituting pseudo-rate constants (defined above) for the rate constants in the homopolymerization scheme. Molecular weight equations have already been given in the review paper by Gao and Penlidis (1996).

3.2 Termination in Copolymerization

The rate of termination in copolymerization is given by equation 3.10 and the cross-termination

factor is defined in equation 3.11. As stated before, from a statistical point of view, ϕ should be one, however many research groups (Walling 1949, Fukui et al. 1961, Ito 1978, 1971) have observed that the ϕ factor deviates from unity. Considerable effort in the literature has been spent on arriving at a clear physical meaning for the ϕ factor with little success. In this section, a literature overview is given and the approach used in this project is described.

Early studies on the rate of termination in copolymerization observed large values of the ϕ factor, implying the significance of cross-termination between the two unlike radicals. Rudin and Chiang (1974) obtained a ϕ value of 1 for Sty/p-MSty and later Chiang and Rudin (1975) reported a ϕ value of 13 for MMA/Sty. Odian (1982) listed ϕ values for many copolymer systems and related the ϕ values to reactivity ratios. An empirical trend between the ϕ factor and the product of r_1r_2 is that the smaller the product of r_1r_2 is the greater the ϕ value. This trend applies to copolymer systems when both reactivity ratios are less than 1. Odian (1982) concluded that such a trend indicates the ϕ factor is somewhat related to the polarity of the copolymer systems. Many other groups (Ito 1971, Wittmer 1979, Russo 1987, Prochazka and Kratochvill 1983, etc.) have also tried to give a physical meaning to ϕ. No conclusive definition of the ϕ factor has been reached among different research groups so far.

More recently, researchers tried to use the penultimate model scheme to give a better description of the rate of termination. Russo and Munari (1968) presented a new expression of the overall kt using the penultimate model scheme, and their expression required two adjustable parameters. Bonta et al.(1975) continued the earlier work of Russo and Munari (1968) and reemphasized the effect of the penultimate unit on the overall kt. Fukuda et al.(1992) in their review paper stated that the penultimate model kt expression fits experimental data better than the terminal model kt expression. Madruga et al.(1981) compared various models of the overall kt. They concluded that the overall kt from the penultimate model had more success in fitting their experimental data. However, Russo (1987) states that the better fit in the experimental data is ascribed to the use of more parameters. Additionally, the two parameters used in the penultimate model expression of kt sometimes are estimated to have negative values. Similar findings were also obtained by Ito

and O'Driscoll (1979). This questions the physical meaning of the two parameters used in the penultimate model expression of kt. Ito and O'Driscoll (1979) eventually confirmed the difficulty to assess any realistic validity of the various models of kt. Similar conclusions were also reached by Wittmer (1979). Finally, O'Driscoll and Huang (1989) stated that the ϕ factor has no physical meaning but remains as an adjustable parameter which enables one to fit experimental data.

After reviewing the work presented in the literature on the modeling of the overall kt, it can be clearly seen that most attempts to clarify the cross-termination factor ϕ have failed, and the comparison of the terminal model expression of kt and the penultimate model expression of kt leads to no definite conclusions. More systematic investigations and statistical model discrimination methods (Burke et al., 1994) should be used in discriminating between the penultimate model kt and the terminal model kt. In this thesis, it is not attempted to give a physical meaning to the cross-termination factor. The terminal model expression of kt (equation 3.12) is used in the simulation package, and the ϕ factor defined in equation 3.11 remains an adjustable parameter. It should also be stated that the significance of the ϕ factor in the simulations is limited to the low conversion range only, since in most copolymer systems exhibit a strong gel effect and the chemically controlled kt becomes diffusion controlled at the early stages of the reaction. With respect to the estimation of ϕ, the empirical relationship between the ϕ factor and the product of the reactivity ratios presented in Odian (1982) can be used as a starting point, with subsequent fine-tuning based on process data and rigorous non-linear parameter estimation techniques.

3.3 Modeling Considerations on Diffusion Controlled Kinetics.

Gel effect and limiting conversion are commonly observed in free radical copolymerization. The onset of the gel effect and limiting conversion in homopolymerization were predicted successfully by Marten and Hamielec (1979, 1982). Detailed implementation of their model has already been described in the review by Gao and Penlidis (1996). In copolymerization, the prediction of the onset of gel effect and limiting conversion is apparently more difficult than its analogue in homopolymerization. Since there are two monomers involved, the reaction characteristics for a

particular copolymer system depend not only on each individual monomer but also on the monomer feed. In this bulk/solution model, an approach similar to what was employed in the homopolymerization simulation package was used. In Marten and Hamielec's model, the overall free volume of the copolymer system is calculated using the following equation,

$$V_F = [0.025+\alpha_p(T-T_{gp})](V_p/V_T)+[0.025+\alpha_m(T-T_{gm})](V_m/V_T) \quad (3.24)$$

where:

V_F: total free volume fraction in the reaction mixture

V_p: total volume of polymer in the reaction mixture

V_m: total volume of monomers in the reaction mixture

V_T: total volume of the reaction mixture

α_p: expansion coefficient for polymer

α_m: expansion coefficient for monomer

T: reaction temperature

Tgp: glass transition temperature of copolymer

Tgm: glass transition temperature of monomer

Both monomer and polymer contribute to the total free volume (contribution from solvent will be included if copolymerization is conducted in solution). It is clear from equation 3.24, that in order to describe the reaction kinetics over the entire conversion range, the appropriate calculation of the glass transition temperature (Tg) of the copolymer is essential. The modeling of Tg for copolymers is thus discussed in the next section.

3.4 Simulation of Copolymer Tg

As stated before, a good estimate of copolymer Tg becomes critical for the calculation of the total free volume of the reaction mixture. In addition, the Tg value of the final polymer product is an important index that reflects many physical properties of the polymer. To produce polymer with desired physical properties, Tg must be controlled throughout the whole course of the reaction.

3.4.1 Literature Review

An extensive literature search has been conducted to collect all available information on the simulation of copolymer Tg. Many Tg models were proposed in the past half century. Although they all differ from each other in their expressions, many were derived from the same theoretical basis, i.e., either from an entropy point of view or from a free volume point of view. Nonetheless, many models are equivalently interchangeable under certain assumptions. The section below will look at all models in three groups.

Models Based on Free Volume Theory

Gordon and Taylor (1952)

Gordon and Taylor (1952) were the first to propose an equation on copolymer Tg based on the assumption of additive free volume. It can be expressed as:

$$Tg = \frac{W_A Tg_A + k W_B Tg_B}{W_A + k W_B} \tag{3.25}$$

In the above equation, as pointed out by Gordon and Taylor, k was considered a constant that reflects the interactions of all diads in the copolymer. Its value can be estimated by taking the ratio of the difference of the specific volume-temperature coefficients above and below Tg of each corresponding monomer, i.e., $k=\Delta\beta_A/\Delta\beta_B$. It is clear that when k=1 and W_A is replaced by a mole fraction, equation 3.25 is equivalent to Dimarzio-Gibbs' model (see equation 3.27 below). Gordon and Taylor (1952) gave values of k for various polymers.

Wood (1958)

Wood (1958) presented an expression for copolymer Tg as:

$$A_1 c_1 (Tg - Tg_1) + A_2 c_2 (Tg - Tg_2) = 0 \tag{3.26}$$

where A is an adjustable parameter, c is a weighting factor, and the subscripts stand for the monomer type. Wood observed some deviation of the original estimate of k given by Gordon and Taylor(1952), and then reestimated the value of k for many copolymer systems. The cause of the deviation of the k value was later discussed by Johnston (1976b), who indicated that since k is an average of the interactions of all diads in the copolymer, larger differences in the interaction

will lead to a less accurate value for k.

Models Based on Entropy

Dimarzio and Gibbs (1959)

It is generally considered that the configurational entropy of a polymer chain is zero at Tg. This can be applied to both homopolymers and copolymers, by assuming that the stiffness energy of the copolymer chain is a linear combination of those of each corresponding homopolymer. Dimarzio and Gibbs (1959) first introduced the following equation

$$Tg = n_A' Tg_A + n_B' Tg_B \tag{3.27}$$

where $n'_{A/B}$ represents the mole fraction of rotatable bonds of monomer A/B in the copolymer chain, and $Tg_{A/B}$ represents the Tg of homopolymer A/B. Dimarzio and Gibbs (1959) also claimed that their model is equivalent to Gordon-Taylor's model when the mole fraction in their model is replaced by a weight fraction. They also stated that the assumption that the stiffness energy of the copolymer is a linear combination of those of each corresponding homopolymer is not always valid, especially if a copolymer has a higher content of AB (alternating) diads. This observation indirectly indicates the fact that microstructure has an appreciable effect on Tg.

Barton (1970)

Dimarzio-Gibbs' model was later extended by Barton (1970) to take the microstructure effect on Tg into account. His model is given as:

$$Tg = n_{AA}' Tg_{AA} + n_{BB}' Tg_{BB} + (n_{AB}' + n_{BA}') Tg_{AB} \tag{3.28}$$

where n'_{ij} is the mole fraction of rotatable bonds contained in ij sequences, which can be calculated by:

$$n_{ij}' = \frac{n_{ij}\alpha_{ij}}{\sum n_{ij}\alpha_{ij}} \tag{3.29}$$

n_{ij} is the probability of forming an ij diad, and α_{ij} is the number of rotatable bonds per sequence. By using equation 3.28, Barton calculated the Tg of 11 different copolymers, many of which exhibit a maximum/minimum in the Tg versus overall composition. In most cases, good

agreement was reached. However, to use equation 3.28, one must know the value of Tg_{AB} and α_{ij}. In Barton's paper, though the value of α_{ij} of the 11 copolymer systems is listed, the method of estimating α_{ij} is unfortunately not mentioned.

Suzuki and Mathot (1989)

More recently, Suzuki and Mathot (1989) derived a new version of Barton's equation and described its characteristics in detail.

$$Tg = n_{aa}Tg_{aa} + n_{bb}Tg_{bb} + \left(\frac{R}{100}\right)\left(Tg_{AB} - Tg_{avg}\right) \qquad (3.30)$$

where $Tg_{avg} = (Tg_{AA}+Tg_{BB})/2$ and R is defined as the average number of both A and B monomer sequences occurring in a copolymer per 100 monomer units. An estimate of R can be directly obtained from composition data and a nuclear magnetic resonance (NMR) study, therefore the Tg of a copolymer can be calculated when Tg_{AB} is known. Suzuki and Mathot (1989) used equation 3.30 to calculate the Tg of styrene/methyl methacrylate, styrene/acrylonitrile and acrylonitrile/butadiene copolymers. The agreement was satisfactory. They also discussed the models by Ham (1975) and Uematsu and Honda (1965), which take triad effects on copolymer Tg into account. It was then concluded that the diad model is adequate to calculate the Tg of most copolymers. The same group (Suzuki and Miyamoto, 1990) later tested styrene/α-methyl styrene with the same equation and obtained good results. Most recently, Suzuki et al.(1994) extended their studies to the effect of sequence length distribution on both heat capacity and Tg.

Other Efforts

Other research groups also proposed equations very similar to Barton's (equation 3.28), but they gave a different definition for n'_{ij}. These groups include Uematsu and Honda (1965) and Hirooka and Kato (1974). All these equations can fit Tg data of certain copolymer systems.

Other Models

Fox (1956)

A simple, early model on the copolymer Tg proposed by Fox (1956) is shown below,

$$\frac{1}{Tg} = \frac{W_A}{Tg_A} + \frac{W_B}{Tg_B} \tag{3.31}$$

where $W_{A/B}$ represents the weight fraction of monomer A/B in the copolymer chain, and $Tg_{A/B}$ represents the Tg of homopolymer A/B. In this equation the copolymer Tg lies between the Tg of the two corresponding homopolymers A and B. The effect of copolymer microstructure on Tg is not considered in Fox's equation. Literature evidence shows that such an expression is not valid for many copolymer systems.

Johnston (1969)

Johnston (1969) independently reported the following equation for copolymer Tg, taking the contribution from sequence distribution into account,

$$\frac{1}{Tg} = \frac{W_A P_{AA}}{Tg_A} + \frac{W_B P_{BB}}{Tg_B} + \frac{W_A P_{AB} + W_B P_{BA}}{Tg_{AB}} \tag{3.32}$$

where P_{AA}, P_{BB} and P_{AB} are probabilities for the corresponding sequences. Johnston (1972, 1973, 1976a) later studied the Tg for a series of copolymer systems with equation 3.32. To use equation 3.32, the Tg of the alternating copolymer (Tg_{AB}) is needed. Since strictly alternating copolymers are not always available, Johnston (1976b) suggested four different methods of estimating the Tg of "diad" polymers.

Couchman (1982)

Couchman (1982) derived his equation from a thermodynamic point of view. Though it is more theoretically sound, it requires additional parameters (ΔCp, the increment of heat capacity at glass transition temperature) to predict the copolymer Tg. The equation is shown below

$$\ln(Tg) = \frac{r_A f_A^2 \Delta Cp_A \ln(Tg_A) + r_B f_B^2 \Delta Cp_B \ln(Tg_B) + 2 f_A f_B \Delta Cp_A}{r_A f_A^2 \Delta Cp_A + r_B f_B^2 \Delta Cp_B + 2 f_A f_B \Delta Cp_{AB}} \tag{3.33}$$

where: r_A: reactivity ratio of monomer A

r_B: reactivity ratio of monomer B

f_A: mole fraction of monomer A in the feed

f_A: mole fraction of monomer B in the feed

Under certain conditions, Couchman's equation can be simplified by assuming ΔCp of polymers A, B and the alternating polymer AB equal, in which case equation 3.33 requires no additional parameter to be estimated. However, Fernandez-Garcia et al.(1994) tested Couchman's equation and showed that it has no apparent advantages over Johnston's and Barton's equations. Nevertheless, the simplified Couchman's equation requires no additional parameter and is easy to implement. Testing results with equation 3.33 from other groups (Fernandez-Garcia et al. 1994, Schellenberg and Vogel 1994) seem to be promising.

3.4.2 Tg Model Implementation and Testing

From all the Tg models discussed so far, none can be claimed as universal. Tg models from many other groups can be derived from equation 3.26. Equation 3.26, when A_2/A_1 is defined as k, and c is defined as the weight fraction, is equivalent to Gordon-Taylor's expression. Dimarzio-Gibbs' model is also equivalent to Gordon-Taylor's model under specific conditions. Additionally, if $A_2/A_1=Tg_1/Tg_2$, and c is defined as the weight fraction, then equation 3.26 becomes Fox's (1956) expression.

Several groups have tested Tg models with various copolymers. Podesva and Prochazka (1979) compared models from Gordon and Taylor (1952) and Fox (1956). Pomposo et al.(1993) also discussed and compared Gordon-Taylor's, Couchman's and Fox's equations. Several acrylate/acrylate copolymer blends were used as testing material. The main observation is that Gordon-Taylor's expression seemed to perform better. Schellenberg and Vogel (1994) recommended Gordon-Taylor and Couchman's equations for the Tg of Sty/butyl methacrylate(BMA) copolymer, while the use of Fox's equation appeared to be unsatisfactory. Arranz et al.(1984) and Sanchez-Chaves et al.(1988) compared Barton's and Johnston's models and stated that both models worked equally well.

A more complete test of various equations was conducted by Fernandez-Garcia et al.(1994). They tested equations from Fox, Gordon-Taylor, Barton, Johnston and Couchman and commented on

other equations in the literature. In their studies, Tg of methyl methacyrlate/methyl acrylate copolymers of different compositions was measured and compared with predictions of copolymer Tg from various equations. The Gordon-Taylor equation was used with different values of k. A sum of squares was used as an index for the comparison. From their testing results, it was concluded that Gordon-Taylor's, Johnston's and the simplified Couchman's equation gave better predictions. They also used the above three equations to calculate the Tg of copolymer samples generated at all conversion levels. Again, good agreement was obtained. Gordon-Taylor's expression was considered to be the best for Tg of copolymer at all conversion levels and compositions. This somehow contradicts what Johnston (1976b) suggested that the parameter k in Gordon-Taylor's expression (see equation 3.25) is unreliable when the interaction is significant. Despite this contradiction, from all the existing testing evidence, Gordon-Taylor's expression can be used to predict copolymer Tg in a very satisfactory way, provided that an appropriate value of k is chosen.

The only other group that monitored the dependence of Tg on conversion is Guillot (1990), Djekhaba and Guillot (1990) and Guillot and Emelie (1991). In Guillot's tests, differential scanning calorimetry (DSC) and NMR were used to determine polymer Tg and microstructure. They also used Johnston's equation to simulate the DSC curves and histograms. There are many other papers providing information on Tg for various copolymer systems. The most useful ones are summarized in Table 3.1.

To summarize:

(1) Johnston's equation appears to be more general than others. This equation has been tested to give satisfactory results for most copolymer systems.

(2) Couchman's equation has more of a theoretical basis, yet ΔCp of polymer is not easy to estimate, and hence its simplified form is easier to implement. Testing results obtained in this laboratory shows that simulation results using Couchman's equation agree well with experimental data and are very close to results using Johnston's model.

Table 3.1 Useful References on Modeling of Copolymer Tg

References	Remarks
Beevers and White (1960, 1963)	MMA/AN, AN/Sty
Beevers (1962)	MMA/Sty
Brar and Sunita (1992)	AN/EA, AN/MA
Comyn and Fernandez (1975)	EA/Vinyl Dichloride
Edwards (1994)	Tg equations in general
Fried (1993)	Tg estimation
Harris and Gilbert (1982)	modified Johnston's model
Lu and Jiang (1991)	Tg and molecular weight
Schneider (1988)	Sty/p-MSty
Schneider and Neto (1983)	Tg and sequence distribution
Stutz et al.(1990)	Tg of crosslinked polymer
Switala-Zeliazkow (1993)	Sty/AA, Sty/methacrylic acid
Tonelli (1977)	AN/VAc alternating polymer

(3) Gordon-Taylor's expression received quite good supporting evidence from the literature, yet there is uncertainty introduced via the parameter k as claimed by Johnston (1976b). So far there is no satisfactory method for estimating k in the literature and its choice remains arbitrary.

(4) Barton's equation has also been tested to give good predictions for various copolymer systems, yet it was not supported by Fernandez-Garcia et al.(1994). Tests carried in this project also show that simulation results for many different copolymer systems usually deviate from actual experimental results, especially at higher conversion levels.

After an extensive testing of all the equations discussed above, equations from Johnston and Couchman seem to perform better, and therefore they have been implemented into the package and set up as user options.

Chapter 4. Bulk/Solution Simulation Package/Database Overview

As mentioned in the introduction, the simulation package includes two models, the bulk/solution model and the emulsion model. In this chapter, the database structure of the bulk and solution model is described. The database for the emulsion polymerization model will be described separately in chapter 16 of volume two.

The bulk/solution model has two major programs: the MASTER and the DATABASE programs. The MASTER program simulates multicomponent polymerizations (homopolymerization, copolymerization as well as terpolymerization) in bulk and solution. When the MASTER program is executed, it uses several screens to receive information on recipes and reaction conditions from the user. These screens are shown in figures 4.1 to 4.4.

The first screen in the MASTER program is the reaction formulation screen, and is shown in figure 4.1 (in figure 4.1, a copolymerization reaction is simulated, therefore the screen shows two monomers. In case of simulation of terpolymerization, there will be three monomers displayed on the same screen). This is the screen for designing reaction recipes. Since this model is used for copolymerization, users have to select two monomers from the database. Other reactants can also be selected on this screen. Users can simply input the amount of each reactant in the recipe with the choice of many different units. As noted earlier, this model is developed based on a previous homopolymerization model, hence it can also be used for homopolymerization simulations. To do this, users simply select the monomer to be simulated and set the second monomer amount to zero.

Figure 4.2 displays the output files screen.

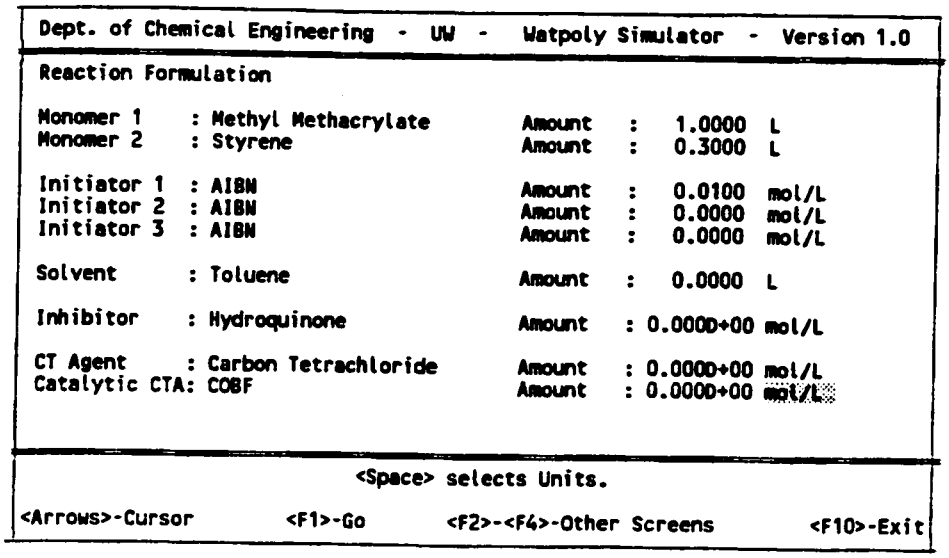

Figure 4.1 Reaction formulation screen

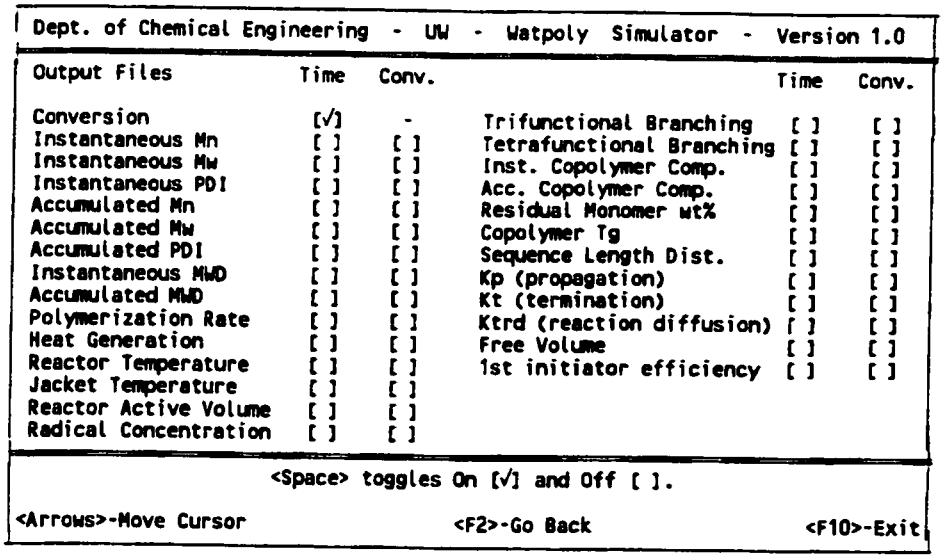

Figure 4.2 Output files screen

Full description of all the output files is given below:

Conversion	:	conversion
Instantaneous Mn	:	instantaneous number average molecular weight
Instantaneous Mw	:	instantaneous weight average molecular weight
Instantaneous PDI	:	instantaneous polydispersity index
Accumulated Mn	:	accumulated number average molecular weight
Accumulated Mw	:	accumulated weight average molecular weight
Accumulated PDI	:	accumulated polydispersity index
Instantaneous MWD	:	instantaneous molecular weight distribution
Accumulated MWD	:	accumulated molecular weight distribution
Polymerization rate	:	rate of polymerization
Heat generation	:	heat generated in polymerization reaction
Reactor Temperature	:	reactor temperature
Jacket Temperature	:	jacket temperature
Reactor Active Volume	:	total volume of reaction mixture
Radical Concentration	:	total concentration of live radicals
Trifunctional Branching	:	number of trifunctional branching points per polymer molecule
Tetrafunctional Branching	:	number of tetrafunctional branching points per polymer molecule
Inst. Copolymer Comp. mol%	:	instantaneous copolymer composition[a]
Acc. Copolymer Comp. mol%	:	accumulated copolymer composition[a]
Residual Monomer. wt%	:	weight percentage of unreacted monomer[a]
Copolymer Tg	:	glass transition temperature of copolymer produced
Sequence Length Dist.	:	sequence length distribution
k_p (Propagation)	:	overall propagation rate constant
k_t (Termination)	:	overall termination rate constant
k_{rd} (Reaction Diffusion)	:	overall reaction diffusion control rate constant
Free Volume	:	total free volume of the reaction mixture
1st Initiator Efficiency	:	efficiency of the first initiator used

a: with respect to the first monomer selected on the reaction formulation screen.

Figure 4.3 displays the computational options screen. It is worth noting that users should be cautious when selecting the penultimate model option and the copolymer Tg model option. The penultimate model option has already been explained in section 2.3. Users should check the database first before activating this option to make sure there is adequate information (six reactivity ratios) stored in the database. As to the option of copolymer Tg model, both Johnston's

and Couchman's models work equally well in many cases. The preference for either model depends on the individual copolymer system, the available information and the user.

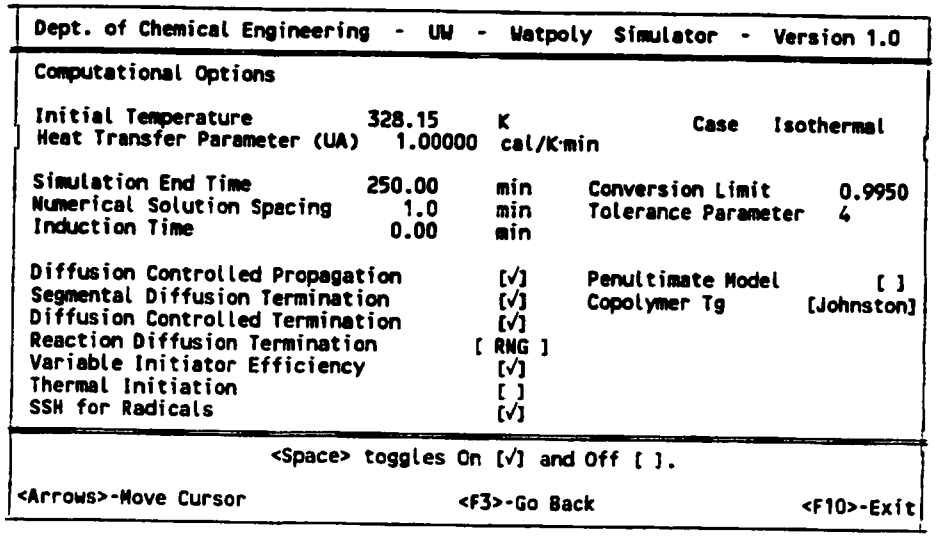

Figure 4.3 Computational options screen

The flow option screen is displayed in figure 4.4. This is the screen for users to input flow rate information when polymerization is carried out in semibatch or CSTR mode.

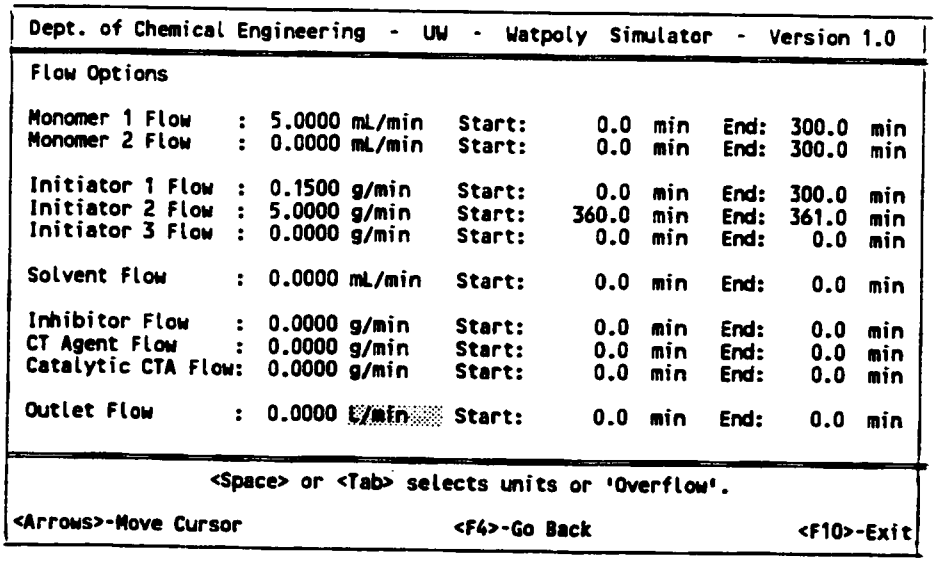

Figure 4.4 Flow options screen

4.1 Database Structure and Items

This bulk/solution model has an extensive database that includes twelve different monomer systems, a wide range of initiators (azo groups, peroxides, etc.), solvents, CTAs, inhibitors, etc. The development of this database took a considerable amount of research effort. The information collected is maintained by the DATABASE program. One can input new information into the database or edit/retrieve/delete existing information in the database. All database items for monomers, initiators, solvents, CTAs and inhibitors have already been described in detail in Gao and Penlidis (1996). In this thesis, emphasis is focused on introducing the new database structure and items that are specifically designed for copolymerization.

Simulation of a homopolymerization requires information on all species included in the reaction recipe, such as monomer, initiator(s), solvent, etc. Additional information is needed to characterize copolymerization kinetics. The simplest way to provide all the necessary information is to build a complete new database for each copolymer system. Most models presented in the literature use this approach. All the rate constants and other parameters are estimated for the specific copolymer system simulated. Apparently such an approach lacks flexibility and generality since each copolymer system requires a specific database of its own.

To overcome this problem, a different approach has been adopted in the database development. The existing homopolymerization database is expanded to store new information that can characterize each copolymer system. Only four new database items are added to the existing homopolymerization database. The four additional database items are the reactivity ratios used in the terminal model, the cross-termination factor ϕ and the Tg of alternating copolymer used. In case the penultimate model option is invoked, a total of six reactivity ratios is needed. The new database structure is illustrated in figure 4.5 (the same database also contains all necessary kinetic information for the simulation of terpolymerization, more details are given in chapter 13). During a simulation, once the recipe is set, the simulator will first search the database for information on the two selected monomers as well as on other reaction ingredients. After retrieving the necessary information from the database, the simulator will then search the database

where copolymerization kinetic information is stored for reactivity ratios, cross termination factor and the alternating copolymer Tg for that specific copolymer pair. After all that information is read from the database, a simulation will subsequently be performed.

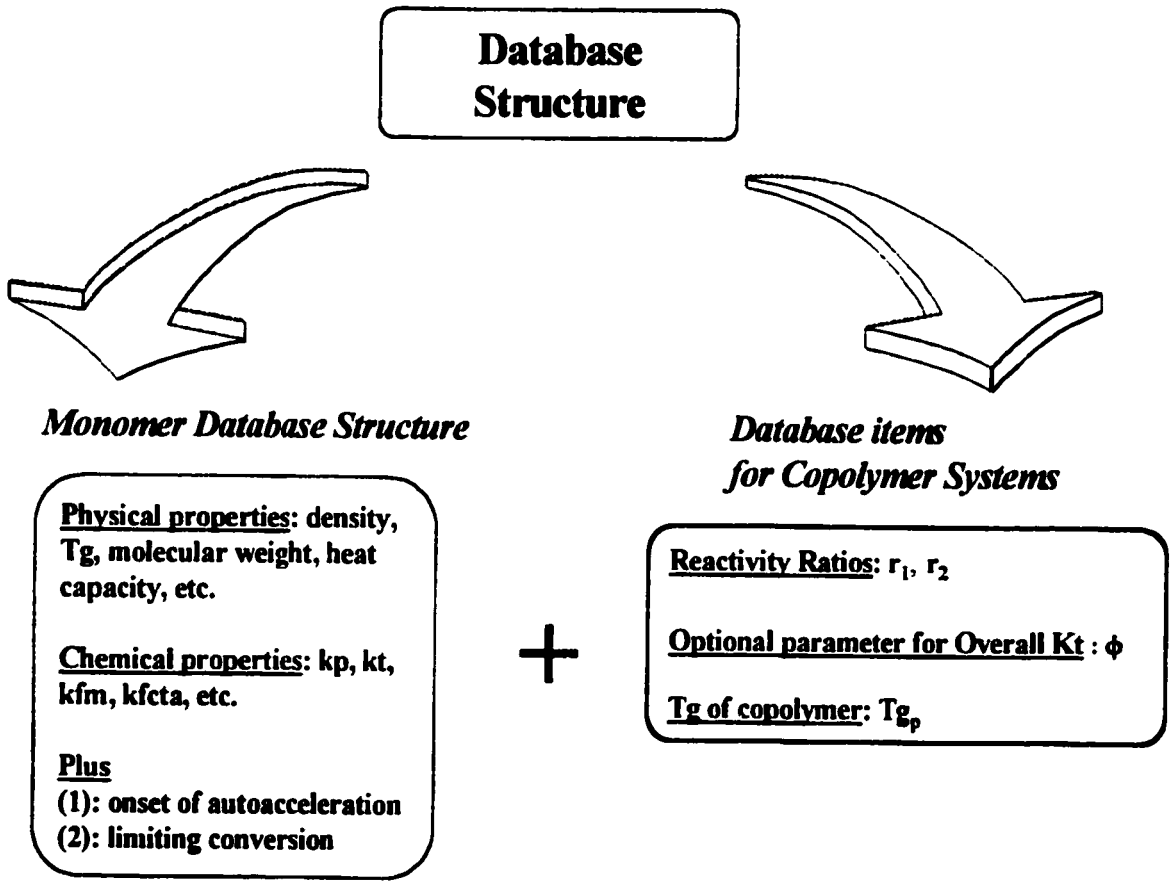

Figure 4.5 Database Structure of the Bulk/Solution Model.

Chapter 5. Model Testing Guidelines and Reactivity Ratio Estimation

The majority of models presented in the literature are not extensively tested for reliability and validity. Experimental data that characterize copolymerization like conversion, molecular weight, composition, etc., are the most useful information for model testing. In this thesis, about 15 copolymer systems are tested. An extensive set of experimental data available in the literature have been collected through literature search. It is common that most literature data are limited to low conversion levels. In such cases, complementary experiments were conducted in this laboratory. These experiments were carefully designed first from a statistical point of view and then were carried out. Polymer samples were subsequently collected over the whole conversion range and characterized. This section outlines procedures for experiments and polymer characterization, and highlights guidelines for model testing.

5.1 Model Testing Guidelines

All simulation results presented in both volumes 1 and 2 (in about 250 figures) have been generated following the guidelines outlined below:

(1) The most important feature is the handling of the database. All model predictions are generated by the same database. This means that once the database for a particular polymer system is set, there will be no more parameter tuning, i.e., the database becomes 'read only'.

(2) The copolymerization database of the bulk/solution model is expanded based on the previous homopolymerization database developed by Gao and Penlidis (1996). With such a database, simulations of a homo-/co-/terpolymerization share the same database information. This implies that all the simulation results on homo-/co-/terpolymerization are generated based on exactly the same database. Most models in the literature do not have such consistency.

(3) Both models have several built-in options (see figures 4.3 and 16.2). The selection of the

different options used in a simulation varies from system to system. This is where the user's process understanding (which is always crucial in modelling) comes into play.

(4) Measurement of co- and terpolymerization molecular weight averages by gel permeation chromatography (GPC) is more difficult than for its homopolymer counterpart. This is because copolymer standards are not as widely available as homopolymer standards (there have been no commercial terpolymer standards available so far). Composition drift presents additional complications. Considering these facts, in this thesis emphasis is primarily placed on the simulation of molecular weight averages of azeotropic composition.

5.2 Brief Experimental Procedure Outline

Many experiments were conducted in our laboratory to provide model testing material. The experimental and polymer sample characterization procedures are briefly outlined here. Most copolymerization experiments were carried out in glass ampoules of 10 cm in length and 1.4 cm in outer diameter. These dimensions were chosen so as to ensure the ampoules had a sufficient surface to volume ratio to keep the polymerization isothermal, according to Zhu and Hamielec (1991). Stock solutions of the monomer and initiator were prepared by weighing appropriate amounts of reagents and then ca 5 mL aliquots were pipetted into the ampoules. Degassing of the monomer solution was done by several vacuum-freeze-thaw cycles. The ampoules were then flame-sealed and stored in liquid nitrogen until ready for use. Polymerizations were carried out by placing the ampoules in a water bath (fitted with a shaker) at the chosen temperature. The ampoules were removed from the water bath after a recorded time interval. They were then frozen by submersion in liquid nitrogen and weighed immediately. Thereafter the ampoules were broken and the contents were transferred into a glass dish or beaker containing hydroquinone and hexyl alcohol. The polymer samples were air-dried to remove the solvent and vacuum-dried for three days at approximately 40°C until a constant weight was reached. Conversion levels were then determined by comparing the weights of products to the weights of the monomer initially added in the ampoules. Molecular weight averages of samples were obtained via GPC (gel

permeation chromatography) along with a molecular weight detector, MALLS (multi-angle laser light scattering) and a mass detector, DRI (differential refractive index detector). The whole setup consisted of a solvent reservoir, a solvent degasser, a pump, a pulse dampener, a sample injector, a bank of three Waters Ultrastyragel columns (10^3, 10^4 and 10^6 Angstroms in size), a MALLS detector (DAWN DSP-F from Wyatt Technology Corp.) and a Waters R401 differential refractive index detector. Chromatographic grade tetrahydrofuran (THF) was the mobile phase in the system and all samples were dissolved in THF for the measurements. Polymer composition was measured with a 300 MHz AC Bruker Fourier-Transform ^{1}H NMR spectrometer. Deuterated chloroform was used as solvent to dissolve the polymer samples at room temperature. The relative amounts of monomer bound in the copolymer chain were estimated from the areas under the appropriate absorption peaks of the spectra.

5.3 Reactivity Ratio Estimation

Reactivity ratios are very important parameters in copolymerization simulation. Appropriate estimates of reactivity ratios are critical for a model to deliver reliable predictions. This subject has been the literature focus in the past decade. There is ample information on reactivity ratios for various copolymer systems in the literature. Ham (1964) and Greenley (1980a, b) presented an extensive listing of reactivity ratio values. The *Polymer Handbook* (Brandrup and Immergut 1989) is also another literature source for reactivity ratios. Though there is a lot of information available, reported literature values of reactivity ratios vary over a wide range. The main reason for this variation is that the estimation methods employed by most research groups are not appropriate. Traditional methods for reactivity ratio determinations, like Fineman and Ross (1950), Braun et al.(1973), Kelen and Tudos (1975), are based on first transforming the instantaneous copolymer composition equation into a form that is linear in the parameters r_1 and r_2 and then estimating the reactivity ratios by graphical plotting or by linear least squares. These approaches are statistically unsound because the "independent variable" has error and the dependent variable does not have constant variance. As a result, they have been shown by Tidwell and Mortimer (1965, 1970) to often lead to very poor estimates with misleading confidence intervals.

More recently, a statistically sound error-in-variables-model (EVM) method or its modifications (Box 1970, Britt and Luecke 1973, Sutton and MacGregor 1977, Patino-Leal et al. 1980, Reilly and Patino-Leal 1981) are used in reactivity ratio estimation. The EVM method allows one to properly take into account all the sources of experimental error. It gives reliable estimates of reactivity ratios and has widely been adopted in this work. Dube et al.(1991), Dube and Penlidis (1995a) and McManus and Penlidis (1996) are representative examples. Burke et al.(1993) further discussed the experimental design for reactivity ratio determination under composition constraints and for the penultimate model, thus extending the work of Tidwell and Mortimer (1965, 1970).

Chapter 6. Simulation of Copolymerization of Styrene and Methyl Methacrylate

6.1 Literature Summary

Like their homopolymers, the MMA/Sty copolymer received much more literature attention compared to other copolymer systems. However, most kinetic studies were focused on the estimation of reactivity ratios and experiments conducted were confined to low conversion ranges. Only a few groups presented full conversion range experimental data. Table 6.1 lists useful literature papers on Sty/MMA.

Table 6.1 Literature References on Methyl Methacrylate/Styrene Copolymer

Reference	Remarks
Balaraman et al.(1986)	nonisothermal CSTR operation, multiplicity and stability studies
Balaraman (1982)	cross termination studies
Balaraman et al.(1983)	CSTR operation, modeling, reactivity ratios
Bamford and Basahel (1980)	chain transfer, penultimate effect
Beldie et al.(1985)	copolymer Tg data
Bevington et al.(1954)	termination reaction studies
Bonta et al.(1975)	low conversion experiments in solvents
Borchardt (1982)	steric and electronic effect on reactivity ratios
Brar and Kapur (1988)	sequence length determination
Chen and Hwang (1982)	full conversion experiments, oligomers
Chiang and Rudin (1975)	cross-termination factor, low conversion experiments
Dionisio and O'Driscoll (1979)*	full conversion experimental data
Fujihara et al.(1979)	solvent effect on reactivity ratios
Fukuda et al.(1985a-b, 1987a-b, 1989)	penultimate effect, reactivity ratios
Fukui et al.(1961)	cross-termination
Ito (1971)	cross-termination rate constant

Johnson et al.(1978)*	full conversion experimental data
Johnson et al.(1983)	temperature effect on reactivity ratios
Khan and Wadehra (1981)	low conversion experiments
Krstina et al.(1992)	solvent effect
Kuo et al.(1989)	composition studies
Kuo and Chen (1981)	low conversion experiments, cross-termination studies
Lewis et al.(1948a,b)	reactivity ratio estimates, temperature and solvent effect on reactivity ratios
Madruga et al.(1979)	solvent effect, reactivity ratio determination
Madruga and Roman (1989)	copolymerization experiments in benzene at low conversion
Madruga et al.(1981)	solvent effect on termination
Madruga (1993)	solvent effect
Mayo and Lewis (1944)	classical terminal model, reactivity ratios
Melville and Valentine (1950)	low conversion experiments and kinetic studies
Meyer (1966)	reactivity ratios
Olaj et al.(1988, 1989)	overall rate constants
O'Driscoll and Huang (1989, 1990)*	full conversion experimental data
O'Driscoll et al.(1984)	reactivity ratio estimates, full conversion composition data
Prochazka and Kratochvil (1983)	termination reaction in copolymerization
Russo and Munari (1968)	cross-termination studies
Schoonbrood et al.(1996)	cross-chain transfer rate constant
Schweer (1993)	penultimate model reactivity ratio estimates penultimate model effect on kp
Sharma and Soane (1988)	full conversion modeling, simulation
Srivastava and Mathur (1981)	copolymerization with complex agent
Suzuki et al.(1959)	low conversion experiments, cross-termination studies

* papers present full conversion experimental data that are used for model testing

6.2 Model Testing Results

Johnson et al.(1978)

Johnson et al.(1978) was the first group that reported full conversion experimental data. MMA/Sty copolymerization was conducted in bulk, benzene and butyl stearate. Styrene content in the initial monomer feed was 35 mol% and 60 mol%. Conversion and copolymer cumulative composition were measured. Johnson et al.(1978) observed a strong gel effect in their two bulk runs. They also noticed that the cumulative composition deviated from predictions by the integrated copolymer composition equation at higher conversion levels. This deviation was ascribed to a steric effect in the case of styrene monomer restricting its mobility at higher conversions. It was thus suggested by Johnson et al.(1978) that the reactivity ratios change with conversion.

Figure 6.1 shows the simulation results for the two bulk runs from Johnson et al.(1978). Gel effect and limiting conversion are present in both runs, with more styrene content in the monomer feed slowing down the overall rate of polymerization. Solution polymerization of MMA/Sty was also conducted in benzene. Figure 6.2 displays the comparison of model predictions and experimental results. Clearly the presence of solvent diluted the reaction mixture and alleviated the gel effect.

Dionisio and O'Driscoll (1979)

Dionisio and O'Driscoll (1979) argued that the deviation observed in the measured copolymer composition from Johnson et al.(1978) was unexpected. To confirm this, they repeated the copolymerization of styrene and MMA in bulk with 60 mol% of styrene in the feed. Copolymer composition was measured by UV analysis. Figure 6.3 shows the model predicted conversion along with reported experimental results. The agreement between model predictions and reported data is very good. The feed ratio is close to an azeotropic feed, thus a nearly constant cumulative composition is expected. However, as shown in figure 6.4, the measured composition did not behave exactly as predicted. In figure 6.4, the model predicts a nearly constant cumulative composition (solid line), while the measured composition showed an obvious (cyclical) variation.

This variation is very similar to what Johnson et al.(1978) reported earlier. Dionisio and O'Driscoll (1979) tried to interpret this deviation by a penultimate model effect, depropagation and charge transfer complex formation, yet all postulations were rejected and no satisfactory explanation was presented. It is likely that the data variation in figure 6.4 is due to systematic experimental error from the UV analysis (see the discussion in the following paragraph).

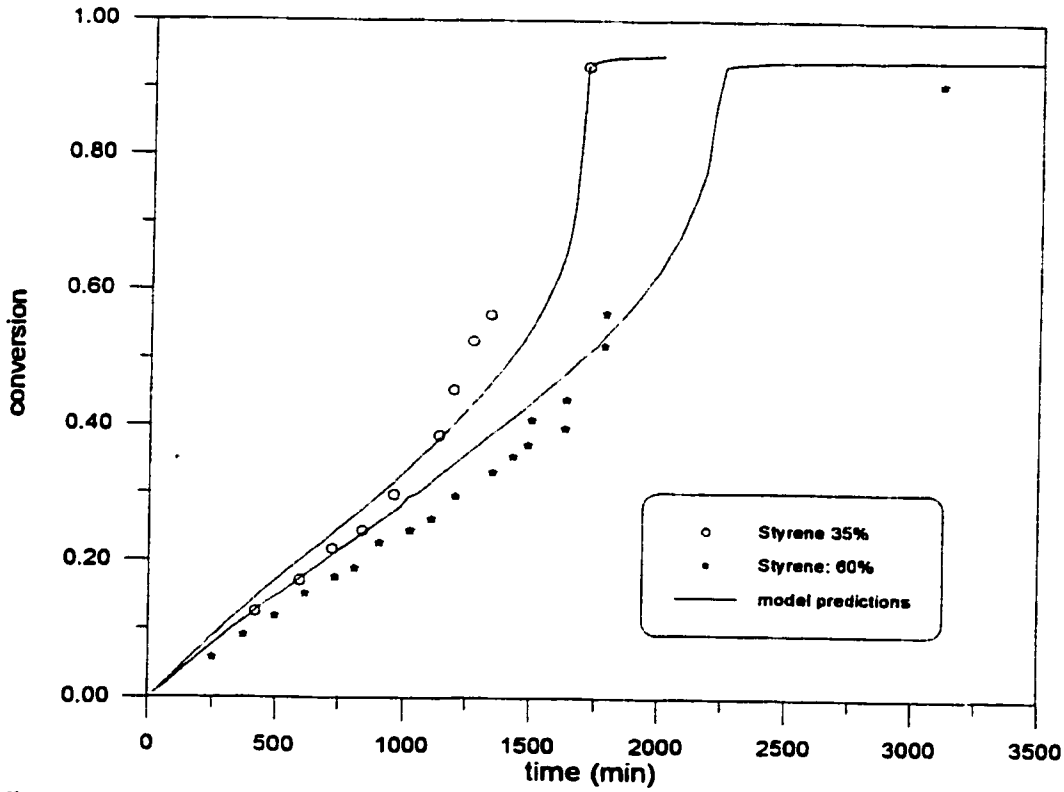

Figure 6.1 Simulation of Methyl Methacrylate and Styrene Bulk Copolymerization at 60°C. BPO: 2 g/L.

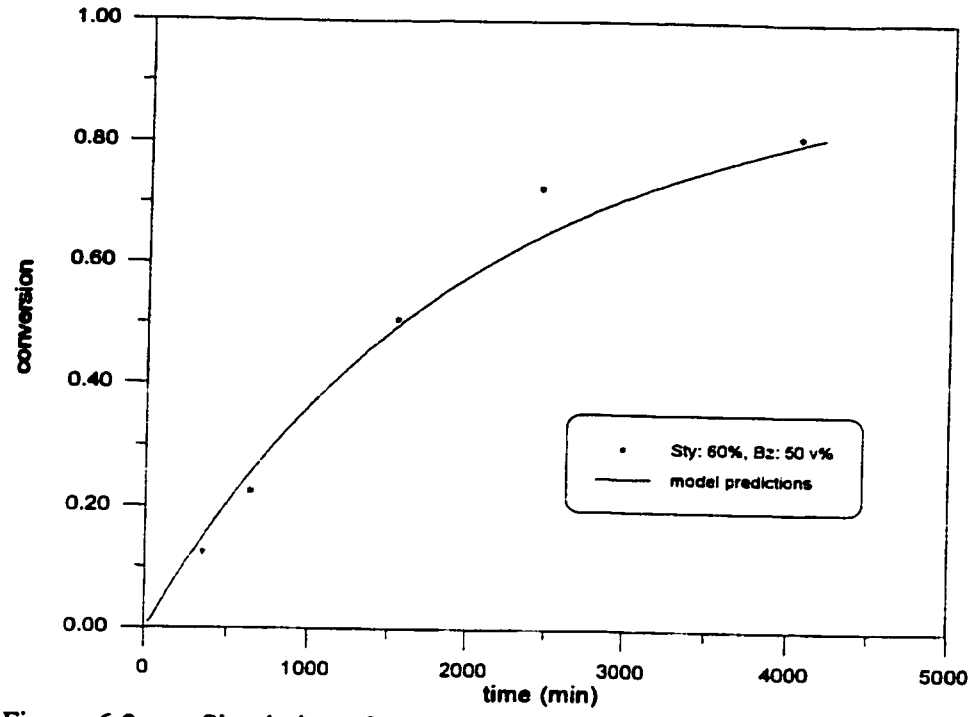

Figure 6.2 Simulation of Methyl Methacrylate and Styrene Solution Copolymerization at 60°C. BPO as initiator: 4 g/L.

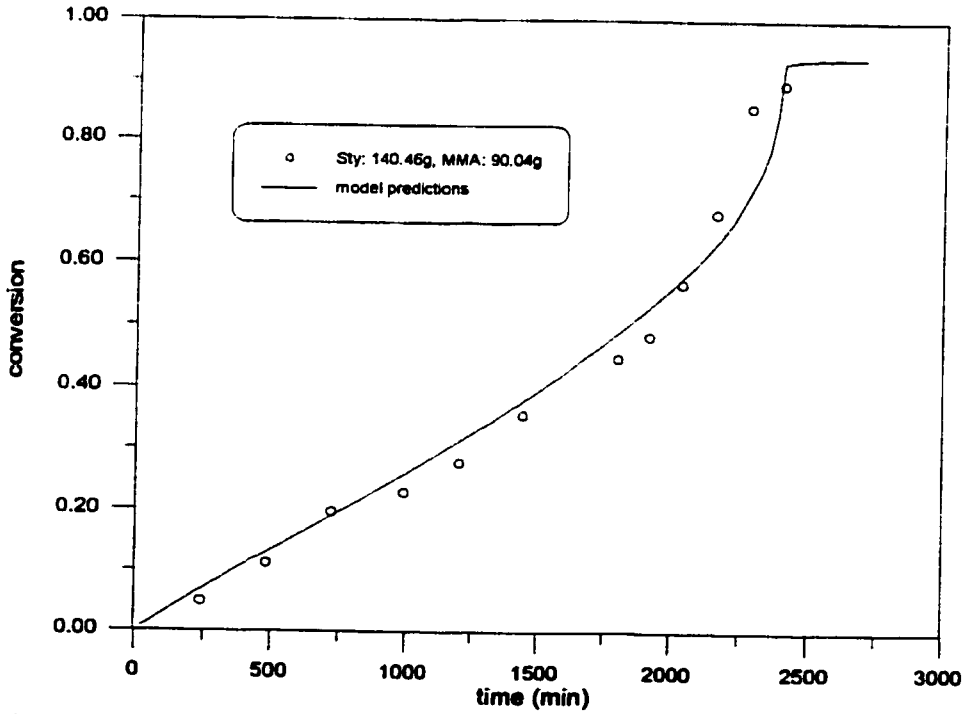

Figure 6.3 Simulation of Methyl Methacrylate/Styrene Copolymerization in bulk at 60°C. BPO: 2g/L

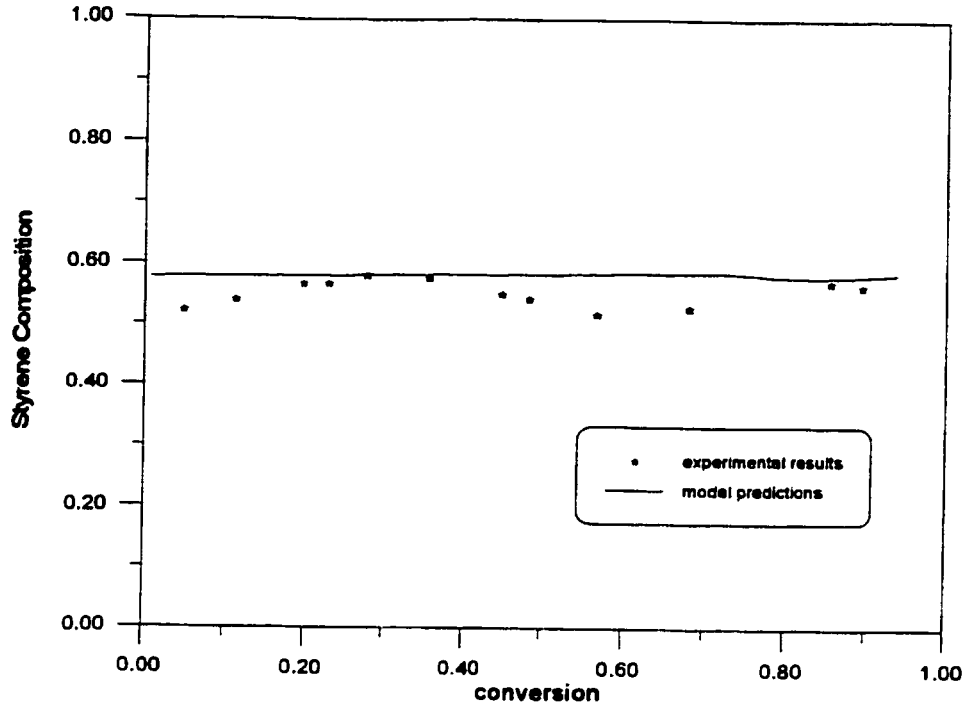

Figure 6.4 Composition Drift in Methyl Methacrylate and Styrene Bulk Copolymerization at 60°C. BPO: 2 g/L.

O'Driscoll et al.(1984)

O'Driscoll et al.(1984) later repeated their previous runs but used a different analytical method for measuring copolymer composition. Copolymerizations of MMA and styrene were conducted at 60°C using benzoyl peroxide (BPO) as initiator. Initial styrene in the feed was 35 mol% and 60 mol%. Copolymer composition was measured by nuclear magnetic resonance (NMR). Figure 6.5 shows the reproduced conversion data. Good reproducibility was obtained and more interestingly, the previously reported copolymer composition deviation was not observed. Figure 6.6 shows the comparison of the previous copolymer composition results by UV and the more recent measurements by NMR. O'Driscoll et al.(1984) compared the two analytical methods and concluded that the previous analysis had error. They stated that earlier UV techniques suffered from consistent deviation from the ideal absorption and this led to the previously observed composition deviation. O'Driscoll et al.(1984) also measured number average molecular weight

by GPC. Their results compared with model predictions are plotted in figure 6.6. Though model predictions are higher than the reported values, this model predicted the correct trend for the molecular weight average profile over the entire conversion range. The discrepancy in figure 6.6 may be due to GPC measurement errors and the approximation used in the calibration curve.

O'Driscoll and Huang (1989, 1990)

O'Driscoll and Huang (1989, 1990) conducted full conversion range experiments with MMA/Sty in bulk. Styrene content in the monomer feed ranged from 30 mol% to 70 mol%, while 52 mol% styrene is the azeotropic feed. Figure 6.7 presents predicted conversion profiles as well as measured conversion for all three bulk runs. It is clear from figure 6.7 that the copolymerization model can describe kinetic characteristics of copolymerization of MMA/Sty over the entire conversion range. The onset of gel effect and limiting conversion are satisfactorily predicted by the model in all three runs with different styrene monomer feed composition. Figure 6.8 is the accumulated copolymer composition. The agreement between model predictions and reported data is very good. For the azeotropic run, the accumulated styrene composition stayed constant throughout up until about 70% conversion. After that point, one can see a slight drift downwards, which is largely due to diffusional limitations on the rate constant of propagation. This trend was successfully picked up by the model.

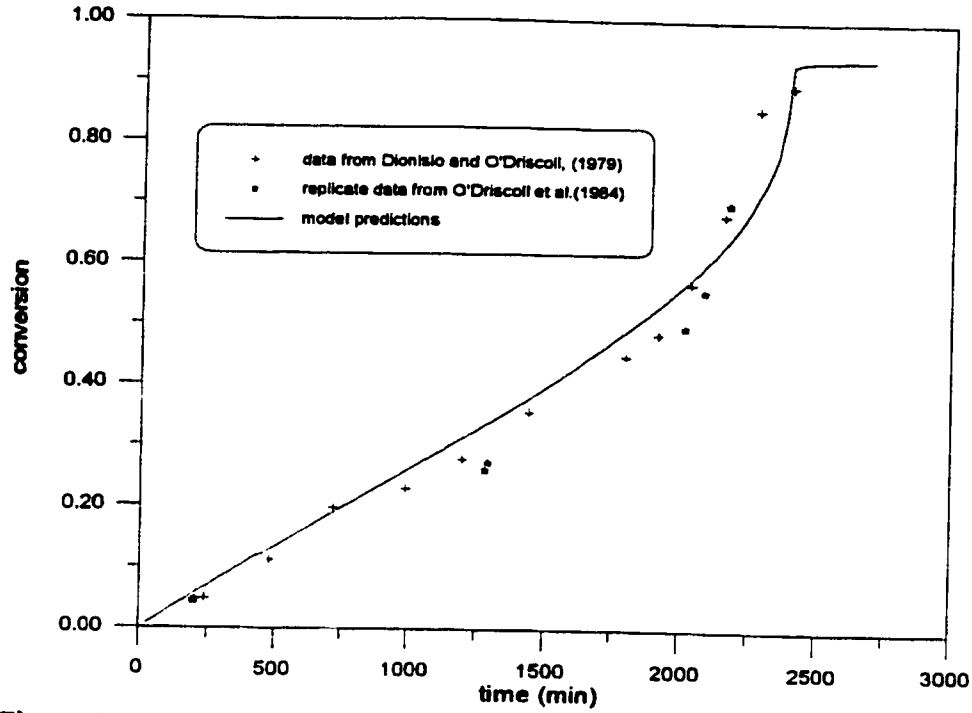

Figure 6.5 Simulation of Methyl Methacrylate and Styrene Copolymerization in Bulk at 60°C.
BPO: 2g/L styrene in monomer feed: 60 mol%

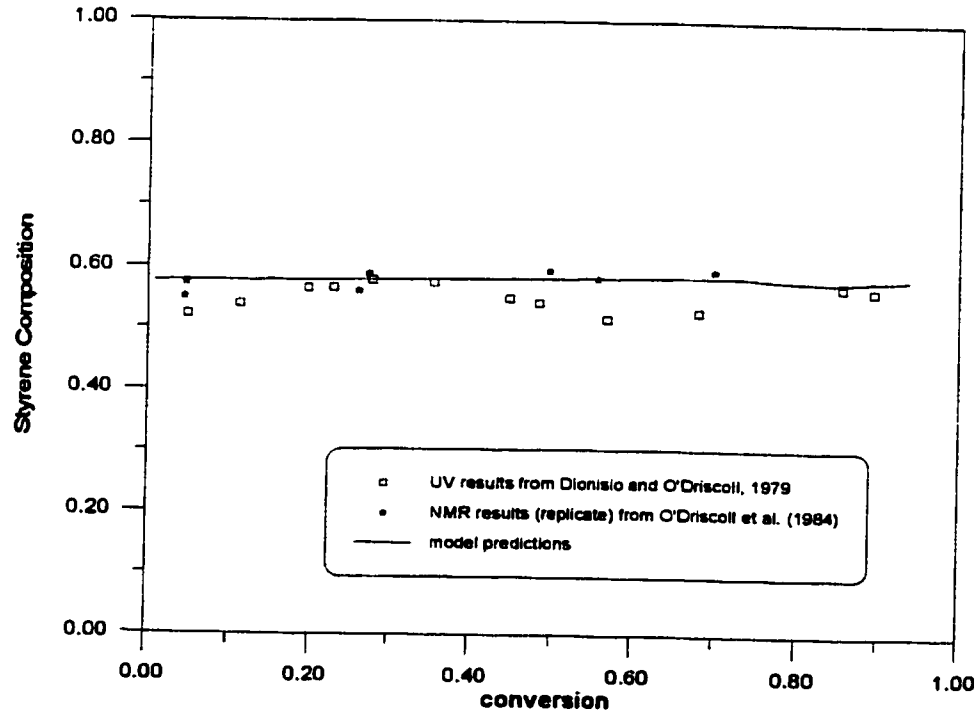

Figure 6.6 Simulation of Methyl Methacrylate and Styrene Bulk Copolymerization at 60°C.
BPO as initiator: 2 g/L, styrene in monomer feed: 60 mol%

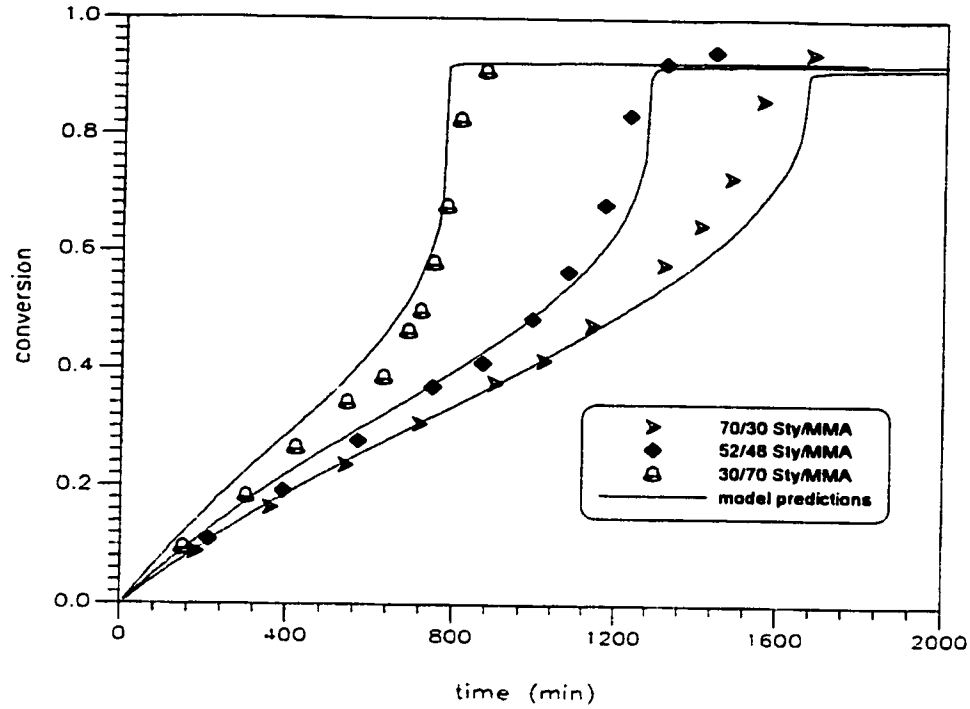

Figure 6.7 Simulation of Methyl Methacrylate and Styrene Copolymerization in Bulk at 60°C. [AIBME]: 0.01 mol/L

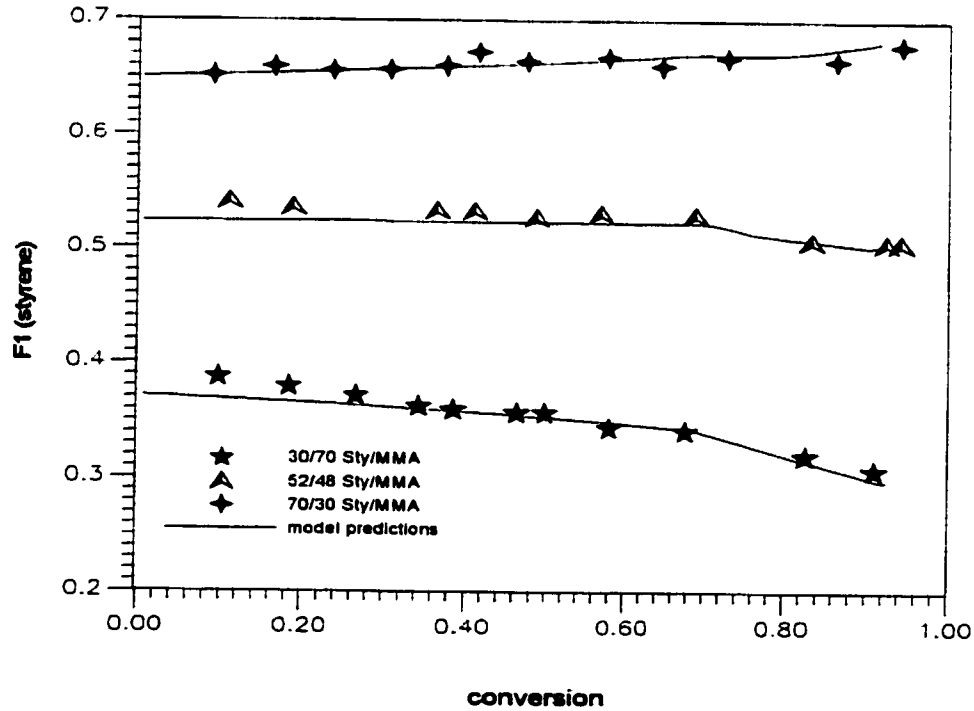

Figure 6.8 Simulation of Composition Drift in Methyl Methacrylate and Styrene in Bulk at 60°C. [AIBME]: 0.01 mol/L

Chapter 7. Simulation of Copolymerization of Styrene and Acrylonitrile

7.1 Literature Review

Styrene and acrylonitrile is another popular copolymer system that received much literature attention in the past due to its commercial importance in the rubber industry. Sty/AN copolymer product is a common thermoplastic with high chemical resistance, tensile strength, easy to process and good mechanical properties. Styrene and acrylonitrile are often polymerized with butadiene to produce ABS rubber. Though this copolymer is of great industrial and academic interest, very few groups only have conducted full conversion experiments or kinetics studies. Table 7.1 below lists references containing useful information for kinetic studies.

Table 7.1 Literature references for Styrene/Acrylonitrile

Reference	Remarks
Arita et al.(1981)	sequence length distribution
Asakura et al.(1981)	reactivity ratios
Balke et al.(1982)	modeling and simulation
Blanks and Shah (1976)	cross-termination studies, reactivity ratios
Cheng and Yan (1989)	reactivity ratios, low conversion experiments
Doak (1948)	reactivity ratios
Farber (1986)	multiple steady state studies, CSTR operation
Garcia-Rubio et al.(1985)*	full conversion data, mathematical modeling
Garcia-Rubio et al.(1982)	modeling and simulation
Hatate et al.(1984)	CSTR operation, low conversion experiments, reactivity ratios
Hayes and Futamura (1981)	reactivity ratios
Hayes (1981)	reactivity ratios
Hill et al.(1982)	sequence length distribution
Hill et al.(1991)	reactivity ratios
Hill et al.(1992)	solvent effect on reactivity ratios

Hill et al.(1989)	reactivity ratio determination from triad fractions, penultimate unit effect
Johnston (1976b)	copolymer Tg
Kirchner and Schlapkohl (1976)	thermal initiation kinetics
Kucher et al.(1978)	low conversion studies on cross-termination
Lin et al.(1979)*	experiments up to 50% conversion, high temperature runs, solution polymerization, modeling
Lord (1984)*	modeling and simulation
Mayo et al.(1948a)	chemical structure and reactivity
Nagaya et al.(1980)	sequence length distribution studies
Santos et al.(1994)	terpolymerization
Schellenberg and Wigand (1992)	oligomers
Sebastian and Biesenberger (1981)*	full conversion experiments, solution polymerization
Tanczos et al.(1982)	low conversion experiments, inhibition

* papers present full conversion experimental data that are useful for model testing

From Table 7.1, one can make the following observations:

(1) Most literature studies limit their work to low conversions and reactivity ratio estimation only. Full conversion range data are very rare.

(2) Sty/AN copolymerization often exhibits heterogeneity. Copolymer may precipitate at a certain stage of the reaction. Discrepancies between model predictions and experimental measurements are due to precipitated polymer, in which case a polymer-rich phase is formed.

(3) Among all the papers in Table 7.1, Garcia-Rubio et al.(1985) and Lord (1984) provide most insightful modeling and simulation information for model testing for this copolymer system.

(4) It was mentioned in Gao and Penlidis (1996) that solvent has a significant effect on the reaction kinetics in acrylonitrile homopolymerization. Acrylonitrile has different rate constants in different solvents. Additionally, homopolymerizations of acrylonitrile in *N, N*-dimenthyl

formamide (DMF) and dimethyl sulfoxide (DMSO) are homogeneous, while in bulk and other solvents precipitation was observed. Most literature data used in model testing were collected from bulk copolymerization, therefore rate constants for acrylonitrile homopolymerization in bulk were used. Caution must be exercised in interpreting comparison of model predictions with experimental data when solvent is used. Nevertheless, in the model testing of Lin et al.(1979) data (toluene was used as a solvent), the solvent effect on reaction kinetics did not seem to be significant.

7.2 Model Testing

Garcia-Rubio et al.(1985)

Garcia-Rubio et al.(1985) is the only group that studied Sty/AN copolymerization up to high conversion. Garcia-Rubio et al.(1985) conducted full conversion range experiments at two different temperature levels. They observed that copolymerization of Sty/AN in bulk is a homogeneous process throughout most of the conversion range if the initial styrene monomer feed composition is greater than 50%. If the initial styrene monomer feed composition is between 10~50%, the reaction mixture remains homogeneous at low conversion levels. Under certain circumstances (high acrylonitrile content in the monomer feed, >50%), the reaction mixture exhibits heterogeneity, and regions of hard and soft polymer in the ampoules are evident, especially at high conversion levels. The heterogeneity in polymerizations involving acrylonitrile has already been discussed in Gao and Penlidis (1996). Copolymerization of Sty/AN in glass ampoules is more like a suspension polymerization rather than a bulk polymerization in cases heterogeneity is observed. In this thesis, we do not attempt to simulate copolymerizations with prevailing heterogeneity. Fortunately, the data reported by Garcia-Rubio et al.(1985) are mostly from runs with high styrene content (above 50%) in which no apparent heterogeneity was observed. Therefore, it can be safely assumed that the use of this copolymerization model to simulate copolymerization of Sty/AN in bulk is appropriate.

Figure 7.1 shows five bulk runs with various styrene contents at 40°C. It is apparent that there is a strong gel effect and limiting conversion (about 90%) in all five runs. The agreement between

model predictions and reported conversion profiles is satisfactory. Figures 7.2 and 7.3 are comparisons of simulated residual styrene in the reaction mixture and measured data. Both plots indicate a considerable composition drift towards the end of the reaction in most runs.

Figures 7.4 and 7.5 show more runs conducted at 60°C. The initiator concentrations in figures 7.4 and 7.5 are 0.01 and 0.05 mol/L, respectively. The effect of initiator on the rate of polymerization is obvious. Higher initiator level increases the rate of polymerization and reduces the limiting conversion relatively. Gel effect is also stronger in the runs with higher initiator concentration. Figures 7.6 and 7.7 are the residual styrene compositions in the runs with the lower initiator concentration, while figures 7.8 and 7.9 are for the runs with the higher initiator concentration. Figures 7.6 to 7.9 indicate that initiator concentration has no apparent effect on polymer composition. Garcia-Rubio et al.(1985) also measured number average molecular weight data by viscometry. Results obtained through this method give an approximate number average molecular weight and are considered less reliable. As a result, their reported molecular weight data are not simulated in this thesis.

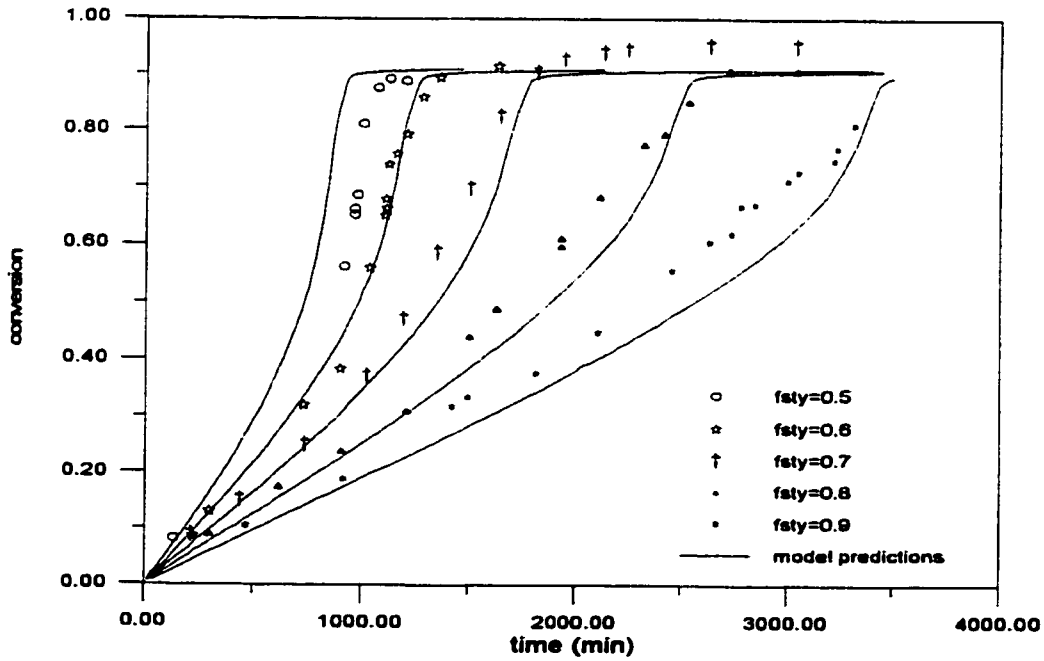

Figure 7.1 Simulation of Styrene and Acrylonitrile Bulk Polymerization at 40°C. [AIBN]=0.05 mol/L.

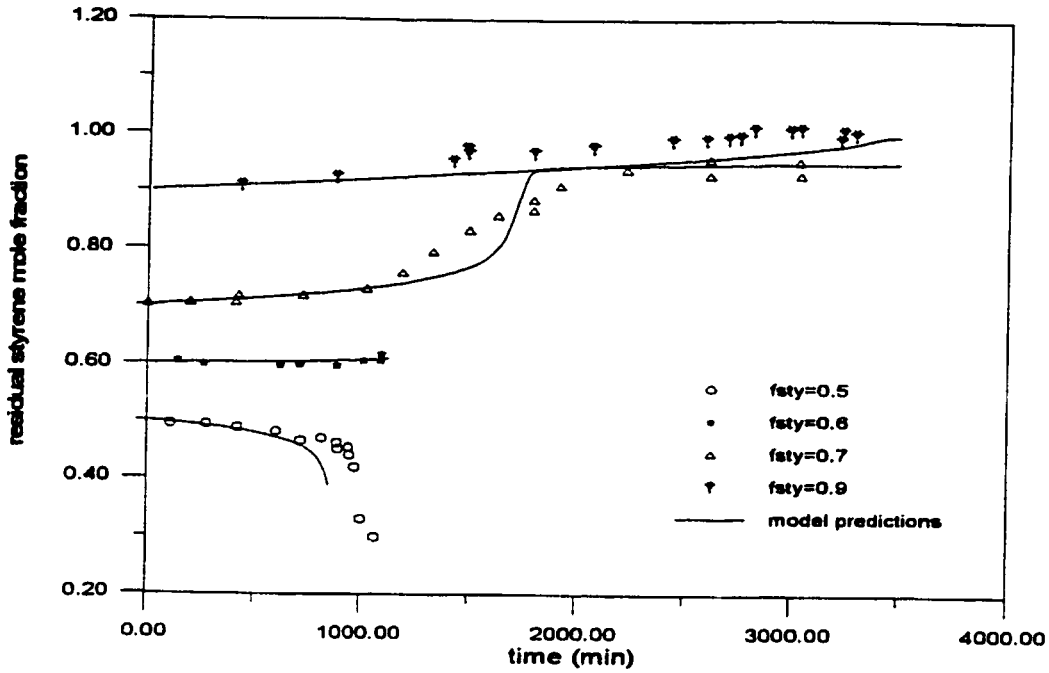

Figure 7.2 Simulation of Monomer Feed Composition in Styrene and Acrylonitrile Bulk Polymerization at 40°C. [AIBN]=0.05 mol/L.

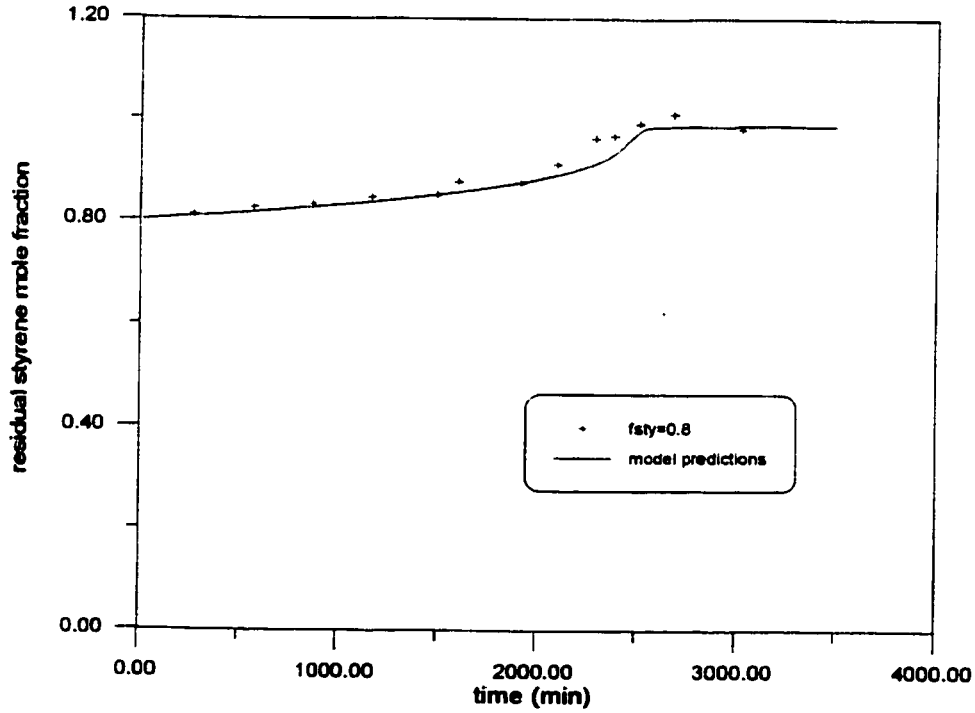

Figure 7.3 Simulation of Monomer Feed Composition in Styrene and Acrylonitrile Bulk Polymerization at 40°C. [AIBN]=0.05 mol/L.

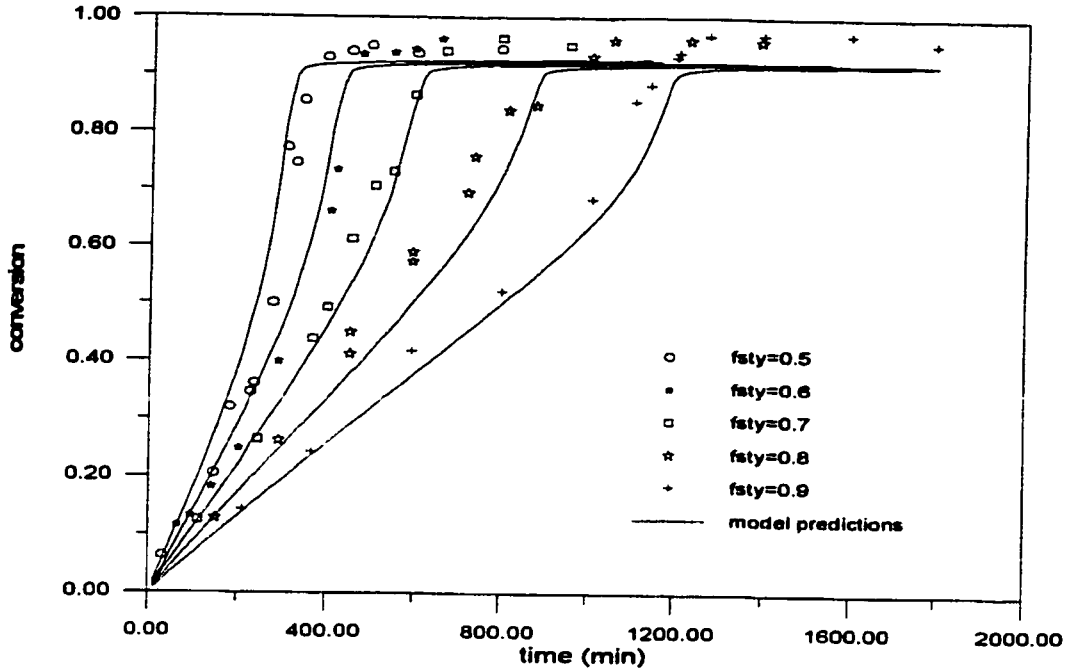

Figure 7.4 Simulation of Styrene and Acrylonitrile Bulk Polymerization at 60°C. [AIBN]=0.01 mol/L.

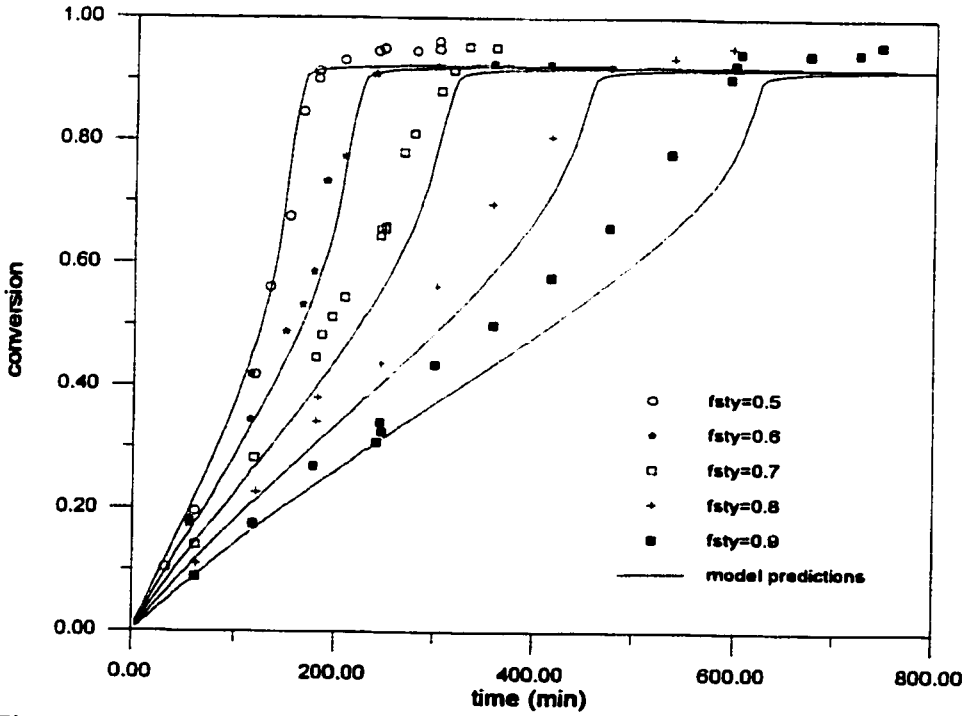

Figure 7.5 Simulation of Styrene and Acrylonitrile Bulk Polymerization at 60°C. [AIBN]=0.05 mol/L.

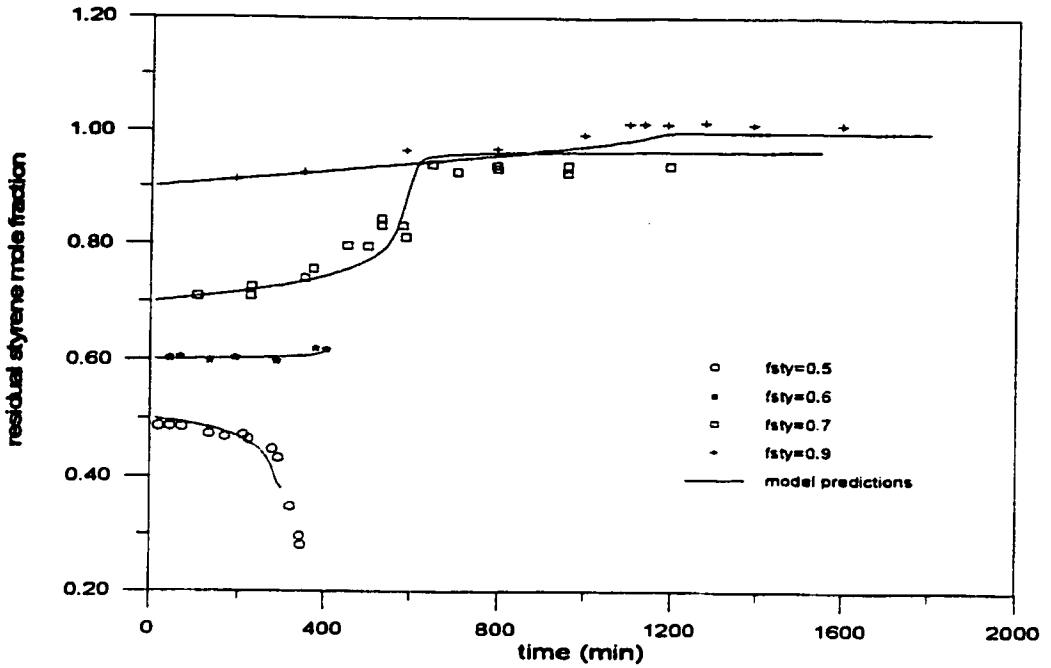

Figure 7.6 Simulation of Monomer Feed Composition in Styrene and Acrylonitrile Bulk Polymerization at 60°C. [AIBN]=0.01 mol/L.

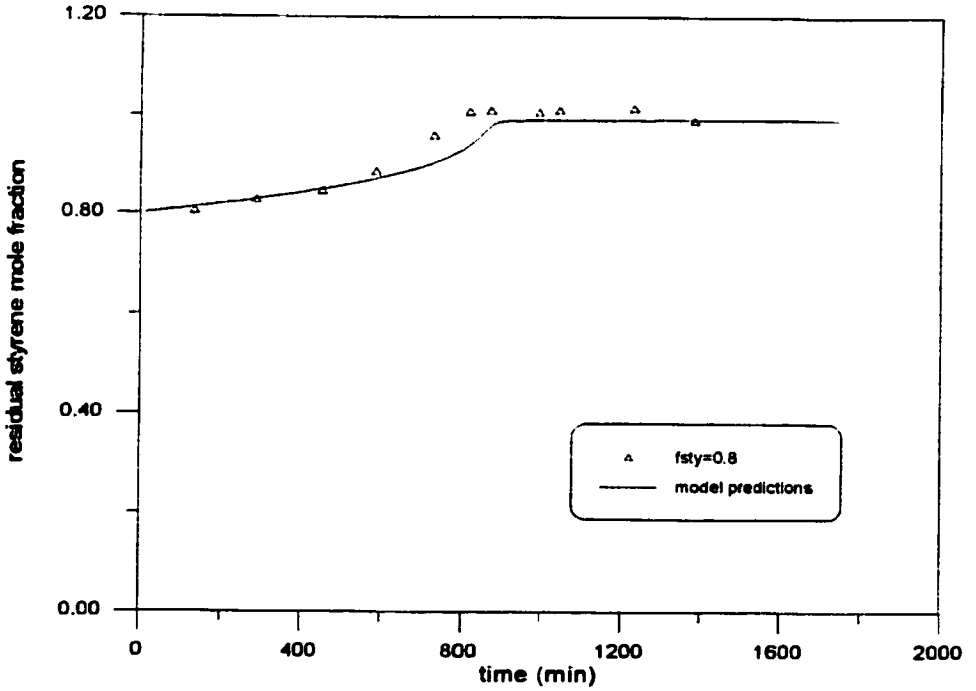

Figure 7.7 Simulation of Monomer Feed Composition in Styrene and Acrylonitrile Bulk Polymerization at 60°C. [AIBN]=0.01 mol/L.

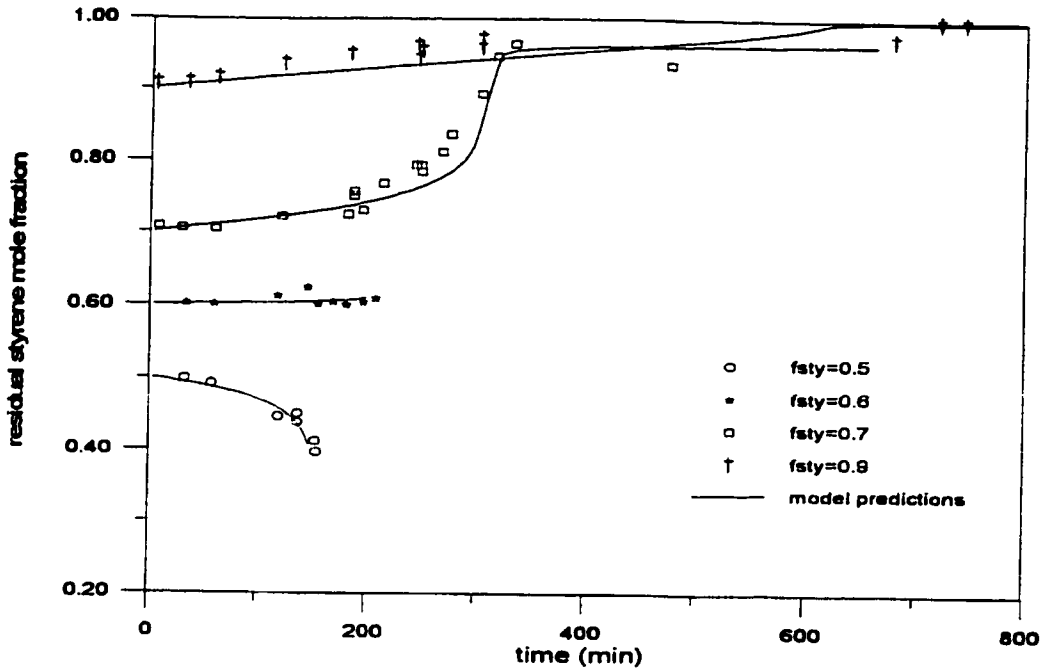

Figure 7.8 Simulation of Monomer Feed Composition in Styrene and Acrylonitrile Bulk Polymerization at 60°C. [AIBN]=0.05 mol/L.

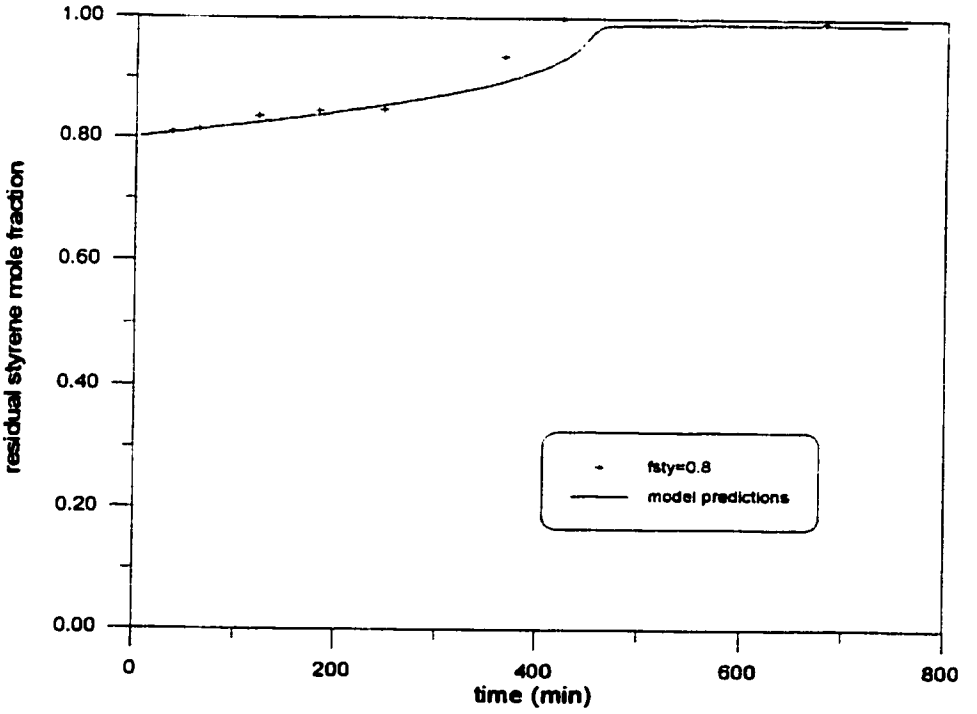

Figure 7.9 Simulation of Monomer Feed Composition in Styrene and Acrylonitrile Bulk Polymerization at 60°C. [AIBN]=0.05 mol/L.

Sebastian and Biesenberger (1981)

Sebastian and Biesenberger (1981) investigated Sty/AN copolymerization at relatively higher temperatures. Their objective was focused on thermal runaway reactions. Differential scanning calorimetry (DSC) was used to detect the rate of heat generation from the reaction and the corresponding conversion was determined. Heterogeneity may occur in the runs with AN content higher than 35%. All the runs reported by Sebastian and Biesenberger (1981) have less than 35% AN in the initial feed, so polymer precipitation can be considered negligible. Figure 7.10 shows three bulk runs with 60% styrene in the feed at 85, 95 and 100°C. It should be noted that in all three runs autoacceleration starts quite early in the reaction and polymerization is nearly completed within a very short period of time. Runs conducted at 95 and 100°C were completed within 15 minutes.

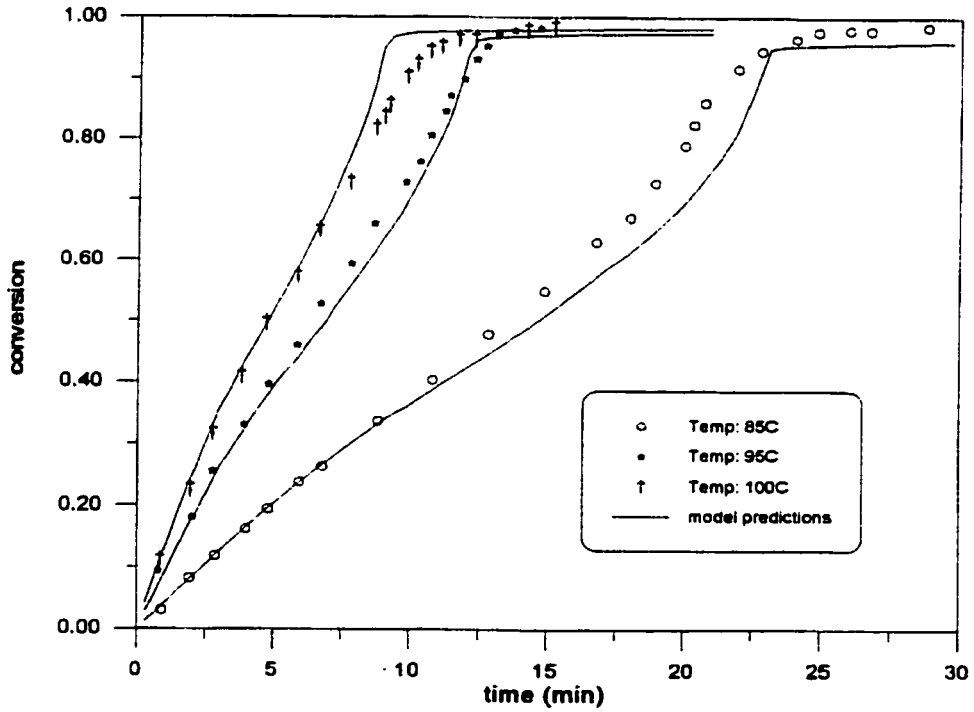

Figure 7.10 Simulation of Styrene and Acrylonitrile Bulk Copolymerization. [AIBN]=0.01 mol/L, 60% styrene.

Lin et al.(1979)

Lin et al.(1979) probably was the first group that published experimental data beyond conversion of 10-20%. In their experiments, Sty/AN copolymerization was carried out in toluene at 80 and 100°C. Due to the presence of solvent, no gel effect was observed. Final conversion level in all their runs was around 50%. Though Lin et al.(1979) did not conduct their experiments to high conversion, their experimental data are good for model testing. Figure 7.11 displays Sty/AN solution copolymerization in toluene at 100°C. Since the reaction temperature is fairly high, thermal initiation may be present. Lin et al.(1979) performed one experiment without any initiator added. The final conversion after 5 hours was around 25%. This confirms that thermal initiation does contribute to monomer radical generation. In model testing, the thermal initiation option was thus used for runs conducted at 100°C. Figure 7.12 demonstrates the effect of temperature on the rate of polymerization. Figure 7.13 demonstrates the effect of initiator level on the rate of polymerization at 80°C. The presence of toluene dilutes the reaction mixture and thus slows down the reaction. The effect of different solvent levels is illustrated in figure 7.14 for the runs at 80°C.

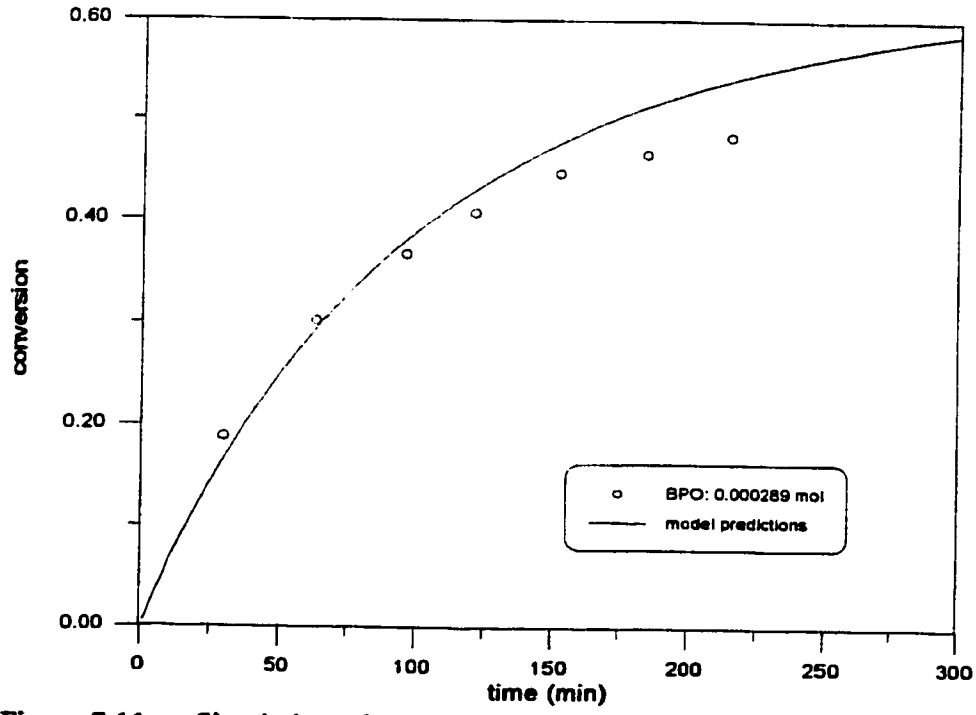

Figure 7.11 Simulation of styrene and acrylonitrile copolymerization in toluene at 100°C. AN: 0.396 mol, Sty: 0.605 mol, toluene: 0.603 mol.

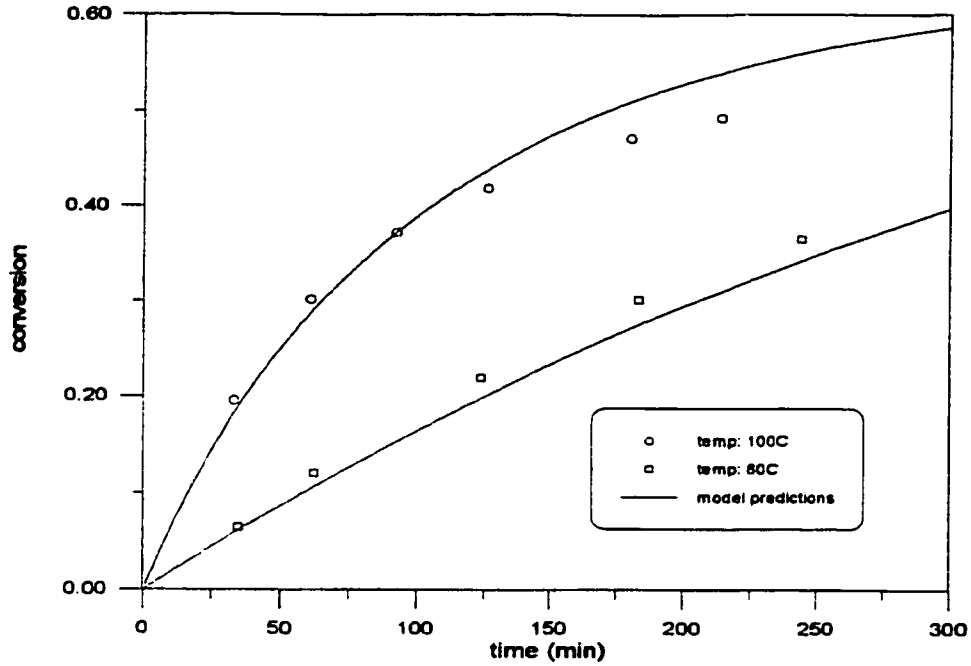

Figure 7.12 Simulation of Styrene and Acrylonitrile Copolymerization in Toluene. AN: 0.396 mol, Sty: 0.605 mol, toluene: 0.603 mol, BPO: 0.000289 mol.

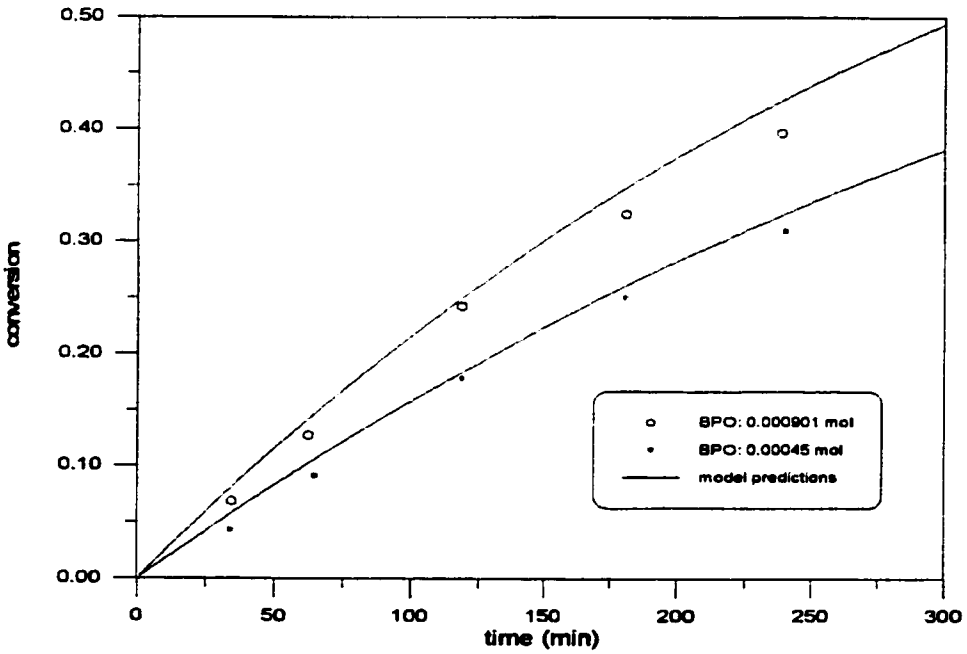

Figure 7.13 Simulation of Styrene and Acrylonitrile Copolymerization in Toluene at 80°C.
AN: 0.396 mol, Sty: 0.605 mol, toluene: 1.413 mol.

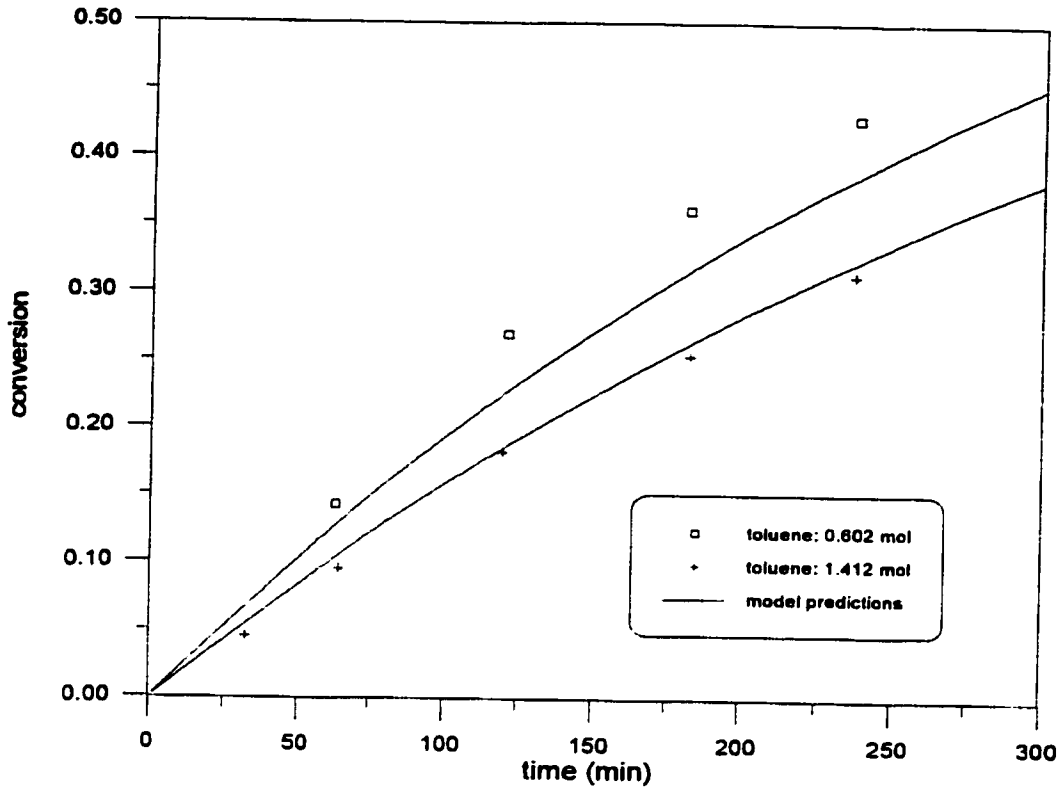

Figure 7.14 Simulation of Styrene and Acrylonitrile copolymerization in Toluene at 80°C.
AN: 0.396 mol, Sty: 0.605 mol, BPO: 0.00045 mol.

Chapter 8. Simulation of Copolymerization of Styrene and Acrylates

Though reactivity ratio estimates of styrene and other acrylates are available from different sources, full conversion range experimental data that can be used for model testing are not found in the literature. To test the model's reliability with regard to various styrene/acrylates copolymer systems, full conversion range experiments have been carried out in this laboratory, and kinetic data collected from these experiments were then used for model testing and database enrichment. The following several sections present model testing results for three styrene/acrylate copolymers.

8.1 Simulation of Copolymerization of Styrene and Butyl Acrylate

8.1.1 Literature Summary

Though styrene/butyl acrylate (Sty/BA) is of industrial importance for various applications, its reaction kinetics was little known. Dube et al.(1990a, b) investigated Sty/BA copolymerization kinetics and carried out full conversion range experiments under a variety of reaction conditions. The experimental data they reported are the only source for model testing. Dube et al.(1990b) summarized the literature information on this copolymer system, and found out that it is mostly limited to low conversion classical theory studies on copolymerization in bulk or emulsion. Reactivity ratios for Sty/BA reported from the literature were listed in Dube et al.(1990b) and hence are not retabulated in this thesis. Bradbury and Melville (1954) measured reactivity ratios and discussed the cross-termination step in Sty/BA copolymerization. Devon and Rudin (1986) attempted to determine the chain transfer to monomer constant of Sty/BA in emulsion polymerization. More recently, Brar et al.(1992) used the EVM method to estimate reactivity ratios. Their reactivity ratio estimates are slightly different from those reported by Dube et al.(1990b), even though both estimates were obtained from the EVM method. It should be emphasized here that the experimental design for reactivity ratio estimation is very important. In Brar et al.'s(1992) estimates, the Tidwell-Mortimer criterion is not applied, as discussed in Burke et al.(1994) and section 5.3. This maybe the reason for the discrepancy. Kostanski and Hamielec (1992) investigated the temperature effect on reactivity ratios. Kostanski and Hamielec (1994) later synthesized Sty/BA oligomers at higher temperatures in a CSTR, with emphasis on the

microstructure of the oligomer produced than on reaction kinetics. Both Fukuda et al.(1989) and Davis et al.(1991) used the PLP method to measure the overall propagation rate constant for Sty/BA. The obtained results were interpreted on the basis of penultimate model kinetics. Discussion on model discrimination was given in section 2.3. Comments on the PLP method were given in Gao and Penlidis (1996). Table 8.1 below gives a list of literature references on Sty/BA, with a star indicating references useful for model development.

Table 8.1 References on Styrene/Butyl Acrylate

References	Remarks
Balaraman et al.(1983)	reaction kinetics, reactivity ratios
Borchardt (1982)	reactivity ratios
Brar et al.(1992)	reactivity ratios
Bradbury and Melville (1954)	low conversion experiments, thermal initiation, solution polymerization
Buback et al.(1994)	reaction diffusion control kinetics
Davis et al.(1991)	propagation rate constant determination by PLP method
Devon and Rudin (1986)	low conversion experiments, kinetic rate constants, emulsion polymerization
Dube et al.(1990a, b)*	full conversion experiments, reactivity ratio determination by EVM, modeling
Fukuda et al.(1989)	rate constant determination, penultimate effect
Kaszas et al.(1985)	low conversion experiments, reactivity ratios
Kostanski and Hamielec (1992)	temperature effect on reactivity ratios
Kostanski and Hamielec (1994)	oligomerization, CSTR operation, thermal initiation
Rizzardo et al.(1995)	chain transfer kinetics, oligomers
Spardans, et al.(1990)	copolymer characterization

* papers present full conversion experimental data and are used for model testing

8.1.2 Model Testing

The reactivity ratios used in the model testing are from Dube et al.(1990b). Figure 8.1 represents three bulk runs with various monomer feed compositions at 50°C. An interesting observation in these three runs is how the monomer feed composition affects the copolymerization characteristics. It is known that BA and styrene are two monomers with very different polymerization characteristics. Firstly, BA homopolymer has a very low Tg around -45°C, and appears to be flexible at room temperature; styrene homopolymer is just the opposite. It has a very high Tg around 105°C, and appears to be fairly hard and tough. Secondly, BA homopolymerization exhibits a strong gel effect at the early stage of the reaction and there is no limiting conversion. Gel effect starts late in the styrene homopolymerization and there is usually a limiting conversion. The overall reaction behaviour for a copolymerization of these two monomers largely depends on which monomer is more dominant in the initial monomer feed. Such characteristics are well reflected in the three runs with styrene content in the monomer feed ranging from 25% to 95%. The azeotropic composition for this copolymer is 94.2 mol% styrene in the feed. In the azeotropic run in figure 8.1, the model predicts a limiting conversion at around 90% as represented by the solid line. This is expected since there is about 95 mol% styrene in the feed. This run is very much like a styrene homopolymerization in which autoacceleration starts late in the reaction and limiting conversion is observed. Such trends are well represented by the open squares in figure 8.1. However, the reported conversion points at the end of the reaction (above 92% conversion) from Dube et al.(1990b) are higher than the model predictions. We suspect experimental error involved in these data points. In the run with the highest BA content (75 mol%), the reaction resembles more closely a BA homopolymerization. Autoacceleration starts relatively early in the reaction and there is no limiting conversion. This is due to the fact that BA has a very low Tg. It is convincing from figure 8.1 that the model predicts copolymerization of Sty/BA satisfactorily over the entire conversion range under a wide variety of monomer feed compositions.

Figure 8.2 is the comparison of model-predicted styrene composition in the copolymer with

measured NMR data. The agreement is fairly good. In the azeotropic run, the accumulated copolymer composition remains the same over the whole conversion range. Composition drift is not severe in the other two runs. Figure 8.3 gives measured molecular weight data of the samples collected in the azeotropic run. As mentioned before, only molecular weight data from azeotropic runs are simulated. In figure 8.3 both number average and weight average molecular weights increase towards the end of the reaction. The increase in the weight average molecular weight is much more significant. These kinetic trends were correctly reflected by the model in figure 8.3. More runs were conducted at the same temperature but at a higher initiator level. Similar reaction characteristics to those of figures 8.1 were observed. The rate of polymerization in the runs of figure 8.4 is higher due to the higher level of initiator. Figure 8.4 displays the comparison of model predictions with experimental data. Again, the agreement is good. Figure 8.5 shows composition drift of styrene monomer bound in the copolymer for all three runs. Comparing experimental results between figures 8.2 and 8.5, it is clear that the initiator level has little effect on the accumulated copolymer composition. Figure 8.6 gives again molecular weight averages from the runs at the higher initiator level.

To summarize, the simulation of Sty/BA copolymerization in bulk is satisfactory. This copolymer system has two monomers with very different physical/chemical properties. The presence of styrene significantly slows down the rate of polymerization, and increases the Tg of the final copolymer product. All experiments were performed at 50°C; more experiments at other temperature levels will definitely test the model's reliability further.

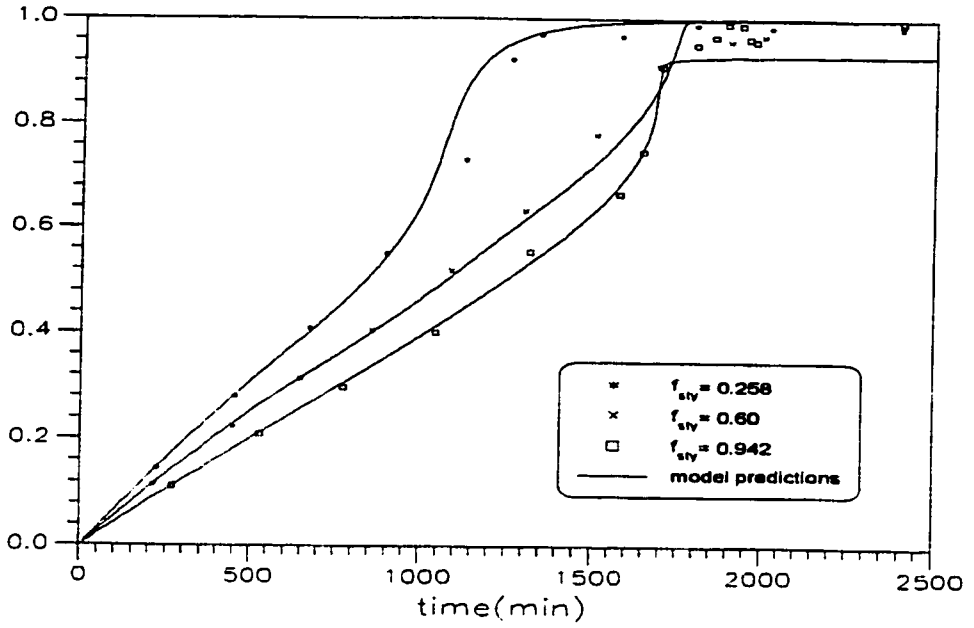

Figure 8.1 Simulation of Styrene and Butyl Acrylate Copolymerization in Bulk at 50°C. [AIBN]: 0.05 mol/L.

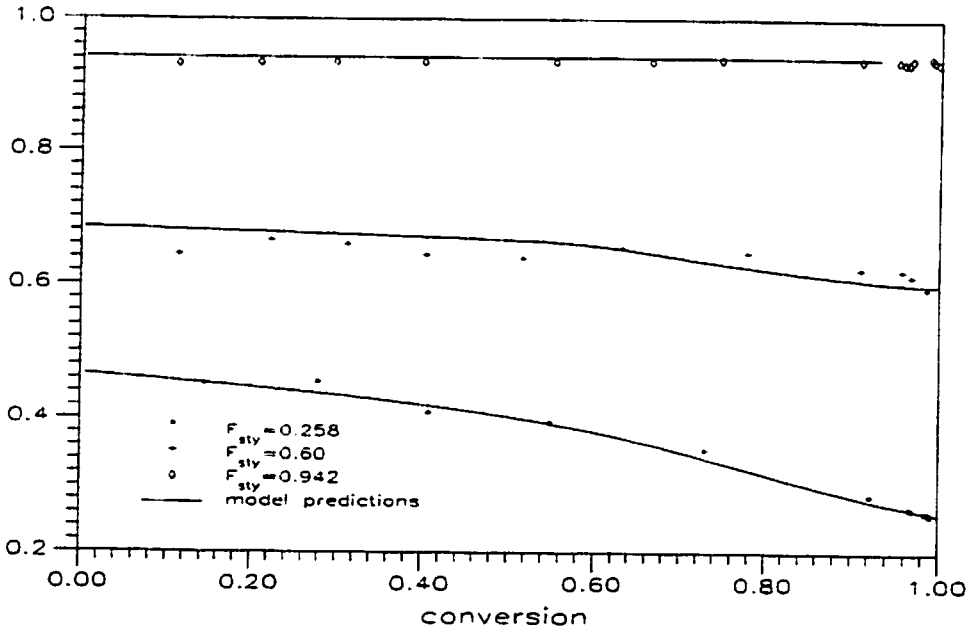

Figure 8.2 Simulation of Composition Drift in Styrene and Butyl Acrylate Copolymerization in Bulk at 50°C. [AIBN]: 0.05 mol/L.

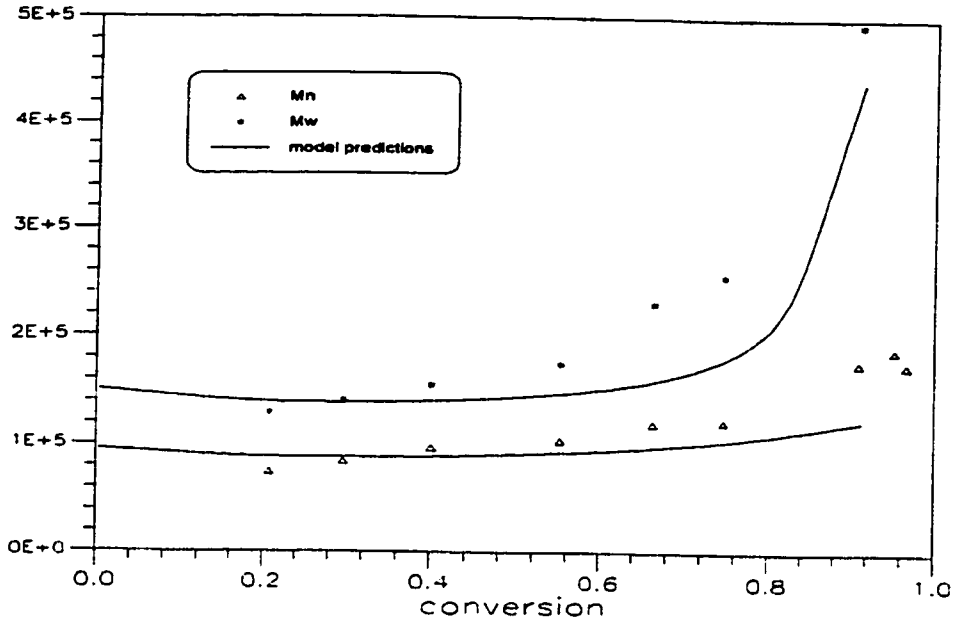

Figure 8.3 Simulation of Molecular Weight in Styrene and Butyl Acrylate Copolymerization in bulk at 50°C. [AIBN]: 0.05 mol/L, f_{sty}: 0.942

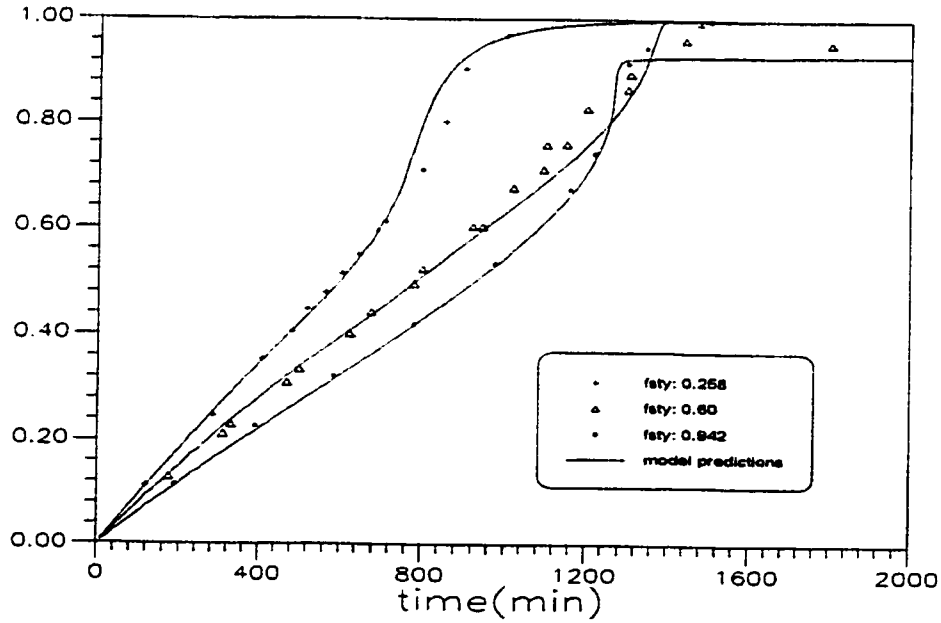

Figure 8.4 Simulation of Styrene and Butyl Acrylate Copolymerization in Bulk at 50°C. [AIBN]: 0.1 mol/L.

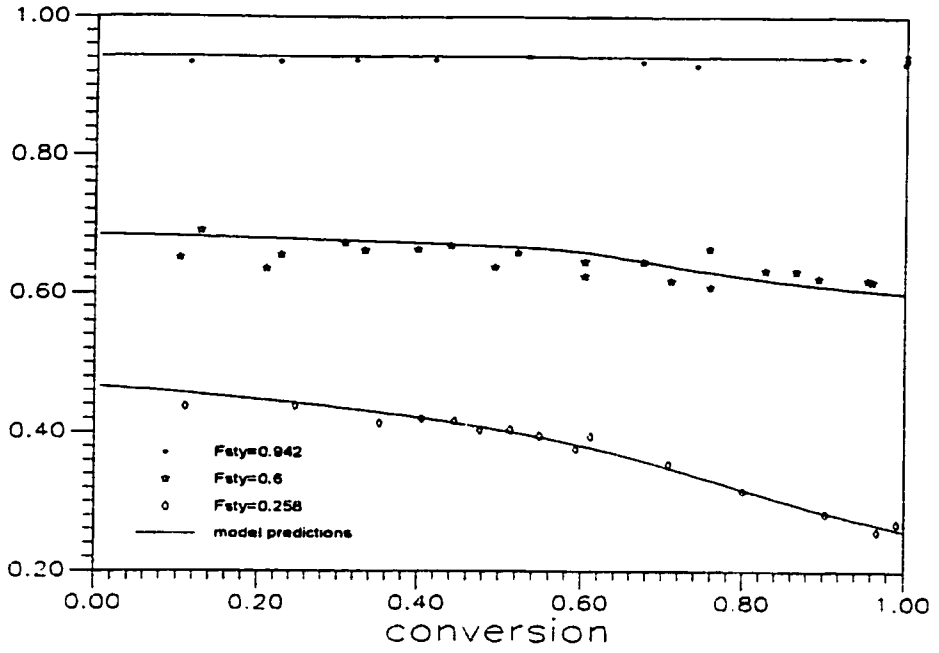

Figure 8.5 Simulation of Composition Drift in Styrene and Butyl Acrylate Copolymerization in Bulk at 50°C. [AIBN]: 0.1 mol/L.

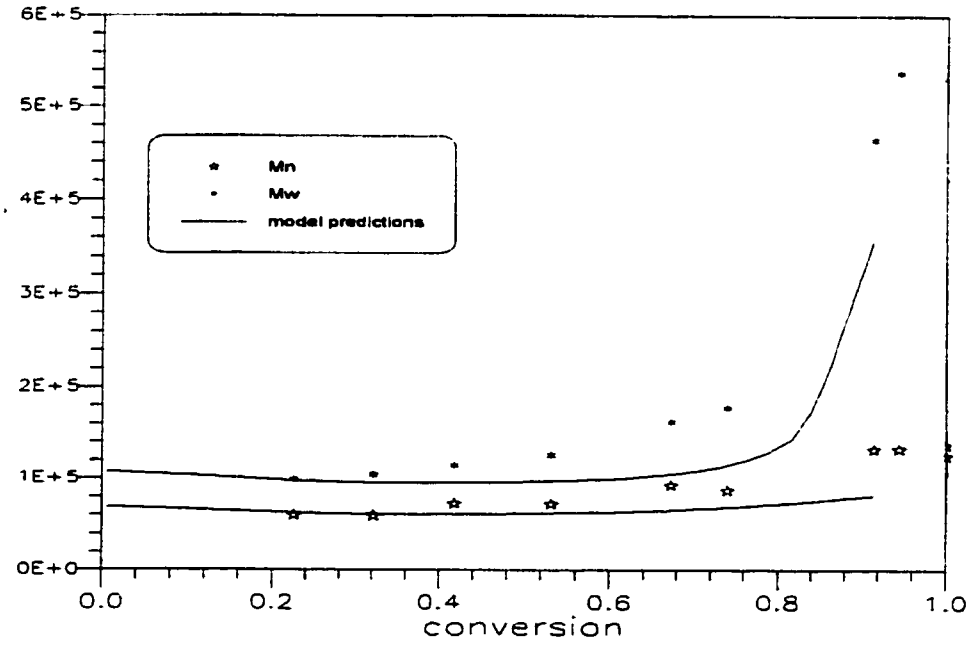

Figure 8.6 Simulation of Molecular Weight in Styrene and Butyl Acrylate Copolymerization in Bulk at 50°C. [AIBN]: 0.1 mol/L, f_{sty}: 0.942

8.2 Simulation of Copolymerization of Styrene and Ethyl Acrylate

8.2.1 Literature Review

Sty/EA copolymerization kinetics is poorly understood and little information is available in the literature. The references collected primarily concentrate on measuring overall copolymerization rate at very low conversion. Fehervari et al.(1982a, b) measured the overall rate of polymerization of Sty/EA in benzene as well as reactivity ratios. Fehervari et al.(1981) also measured the rate of initiation of the same copolymer system in benzene. Wittmer (1979) measured the overall rate of polymerization at various monomer feed compositions and attempted to interpret the data using the penultimate model. More recently, the PLP method was used by many groups to directly determine the rate constant for propagation. Ma et al.(1994) investigated the copolymerization of styrene and EA in bulk at 40°C. They determined the values of the rate constant of propagation (k_p) and termination (k_t) of both EA and styrene at low conversion. The values of k_p and k_t of EA reported are 4700 and 11×10^6 L/mol·s, respectively. These values are much higher than those from other research groups. Several sources of error involved in their measurements are suspected. Hutchinson et al.(1993) pointed out that an accurate measurement of k_p using PLP largely depends on a proper numerical treatment of the data, as well as on the analysis and interpretation of the experimental gel permeation chromatography traces. Inappropriate experimental and numerical analysis may easily result in erroneous results and misleading statements. Ma et al.(1994) stated that the measurement of k_p of EA was unsuccessful because the gel effect started very early in EA homopolymerization, thus it was suggested that extra caution should be exercised in the use of k_p and k_t values they reported.

Due to this lack of information, full conversion range experiments were conducted in this laboratory by McManus and Penlidis (1996). This is the first time that full conversion range experimental data for this copolymer system are reported. McManus and Penlidis (1996) estimated reactivity ratios by the EVM method using copolymer composition data collected from designed experiments. The reported conversion, composition and molecular weight data are the only source for model testing. Table 8.2 lists literature references, with a star indicating data sources useful for model development.

Table 8.2 References on Sty/EA Copolymerization

References	Remarks
Borchard (1982)	steric and electronic effects on reactivity ratios
Brar (1993)	microstructure and copolymer Tg
Fehervari and Foides-Berezsnich (1982a, b)	low conversion experiments in benzene, reactivity ratios
Fehervari et al.(1981)	rate of initiation in bulk and benzene
Fukuda et al.(1989)	penultimate effect on overall copolymer kp
Gao et al.(1997)	ethyl acrylate homopolymerization, modeling
Ma et al.(1994)	overall copolymer kp measurement by PLP method
McManus and Penlidis (1996)*	full conversion range experiments
Wittmer (1979)	classical copolymerization theory, cross-termination

* data source useful for model developing

8.2.2 Model Testing

McManus and Penlidis (1996) conducted full conversion range Sty/EA copolymerization in bulk using AIBN as initiator. Their experimental plan was based on a modified 2^3 factorial design. Effects of temperature, initiator level and monomer feed composition on reaction kinetics were examined. Reactivity ratios were estimated using EVM. The azeotropic composition of Sty/EA copolymer is f_{sty} equal to 76.2 mol%. Figure 8.7 represents four bulk runs (including one replicate run) with different initial styrene feed compositions, and AIBN concentration of 0.05 mol/L. Similar to Sty/BA copolymer, styrene and ethyl acrylate are two monomers with very different physical/chemical properties. Ethyl acrylate is a very fast-reacting monomer with strong autoacceleration and its homopolymer has a low Tg (-24°C) which leads to no limiting conversion, while styrene is just the opposite (slow polymerization and high homopolymer Tg). The conversion profiles of these runs resemble those in Sty/BA copolymerization, i.e., more styrene content in the monomer feed slows down the overall rate of polymerization. Figure 8.7 shows model predictions for all these runs, and the agreement is good. One replicate run was performed at styrene feed composition of 45.3 mol%. The reproducibility is very satisfactory.

Figure 8.8 shows composition change in the runs displayed in figure 8.7. The azeotropic run exhibits no composition drift over the entire conversion range, while the run with 15.2 mol% styrene in the feed exhibits severe composition drift starting at around 40% conversion. It was observed by McManus and Penlidis (1996) that the large composition drift changed the Sty/EA copolymer's opacity. The copolymer changed from transparent to completely white, and also became more brittle. However, such a phenomenon did not occur in samples of azeotropic composition. Figure 8.8 displays more replicate data. Again, the reproducibility is good. Figure 8.9 shows measured molecular weights for the azeotropic run along with model predictions. Figure 8.9 shows the effect of autoacceleration on the molecular weight of the final copolymer product: the number average molecular weight changes little during the course of the polymerization while the weight average molecular weight increases markedly towards the end of the reaction. These trends are correctly reflected by the model's predictions. Figure 8.10 represents more bulk runs under similar reaction conditions but with higher AIBN concentration, 0.1 mol/L. Clearly, the overall rate of polymerization in all three runs is faster compared with that in the runs with lower initiator amount. Composition drift in these three runs is illustrated in figure 8.11. Higher initiator level has no apparent effect on copolymer composition, as expected. Figure 8.12 shows the molecular weight picture from the azeotropic run with 0.1 mol/L AIBN. If figure 8.12 is compared to figure 8.9, one can see that both molecular weight averages in figure 8.12 are lower than those in figure 8.9. This is due to the higher initiator level used in the runs of figure 8.12. The rate autoacceleration exhibits a similar effect on the molecular weights in figure 8.12, i.e., the weight average molecular weight increases markedly at the end of the reaction while the number average molecular weight increases only very slightly.

McManus and Penlidis (1996) conducted more experiments at a higher temperature of 60°C. Figure 8.13 displays three runs of the same monomer feed compositions at 60°C (AIBN concentration is 0.05 mol/L). If compared to the runs of figure 8.7, the overall rate of polymerization is faster. Molecular weight averages of the azeotropic run in figure 8.15 are relatively lower than those in figure 8.9. Copolymer composition from the corresponding runs (figures 8.14 and 8.8) is however unaffected by the elevated reaction temperature. Experimental

results from an azeotropic run at higher temperature (60°C) and initiator levels (0.1 mol/L) are displayed in figures 8.16 to 8.18. Similar reaction characteristics are observed in these figures.

McManus and Penlidis (1996) examined also the effect of CTA on reaction kinetics in a set of additional experiments. Three additional experiments were performed at azeotropic monomer composition with various levels of *p*-octyl mercaptan (octane thiol) added as a CTA. Reaction temperature was 60°C and initiator concentration 0.05 mol/L. Figures 8.19 to 8.21 illustrate experimental conversion profiles at three different levels of CTA as well as model predictions. It is convincing from these figures that the polymerization kinetic behaviour with added CTA in all three runs is well captured by the model. Conversion profiles with the lowest and highest CTA levels from figures 8.19 and 8.21 are plotted together in figure 8.22 for comparative purposes. It is clear from figure 8.22 that the presence of CTA slows down the overall rate of polymerization. The rate of polymerization in the run with the highest CTA level is obviously suppressed. In contrast, CTA has no apparent effect on copolymer composition as demonstrated in figure 8.23 (compare, for instance, with figures 8.17 or 8.14). Copolymer composition stays constant throughout the reaction. The most significant effect of CTA is on the molecular weight averages. Figures 8.24 and 8.25 display molecular weight averages from runs with and without CTA. Both number average and weight average molecular weights are significantly reduced by the presence of CTA. Model predictions in both figures agree with experimental data in a satisfactory way. Some discrepancies are observed in figure 8.25 for the weight average molecular weight with CTA. It should be understood that molecular weight data from these runs are in the range of a few thousands, which is the low limit of the GPC columns. Hence, these measurements are more prone to experimental error. Overall, the simulation of Sty/EA copolymerization in bulk is satisfactory, and the effects of temperature, initiator concentration, monomer feed composition and CTA on reaction kinetics are well described by this model.

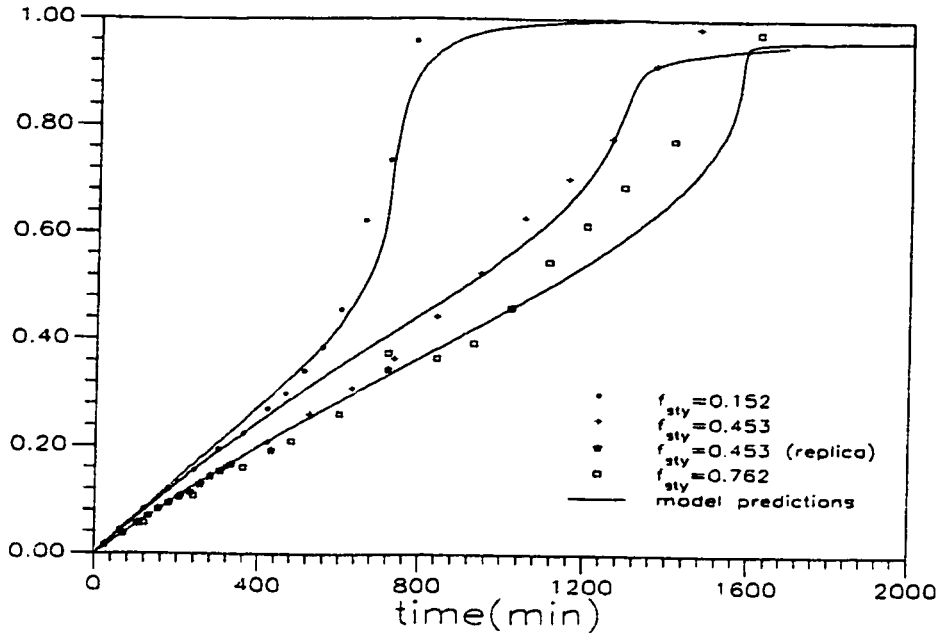

Figure 8.7 Simulation of Styrene and Ethyl acrylate Copolymerization in Bulk at 50°C. [AIBN]: 0.05 mol/L.

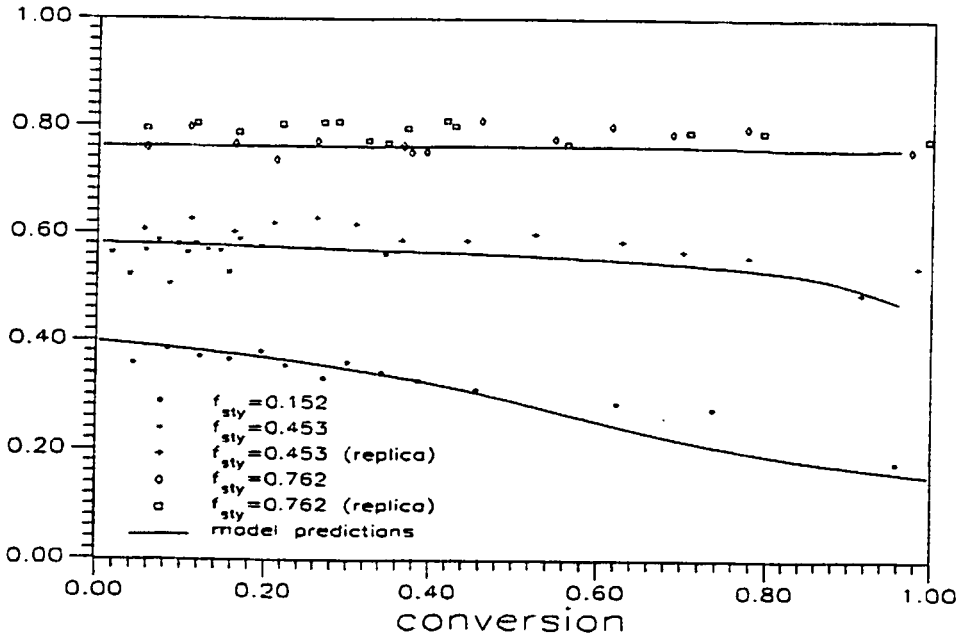

Figure 8.8 Simulation of Composition Drift in Styrene and Ethyl Acrylate Copolymerization in bulk at 50°C. [AIBN]: 0.05 mol/L.

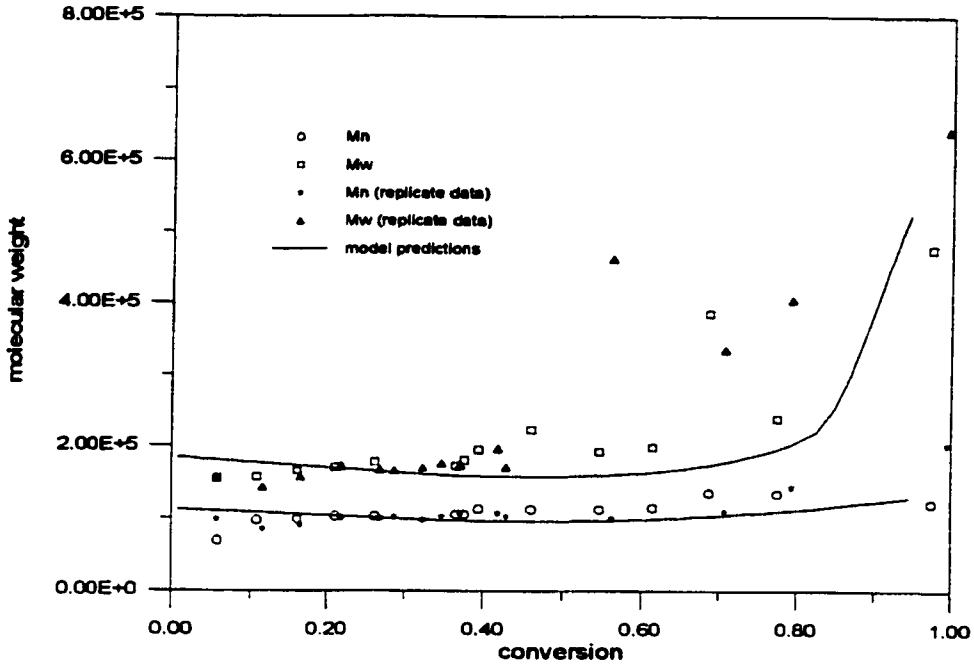

Figure 8.9 Simulation of Molecular Weight in Styrene and Ethyl Acrylate Copolymerization in Bulk at 50°C. [AIBN]: 0.05 mol/L, f_{sty}=0.762.

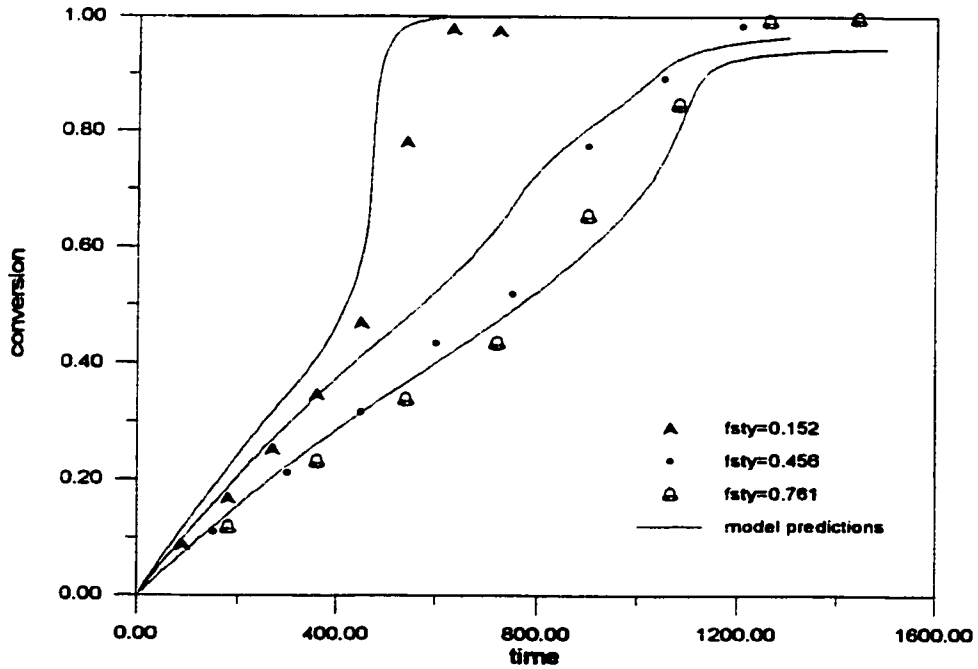

Figure 8.10 Simulation of Styrene and Ethyl Acrylate Copolymerization in Bulk at 50°C. [AIBN]: 0.1 mol/L

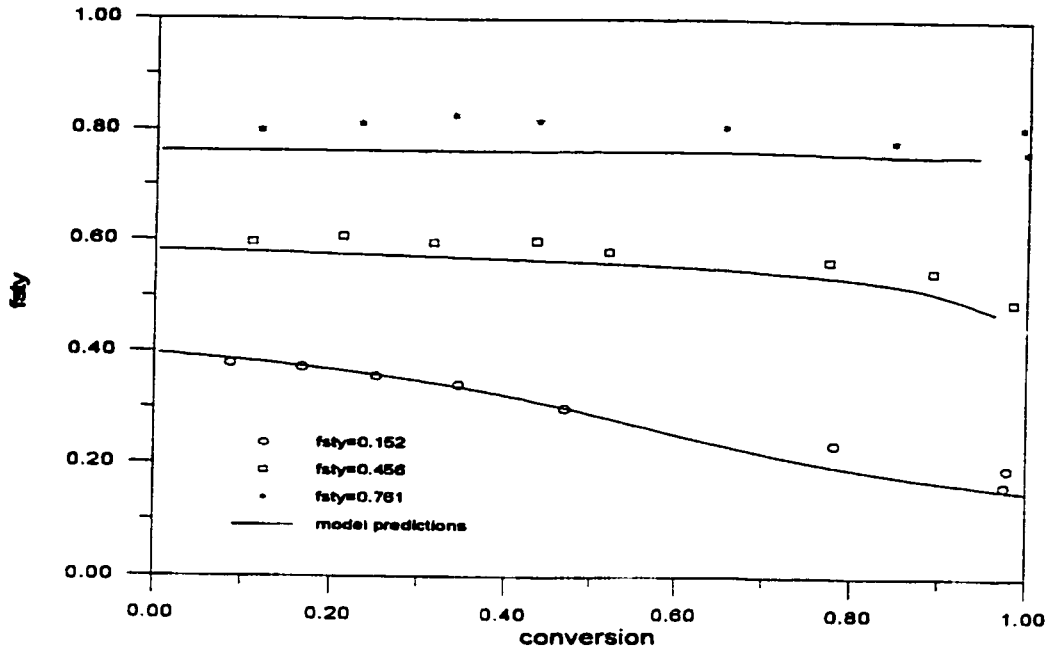

Figure 8.11 Simulation of Composition Drift in Styrene and Ethyl Acrylate Copolymerization in Bulk at 50°C. [AIBN]: 0.1 mol/L.

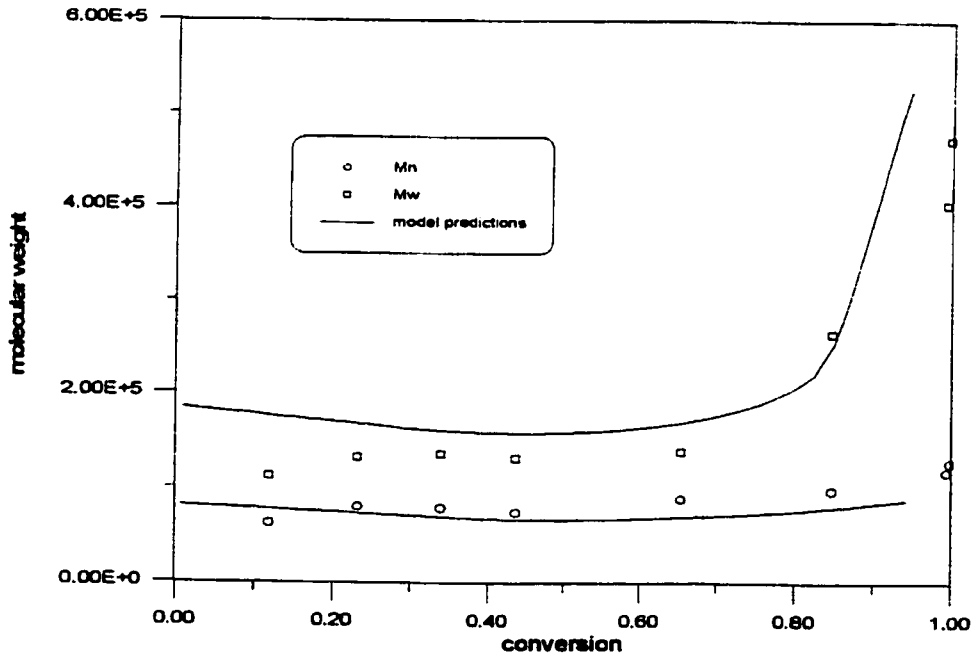

Figure 8.12 Simulation of Molecular Weight in Styrene and Ethyl Acrylate Copolymerization in Bulk at 50°C. [AIBN]: 0.1 mol/L, f_{sty}=0.762.

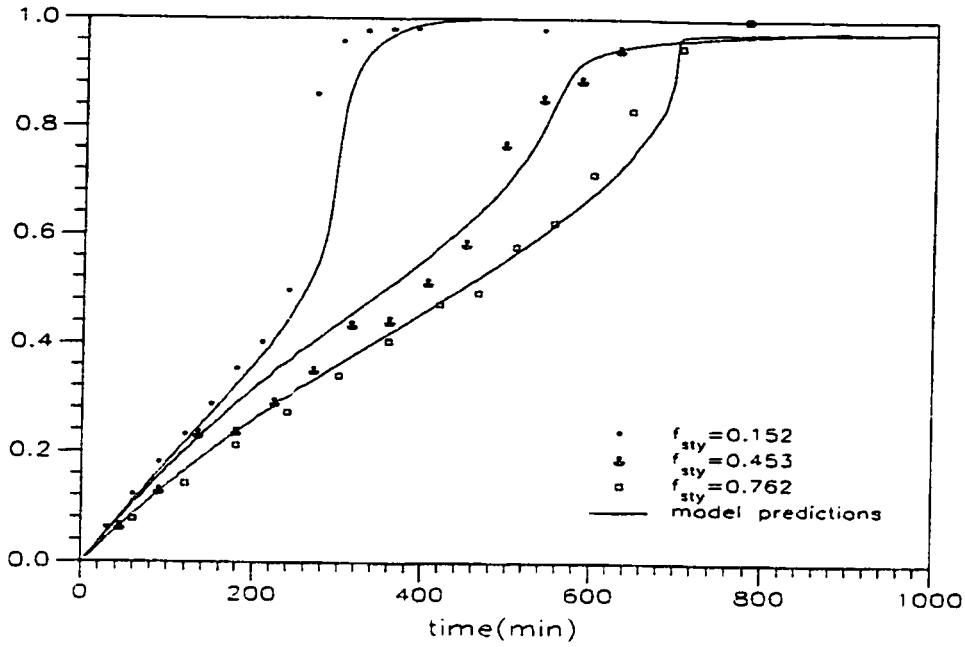

Figure 8.13 Simulation of Styrene and Ethyl Acrylate Copolymerization in Bulk at 60°C. [AIBN]: 0.05 mol/L.

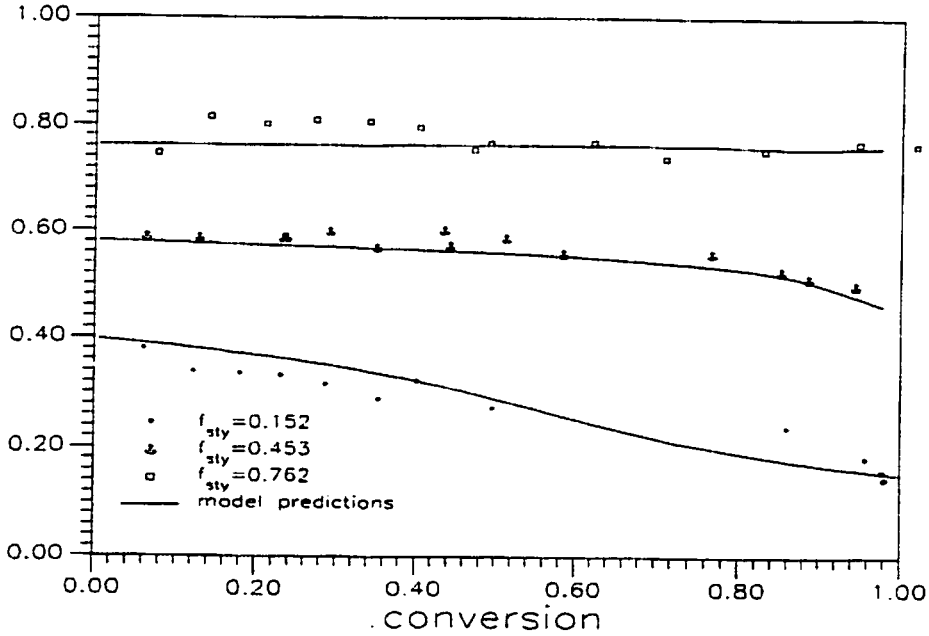

Figure 8.14 Simulation of Composition Drift in Styrene and Ethyl Acrylate Copolymerization in Bulk at 60°C. [AIBN]: 0.05 mol/L.

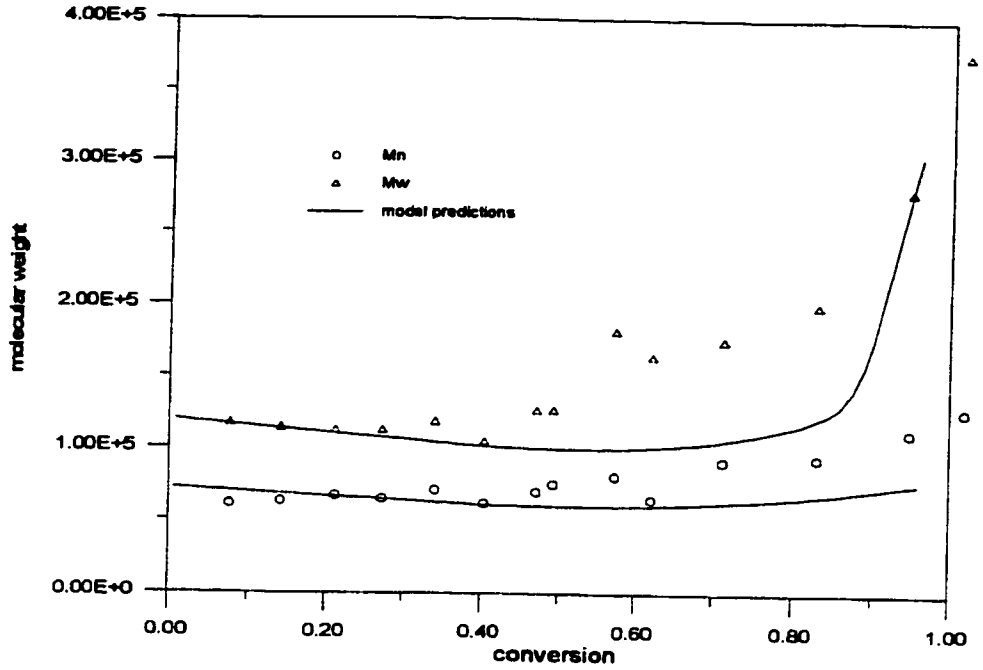

Figure 8.15 Simulation of Molecular Weight in Styrene and Ethyl Acrylate Copolymerization in Bulk at 60°C. [AIBN]: 0.05 mol/L.

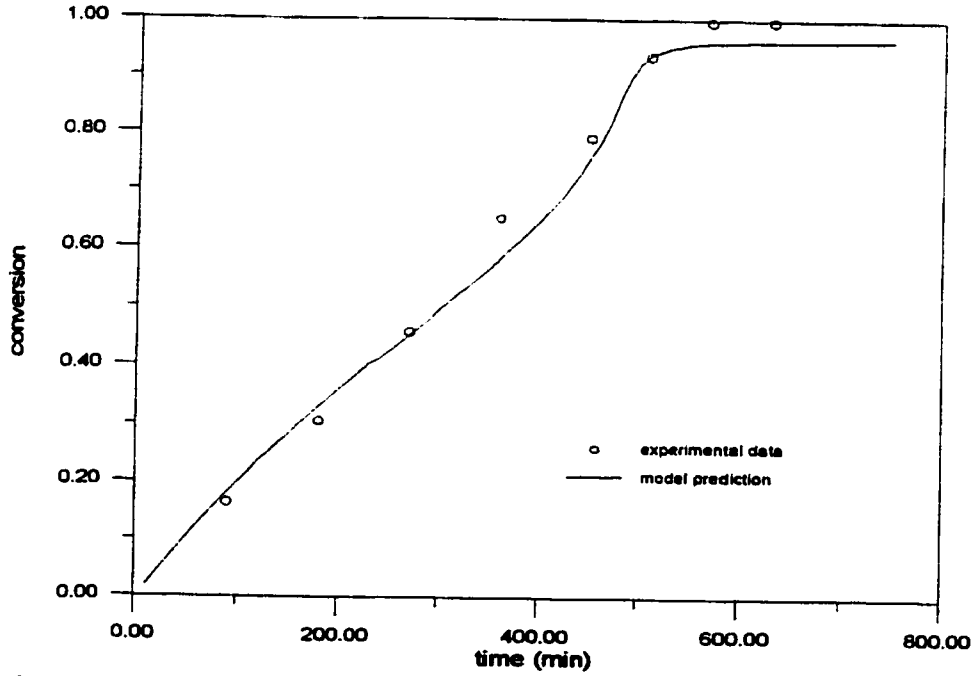

Figure 8.16 Simulation of Styrene and Ethyl Acrylate Copolymerization in Bulk at 60°C. [AIBN]: 0.1 mol/L.

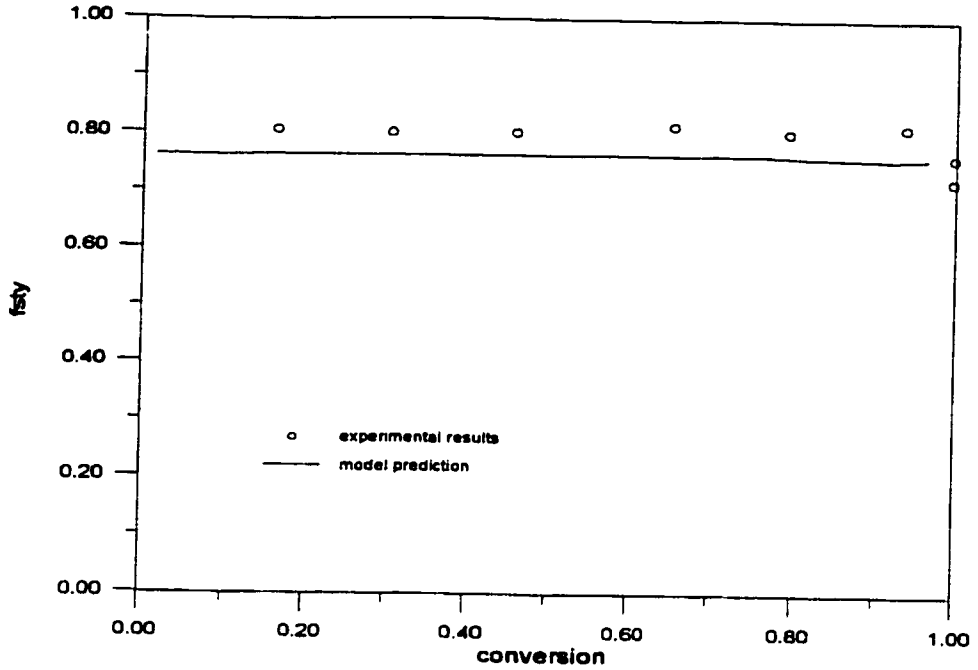

Figure 8.17 Simulation of Composition Drift in Styrene and Ethyl Acrylate Copolymerization in Bulk at 60°C. [AIBN]: 0.1 mol/L.

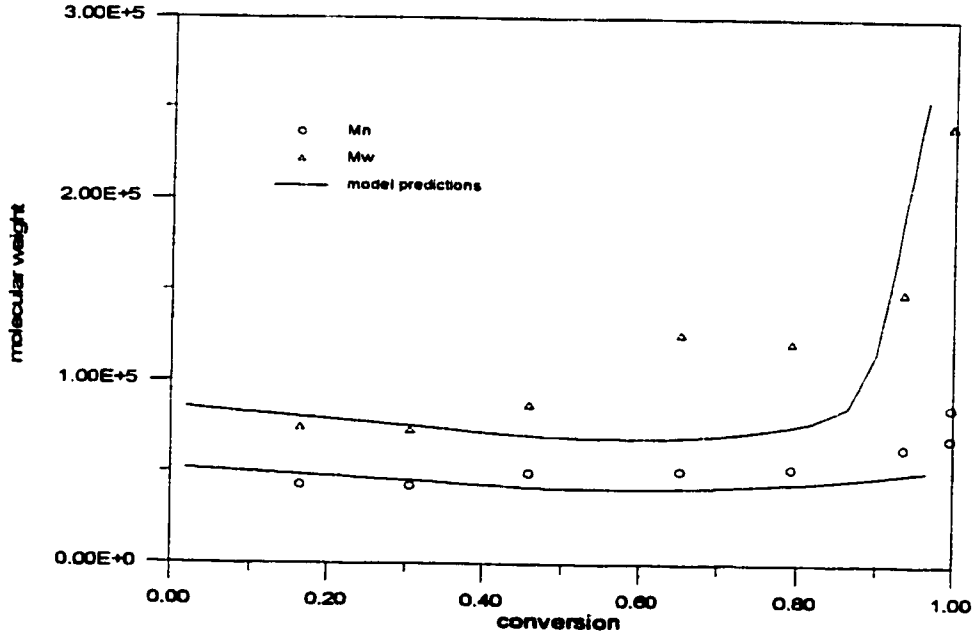

Figure 8.18 Simulation of Molecular Weight in Styrene and Ethyl Acrylate Copolymerization in Bulk at 60°C. [AIBN]: 0.1 mol/L.

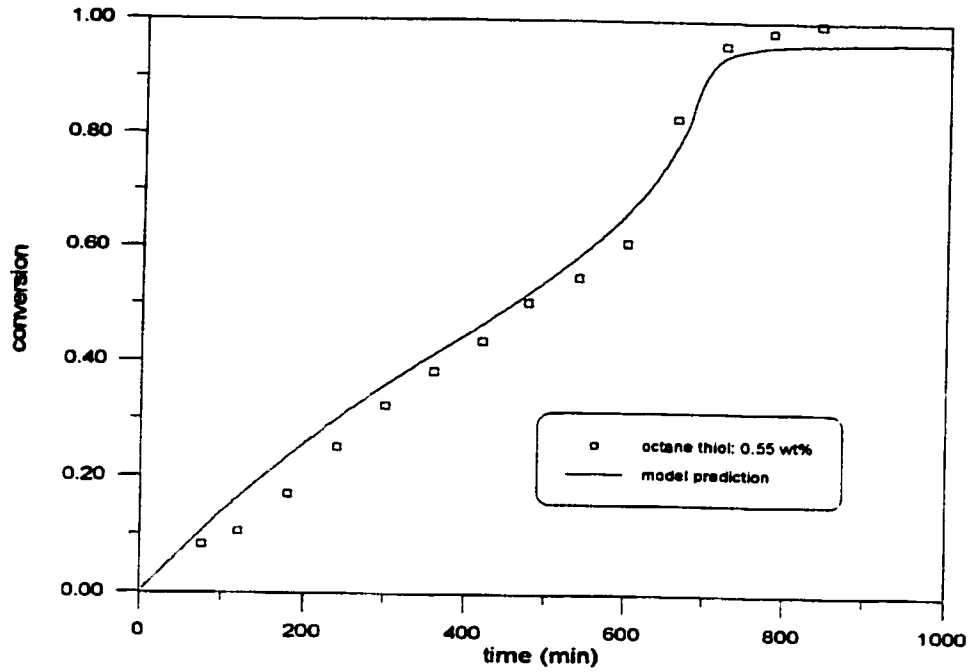

Figure 8.19 Simulation of Styrene and Ethyl Acrylate Copolymerization with CTA in Bulk at 60°C. [AIBN]: 0.05 mol/L, f_{sty}=0.762.

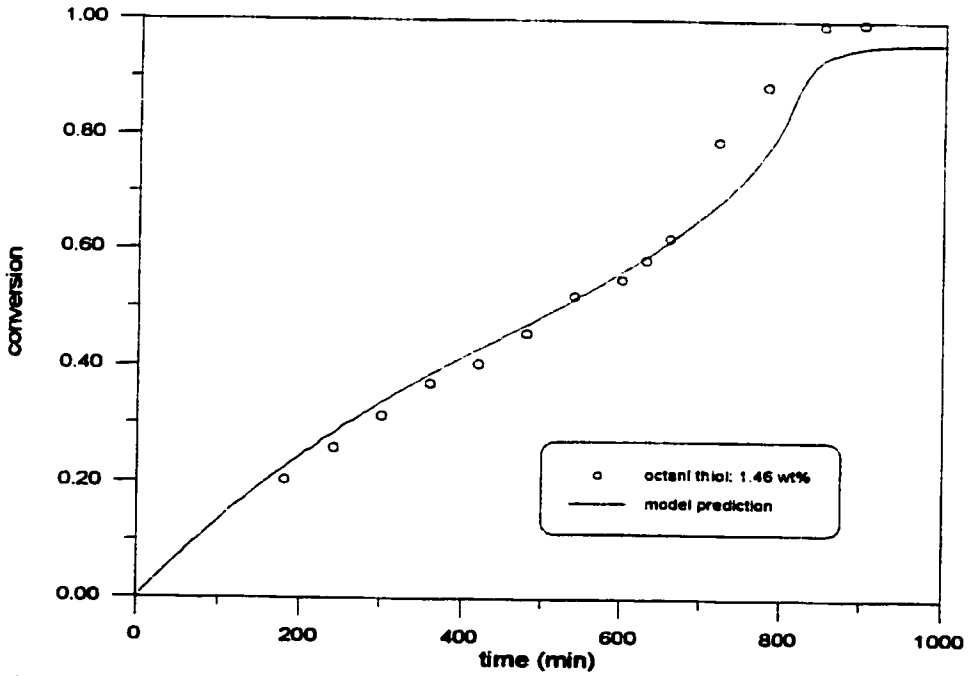

Figure 8.20 Simulation of Styrene and Ethyl Acrylate Copolymerization with CTA in Bulk at 60°C. [AIBN]: 0.05 mol/L, f_{sty}=0.762.

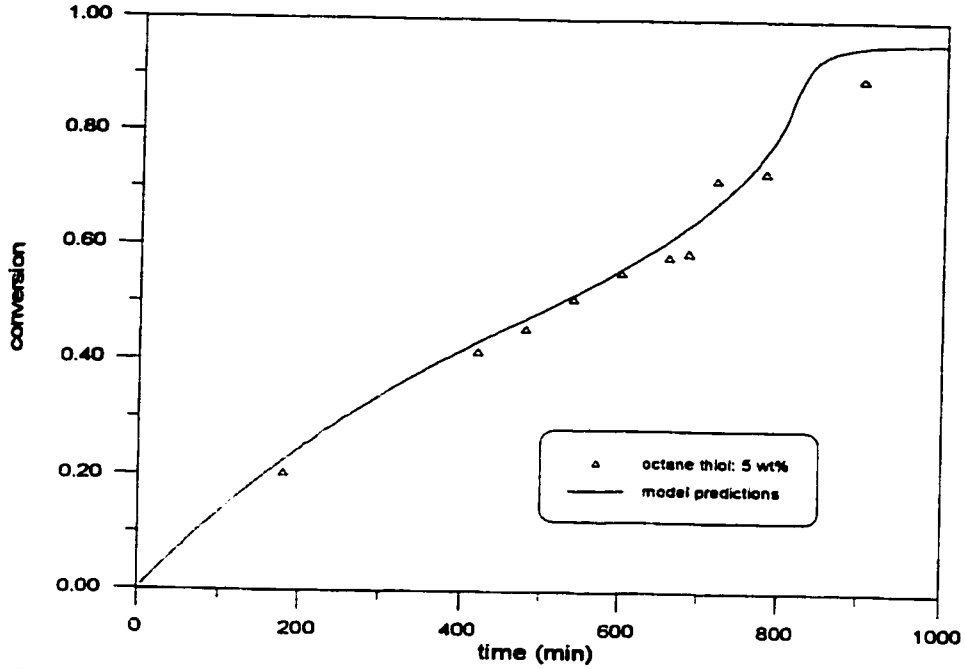

Figure 8.21 Simulation of Styrene and Ethyl Acrylate Copolymerization with CTA in Bulk at 60°C. [AIBN]: 0.05 mol/L, f_{sty}=0.762.

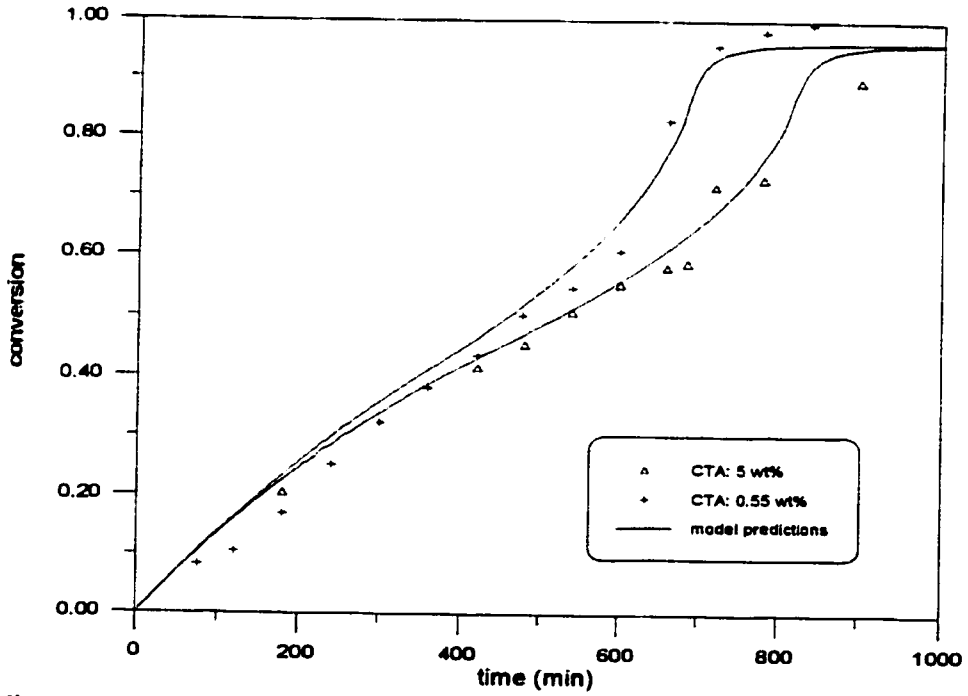

Figure 8.22 Simulation of Styrene and Ethyl Acrylate Copolymerization with CTA in Bulk at 60°C. [AIBN]: 0.05 mol/L, f_{sty}=0.762.

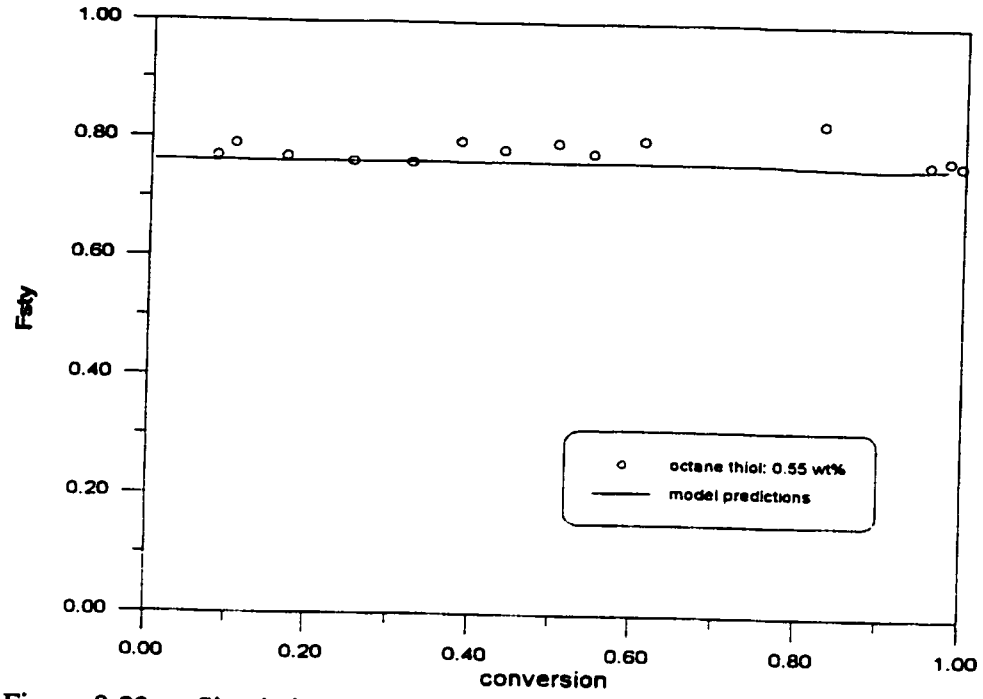

Figure 8.23 Simulation of Copolymer Composition in Styrene and Ethyl Acrylate Copolymerization with CTA in Bulk at 60°C. [AIBN]: 0.05 mol/L, f_{sty}=0.762.

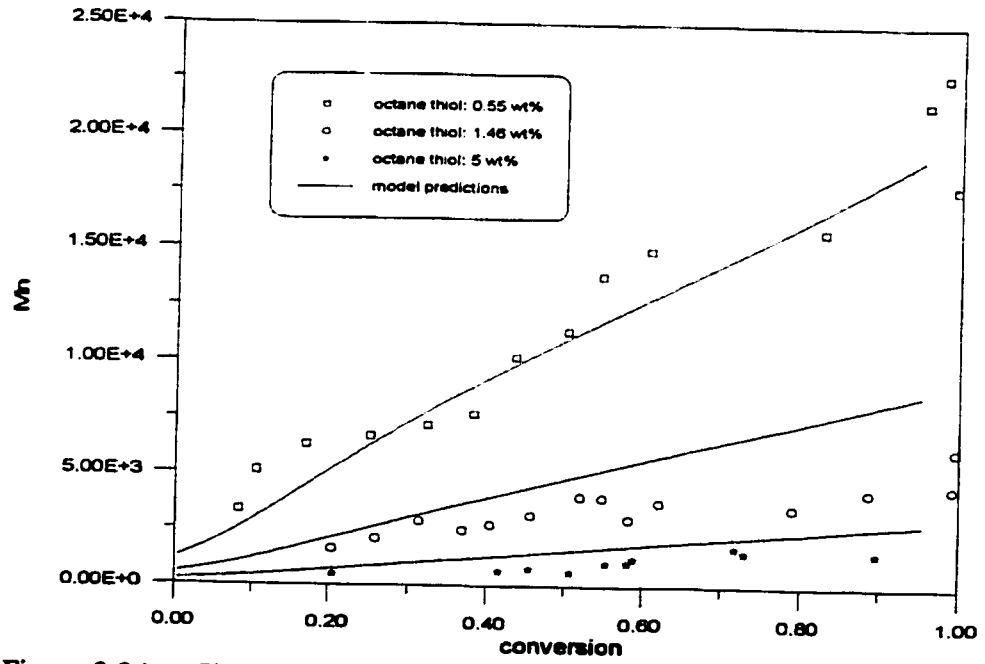

Figure 8.24 Simulation of Number Average Molecular Weight in Styrene and Ethyl Acrylate Copolymerization in Bulk at 60°C. [AIBN]: 0.05 mol/L, f_{sty}=0.762.

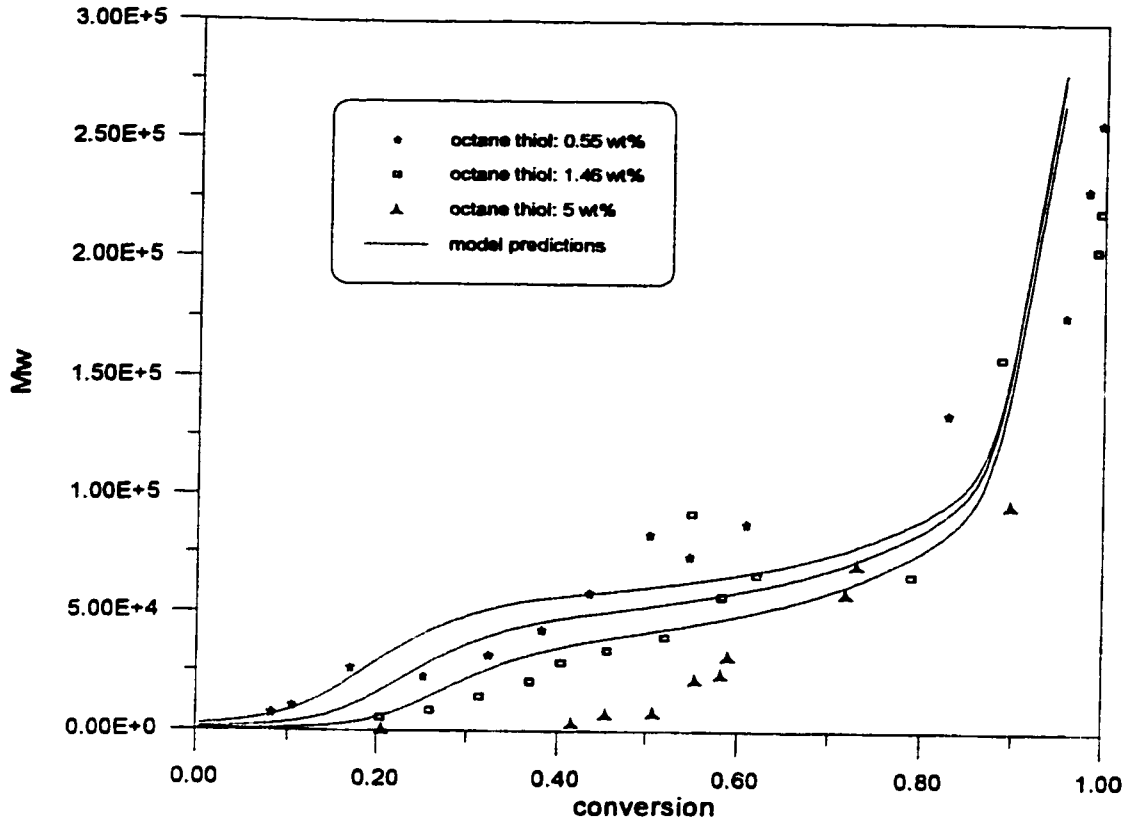

Figure 8.25 Simulation of Weight-Average Molecular Weight in Styrene and Ethyl Acrylate Copolymerization in Bulk at 60°C with [AIBN]=0.05 mol/L and f_{sty}=0.762.

8.3 Simulation of Copolymerization of Styrene and 2-Hydroxyethyl Acrylate

8.3.1 Literature Review

Styrene and 2-hydroxyethyl acrylate copolymer has a variety of commercial applications such as adhesives, coatings, and many medical applications. Nevertheless, this is almost an "exotic" copolymer system with almost no literature information. Except for very limited studies on reactivity ratio estimates, no detailed kinetic investigation and experimental results could be found in the literature. Table 8.3 lists all the references that are somehow related to 2-hydroxyethyl acrylate polymerization.

Among the references of Table 8.3, none gives kinetic information that can be used directly in the modeling of Sty/2-HEA copolymerization. McGinnis and Ting (1975) measured the volume change in several acrylates homopolymerization. It was found that 2-HEA reacts faster than 2-ethyl hexylacrylate. This is probably the only indication in the literature of how fast 2-HEA reacts. Chow (1975) calculated reactivity ratios using Q-e values. Chow (1975) noticed the effect of solubility of Sty/2-HEA copolymer on the estimates. This problem will be addressed in more detail in the next section. Catala et al.(1986) estimated reactivity ratios of 2-HEA and EA, BA and MA copolymers using the Fineman-Ross method. Based on the reactivity ratios of the three copolymer systems, Catala et al.(1986) stated that an increase in the size of the ester group favours the introduction of the 2-HEA monomer into the copolymer. However, all of the above observations are only approximate trends since the estimation used was not statistically sound.

Table 8.3 References on 2-hydroxyethyl acrylate polymerization

Reference	Remarks
Catala et al.(1986)	reactivity ratio estimates
Chow (1975)	reactivity ratios, Q-e values
Galbraith et al.(1987)	2-HEA/Sty/BA terpolymerization
Lebduska et al.(1986)	solvent effect on Sty/2-HEA reactivity ratios
McGinniss and Ting (1975)	photopolymerization
Yocum and Nyquist (1973)	crosslinking

8.3.2 Sty/2-HEA Copolymerization --- A Problematic System

Since no direct literature information can be used in model testing, reactivity ratios were estimated in this laboratory by Kim (1994). The Tidwell-Mortimer D-optimality criterion was used in designing experiments for the reactivity ratio estimation. Full conversion range experiments were also conducted and polymer samples were characterized. A total of eight sets of experiments plus one replica were performed based on a 2^3 factorial design. The effects of initiator, temperature, and monomer feed composition on the reaction kinetics were examined. Additional runs were also carried out at the determined azeotropic composition.

Reactivity Ratio Estimation

The Tidwell-Mortimer criterion was used to design experiments for reactivity ratio estimation. Reported reactivity ratios in the literature were first used to determine the initial monomer feed compositions in the first set of experiments. Reactivity ratios were thus estimated using EVM. The final reactivity ratio values for Sty/2-HEA were: r_{sty}=0.254, $r_{2\text{-HEA}}$=0.279. The 95% joint confidence region showed greater variation in $r_{2\text{-HEA}}$, especially in runs with higher 2-HEA content in the monomer feed. This indicates difficulties in handling this monomer.

8.3.3 Full Conversion Range Experiments and Model Testing

Full conversion range experiments conducted by Kim (1994) were simulated by the model. It should be pointed out that it is difficult to set up a reliable database for 2-HEA based on the available copolymerization data. Sty/2-HEA is a problematic copolymer system, and experimental results in some runs have poor reproducibility. Model testing for this monomer is limited in simulating only the trends in polymerization kinetics. We selectively simulated four runs at the azeotropic composition. Figure 8.26 shows the simulation of Sty/2-HEA copolymerization in bulk at 40°C. AIBN was used as initiator. The model predictions in figure 8.26 follow the measured conversion profiles over the entire range. It is also noticed that there is a discrepancy in the run with the lower initiator level. There might be several factors contributing to this disagreement. Firstly, nonisothermality may be present. Kim (1994) reported that 2-HEA is a very 'fast'

monomer and its polymer is very viscous. This may hinder heat transfer between the reaction mixture and the surroundings and lead to a nonisothermal reaction. Secondly, 2-HEA monomer usually contains crosslinking agents if it is not completely purified. Crosslinking agents are a common side product in 2-HEA monomer synthesis. Thirdly, residual 2-HEA may continue to polymerize when polymer samples are being dried.

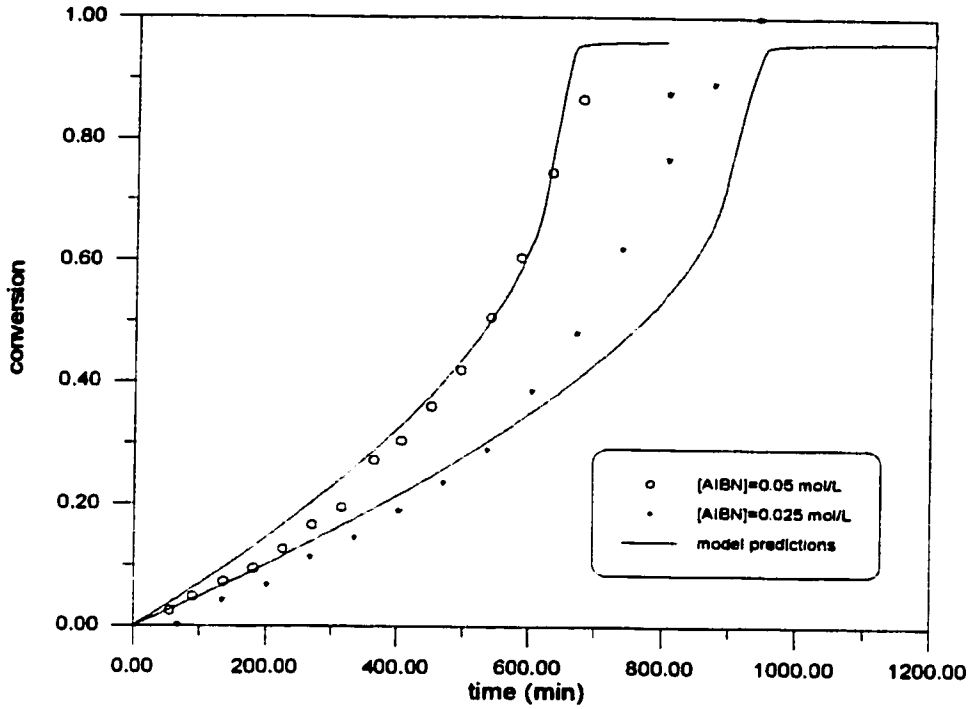

Figure 8.26 Simulation of Sty/2-HEA Copolymerization in Bulk at 40°C. f_{sty}: 0.515

Figure 8.27 displays the simulation of Sty/2-HEA at 50°C. The overall agreement between model predictions and experimental data is good. According to the estimated reactivity ratios by Kim (1994), all four runs in figures 8.26 and 8.27 are supposed to be at azeotropic composition. However, measured composition data are very scattered due to experimental difficulties. This inevitably makes it difficult to test the model's reliability, therefore further model testing was not pursued.

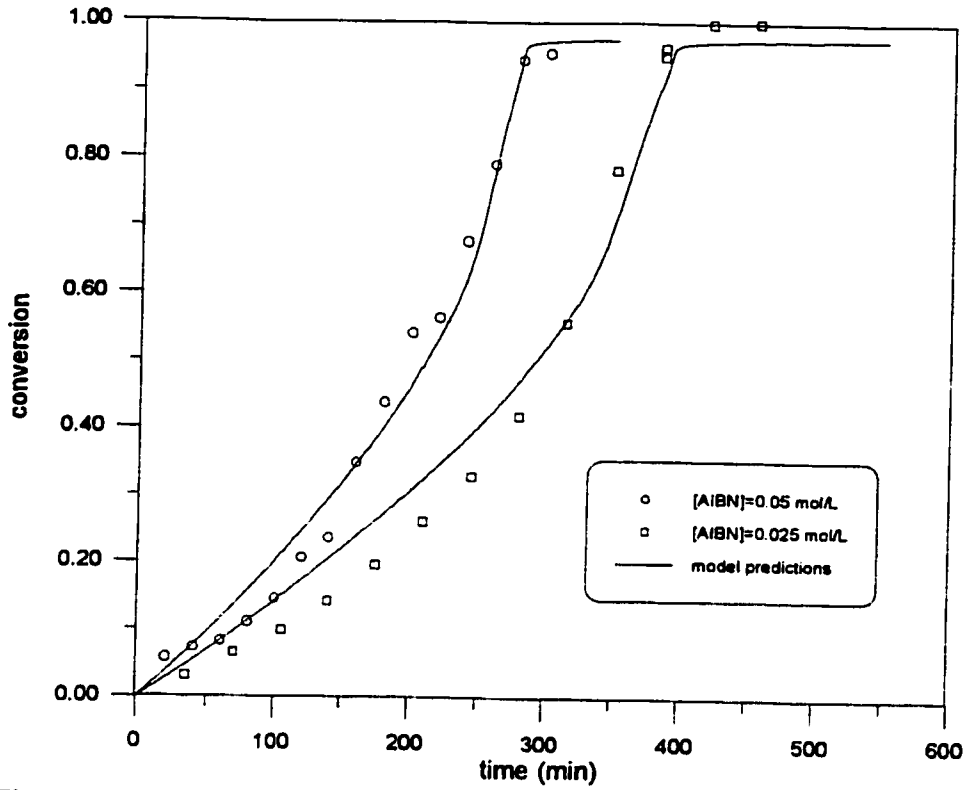

Figure 8.27 Simulation of Sty/2-HEA copolymerization in bulk at 50°C. f_{sty}: 0.515

8.3.4 Summary

The kinetic investigation and simulation on the copolymerization of Sty/2-HEA in this thesis presents the first attempt so far in the literature to understand polymerization characteristics of this copolymer system. Many difficulties were encountered in monomer purification, experimentation and polymer characterization. Some experimental results reported by Kim (1994) have poor reproducibility, especially in the NMR analysis. In order to set up a database for the problematic 2-HEA monomer, further kinetic investigations are underway in this laboratory. Kim (1994) made several recommendations that might be useful for future work on this system.

Chapter 9. Simulation of Copolymerization of Methyl Methacrylate/Methyl Acrylate and Methyl Methacrylate/Ethyl Acrylate

Methyl methacrylate and other acrylate copolymers have good mechanical and optical properties, and various applications in pharmaceutical and optical products. Despite their commercial applications, copolymerizations of methyl methacrylate with other acrylates are largely unstudied in the literature. In the following several sections, we will discuss the reaction kinetics and simulation of MMA/EA and MMA/MA copolymerizations.

9.1 Literature Review on MMA/EA Copolymerization

Information on this copolymer pair is very limited. Some reactivity ratios have been reported in the literature. In early studies, Bevington and Harris (1967) used the Fineman-Ross method to calculate r_{MMA} and r_{EA} as 1.83 and 0.47, respectively. Madruga et al.(1983a, b) performed many MMA/EA copolymerizations under various conditions. They determined reactivity ratios using the Fineman-Ross method. The temperature effect on reactivity ratios was studied by Madruga et al.(1982). Their estimated reactivity ratios at three different temperatures are listed in Table 9.1.

Table 9.1 Reactivity Ratios of MMA/EA

Temperature (°C)	r_{MMA}	r_{EA}
35	2.13	0.11
50	2.11	0.14
65	2.52	0.16

Other references related to this copolymer system are by Borchardt (1982) and Bressers and Kloosterboer (1980).

9.2 Model Testing on MMA/EA Copolymerization

Wang and Ruckenstein (1993) is the only group that carried out full conversion range MMA/EA

experiments in bulk. In their studies, MMA and EA were polymerized at 80°C in bulk, and *n*-butyl mercaptan was added as a CTA to investigate its effect on reaction kinetics. Both experimental results and model predictions are presented in figure 9.1. It can be seen from figure 9.1 that MMA/EA copolymerization exhibits a strong gel effect and reaches full conversion. This is not surprising because ethyl acrylate homopolymer has a very low Tg around -24°C and the reaction temperature is fairly high. The presence of CTA delays the onset of autoacceleration but has little effect on the final conversion level.

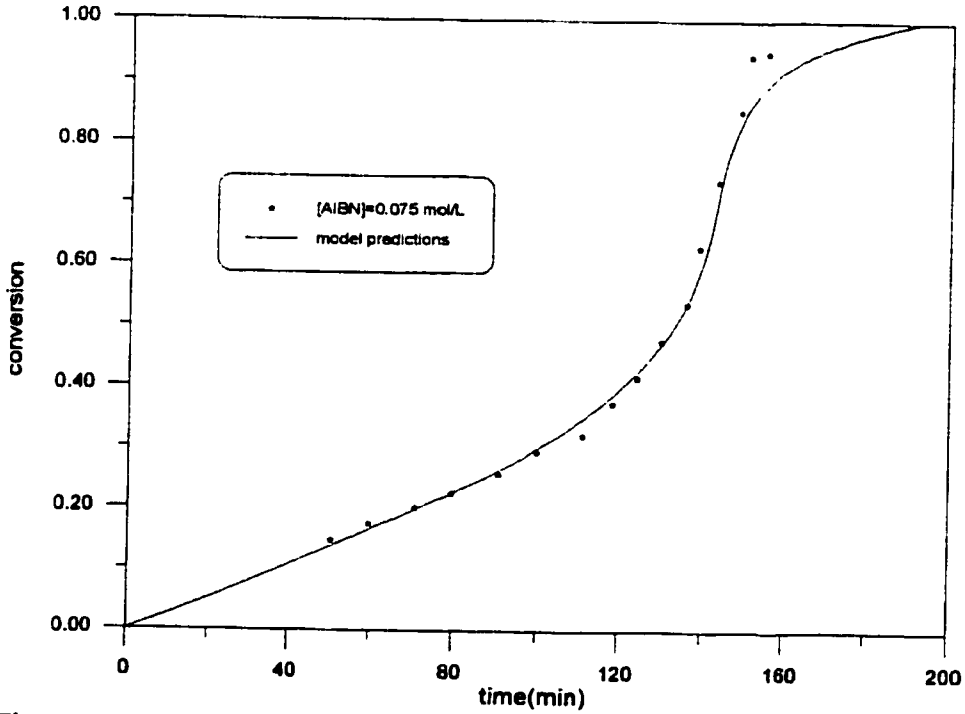

Figure 9.1 Simulation of MMA/EA Copolymerization at 80°C. MMA:EA=100:15 in the Feed, n-Butyl Mercaptan as CTA, [CTA]: 0.4 v%.

9.3 Literature Review on MMA/MA Copolymerization

Little information is available for this copolymer system. In early studies, Bevington and Harris (1967) used the Fineman-Ross method to estimate reactivity ratios for this copolymer system as r_{MMA}=0.34, r_{MA}=1.69. Recently, Arias et al.(1993) listed all the reported reactivity ratios available in the literature. They used the Kelen-Tudos method and estimated reactivity ratios as r_{MMA}=0.42, r_{MA}=2.36, based on copolymer composition data. Lopez-Gonzalez et al.(1993) from the same group used the estimated reactivity ratios and successfully predicted triad fractions in the copolymer chain over the entire conversion range. They thus stated that the terminal model can give a precise description of copolymerization for MMA/MA. As discussed before, these two linearization methods are statistically unsound and additionally the experiments were not statistically designed either, hence the reported reactivity ratios may contain errors. Madruga and Fernandez-Garcia (1996) later used improved non-linear least squares methods to recalculate the reactivity ratios of MMA/MA copolymer. The revised values are r_{MMA}=0.407, r_{MA}=2.241. These values are probably the best available in the literature.

Fernandez-Garcia et al.(1994) conducted an extensive study on MMA/MA copolymer Tg and carried out copolymerizations in benzene up to high conversion. They reviewed and compared many Tg models proposed in the literature. They concluded that Johnston's and Couchman's Tg models are superior to others. Most importantly, they are probably the only group that presented copolymer Tg profiles over the entire conversion range. Johnston's Tg model seemed to fit measured Tg data very well. Table 9.2 lists the most useful references for MMA/MA copolymerization.

Table 9.2 Literature Listing for MMA/MA Copolymerization

References	Remarks
Arias et al.(1993)*	solution copolymerization in benzene, low-mid conversion range
Bevington and Harris (1967)	reactivity ratios
Borchardt (1982)	steric and electronic effects on reactivity ratios

Chaudhuri and Palit (1968)	termination mode
Fernandez-Garcia et al.(1994)*	modeling of copolymer Tg
Fukui et al.(1961)	cross-termination
Lewis et al.(1948a)	temperature effect on reactivity ratios
Lopez-Gonzalez et al.(19993)	solution copolymerization in benzene, sequence length distribution
Madruga and Fernandez-Garcia (1996)	solution copolymerization in benzene
Wang and Ruckenstein (1993)*	full conversion experiment with CTA

* papers used for model testing

9.4 Model Testing on MMA/MA Copolymerization

Arias et al.(1993) performed MMA/MA copolymerizations in benzene at 50°C. Figure 9.2 shows one experiment with 30% MA in the feed, with final conversion level around 40%. No gel effect was observed due to the presence of benzene solvent. Figure 9.3 displays composition drift for several runs with various initial monomer feed compositions. In all cases, MMA monomer is depleted faster than MA, and this behaviour is well captured by this model.

Wang and Ruckenstein (1993) conducted MMA/MA bulk polymerization using n-butyl mercaptan as CTA. Figure 9.4 illustrates one bulk run with 15% MA in the feed. One can see the gel effect in MMA/MA copolymerization but no limiting conversion was observed. Figure 9.5 shows three MMA/MA runs at various initial MA monomer feed compositions. Since MA is 'faster' than MMA, higher MA content in the monomer feed will increase the overall rate of polymerization. In both figures, the agreement between this model predictions and experimental data is quite satisfactory.

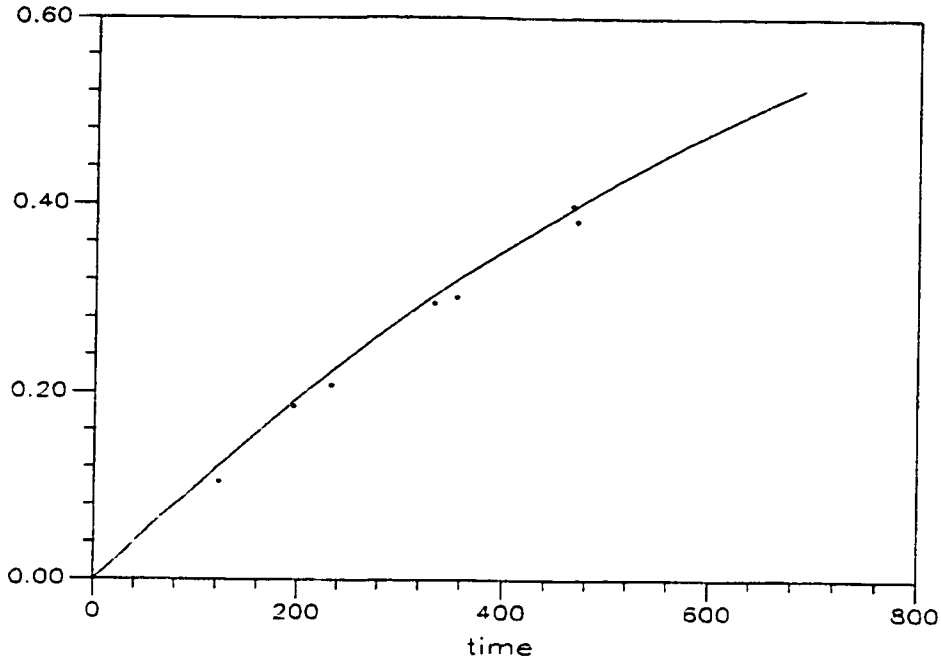

Figure 9.2 Simulation of MMA/MA Copolymerization in Benzene at 50°C. [AIBN]=0.015 mol/L

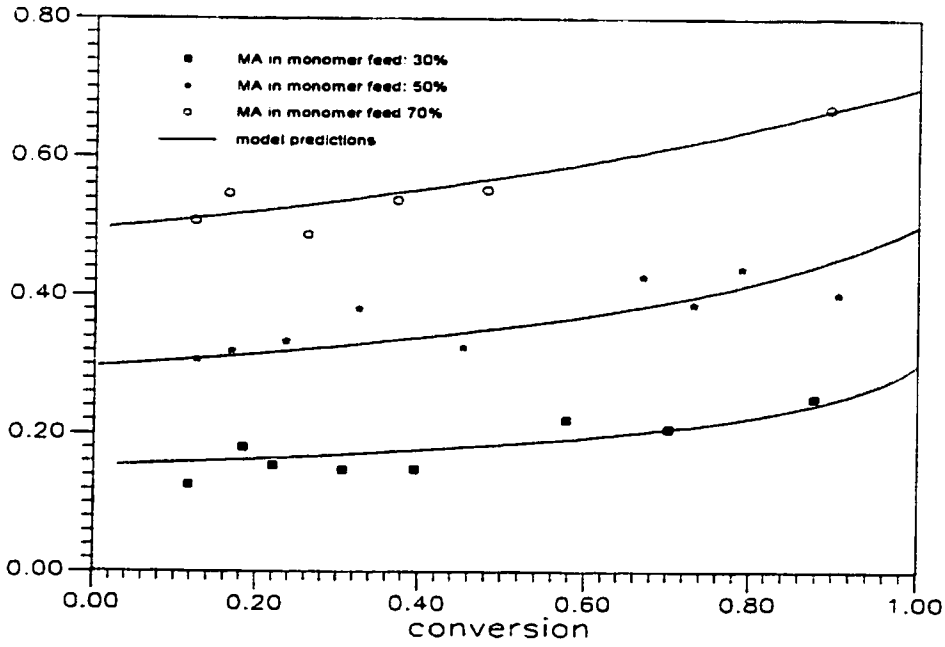

Figure 9.3 Simulation of composition drift in MMA/MA copolymerization in benzene at 50°C. [AIBN]=0.015 mol/L

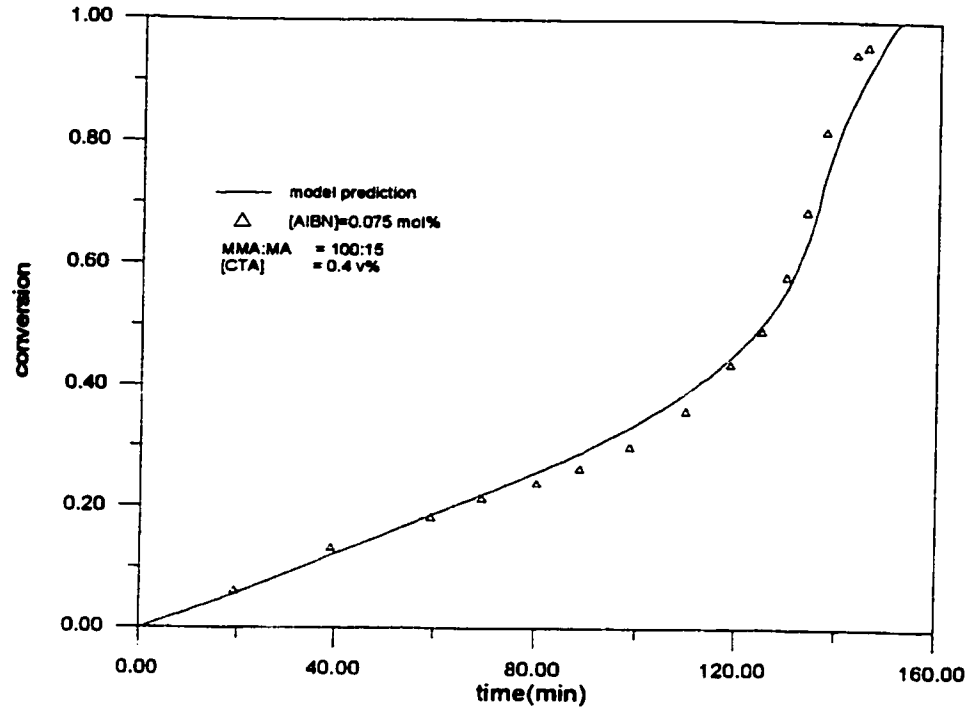

Figure 9.4 Simulation of MMA/MA Copolymerization in Bulk at 80°C.

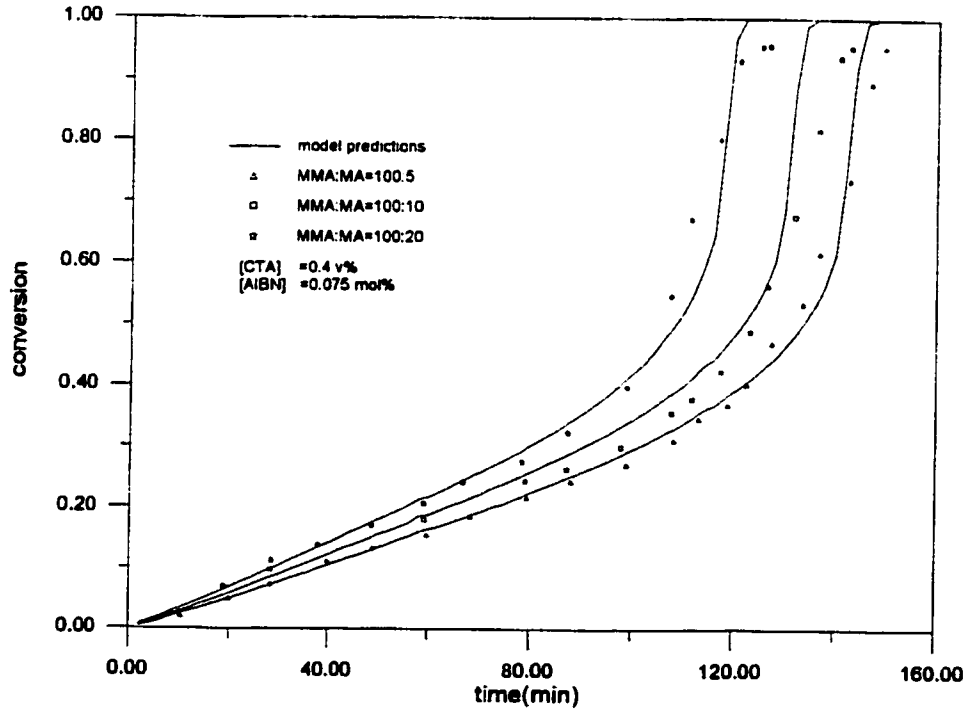

Figure 9.5 Simulation of MMA/MA Copolymerization at Various Monomer Feed Ratio at 80°C.

Chapter 10. Simulation of Copolymerization of Methyl Methacrylate/Vinyl Acetate, Butyl Acrylate/Vinyl Acetate and Methyl Methacrylate/Butyl Acrylate

The butyl acrylate/methyl methacrylate/vinyl acetate (BA/MMA/VAc) terpolymer is an important industrial product of many applications, however, its kinetic behaviour is not well understood. Dube and Penlidis (1995a, b) used a systematic approach to investigate this system. Experiments on each copolymer pair were carried out in bulk. Data from this work are the major source for model testing. The following sections present kinetic studies on each copolymer system.

10.1 Simulation of Copolymerization of MMA/BA

10.1.1 Literature Summary

MMA/BA copolymer product has a much lower Tg compared to that of MMA/MA or MMA/EA copolymers. This is because BA homopolymer has a low Tg of -50°C. MMA/BA copolymer is thus more flexible. Like many other copolymer systems, MMA/BA copolymerization received little attention in the literature. Table 10.1 below gives a list of papers that are related to MMA/BA copolymerization in bulk, with a star indicating papers providing full conversion range experimental data useful for model testing.

Most of the kinetic studies on MMA/BA copolymer included were only reactivity ratio estimations (Bevington and Harris, 1965; Aerdts et al., 1994). More references can be found on emulsion MMA/BA copolymerization, however they are not cited here. Wang and Ruckenstein (1993), and Dube and Penlidis (1995a) performed full conversion range experiments.

10.1.2 Model Testing

Wang and Ruckenstein (1993) performed MMA/BA copolymerizations in bulk using n-butyl mercaptan as CTA up to high conversion. Conversion was measured by dilatometery. Figure 10.1 displays both experimental results and model predictions. The overall agreement is good except

for discrepancies at the lower conversion range. The MMA/BA copolymerization exhibits strong autoacceleration but reaches full conversion. This is expected since the butyl acrylate homopolymer has a low Tg.

Table 10.1 Literature Reference on MMA/BA Copolymerization

References	Remarks
Aerdts et al.(1994)	reactivity ratio estimates, sequence length distribution, stereoregularity
Bevington and Harris (1967)	reactivity ratios
Borchard (1982)	steric and electronic effects on reactivity ratios
Dube and Penlidis (1995a)*	full conversion range experiments, reactivity ratio estimation
Fukuda et al.(1989)	penultimate effect
Gunesin and Piirma (1981)	block MMA/BA copolymer synthesis
Kobayashi (1988a)	Sty/MMA/BA terpolymer characterization
Kobayashi (1988b)	sequence distribution effect on Sty/MMA/BA terpolymer Tg
Rajatapiti et al.(1996)	bulk and emulsion experiments
Rizzardo et al.(1995)	chain transfer reaction
Wang and Ruckenstein (1993)*	full conversion range experiments with CTA

* papers providing full conversion range experimental data useful for model testing

Dube and Penlidis (1995a) took a systematic approach to investigate this copolymer system. The Tidwell-Mortimer criterion was used to design experiments for reactivity ratio estimation. The estimated reactivity ratios were r_{BA}=0.297, r_{MMA}=1.789. These reactivity ratio values indicate that there is no azeotropic composition for this copolymer system. Composition drift is expected for all monomer feed compositions. Full conversion range experiments based on a 2^3 factorial design were carried out. The feed compositions were chosen based on a number of criteria. The first composition, f_{BA}=0.439, corresponded to a 1:1 weight ratio of the two monomers. The second composition, f_{BA}=0.163, was chosen in order to minimize the composition drift. This was done in order to simplify the molecular weight analysis.

Figures 10.2 and 10.3 show experimental results as well as model predictions for two different monomer feed compositions. One replicated run at the lower initiator concentration is shown in figure 10.2. Discrepancy exists between the two runs. It should be understood that experiments carried out at lower initiator levels are more likely to suffer from impurities which may lead to a slower rate. All experiments conducted exhibited strong gel effect and reached full conversion. In figure 10.3, the measured conversion level of the samples at the final stage of the reaction exceeded 100%, which is due to experimental errors. One interesting phenomenon is observed when the conversion profiles in figures 10.2 and 10.3 are compared carefully. The conversion profiles in the runs of figure 10.2 at the final stage of the reaction appear to be smoother than those in figure 10.3. Such 'smoothness' is more pronounced in BA homopolymerization. Runs in figure 10.2 have a higher BA content in the monomer feed, hence their reaction characteristics resemble closer those of BA homopolymerization, while on the other hand, experiments shown in figure 10.3 have higher MMA monomer feed composition and behave more like a MMA homopolymerization. Figure 10.4 is a plot of the composition data for all runs. The predictions of the data are quite good. The predictions are generated using the reactivity ratios estimated by Dube and Penlidis (1995a). In all cases, the observed composition drift is relatively small, especially in the lower conversion range.

Figures 10.5 and 10.6 show the measured molecular weight averages for runs with lower BA content in the monomer feed. It must be stated that due to the composition drift in the experiments, the measured molecular weight averages reflect only a *trend* of the molecular weight profile. Nevertheless, as can be seen from figure 10.4, composition drift is relatively small, and the measured molecular weight averages should be quite reasonable. Comparing results in figures 10.5 and 10.6, it is clear that a higher initiator amount (figure 10.6) reduces both number and weight average molecular weights. There is a marked increase in weight average molecular weight at the final stage of the reaction. Model predictions are in close range of the measured results. Figures 10.7 and 10.8 are the simulation and experimental molecular weight results for the runs with higher BA content in the monomer feed. Again, satisfactory trends are described.

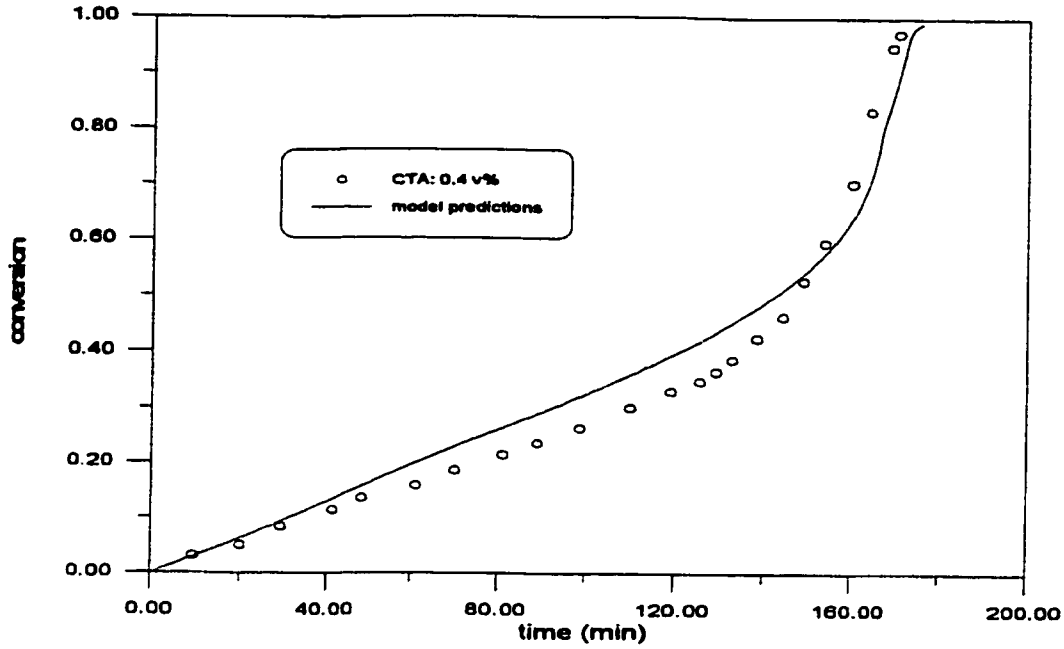

Figure 10.1 Simulation of MMA/BA Copolymerization in Bulk at 80°C. MMA:BA=100:15 mol ratio, AIBN: 0.075 mol% of monomers

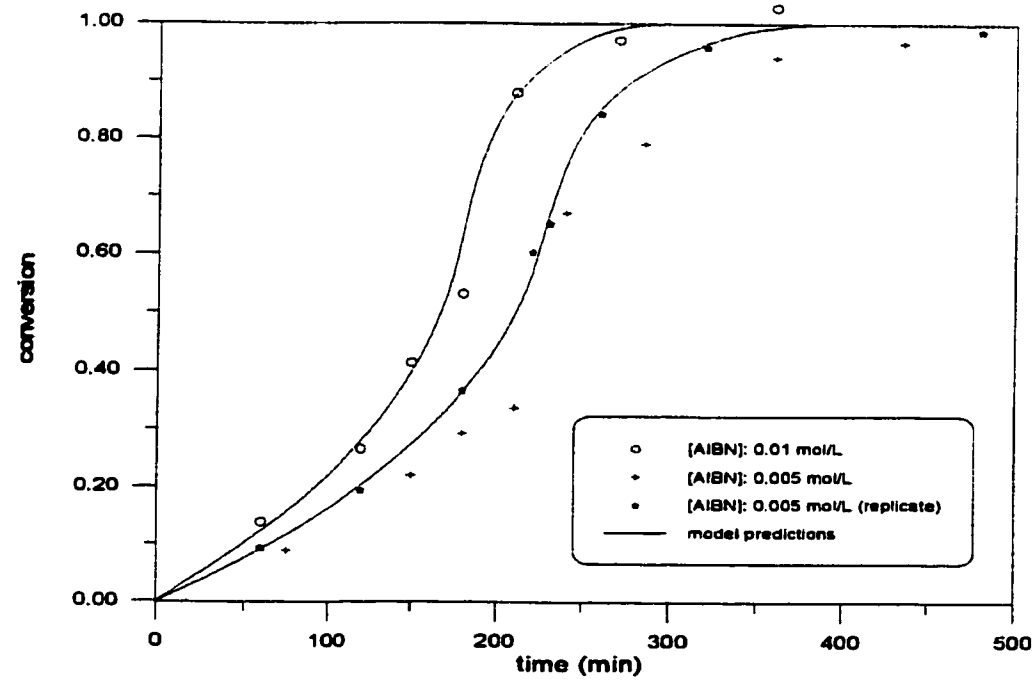

Figure 10.2 Simulation of MMA/BA Copolymerization in Bulk at 60°C. f_{BA}=0.439

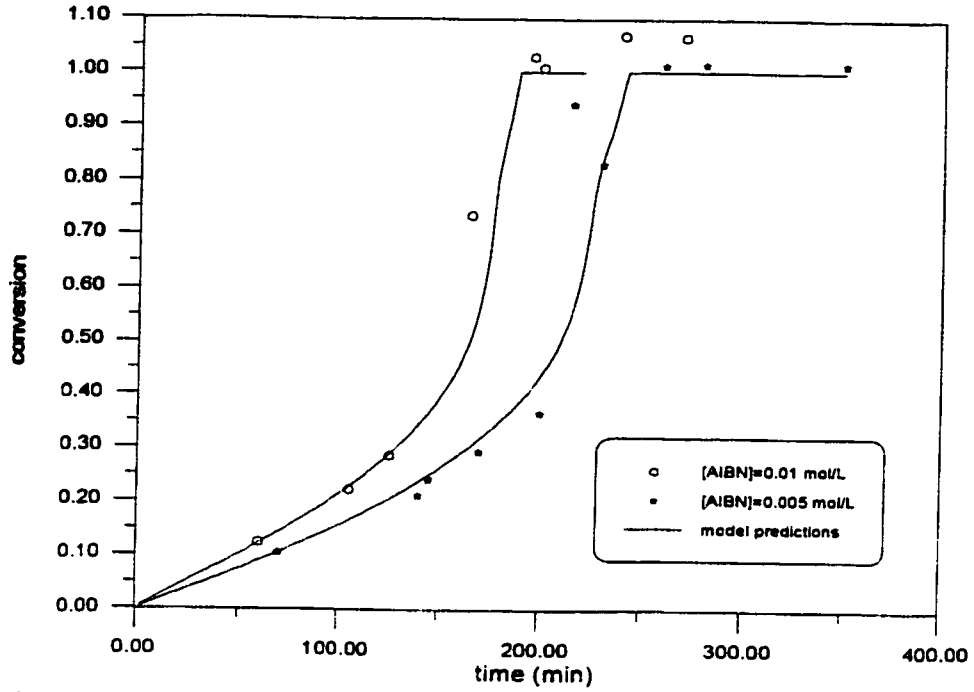

Figure 10.3 Simulation of MMA/BA Copolymerization in Bulk at 60°C. f_{BA}=0.163

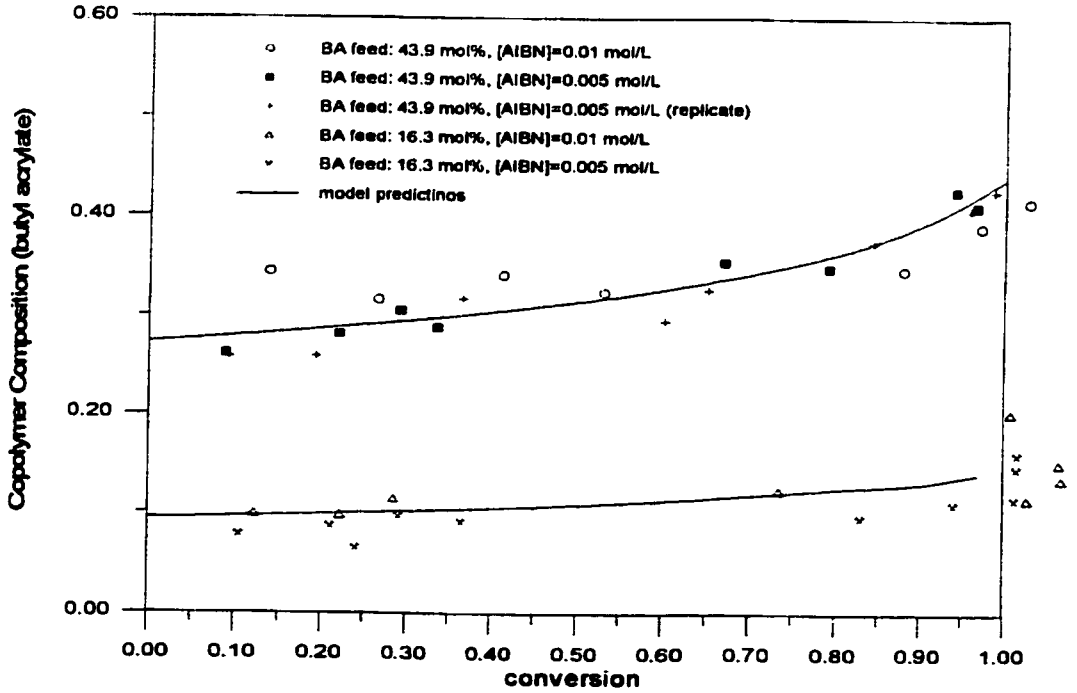

Figure 10.4 Composition Drift in MMA/BA Copolymerization in Bulk at 60°C.

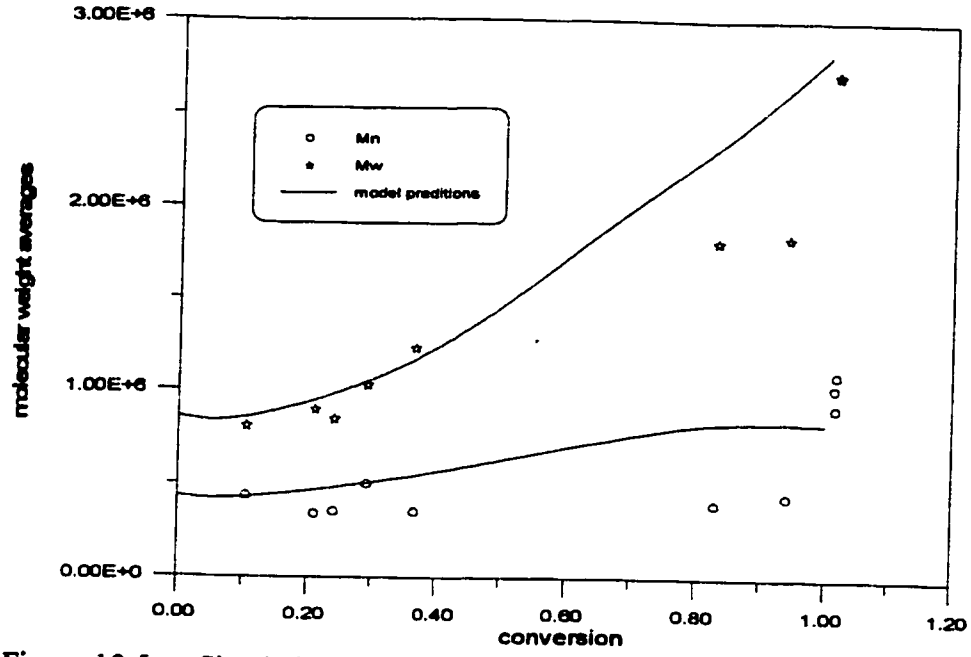

Figure 10.5 Simulation of MMA/BA Copolymerization in Bulk at 60°C. f_{BA}=0.163, [AIBN]=0.005 mol/L

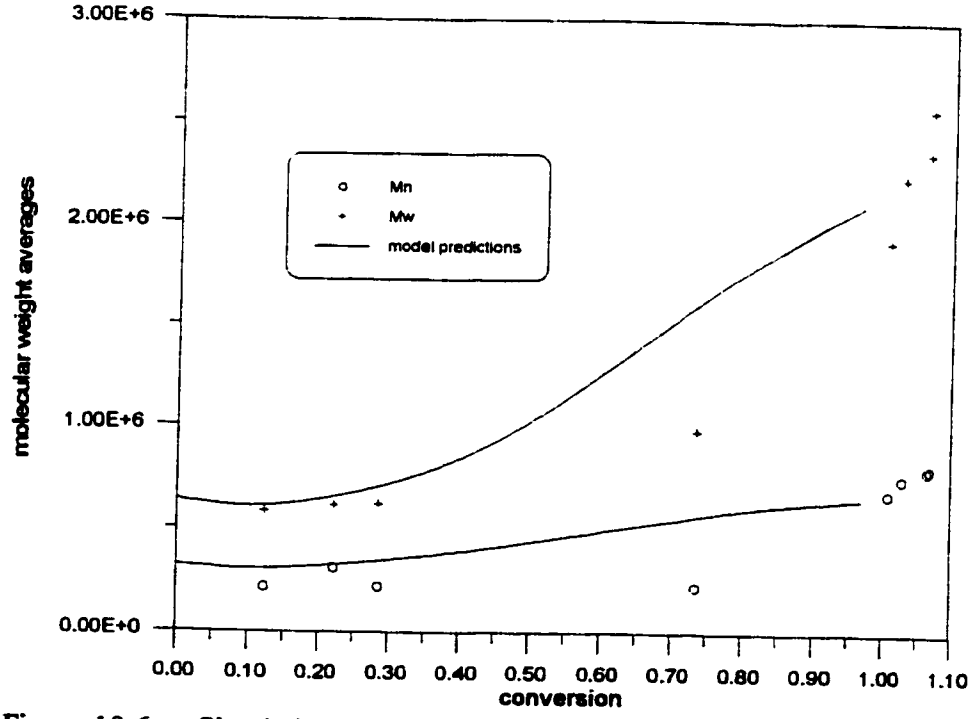

Figure 10.6 Simulation of MMA/BA Copolymerization in Bulk at 60°C. f_{BA}=0.163, [AIBN]=0.01 mol/L

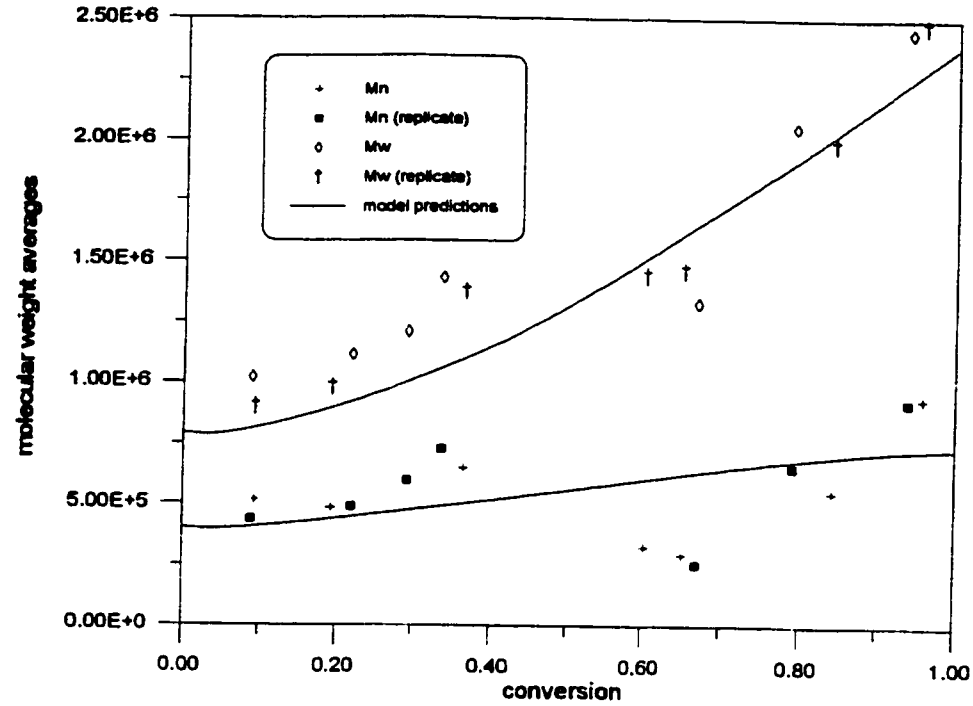

Figure 10.7 Simulation of MMA/BA Copolymerization in Bulk at 60°C. f_{BA}=50 wt%, [AIBN]=0.005 mol/L

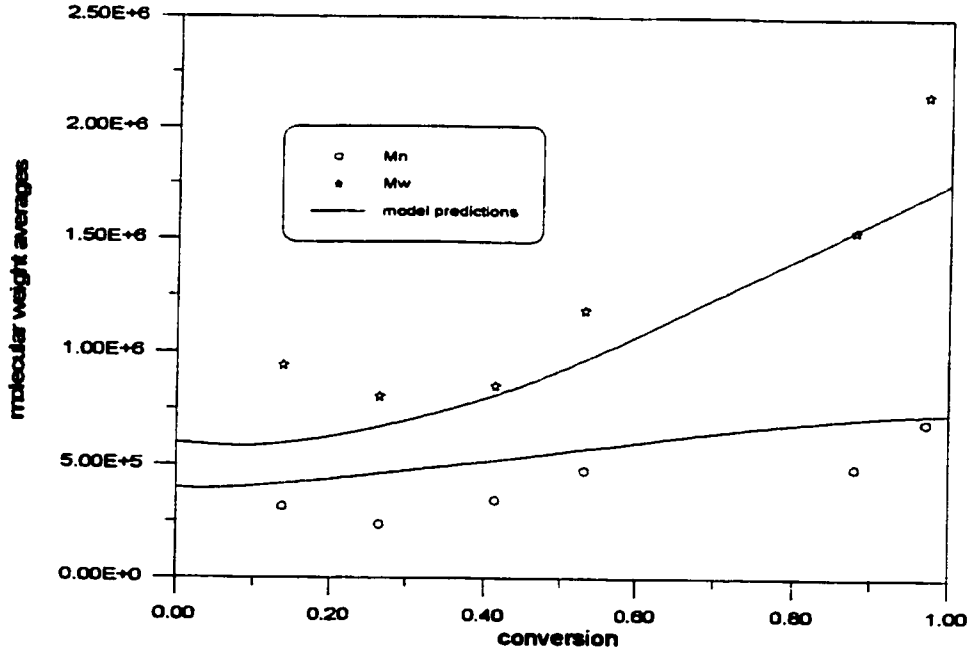

Figure 10.8 Simulation of MMA/BA copolymerization in bulk at 60°C. f_{BA}=50 wt%, [AIBN]=0.01 mol/L

10.2 Simulation of Copolymerization of MMA/VAc

MMA and VAc are two monomers of fairly different kinetic characteristics. VAc reacts much faster than MMA and it has significant long chain branching, while the MMA polymer is a linear chain. Literature references related to copolymerization of these two monomers are in Table 10.2.

Table 10.2 References on MMA/VAc Copolymerization

References	Remarks
Atherton and North (1962)	classical theory, termination reaction
Borchardt (1982)	steric and electronic effects on reactivity ratios
Brar and Charan (1993)*	reactivity ratio estimation using EVM method
Busfield and Low (1975)	solvent effect on reactivity ratios
Chiang and Rudin (1975)	studies on termination in copolymerization
Choi and Butala (1991)	solution copolymerization
Dube and Penlidis (1995a)*	systematic approach on kinetic studies, full conversion experimental results
Farber (11986)	studies on steady states in CSTR operation
Fukuda et al.(1989)	penultimate effect on rate constants
Hamer et al.(1981)	multiple steady state studies in CSTR operation
Krstina et al.(1992)	solvent effect
Kuo et al.(1989)	calculation of composition in copolymerization
Ma et al.(1993)	penultimate effect on rate constants
Mayo et al.(1948a)	chemical structure effect on reactivity ratios
Mayo et al.(1948b)	classical theory studies
Prochazka and Kratochvil (1983)	termination kinetics in copolymerization
Suzuki et al.(1958)	rate constant determination

* papers found to be more useful

Not many references from Table 11 provide information that can be directly used in simulation and model testing on this copolymer systems. Earlier studies (Atherton and North, 1962; Suzuki

et al., 1958; Chiang and Rudin, 1975; Prochazka and Kratochvil, 1983) were focused on the termination mechanism in copolymerization. Brar and Charan (1993) estimated reactivity ratios using EVM. Ma et al.(1993) discussed the propagation rate constant for MMA/VAc copolymerization for different monomer feed compositions. Their work primarily stresses the penultimate effect on copolymerization kinetics. Their estimated rate constant for propagation for VAc is 6800 L/mol·s at 40 °C. We find this value exceptionally higher than any other reported values in the literature. Ma et al.(1993), however, did not offer any explanation. The most informative reference is by Dube and Penlidis (1995a). Reactivity ratios were estimated using EVM and full conversion range experiments were carried out. The estimated reactivity ratios are r_{MMA}=24.0254, r_{BA}=0.026107. The large difference in the two reactivity ratios indicates both radicals prefer to react with MMA monomer, hence this fact will lead to a significant composition drift and another unique kinetic behaviour with respect to the rate of polymerization (see below).

10.2.1 Model Testing

Figure 10.9 displays the measured conversion as well as model predictions. It is noted that there is a drastic and rapid increase in conversion level starting at about 40%. This phenomenon was called the 'double rate phenomenon'. As the reactivity ratios indicated that both radicals prefer to react with MMA monomer, MMA disappears at a much faster rate than VAc. This can be verified from the composition change shown in figure 10.10. In figure 10.10, the accumulated MMA polymer composition is relatively high (about 90%) at the beginning of the reaction, and then drops quickly to around 30% after 40% conversion. This indicates that most MMA monomer is consumed in the first 40% conversion, with the second stage dominated by the polymerization of VAc. This drastic composition drift makes MMA/VAc copolymerization rather a two stage homopolymerization. Since the rate constant of propagation of VAc is about an order of magnitude higher than that of MMA, the rate of polymerization accelerates significantly after 40% conversion as demonstrated in figure 10.9. This unique 'double rate phenomenon' characteristic in MMA/VAc copolymerization is captured nicely by this model in figures 10.9 and 10.10. Figure 10.11 shows molecular weight averages for this system. It should be stressed again

that these data points reveal only the *trend* of molecular weight average changes in the reaction rather than true values due to the large composition drift. The model predictions are in the correct range and follow the trend nicely. The simulated weight average molecular weight increases significantly indicating long branching commonly observed in VAc homopolymerization.

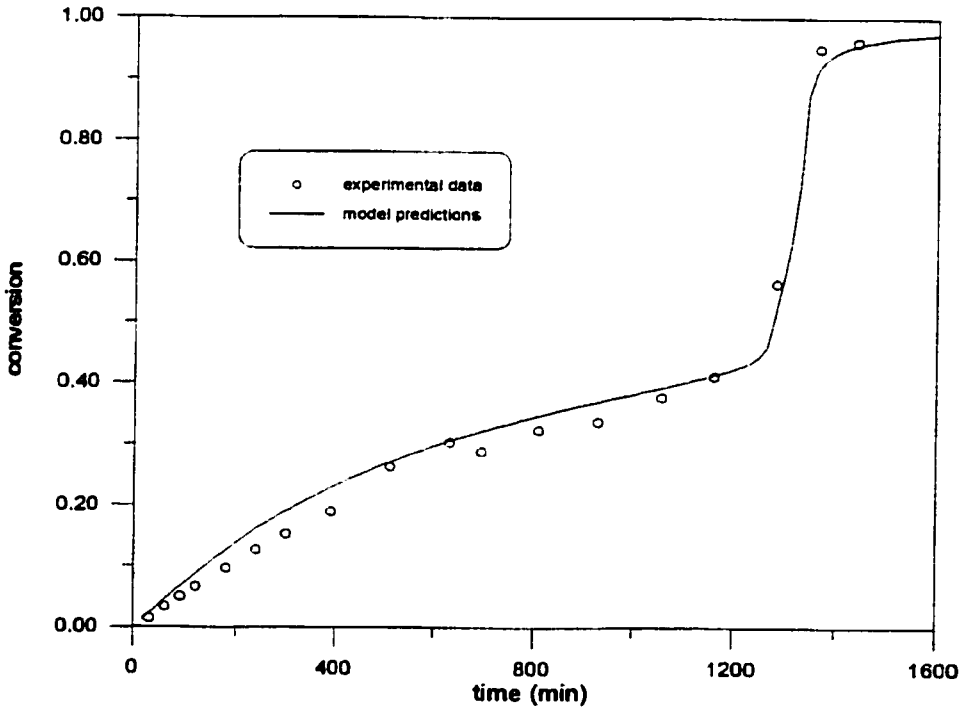

Figure 10.9 Simulation of MMA/VAc Copolymerization in Bulk at 60°C. f_{MMA}=30 mol%, [AIBN]=0.01 mol/L

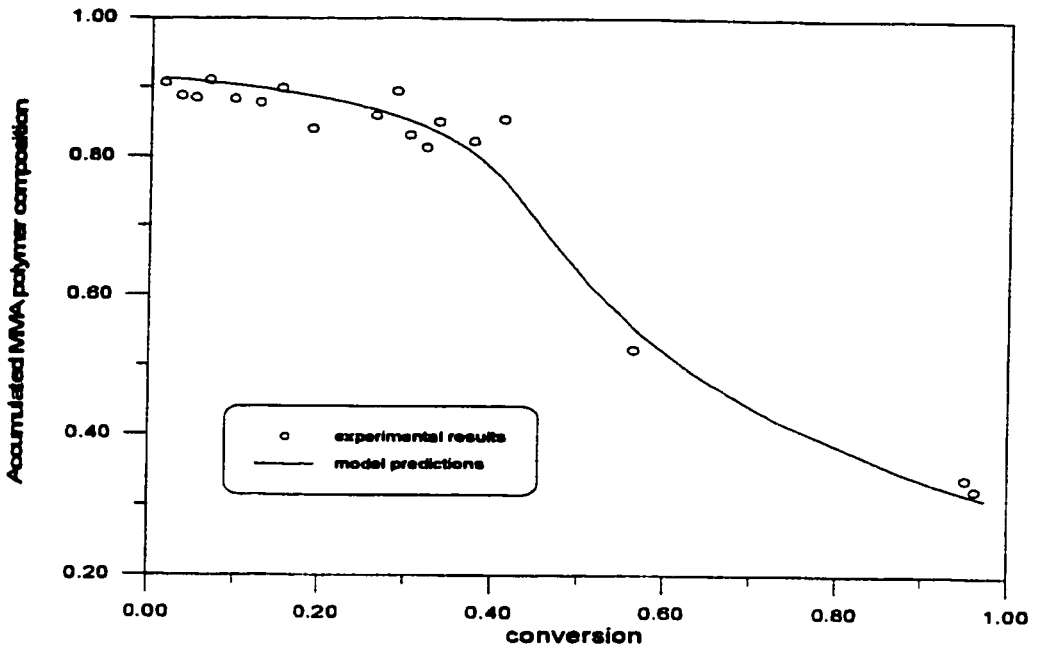

Figure 10.10 Simulation of MMA/VAc Copolymerization in Bulk at 60°C. f_{MMA}=30 mol%, [AIBN]=0.01 mol/L

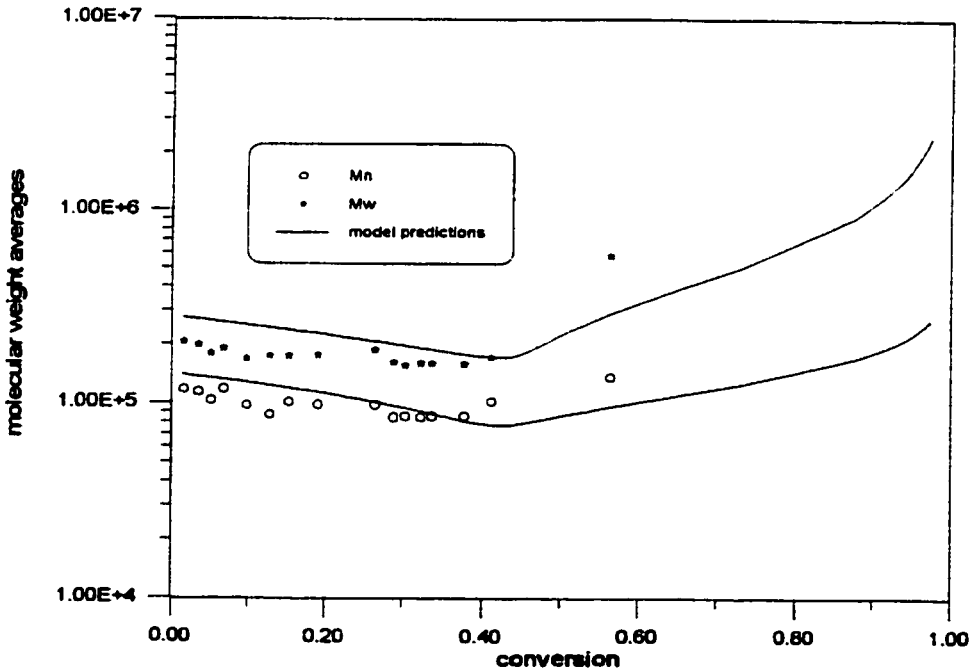

Figure 10.11 Simulation of MMA/VAc copolymerization in Bulk at 60°C. f_{MMA}=30 mol%, [AIBN]=0.01 mol/L

10.3 Simulation of Copolymerization of BA/VAc

10.3.1 Literature Summary

Very few papers can be found for this copolymer system. Most literature information is concentrated on the copolymerization in emulsion. Bataille and Bourassa (1989) used the Finneman-Ross method to estimate reactivity ratios as: r_{BA}=0.024, r_{BA}=10.67. McKenna et al.(1995) carried out both homo- and copolymerization of VAc and BA in solution. Their investigation was focused on the effect of dissolved oxygen on reaction kinetics. Two semibatch copolymerization runs were performed in a 7-liter reactor at 70°C. Ethyl acetate was used as the solvent. It was concluded that the rate of polymerization was very sensitive to the dissolved oxygen. McKenna et al.(1995) measured the conversion levels in these runs and attempted to estimate the rate constant of transfer to inhibitor (oxygen). Their data are useful for studies on the effect of inhibitors on copolymerization kinetics. Unfortunately, their results were not used for model testing in this thesis since it is very difficult to approximate the dissolved amount of oxygen in the reaction mixture.

10.3.2 Model Testing

Dube and Penlidis (1995a) were the only group that investigated BA/VAc copolymerization kinetics and performed full conversion range experiments. Their estimated reactivity ratios for BA and VAc are r_{BA}=0.026, r_{VAc}=5.938 and they were used for model testing. Figure 10.12 shows a full conversion run at 60°C and figure 10.13 is the composition change versus conversion. Unlike MMA/VAc copolymerization, the composition drift in BA/VAc is not as severe. Model predictions generally follow the trend of composition change over the entire range of copolymerization. The 'double rate phenomenon' is not observed in BA/VAc copolymerization mainly due to the marginal composition drift. The picture shown in figure 10.12, however, is not satisfactory. No obvious evidence has been found to interpret the discrepancy. One possible reason could be nonisothermality due to poor heat transfer during the specific run. Since little information is available for BA/VAc, further kinetic investigations and experimental verification will definitely be helpful.

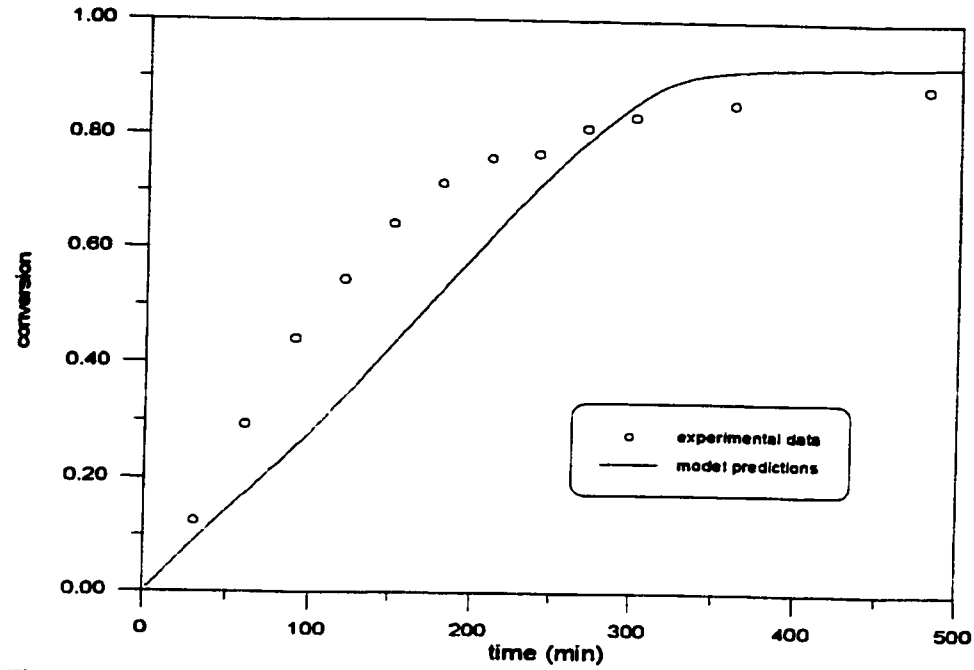

Figure 10.12 Simulation of BA/VAc Copolymerization in Bulk at 60°C. f_{BA}=80 mol%, [AIBN]=0.00054 mol/L

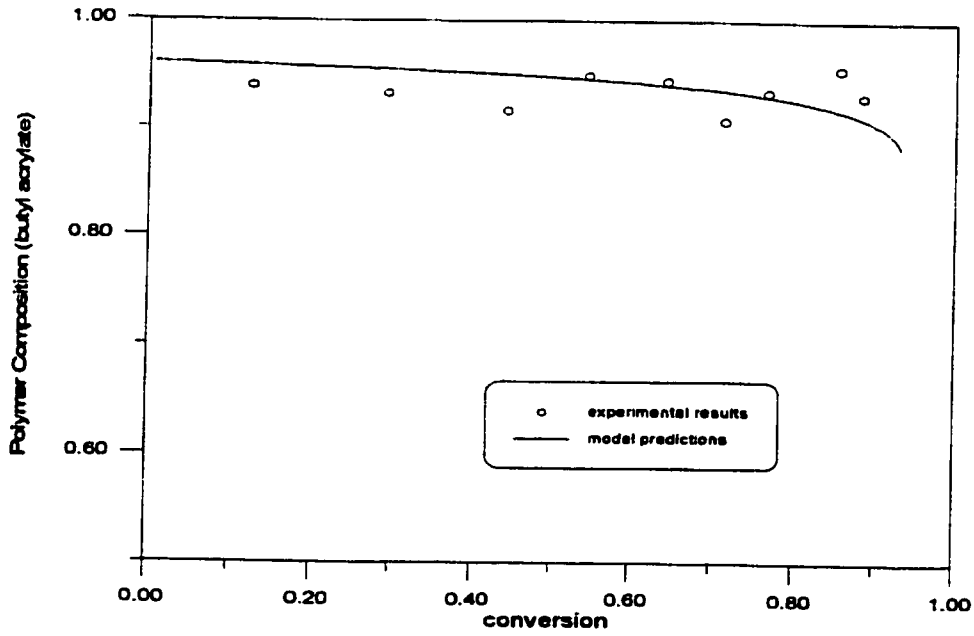

Figure 10.13 Simulation of BA/VAc Copolymerization in Bulk at 60°C. f_{BA}=80 mol%, [AIBN]=0.00054 mol/L

Chapter 11. Simulation of Copolymerization of Styrene and Carboxylic Acids

11.1 Monomer Characteristics

Acrylic acid (AA) and methacrylic acid (MAA) monomers are relatively weak acids. It is well known that both monomers can be dissociated or ionized by losing the H atom in their -COOH group. Homopolymerization of AA and MAA is very strongly medium pH-dependent. A small increase in the pH of the reaction medium will decrease the rate of polymerization sharply (in the low and middle pH range, pH < 7). Another characteristic of the homopolymerization of AA and MAA is its heterogeneity. The polymers of AA and MAA do not dissolve in their own monomer. The polymer precipitates as a fine powder and a polymer phase is formed after the reaction starts. Detailed discussion and modelling of AA and MAA homopolymerization were given in the previous review paper by Gao and Penlidis (1996).

11.2 Copolymerization of Styrene/AA

Much information on Sty/AA and Sty/MAA kinetics available in the literature is for emulsion copolymerization. Blackley et al.(1987) investigated the influence of surfactant type on the copolymerization of styrene with low levels of acrylic acid. Shoaf and Poehlein (1991) developed a model for Sty/AA copolymerization up to high conversion in emulsion. Their model predictions agree with experimental results well up to high conversion levels. Guillot (1990) investigated the pH effect on reaction kinetics. Ionized and nonionized carboxylic acid monomers were considered to have different reactivities.

Kinetic studies on bulk and solution copolymerization of Sty/AA are mostly limited to reactivity ratio estimation and solvent effects. Chapin et al.(1949) in their early work measured reactivity ratios of Sty/AA and Sty/MAA by fitting the measured composition curve. Kerber (1966) estimated Sty/AA reactivity ratios in bulk as well as in four different solvents, methyl ethyl ketone, dioxane, tetrahydrofuran (THF) and dimethylformamide (DMF). It is noted in their work that solvents have a considerable effect on the value of reactivity ratios. Table 11.1 lists reactivity ratios for Sty/AA from different sources.

Table 11.1 List of Reactivity Ratios for Sty/AA

r_{Sty}	r_{AA}	Remarks	Sources
0.25	0.15	Bulk	Chapin et al.(1949)
0.25	0.07	Bulk	Kerber (1966)
0.7	0.15	methyl ethyl ketone	idid
0.75	0.13	dioxane	idid
0.9	0.14	THF	idid
1.03	0.15	DMF	idid
0.25	0.05	bulk	Ryabov et al.(1970)
1.1	0.08	dimethylformamide	idid
0.3	0.13	Bulk	Toppet et al.(1975)
1.6	0.05	Dimethylformamide	idid
0.3	0.2	benzene	Switala et al.(1986a-b)
0.25	0.18		Cheng et al.(1991)
1.16	0.81	thermal polymerization	Cheng et al.(1991)

It is apparent that reactivity ratios from literature sources are quite different from each other. Relatively speaking, reactivity ratio values in bulk are more consistent, especially for styrene. Values for AA are much more scattered. This implies AA is a more difficult monomer to estimate its characteristics. Hamielec et al.(1986) possibly is the only group that performed Sty/AA copolymerization in bulk up to high conversion. The reaction temperature in their experiments was between 230 and 300°C. Sty/AA copolymer of low molecular weight with a narrow distribution was produced in a CSTR. In some runs, the CSTR was followed by a tubular reactor to obtain higher conversions and copolymer of lower molecular weights. The kinetics of thermal initiation was studied in detail. Spychaj and Hamielec (1991) later further extended the previous work and concluded that the thermal initiation in Sty/AA copolymerization is mainly due to styrene radicals rather than acrylic acid radicals.

11.3 Copolymerization of Sty/MAA

Like Sty/AA copolymerization, kinetic studies on Sty/MAA are limited to reactivity ratio estimation and solvent effects. Sty/MAA copolymerization is more commonly carried out in emulsion rather than in bulk or solution. Ruckenstein and Kim (1989) performed Sty/MAA copolymerization in a non-conventional emulsion process known as concentrated emulsion. In contrast to the conventional emulsion process which has a large amount of water as the continuous phase, only a small amount of water (about 5-25 v%) was used in concentrated emulsion. This is to minimize the loss of MAA dissolved in the water phase. They found that the surface density of the carboxylic groups on the latex surface increases linearly with the feed molar ratio of methacrylic/styrene and about 5% of carboxylic groups of the copolymer latex are located on its surface.

Plochocka and Harwood (1978) estimated reactivity ratios for Sty/MAA copolymer in dioxane and carbon tetrachloride based on composition as well as sequence distribution data. They found that reactivity ratio values estimated based on sequence distribution data are more consistent in both solvents than those based on composition data. Boudevska and Todorova (1985) conducted a more extensive investigation of solvent effects on reactivity ratios. Reactivity ratios were estimated using the Kelen-Tudos method from runs in bulk and various solvents. Their estimated reactivity ratios are listed in Table 11.2.

Table 11.2 Listing of Reactivity Ratios for Sty/MAA

Solvent	r_{sty}	r_{MAA}
Carbon tetrachloride	0.06	0.54
Chloroform	0.08	0.51
Acetone	0.65	0.43
1-4 dioxane	0.59	0.41
Acetonitrile	0.29	0.06

From the values of Table 11.2, the solvent effect on the reactivity ratio estimates is obvious. So

far no satisfactory kinetic models are available in the literature to describe the solvent effect. The sequence length distribution effect on glass transition temperature of Sty/MAA was studied by Switala-Zeliazkow (1993). Other papers that are of interest with respect to this copolymer system are Ryabov et al.(1970), Semchikov et al.(1979, 1984, 1990, 1991), and Egorochkin et al.(1992).

11.4 Remarks

Styrene and carboxylic acid copolymers are widely used in latex, coating materials, adhesives, etc., and are more commonly produced in emulsion rather than in bulk and solution. Despite their commercial importance, little is known on the reaction kinetics of this group of copolymers. Despite literature search on this group of copolymers, no experimental data have been found, therefore model testing can not be performed. For future work in this area, we make several recommendations below.

(1) Reactivity ratios of Sty/AA and Sty/MAA in bulk should be estimated using the Tidwell-Mortimer criterion. The statistically sound EVM method should be used in the calculation. The estimated reactivity ratios may be used for simulation of Sty/AA and Sty/MAA copolymerization in emulsion.

(2) Full conversion range experiments at different temperatures should be carried out. These experiments would help to estimate important kinetic parameters, for modeling and simulation. Composition and molecular weight averages of the polymer produced should be measured for all runs.

(3) It should be understood that some rate constants of carboxylic acids in bulk, especially the rate constant of propagation, are very different from those in water phase. Simulation of styrene and carboxylic acids copolymerization in emulsion presents a very challenging task since carboxylic acid monomers are soluble in the water phase and their rate constants of propagation are affected greatly by the pH value of the medium. Previous work (Gao and Penlidis, 1996) on carboxylic acid homopolymerization can be utilized along with modern emulsion kinetic theory as a starting point for modeling of these peculiar copolymer systems.

Chapter 12. Simulation of Copolymerization of *p*-Methyl Styrene and Various Monomers.

Hamielec's group (Bhattacharya and Hamielec, 1986; Jones et al., 1986; Yaraskavitch et al., 1987) is one of very few groups that has conducted a series of experiments with *p*-MSty/Sty, *p*-MSty/MMA, and *p*-MSty/AN copolymerization in bulk up to high conversion. They also developed a model to describe the kinetic behaviour of copolymerization based on free volume theory. Segmental diffusion control, translational diffusion control as well as reaction diffusion control mechanisms were all included into their model. The mathematical model frame and approach in this simulation package are very similar to those used in their models. In all their experiments, conversion, polymer composition and molecular weight averages were measured at all conversion levels. These data are the main source for model testing. Other references found to be useful are listed in Table 12.1.

Table 12.1 Reference List for copolymerization of *p*-Methyl Styrene and Other Monomers

References	Remarks
Achilias and Kiparissides (1987)	modeling and simulation
Bhattacharya and Hamielec (1985)*	p-methyl styrene/styrene copolymerization full conversion experiments, modeling and simulation, modeling of thermal initiation in copolymerization
Bhattacharya and Hamielec (1986)*	p-methyl styrene/styrene copolymerization full conversion experiments, modeling and simulation
Gyongyhalmi et al.(1993)	p-methyl styrene homopolymerization at high temperatures
Jones et al.(1986)*	p-methyl styrene/methyl methacrylate copolymerization full conversion experiments, modeling and simulation
Kozorezov and Shilyaeva (1996)	thermal polymerization of p-methyl styrene
Lin et al.(1987)	p-methyl styrene/methyl methacrylate copolymerization
Maxwell and Russel (1993)	diffusion controlled copolymerization kinetics

Paoletti and Billmeyer (1964)	rate constants for p-methyl styrene
Schroder (1987)	p-methyl styrene/styrene crosslinking copolymerization
Wittmer (1979)	classical copolymerization kinetics
Yaraskavitch et al.(1987)*	p-methyl styrene/acrylonitrile copolymerization full conversion experiments, modeling and simulation

* papers found of greater usefulness and used for model testing

12.1 Simulation of Copolymerization of Styrene and *p*-Methyl Styrene

The most distinctive characteristic of this copolymer system is its thermal self-polymerization at temperatures above 100°C. The thermal initiation mechanism in the homopolymerization of both monomers was described in Hui and Hamielec (1972), Husain and Hamielec (1978) and Ito (1986). Paoletti and Billmeyer (1964) reported rate constants of propagation for styrene, p-methyl styrene and o-methyl styrene in emulsion. Rudin and Chiang (1974) studied copolymerization of styrene and p-methyl styrene at 60°C. Achilias and Kiparissides (1987) used the model presented by Bhattacharya and Hamielec (1986) to simulate the experimental data from the same group. Bhattacharya and Hamielec (1985, 1986) were the only group that reported high conversion range experimental data. They also presented a kinetic model for thermal initiation in the copolymerization of these two monomers. The initiation rate is believed to be third-order with respect to monomer concentration and is expressed as equation 12.1:

$$R_{It} = K[M]^3 \tag{12.1}$$

In the equation above, [M] is the total monomer concentration, and K is an overall rate constant for thermal initiation, which is a function of monomer feed composition. Equation 12.1 was implemented into this model for the simulation of p-MSty/Sty thermal copolymerization. In all model testing for this copolymerization, the thermal initiation option was activated. Bhattacharya and Hamielec (1985, 1986) estimated the reactivity ratios of these two monomers as r_{Sty}=0.971, $r_{p\text{-}MSty}$=0.901. The two reactivity ratios are close to 1. This indicates these two monomers very closely resemble each other due to their similar molecular structure. The reported reactivity ratios

were used in model testing, and simulation results are presented in the section below.

12.1.1 Model Testing

Bhattacharya and Hamielec (1986) conducted p-MSty/Sty copolymerizations at four high temperature levels, 120, 140, 160 and 180°C . Copolymerization was initiated thermally without any chemical initiator present. Figures 12.1 to 12.4 present simulation results as well as reported conversion data. In figures 12.1 and 12.2, experiments were conducted at 160 and 180°C with different monomer feed compositions. The rates of polymerization in the runs at the same temperature but different monomer feed composition are close to each other. This implies that the chemical characteristics of styrene and p-methyl styrene are very similar to each other. Temperature effects on the rate of polymerization are as expected; higher temperature leads to a faster copolymerization as well as higher final conversion levels. Same observations can also be made for figures 12.3 and 12.4.

Figures 12.5 to 12.7 show weight average molecular weight data and figures 12.8 and 12.9 show number average molecular weight data. The weight average molecular weight data were measured by both size exclusion chromotography (SEC) and low angle laser light scattering photometry (LALLSP). It is evident from figures 12.5 to 12.7 that LALLSP gives higher weight average molecular weight data values than the SEC measurements. All the figures clearly demonstrate the temperature effect on molecular weight averages. The higher the temperature, the lower the molecular weight averages are.

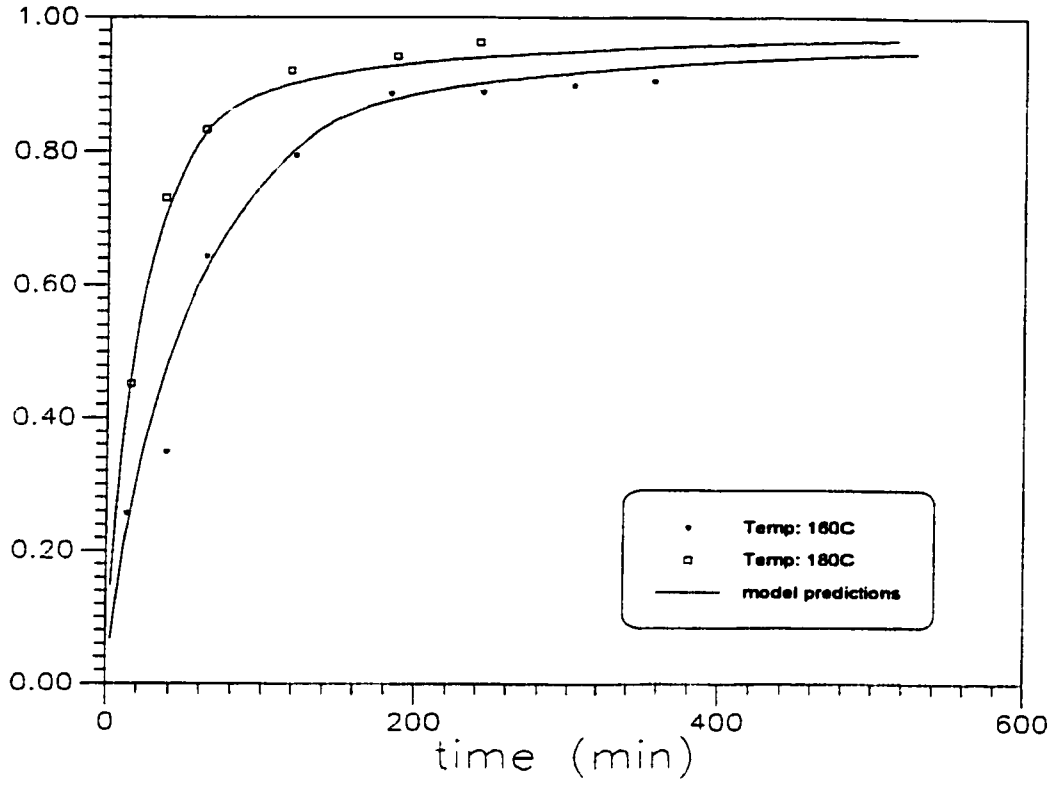

Figure 12.1 **Simulation of Sty/*p*-MSty Copolymerization in Bulk. f_{Sty}=20 mol%.**

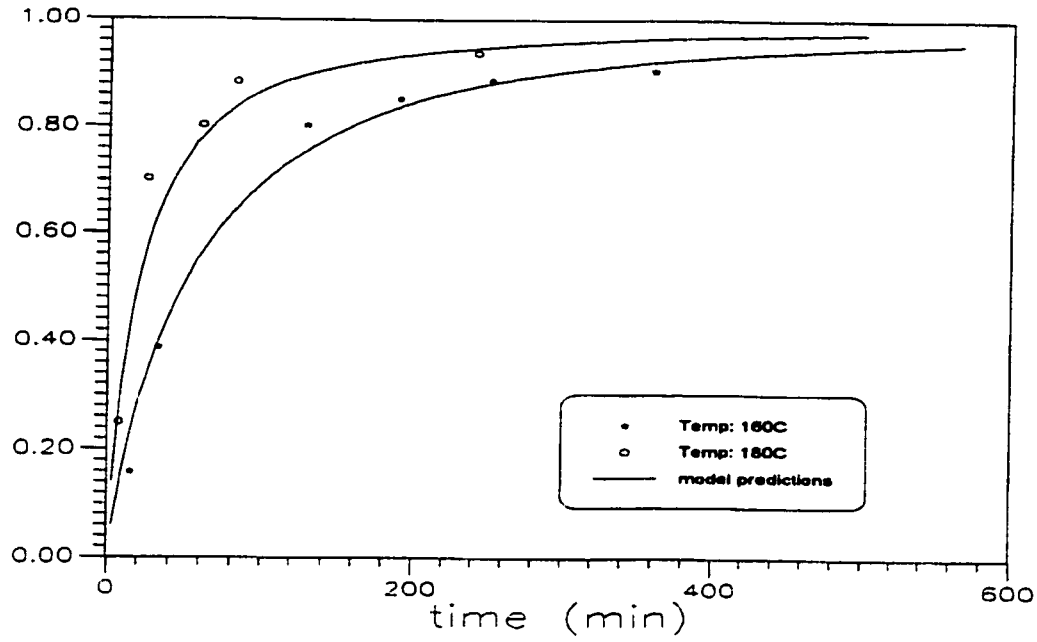

Figure 12.2 Simulation of Sty/*p*-MSty Copolymerization in Bulk. f_{Sty}=75 mol%.

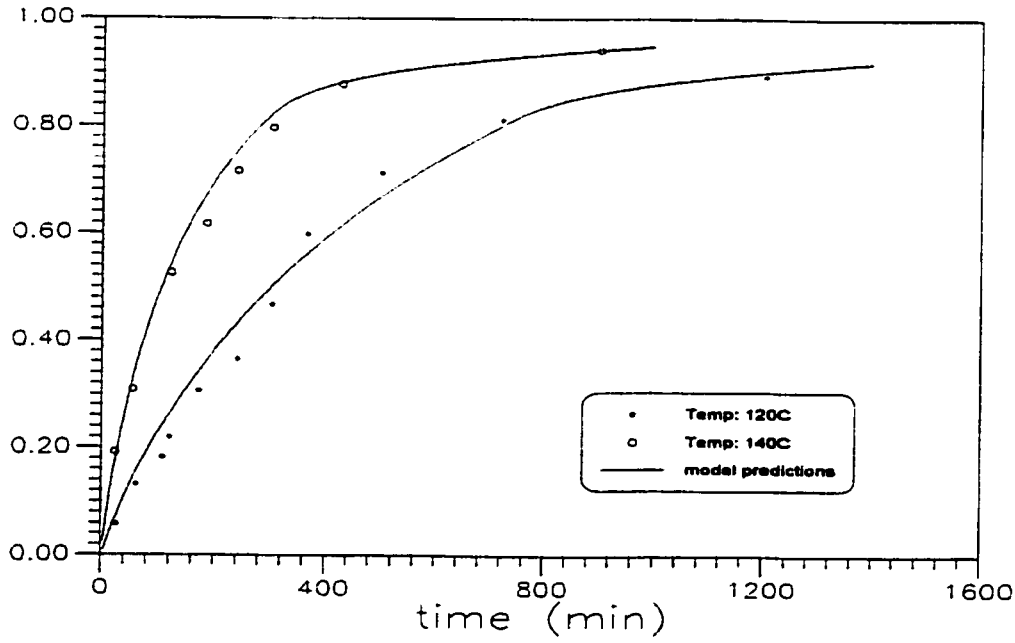

Figure 12.3 Simulation of Sty/*p*-MSty Copolymerization in Bulk. f_{Sty}=20 mol%.

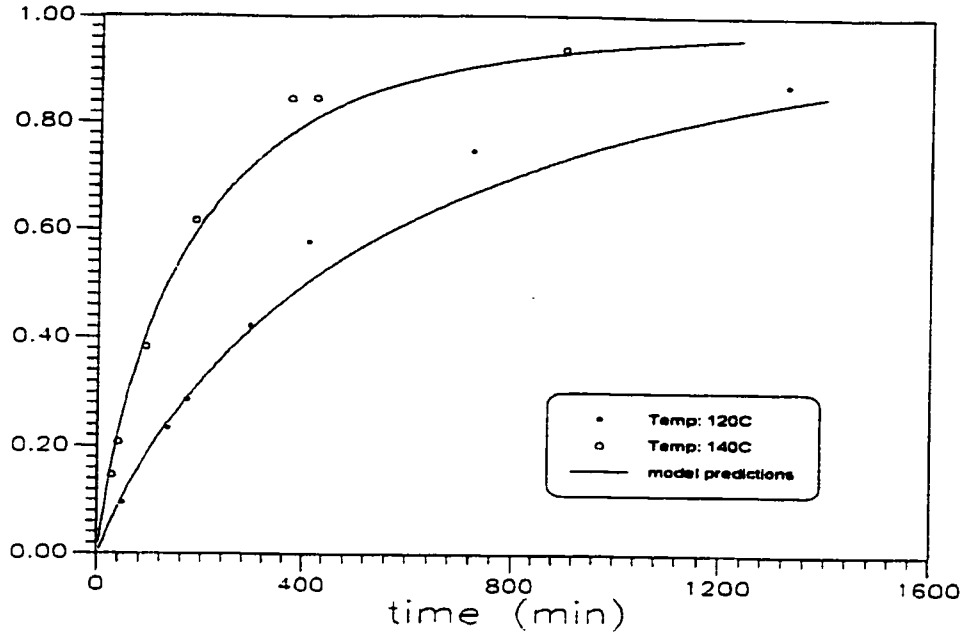

Figure 12.4 Simulation of Sty/*p*-MSty Copolymerization in Bulk. f_{Sty}=75 mol%.

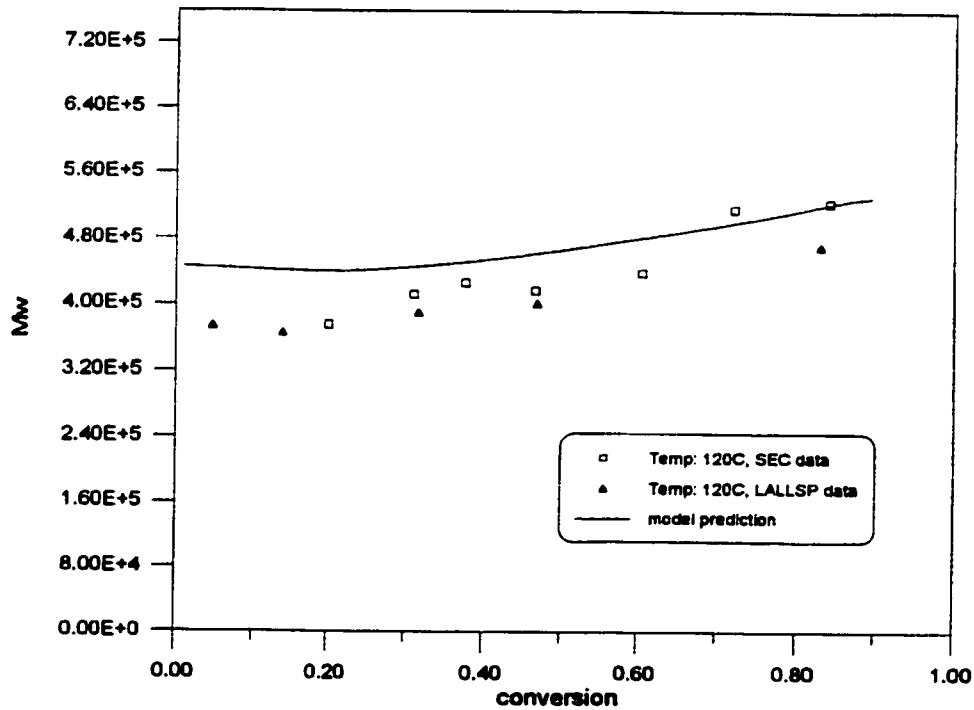

Figure 12.5 Simulation of Weight Average Molecular Weight in Sty/*p*-MSty Copolymerization in Bulk at 120°C. f_{Sty}=20 mol%.

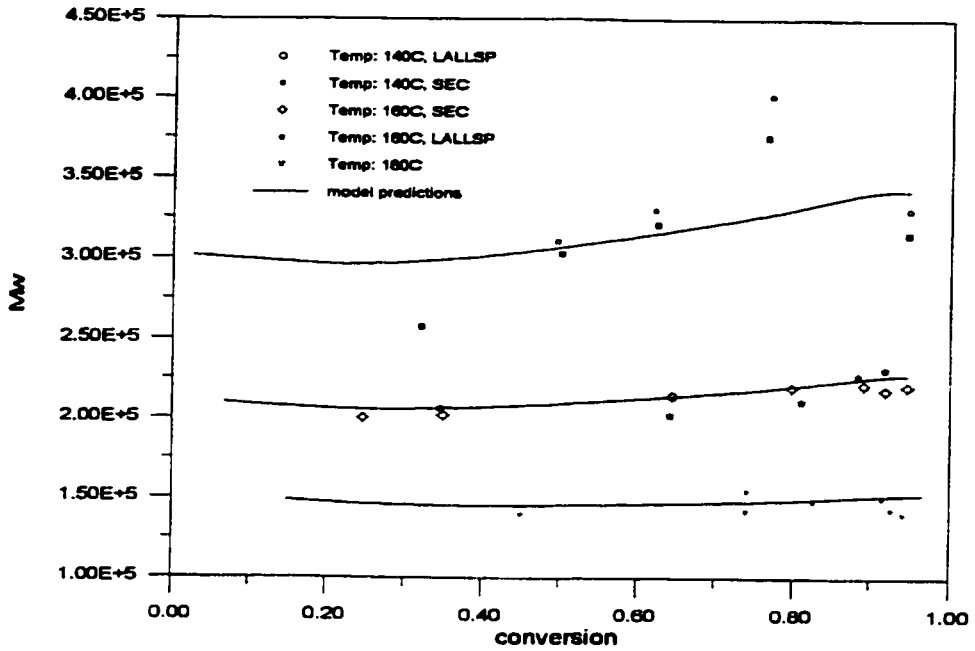

Figure 12.6 Simulation of Weight Average Molecular Weight in Sty/*p*-MSty Copolymerization in bulk. f_{Sty}=20 mol%.

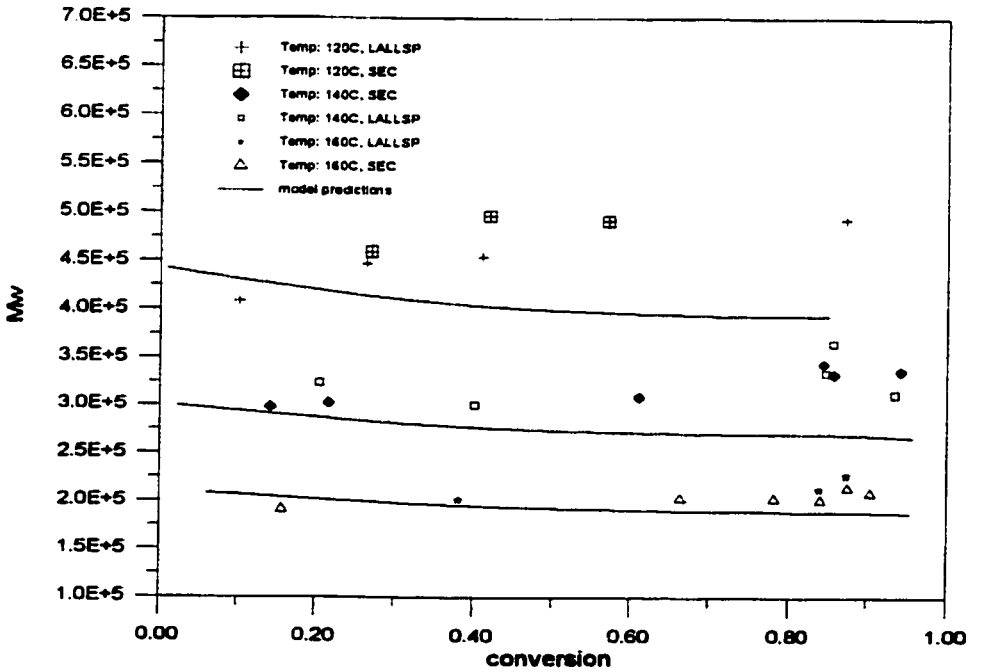

Figure 12.7 Simulation of Weight Average Molecular Weight in Sty/*p*-MSty Copolymerization in Bulk. f_{Sty}=75 mol%.

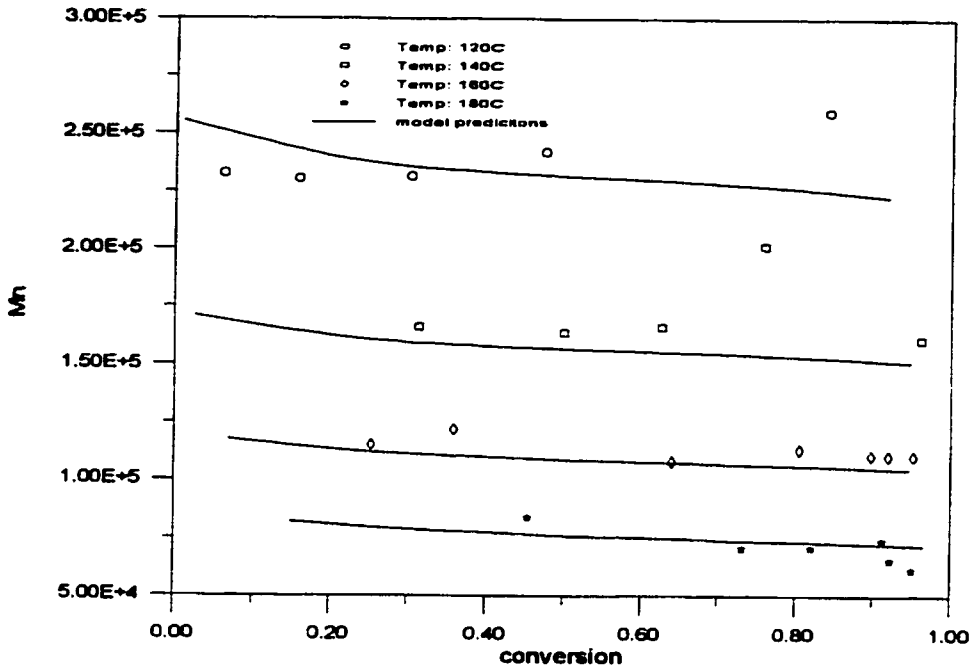

Figure 12.8 Simulation of Number Average Molecular Weight in Sty/*p*-MSty Copolymerization in Bulk. f_{Sty}=20 mol%.

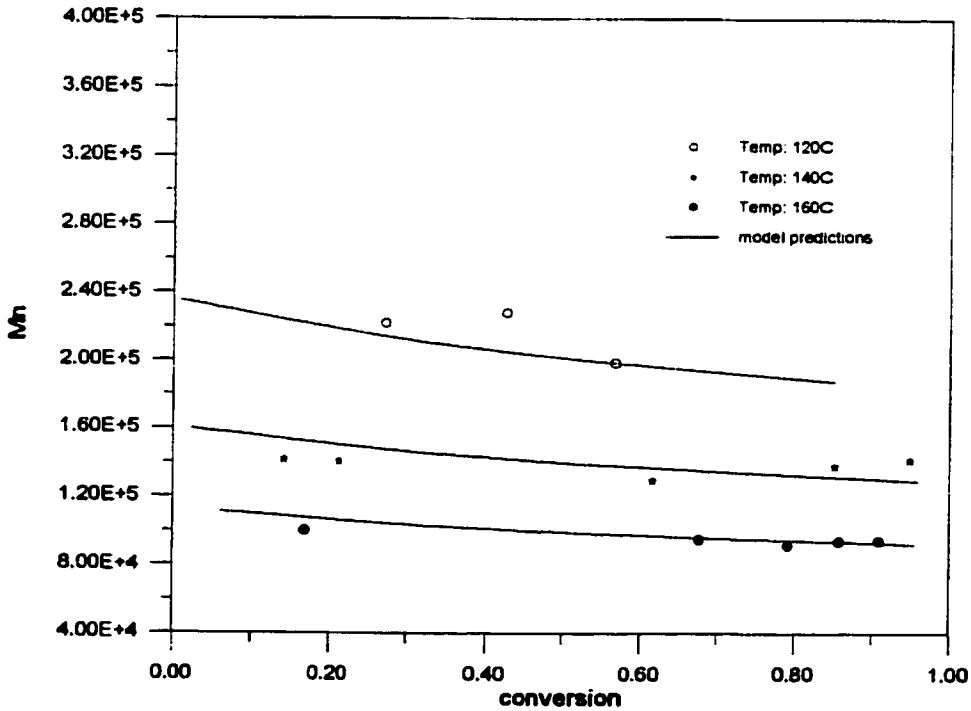

Figure 12.9 Simulation of Number Average Molecular Weight in Sty/*p*-MSty Copolymerization in Bulk. f_{Sty}=75 mol%.

12.2 Simulation of Copolymerization of Methyl Methacrylate and *p*-Methyl Styrene

Jones et al.(1986) is the only source of information available in the literature for this copolymer system. Full conversion range bulk experiments were carried out at two temperature levels. Kinetic parameters were estimated based on the obtained experimental data (conversion, composition and molecular weight averages). Their estimated parameters provide very useful information for simulation and model testing. The estimated reactivity ratios are r_{MMA}=0.498, $r_{p\text{-}MSty}$= 0.419 and were used in model testing. The corresponding azeotropic feed composition is f_{MMA}=0.54.

Figures 12.10 to 12.13 show the comparison of predicted and measured conversion versus time curves from runs conducted at different reaction conditions. Figure 12.10 displays four azeotropic runs at two temperatures and two initiator levels. MMA/p-MSty copolymerization is much like MMA/Sty copolymerization, i.e., there is a strong gel effect and limiting conversion at the end of the reaction. Figure 12.11 illustrates two runs with higher MMA content in the monomer feed, while figures 12.12 and 12.13 display three runs at a lower MMA content in the feed. The effect of initial monomer feed composition on reaction kinetics is very apparent; higher MMA content will lead to a strong gel effect and a faster rate of polymerization. In all cases, model predicted conversion curves agree with measured data points reasonably well, except for the two runs with the lower initiator level at the lower temperature in figures 12.10 and 12.13. Such a discrepancy was also discussed before in this thesis and is commonly observed in reactions with lower initiator amounts since these reactions are more vulnerable to impurities.

Figures 12.14 and 12.15 show the composition drift of residual monomer versus conversion at 60 and 80°C. Residual monomer composition for the runs with the azeotropic monomer feed composition remains constant during the reaction up to a conversion level of about 75%. Towards the very end of the reaction, it starts to drift away from the initial value. This is because each individual rate constant of propagation may become diffusion controlled at slightly different stages of the reaction. This will in turn cause the 'apparent reactivity ratio' to change and result in the 'drift' observed at the end of the reaction. This model is good at capturing the evolution

of copolymer composition in all runs.

Figures 12.16 and 12.17 are the simulation of weight average molecular weight measured from runs with azeotropic monomer feed compositions. The model predicts weight average molecular weight from runs at 80°C reasonably well, while it underestimates the weight average molecular weight from runs at 60°C at the final conversion level. No reasonable explanation can be given at this stage, it could be due to experimental error or improper parameter values. Overall, this model can describe kinetic behavior of MMA/*p*-MSty copolymerization quite well.

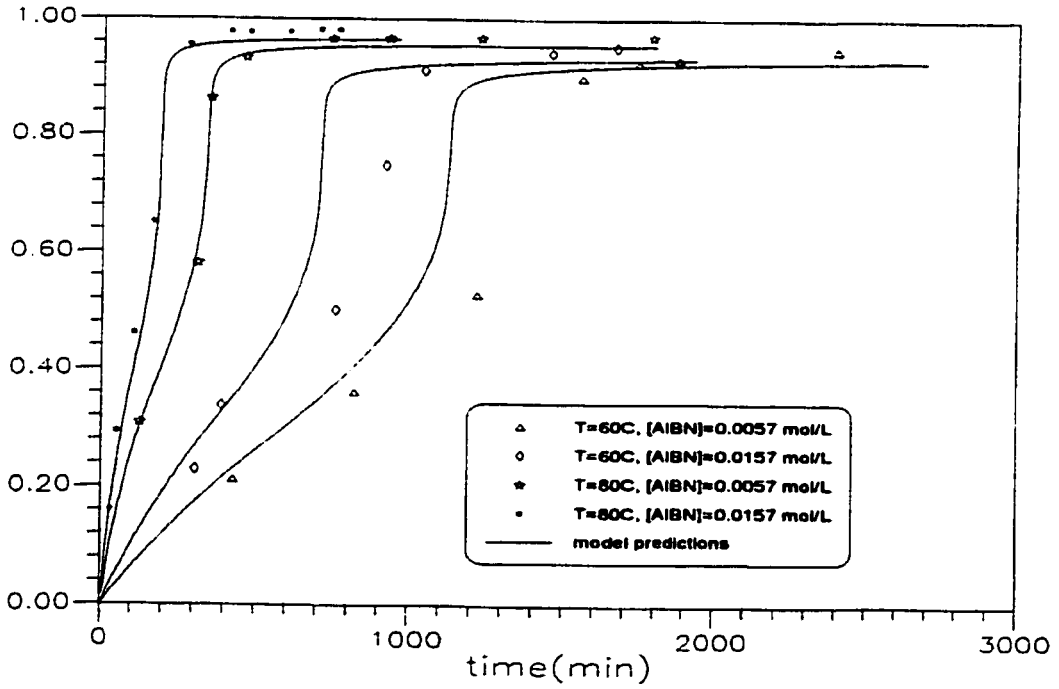

Figure 12.10 Simulation of MMA/*p*-MSty copolymerization in bulk. f_{MMA}=54 mol%.

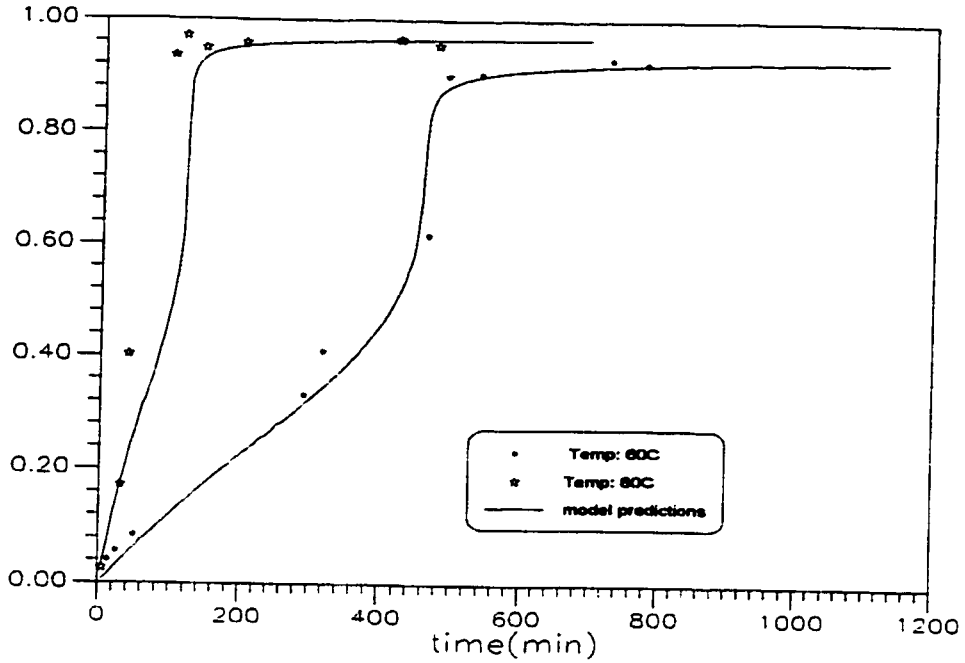

Figure 12.11 Simulation of MMA/*p*-MSty Copolymerization in Bulk. f_{MMA}=83 mol%, [AIBN]=0.0157 mol/L.

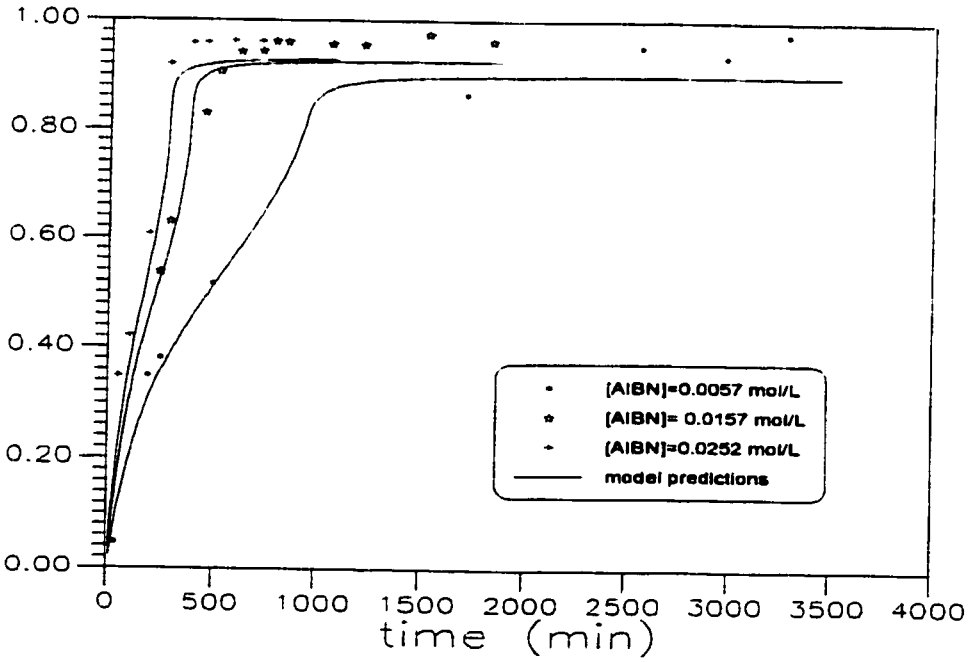

Figure 12.12 Simulation of MMA/*p*-MSty Copolymerization in Bulk at 80°C. f_{MMA}=21 mol%.

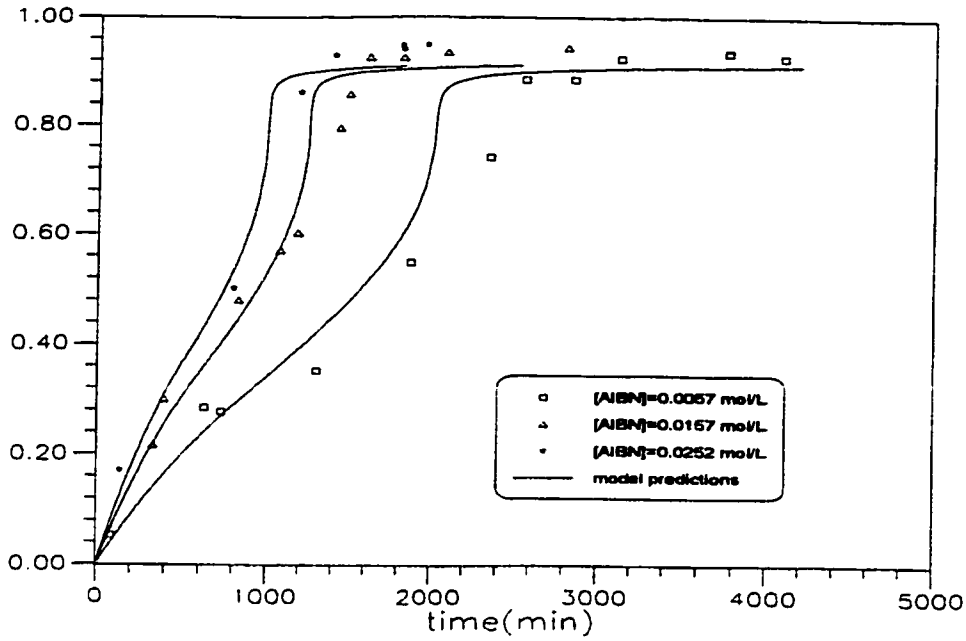

Figure 12.13 Simulation of MMA/*p*-MSty Copolymerization in Bulk at 60°C. f_{MMA}=21 mol%.

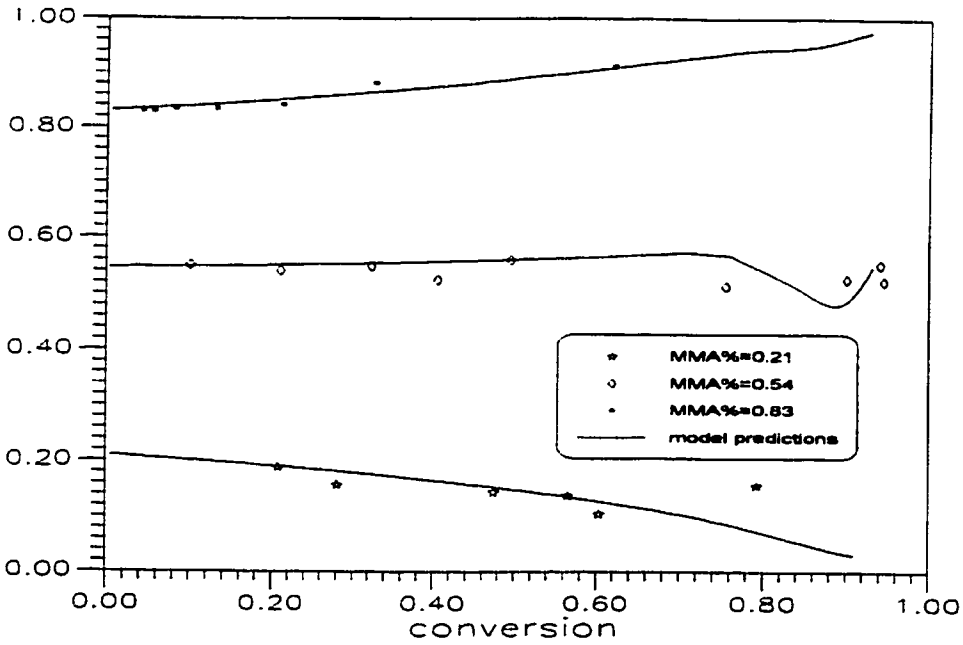

Figure 12.14 Simulation of Residual Monomer Composition in MMA/*p*-MSty Copolymerization in Bulk at 60°C. [AIBN]=0.0157 mol/L

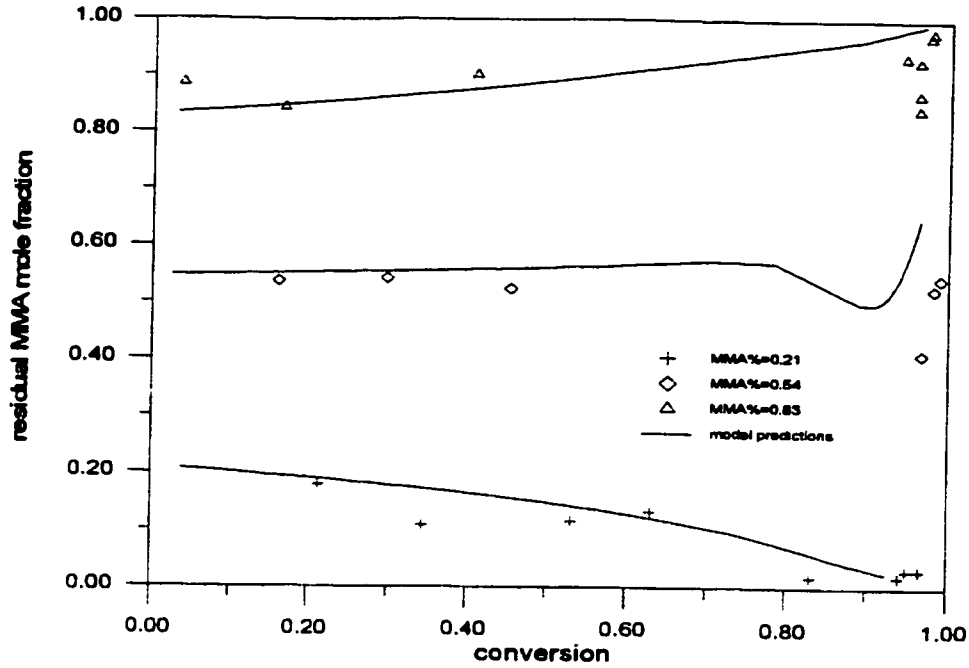

Figure 12.15 Simulation of Residual Monomer Composition in MMA/*p*-MSty Copolymerization in Bulk at 80°C. [AIBN]=0.0157 mol/L

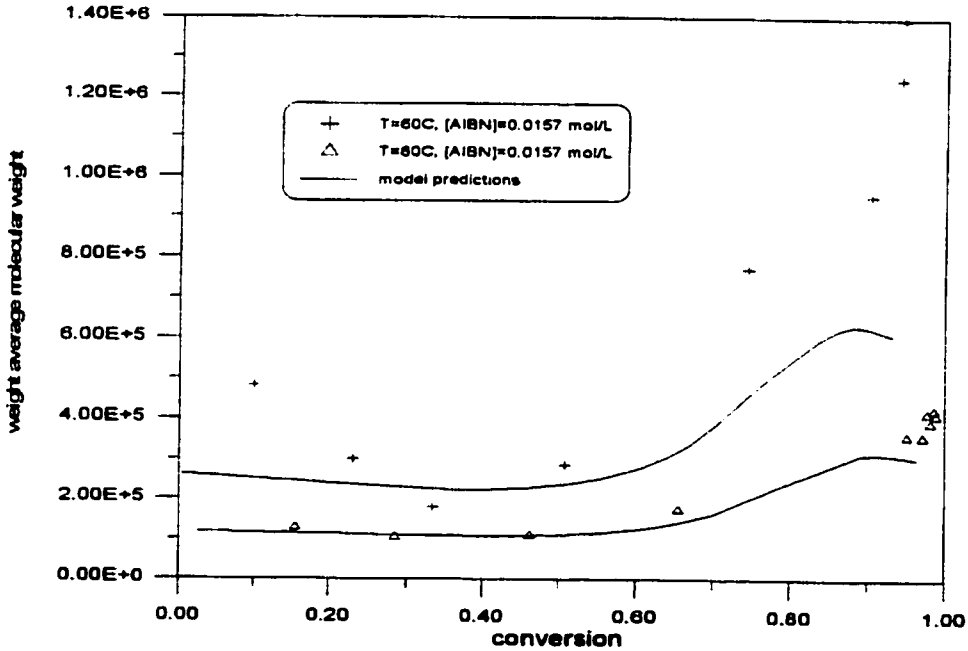

Figure 12.16 Simulation of Weight Average Molecular Weight in MMA/*p*-MSty Copolymerization in Bulk. [AIBN]=0.0157 mol/L

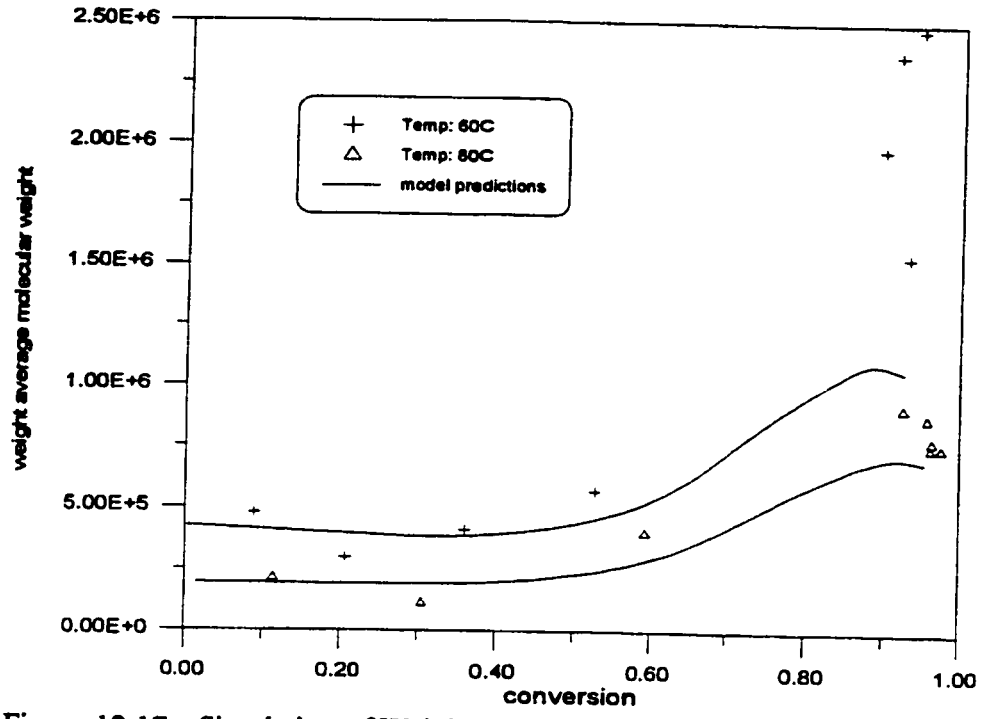

Figure 12.17 Simulation of Weight Average Molecular Weight in MMA/*p*-MSty Copolymerization in Bulk. [AIBN]=0.0157 mol/L

12.3 Simulation of Copolymerization of Acrylonitrile and *p*-Methyl Styrene

Yaraskavitch et al.(1987) investigated the kinetics of AN/*p*-MSty copolymerization in bulk at three temperatures over the entire conversion range. Two levels of initiator (AIBN) concentration and three initial monomer compositions were studied. They also developed a model that is similar to those proposed by Bhattacharya and Hamielec (1986) and Jones et al.(1986). Their model used free-volume theory to describe the autoacceleration and limiting conversion in AN/*p*-MSty copolymerization. Kinetic parameters related to segmental diffusion control and reaction diffusion control were estimated based on experimental results. The reported reactivity ratios are $r_{p\text{-MSty}}$=0.26, r_{AN}=0.066. The resulting azeotropic monomer composition is $f_{p\text{-Msty}}$=0.56.

The comparison of model predictions and measured conversion data from Yaraskavitch et al.(1987) can be seen in figures 12.18 to 12.22. Figure 12.18 demonstrates temperature and initiator effects on the conversion curve from runs with azeotropic monomer composition.

Copolymerization of AN/*p*-MSty exhibits a strong gel effect. Yarashavitch et al.(1986) estimated the Tg of AN/*p*-MSty copolymer as 378.2K, which is higher than the highest reaction temperature. Such high copolymer Tg results in a limiting conversion in all runs performed. Figures 12.19 and 12.20 demonstrate temperature effects on reaction kinetics. Figures 12.21 and 12.22 show conversion profiles for runs with different initiator levels. In general, this model delivers good predictions in all cases with very minor discrepancies. It is worth mentioning that in the non-azeotropic runs, severe composition drift occurs (see figures 12.23 to 12.25). This may produce incompatible copolymer chains and lead to microphase separation. This phenomenon would considerably change the kinetic behaviour of the reaction.

Figures 12.23 to 12.25 show simulated and measured residual monomer composition profiles for all runs. Acrylonitrile is incorporated into the copolymer chain at a faster rate than *p*-MSty. For runs with 80 and 90% p-MSty in the feed, at around 75% conversion, most of the acrylonitrile monomer is depleted. The residual monomer composition for the azeotropic runs remains constant throughout most of the reaction, which is as expected.

Molecular weight data from the azeotropic runs at 60 and 80°C were also reported by Yaraskavitch et al.(1987) and are plotted in figures 12.26 to 12.28. Weight average molecular weight was measured by both SEC and LALLS. This model gives reasonably good predictions while discrepancy exists at the higher conversion level, where this model generally underestimates weight average molecular weight. It is suspected that there could be some degree of branching occurring at the later stage of the copolymerization. No conclusive evidence can be obtained from Yaraskavitch et al.'s (1987) work, but at least that is the indication from the fact that the LALLS measurements are higher than the corresponding SEC values. This was also observed in subsection 12.1.1 (figures 12.6 to 12.7).

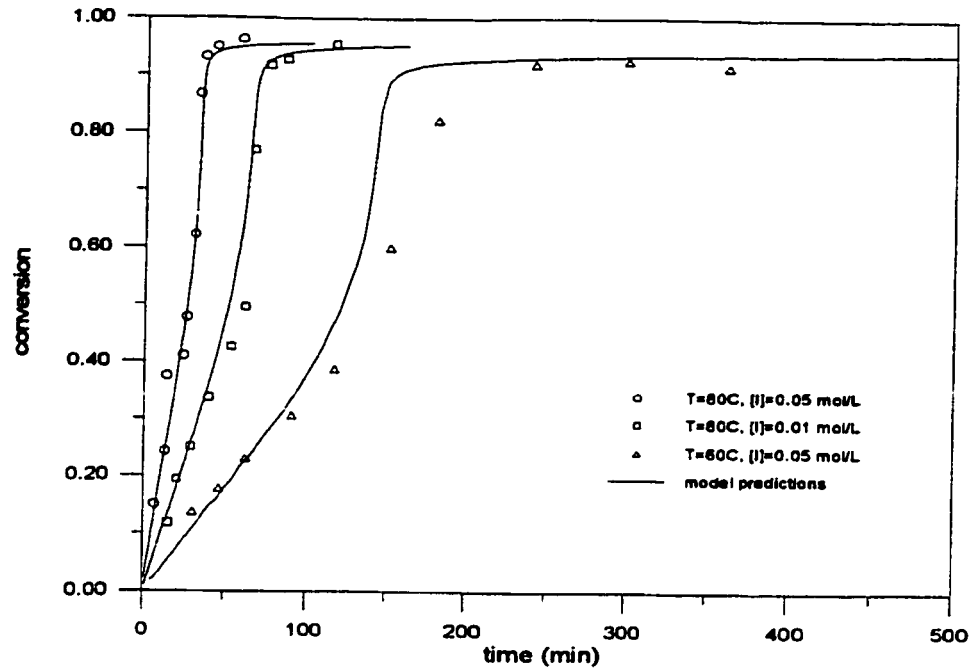

Figure 12.18 Simulation of AN/*p*-MSty Copolymerization in Bulk. [AIBN] as initiator, $f_{p\text{-MSty}}$=56 mol%.

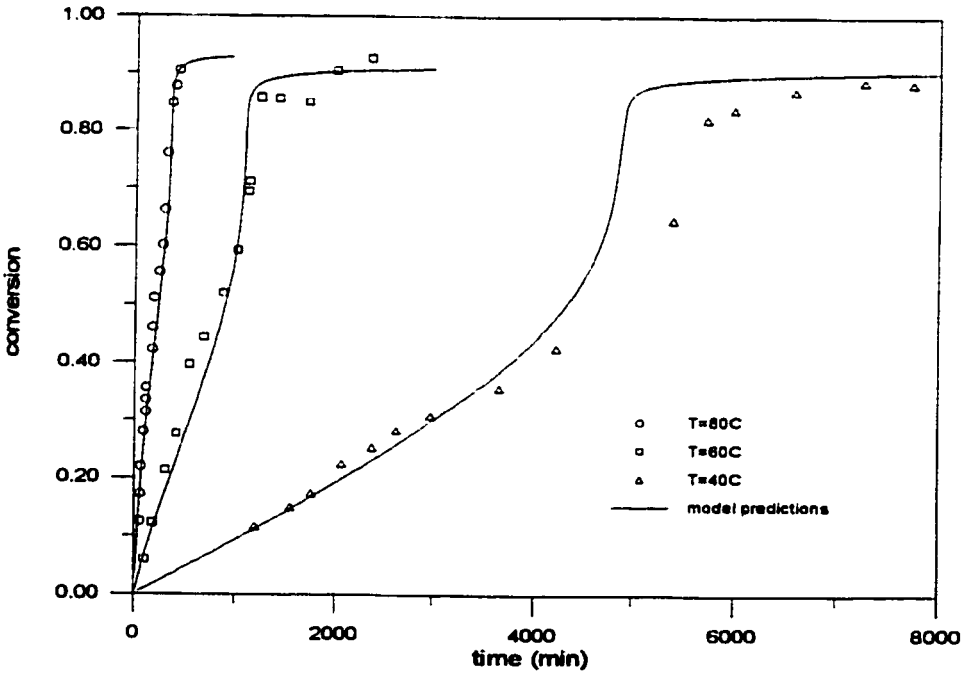

Figure 12.19 Simulation of AN/*p*-MSty Copolymerization in Bulk at Different Temperatures.
[AIBN]=0.01 mol/L, $f_{p\text{-MSty}}$=90 mol%.

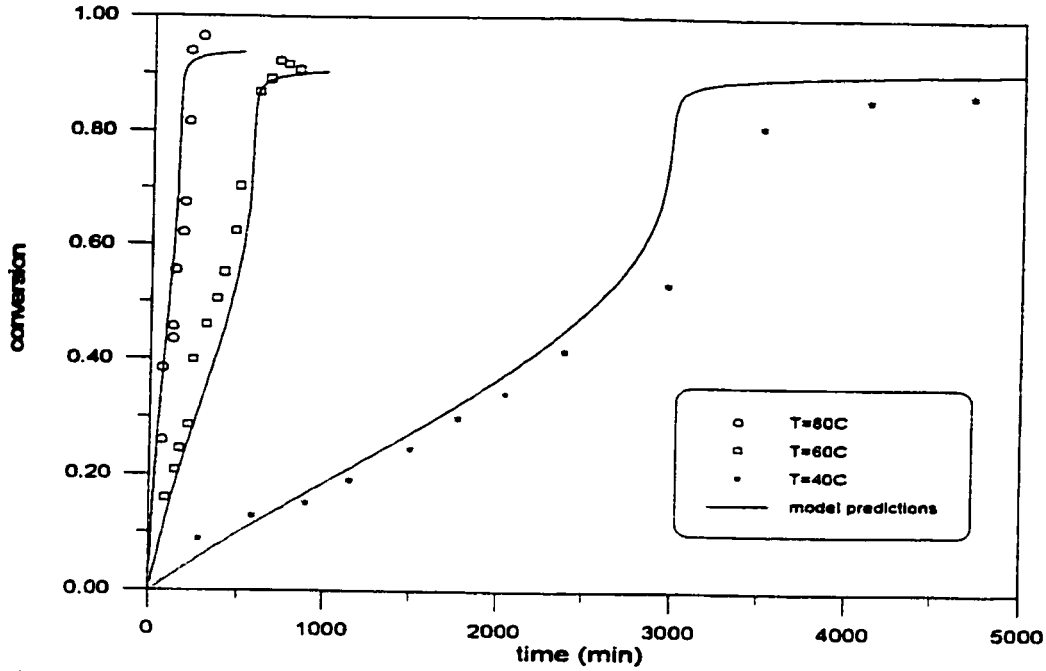

Figure 12.20 Simulation of AN/*p*-MSty Copolymerization in Bulk at Different Temperatures. [AIBN]=0.05 mol/L, $f_{p\text{-MSty}}$=90 mol%.

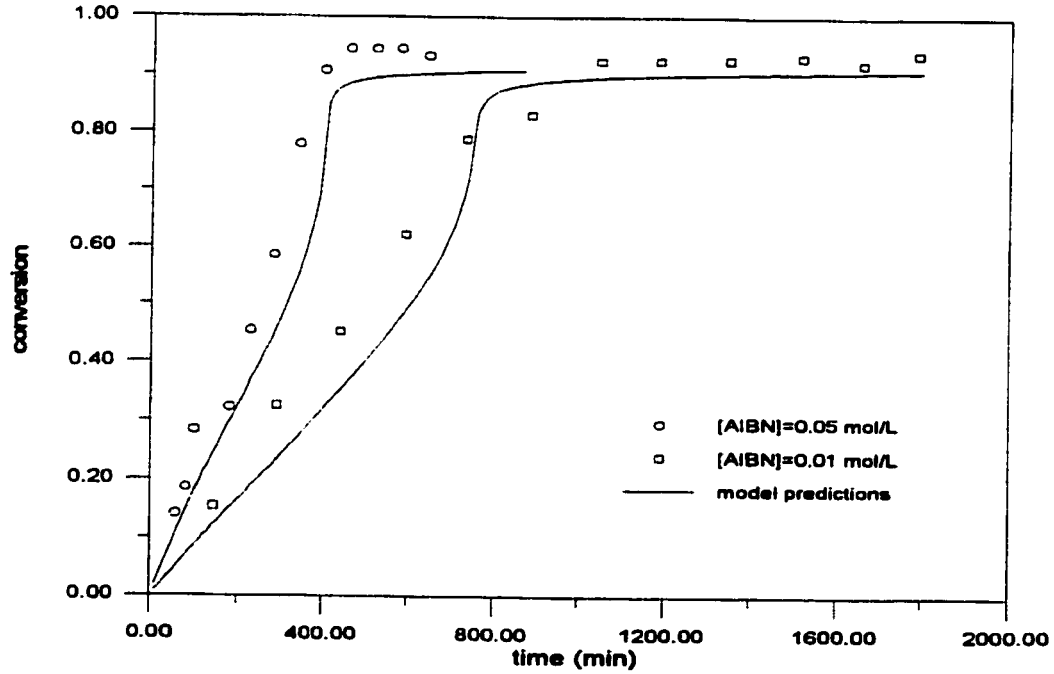

Figure 12.21 Simulation of AN/*p*-MSty Copolymerization in Bulk at 60°C. $f_{p\text{-MSty}}$=80 mol%.

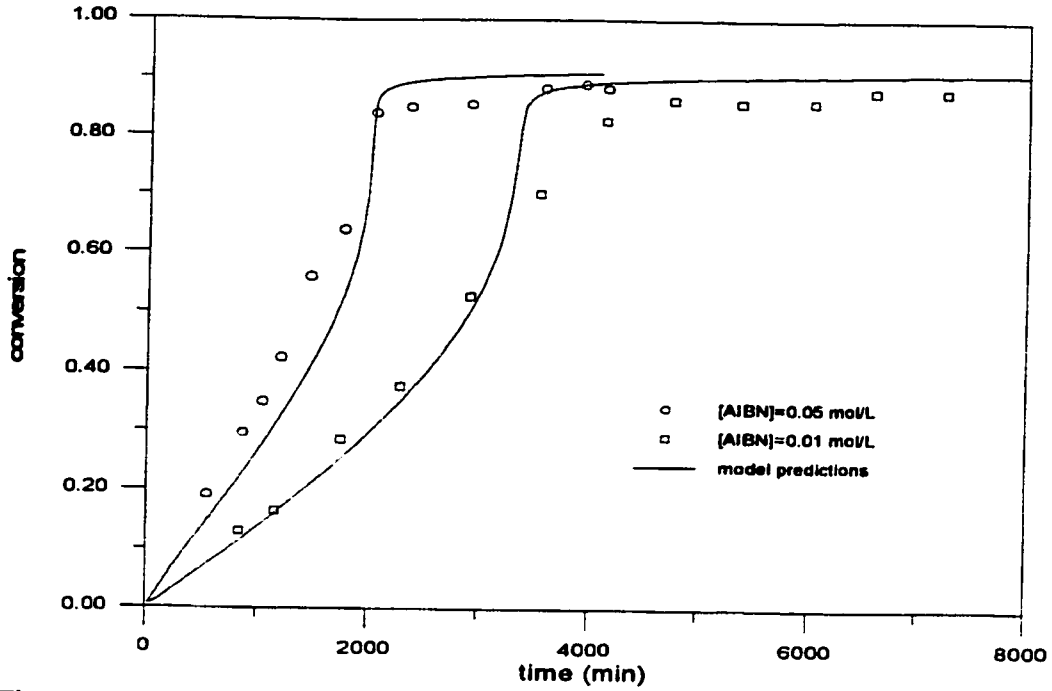

Figure 12.22 Simulation of AN/*p*-MSty Copolymerization in Bulk at 64°C. $f_{p\text{-MSty}}$=80 mol%.

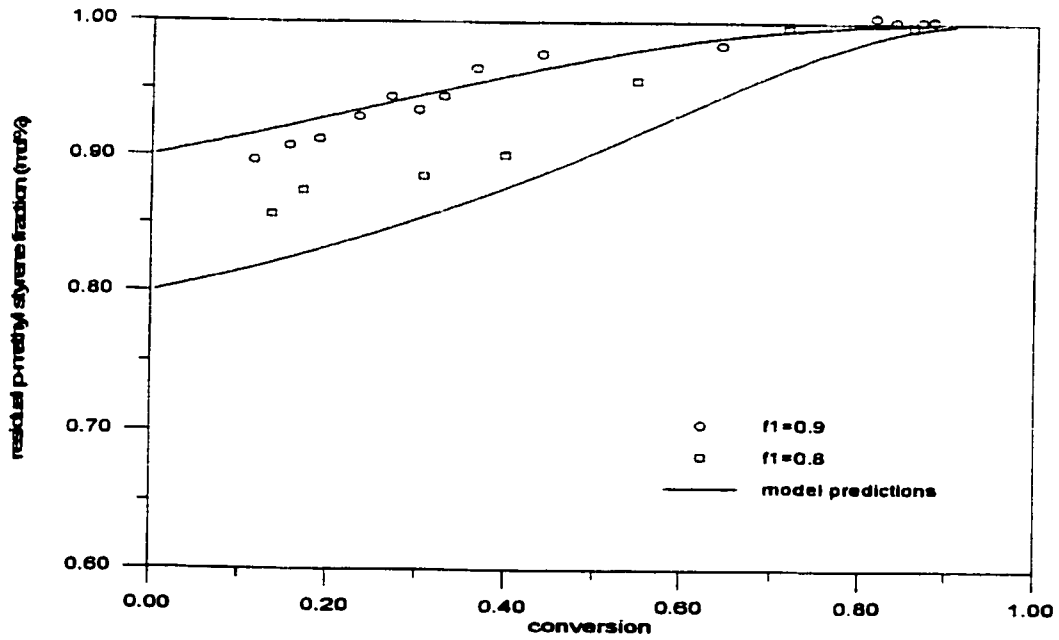

Figure 12.23 Simulation of Composition in AN/*p*-MSty Copolymerization in Bulk at 40°C. [AIBN]=0.01 mol/L

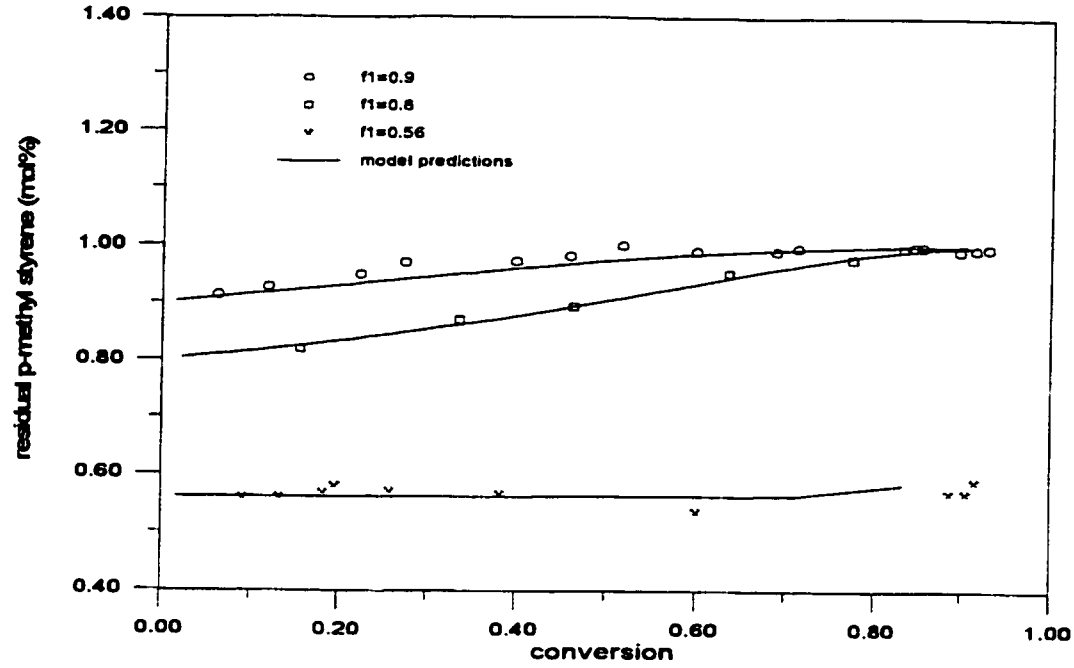

Figure 12.24 Simulation of Composition in AN/*p*-MSty Copolymerization in Bulk at 60°C. [AIBN]=0.01 mol/L

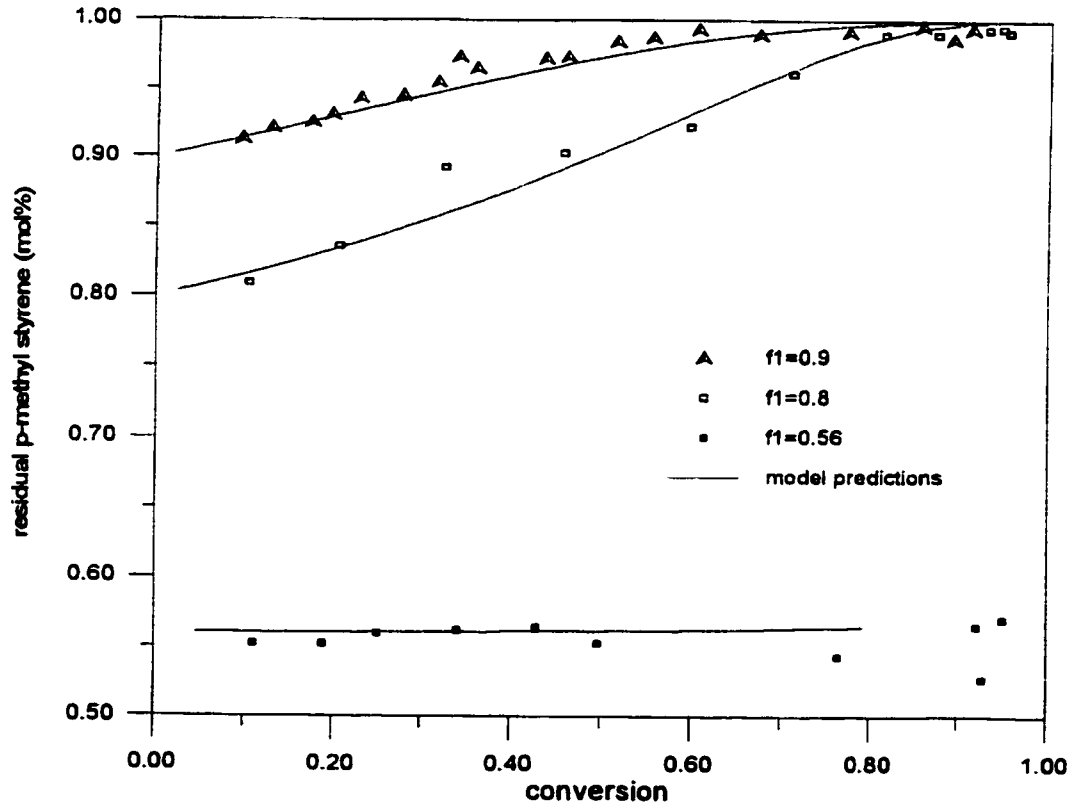

Figure 12.25 Simulation of Composition in AN/*p*-MSty Copolymerization in Bulk at 80°C. [AIBN]=0.01 mol/L

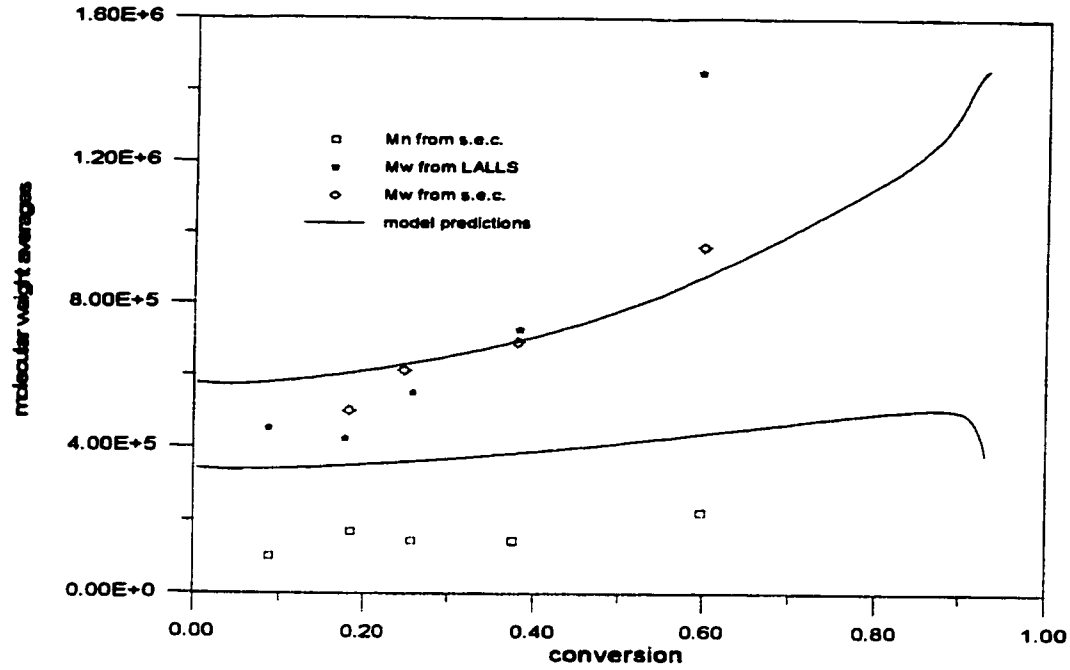

Figure 12.26 Simulation of Molecular Weight in AN/*p*-MSty Copolymerization in Bulk at 60°C. [AIBN]=0.01 mol/L, $f_{p\text{-MSty}}$=56 mol%.

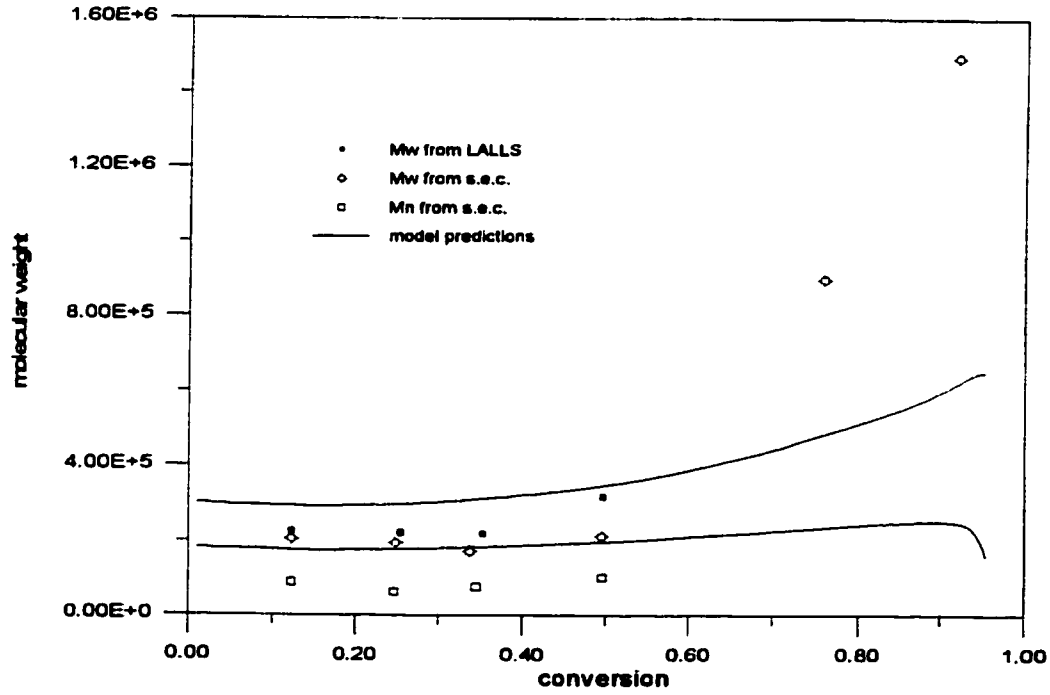

Figure 12.27 Simulation of Molecular Weight in AN/*p*-MSty Copolymerization in Bulk at 60°C. [AIBN]=0.05 mol/L, $f_{p\text{-MSty}}$=56 mol%.

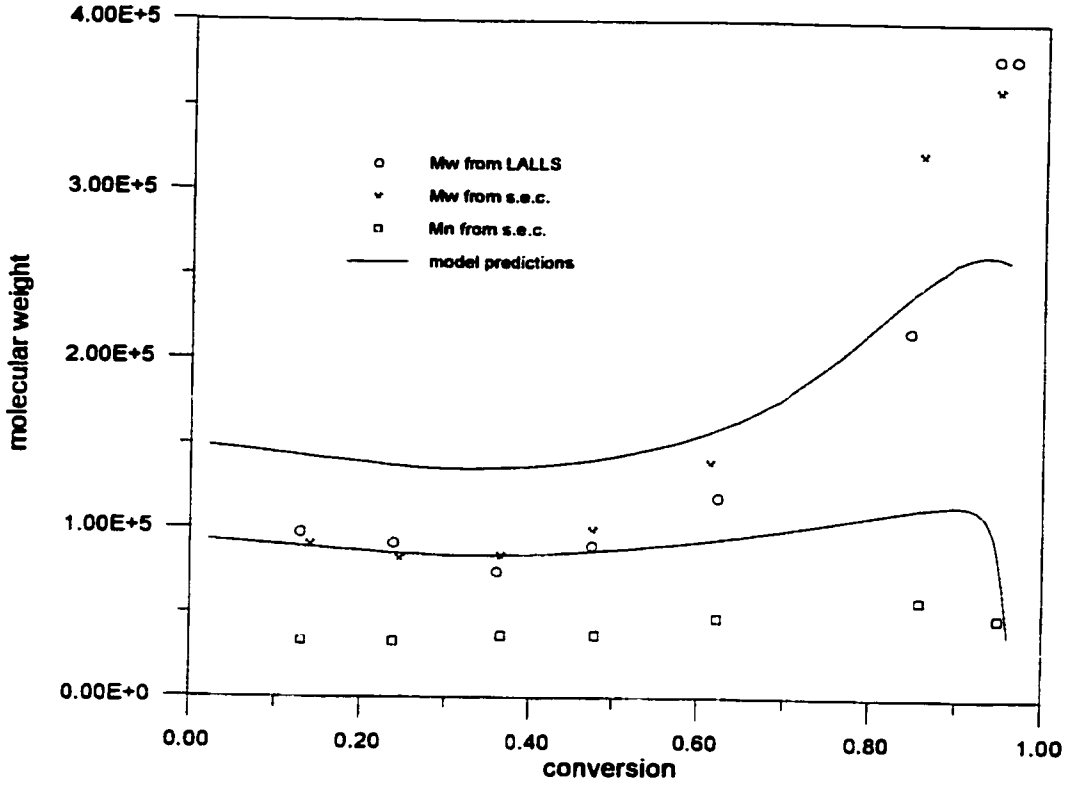

Figure 12.28 Simulation of Molecular Weight in AN/*p*-MSty Copolymerization in Bulk at 80°C. [AIBN]=0.01 mol/L, $f_{p\text{-MSty}}$=56 mol%.

Chapter 13. Simulation of Terpolymerization in Bulk and Solution.

Previous research effort was focused on the simulation of homo- and copolymerizations in bulk and solution. Model development and testing results have been summarized in the extensive papers by Gao and Penlidis (1996, 1998). The final step in our long-term project described before (Gao and Penlidis, 1996) is to simulate free-radical terpolymerization in bulk and solution. This paper gives an overview on model development and model testing for terpolymerizations. The development of this model and the accompanying simulator/database package marks the culmination of our work in the area of modelling multicomponent polymerizations with two significant points: (1) it is the first time in the open literature that simulation of free-radical terpolymerizations is published; and (2) the ultimate objective in our long-term project of developing a general simulation package which is able to simulate multicomponent polymerizations in bulk and solution has been achieved.

The simulation of terpolymerization is accomplished by applying the "pseudo-kinetic rate constant" method. The validity of this method has already been examined and demonstrated by Tobita and Hamielec (1991) and Xie and Hamielec (1993a-b), and further confirmed by our copolymerization model testing results (Gao and Penlidis, 1998). Similar to the model for homo- and copolymerization, free-volume theory was used to describe the kinetic behaviour of terpolymerization at high conversion levels. To test a model's reliability, experimental data are essential. Unfortunately, kinetic studies on terpolymerization are very limited, let alone full conversion range experimental data. The only full conversion range experimental data available in the literature have been generated in our own laboratory by Dube and Penlidis (1995a-b) as part of the effort of completing this long-term project. Butyl acrylate/methyl methacrylate/vinyl acetate (BA/MMA/VAc) has been selected as the terpolymer system to be investigated. The BA/MMA/VAc system is both extremely challenging (as shown by Dube and Penlidiss (1995a-b), due to extreme composition drift and the "double-rate phenomenon") and widely used commercially (yet not very well understood). Terpolymerizations of this system were conducted in both bulk and solution. Collected experimental data not only reconfirmed the "double-rate

phenomenon" observed earlier by Dube and Penlidis (1995b), but also revealed a strong solvent effect.

The same database developed for the copolymerization simulation package was used in all our terpolymerization simulations without any further changes. Such a unique database structure (for a detailed description of the database structure, see Gao and Penlidis, 1998) is of great advantage, since it enables one to simulate multicomponent polymerizations based on simple homopolymerization characteristics without the price of adding new parameters for each specific system. This makes the model and simulator very general in their applicability.

13.1 Brief Background on Terpolymerization.

Terpolymerization in bulk and solution involves three different monomers, hence there is a total of nine propagation reactions as shown below:

$$R_{r,1}\cdot + M_1 \xrightarrow{kp_{11}} R_{r+1,1}\cdot \qquad (13.1)$$

$$R_{r,1}\cdot + M_2 \xrightarrow{kp_{12}} R_{r+1,2}\cdot \qquad (13.2)$$

$$R_{r,1}\cdot + M_3 \xrightarrow{kp_{13}} R_{r+1,3}\cdot \qquad (13.3)$$

$$R_{r,2}\cdot + M_1 \xrightarrow{kp_{21}} R_{r+1,1}\cdot \qquad (13.4)$$

$$R_{r,2}\cdot + M_2 \xrightarrow{kp_{22}} R_{r+1,2}\cdot \qquad (13.5)$$

$$R_{r,2}\cdot + M_3 \xrightarrow{kp_{23}} R_{r+1,3}\cdot \qquad (13.6)$$

$$R_{r,3}\cdot + M_1 \xrightarrow{kp_{31}} R_{r+1,1}\cdot \qquad (13.7)$$

$$R_{r,3}\cdot + M_2 \xrightarrow{kp_{32}} R_{r+1,2}\cdot \qquad (13.8)$$

$$R_{r,3}\cdot + M_3 \xrightarrow{kp_{33}} R_{r+1,3}\cdot \qquad (13.9)$$

where kp_{11}, kp_{12}, kp_{13}, kp_{21}, kp_{22}, kp_{23}, kp_{31}, kp_{32} and kp_{33} are the propagation rate constants for

reactions 1 to 9, respectively. Subscripts 1, 2 and 3 used in the above reactions denote radical/monomer of type 1, 2 and 3. The so-called long chain approximation of type II (LCA II) used in copolymerization can equally be applied to terpolymerization and this would lead to the following assumptions,

$$kp_{12}[R_1\cdot][M_2] + kp_{13}[R_1\cdot][M_3] = kp_{21}[R_2\cdot][M_1] + kp_{31}[R_3\cdot][M_1] \qquad (13.10)$$

$$kp_{21}[R_2\cdot][M_1] + kp_{23}[R_2\cdot][M_3] = kp_{12}[R_1\cdot][M_2] + kp_{32}[R_3\cdot][M_2] \qquad (13.11)$$

$$kp_{31}[R_3\cdot][M_1] + kp_{32}[R_3\cdot][M_2] = kp_{13}[R_1\cdot][M_3] + kp_{23}[R_2\cdot][M_3] \qquad (13.12)$$

where $[R_i\cdot]$ denotes concentration of radicals of type i, and $[M_i]$ is the corresponding monomer concentration. Alfrey and Goldfinger (1944, 1946) were the first group to derive the instantaneous terpolymer composition for each monomer, given by:

$F_1 : F_2 : F_3 =$

$$f_1\left[\frac{f_1}{r_{31}r_{21}} + \frac{f_2}{r_{21}r_{32}} + \frac{f_3}{r_{31}r_{23}}\right]\left[f_1 + \frac{f_2}{r_{12}} + \frac{f_3}{r_{13}}\right]$$

$$: f_2\left[\frac{f_1}{r_{12}r_{31}} + \frac{f_2}{r_{12}r_{32}} + \frac{f_3}{r_{32}r_{13}}\right]\left[f_2 + \frac{f_1}{r_{21}} + \frac{f_3}{r_{23}}\right] \qquad (13.13)$$

$$: f_3\left[\frac{f_1}{r_{13}r_{21}} + \frac{f_2}{r_{23}r_{12}} + \frac{f_3}{r_{13}r_{23}}\right]\left[f_3 + \frac{f_1}{r_{31}} + \frac{f_2}{r_{32}}\right]$$

where f_i is the mole fractions of monomer of (free) monomer i in the reactor, F_i is the mole fraction of (bound) monomer i incorporated in the terpolymer, and r_{ij} denotes reactivity ratios. Equation 13.13 is commonly referred to as the Alfrey-Goldfinger equation.

In the literature, there is only a very limited number of papers published on terpolymerization kinetics. Most focus on verifying the validity of the Alfrey and Goldfinger equation. Rudin et al. (1973) estimated reactivity ratios for several terpolymer systems by using equation 13.13. They stated that the estimated reactivity ratios are not much different from those estimated in the corresponding copolymerization experiments, therefore the Alfrey and Goldfinger equation is

applicable to multicomponent polymerizations and it thus predicts experimental data (terpolymer composition at low conversion levels) reasonably well. Though Rudin et al.(1973) were probably the earliest group that estimated reactivity ratios directly based on the terpolymer equation, their estimates may contain errors as pointed out by Duever et al.(1983). Since Rudin et al.(1973) used a least squares method, instead of the more statistically sound error-in-variables-model (EVM) method, the confidence regions of their estimates are always smaller than those resulting from EVM and some of their point estimates are erroneous. Duever et al.(1983) reestimated reactivity ratios for the same terpolymer system using the EVM method. The advantages of using the EVM method have already been discussed widely in the last decade or so, hence they will not be reemphasized here again.

Chien and Finkenaur (1985) derived a simplified equation for instanteous terpolymer composition. Their equation is limited to systems in which the concentration of two monomers is much less than the third monomer. Apparently, such a limited expression can not be applied to terpolymer systems in general. Janovic et al.(1983) investigated acrylonitrile/styrene/tribromophenyl acrylate terpolymer system. Their measured terpolymer composition data agree with calculations from the Alfrey-Goldfinger's equation. More recently, Hocking and Klimchuk (1996) revisited the derivation of the instantaneous terpolymer composition equation. In their paper, they refined the derivation by arriving at a more symmetrical form. They illustrated the validity of their version of the terpolymer equation via numerical comparisons with previous versions. Based on our literature review, we can state that overall the Alfrey-Goldfinger equation (or its more recent refined versions) is still adequate for describing terpolymer composition.

In other publications concerning terpolymerizations, Tsuchida et al.(1974) looked at the system styrene/butyl methacrylate/methacrylic acid, with limited data in the low molecular weight region. Padwa and Schwier (1991) dealt with an efficient algorithm to solve the Alfrey-Goldfinger equation in an iterative way. Angelovici and Kohn (1991) investigated adhesive properties of ethyl acrylate/ethyl α-cyanocinnamate/styrene terpolymerized at 60°C to low conversion (less than 6%). Buback and Panten (1993) reported results on the high pressure, high temperature

terpolymerization of ethylene/acrylonitrile/vinyl acetate in a continuous tubular reactor and looked at the validity of reactivity ratio estimates. Engelmann and Schmidt-Naake (1993, 1994) investigated the influence of reactor type on chemical composition distributions for methyl methacrylate/styrene/maleic anhydride semi-batch reactors gave products with homogeneous properties, if appropriate operation feeding policies were applied. Shukla and Srivastava (1994) calculated reactivity ratios for solution terpolymerization of styrene/acrylonitrile/chromium acrylate and determined the glass transition temperature. Olaj and Schnoll-Bitai (1995) extended their work on penultimate schemes from copolymerization to terpolymerization, whereas Schoonbrood et al.(1995) argued on behalf of the penultimate effect for the terpolymerization of styrene/methyl methacrylate/methyl acrylate, studied via pulsed laser techniques. Finally, Chylla et al.(1997) looked at semi-batch flow scheduling strategies and related practical considerations for the terpolymerization of styrene/α-methyl styrene/acrylic acid.

As mentioned earlier, the general characteristic of all these literature references is that they mainly deal with terpolymer composition issues (related to the Alfrey-Goldfinger equation and/or modifications of it), without any complete attempts to look at terpolymerization kinetic behaviour over the full conversion range.

13.2 Mathematical Modelling of Terpolymerization

The fundamental mechanism of terpolymerization is not different from that of homo/copolymerization, therefore terpolymerization can be modelled in an analogous way. If radical reactivity is only determined by the terminal unit, then terpolymerization will have nine propagation rate constants and six corresponding reactivity ratios. The rate of polymerization can be expressed as:

$$Rp = -\frac{d[M_1]}{dt} - \frac{d[M_2]}{dt} - \frac{d[M_3]}{dt} = \sum_{i=1}^{3}\sum_{j=1}^{3} kp_{ij}[R_i][M_j] \qquad (13.14)$$

The pseudo-overall rate constant of propagation is

$$k_p = \sum_{i=1}^{3}\sum_{j=1}^{3} kp_{ij}\phi_i f_j \tag{13.15}$$

where ϕ_1, ϕ_2 and ϕ_3 are the mole fractions of radicals of type 1, 2 and 3, respectively. Unlike other groups in the literature, the instantaneous terpolymer composition can easily be obtained by using the equation below while avoiding using the more complicated Alfrey-Goldfinger equation.

$$F_1 : F_2 : F_3 = Rp_1 : Rp_2 : Rp_3 \tag{13.16}$$

where:

$$Rp_i = -\frac{d[M_i]}{dt} = \sum_{j=1}^{3} kp_{ji}\phi_j f_i \tag{13.17}$$

where i=1, 2, 3.

The kinetic scheme of copolymerization can easily be extended to terpolymerization without major modifications. More importantly, from a modelling point of view, the simulation of terpolymerization theoretically requires no additional information than needed to describe three copolymerization systems. This is extremely helpful since it implies that the simulation of a multicomponent polymerization can be obtained by utilizing the existing copolymerization database (Gao and Penlidis, 1998).

Simulation of Terpolymerization at High Conversion

In order to simulate terpolymerization over the entire conversion range, diffusion control must be tackled for termination, propagation and initiator efficiency. In a way similar to the simulation of copolymerization (Gao and Penlidis, 1998), the free volume approach (Marten and Hamielec 1982, Gao and Penlidis, 1996) was employed and further extended to cover terpolymerization. The expression for the free volume of the polymerizing system is the same as for copolymerizations, only extended to three monomers:

$$\begin{aligned} V_F = {} & [0.025+\alpha_p(T-T_{gp})](V_p/V_T) + [0.025+\alpha_s(T-T_{gs})](V_s/V_T) \\ & + \sum_{i=1}^{3} [0.025+\alpha_{m,i}(T-T_{gm,i})](V_{m,i}/V_T) \end{aligned} \tag{13.18}$$

In equation 13.18, T is the polymerization temperature, V_t is the total volume of the polymerizing mixture, α denotes the expansion coefficient, subscripts p, s and m refer to polymer, solvent and monomers (i=1,2,3), respectively, V is the volume of the different ingredients(p, s and m), and Tg denotes glass transition temperature for the different ingredients.

Note a lot of information can be found for the prediction of Tg_p, the glass transition temperature of the terpolymer being synthesized at some conversion level. From our previous investigations on Tg_p (Gao and Penlidis, 1998), the equation by Johnston (1969) was used and extended to the terpolymer case, as:

$$\frac{1}{Tg_p} = \sum_{i=1}^{3} \frac{w_i P_{ii}}{Tg_{pi}} + \frac{w_1 P_{12} + w_2 P_{21}}{Tg_{p_{12}}} + \frac{w_1 P_{13} + w_3 P_{31}}{Tg_{p_{13}}} + \frac{w_2 P_{23} + w_3 P_{32}}{Tg_{p_{23}}} \qquad (13.19)$$

In the above equation, Tg_{pi} is the glass transition temperature for homopolymer of monomer type i, $Tg_{p,ij}$ is the glass transition temperature of alternating copolymer of monomers i and j, w_i is the weight fraction of monomer i bound in the terpolymer chain and finally P_{ij} is the probability of forming a diad of monomer i and j. Equation 13.19 is analogous to the copolymer equation for Tgp (Gao and Penlidis, 1998) and hence requires no additional information. This enables one to simulate terpolymer Tg at any conversion level based on existing information for copolymer Tg from the same database. Equation 13.19 above, being a direct extension of Johnston's equation for copolymers, is a practical starting point.

Importance of Design of Experiments

Terpolymerizations are multivariable systems and hence involve many experimental factors that may be manipulated during experiments. These experimental factors have been discussed in detail in dube and Penlidis (1995a-b). Special care should be exercised when collecting data from such multivariable systems, and use of statistically sound techniques for the design and analysis of the experiments is of paramount importance. Very systematic approaches are indeed, such the ones described in Dube et al.(1996) and Dube and Penlidis (1996). In the former, an optimal sequential

design of experiments methodology is illustrated and applied to the BA/MMA/VAc system in bulk/solution/emulsion. In the latter, a hierarchical data analysis of a replicate experiment is described and discussed. Such hierarchical analyses are extrememly helpful complementary steps for any kinetic investigation of a reactive system. Detailed experimental procedures are given in Dube and Penlidis (1995a-b, 1996).

13.3 Results and Discussion

BA/MMA/VAc Terpolymerization in Bulk

As discussed previously, simulation of terpolymerization can be obtained by utilizing the existing copolymerization database without any additional changes. This is of great advantage from a modelling point of view. It implies that if one can simulate copolymerizations of BA/MMA, MMA/VAc and BA/VAc satisfactorily, he/she should be able to simulate terpolymerization equally well without adjusting any database items. Such characteristics are both beneficial and challenging. All model predictions shown below are obtained based on the copolymerization simulation package database without any further tuning. The feed composition ratio is 30/30/40 wt% BA/MMA/VAc.

Figure 13.1 shows one run at 50°C. It is apparent that there was an acceleration effect starting at about 60% conversion. Similar to copolymerization of BA/VAc and MMA/VAc, there was a severe composition drift in this run as shown in figure 13.2. At the early stage of the reaction, there was little vinyl acetate being incorporated into the terpolymer chain, thus the terpolymerization at this stage was more like a copolymerization of BA and MMA in a VAc solution. After about 60% conversion, the majority of BA and MMA were consumed and vinyl acetate dominated the reaction. Due to the high kp of vinyl acetate, the rate of polymerization increased considerately. At high conversion level, vinyl acetate dominated the reaction, and this trend was confirmed by the composition profile displayed in figure 13.2. The accumulated terpolymer composition of BA and MMA decreased drastically while the vinyl acetate content increased. This unique "two-stage" kinetic characteristic exhibited by BA/MMA/VAc was

described satisfactorily by the model. Such agreement indicates: (1) the assumption that simulation of terpolymerization can be obtained by extending the kinetic mechanism of copolymerization is justified; (2) terpolymerization can be described adequately by utilizing information for the three corresponding copolymer systems; (3) the model database for BA/MMA, BA/VAc, and MMA/VAc copolymers is reliable.

Figure 13.3 is the simulation of molecular weight averages for the same run. It should be noted that due to the lack of an accurate value for the refractive index increment (dn/dc) for this specific terpolymer system, the measurements should be considered as a general trend of the molecular weight averages profile rather than exact values. Overall, the molecular weight averages for this run are satisfactorily described by the model.

Figure 13.4 displays a run at 50°C but at a higher initiator concentration. The initiator concentration effect is obvious: the same terpolymer system reached about 80% conversion within 10 hours compared to more than 20 hours in figure 13.1. Also, the higher level of initiator concentration brought down both molecular weight averages (see figure 13.5). The "two-stage" phenomenon was also observed in this run. The terpolymer composition profile displayed in figure 13.6 has confirmed the severe terpolymer composition drift. In all cases, the model delivered reliable predictions.

Two runs including one replica were performed at a higher temperature level (70°C) and the conversion results are displayed in figure 13.7. Large discrepancies in the mid- and high conversion range between model predictions and experimental data (conversion) were observed. Certain troubleshooting was conducted to explain such a disagreement. Based on the simulation results on copolymerization of the three corresponding copolymers and on terpolymerization of this system at a lower temperature level, it is confirmed that the model's database was reliable. The actual experimental points might be the culprit. Dube and Penlidis (1995b) observed that "... some samples were surrounded by a lower viscosity liquid". It was believed that the terpolymer at the center of the ampoule had a higher conversion due to a higher temperature level. This was

a clear indication of non-isothermality. To take the non-isothermality into account, the same run was simulated under non-isothermal conditions. A new prediction is presented in figure 13.8, and very satisfactory results are achieved. Simulations for both terpolymer composition and molecular weight averages are presented in figures 13.9 and 13.10, respectively. The agreement between model predictions and experimental data is good.

Model testing results on the bulk run conducted at high temperature and high initiator level (70°C, 0.071 mol/L) are displayed in figures 13.11 to 13.13. The agreement between model predictions and experimental data in general is good. In figure 13.11, some discrepancies were observed around 70% conversion level. It was noted that the discrepancies appeared at the peak of the gel effect, and again some nonisothermality might have actually occurred. It was also observed in all runs that the weight average molecular weight increased significantly at high conversion levels, especially in the high temperature runs. This trend indicates that the gel effect results in higher weight average molecular weight. Another reason for this dramatic increase is that since vinyl acetate dominated the late stage of the polymerization, there could be considerable transfer to polymer reactions taking place, which leads to higher weight average molecular weight. In all cases, the simulation of molecular weight averages was good.

So far the simulation of terpolymerization in bulk has been satisfactory. The severe composition drift as well as the "two-stage" phenomenon were observed in all runs. For all runs, the model consistently delivered reliable predictions on conversion, composition and molecular weight averages.

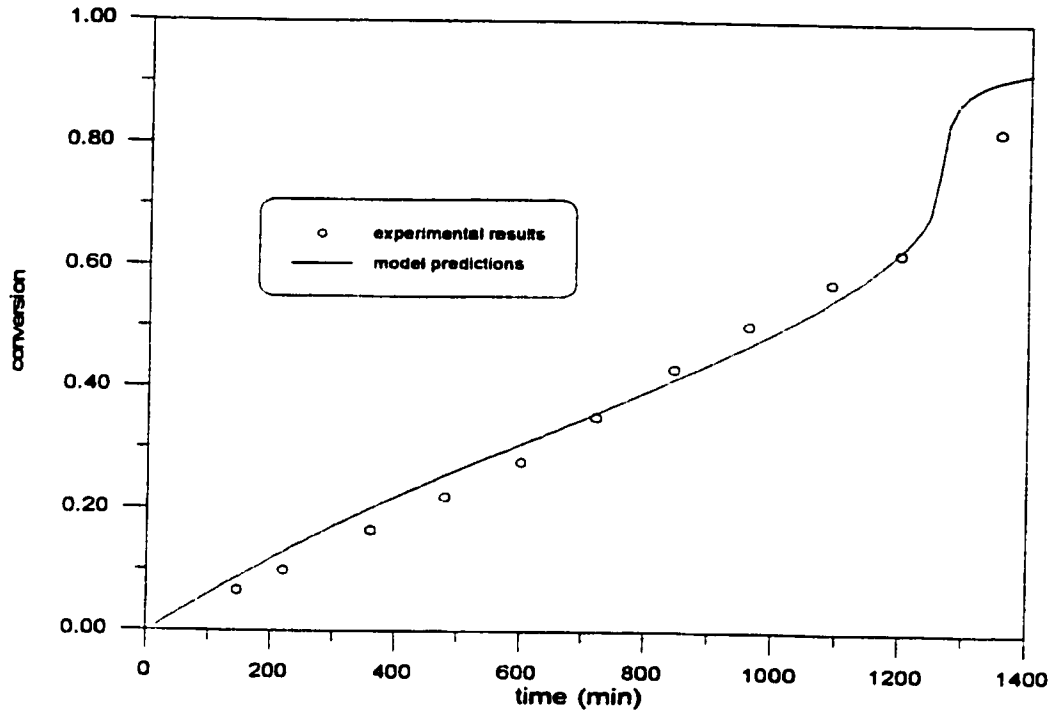

Figure 13.1 Simulation of BA/MMA/VAc Terpolymerization in Bulk at 50°C. [AIBN]=0.01 mol/L

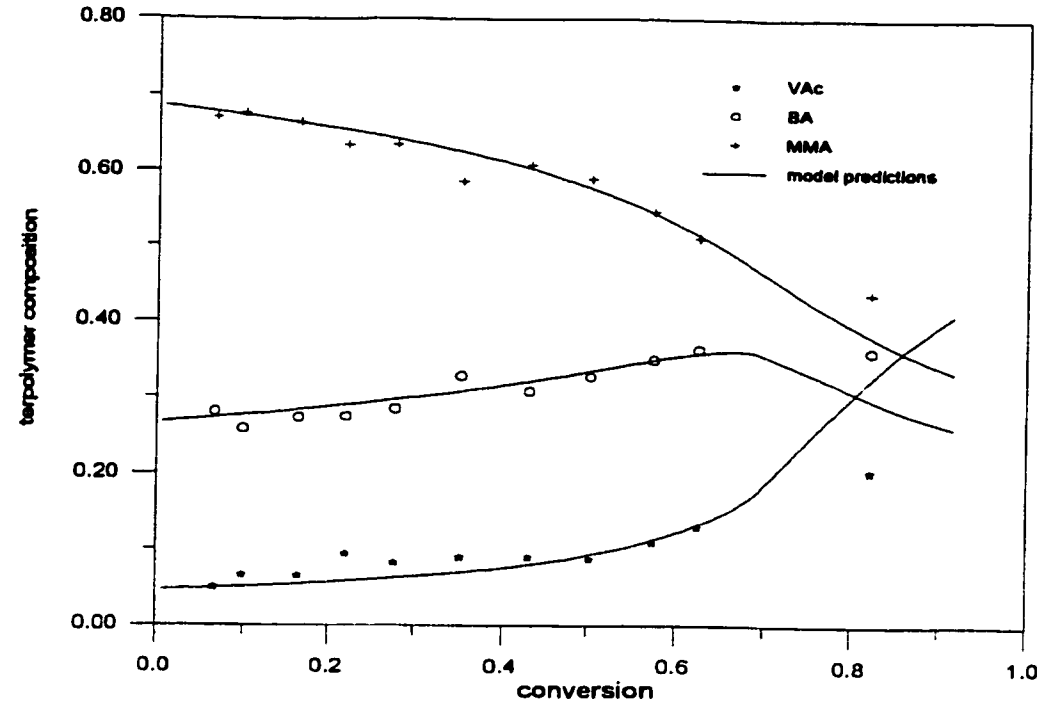

Figure 13.2 Simulation of Terpolymer Composition in BA/MMA/VAc Terpolymerization in Bulk at 50°C. [AIBN]=0.01 mol/L

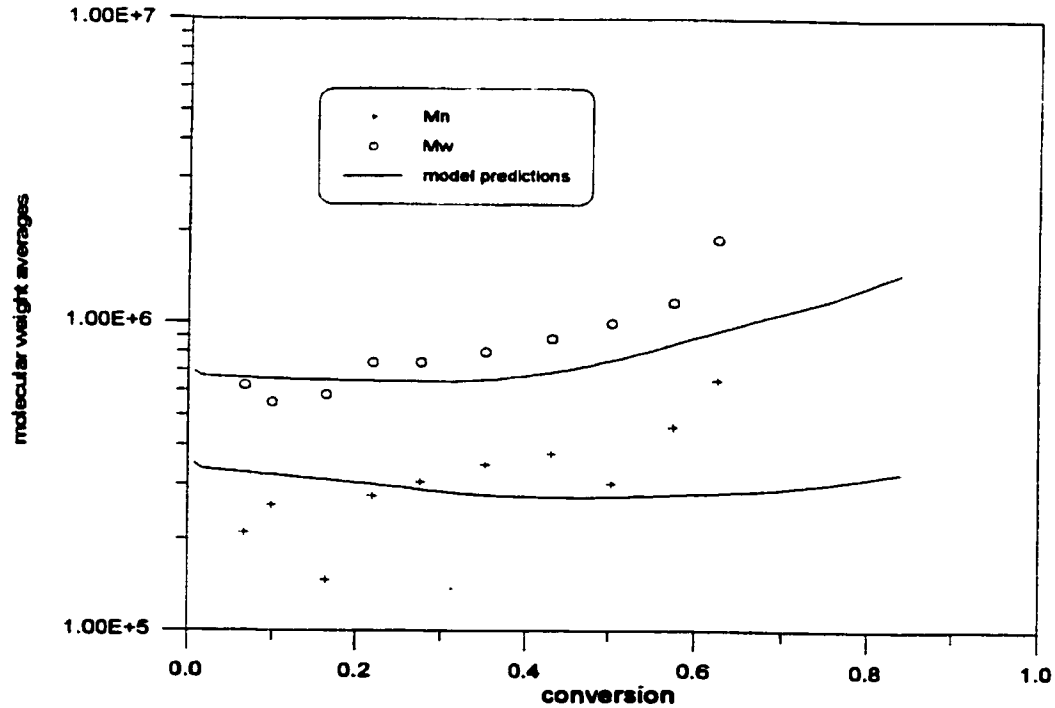

Figure 13.3 Simulation of Molecular Weight Average in BA/MMA/VAc Terpolymerization in Bulk at 50°C. [AIBN]=0.01 mol/L

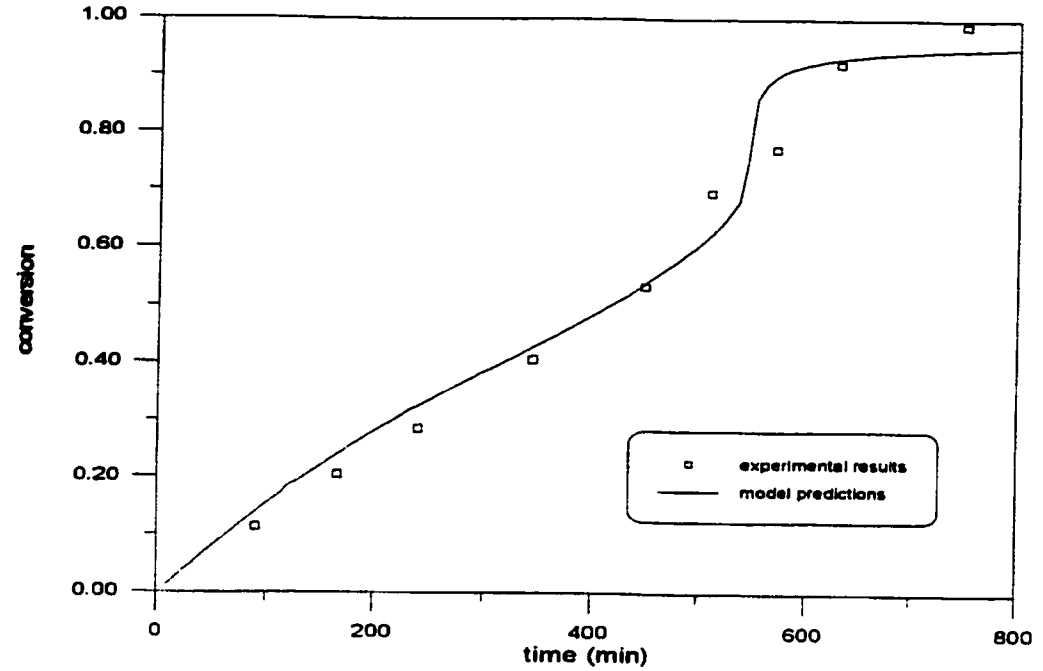

Figure 13.4 Simulation BA/MMA/VAc Terpolymerization in Bulk at 50°C. ([AIBN]: 0.071 mol/L)

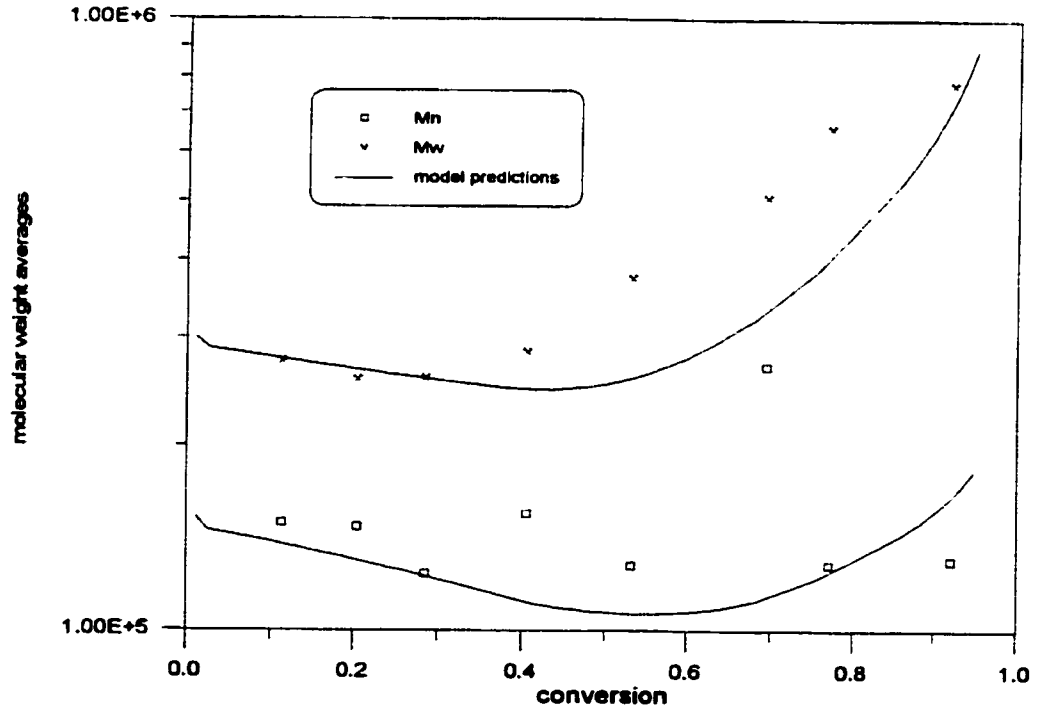

Figure 13.5 Simulation of Molecular Weight Average BA/MMA/VAc Terpolymerization at 50°C. ([AIBN]: 0.071 mol/L)

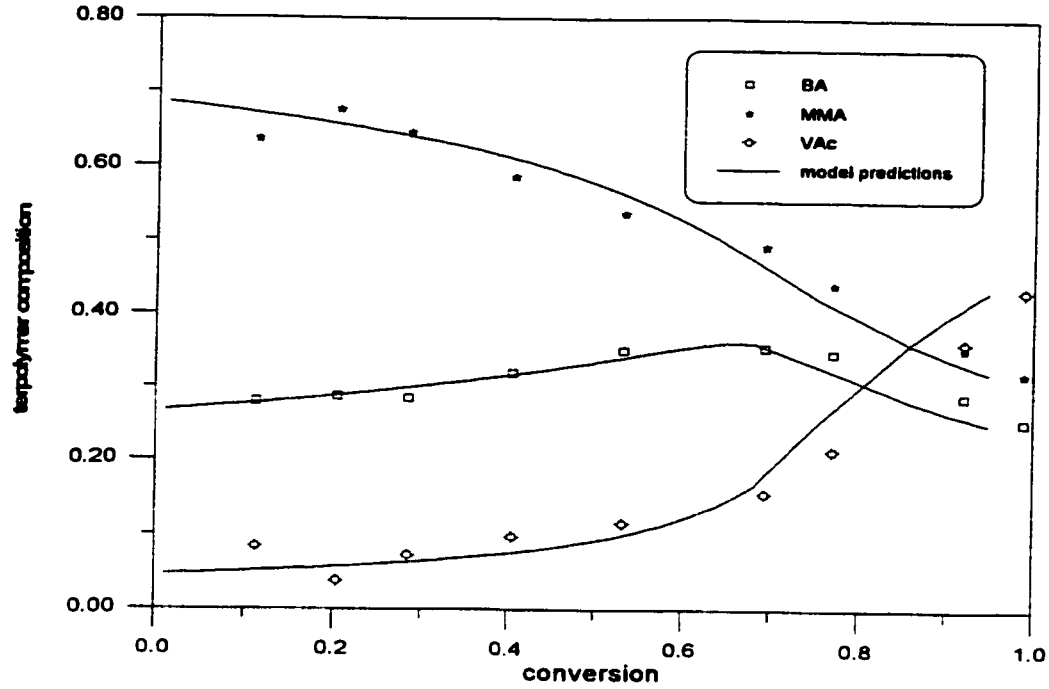

Figure 13.6 Simulation of Terpolymer Composition in BA/MMA/VAc Terpolymerization at 50°C. ([AIBN]: 0.071 mol/L)

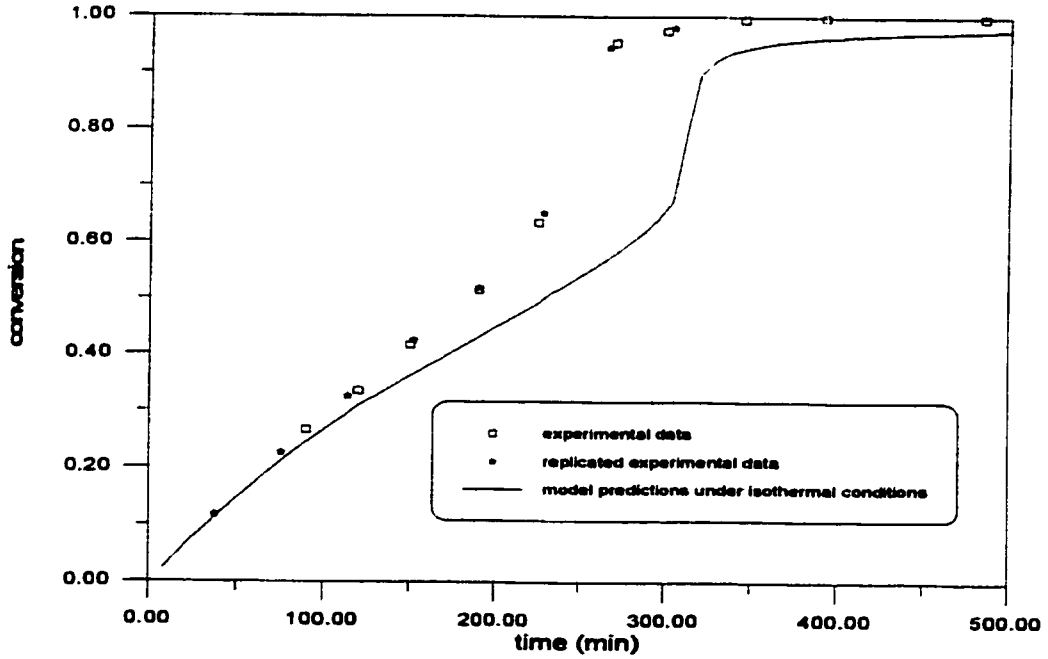

Figure 13.7 Simulation of BA/MMA/VAc Terpolymerization in Bulk at 70°C. [AIBN]=0.01 mol/L

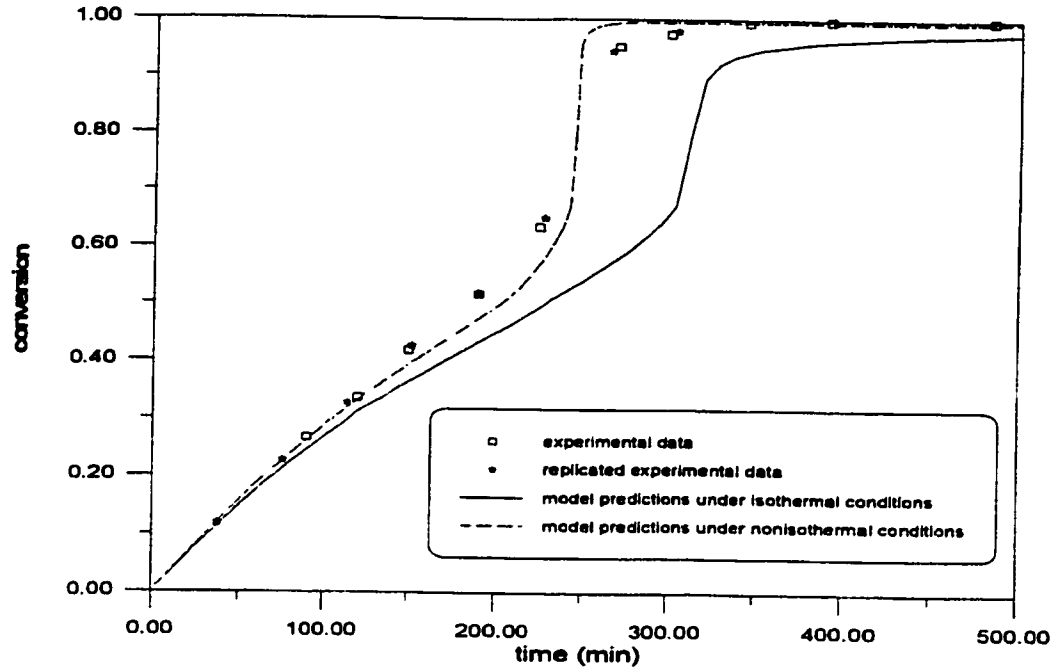

Figure 13.8 Simulation of BA/MMA/VAc Terpolymerization in Bulk at 70 °C. [AIBN]=0.01 mol/L

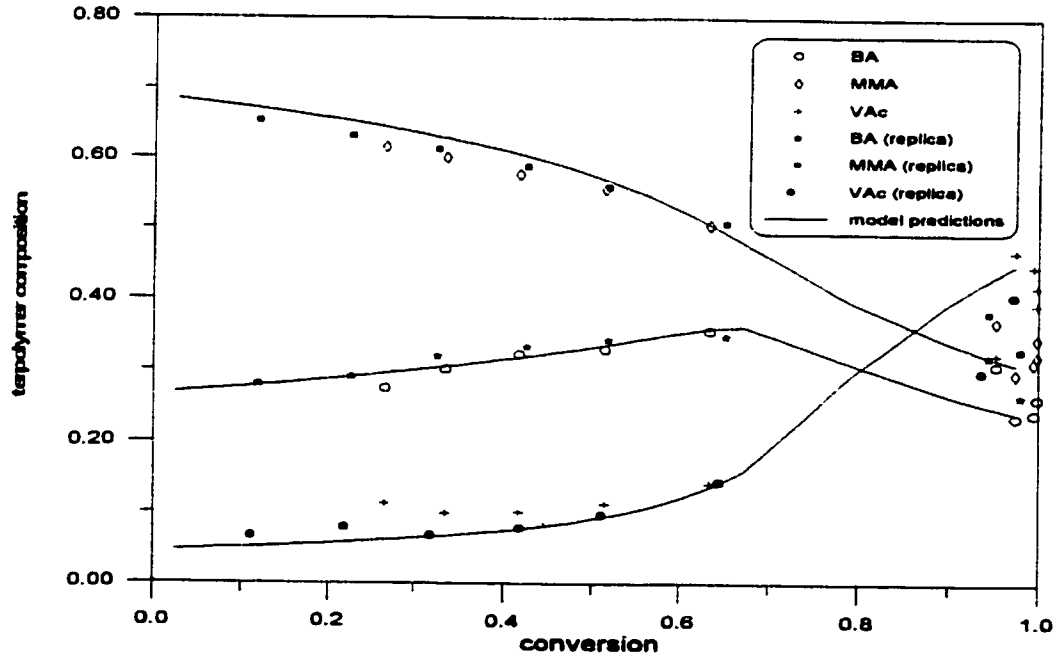

Figure 13.9 Simulation of Terpolymer Composition of BA/MMA/VAc Terpolymerization in Bulk at 70°C. [AIBN]= 0.01 mol/L

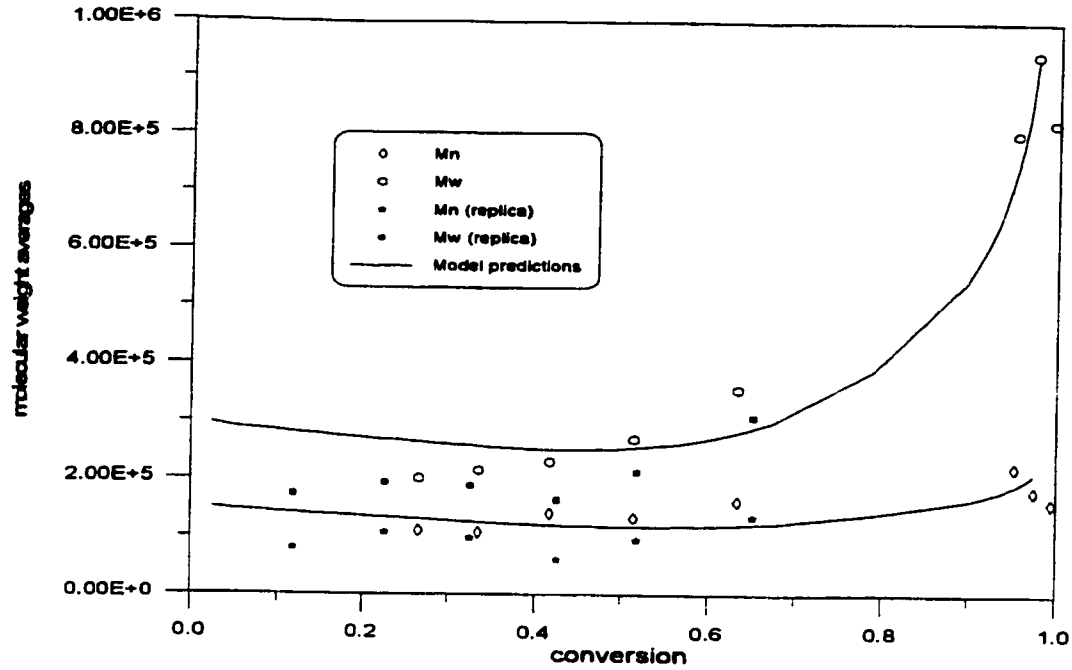

Figure 13.10 Simulation of Molecular Weight Averages of BA/MMA/VAc Terpolymerization in Bulk at 70°C. [AIBN]= 0.01 mol/L

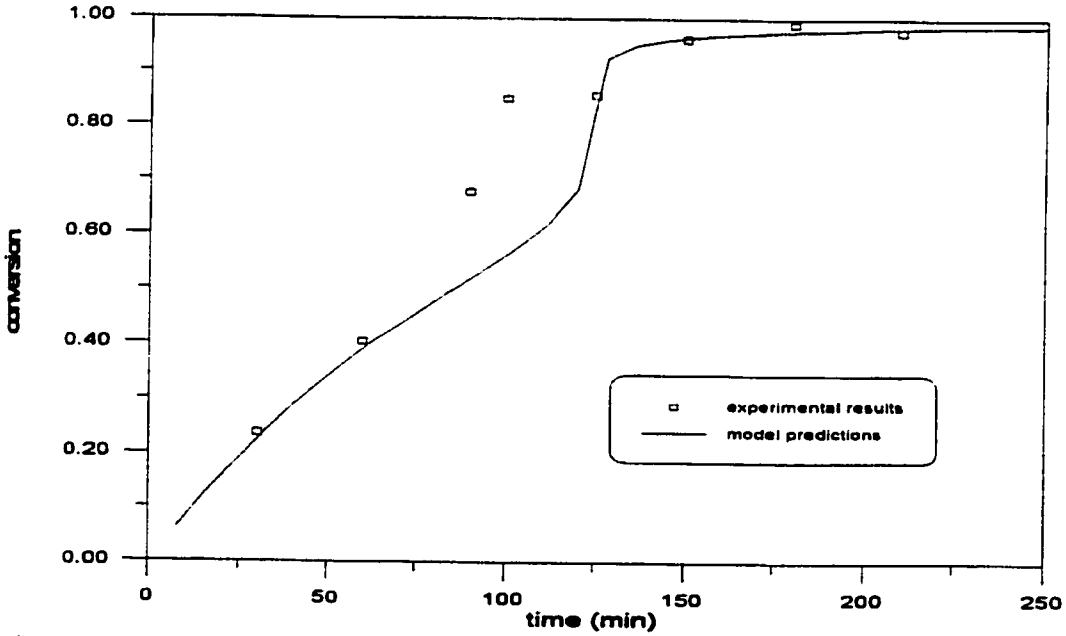

Figure 13.11 Simulation of Molecular Weight Averages of BA/MMA/VAc Terpolymerization in Bulk at 70°C. [AIBN]= 0.071 mol/L

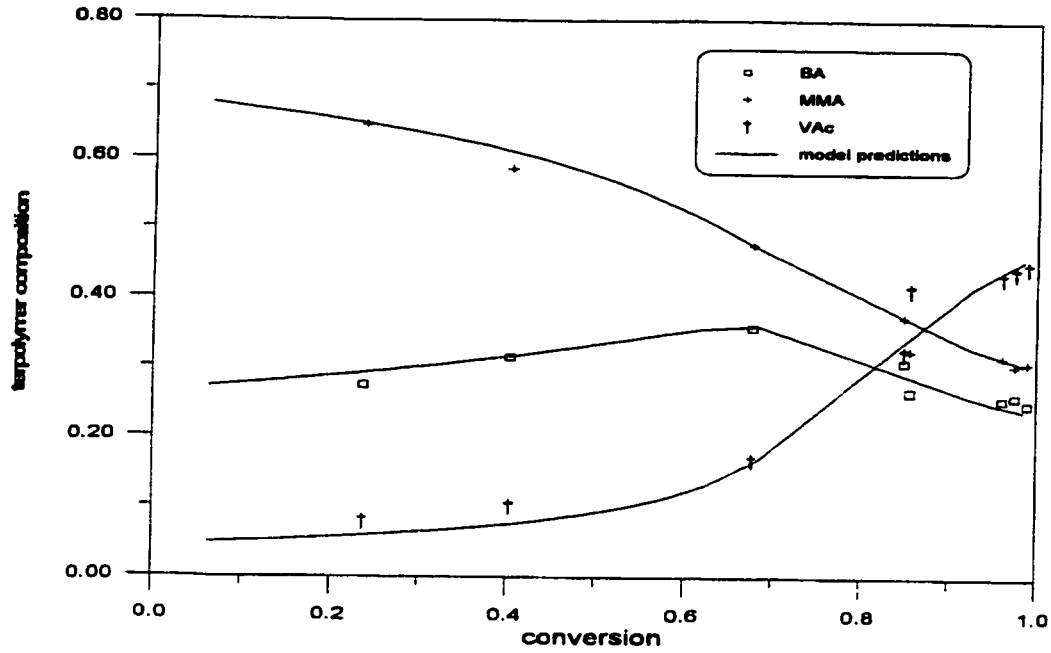

Figure 13.12 Simulation of Terpolymer Composition of BA/MMA/VAc Terpolymerization in Bulk at 70°C. ([AIBN]: 0.071 mol/L)

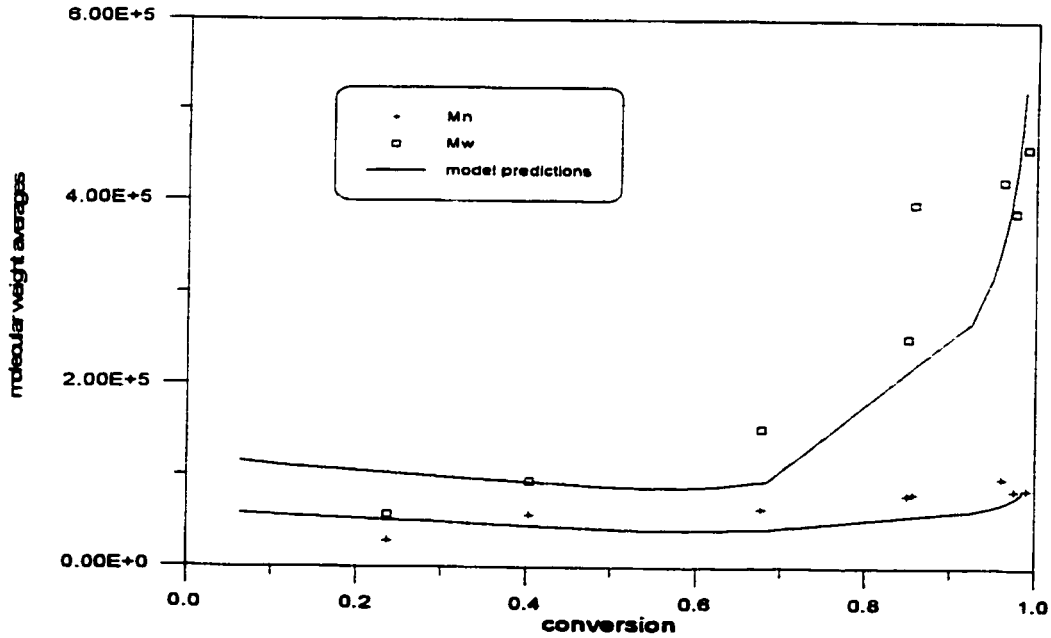

Figure 13.13 Simulation of Molecular Weight Averages of BA/MMA/VAc Terpolymerization in Bulk at 70°C. [AIBN]= 0.071 mol/L

BA/MMA/VAc Terpolymerization in Toluene

BA/MMA/VAc terpolymerization was also conducted in toluene at 70°C. The same monomer feed ratio and 40wt% toluene in the mixture was used in this run. As can be seen in figure 13.14, the overall rate of polymerization was much slower than its bulk counterpart (compare with figure 13.11). The model predictions for the conversion profile were in good agreement with the data up to 60% conversion, but afterwards, the model predicted a much faster rate of polymerization than actually observed in the run. Such a large discrepancy was never present in the bulk run simulations.

The simulation of terpolymer composition was inspected next. As expected, the presence of toluene did not appear to affect terpolymer composition, and the same trend, i.e., severe composition drift, was apparent after 60% conversion as shown in figure 13.15. It was obvious again that before 60% conversion, the reaction was dominated by copolymerization of BA and MMA, and at the late stage of the reaction, the terpolymerization was dominated by vinyl acetate. Based on the fact that there was a good agreement between model predictions and measured conversion data at the early stages of the run, it was reasonable to think that the large discrepancy could be mainly attributed to vinyl acetate polymerization. Toluene was suspected to have a profound effect on vinyl acetate polymerization. To confirm this suspicion, the rate constant of propagation for vinyl acetate was subsequently readjusted to take the solvent effect into account (Gao and Penlidis, 1996). The new model predictions were in a much better agreement as demonstrated in figure 13.16. The presence of toluene not only alleviated the gel effect significantly but also slowed down the rate of polymerization of vinyl acetate considerably.

More evidence can be obtained via the simulation of weight-average molecular weight in figure 13.17. If there were no solvent effect from toluene, the model would predict an increase in the weight average molecular weight as observed in all the bulk runs. However, experimental data did not support such a prediction. As displayed in figure 13.17, the weight average molecular weight remained low at the end of reaction, typical of the behaviour in solution polymerization. The new predictions given by the model using the readjusted rate constant of propagation were

in a much better agreement with the actual experimental data.

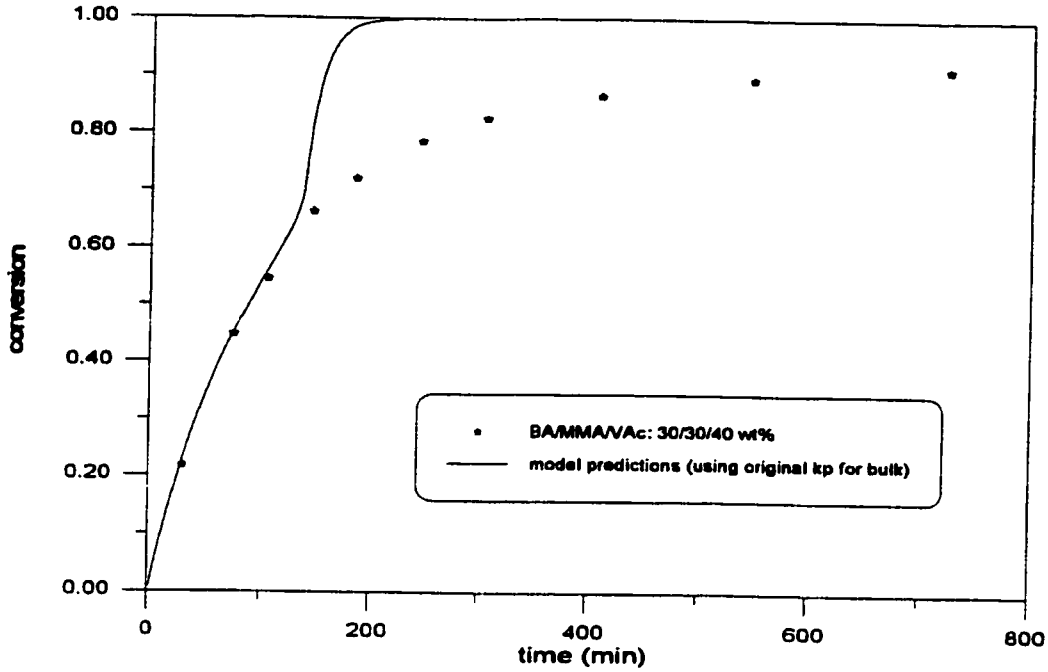

Figure 13.14 Simulation of BA/MMA/VAc Terpolymerization in Toluene at 70°C. [AIBN]=0.071 mol/L

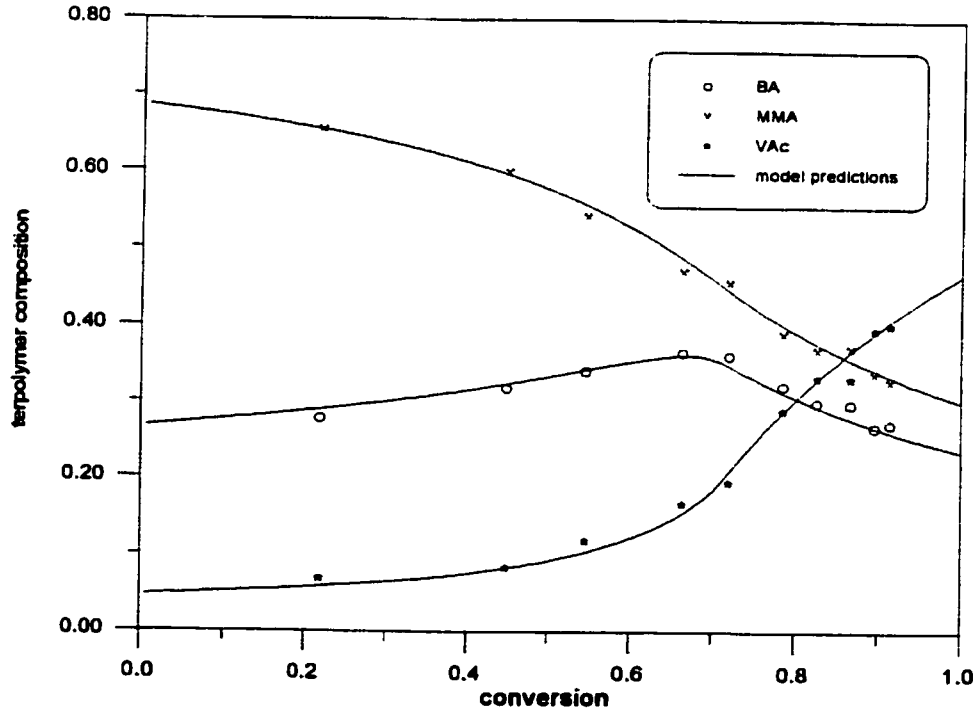

Figure 13.15 Simulation of Composition Drift in BA/MMA/VAc Terpolymerization in Toluene at 70°C. [AIBN]=0.071 mol/L

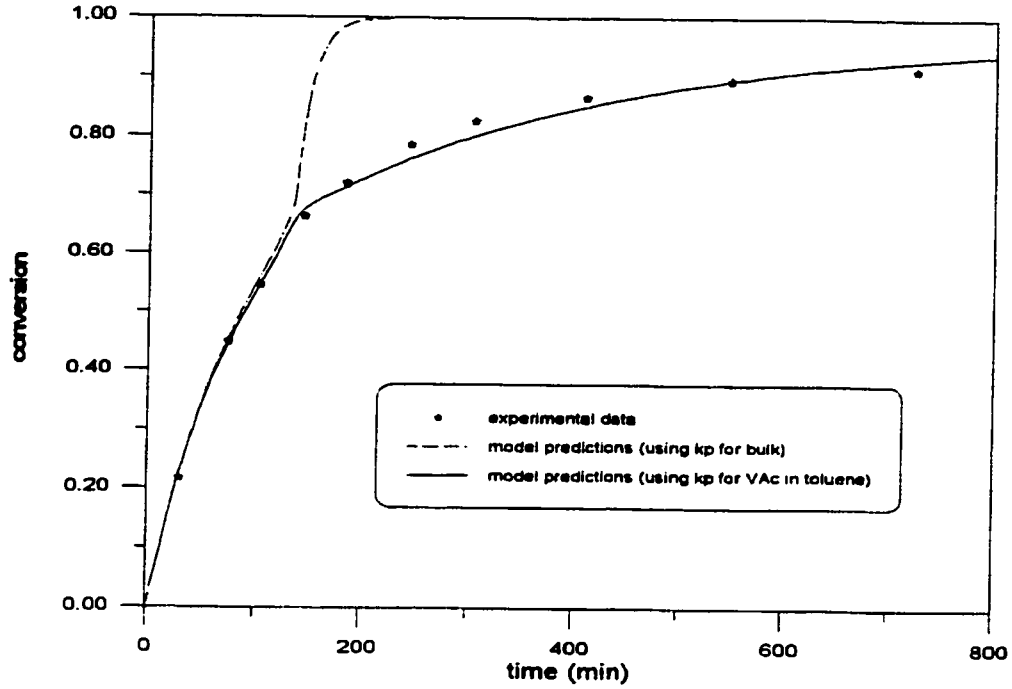

Figure 13.16 Simulation of BA/MMA/VAc Terpolymerization Rate in Toluene at 70°C. [AIBN]=0.071 mol/L

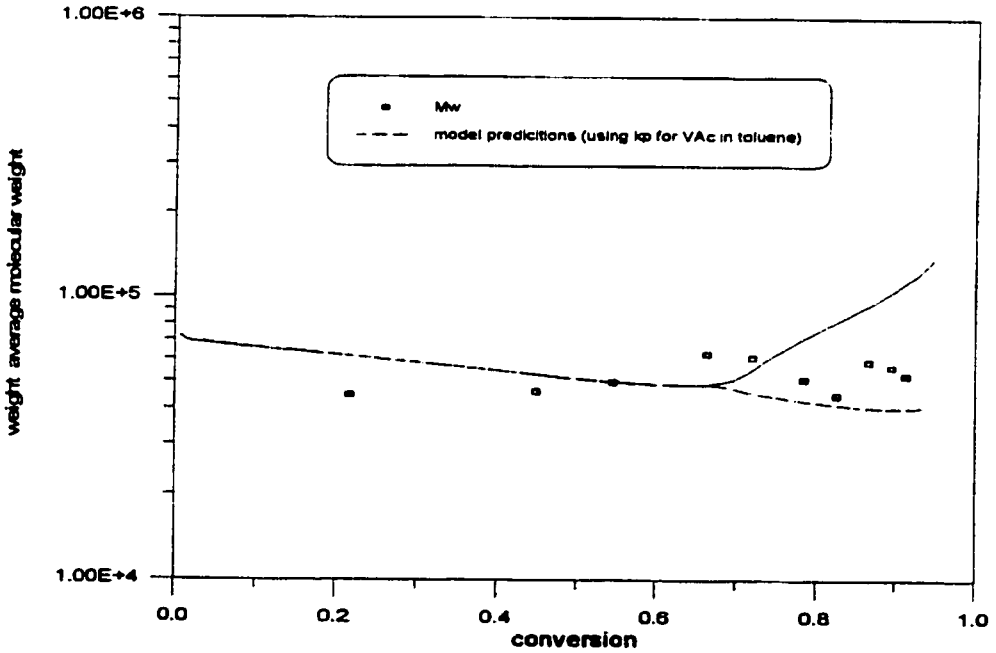

Figure 13.17 Simulation of Weight-Average Molecular Weight in BA/MMA/VAc Terpolymerization in Toluene at 70°C. [AIBN]=0.071 mol/L

References on Bulk/Solution (Volume 1)

Achilias D. S. and Kiparissides C. (1987) Mathematical Modelling of Thermal Copolymerization of Styrene/*p*-MethylStyrene. *Polym. Proc. Eng.* **5**, 23-36.

Achilias D. S. and Kiparissides C. (1992) Towards the Development of a General Framework for Modelling Molecular Weight and Compositional Changes in Free-Radical Copolymerization Reactions. *J. Macromol. Sci. Revs. Chem. Phys.* **C32**, 183-234.

Aerdts A. M., German A. L. and van der Velden G. P. M. (1994) Determination of the Reactivity Ratios, Sequence Distribution and Stereoregularity of Butyl Acrylate - Methyl Methacrylate Copolymers by Means of Proron and Carbon-13 NMR. *Magnetic Resonance in Chemistry* **32**, 80-88.

Alfrey T. and Goldfinger G. (1944) The Mechanism of Copolymerization. *J. Chem. Phys.* **12**, 205-209.

Alfrey T. and Goldfinger G. (1944) *J.Chem.Phys.* Copolymerization of Systems of Three and More Components. **12**, 322-322.

Alfrey T. and Goldfinger G. (1946) *J.Chem.Phys.* Copolymerization of Systems Containing Three Components. **14**, 115-116.

Allen P. E. M. and Patrick C. R. (1974) *Kinetics and Mechanisms of Polymerization Reactions.* John Wiley&Sons, New York, London, Syndey, Toronto.

Angelovici M.E. and Kohn D.H.(1991). Terpolymerization Studies: IV. Terpolymerization of Ethyl Acrylate, Ethyl α-Cyanocinnamate, and Styrene. *J.Appl.Polym.Sci.* **42**, 1121-1124.

Arias C., Lopez-Gonzalez M. M., Fernandez-Garcia M., Barrales-Rienda J. M. and Madruga E. L. (1993) Free-Radical Copolymerization of Methyl Acrylate with Methyl Methacrylate in Benzene Solution. *Polymer* **34**, 1786-1789.

Arita K., Ohtomo T. and Tsurumi Y. (1981) Analysis of the Monomer Sequence Distribution in Alternating Acrylonitrile-Styrene Copolymers by ^{13}C-NMR. *J. Polym. Sci. Polym. Lett.* **19**, 211-216.

Arranz F., Sanchez-Chaves M. and Molinero A. (1984) Sequence Distribution and Glass Transition of Vinyl Alcohol/n-Alkyl Vinyl Carbonate Copolymers. *Makromol. Chem.* **185**, 2153-2159.

Arriola D. J. (1989) PhD Thesis, Dept. of Chemical Engineering, University of Wisconsin.

Asakura J. I., Yoshihara M., Matsubara Y. and Maeshima T. (1981) Effect of Solvent on the Radical Copolymerizability of Styrene with Acrylonitrile. *J. Macromol. Sci. Chem.* **A15**, 1473-1478.

Atherton J. N. and North A. M. (1962) Diffusion-Controlled Termination in Free Radical Copolymerization. *Trans. Faraday. Soc.* **58**, 2049-2057.

Balaraman K. S. (1982) Comments on the Kinetic Mechanism of Free Radical Bulk Copolymerization of Styrene-Methyl Methacrylate. *Polymer* **23**, 1245-1246.

Balaraman K. S., Kulkarni B. D. and Mashelkar R. A. (1983) Bulk Copolymerization of Styrene-Acrylic Esters: Some Analysis and Design Considerations. *Polym. Eng. Sci.* **23**, 719-725.

Balaraman K. S., Kulkarni B. D. and Mashelkar R. A. (1986) Nonisothermal Bulk Copolymerization of Styrene and Methyl Methacrylate in a CSTR: Multiplicity and Stability Analysis. *J. Appl. Polym. Sci.* **31**, 885-900.

Balke S., Garcia-Rubio L. and Patel R. (1982) Conversion Prediction in High Conversion Free-Radical Polymerizations. *Polym. Eng. Sci.* **22**, 777-787.

Bamford C. H. and Basahel S. N. (1980) Moderated Copolymerization. Part 4.--- Penultimate Unit Effect in Chain-Transfer: System Styrene/Methyl Methacrylate/1-Butane Thiol. *J. Chem. Soc. Faraday. I.* **76**, 107-111.

Barton J. M. (1970) Relation of Glass Transition Temperature to Molecular Structure of Addition Copolymers. *J. Polym. Sci. Part C.* **30**, 573-597.

Bataille P. and Bourassa H. (1989) Determination of the Reactivity Parameters for the Copolymerization of Butyl Acrylate with Vinyl Acetate. *J. Polym. Sci. Chem.* **27**, 357-365.

Beevers R. B. (1962) Physical Properties of Vinyl Polymers. Part 4. - Glass-Transition Temperature of Methyl Methacrylate + Styrene Copolymers. *Trans. Faraday Soc.* **58**, 1465-1472.

Beevers R. B. and White E. F. T. (1960) Physical Properties of Vinyl Polymers. Part 2. - The Glass-Transition Temperature of Block and Random Acrylonitrile + Methyl Methacrylate Copolymers. *Trans. Faraday Soc.* **56**, 1529-1534.

Beevers R. B. and White E. F. T. (1963) A Note on the Glass-Transition Temperatures of Acrylonitrile + Styrene Copolymers. *Polymer Lett.* **1**, 171-176.

Beldie C., Onu A., Bourceanu G. and Poinescu I. C. (1985) Glass Transition Temperatures of Some Copolymers of Styrene with Methyl Methacrylate Using DTA and Chromatographic Data.

Eur. Polym. J. **21**, 321-323.

Bevington J. C., Melville H. W. and Taylor R. P. (1954) The Termination Reaction in Radical Polymerizations. II. Polymerizations of Styrene at 60°C and of Methylate at 0 and 60°C, and the Copolymerization of These Monomers at 60°C. *J. Polym. Sci.* **XIV**, 463-476.

Bevington J. C. and Harris D. O. (1967) Reactivity of Acrylates and Methacrylates. *Polymer Lett.* **5**, 799-802.

Bhattacharya D. and Hamielec A. E. (1985) Thermal Copolymerization of Styrene/*p*-Methylstyrene at High Conversion and Temperatures. *Polym. Proc. Eng.* **3**, 219-246.

Bhattacharya D. and Hamielec A. E. (1986) Bulk Thermal Copolymerization of Styrene/p-Methylstyrene: Modelling Diffusion-Controlled Termination and Propagation Using Free-Volume Theory. *Polymer* **27**, 611-618.

Blackley C. D., Andries S. and Sebastian R. D. (1987) Influence of Surfactant Type and Purity upon Emulsion Copolymerization of Styrene and Acrylic Acid. *Brit. Polym. J.* **19**, 25-30.

Blanks R. F. and Shah B. N. (1976) Kinetics of Bulk Polymerization of Styrene-Acrylonitrile Copolymers. *J. Polym. Sci. Chem.* **14**, 2589-2593.

Bonta G., Gallo B. M. and Russo S. (1975) Chemical Reactivity and Conformational Properties of Growing Chains. *J. Chem. Soc. Faraday Trans.* **71**, 1727-1732.

Borchardt J. K. (1982) Steric and Electronic Effects of Alkyl Substituents on Reactivity Ratios in Copolymerization Reactions of Acrylates and Methacrylates. *Polymer Prep.* **23**, 209-211.

Boudevska H. and Todorova O. (1985) The Influence of Molecular Interaction on Polymerization. 10a. On the Copolymerization of Methacrylic Acid and Styrene. *Makromol. Chem.* **186**, 1711-1720.

Box M. J. (1970) Improved Parameter Estimation. *Technometrics* **12**, 219-229.

Bradbury J. H. and Melville H. W.,F.R.S. (1954) The Co-Polymerization of Styrene and Butyl Acrylate in Benzene Solution. *Proc. Roy. Sci. (London)* **A222**, 456-470.

Brar A. S. and Kapur G. S. (1988) Sequence Determination in Styrene-Methyl Methacrylate Copolymers by ^{13}C NMR Spectroscopy. *Polymer J.* **20**, 371-376.

Brar A. S., Sunita and Satyanarayana C. V. V. (1992) Microstructure Determination of Styrene-Butyl Acrylate Copolymers by NMR Spectroscopy. *Polymer J.* **24**, 879-887.

Brar A. S. and Sunita (1992) Determination of Microstructure and Glass-Transition Temperature of Acrylonitrile-Methyl Acrylate Copolymers by ^{13}C-NMR Spectroscopy. *J. Polym. Sci. Chem.* **30**, 2549-2557.

Brar A. S. (1993) Microstucture Determination of Styrene/Ethyl Acrylate Copolymers by NMR Spectroscopy and Its Correlation with Glass Transition Temperature. *Makromol. Chem.* **194**, 1707-1720.

Brar A. S. and Charan S. (1993) Reactivity Ratios and Microstructure Determination of (Vinyl Acetate)-(Methyl Methacrylate) Copolymers. *Eur. Polym. J.* **29**, 755-759.

Braun D., Bendlein W. and Mott G. (1973) A Simple Method of Determining Copolymerization Reactivity Ratios by Means of A Computer. *Eur. Polym. J.* **9**, 1007-1012.

Bressers H. J. L. and Kloosterboer J. G. (1980) Thermally and Light-Induced Polymerization of Ethyl Acrylate and Methyl Methacrylate, Studied by DSC. *Polymer Bull.* **2**, 201-204.

Britt H. I. and Leucke R. H. (1973) The Estimation of Parameters in Nonlinear, Implicit Models. *Technometrics* **15**, 233-247.

Broadhead T. D., Hamielec A. E. and MacGregor J. F. (1985) Dynamic Modelling of the Batch, Semi-Batch and Continuous Production of Styrene/Butadiene Copolymers by Emulsion Polymerization. *Makromol. Chem. Suppl.* **10/11**, 105-128.

Brandrup J. and Immergut E.H.(eds.)(1989) *Polymer Handbook* John Wiley & Sons, New York.

Buback M. and Panten K. (1993) Terpolymerization of Ethene, Acrylonitrile and Vinyl Acetate. *Makromol.Chem.* **194**, 2471-2481.

Buback M., Huckestein B. and Russel G. T. (1994) Modelling of Termination in Intermediate and High Conversion Free Radical Polymerization. *Macromol. Chem. Phys.* **195**, 539-554.

Burke A. L., Duever T. A. and Penlidis A. (1997) Discrimination between the Terminal and Penultimate Models Using Designed Experiments: An Overview. *Ind. Eng. Chem. Res.* **36(4)**, 1016-1035.

Burke A. L., Duever T. A. and Penlidis A. (1994) Model Discrimination via Designed Experiments: Discriminating between the Terminal and Penultimate Models on the Basis of Composition Data. *Macromolecules* **27**, 386-399.

Burke A. L., Duever T. A. and Penlidis A. (1993) Revisiting the Design of Experiments for Copolymer Reactivity Ratio Estimation. *J. Polym. Sci. Chem.* **31**, 3065-3072.

Busfield W. K. and Low R. B. (1975) Solvent Effects in the Free Radical Copolymerization of Vinyl Acetate and Methyl Methacrylate. *Eur. Polym. J.* **11**, 309-312.

Buzzi-Ferraris G. and Forzatti P. (1983) A New Sequential Experimental Design Procedure for Discriminating Among Rival Models. *Chem. Eng. Sci.* **38**, 225-232.

Catala J. M., Nonn A., Pujot J. M. and Bross J. (1986) Radical Copolymerization of 2-Hydroxyethyl Acrylate with Alkylacrylate-Determination of the Reactivity Ratios. *Polymer Bull.* **15**, 311-315.

Chapin E. C., Ham G. E. and Mills C. L. (1949) Copolymerization. VII. Relative Rates of Addition of Various Monomers in Copolymerization. *J. Polym. Sci.* **4**, 597-604.

Chaudhuri A. K. and Palit S. R. (1968) Mode of Termination in the Copolymerization of Vinyl Acetate---Isobutyl Methacrylate and Methyl Methacrylate---Methyl Acrylate at 60°C. *J. Polym. Sci. A-1* **6**, 2187-2196.

Chen S. A. and Hwang C. C. (1982) Kinetics of Free Radical Oligomerization, 2[a] Cooligomerization of Styrene and Methyl Methacrylate in Carbon Tetrachloride. *Makromol. Chem.* **183**, 1485-1495.

Cheng H., Yamada B. and Otsu T. (1991) Polymerization and Copolymerization of α-alkylacrylic Acid and Characterization of Their Polymers. *J. Polym. Sci. Chem.* **29**, 1837-1843.

Cheng H. and Yan D. (1989) Copolymerization of Styrene with Acrylonitrile Initiated by 2-methyl-2-undecanethiol. *Makromol. Chem.* **190**, 2287-2291.

Chiang S. S. M. and Rudin A. (1975) Termination Rates in Free Radical Copolymerizations. *J. Macromol. Sci. Chem.* **A9**, 237-256.

Chien, J.C.W. and Finkenaur, A.L. (1985) A Simplification of the Terpolymerization Equation. *J.Polym.Sci.Chem.* **23**, 2247-2254.

Chiu W. Y., Carratt G. M. and Soong D. S. (1983) A Computer Model for the Gel Effect in Free-Radical Polymerization. *Macromolecules* **16**, 348-357.

Choi K. Y. and Butala D. N. (1991) An Experimental Study of Multiobjective Dynamic Optimization of a Semibatch Copolymerization Process. *Polym. Eng. Sci.* **31**, 353-364.

Chow C. D. (1975) Monomer Reactivity Ratio and Q-e Values for Copolymerization of Hydroxyalkyl Acrylates and 2-(1-Aziridinyl) Ethyl Methacrylate with Styrene. *J. Polym. Sci. Chem.* **13**, 309-313.

Christiansen R. L. (1990) PhD Thesis, Dept. of Chemical Engineering, University of Wisconsin.

Chylla R.W., Campbell J.D., and Teymour F.(1997). Dynamics of Semibatch Polymerization Reactors: II. Pilot-Plant Study. *AIChE J.* **43**, 157-165.

Comyn J. and Fernandez R. A. (1975) Glass Transition Temperatures of Copolymers of Ethyl Acrylate and Vinlyidene Chloride. *Eur. Polym. J.* **11**, 149-151.

Couchman P. R. (1982) Compositional Variation of Glass-Transition Temperatures. 7. Copolymers. *Macromolecules* **15**, 770-773.

Davis T. P., O'Driscoll K. F., Piton M. C. and Winnik M. A. (1991) Copolymerization Propagation Kinetics of Styrene with Alkyl Acrylates. *Polym. Int.* **24**, 65-70.

Devon M. J. and Rudin A. (1986) Monomer Chain Transfer in the Copolymerization of Styrene and Butyl Acrylate. *J. Polym. Sci. Chem.* **24**, 2191-2198.

Dimarzio E. A. and Gibbs J. H. (1959) Glass Temperature of Copolymers. *J. Polym. Sci.* **XL**, 121-131.

Dionisio J. M. and O'Driscoll K. F. (1979) High-Conversion Copolymerization of Styrene and Methyl Methacrylate. *J. Polym. Sci. Polym. Lett.* **17**, 701-707.

Djekhaba S. and Guillot J. (1990) Batch Emulsion Copolymers Styrene with Ethyl Acrylate: Microstructure and Glass Transition Temperature. *Eur. Polym. J.* **26**, 1017-1025.

Doak K. W. (1948) Copolymerization. VI. The Copolymerization of Chloroethylenes with Other Monomers. *J. Am. Chem. Soc.* **70**, 1525-1527.

Dube M. A., Penlidis A. and O'Driscoll K. F. (1990a) Mathematical Modelling of Styrene/Butyl Acrylate Copolymerization. *Chem. Eng. Sci.* **45**, 2785-2792.

Dube M. A., Penlidis A. and O'Driscoll K. F. (1990b) A Kinetic Investigation of Styrene/Butyl Acrylate Copolymerization. *Can. J. Chem. Eng.* **68**, 974-987.

Dube M. A., Amin Sanayei R., Penlidis A., O'Driscoll K. F. and Reilly P. M. (1991) A Microcomputer Program for Estimation of Copolymerization Reactivity Ratios. *J. Polym. Sci. Chem.* **29**, 703-708.

Dube M. A. and Penlidis A. (1995a) A Systematic Approach to the Study of Multicomponent Polymeirzation Kinetics---the Butyl Acrylate/Methyl Methacrylate/Vinyl Acetate Example: 1. Bulk Copolymerization. *Polymer* **36**, 587-598.

Dube M. A. and Penlidis A. (1995b) A Systematic Approach to the Study of Multicomponent Polymeirzation Kinetics: the Butyl Acrylate/Methyl Methacrylate/Vinyl Acetate Example: $2^{a)}$. *Macromol. Chem. Phys.* **196**, 1101-1112.

Dube M. A., Soares, J.B.P. and Penlidis A. (1997) Mathematical Modelling of Multicomponent Chain-Growth Polymerizations in Batch, Semi-Batch and Continuous Reactors: A Review. *Ind. Eng. Chem. Res.* **36(4)**, 966-1015.

Dube M. and Penlidis A.(1996) A Hierarchical Data Analysis of a Replicate Experiment in Emulsion Terpolymerization. *AIChE J.*, **42**, 1985

Dube M., Penlidis A. and Reilly P.M.(1996) A Systematic Approach to the Study of Multicomponent Polymerization Kinetics: The Butyl Acrylate/Methyl Methacrylate/Vinyl Acetate Example IV. Optimal Bayesian Design of Emulsion Terpolymerization Experiments in a Pilot Plant Reactor. *J. Polym. Sci., Polym. Chem.*, **34**, 811-831

Duever T.A., O'Driscoll K.F., and Reilly P.M.(1983). The Use of the Error-in-Variables Model in Terpolymerization. *J.Polym.Sci.Chem.* **21**, 2003-2010.

Edwards S. F. (1994) The Glass Transition in Polymers. *Polymer* **35**, 3827-3830.

Egorochkin G. A., Semchikkov Y. D., Smirnova L. A., Karyakin N. V. and Kutin A. M. (1992) Thermodynamics of Mixing of Some Vinyl Monomers on the Possibility of Predicting Deviations from the Classical Scheme of Copolymerization. *Eur. Polym. J.* **28**, 681-684.

Engelmann U. and Schmidt-Naake G. (1993) Free-Radical Mulcomponent Polymerization Reactors and Chemical Composition Distribution. *Macromol.Theory Simul.*, **2**, 275-297

Engelmann U. and Schmidt-Naake G. (1994) Influence of Reactor Operational Policies on Distributions of Chemical Composition, Molar Mass, Sequence Length and Sequence Frequency of Multicomponent Polymers Obtained by Free-Radical Polymerization. *Macromol.Theory Simul.*, **3**, 219-239

Farber J. N. (1986) Steady State Multiobjective Optimization of Continuous Copolymerization Reactors. *Polym. Eng. Sci.* **26**, 499-507.

Fehervari A., Foldes-Berezsnich T. and Tudos F. (1981) Kinetics of Free Radical Copolymerization. IV. Rate of Initiation in the Copolymerization System Ethyl Acrylte-Styrene-Benzene. *J. Macromol. Sci. Chem.* **A16**, 993-1002.

Fehervari A., Foldes-Berezsnich T. and Tudos F. (1982a) Kinetics of Free Radical Copolymerization. V. Copolymerization of Ethyl Acrylate with Styrene. Composition of Copolymers. *J. Macromol. Sci. Chem.* **A18**, 337-346.

Fehervari A., Foldes-Berezsnich T. and Tudos F. (1982b) Kinetics of Free Radical Copolymerization. VII. Kinetics Analysis of Ethyl Acrylate-Styrene Copolymerization in Inert Solvent. *J. Macromol. Sci. Chem.* **A18**, 337-346.

Fernandez-Garcia M., Lopez-Gonzalez M. M., Barrales-Rienda J. M., Madruga E. L. and Arias C. (1994) Effect of Copolymer Composition and Conversion on the Glass Transition of Methyl Acrylate-Methyl Methacrylate Copolymers. *J. Polym. Sci. Phys.* **32**, 1191-1203.

Fineman M. and Ross S. D. (1950) Linear Method for Determining Monomer Reactivity Ratios in Copolymerization. *J. Polym. Sci.* **5**, 259-265.

Fox T. G. (1956) *Bull Am. Phys. Soc.* **1**, 123

Fried J. R. (1993) Correlative Techniques for the Estimation of the Glass-Transition Temperature. *Comp. Poly. Sci.* **3**, 47-58.

Fujihara H., Yamazaki K., Matsubara Y., Yoshihara M. and Maeshima T. (1979) Radical Copolymerization of Methyl Methacrylate with Styrene in Several Solvents. *J. Macromol. Sci. Chem.* **13**, 1081-1088.

Fukuda T., Ma Y. D. and Inagaki H. (1982) Free-Radical Copolymerization I. Reactivity Ratios in Bulk-Copolymerization of p-Chlorostyrene and Methyl Acrylate. *Polymer J.* **14**, 705-711.

Fukuda T., Ma Y. D. and Inagaki H. (1985a) Re-Examination of Free-Radical Copolymerization Kinetics. *Makromol. Chem. Suppl.* **12**, 125-132.

Fukuda T., Ma Y. D. and Inagaki H. (1985b) Free-Radical Copolymerization. 3. Determination of Rate Constants of Propagation and Termination for the Styrene/Methyl Methacrylate System. A Critical Test of Termination-Model Kinetics. *Macromolecules* **18**, 17-26.

Fukuda T., Kubo K., Ma Y. D. and Inagaki H. (1987a) Free-Radical Copolymerization V. Rate Constants of Propagation and Termination for a Styrene/Methyl Methacrylate/Toluene System. *Polymer J.* **19**, 523-530.

Fukuda T., Ma Y. D. and Inagaki H. (1987b) Free-Radical Copolymerization, 6[a)] New Interpretation for the Propagation Rate versus Composition Curve. *Makromol. Chem. Rapid Commun.* **8**, 495-499.

Fukuda, T., Ma, Y.D., Kudo, K., and Takada, A.(1989). Free-Radical Copolymerization VII. Reinterpretation of Velocity-of-Copolymerization Data. *Polymer J.* **12**, 1003-1009

Fukuda T., Kubo K. and Ma Y. D. (1992) Kinetics of Free Radical Copolymerization. *Prog. Polym. Sci.* **17**, 875-916.

Fukui K., Yonezawa T. and Morokuma K. (1961) On Cross Termination in Radical Polymerization. *J. Polym. Sci.* **XLIX**, 511-515.

Galbraith M. N., Moad G., Solomon D. H. and Spurling T. H. (1987) Influences of the Initiation and Termination Reactions on the Molecular Weight Distribution and Compositional Heterogeneity of Functional Copolymers: An Application of Monte Carlo Simulation. *Macromolecules* **20**, 675-679.

Gao J. and Penlidis A. (1996) A Comprehensive Simulator/Database for Reviewing in Free-Radical Homopolymerization. *J. Macromol. Sci. Revs. Chem. Phys.* **C36**, 199-404.

Gao, J. and Penlidis, A.(1998) A Comprehensive Simulator/Database Package for Reviewing Free-Radical Comopolymerizations. *J. Macromol. Sci. Rev. Macromol. Chem. Phy.* **C38**, 651-780

Gao J., McManus N. T. and Penlidis A. (1997) Experimental and Simulation Studies on Ethyl Acrylate Polymerization. *Macromol. Chem. Phys.* **198**, 843-859.

Garcia-Rubio L. H., MacGregor J. F. and Hamielec A. E. (1982) Modelling and Control of Copolymerization Reactors. In *Computer Applications in Applied Polymer Science* (Edited by Provder T.), p. 87.

Garcia-Rubio L. H., Lord M. G., MacGregor J. F. and Hamielec A. E. (1985) Bulk Copolymerization of Styrene and Acrylonitrile: Experimental Kinetics and Mathematical Modelling. *Polymer* **26**, 2001-2013.

Gordon M. and Taylor J. S. (1952) Ideal Copolymers and the Second-order Transitions of Synthetic Rubbers. I. Non-Crystalline Copolymers. *J. Appl. Chem.* **2**, 493-500.

Greenley R. Z. (1980b) Recalculation of Some Reactivity Ratios. *J. Macromol. Sci. Chem.* **A14**, 445-515.

Greenley R. Z. (1980a) An Expanded Listing of Revised Q and e Values. *J. Macromol. Sci. Chem.* **A14**, 427-443.

Guillot, J. and Rios Guerrero, L. (1982) Terpolymerisation Acrylonitrile/Styrene/Acrylate de Methyle, 3[a)] Etude du Mecanisme de la Copolymerisation en Emulsion. *Makromol. Chem.* **183**, 1979-2008.

Guillot J. (1990) Modelling and Simulation of Emulsion Copolymerization of Monomers of Different Polarities - Relationship Polymerization Process-Microstructure-Properties. *Makromol. Chem. Macromol. Symp.* **35/36**, 269-289.

Guillot J. and Emelie B. (1991) Modelling of the Glass Transition of Random Copolymers. *Makromol. Chem. Rapid Commun.* **12**, 117-126.

Gunesin B. Z. and Piirma I. (1981) Block Copolymers Obtained by Free Radical Mechanism. II. Butyl Acrylate and Methyl Methacrylate. *J. Appl. Polym. Sci.* **26**, 3103-3115.

Gyongyhalmi I., Nagy A., Foldes-Berezsnich T. and Tudos F. (1993) Kinetics of Radical Polymerization, 55[a)] The Polymerization of p-Methylstyrene in Solution. *Makromol. Chem.* **194**, 3357-3368.

Ham G. E. (1975) Role of Triad Concentration in Glass Transition Temperatures of Copolymers. *J. Macromol. Sci. Chem.* **A9**, 461-467.

Ham G. E. (1964) *Copolymerization*. Interscience Publishers, New York, London, Sydney.

Hamer J. W., Akramov T. A. and Ray W. H. (1981) The Dynamic Behavior of Continuous Polymerization Reactors ---II. Nonisothermal Solution Homopolymerization and Copolymerization in CSTR. *Chem. Eng. Sci.* **36**, 1897-1914.

Hamielec A. E. and MacGregor J. F. (1983) *Polymer Reaction Engineering* (Edited by Reichert K. H. and Geiseler W.), p. 21. Hanser Publishers, New York.

Hamielec A. E., MacGregor J. F., Webb S. and Spychaj T. (1986) Thermal and Chemical-Initiated Copolymerization of Styrene/Acrylic Acid at High Temperatures and Conversions in a Continuous Stirred Tank Reactor. In *Polymer Reaction Engineering* (Edited by Reichert K. H. and Geiseler W.), p. 185. Huthig & Wepf, New York.

Hamielec A. E., MacGregor J. F. and Penlidis A. (1987) Multicomponent Free-Radical Polymerization in Batch, Semi-Batch and Continuous Reactors. *Makromol. Chem. Macromol. Symp.* **10/11**, 521-570.

Hamielec A. E., MacGregor J. F. and Penlidis A. (1989) Copolymerization. In *Comprehensive Polymer Science* (Edited by Allen G. and Bevington J. C.), p. 17. Pergamon Press, Oxfor, NewYork.

Harris S. H. and Gilbert R. D. (1982) Acrylonitrile-4-Vinylpyridine Copolymers Effect of Comonomer Sequence Distribution on Properties. *J. Polym. Sci. Chem.* **20**, 1653-1667.

Hatate Y., Otake T. A., Ikari A. and Nakashio F. (1984) The Rate of Styrene and Acrylonitrile Copolymerization Involving a Minute Amount of Either Monomer. *J. Chem. Eng. Jpn.* **17**, 158-165.

Hayes R. A. (1981) Determination of Reactivity Ratios for the Copolymerization of Styrene and

Styrene-Acrylonitrile with Polybutadienes. *J. Polym. Sci. Chem.* **19**, 993-997.

Hayes R. A. and Futamura, S. (1981) Kinetics and Mechanism of the Polymerization of Styrene-Acrylonitrile in the Presence of Polybutadiene. *J. Polym. Sci. Chem.* **19**, 985-991.

Hill D. J. T., O'Donnell J. H. and O'Sullivan P. W. (1982) Analysis of the Mechanism of Copolymerization of Styrene and Acrylonitrile. *Macromolecules* **15**, 960-966.

Hill D. J. T., Lang A. P., O'Donnell J. H. and O'Sullivan P. W. (1989) Determination of Reactivity Ratios from Analysis of Triad Fractions - Analysis of the Copolymerization of Styrene and Acrylonitrile as Evidence for the Penultimate Model. *Eur. Polym. J.* **25**, 911-915.

Hill D. J. T., Lang A. P. and O'Donnell J. H. (1991) The Study of the Copolymerization of Styrene and Acrylonitrile to High Converstion. Application of Low Conversion Reactivity Ratios. *Eur. Polym. J.* **27**, 765-772.

Hill D. J. T., Lang A. P., Munro P. D. and O'Donnell J. H. (1992) The Effect of Solvent on the Styrene-Acrylonitrile Copolymerization. *Eur. Polym. J.* **28**, 391-398.

Hirooka M. and Kato T. (1974) Glass Transition Temperature and Sequential Structure of Equimolar Copolymers. *Polymer Lett.* **12**, 31-37.

Hocking, M.B. and Klimchuk, K.A. (1996) A Refinement of the Terpolymer Equation and Its Simple Extension to Two- and Four-Component Systems. *J.Polym.Sci.Chem.* **34**, 2481-2497.

Hsiang T. and Reilly P. M. (1971) A Practical Method for Discriminating among Mechanistic Models. *Can. J. Chem. Eng.* **49**, 865-871.

Hui A. W. and Hamielec A. E. (1972) Thermal Polymerization of Styrene at High Conversions and Temperatures: An Experimental Study. *J. Appl. Polym. Sci.* **16**, 749-769.

Husain J. R. and Hamielec A. E. (1978) Thermal Polymerization of Styrene. *J. Appl. Polym. Sci.* **22**, 1207-1223.

Hutchinson R. A., Richards J. R. and Aronson M. T. (1993) Analysis of Pulsed-Laser-Generated Molecular Weight distribution for the Determination of Propagation Rate Coefficient. *Macromolecules* **26**, 6410-6415.

Hutchinson R.A., Paquet D.A., McMinn Jr. J.H. and Fuller R.E.(1995) Measurement of Free-Radical Propagation Rate Coefficients for Ethyl, Butyl, and Isobutyl Methacrylates by Pulsed-Laser Polymerization. *Macromol.* **28**, 4023-4028

Hutchinson R.A., Beuermann S., Paquet D.A., and McMinn J.H. (1997) Determination of Free-

Radical Propagation Rate Coefficients for Alkyl Methacrylates by Pulsed-Laser Polymerization. *Macromol.* **30**, 3490-3493

Ito K. (1971) Cross-Termination Rate Constants in Copolymerizations of Some Methacrylates and Styrene. *J. Polym. Sci. A-1* **9**, 867-871.

Ito K. (1978) An Approach to the Termination Rate in Radical Copolymerization. *J. Polym. Sci. Chem.* **16**, 2725-2728.

Ito K. and O'Driscoll K. F. (1979) The Termination Reaction in Free Radical Copolymerization. I. Methyl Methacrylate and Butyl- or Dodecyl Methacrylate. *J. Polym. Sci. Chem.* **17**, 3913-3921.

Ito K. (1986) Evidence for Third Order Initiation in Monomer in Thermal Polymerization of Styrene. *Polymer J.* **18**, 877-879.

Janovic, Z., Saric, K., and Vogl, O.(1983). Terpolymerization of Acrylonitrile, Styrene, and 2,4,6-Tribromophenyl Acrylate. *J.Polym.Sci.Chem.* **21**, 2713-2725.

Johnson A. F., Khaligh B., Ramsay J. and O'Driscoll K. F. (1983) Temperature Effects in Free Radically Initated Copolymerization Reactions. *Polymer Commun.* **24**, 35-37.

Johnston N. W. (1969) Sequence Distribution Effects on Glass Transition Temperatures. *Polymer Prep.* **10**, 608-613.

Johnston N. W. (1972) Sequence Distribution-Glass Transition Effects III; αMS/AN Copolymers. *Polymer Prep.* **13**, 1029-1040.

Johnston N. W. (1973) Sequence distribution-Glass Transition Effects. II. Alkyl Methacrylate/Vinyl Chloride Copolymers. *J. Macromol. Sci. Chem.* 7, 531-545.

Johnston N. W. (1976a) The use of Alternating Copolymers in Sequence Distribution -Glass Transition Predictions. *Polymer Prep.* **14**, 46-51.

Johnston N. W. (1976b) Sequence Distribution - Glass Transition Effects. *J. Macromol. Sci. Revs. Chem.* **C14**, 215-250.

Johnson M., Karmo T. S. and Smith R. R. (1978) High Conversion Copolymerization of Styrene with Methyl Methacrylate. *Eur. Polym. J.* **14**, 409-414.

Jones K. M., Bhattacharya D., Brash J. L. and Hamielec A. E. (1986) An Investigation of the Kinetics of Copolymerization of Methyl Methacrylate/p-Methyl Styrene to High Conversion: Modelling Diffusion-Controlled Termination and Propagation by Free-Volume Theory. *Polymer* **27**, 602-610.

Jones S. A., Prementine G. S. and Tirrell D. A. (1985) Model Copolymerization Reactions. Direct Observation of a "Penultimate Effect" in a Model Styrene/Acrylonitrile Copolymer. *J. Am. Chem. Soc.* **107**, 5275-5276.

Kaszas G., Foldes-Berezsnich T. and Tudos F. (1985) Kinetics of Radical Copolymerization. XII. Investigation of the Rate of Polymerization of the System Styrene-Butyl Acrylate-Benzene. *J. Macromol. Sci. Chem.* **A22**, 1571-1592.

Kelen T. and Tudos F. (1975) Analysis of the Linear Methods for Determining Copolymerization Reactivity Ratios. I. A New Improved Linear Graphic Method. *J. Macromol. Sci. Chem.* **A9**, 1-27.

Kerber V. R. (1966) Anderung der Copolymerisations Parameter im System Styrol/acrylsaure durch Losungsmitteleffekte. *Makromol. Chem.* **96**, 30-40.

Khan H. U. and Wadehra B. M. (1981) Kinetic Study of Free Radical Bulk Copolymerization of Styrene-Methyl Methacrylate. *Polymer* **22**, 488-490.

Kim J. D. (1994) M.A.Sc. Thesis, Dept. of Chemical Engineering, Univeristy of Waterloo.

Kirchner K. and Schlapkohl H. (1976) The Formation of Oligomers in the Thermal Copolymerization of the Styrene/Acrylonitrile System. *Makromol. Chem.* 177, 2031-2042.

Klumperman B. and Kraeger I. (1994) Effect of Solvent on the Copolymerization of Styrene and Acrylonitrile. Application of the Bootstrap Effect to the Penultimate Unit Model. *Macromolecules* **27**, 1529-1534.

Kobayashi M. (1988a) Characterization of Styrene-Methyl Methacrylate-*n*-Butyl Acrylate Terpolymers. I. Average Diad Concentration Determined by ^{1}H-NMR. *J. Appl. Polym. Sci.* **35**, 299-309.

Kobayashi M. (1988b) Characterization of Styrene-Methyl Methacrylate-*n*-Butyl Acrylate Terpolymers. II. Effects of Sequence Distribution on Glass Transition Temperature. *J. Appl. Polym. Sci.* **35**, 311-319.

Kostanski L. K. and Hamielec A. E. (1994) Thermal Styrene/Butyl Acrylate Co-Oligomerization in a Continuous Stirred Tank Reactor. *Polymer* **35**, 4168-4174.

Kostanski L. K. and Hamielec A. E. (1992) Influence of Temperature on Butyl Acrylate Styrene Copolymerization Parameters. *Polymer* **33**, 3706-3710.

Kozorezov Y. I. and Shilyaeva I. Y. (1996) Thermal Polymerization of p-Methyl Styrene. *Int. Polym. Sci. Tech.* **22**, 58-60.

Krstina J., Moad G. and Solomon D. H. (1992) Effects of Solvent on Model Copolymerization Reactions. A ^{13}C-NMR Study. *Eur. Polym. J.* **28**, 275-282.

Kucher R. V., Anisimova L. N., Zaitsev Y. S., Lachinov M. B. and Zubov V. P. (1978) The Termination Stages in the Styrene-Acrylonitrile Copolymerization. *Polym. Sci. U. S. S. R.* **A20**, 2488-2493.

Kuo J. F. and Chen C. Y. (1981) Studies on the Radical Chain Copolymerization of Methyl Methacrylate and Styrene at Their Azeotropic Composition. *Macromolecules* **14**, 335-339.

Kuo J. F., Chen C. Y. and Luo S. H. (1989) A Method for the Calculation of Compositions of Radical-Chain Copolymerizations. *J. Appl. Polym. Sci.* **38**, 529-537.

Lebduska J., Snuparek J. and Kaspar K. (1986) Solution Copolymerization of Styrene and 2-Hydroxyethyl Methacrylate. *J. Polym. Sci. Chem.* **24**, 777-791.

Lewis F. M., Walling C., Cummings W., Briggs E. R. and Wenisch W. J. (1948b) Copolymerization. VII. Copolymerizations of Some Further Monomer Pairs. *J. Am. Chem. Soc.* **70**, 1527-1529.

Lewis F. M., Walling C., Cummings W., Briggs E. R. and Mayo F. R. (1948a) Copolymerization. IV. Effects of Temperature and Solvents on Monomer Reactivity Ratios. *J. Am. Chem. Soc.* **70**, 1519-1523.

Lin D. J., Petit A. and Neel J. (1987) Copolymerisation Radicalaire du Methyl-r Styrene avec le methacrylate de Methyle ou l'acrylonitrile. Determination des Rapports de Reactivite. *Makromol. Chem.* **188**, 1163-1175.

Lin C. C., Chiu W. Y. and Wang C. T. (1979) Simulation Model for the Solution Copolymerization of Acrylonitrile and Styrene in Azeotropic Composition. *J. Appl. Polym. Sci.* **23**, 1203-1222.

Lopez-Gonzalez M. M., Fernandez-Garcia M., Barrales-Rienda J. M. and Madruga E. L. (1993) Sequence Distribution and Stereoregularity in Methyl Methacrylate --- Methyl Acrylate Copolymers at High Conversions. *Polymer* **34**, 3123-3128.

Lord M. G. (1984) M.A.Sc. Thesis, Dept. of Chemical Engineering, University of McMaster.

Lu X. and Jiang B. (1991) Glass Transition Temperature and Molecular Parameters of Polymer. *Polymer* **32**, 471-478.

Ma Y. D., Won Y. C., Kubo K. and Fukuda T. (1993) Propagation and Termination Processes in the Free-Radical Copolymerization of Methyl Methacrylate and Vinyl Acetate.

Macromolecules **26**, 6766-6770.

Ma Y. D., Kim P. S., Kubo K. and Fukuda T. (1994) Propagation and Termination Processes in Free-Radical Copolymerization of Styrene and Ethyl Acrylate. *Polymer* **35**, 1375-1381.

Madruga E. L., Roman J. S. and Del Puerto M. A. (1979) Radical Copolymerization of Acrylic Monomers. II. Effect of Solvent on Radical Copolymerization of Methyl Methacrylate and Styrene. *J. Macromol. Sci. Chem.* **13**, 1105-1115.

Madruga E. L., Roman J. S. and der Puerto M. A. (1981) Effect of Solvent on the Termination Step for the Radical Copolymerization of Methyl Methacrylate and Styrene. *Polymer* **22**, 951-955.

Madruga E. L., San Roman J. and Rodriguez M. J. (1982) The Effect of Temperature on the Free Radical Copolymerization of Methyl Methacrylate with Ethyl Acrylate. *Eur. Polym. J.* **18**, 1011-1013.

Madruga E. L., San Roman J. and Rodriguez M. J. (1983a) Radical Polymerization in the Presence of Complexing Agents. V. Effect of Low Concentrations of $ZnCl_2$ on the Rate of Copolymerization of Methyl Methacrylate with Ethyl Acrylate. *J. Polym. Sci. Chem.* **21**, 2739-2748.

Madruga E. L., San Roman J. and Rodriguez M. J. (1983b) Radical Polymerization in the Presence of Complexing Agents. VI. Effect of Low Concentrations of $ZnCl_2$ on the Overall Rate of Copolymerization of Methyl Methacrylate with Ethyl Acrylate. *J. Polym. Sci. Chem.* **21**, 2749-2754.

Madruga E. L. and Roman J. S. (1989) Kinetic Study of the Free Radical Copolymerization of Styrene with Methl Methacrylate in Benzene. *Eur. Polym. J.* **25**, 1269-1272.

Madruga E. L. (1993) Solvent Effects on the Overall Rate of Copolymerization for the Methyl Methacrylate-Styrene System. *Makromol. Chem. Rapid Commun.* **14**, 581-589.

Madruga E. L. and Fernandez-Garcia M. (1996) Kinetic Study of Free-Radical Copolymerization of Methyl Acrylate and Methyl Methacrylate in Benzene. *Macromol. Chem. Phys.* **197**, 1185-1191.

Mahabadi H. K. and O'Driscoll K. F. (1977a) Termination Rate Constant in Free-Radical Polymerization. *J. Polym. Sci. Chem.* **15**, 283-300.

Mahabadi H. K. and O'Driscoll K. F. (1977b) Termination Rate Constant in Free-Radical Polymerization. *Macromolecules* **10**, 55-58.

Mahabadi H. K. and O'Driscoll K. F. (1977c) Termination Rate Constant in Free-Radical Polymerization. III. Determination of Propagation and Termination Rate Constants for Styrene and Methyl Methacrylate. *J. Macromol. Sci. Chem.* **A11**, 967-976.

Mahabadi H.K. and O'Driscoll K.F.(1976). Dependence of the Termination Rate Constant on Monomer Size in Free-Radical Polymerization. *Polymer Lett. Ed.* **14**, 671-673.

Marten F. L. and Hamielec A. E. (1979) High Conversion Diffusion-Controlled Polymerization. In *Polymer Reactors and Processes. ACS Symposium Series, 104* (Edited by Henderson J. N. and Bouton T. C.

Marten F. L. and Hamielec A. E. (1982) High-Conversion Diffusion-Controlled Polymerization of Styrene. I. *J. Appl. Polym. Sci.* **27**, 489-505.

Maxwell I. A. and Russel G. T. (1993) Diffusion Controlled Copolymerization Kinetics. *Makromol. Chem. Theory Simul.* **2**, 95-128.

Mayo F. R. and Walling C. (1950) Copolymerization. *Chem. Rev.* **46**, 191-287.

Mayo F. R. and Lewis F. M. (1944) Copolymerization. I. A Basis for Comparing the Behavior of Monomers in Copolymerization; The Copolymerization of Styrene and Methyl Methacrylate. *J. Am. Chem. Soc.* **66**, 1594-1601.

Mayo F. R., Lewis F. M. and Walling C. (1948a) Copolymerization. VIII. The Relation Between Structure and Reactivity of Monomers in Copolymerization. *J. Am. Chem. Soc.* **70**, 1529-1533.

Mayo F. R., Walling C., Lewis F. M. and Hulse W. F. (1948b) Copolymerization. V. Some Copolymerizations of Vinyl Acetate. *J. Am. Chem. Soc.* **70**, 1523-1525.

McGinniss V. D. and Ting V. W. (1975) Acrylate Systems for U.V. Curing. *J. Rad. Cur.* **2**, 14-18.

McIsaac, S.L. (1994) M.A.Sc. Thesis, Dept. of Chemical Engineering, University of Waterloo.

McKenna T. K., Graillat C. and Guillot J. (1995) Contributions to Defining the Rate Constants for the Homo- and Copolymerization of Butyl Acrylate and Vinyl Acetate. *Polymer Bull.* **34**, 361-368.

McManus N. T. and Penlidis A. (1996) A Kinetic Investigation of Styrene/Ethyl Acrylate Copolymerization. *J. Polym. Sci. Chem.* **34**, 237-248.

Melville H.W. and Valentine L. (1950) Studies in Copolymerization 1. The Evaluation of the Kinetic Coefficients for the Copolymerization of Styrene and Methyl Methacrylate. *Proc. Royal*

Soc. (London) **200**, 337-358

Merz E., Alfrey T. and Goldfinger G. (1946) Intramolecular Reactions in Vinyl Polymers as a Mean of Investigation of the Propagation Step. *J. Polym. Sci.* **1**, 75-82.

Meyer V. E. (1966) Copolymerization of Styrene and Methyl Methacrylate. Reactivity Ratios from Conversion-Composition Data. *J. Polym. Sci. A-1* **4**, 2819-2830.

Nagaya T., Sugimura Y. and Tsuge S. (1980) Studies on Sequence Distribution in Acrylonitrile — Styrene Copolymers by Pyrolysis-Glass Capillary Gas Chromatography. *Macromolecules* **13**, 353-357.

O'Driscoll K. F., Kale L. T., Garcia-Rubio L. H. and Reilly P.M. (1984) Applicability of Mayo-Lewis Equation to High-Conversion Copolymerization of Styrene and Methyl Methacrylate. *J. Polym. Sci. Chem.* **22**, 2777-2788.

O'Driscoll K. F. and Huang J. F. (1989) The Rate of Copolymerization of Styrene and Methyl Methacrylate --- I. Low Conversion Kinetics. *Eur. Polym. J.* **25**, 629-633.

O'Driscoll K. F. and Huang J. F. (1990) The Rate of Copolymerization of Styrene and Methyl Methacrylate --- II. The Gel Effect in Copolymerization. *Eur. Polym. J.* **26**, 643-647.

Odian G. (1982) *Principles of Polymerization*. Wiley-Interscience, New York, Chichester, Brisbane, Toronto, Singapore.

Olaj O. F., Bitai I. and Gleixner G. (1985) The Laser Flash-Initiated Polymerization as a Tool of Evaluating (Individual) Kinetic Constants of Free Radical Polymerization. 1. *Makromol. Chem.* **186**, 2569-2580.

Olaj O. F., Schnoll-Baitai I. and Kremminger P. (1989) Evaluation of Individual Rate Constants from the Chain-Length Distribution of Polymer Samples Prepared by Intermittent (Rotating Sector) Photopolymerization --- 2. The Copolymerization System Styrene-Methyl Methacrylate. *Eur. Polym. J.* **25**, 535-541.

Olaj O.F. and Schnoll-Baitai I. (1995) The Extension of the "Restricted" Penultimate Scheme of Binary Copolymerization to Ternary Systems. *Makromol.Theory Simul.* **4**, 577-584.

Olaj O. F., Kremminger P. and Schnoll-Baitai I. (1988) Evaluation of Individual Rate Constants from the Chain-Length Distribution of Polymer Samples Prepared by Intermittant (Rotating Sector) Photo-Polymerization, 1. First Experiences with Styrene and Methyl Methacrylate. *Makromol. Chem. Rapid Commun.* **9**, 771-779.

O'Neil, G.A. and Torkelson J.M. (1997) Recent Advances in the Understanding of the Gel Effect

in Free-Radical Polymerization. *TRIP.* **5**, 349-355.

Padwa A.R. and Schwier C.E. (1991) Prediction of Monomer Compositions in Terpolymerization. *J.Appl.Polym.Sci.* **42**, 2987-2988.

Paoletti K. P. and Billmeyer F. W.,Jr. (1964) Absolute Propagation Rate Constants for the Radical Polymerization of Substituted Styrenes. *J. Polym. Sci. A-1* **2**, 2049-2062.

Patino-Leal H., Reilly P. M. and O'Driscoll K. F. (1980) On the Estimation of Reactivity Ratios. *J. Polym. Sci. Chem.* **18**, 219

Plochocka K. and Harwood H. J. (1978) Solvent Effect in Radical Copolymerization and Sequence Distribution of Monomers in Copolymers of Styrene with Methacrylic Acid. *Polymer Prep.* **19**, 240-244.

Podesva J. and Prochazka O. (1979) A Method for Evaluating the Copolymer Glass Transition Data. *Makromol. Chem.* **180**, 2525-2530.

Pomposo J. A., Eguiazabal I., Calahorra E. and Cortazar M. (1993) Glass Transition Behaviour and Interactions in Poly(p-Vinyl Phenol)/Polymethacrylate Blends. *Polymer* **34**, 95-102.

Prementine G. S. and Tirrell D. A. (1989) Model Copolymerizations. Determination of the Relative Rates of Addition of Styrene and Acrylonitrile to the Benzyl Radical. *Macromolecules* **22**, 52-55.

Prochazka O. and Kratochvil P. (1983) Termination in Radical Copolymerization: Correlation of Experimental Data. *J. Polym. Sci. Chem.* **21**, 3269-3279.

Rajatapiti P., Dimonie V. L. and El-Aasser M. S. (1996) Bulk and Emulsion Copolymerizations of *n*-Butyl Acrylate and Poly(methyl methacrylate) Macromonomer. *J. Appl. Polym. Sci.* **61**, 891-900.

Reilly P. M. (1970) Statistical Methods in Model Discrimination. *Can. J. Chem. Eng.* **52**, 103-109.

Reilly P. M. and Patino-Leal H. (1981) A Bayesian Study of the Error-in-Variable Model. *Technometrics* **23**, 221-231.

Rizzardo E., Meijs G. F. and Thang S. H. (1995) Chain Transfer by Radical Addition-Fragmentation Mechanisms: Synthesis of Macromonomers and End-Functional Oligomers. *Makromol. Chem. Macromol. Symp.* **98**, 101-123.

Ruckenstein E. and Kim K. (1989) Copolymerization of Styrene and Methacrylic Acid in

Concentration Emulsions. *J. Polym. Sci. Chem.* **A27**, 4375-4388.

Rudin A. and Chiang S. S. M. (1974) Kinetics of Free-Radical Copolymerization of α-Methylstyrene and Styrene. *J. Polym. Sci. Chem.* **12**, 2235-2254.

Rudin, A., Ableson, W.R., Chiang, S.S.M. and Bennett, G.W. (1973) Estimation of Reactivity Ratios from Multicomponent Copolymerizations. *J.Macromol.Sci.Chem.* **A7**, 1203-1230

Russell G. T., Napper D. H. and Gilbert R. D. (1988) Termination in Free-Radical Polymerization Systems at High Conversion. *Macromolecules* **21**, 2133-2140.

Russo S. and Munari S. (1968) A Model for the Termination Stage of Some Radical Copolymerizations. *J. Macromol. Sci. Chem.* **A2**, 1321-1332.

Russo S. (1987) Initiation, Propagation and Termination in Free Radical Copolymerization. *Makromol. Chem. Macromol. Symp.* **10/11**, 395-414.

Ryabov A. V., Semchikkov Y. D. and Slavniskaya N. N. (1970) Effect of the Medium on the Homogeneous Radical Copolymerization of Unsaturated Carboxylic Acid with Vinyl Monomers. *Vysokomol. Soyed* **A12**, 553-559.

Sanchez-Chaves M., Arranz F. and Montes M. (1988) Vinyl Alcohol-Vinyl Propionate Copolymers: Sequence Distribution and Glass Transition. *Polymer* **29**, 2244-2248.

Santos R. d. J., Soares B. G. and Gomes A. S. (1994) Copolymerization of Styrene, Maleic Anhydride and Acrylonitrile up to high Conversion. *Macromol. Chem. Phys.* **195**, 2517-2521.

Schellenberg G. and Vogel J. (1994) On the Glass Transition Temperature of Styrene-n-Butyl Methacrylate Copolymers in Dependence on Chemical Composition, Molecular Weight, and Mixtures. *J. Polym. Sci. Phys.* **32**, 1969-1975.

Schellenberg J. and Wigand G. (1992) The Formation of Oligomers in the Inhibited Thermal Copolymerization of Styrene and Acrylonitrile. *Makromol. Chem.* **193**, 3063-3071.

Schneider H. A. (1988) The Gordon-Taylor Equation. Additivity and Interaction in Compatible Polymer Blends. *Makromol. Chem.* **189**, 1941-1955.

Schneider H. A. and Neto H. N. (1983) The Effect of Sequence Distribution on Glass Transition of Donor-Acceptor Copolymer Systems. *Polymer Bull.* **9**, 457-463.

Schoonbrood H. A. S., Pierik S. C. J., van den Reijen B., Heuts J. P. A. and German A. L. (1996) Cross-Chain Transfer Rate Constants of Styrene-Terminated Radicals to Methyl Acrylate and Methyl Methacrylate. *Macromolecules* **29**, 6717-6723.

Schoonbrood, H.A.S., van den Reijen, B., de Kock, J.B.L., Manders, B.G., Van Herk, A.M. and German, A.L. (1995) Pulsed Laser Terpolymerization of Styrene, Methyl Methacrylate and Methyl Acrylate. *Makromol.Chem.Rapid Commun.* **16**, 119-124.

Schroder U. K. O. (1987) Thermal Crosslinking of Styrene/p-Methylstyrene Copolymers. *Makromol. Chem.* **188**, 2775-2787.

Schweer J. (1993) Penultimate Model Description of the Propagation Kinetics for the Free Radical Copolymerization of Styrene and Methyl Methacrylate. *Makromol. Chem. Theory Simul.* **2**, 485-502.

Sebastian D. H. and Biesenberger J. A. (1981) A Kinetic Study of Free-Radical Styrene-Acrylonitrile Copolymerization by Differential Scanning Calorimeter. *J. Macromol. Sci. Chem.* **15**, 553-584.

Semchikkov Y. D., Ryabov A. V., Smirnova L. A., Yegorochkin A. N., Sukhova T. Y., Kuznetsov V. A. and Laptev A. Y. (1979) The Effect of Catalytic Amounts of Thiols on the Compositions of Unsaturated Acid Copolymers. *Vysokomol. Soyed* **A21**, 327-332.

Semchikkov Y. D., Smirnova L. A., Knyazeva T. Y., Bulgakova S. A., Voskikoinik G. A. and Sherstyanykh V. I. (1984) General Nature of the Effect of Molecular Weight on the Composition of a Copolymer on Homogeneous Radical Copolymerization. *Vysokomol. Soyed* **A26**, 704-710.

Semchikkov Y. D., Knyazeva T. Y., Smirnova L. A. and Bulgakova S. A. (1990) Dependence of Copolymer Composition upon Molecular Weight in Homogeneous Radical Copolymerization. *Eur. Polym. J.* **26**, 883-887.

Semchikkov Y. D., Gromov V. F. and Teleshov E. N. (1991) Macromolecular Effects in Radical Polymerizations. *Vysokomol. Soyed* **A33**, 1428-1144.

Sharma D. K. and Soane D. S. (1988) High-Conversion Diffusion-Controlled Copolymerization Kinetics. *Macromolecules* **21**, 700-710.

Shoaf L. G. and Poehlein G. W. (1991) Kinetics of Emulsion Copolymerization with Acrylic Acids. *J. Appl. Polym. Sci.* **42**, 1213-1237.

Shukla, P., Srivastava, K.A., and '(1994). Terpolymerization of Styrene, Acrylonitrile and Chromium Acrylate: Synthesis and Properties. *Polymer* **35**, 4665-4670.

Soh, S.K., and Sundberg, D.C.(1982) Diffusion-Controlled Vinyl Polymerization. II. Limitations on the Gel Effect. *J. Polym. Sci. Polym. Chem.*, **20**, 1315-1329

Soh S. K. and Sundberg D. C. (1982a) Diffusion-Controlled Vinyl Polymerization. I. The Gel

Effect. *J. Polym. Sci. Chem.* **20**, 1299-1313.

Soh S. K. and Sundberg D. C. (1982b) Diffusion-Controlled Vinyl Polymerization. II. Limitations on the Gel Effect. *J. Polym. Sci. Chem.* **20**, 1315-1329.

Soh S. K. and Sundberg D. C. (1982c) Diffusion-Controlled Vinyl Polymerization. III. Free Volume Parameters and Diffusion-Controlled Propagation. *J. Polym. Sci. Chem.* **20**, 1331-1344.

Soh S. K. and Sundberg D. C. (1982d) Diffusion-Controlled Vinyl Polymerization. IV. Comparison of Theory and Experiment. *J. Polym. Sci. Chem.* **20**, 1345-1371.

Sparidans R. W., Claessens H. A., Van Doremaele G. H. J. and Van Herk A. M. (1990) Analysis of Poly(styrene-co-methyl acrylate) and Poly(styrene-co-butyl acrylate) by High-Performance Liquid Chromatography. *J. Chromatography* **508**, 319-331.

Spychaj, T. and Hamielec, A. E. (1991) High Temperature Continuous Bulk Copolymerization of Styrene and Acrylic Acid: Thermal Behavior of the Reactants. *J. Appl. Polym. Sci.* **20**, 2111-2119.

Srivastava N. and Mathur G. N. (1981) A Kinetic Study on Copolymerization of Styrene with Methyl Methacrylate in the Presence of Zinc Chloride. *Polymer* **22**, 391-394.

Stickler, M.(1983) Free-Radical Polymerization Kinetics of Methyl Methacrylate at Very High Conversions, *Makromol. Chem.*, **184**, 2563-2579

Stutz H., Illers K.-H. and Mertes J. (1990) A Generalized Theory for the Glass Transition Temperature of Crosslinked and Uncrosslinked Polymers. *J. Polym. Sci. Phys.* **28**, 1483-1498.

Sutton T. L. and MacGregor J. F. (1977) The Analysis and Design of Binary Vapour-Liquid Equilibrium Experiments. Part I. Parameter Estimation and Consistency Tests. *Can. J. Chem. Eng.* **55**, 602-608.

Suzuki M., Miyama H. and Fujimoto S. (1958) A Thermoistor Method of Determing the Rate Constant for the Copolymerization of Vinyl Acetate and Methyl Methacrylate. *J. Polym. Sci.* **XXXII**, 445-455.

Suzuki M., Miyama H. and Fujimoto S. (1959) Copolymerization of Styrene with Vinyl Acetate and Methyl Methacrylate. *J. Polym. Sci.* **XXXVII**, 533-540.

Suzuki H. and Mathot V. B. F. (1989) An Insight into the Barton Equation for Copolymer Glass Transition. *Macromolecules* **22**, 1380-1384.

Suzuki H. and Miyamoto T. (1990) Glass Transition Temperatures of Compatible Block

Copolymers. *Macromolecules* **23**, 1877-1879.

Suzuki H., Nishio Y., Kimura N., Mathot V. B. F., Pijpers M. F. J. and Murakami Y. (1994) Effects of Sequence Length Distribution on Heat Capacity and Glass Transition Temperature of Styrene-Methyl Methacrylate Copolymers. *Polymer* **35**, 3698-3702.

Switala-Zeliazkow M. and Wojtczak (1986a) Microsture of Styrene-Methacrylic Acid and Styrene-Acrylic Acid Copolymers, 1[a]: ^{1}H NMR Study of Methlated Styrene-Acrylic Acid Copolymers. *Makromol. Chem.* **187**, 2411-2418.

Switala-Zeliazkow M. and Wojtczak (1986b) Microsture of Styrene-Methacrylic Acid and Styrene-Acrylic Acid Copolymers, 2[a]: ^{1}H NMR Study of Methlated Styrene-Acrylic Acid Copolymers. *Makromol. Chem.* **187**, 2419-2426.

Switala-Zeliazkow M. (1993) Microstructure of Styrene-Methylacrylic Acid and Styrene-Acrylic Acid Copolymers, 6[a] Relation of the Glass Transition Temperature to the Microstucture of (Meth)acrylic Acid-Styrene Copolymers. *Makromol. Chem.* **194**, 1505-1511.

Tanczos I., Foldes-Berezsnich T. and Tudos F. (1982) Kinetics of Radical Copolymerization --- VIII. Investigation of the Effect of Molecular Inhibitors in Copolymerization --- 1. Bulk Copolymerization. *Eur. Polym. J.* **18**, 487-491.

Tidwell P. W. and Mortimer G. A. (1970) Science of Determining Copolymerization Reactivity Ratios. *J. Macromol. Sci. Rev.* **C4**, 281-312.

Tidwell P. W. and Mortimer G. A. (1965) An Improved Method of Calculating Copolymer Reactivity Ratios. *J. Polym. Sci. Chem.* **3**, 369-387.

Tobita H. and Hamielec A. E. (1991) Kinetics of Free-Radical Copolymerization: the Pseudo-Kinetcs Rate Constant Method. *Polymer* **32**, 2641-2647.

Tobita H. and Hamielec A. E. (1988) A Kinetic Model for Network Formation in Free Radical Polymerization. *Makromol. Chem. Macromol. Symp.* **20/21**, 501-543.

Tonelli A. E. (1977) Glass Transition Temperatures of Requlary Alternating Acrylonitrile-Vinyl Acetate Copolymers. *Macromolecules* **10**, 716-717.

Toppet S. M., Slinckx M. and Smets G. (1975) Influence of the Reaction Medium on the Composition and the Microstructure of Styrene-Acrylic Acid Copolymers. *J. Polym. Sci. Chem.* **12**, 1879-1887.

Tsuchida, E., Aoyagi, J., Shinzo, K. and Shinohara, I. (1974) Simulation of Kinetic analysis on Terpolymerization of Styrene/Butyl Methacrylate/Methacrylic Acid System. *Polymer* **15**, 479-

484.

Uematsu I. and Honda K. (1965) The Glass Transition Temperature of Copolymer. *Report on Prog. in Poly. Phys. in Japan* **VIII**, 111-114.

Walling C. (1949) Copolymerization. XIII. Over-all Rates in Copolymerization. Polar Effects in Chain Initiation and Termination. *J. Am. Chem. Soc.* **71**, 1930-1935.

Wang C. and Ruckenstein E.(1993) On the Gel Effect in the Presence of a Chain Transfer Agent in Methyl Methacrylate Polymerization and Its Copolymerization with Various Acrylates. *J. Appl. Polym. Sci.* **49**, 2179-2188.

Wittmer P. (1979) Kinetics of Copolymerization. *Makromol. Chem. Suppl.* **3**, 129-156.

Wood L. A. (1958) Glass Transition Temperatures of Copolymers. *J. Polym. Sci.* **XXVIII**, 319-330.

Xie T. Y. and Hamielec A. E. (1993a) Modelling Free-Radical Copolymerization Kinetics --- Evaluation of the Pseudo-kinetic rate constant method, 2[a)] Molecular Weight Calculation for Copolymers with Long Chain Branching. *Makromol. Chem. Theory Simul.* **2**, 455-483.

Xie T. Y. and Hamielec A. E. (1993b) Modelling Free-Radical Copolymerization Kinetics --- Evaluation of the Pseudo-kinetic rate constant method, 1 Molecular Weight Calculation for Linear Copolymers. *Makromol. Chem. Theory Simul.* **2**, 421-454.

Yaraskavitch I. M., Brash J. L. and Hamielec A. E. (1987) An Investigation of the Kinetics of Copolymeriztion of p-Methylstyrene/acrylonitrile to High Conversion: Modelling Diffusion-Controlled Termination and Propagation by Free-Volume Theory. *Polymer* **28**, 489-496.

Yocum R. H. and Nyquist E. B. (1973) *Functional Monomers: Their Preparation, Polymerization and Application.* Marcel Dekker, New York.

Zhu S. and Hamielec A. E. (1991) Heat Effects for Free-Radical Polymerization in Glass Ampoule Reactors. *Polymer* **32**, 3021-3025.

14. Simulation of Emulsion Polymerization

Volume 2 of the thesis focuses on simulation of emulsion homo/copolymerization. As mentioned in chapter 1, emulsion polymerization is a complex heterogeneous process involving transport of monomers and free radicals between aqueous and organic phases. Compared to other heterogeneous polymerizations, like suspension or precipitation, emulsion polymerization is likely the most complicated system since reactions occur simultaneously in both phases. The rate of polymerization in the organic phase is not only controlled by monomer partitioning but also affected by other phenomena like particle nucleation, and radical absorption and desorption. Particle stability is affected by emulsifier type, amount of emulsifier and ionic strength of the dispersion media. All these factors make modelling of this system very difficult. Other difficulties encountered in modelling emulsion polymerization include numerical intensity in solving sets of nonlinear ordinary differential equations coupled with algebraic equations and estimation of model parameters. Though emulsion polymerization has been commercialized for more than half a century, some important aspects like particle nucleation, coagulation, etc. are still not well-understood. To simulate this complicated process, a general approach has been adopted. Information from classical modelling sources in the literature (e.g., Min and Ray, 1978; Lichti et al., 1981; Kiparissides and Ponnuswamy, 1981; Penlidis et al., 1986, etc.) has been carefully reviewed and general mass (molar), energy, population (dead polymer molecules and radicals) and particle balances have been written and evaluated, with the final aim to develop a model that is flexible, reliable and practical at the same time.

14.1 Brief Overview of the Classical Smith-Ewart Theory

Advances in achieving a basic understanding of emulsion polymerization have been made by many researchers. Because of the complexity of the system, contradictory conclusions often exist in early studies. It is not the scope of this thesis to give a complete and thorough literature review on all aspects of emulsion polymerization. Instead, emphasis was focused on more recent developments. The basic mechanism of emulsion polymerization was first postulated by Harkins (1947). A typical emulsion polymerization recipe usually includes a dispersion medium (water), monomer, water soluble initiator and emulsifier. Figure 14.1 is an illustrative diagram of this heterogeneous system.

Emulsifier dissolves in water at very low concentration, whereas at higher concentrations (above the critical micelle concentration, cmc), it will form aggregates called micelles. Sodium dodecyl sulfate (SDS) is a typical emulsifier, with a hydrophobic and a hydrophillic end. When micelles are formed, the hydrophillic end of each emulsifier molecule on the surface points towards the aqueous phase while its hydrophobic end points inwards. Hence, the interior of each micelle is highly hydrophobic. Monomers can exist inside micelles, or form large monomer droplets (compared to micelles) stabilized by emulsifier.

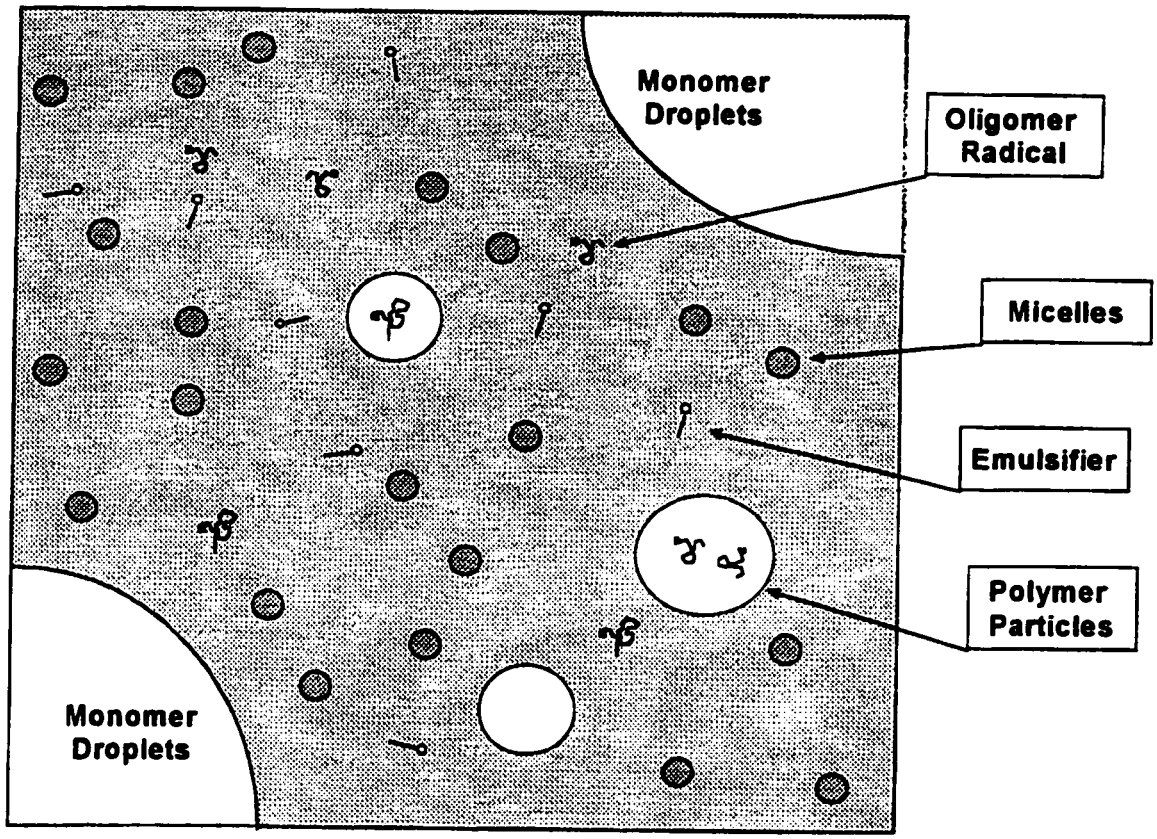

Figure 14.1 Emulsion Polymerization Diagram (stages I and II)

Conventional emulsion polymerization starts in the aqueous phase, where water soluble initiators decompose and generate primary radicals. These primary radicals will propagate in the aqueous phase first and then will enter surrounding micelles. Emulsion polymerization is considered to go through

three intervals. In the first interval, polymer particles are generated. Polymer particles continue to grow in the second stage by absorbing more monomer from the monomer droplets, which serve as a monomer reservoir. Based on thermodynamic equilibrium, the monomer concentration in the polymer particles during the first and second intervals remains relatively constant. The second interval ends when all monomer droplets are consumed. In the third interval, polymerization is completed when all the monomer left in the particles is consumed or a limiting conversion is reached. Figure 14.2 shows the three intervals, and displays the most important phenomena in a typical emulsion reaction.

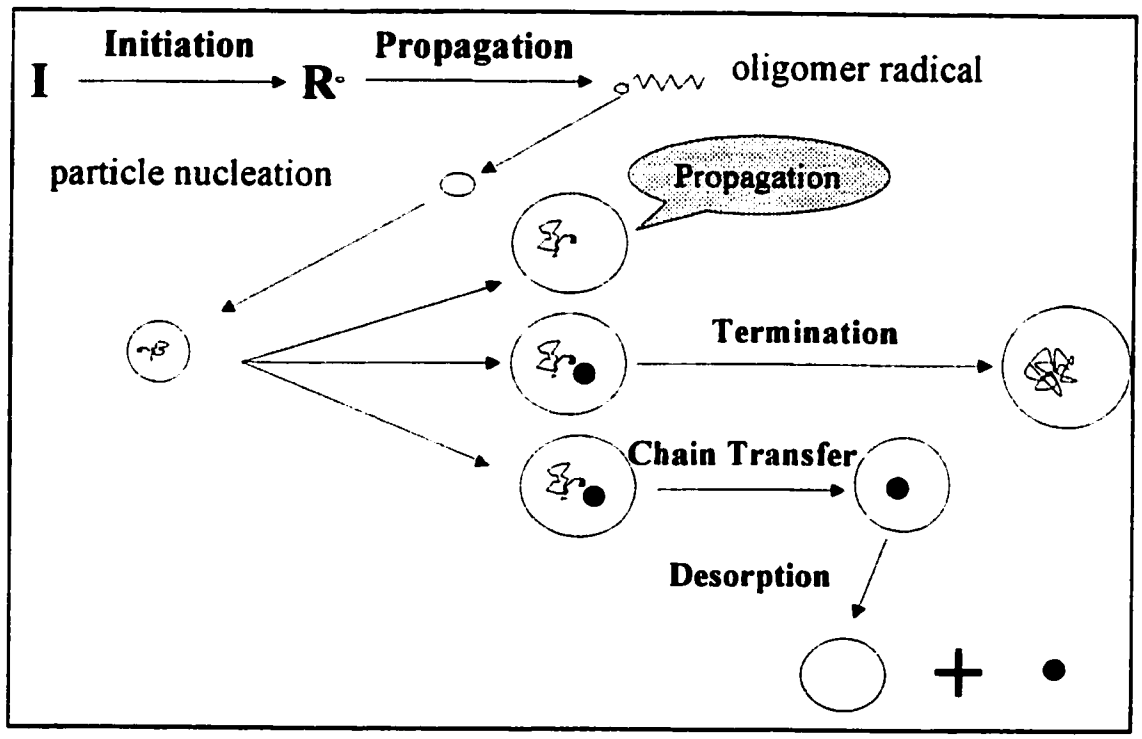

Figure 14.2 Emulsion Polymerization Diagram

Early studies on emulsion polymerization kinetics were limited to aspects like the effect of initiator and emulsifier on number of particles and rate in a qualitative way. Smith and Ewart (1948) were the first group that quantitatively expressed Harkins' postulation in an empirical formulation that related number of particles to the rate of initiation and emulsifier concentration as shown below:

$$Np = 0.37(\rho/\mu)^{2/5}(a_s S)^{3/5} \tag{14.1}$$

where:

Np: number of particles per liter of water

a_s: surface area occupied by unit weight of emulsifier

S: weight concentration of surfactant

ρ: rate of aqueous radical generation by initiation

μ: particle volume growth rate

Models in the 60's and 70's were more or less extended/modified versions of the Smith and Ewart's expression but applied to different monomer systems. Representative ones are Gardon (1968a, b, c, d, e) and Harada et al.(1972).

Equation 14.1 is widely referred to as the Smith-Ewart equation and it indicates the important relationship that the particle number depends on the 0.6 power of the emulsifier concentration and on the 0.4 power of the initiator concentration.

In a way similar to bulk and solution polymerization ($Rp = k_p[M][R\cdot]$), the rate of polymerization in emulsion polymerization can be written as:

$$R_p = k_p[M]_p \frac{N_p \bar{n}}{N_A V_p} \tag{14.2}$$

where $[M]_p$ is the monomer concentration in particles, N_p is the total number of particles in the reaction mixture, $\bar{n}$ is the average number of radicals per particle, V_p is the total volume of particles and N_A is Avogadro's number. $N_p\bar{n}/N_AV_p$ gives the total radical concentration in the particles. To calculate the rate of polymerization, it is necessary to know the values of all four variables $[M]_p$, N_p, V_p and $\bar{n}$ in equation 14.2.

According to the Smith-Ewart scheme, Rp in interval I increases due to the increasing number of newly formed particles, however Rp will remain relatively constant during interval II, since no new particles are formed and the monomer concentration inside the particles $[M]_p$ remains constant based on thermodynamic equilibrium. The conversion versus time curve in this interval appears to be linear. The Smith-Ewart equation has been applied successfully to monomers with very low water solubility (like styrene). However, many monomers with higher water solubility deviate from the Smith-Ewart classical kinetic scheme. The most important reasons for these discrepancies are listed below:

(1): If the monomer is water soluble like acrylonitrile, vinyl acetate, methyl acrylate, etc., there will be additional water phase polymerization.

(2): If there is significant radical desorption present, the average number of radicals per particle $\bar{n}$ will be lower than 0.5. Whenever $\bar{n}$ is less than 0.5, the response of rate of polymerization to changes in emulsifier concentration will be less than predicted. Several commercially important monomer systems fall into this class, which includes vinyl chloride, vinylidene chloride, methyl acrylate and vinyl acetate.

(3): The Smith-Ewart model can only be applied to intervals I and II. At high conversion levels, there are maybe several radicals coexisting in a large particle, and $\bar{n}$ may well be above 0.5. Each particle is like a mini-bulk reactor and bulk kinetics can be applied. The rate of polymerization is higher in stage III than it is in stage II. Examples of this deviation can be observed in methyl methacrylate and butyl acrylate emulsion polymerization.

A large body of evidence from many experiments confirms the above deviations, thus the Smith-Ewart scheme is limited to systems like styrene at low to mid-range of conversion. Ugelstad and Hansen (1976), Min and Ray (1974), Alexander and Napper (1971), and Gilbert and Napper (1983) gave extensive reviews on earlier kinetic studies and further discussed deviations from the Smith-Ewart scheme in great depth.

14.2 Recent Advances

It is clear that early research investigated only specific aspects in emulsion polymerization. With recent advances in both emulsion kinetics and polymer characterization, more in-depth studies have been carried out on important aspects in emulsion polymerization and better understanding has been achieved. A good review on recent advances in emulsion kinetics is given by Gilbert (1995). Researchers have also expanded their work from homopolymerization to copolymerization and even terpolymerization. Several models have been developed by different research groups, and these models have been extended to predict long chain branching, particle size, sequence length and molecular weight characteristics.

There is a large body of models in the literature that describe certain aspects of emulsion polymerization. This thesis does not intend to give a thorough review on all models presented; rather, it focuses on the research work from the most prominent groups. Table 14.1 lists most comprehensive models presented in recent years. Models that can predict molecular weight characteristics are marked as MWD, and models that can deliver particle size characteristics are marked as PSD.

Though there are a number of models available in the literature, most of them deal only with specific aspects in emulsion polymerization and are far from being general. Only models that are comprehensive in nature are selected to be listed in Table 14.1. Among them, models from Ray's and Hamielec's groups are worth noting. Their models are not only the most comprehensive but, more importantly, they are being continuously improved over the years. Min and Ray (1974) was the first group that presented a comprehensive mathematical model that includes particle nucleation (both micellar and homogeneous), desorption, scission, backbiting and transfer to monomer and polymer, while particle size and molecular weight characteristics are calculated based on a population balance approach. Their model was first tested with MMA homopolymerization in Min and Ray (1976, 1978), and was further enhanced by Rawlings and Ray (1988a,b).

Table 14.1 Models of Emulsion Homo-/Copolymerization

Groups	Remarks	Systems
Ballard et al.(1981)	copolymerization model for 0-1 systems	
Broadhead et al.(1985)	copolymerization model, CSTR operation, PSD, long chain branching frequency	Sty/BD
Congalidis et al.(1989)	PSD, copolymerization model	MMA, Sty
Dougherty (1986a,b)	comprehensive model, MWD, PSD, copolymerization model	Sty/MMA
Dube et al.(1996)	monodispersed particle size, long-chain branching, copolymerization model	BD/AN
Forcada and Asua (1990, 1991)	sequence length, monodispersed particle size	Sty/MMA
Giannetti et al.(1988)	reviews on PSD	
Giannetti (1989)	copolymerization model using pseudo-homopolymerization approach	
Guillot et al.(1986)	thermodynamic aspects in copolymerization	Sty/AN
Hamielec et al.(1983,1987)	branching, crosslinking, PSD, MWD	
Lichti et al.(1982)	reviews on PSD, MWD	
Lin et al.(1981)	azeotropic composition, copolymerization model	Sty/AN
Mead and Pochlein (1988, 1989)	copolymerization model, monodispersed particle size	Sty/MA, Sty/AN
Min and Ray (1974, 1976, 1978)	comprehensive model, PSD, MWD	MMA
Nomura et al. (1982, 1983, 1985, 1989)	monodispersed particle size, copolymerization model	MMA/Sty
Penlidis et al.(1984)	polyvinyl chloride (PVC) emulsion polymerization in CSTR reactor, PSD, MWD	PVC
Penlidis et al.(1985a)	batch reactor, PSD, MWD, model testing results	VAc
Penlidis et al.(1985b)	dynamic and steady-state modelling of batch, semibatch and CSTR latex reactors, PSD	
Penlidis et al.(1986)	comprehensive review, copolymerization model, PSD, MWD	PVC, VAc/PVC

Rawlings (1985)	comprehensive model, PSD, MWD, CSTR stability	MMA, Sty, VAc
Richards et al.(1989)	an updated version of the early model of Congalidis et al.(1989), copolymerization model, no micellar nucleation assumed, MWD, PSD	MMA MMA/Sty
Rawlings and Ray (1988a,b)	an updated version of the early Min and Ray's model, PSD, MWD, CSTR operation, studies on CSTR oscillation	MMA
Saldivar et al.(1998)	most recent version of Min and Ray's model, PSD, MWD, copolymerization model	MMA/Sty, Sty/α-methyl Sty, Sty/BD
Storti et al.(1989)	copolymerization model using pseudohomopolymerization approach	AN/Sty/ MMA
Urretabizkaia et al.(1994a, b)	terpolymerization model	MMA/BA/ VAc

Rawlings and Ray (1988b) tested the simulation of homopolymerization of MMA, styrene and vinyl acetate in their work. The most recent development from Ray's group is published by Saldidar et al.(1998). They reviewed previous models in the literature (post Smith-Ewart period). They extended their model to simulate copolymerization in emulsion, and their model was tested with three copolymer systems, MMA/Sty, Sty/α-M Sty and Sty/BD. Other major research work from Ray's group is the studies of the dynamics of emulsion polymerization in CSTR operation (reactor startups, oscillations, and steady-state operation). In summary, the model from Ray's group is probably the most sophisticated and detailed among all available at the cost of a very complex mathematical model structure. To keep it tractable yet still rigorous, simplifications are given by Saldidar et al.(1998).

Hamielec's group also developed a comprehensive model which can describe particle size as well as molecular weight characteristics of emulsion homo- and copolymerization. The first version of a comprehensive model was presented by Hamielec et al.(1983). Their model predicts rate of polymerization, particle size, molecular weights, copolymer composition, branching, crosslinking,

etc.. Unlike Ray's model in which the molecular weight distribution was coupled with the particle size distribution, Hamielec et al.(1982, 1983) modelled the particle size distribution by using particle birth time as an internal cordinate. According to this definition, the growth rate of every newly formed particle generation depends on the birth time of the first generation of particles. This approach avoids solving full population balance equations which can be very intensive mathematically and reduces the full population balance equations to ordinary differential equations, thus making predicting particle size characteristics much easier. Nevertheless, Saldivar et al.(1998) commented that such a method does not account for the effect of particle size on rate of polymerization and molecular weight distribution at various stages of the reaction. Though Hamielec's model does not have the sophistication Ray's model has, it's very easy to implement without losing details. Hamielec's group is also one of the very few that investigated the gel effect in emulsion polymerization. The detailed mathematical model frame was described in Penlidis et al.(1985a, 1986) and simulation results for emulsion polymerization of vinyl acetate, and vinyl acetate/vinyl chloride were presented. Literature models were reviewed by Penlidis et al.(1985b). Hamielec model was also applied to simulate copolymerization in emulsion. Broadhead et al.(1985) presented a copolymerization model which can predict particle size distribution, molecular weight averages and long chain branching of Sty/BD copolymerization in emulsion. The original Hamielec model was further improved by Penlidis' group, and a more recent version was presented by Dube et al.(1996). This model was used to simulate the NBR rubber (acrylonitrile/butadiene) production process.

Gilbert's group (Congalidis et al. 1989, Richards et al. 1989) has also been attempting to develop a comprehensive model for emulsion polymerization. In their work, particles are assumed to be generated homogeneously even though the emulsifier concentration is above the critical micelle concentration (CMC). This assumption is still of controversial. Their model has been tested to simulate homopolymerization of styrene and copolymerization of MMA/Sty, but limited simulation results were presented in Richards et al.(1989). Dougherty et al.(1986a, b) presented a detailed model to simulate MMA/Sty copolymerization, and their model was then used with online process measurements for process control purposes.

15. Development of Emulsion Polymerization Simulation Package

The objective here is to build a general model that covers the entire spectrum of important physical-chemical phenomena in emulsion polymerization. The comprehensive model consists of a set of differential equations as well as algebraic equations based on mass and energy balances. The following sections cover each important aspect in emulsion polymerization.

The model was constructed based on a set of assumptions. These assumptions are:

(1): Particle size is monodisperse. If particles are generated in stage I in a relatively short period of time, this assumption holds. This assumption will not be valid if more emulsifier is added into the system in a semibatch or CSTR operation.

(2): Reactor is perfectly mixed.

(3): The main loci of polymerization is inside polymer particles. The assumption is usually justified unless we deal with mini- or microemulsion cases.

15.1 Initiation

A water soluble initiator I, like potassium persulfate (KPS), is commonly used in emulsion polymerization. When heated, it will decompose into two highly reactive free radicals $R\cdot_o$ which then react with monomers available in the water phase,

$$S_2O_8^{-2} \xrightarrow{k_d} 2SO_4^{-}\cdot \tag{15.1}$$

$$SO_4^{-}\cdot + M \xrightarrow{k_p} R_1\cdot \tag{15.2}$$

where k_d is the rate constants for reaction 15.1. The rate of initiation is:

$$R_I = 2fk_d[I] \tag{15.3}$$

Redox initiation can be used when emulsion polymerization is especially conducted at low temperatures. A typical example of this is the acrylonitile/butadiene rubber production at 5~10°C. A redox system includes a water soluble initiator, a reducing agent (RA) and an oxidation agent. A

typical initiation mechanism involving a redox system as proposed by Anderson and Proctor (1965) follows:

$$S_2O_8^{2-} + Fe^{2+} \xrightarrow{k_1} SO_4^{\cdot-} + Fe^{3+} + SO_4^{2-} \tag{15.4}$$

$$RA + Fe^{3+} \xrightarrow{k_2} Fe^{2+} + X \tag{15.5}$$

$$SO_4^{\cdot-} + M \xrightarrow{kp} R_1\cdot \tag{15.6}$$

The mass balances for the reacting species involved in reactions 15.4~15.6 are:

$$\frac{dN_I}{dt} = F_I^{in} - k_1[I]_w N_{Fe^{2+}} + F_I^{out} \tag{15.7}$$

$$\frac{dN_{RA}}{dt} = F_{RA}^{in} - k_2[RA]_w N_{Fe^{3+}} + F_{RA}^{out} \tag{15.8}$$

$$\frac{dN_{Fe}^{2+}}{dt} = -k_1[I]_w N_{Fe^{2+}} + k_2[RA]_w N_{Fe^{3+}} \tag{15.9}$$

$$\frac{dN_{Fe}^{3+}}{dt} = k_1[I]_w N_{Fe^{2+}} - k_2[RA]_w N_{Fe^{3+}} \tag{15.10}$$

$$\frac{dN_{SO_4^{\cdot-}}}{dt} = k_1[I]_w N_{Fe^{2+}} - N_{SO_4^{\cdot-}} kp[M]_w \tag{15.11}$$

where N stands for the number of moles of a particular species denoted by the subscript, and F is the flow rate of a particular reactant. The total mass of iron (both Fe^{2+} and Fe^{3+}) remains constant as can be seen in reactions 15.4 and 15.5, and this leads to:

$$\frac{dN_{Fe}}{dt} = \frac{dN_{Fe}^{2+}}{dt} + \frac{dN_{Fe}^{3+}}{dt} \tag{15.12}$$

and

$$N_{Fe} = N_{Fe^{2+}} + N_{Fe^{3+}} \tag{15.13}$$

If we assume that dN_{Fe2+}/dt is negligible, through a mass balance on Fe^{2+}, the number of moles of Fe^{2+} can be obtained as:

$$N_{Fe^{2+}} = \frac{k_2 N_{Fe}[RA]_w}{k_1[I]_w + k_2[RA]_w} \tag{15.14}$$

Finally, the total rate of initiation R_i including both thermal decomposition of a water soluble initiator and redox initiation systems is expressed as:

$$R_i = 2fkd[I]_w + k_1 \frac{N_{Fe^{2+}}}{V_w}[I]_w \qquad (15.15)$$

V_w is the total volume of water in liters.

15.2 Particle Nucleation and Growth

Particle nucleation by far is the most important phenomenon in emulsion polymerization. It has generated a lot of research interest and remains the most discussed and sought-after subject in emulsion kinetics. This is because not only the rate of polymerization is directly related to the total number of particles but particle size distribution is a key indicator of emulsion latex physical properties. Despite of countless efforts made by various groups so far, the understanding of particle generation is poor, and the prediction of particle number and size is still not very successful. There are several reasons for this:

(1): the measurement of number and size of polymer particle nuclei which are in the region of a few hundred angstroms presents extremely difficult experimental problems.

(2): there are many complex microprocesses occurring simultaneously, e.g., radical absorption, precipitation, coagulation, etc., and each microprocess itself is difficult to understand and model.

In the early studies, it was accepted that particles are generated by micelles absorbing radicals from the water phase. This is the so-called micellar nucleation. Smith and Ewart (1948) stated that the rate of particle nucleation with the presence of micelles is controlled by the laws of diffusion. They then used equation 14.1 to calculate the total particle number as a function of emulsifier concentration and initiation rate.

A new particle nucleation mechanism was proposed by Hansen and Ugelstad (1978) as well as by

Fitch and Tsai (1971a,b) after the original Smith-Ewart's postulation. It was stated by these two groups that particles can be generated by precipitated water phase oligomer radicals. This is the so-called homogeneous particle nucleation. It is now widely accepted that both phenomena coexist in most emulsion polymerizations. Both mechanisms are discussed in the following sections.

15.2.1 Micellar Nucleation

There are basically two different theories that describe radical absorption by micelles or particles. Smith and Ewart (1948) postulated that this phenomenon is a diffusion process, however the Smith and Ewart scheme (equation 14.1) actually reflects a collision process. Micellar nucleation can also be described as a collision process (Gardon 1968a, b, c, d, e, f). The expression for the rate of micellar nucleation (Rc) based on diffusion and collision theories is given in equations 15.16 and 15.17, respectively:

$$R_c = 4\pi r D_w [R\cdot]_w \tag{15.16}$$

$$R_c = 4\pi r^2 k_{mp} [R\cdot]_w \tag{15.17}$$

where D_w in equation 15.16 is the diffusivity coefficient of the radicals in the water phase and k_{mp} in equation 15.17 is the mass transfer coefficient for water phase radical oligomers. In both equations, r is the radius of the micelle/particle and $[R\cdot]_w$ is the concentration of water phase radical oligomers. It is very obvious that the only difference in the two equations is that the rate of absorption of radicals is proportional to the micelle/particle radius according to diffusion theory, whereas according to collision theory, it is proportional to the micelle/particle surface area.

Both diffusion theory and collision theory have been used to describe particle nucleation by a number of authors. Hansen and Ugelstad (1978, 1982) and Song and Poehlein (1988a, b) used the diffusion theory to calculate rate of radical absorption. Groups using collision include Fitch and Tsai (1971a,b), Min and Ray (1974), Dickinson (1976) and Kiparissides (1978). Generally speaking, it is difficult to distinguish which theory is more of advantage over the other. Barrett (1975) pointed out that radicals are assumed to travel in a straight line in the collisional approach and this underestimates the

probability of collision with a particle. Fitch and Tsai (1971a,b) were the first to used the collision theory to quantify the rate of radical capture, and in a later study, Fitch and Shih (1975) measured the radical capture rate for MMA seeded polymerization. Their experimental data support the conclusion that R_c is proportional to the first power of particle radius, thus it should be considered as a diffusional process. From a theoretical point of view, it is unlikely that the mass transfer coefficient k_{mp} in equation 15.17 is a constant, since its value depends on many factors like particle size, ionic strength of the media, radical chain length of radical and surface charge of the particle. Therefore, equation 15.17 is a very simplified formulation to describe the particle nucleation process. However, this does not imply that the diffusion approach is of any advantage over the collision approach. As a matter of fact, the micellar particle nucleation process is neither a pure diffusional nor a collisional process, but rather a combination of both. The approach adopted in this thesis is based on the diffusion theory simply because there is more kinetic information available in the literature.

Hansen and Ugelstad (1978, 1982) were the only group that attempted to quantify effects of radical chain length, particle size and surface charge density on the rate of particle absorption. They proposed a concept of reversible/irreversible absorption, which postulated that an absorbed radical may escape out of the particle many times before it is irreversibly absorbed. An improved version of equation 15.16 for the rate of particle nucleation is:

$$R_c = 4\pi r D_w [R\cdot]_w F \tag{15.18}$$

F in the above equation is an efficiency factor for radical absorption. It takes the effects of radical solubility, particle surface electrical potential and particle size into account. The detailed calculation of F is complicated and requires many additional parameters that are difficult to obtain. The conclusions from Hansen and Ugelstad's (1982) study are: (1) when radicals are large and hydrophobic, adsorption is irreversible, i.e., $F \approx 1$ (2) when particles are small, the electrostatic effects are negligible (3) if small radicals are more hydrophilic, absorption is more likely to be reversible, i.e., $F \to 0$. Though Hansen and Ugelstad's (1978, 1982) approach is more theoretically sound, the absorption efficiency is nevertheless very difficult to estimate, and its complexity makes it somewhat impractical to use. In this emulsion model, equation 15.16 is used without implementing the capture

efficiency F. D_w in equation 15.16 should be considered as a lumped parameter which combines many factors rather than a pure diffusivity coefficient. This probably is the reason why reported values of D_w in the literature vary considerably.

There are some other approaches to model the particle nucleation process. A method that is similar to the collision theory, because it postulates that the rate of particle nucleation is proportional to the total micelle surface area, suggests:

$$\frac{dNp}{dt} = N_A\left(k_{cm}\frac{[R\cdot_{tot}]_{capt}}{r_{mic}}\right)\frac{A_m}{A_m+\varepsilon A_p} \qquad (15.19)$$

The ε in the above equation represents the ratio of radical absorption between micelles and particles. A_p is the total surface area of particles, A_m is the free micellar area, $[R\cdot_{tot}]_{capt}$ is the concentration of water phase radicals that can be absorbed by either micelles or particles, k_{cm} is the rate constant for radical absorption by micelles and r_{mic} is the radius of a micelle. It is also assumed that each particle surface is entirely covered by emulsifier molecules. Several groups including Dougherty (1986a), Penlidis et al.(1986) and Dube et al.(1996) used equation 15.19 to calculate Np. Parameters k_{cm} and ε have to be estimated experimentally. The free micellar area available for micelle formation (and hence, for particle formation via micellar nucleation) can be calculated as:

$$A_{mic} = ([S]_t-[S]_{cmc})S_a V_w N_A - A_p - A_{md} \qquad (15.20)$$

where S_a is the area covered by a single emulsifier molecule. $[S]_t$ is the total concentration of emulsifier, and $[S]_{cmc}$ is the critical micelle concentration. The value of all these three variables can be calculated for a specific emulsifier. A_{md} is the total surface area of monomer droplets, and since A_{md} is several orders of magnitude smaller than the total surface area of particles, it can safely be omitted. The area of particles A_p can be calculated by the expression below, if a particle is considered spherical,

$$A_p = (36\pi N_p)^{1/3}(V_p)^{2/3} \qquad (15.21)$$

15.2.2 Homogeneous Nucleation

Priest (1952) first observed that particles can still be formed without the presence of micelles (in this

case there is either no emulsifier or its concentration is below CMC). When a radical in the aqueous phase propagates beyond its solubility (due to the continuous addition of monomer units), it becomes a primary particle, also called a particle precursor. A primary particle is stabilized by either the initiator segments at the chain ends or available emulsifier in the system. Napper and Alexander (1962) later confirmed Priest's observation and described the homogenous particle nucleation qualitatively. Fitch and Tsai (1971a,b) was the first group that proposed a detailed mechanism for this self-nucleation process and gave a quantitative calculation for the rate of homogeneous particle nucleation. They assumed that a water phase radical will travel a distance L before it becomes a primary particle. The longer the distance, the more likely it will be absorbed by an existing particle. If it is absorbed by an existing particle, no new particle is formed. These primary particles will subsequently undergo extensive flocculation. According to Fitch and Tsai's (1971a) postulation, the rate of particle nucleation is then:

$$\frac{dNp}{dt} = R_i - R_c - R_f \tag{15.22}$$

where R_c is the rate of absorption of radicals, R_i is the rate of radical generation through initiation and R_f is the rate of flocculation. When there is sufficient emulsifier in the system, primary particles are stable and flocculation is nearly negligible. This makes the rate of particle nucleation directly related to R_i and R_c, and R_f can be dropped in equation15.22.

Fitch and Tsai (1971a) derived an expression for the rate of radical absorption as:

$$R_c = \pi r_p^2 L R_i Np \tag{15.23}$$

where:

L: the average distance of diffusion a water phase radical travels before it has grown to a size at which it precipitates as primary particle

r_p: particle radius

The above equation suggests that the rate of radical absorption is proportional to the cross-section area of the radical and the particle, therefore the radical absorption process can be described as a collision process. Another key parameter in Fitch and Tsai's model is the average distance L. Fitch

and Tsai's (1971a) demonstrated that L is in the magnitude of 2.8×10^{-3} cm, and it is obvious that L is very sensitive to monomer solubility in the water phase. In a later publication, Fitch (1981) treated the radical absorption as a diffusion process, and the rate of radical absorption was expressed as:

$$R_c = 4\pi r_p D_w Np[R\cdot]_w \tag{15.24}$$

$[R\cdot]_w$ is the number of radicals per liter water and Np is the total number of particles per liter water. After the original work on homogeneous particle nucleation by Fitch and Tsai (1971a,b), a number of research groups have attempted to quantify the homogeneous particle nucleation process using different approaches. A more rigorous model was proposed by Hansen and Ugelstad (1978). This group modeled the homogeneous nucleation by using a population balance on water phase oligomer radicals with chain length less than j_{cr} which is the critical chain length beyond which an oligomer radical will precipitate and form a primary particle. Using this approach, Hansen and Ugelstad (1978) successfully calculated $[R]_w$, which is needed to calculate the rate of radical absorption. In order to understand Hansen and Ugelstad's more rigorous approach, a visualization of all water phase phenomena is essential. Such visualization will help one to establish a mass balance of oligomer radicals of various chainlengths. Figure 15.1 elucidates how a particle is formed either by homogeneous particle nucleation or by micellar absorption.

15.2.3 Mass Balances of Radicals in the Water Phase

The mass balance of radicals in the water phase is affected by radicals entering the water phase, radicals leaving the water phase and reactions involving water phase radicals. A complete list of possible reactions of radicals in the aqueous phase is given in Table 15.1.

Table 15.1 Water phase phenomena involving radicals

Process	Results
radicals entering the water phase	
initiation	*major source of radical generation*
desorption	*small radicals entering water phase*

radicals leaving the water phase	
radical captured by a micelle	*micellar particle nucleation*
radical captured by a particle	*does not change total particle number*
radical captured by a monomer droplet	*negligible in conventional emulsion polymerization*
reactions involving radicals	
radical propagates with monomers	*no effect on total number of radicals*
radical termination	*produces oligomeric polymer in water phase*
radical reacts with impurities	*reduces total number of radicals in water phase*
radical reacts with small molecules	*chain transfer reaction, produces monomeric radicals*
radicals form a particle	*homogeneous particle nucleation*

(1) Radical generation by initiation

Chemical initiator decomposition is the major source for radicals entering the water phase. As long as there is initiator present, there will always be radicals generated. The mechanism and rate expressions have already been given in section 15.1.

(2) Radical desorption from particles

Chain transfer reactions like transfer to monomer and to CTA in a polymer particle will produce a monomeric or CTA radical. Such small radicals may desorb into the water phase, especially when monomer or CTA radicals are more water soluble.

(3) Radicals captured by a micelle

If a micelle captures a radical, it then becomes a particle. This is the so-called micellar nucleation discussed above. Most particles are generated this way.

(4) Radicals captured by a particle

Particles compete with micelles in absorbing water phase radicals. The ratio of radicals entering particles is proportional to the total particle surface area.

(5) Radical propagates with monomers

Primary radicals generated either by initiation or by chain transfer reaction will propagate with monomer dissolved in the aqueous phase and grow into oligomers. This reaction consumes a very small percentage of monomers, but oligomers produced in this step may form particles when they reach a critical size.

(6) Radical terminates with another radical

This reaction stops water phase radical growth and produces oligomeric polymer. This reaction is usually considered unimportant by many groups.

(7) Radical reacts with impurities

Water soluble impurities kill active radicals and generate a dead molecule. The overall effect is the delay of the start of emulsion polymerization. This reaction is usually neglected by most models in the literature. More in-depth studies of impurity effects on reaction kinetics can be found in Appendix 2.

(8) Reaction involves small molecules

In general, chain transfer to small molecules has little effect on the overall particle number and size. However, chain transfer to small molecules actually produces emulsifier-like oligomers which may have some effect in emulsifier-free reactions.

(9) Radicals precipitate and form a particle

This is another source of particle nucleation. A lot of research effort has been put into the modeling of homogeneous nucleation. Representative efforts are the micro-approach by Hansen and Ugelstad (1978) and the macro-approach by Fitch and Tsai (1971a,b).

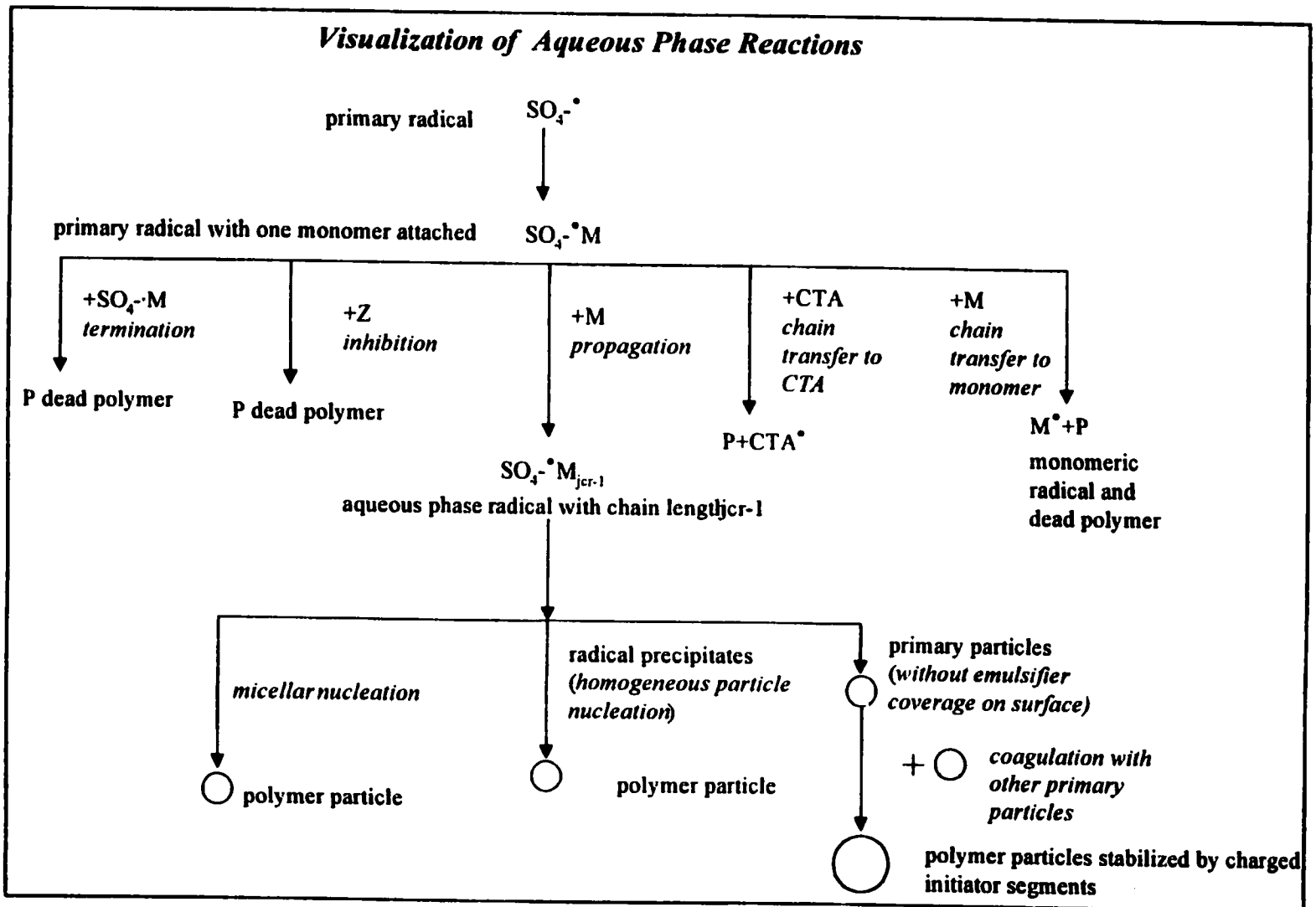

Figure 15.1 Particle formation in aqueous phase

The method used in this thesis to model homogeneous particle nucleation is analogous to the postulation in Hansen and Ugelstad (1978), but it is more general by including reactions like chain transfer to CTA and inhibitor, as shown in figure 15.1. One very important reaction which is not displayed in figure 15.1 is the desorption process. The original Hansen and Ugelstad's (1978) postulation is based on styrene emulsion polymerization, a monomer with negligible desorption, therefore desorption was not included in their model. To develop a general and yet comprehensive model, desorption was considered when constructing the mass balances for radicals of various chain length, as illustrated below. The mass balances for radicals with chain length from 1 to j_{cr-1} are:

$$\frac{d[R\cdot_o]_w}{dt} = R_I + \frac{k_{des} N p \bar{n}}{N_A V_w} - k_{pw}[M]_w[R\cdot_o]_w - k_z[R\cdot_o]_w[Z]_w - k_{tw}[R\cdot_o]_w[R\cdot_{tot}]_w \tag{15.25}$$

$$\frac{d[R\cdot_1]_w}{dt} = k_{pw}[M]_w[R\cdot_o]_w - k_{pw}[M]_w[R\cdot_1]_w - k_{cp}[N_p][R\cdot_1]_w - k_{cm}[MIC][R\cdot_1]_w - k_z[R\cdot_1][Z]_w - k_{fcta}[R\cdot_1][CTA]_w - k_{tw}[R\cdot_1]_w[R\cdot_o]_w \tag{15.26}$$

$$\frac{d[R\cdot_j]_w}{dt} = k_{pw}[M]_w[R\cdot_{j-1}]_w - k_{pw}[M]_w[R\cdot_j]_w - k_{cp}[N_p][R\cdot_j]_w - k_{cm}[MIC][R\cdot_j]_w - k_z[R\cdot_j][Z]_w - k_{fcta}[R\cdot_j][CTA]_w - k_{tw}[R\cdot_j]_w[R\cdot_o]_w \tag{15.27}$$

$$\frac{d[R\cdot_{jcr-1}]_w}{dt} = k_{pw}[M]_w[R\cdot_{jcr-2}]_w - k_{pw}[M]_w[R\cdot_{jcr-1}]_w - k_{cp}[N_p][R\cdot_{jcr-1}]_w - k_{cm}[R\cdot_{jcr-1}]_w[MIC] - k_z[R\cdot_{jcr-1}][Z]_w - k_{fcta}[R\cdot_{jcr-1}][CTA]_w - k_{tw}[R\cdot_{jcr-1}]_w[R\cdot_{tot}]_w \tag{15.28}$$

In the above equations:

k_{pw}: rate constant for propagation in the water phase, L/mol·min

k_{cp}: rate constant for radical capture by particles, L/mol·min

k_{cm}: rate constant for radical capture by micelles, L/mol·min

k_{des}: rate constant for radical desorption, L/mol·min

k_{tw}: rate constant for termination in the water phase, L/mol·min

k_{fcta}: rate constant for chain transfer to (water soluble) CTAs, L/mol·min

k_z: rate constant for chain transfer to inhibitor dissolved in water, L/mol·min

$[CTA]_w$: CTA concentration in water, mol/L

$[M]_w$: monomer concentration in water, mol/L

$[MIC]_w$: micelle concentration in water, mol/L

$[Z]_w$: concentration of water soluble inhibitor, mol/L

$[R\cdot_o]_w$: concentration of primary radicals (without monomer unit) in the water phase, mol/L

$[R\cdot_j]_w$: concentration of radicals of chain length j in the water phase, mol/L

$R\cdot_{o,w}$: primary radical (without monomer unit) in the water phase

$R\cdot_{j,w}$: radical of chain length j in the water phase, ($j=1\sim j_{cr-1}$)

In homogeneous particle nucleation, a particle is formed by a precipitated radical whose chain length is at the critical chain length j_{cr}. The last propagation step involving a radical of chain length j_{cr-1} and a monomer can actually be considered as the particle formation step, thus the rate of homogeneous particle nucleation is expressed as:

$$\frac{d[N_{phomo}]}{dt} = k_{pw}[M]_w[R\cdot_{jcr-1}]_w \tag{15.29}$$

The concentration of all water phase radicals of various chain lengths can be expressed as:

$$[R\cdot]_w = \sum_{j=0}^{jcr-1}[R\cdot_j] \tag{15.30}$$

In the above equation, when j=0, R· is the decomposed initiator fragment. Adding equations 15.25 to 15.28 gives:

$$\frac{d[R\cdot]_w}{dt} = R_I + k_{des}\frac{Np\bar{n}}{N_A V_w} - k_{pw}[M]_w[R\cdot_{jc-1}]_w - k_{cp}[N_p][R\cdot]_w - k_{cm}[MIC][R\cdot]_w$$
$$- k_{fz}[Z]_w[R\cdot]_w - k_{fcta}[CTA][R\cdot]_w - k_{tw}[R\cdot]_w^2 \tag{15.31}$$

If the steady-state hypothesis is applied to all radicals in the water phase, i.e., set left side of equations 15.25 to 15.28 to zero, one obtains the following equations:

$$[R\cdot_o]_w = \frac{R_I + k_{des} N p \bar{n}/(N_A V_w)}{k_{pw}[M]_w + k_z[Z]_w + k_{tw}[R\cdot]_w} \tag{15.32}$$

$$[R\cdot_j]_w = \frac{k_{pw}[M]_w}{k_{pw}[M]_w + k_{cp}[N_p] + k_{cm}[MIC] + k_{tw}[R\cdot]_w + k_z[Z]_w + k_{fcta}[CTA]_w} \times [R\cdot_{j-1}]_w \tag{15.33}$$

Equation 15.33 is valid for radicals with chain length of 1 to jcr-1, hence equations 15.32 and 15.33 can be backsubstituted into equation 15.29 and one can express the rate of particle formation as the following:

$$\frac{d[N_{homo}]}{dt} = \left[\frac{(R_I k_p[M]_w + k_{des} N p \bar{n}/(N_A V_w)) k_p[M]_w}{k_{pw}[M]_w + k_{tw}[R\cdot]_w + k_z[Z]_w}\right] \times \prod_{j=1}^{J_{cr}-1}\left[\frac{k_p[M]_w}{k_{pw}[M]_w + k_{cp}[N_p] + k_{cm}[MIC] + \pi k_z[Z]_w + k_{fcta}[CTA]_w + k_{tw}[R\cdot]_w}\right] \tag{15.34}$$

A close examination of the denominator of the first term in equation 15.34 would lead to the assumption that $k_p[M]_w >> k_{tw}[R_{tot}]_w + k_z[Z]_w$. This assumption can be justified based on the comparison displayed below:

kp_w	$[M]_w$	kz	$[Z]_w$	kt_w	$[R_{tot}]_w$
10^2~10^3	10^{-2}~10^{-3}	10^{-2}~10^{-3}	10^{-3}~10^{-5}	10^7~10^9	10^{-10}~10^{-12}

If the denominator of equation 15.34 can be safely reduced to $kp_w[M]_w$, then equation 15.34 is simplified as:

$$\frac{d[N_{homo}]}{dt} = (R_I + k_{des} N p \bar{n}/(N_A V_w)) \times \prod_{j=1}^{J_{cr}-1}\left[\frac{k_{pw}[M]_w}{k_{pw}[M]_w + k_{cp}[N_p] + k_{cm}[MIC] + k_z[Z]_w + k_{fcta}[CTA]_w + k_{tw}[R\cdot]_w}\right] \tag{15.35}$$

Equation 15.35 is the ultimate expression used to calculate homogeneous particle nucleation. However, the total radical concentration $[R\cdot_{tot}]_w$ still remains unknown. This can be obtained by applying the steady state hypothesis to equation 15.31, which yields:

$$[R\cdot]_w = \frac{-B+\sqrt{B^2+4(R_I+k_{des}Np\bar{n}/(N_AV_w))k_{tw}}}{2k_{tw}} \tag{15.36}$$

where:

$$B = k_{cp}Np/(N_AV_w)+k_{cm}[MIC]+k_z[Z]_w+k_{fcta}[CTA] \tag{15.37}$$

$[R\cdot_{tot}]_w$ is the positive root of equation 15.36. Now, if we substitute $[R\cdot_{tot}]_w$ back in equation 15.35, the rate of homogeneous particle nucleation can be readily calculated. Equation 15.35 is interesting from a statistical point of view, since the second term of equation 15.35 represents the probability of a water soluble radical adding a monomer unit and is always less than 1. Equation 15.35 also reveals the fact that the more water soluble the radicals (which implies a higher j_{cr}), the lower the rate of homogeneous particle nucleation. Similar conclusions were also made in Song and Poehlein (1988a).

It should also be stated that in the calculation of the rate of homogeneous particle nucleation, the rate constants for radical absorption by micelles and particles, if based on diffusion theory, are:

$$k_{cm} = N_A 4\pi D_w r_{mic} \tag{15.38}$$

$$k_{cp} = N_A 4\pi D_p r_p \tag{15.39}$$

r_{mic} and r_p are the radius for micelles and particles, and D_w, D_p are the diffusivities of radicals in the water phase and inside the polymer particle, respectively. The literature values for both diffusivity coefficients vary widely and are somewhat difficult to obtain. Values of D_w for styrene and vinyl acetate can be found in Song and Poehlein (1988a) and Zollars (1979), respectively, yet caution should be exercised when citing these literature values. Song and Poehlein (1988b) did an extensive investigation on homogeneous particle nucleation for a number of monomers including Sty, BA, MMA, VAc and VCl.

The calculation for the total concentration of micelles is now shown below. Each micelle is an aggregation of a number of emulsifier molecules. The concentration of micelles in mol/L is calculated by:

$$[MIC] = \frac{A_{mic}}{4\pi r_{mic}^2 N_A V_W} \tag{15.40}$$

A_{mic} in the above equation is the total surface area of all micelles which can be obtained by equation 15.20.

Other reacting species like CTAs and impurities also play an important role in the particle nucleation process. The overall effect of each individual species depends largely on their water solubility, which implies that partitioning is very important.

Finally, in a conventional emulsion polymerization, i.e., when the emulsifier concentration is above its CMC, particles are generated both homogeneously and by micelle absorption, and the following expression calculates the rate of change of the number of particles:

$$\frac{dN_p}{dt} = \frac{dN_{p_{homo}}}{dt} + \frac{dN_{p_{mic}}}{dt} \tag{15.41}$$

15.2.4 Recent Modelling Efforts on Particle Nucleation

More recent investigations on particle formation were conducted by Gilbert's groups (Hawkett et al. 1980, Gilbert and Napper 1983, Maxwell et al., 1991). In one of their most recent publications on particle nucleation, Maxwell et al.(1991) stated that radical absorption by particles is not a collisional process because: (1) particle surface charge density does not affect radical absorption; and (2) ionic strength of the media exhibits no influence on radical absorption. Based on their previous experimental evidence, Maxwell et al.(1991) summarized their previous experimental finding and proposed a new model for particle formation. They claimed that the propagation of a water phase radical to its critical chain length z is the rate-determining step in the radical absorption process, thus radical absorption should be considered as a diffusional process. Gilbert's group also observed in their experiments that water phase radicals with chain length less than the critical chain length z are reversibly absorbed, i.e., small radicals can enter and escape a particle many times before they can be irreversibly absorbed. This phenomenon directly indicates that the absorption efficiency F is very small

for radicals with chain length less than z. Their statement is in agreement with Hansen and Ugelstad's (1978) conclusion that the radical absorption efficiency is rather small for smaller radicals. It is now commonly accepted that not all radicals of any size can be irreversibly adsorbed. This finding suggests some modification of equations 15.26 and 15.27. Radicals with short chain length (say, less than $j_{cr}/2$) are not included in $[R_j^{\cdot}]_w$ in the terms such as $k_{cp}[Np][R_j^{\cdot}]_w$ and $k_{cm}[MIC][R_j^{\cdot}]_w$. Some groups have already implemented such a modification in their model (Dube et al., 1996) assuming that radicals of chain length less than half of the critical chain length j_{cr} do not prefer to be captured. This assumption is an empirical approximation. Maxwell et al.(1991) attempted to theoretically calculate the minimum chain length z for which radicals can be captured. Based on thermodynamics, Maxwell et al.(1991) calculate the minimum z for styrene about 2. The commonly accepted j_{cr} for styrene is 3~5 (presented in Hansen and Ugelstad, 1978), therefore Maxwell's calculation is in agreement with what Dube et al.(1996) have practiced in their modelling effort. Maxwell et al.(1991) also calculated z for a number of other monomers like BA, MMA, VAc and VCl. Their calculated z for MMA is 4~5 which is much smaller than the ½ of j_{cr} for MMA (j_{cr} for MMA is about 50). Though there is still discrepancy in the actual value of z for a number of monomers, recent kinetic investigations reveal the fact that not all radicals of any size can be irreversibly absorbed. It is thus reasonable to assume that z is approximately equal to half the value of j_{cr} for most monomers. Though this may seem to be a crude measure, it is the best starting point at our current level of understanding of particle nucleation kinetics. Kshirsagar and Poehlein (1994) attempted to validate Maxwell's et al.(1991) postulation. They measured the critical chain length z for vinyl acetate using bombardment-mass spectroscopy. They reported a value of 5~6 for z for VAc, which is very close to the theoretical prediction (7~8) given by Maxwell et al.(1991) based on thermodyanmics. Kshirsagar and Poehlein's (1994) measurement of z indirectly suggested that the colloidal theory may not be applicable to describe the radical absorption process. In order for the colloidal theory to be valid, the size of oligomer radicals must be quite large, and this is clearly not supported by the experimental measurements from Kshirsagar and Poehlein (1994).

Table 15.2 below is a summary of all kinetic models on particle nucleation.

Table 15.2 Summary of Particle Nucleation Models

Model	Authors	Formula
Collisional Process	Fitch and Tsai (1971a,b)	$Rc=4\pi r_p^2 k_{cm}[Np][R\cdot]_w$
Diffusional Process	Hansen and Ugelstad (1978, 1982)	$Rc=4\pi r_p D_w[Np][R\cdot]_w$
Diffusion/Propagational	Maxwell et al.(1991)	$Rc \propto kp[M]_w[R\cdot]_w$
Collisional/Empirical	Dougherty et al.(1986a) Penlidis et al.(1986)	Rc∝total particle surface area
Surface Coverage	Yeliseeva (1982)	Rc∝surface charge density
Colloidal	Penboss et al.(1983)	DLVO-type colloidal

15.2.5 Specific Modelling Considerations on Particle Nucleation

(1) Steady-State Hypothesis on Aqueous Phase Radicals

The diffusional approach this model adopted was an improved version of Hansen and Ugelstad's (1978) original postulation. After it was implemented into the model, it was tested to reproduce Hansen and Ugelstad's calculations. The comparison of our model's prediction (generated by using exactly the same parameter values and reaction conditions indicated in Hansen and Ugelstad, 1978) with that from Ugelstad and Hansen (1978) is displayed in figure 15.2. It is very clear in figure 15.2 that our model reproduced exactly the results given by Hansen and Ugelstad (1978). Figure 15.2 also reveals the effect of critical chain length on particle generation. More water soluble monomers have a higher critical chain length, which consequently results in a slower particle nucleation rate. This is simply because more water soluble monomers (oligomers) are more likely to stay in the water phase for longer periods of time before they are absorbed by micelles or existing particles. In Hansen and Ugelstad's original study, the validity of the steady-state hypothesis was also carefully examined. Hansen and Ugelstad have demonstrated that the prediction generated under the steady-state hypothesis differs from that generated without the steady-state hypothesis only in the first 10 seconds,

whereas afterwards both curves become indistinguishable. Therefore it is reasonable to state that the steady-state hypothesis can be safely used. Asua et al.(1990) also independently verified the validity of the steady-state hypothesis. More detailed studies on both steady-state and nonsteady-state particle nucleation can be found in Song and Poehlein (1988a,b).

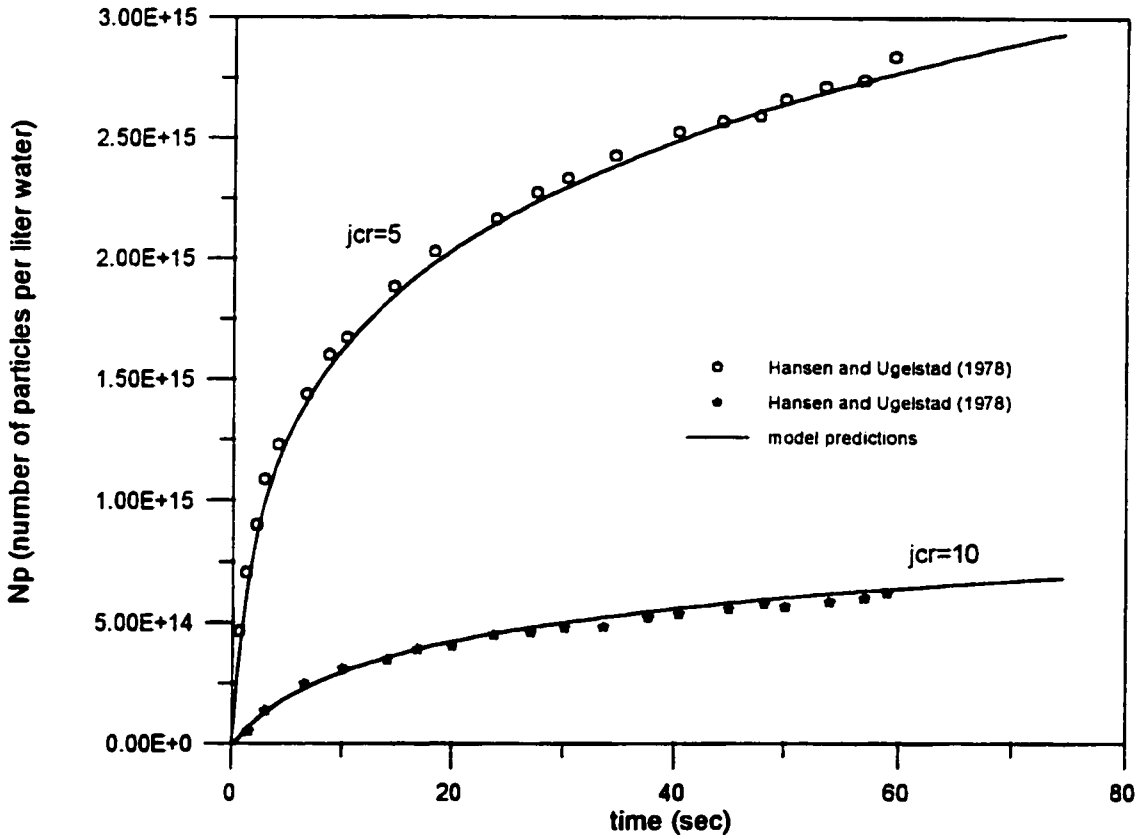

Figure 15.2 Model testing on homogeneous particle nucleation

(2) Model Discrimination

More details were considered in modelling particle nucleation by Hansen and Ugelstad (1982). Water phase radicals derived from initiator decomposition have an ionic initiator fragment attached, which makes these radicals surface active. In contrast, radicals generated by chain transfer to monomers and CTAs do not have an ionic chain end. Hansen and Ugelstad (1982) treated these two types of radicals differently by using different propagation rate constants for propagation and absorption. Maxwell et al.(1991) also assumed that radicals of any chain length without ionic initiator attached can be irreversibly absorbed. It is obviously theoretically advantageous to take this effect into modelling considerations, but it inevitably increases the model's complexity because many more additional rate constants must be estimated. Although Hansen and Ugelstad (1982) presented a model by considering the effect of ionic initiator at the radical chain end on absorption, desorption and propagation, they did not present any estimated values for all rate constants in their model. Recently, de Arbina et al.(1996) compared three models of various levels of complexity, which are: (1) a simple model that does not consider the effect of ionic initiator at radical chain end; (2) a model that considers the effect of ionic initiator at the radical chain end, but assumes no irreversible absorption for radicals of chain length less than z; (3) a model that considers the effect of ionic initiator at radical chain end, but assumes irreversible absorption. They found that all three models fitted the experimental data in a similar way with little difference and they should be considered equivalent. They thus conclude that there is no advantage gained by increasing the model's complexity.

15.3 Monomer Partitioning in Emulsion Homopolymerization

Another important reason why emulsion polymerization is such a complex system is that all reaction ingredients partition themselves in all phases. To keep track of monomer concentration in each phase throughout the reaction is a difficult task simply because there is a lack of satisfactory theory that can fully describe the partitioning phenomenon. To make matters worse, monomer partitioning becomes even more complicated in co-/terpolymerization when several monomers as well as polymer coexist in the same phase. An extensive literature search reveals that most research groups focus on solving this problem empirically, which implies that monomer concentration in both water and polymer

particle phases is measured experimentally. This approach was very popular in early studies and is still the most widely used method nowadays. It is relatively easy to measure monomer concentrations in all phases. From a modelling point of view, a partitioning coefficient is very easy to implement in a model. However, this method becomes increasingly cumbersome and unreliable when more than one monomers are involved in the reaction. Additionally, it is desirable for a model to be capable of predicting monomer concentration for a new emulsion system without measuring the partitioning coefficient each time. In such a case, a theoretical approach is certainly advantageous. It was first demonstrated by Morton et al.(1954) that monomer partitioning can be described by solving the thermodynamic equilibrium equations of participating species in each phase. The principle behind it is the thermodynamic law which states that at the equilibrium state, the chemical potential of each species is the same in all phases under the assumption that thermodynamic equilibrium can be quickly established without mass transfer limitations. Later on, Guillot (1985) presented a similar thermodynamic equilibrium equation for copolymers. It is obvious that calculating monomer concentration based on thermodynamic equilibrium is more theoretically sound but it certainly requires more parameters that are difficult to obtain. Both empirical and theoretical approaches have their own merits and drawbacks. Table 15.3 gives a comparison of the two approaches.

Table 15.3 Comparison of Methods for Monomer Partitioning in Emulsion Polymerization.

	Empirical Approach	Theoretical Approach
Advantages	easy to implement.	theoretically sound, general, can be applied to partitioning involving *n* number of monomers.
Disadvantages	lack of generality. limited to specific monomer system. lack of information for copolymer systems.	numerically difficult to solve sets of nonlinear equilibrium equations; parameters are not available for many systems and are difficult to estimate.

The following two sections describe each approach in greater detail. Because the empirical approach

is rather straightforward, emphasis will be placed on the theoretical approach.

15.3.1 Empirical Approach

Based on a mass balance for monomer, it is easy to express the concentration of monomer in the polymer particle phase as:

$$[M]_p = \frac{N_m}{V_p} \tag{15.42}$$

V_p is the total volume of all polymer particles, which can be expressed as :

$$V_p = \left(\frac{x_c}{\rho_p} + \frac{1-x_c}{\rho_m} \right) N_{m_o} MW_M \tag{15.43}$$

The number of moles of monomer can be calculated as $N_m=(1-x)/N_{mo}$, where N_{mo} is the initial number of moles of monomer and x_c is the so-called critical conversion at which monomer droplets disappear. Substitue equations 15.43 and the one for N_m back to equation 15.42 to obtain the expression for the particles as :

$$[M]_p = \frac{(1-x_c)}{1-x_c(1-\rho_m/\rho_p)MW_M} \tag{15.44}$$

In the above equations, ρ_m and ρ_p are the density for monomer and polymer, respectively. Many physical properties of the emulsion system will change drastically at the critical conversion, thus x_c can be experimentally determined by measuring the sudden change of vapor pressure, conductivity, etc. In stages I and II, the polymer particle composition remains relatively the same, so it is reasonable to assume that monomer concentration also remains the same, thus equation 15.44 provides a formula for calculating the monomer concentration in stages I and II. Equation 15.44 was used by Dougherty (1986a) in his model for predicting monomer partitioning.

In interval III, $x_c<x<1$, and similarly:

$$[M]_p = \frac{(1-x)\rho_M}{(1-x+x\rho_M/\rho_p)MW_M} \tag{15.45}$$

Equation 15.45 is the expression for monomer concentration in particles after the monomer droplets disappear, and x in the above equation is the overall conversion.

Another way of obtaining monomer concentration in the particle phase is the use of an empirical partitioning coefficient. This explicit method obviously is the most straightforward. The partition coefficient is defined as:

$$k_{wp} = \frac{[M]_w}{[M]_p} \tag{15.46}$$

k_{wp} is the ratio of monomer concentration in the water phase over monomer concentration in the polymer phase. k_{wp} values for certain monomer systems and for a very limited number of copolymer systems are available in the literature.

Despite the simplicity, the above two methods are limited in certain ways. First of all, both methods lead to a constant monomer concentration inside the particles throughout stages I and II. This is unlikely, because particle size definitely affects monomer partitioning. Additionally, the empirical method becomes more and more implausible when it is applied to copolymer systems. Partitioning coefficients for each monomer must be estimated. These limitations of the empirical approach can be overcome by using the theoretical approach to a certain extent, which is discussed in the next section.

15.3.2 Theoretical Approach: Thermodynamic Equilibrium

The theoretical approach is established based on two principles: (1) the Flory (1953) and Huggins (1958) mixing model of small molecules and long polymer chains; (2) the thermodynamic law of chemical potential at equilibrium. Applying these two principles to emulsion homopolymerization, it is relatively easy to write down the chemical potential of monomer in the polymer particle phase. Morton (1954) first proposed the following expression:

$$\Delta G_{i,particle}/RT = \mu_i = \mu_{m,p} + \mu_{s,p} = Ln(1-\phi_p) + \phi_p + \chi_{ip}\phi_p^2 + \frac{2\sigma \bar{V}_m}{RTr_p} \tag{15.47}$$

where,

ϕ_p: volume fraction of polymer inside the particle

σ: surface tension

r_p: particle radius

χ_{ip}: interaction parameter between monomer *i* and its homopolymer

$\bar{V}_m$: molar volume of monomer *i*

The chemical potential of monomer *i* in equation 15.47 contains two terms: the free energy due to mixing $\mu_{m,p}$, and the interfacial free energy due to the increasing surface area, $\mu_{s,p}$. For monomer *i* in monomer droplets, a similar term can be written as:

$$\Delta G_{i,droplet}/RT = \mu_{i,d} = \mu_{m,d}+\mu_{s,d} = Ln(1-\phi_p)+\phi_p+\chi_{ip}\phi_p^2+\frac{2\sigma\bar{V}_m}{RTr_d} \qquad (15.48)$$

The chemical potential of monomer *i* in monomer droplets contains the same terms as in a polymer particle. In emulsion homopolymerization, there is only one component in a monomer droplet (monomer), therefore, ϕ_p is zero, and this would make the first three terms equal to zero. The last term represents the free energy of interface between monomer droplets and aqueous phase. The diameter r_d of a monomer droplet is in the range of 10^4~10^5Å. This is rather large compared to the diameter of particles which is about 10^2~10^3 Å, hence, the contribution from the last term in equation 15.48 is very small, and this leads to the free energy of monomer *i* in a monomer droplet to be near zero. As to monomer dissolved in the aqueous phase, its free energy can be written as:

$$\frac{\Delta G_{i,aqueous}}{RT} = \mu_{i,w} = Ln\left(\frac{[M]_w}{[M]_{w,sat}}\right) \qquad (15.49)$$

$[M]_{w,sat}$ is the solubility of monomer in the water phase. In stages I and II, the aqueous phase is saturated with monomer, so $[M]_w$ is equal to $[M]_{w,sat}$, and this makes $\Delta G_{i,droplet}/RT$ equal to zero. According to thermodynamic equilibrium, the chemical potential of monomer in each phase must be equal, e.g.,

$$\left[\frac{\Delta G_i}{RT}\right]_{particle} = \left[\frac{\Delta G_i}{RT}\right]_{droplet} = \left[\frac{\Delta G_i}{RT}\right]_{aqueous} \qquad (15.50)$$

Since both $\Delta G_{i,droplet}/RT$ and $\Delta G_{i,aqueous}/RT$ are zero, equation 15.50 can be rewritten as:

$$\Delta G_{i,particle}/RT = Ln(1-\phi_p)+\phi_p+\chi_{ip}\phi_p^2+\frac{2\sigma\rho_m}{RTr_p} = 0 \qquad (15.51)$$

Equation 15.51 is the well-known theoretical expression for monomer partitioning in stages I and II when there is existence of monomer droplets. Equation 15.51 is a nonlinear equation and the root ϕ_p must be solved for iteratively. While in stage III, when all monomer droplets disappear, the aqueous

phase is no longer saturated with monomer, which implies that $[M]_w < [M]_{w,sat}$ and the thermodynamic equilibrium must be rewritten as:

$$\left[\frac{\Delta G_i}{RT}\right]_{particle} = \left[\frac{\Delta G_i}{RT}\right]_{aqueous} \tag{15.52}$$

Subsequently,

$$Ln(1-\phi_p)+\phi_p+\chi_{ip}\phi_p^2+\frac{2\sigma\rho_m}{RTr_p} = Ln\left(\frac{[M]_w}{[M]_{w,sat}}\right) \tag{15.53}$$

There are two unknows in the above equation, the polymer volume fraction ϕ_p and the monomer concentration in the water phase $[M]_w$. $[M]_w$ can be rewritten based on its definition,

$$\frac{N_m - Vp(1-\phi_p)\rho_m/MW_M}{V_w} = [M]_w \tag{15.54}$$

In order to obtain the roots of ϕ_p and $[M]_w$, equation 15.53 and 15.54 must be solved simultaneously at each iteration (time step).

Equation 15.51 reflects the contribution of mixing as well as of surface energy to the free energy of the monomer. Compared to the empirical approach described in section 15.3.1, equation 15.51 represents a more sophisticated approach. It also indicates that the chemical potential of monomer *i* in the particle phase is affected by three factors, i.e., (1) the miscibility of polymer and monomer *i* through χ_{ip} ; (2) the surface tension effect through σ, where the value of σ is influenced by the choice of emulsifier, monomer and ionic strength; (3) the size of particle through r_p. Clearly equation 15.51 is more theoretically sound than its empirical analog, however the additional sophistication is obtained at the expense of introducing parameters like σ and χ_{ip} that are difficult to obtain. There is only a very limited number of sources that give values of σ and χ_{ip}. In early studies, Morton et al.(1954) used a tensiometer to measure surface tension for styrene. They reported a value of 4.5 dynes/cm for σ for styrene. The value of the interaction parameter χ_{ip} they reported for styrene monomer and its homopolymer is 0.43. Gardon (1968f) extended Morton's original work to more monomer systems, and a number of monomer saturated swelling ratios (swelling ratio is an indication of how much monomer can be dissolved in the polymer particle), parameters χ_{ip} and σ, as well as solubility were

measured in his work. He found that the values of χ_{ip} and σ for styrene and MMA are the most consistent, despite variation of particle size, emulsifier level and temperature. Gardon (1968f) reported exactly the same values for both χ_{ip} and σ for styrene as those given by Morton et al.(1954). For MMA, the value of χ_{ip} is 0.585±0.005, and σ is 1.6±0.4 dyn/cm. Gardon (1968f) considered the interaction coefficient χ_{ip} to be between 0.2~0.6 and σ to range from 1~30 dyne/cm. One interesting finding discussed in Gardon (1968f) is that the surface tension should be lower in stage I during which most particles are small and completely covered by emulsifier. When in stage II particles grow bigger and are less covered by emulsifier, such partial coverage will result in a larger surface tension. However, Gardon (1968f) offered no solution on how to quantify the partial coverage effect. Perhaps the most important conclusion in Gardon (1968f) is that monomer concentration in particles varies little with conversion during stages I and II as long as thermodynamic equilibrium is maintained. This conclusion is in agreement with experimental observations from many other groups.

Though the thermodynamics of monomer partitioning has been discussed by a number of groups (Harvey and Leonard, 1972, Rawling and Ray 1988a and Dimitratos 1989), only very few actually applied it to predict monomer concentration changes in particles during the entire course of the reaction. Guillot (1985) developed a computer simulation program to describe monomer partitioning in AN/Sty copolymerization in emulsion based on thermodynamics principles. Guillot (1985) presented expressions for monomer chemical potential in all phases for both homopolymerization and copolymerization. Compared to equation 15.51, Guillot's(1985) expression for chemical potential included more terms to take the elasticity effect and electric work into account. Such practice nevertheless makes solving the thermodynamic equations much more complicated and introduces many unknown parameters. Unfortunately, Guillot (1985) didn't give values for the parameters used in his equation. Additional results for AN/Sty and VAc/BA copolymerization were given in a later publication by the same author (Guillot, 1986).

15.3.3 Numerical Methods: Selection and Implementation

Equations 15.51 and 15.53 are nonlinear and can only be solved numerically. Solving equations 15.51

or 15.53 is hardly discussed in the literature. Due to the unique characteristics of equations 15.51 and 15.53, the selection of numerical methods and the implementation are worth extra discussion. The comparison and implementation of various numerical methods used in this model is discussed in this section.

Morton et al.(1954) reported that equation 15.51 can be solved iteratively by using the Newton-Ralphson algorithm (the free energy of monomer in equation 15.51 can be expressed as $f(\phi_p)$). This can be done by taking the first order derivative of equation 15.51 (or $f'(\phi_p)$) with regard to the independent variable ϕ_p. Such implementation is correct from a mathematical point of view if the last term in equation 15.51 can be considered as being independent of ϕ_p. However, if equation 15.51 is examined closely, one may find that ϕ_p is related to both particle radius r_p and surface tension σ. Therefore, the mathematical form of $f'(\phi_p)$ is not necessarily correct. Due to such a concern, the Newton-Raphson method was not adopted in this model, in order to avoid direct evaluation of the derivative function $f'(\phi_p)$. An alternative method, the Secant method, was tested. In the Secant method, the derivative function $f'(\phi_p)$ was approximated by a finite difference, as shown in equation 15.55:

$$f'(x_i) = \frac{f(x_{i-1}) - f(x_i)}{x_{i-1} - x_i} \tag{15.55}$$

The root of the equation in the Secant method is given by the following formula:

$$x_{i+1} = x_i - \frac{f(x_i)(x_{i-1} - x_i)}{f(x_{i-1}) - f(x_i)} \tag{15.56}$$

i in the above two equations is an index of iteration number, x_i is the root of equation 15.51, which is ϕ_p, and $f(x)$ is the chemical potential of monomer in the polymer particles. Equation 15.51 can be solved iteratively until a convergence criterion is met.

It would be illustrative if equation 15.51 is plotted, as demonstrated in figure 15.3. In figure 15.3, the Gibbs free energy of monomer (styrene is used as an example in this case) in stages I and II is plotted against ϕ_p for various particle sizes. The interaction parameter $\chi_{i,p}$ for styrene and its homopolymer is 0.4. Sodium dodecyl sulfate was used as emulsifier and the surface tension σ is 4.5 dyn/cm. Particle

radius ranges from 25 Å to 400 Å. The root of equation 15.51 lies on the grid line at which the Gibbs free energy is zero. It is very clearly demonstrated in figure 15.3 that the larger the particle size, the lower the volume fraction of polymer, which indicates that larger particles are more swollen with monomer.

A specific flag was set up in the simulation program to constantly check for the existence of monomer droplets. When monomer droplets disappear, the program uses equations 15.53 and 15.54 instead of 15.51 to solve for monomer partitioning.

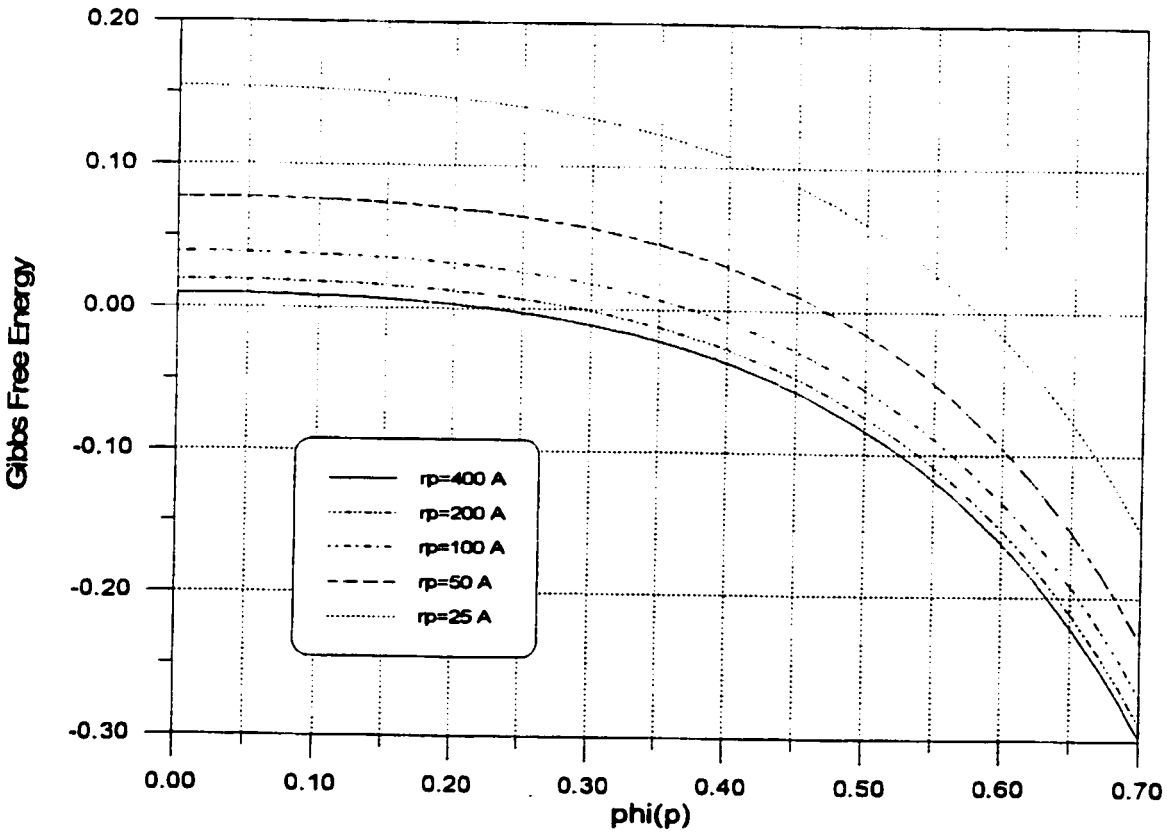

Figure 15.3 Gibbs Free Energy in Stages I and II in Styrene Homopolymerization in Emulsion

When in stage III, equations 15.53 and 15.54 replace equation 15.51 and they must be solved simultaneously. The Gibbs free energy expressed in equation 15.53 is plotted in figure 15.4 at four different levels of conversion, while other conditions are the same as those in figure 15.3. In figure 15.4, the root of the equations 15.53 and 15.54 ϕ_p resides on the line at which the Gibbs free energy is zero, and ranges from 30% to 90%. The mathematical format of both equations 15.53 and 15.51 is very similar to each other, thus the initial attempt was to substitute the monomer concentration in the aqueous phase $[M]_w$ in equation 15.53 by equation 15.54, and then use the Secant method to solve equation 15.53. Unfortunately this method fails to find the root in all cases. This is due to the nature of equations 15.53 and 15.54. Figure 15.4 displays the characteristics of the Gibbs free energy of monomer in stage III, and we can observe that all four curves are nearly vertical in their respective root region, which indicates that even a very small variation of the independent variable x_i (ϕ_p in this case) will result in large changes in the Gibbs free energy. Furthermore, the left side of equation 15.54 must remain positive. If a x_i chosen by the Secant method is somewhat small, that will result in a negative $[M]_w$ and the program will crash if $[M]_w$ in equation 15.53 is substituted by a negative value derived from equation 15.54. Since the Secant method has no restriction on either the direction of root-searching or the step size of x_i, unless x_i varies by a very small step at each iteration, will inevitably result in very large values of the Gibbs free energy, which consequently causes the simulation program to crash. To avoid such pitfalls, different root-finding methods were sought. The Bisection method was eventually chosen because it places restrictions on the range of x_i. Compared to the Secant method, the Bisection method has slower convergence, but it avoids numerical problems that the Secant method may cause. When implementing the Bisection method, the important thing is to first define the range of x_i that includes the root. In our emulsion polymerization model, the Bisection method was implemented, and additional code was written to define the appropriate range of x_i. The logic behind the code of this function is displayed below:

assign an initial value for x_1
set $z=Nm-Vp(1-x_1)\rho_m/(MW_M V_w)$
If $z<0$ then
    Do
      $x_1 = x_1+0.0001$
      recalculate z
    Loop until $z>0$

Calculate equation 15.34

Else

Calculate equation 15.34

If $\Delta G_1 > 0$ then

$x_2 = x_1 + 0.0001$

Do

$x_2 = x_2 + 0.0001$

Calculate ΔG_2

Loop while $\Delta G_2 > 0$

Else

Do

$x_2 = x_2 - 0.0001$

Calculate ΔG_2

Loop while $\Delta G_2 < 0$

x_1 and x_2 derived at the end of each loop in the above pseudo-code are the range of ϕ_p including the root, and ΔG_1 and ΔG_2 are the functions calculated using equation 15.53. As can be seen above, x_1 and x_2 are derived using very small increments (0.0001) to ensure the validity of equation 15.54. Once x_1 and x_2 are derived, the Bisection method can be subsequently applied to find the root of equations15.53 and 15.54.

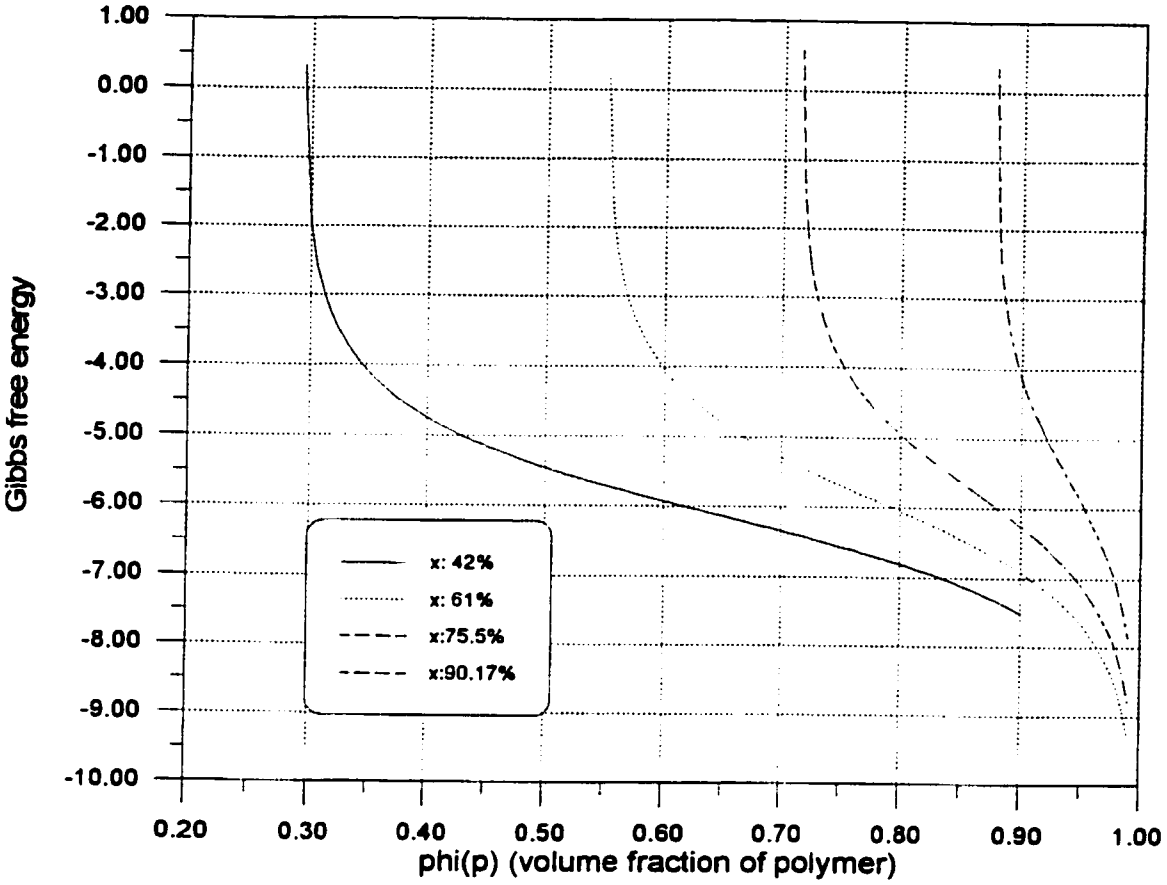

Figure 15.4 Gibbs Free Energy of Styrene in Stage III.

15.4 Desorption

As was first briefly mentioned in the particle nucleation section, absorbed radicals may desorb from polymer particles. The driving forces behind desorption are likely to be the radical's solubility, mobility and several other factors. The smaller the polymer particle, the easier the radical may desorb. Desorption is an important phenomenon in emulsion polymerization. Deviations from the early Smith-Ewart's model are largely caused by desorption. It has been commonly accepted nowadays that desorbed radicals are single monomeric radicals which are the product directly from chain transfer to monomer. These radicals (without an initiator fragment attached) are very small and mobile. Once they desorb out of a particle, they are likely to stay in the vicinity of the particle and may be reabsorbed into the particle. In section 15.2, an expression was already given for the rate of desorption:

$$\rho_{des} = \frac{k_{des} N_p \bar{n}}{N_A V_w} \tag{15.57}$$

The key thing in the above equation is to evaluate the rate constant for desorption, k_{des}. Expressions for k_{des} have been continuously developed by a number of research groups including Harada et al.(1971), Nomura et al.(1971a, 1976), Ugelstad et al.(1976), Nomura and Harada (1981) and Asua et al.(1989). Harada et al.(1971) used a stochastic approach and derived an expression for k_{des} given below:

$$k_{des} = \left(\bar{n} + \frac{k_p [M]_p m_d d_p^2}{12 D_w \delta} \right)^{-1} \left(\frac{k_{fm}}{kp} + \frac{k_{fcta}[CTA]_p}{kp[M]_p} + \frac{R_i(1-\bar{n})}{N_p k_p [M]_p \bar{n}} \right) k_p [M]_p \tag{15.58}$$

where δ is:

$$\delta = \frac{m_d D_p}{m_d D_p + 6 D_w} \tag{15.59}$$

m_d in both equations 15.58 and 15.59 is a partitioning coefficient, which is equivalent to k_{wp}^{-1} in equation 15.46, d_p is the average diameter of polymer particles and D_p is the diffusivity of radical inside the polymer particles. Equation 15.58 indicates that desorption should be considered consisting of several complex processes including chain transfer to monomer, CTA and/or initiator. Harada et al.(1971) tested their expression for several monomers and achieved good agreement. Nomura et

al.(1971a) simplified Harada's equation by assuming the majority of desorbed radicals are monomeric radicals derived from chain transfer to monomer, and if $\bar{n} << 0.5$, equation 15.58 is then reduced to:

$$k_{des} = \left(\frac{12 D_w \delta}{m_d d_p^2} \right) \frac{k_{fm}}{k_p} \tag{15.60}$$

Equation 15.60 was later on verified by Nomura and Harada (1981) using a deterministic approach and it was successfully applied to vinyl acetate and vinyl chloride. When using equation 15.60, users must be cautious that it was derived based on several assumptions, like no re-entry of desorbed radicals, instantaneous termination inside polymer particles, negligible water phase termination and polymer particles containing at most one radical. These assumptions are subject to further justification at higher conversion levels when the interior of a polymer particle becomes very viscous or for monomers that are very water soluble (i.e., water phase termination cannot be neglected).

Ugelstad and Hansen (1976) also investigated the desorption kinetics and proposed a similar expression for k_{des}:

$$k_{des} = \frac{k_{fm}}{k_p'} \left[\frac{12 D_w}{(a + D_w/D_p) d_p^2} \right] \tag{15.61}$$

where k_{fm} is the chain transfer to monomer rate constant, k_p' is the propagation rate constant for radicals generated by the transfer reaction, and a is the partition coefficient for monomer radicals between water phase and particles (a is identical to m_d of equation 15.60, so it can be concluded that equations 15.60 and 15.61 are equivalent. If appropriate values are assigned to parameters in each expression, one should come up with the same value for k_{des}).

Both Nomura's and Ugelstad's expressions have been used by a number of authors for the emulsion polymerization of vinyl acetate (Ugelstad et al. 1969, Friis and Nyhagen 1973, Kiparissides et al. 1980a,b,c, Pollock et al. 1981). Asua et al.(1989) examined Nomura's model and found it deviated from experimental findings reported by Adams et al.(1986). Asua et al.(1989) suspected the validity

of the assumptions of instantaneous termination inside polymer particles and negligible water phase termination utilized in Nomura's model. It was considered in Asua's postulation that a reabsorbed monomer radical is more likely to redesorb instead of undergoing instantaneous termination, and additionally, a desorbed monomer radical like vinyl acetate may propagate in the water phase. Finally, re-entry of desorbed radicals was also included in Asua's model. In their attempt to overcome previous limitations, Asua et al.(1989) derived the following expression:

$$k_{des} = k_{fm}[M]_p \frac{K_o}{\beta K_o + k_p[M]_p} \tag{15.62}$$

where:

$$K_o = \frac{12 D_w / m_d d_p^2}{1 + 2 D_w / m_d D_p} \tag{15.63}$$

$$\beta = \frac{k_{pw}[M]_w + k_{rw}[R\cdot]_w}{k_{pw}[M]_w + k_{rw}[R\cdot]_w + k_{cp} Np/(N_A V_w) + k_{cm}[MIC] + k_z[Z]_w} \tag{15.64}$$

β in equation 15.64 is the probability of a single monomeric unit desorbed radical undergoing water phase propagation or termination and k_{cp} is the rate constant for radical absorption by polymer particles. When β=0, a desorbed radical will be reabsorbed back to the particle. When β=1, a desorbed radical will undergo water phase termination or propagation instead of being reabsorbed. Asua et al.(1989) rewrote Nomura's model as:

$$k_{des} = k_{fm}[M]_p \frac{K_o}{K_o \bar{n} + k_p[M]_p} \tag{15.65}$$

A close comparison of equation 15.62 with equation 15.65 indicates that they are very close to each other. Equations 15.62 and 15.65 become completely identical when both β and $\bar{n}$ become zero. This implies that both Asua's and Nomura's models give the same prediction for monomers with very low water solubility ($\beta \to 0$), however in the case of more water soluble monomers like vinyl acetate or methyl acrylate ($\beta > 0$), Nomura's model predicts a higher rate constant for desorption. Since β has a value between 0 and 1, the previous Nomura's and Ugelstad's models can be considered as a special case of Asua's model when $\bar{n}$ is in the same range of 0 and 1. Asua et al.(1989) stated that their model is advantageous over Nomura's model because it is more general. Adams' et al.(1986) used a γ-

radiolysis relaxation technique to directly determine the desorption rate constant k_{des}, and their measured k_{des} is better predicted by Asua's model. After evaluating all the models discussed above, Asua's model for desorption (equation 15.62) was selected in this thesis due to its apparent advantages.

It is worth mentioning that all authors discussed above assumed a constant δ in their expressions. This is unlikely the case, especially at the late stages of polymerization, because the interior of a polymer particle becomes very viscous, and hence the desorption process becomes diffusion controlled. To quantify the diffusion limitation on desorption, D_p should be treated as a function of viscosity. This subject has not been discussed so far in a quantitative way. Only Friis and Hamielec (1975b) used an empirical expression to calculate the decrease in D_p:

$$D_p = D_{po}\left(0.0017x + \left(\frac{1-x}{1-0.19x}\right)^2\right) \tag{15.66}$$

The above expression was used for vinyl acetate emulsion polymerization. To develop a more general model, the free-volume theory is used in this thesis. In a way similar to the treatment of diffusion controlled rate constant of propagation, k_p, D_p is calculated as:

$$D_p = D_{po}\exp\left(-B\left(\frac{1}{V_F} - \frac{1}{V_{Fpcrit}}\right)\right) \tag{15.67}$$

The modelling of desorption phenomenon was recently reviewed by Gilbert's group in Casey et al.(1994) and Morrison et al.(1994). They presented a detailed model for emulsion polymerization including radical desorption and reabsorption. It was assumed in their model that only monomeric radicals can desorb. This assumption was justified with the fact that the solubilities and diffusivity of dimeric and trimeric radicals are much lower than monomeric radicals. Casey et al.(1989) treated initiator-derived radicals differently from transfer reaction derived radicals, and this was done by using a separate rate constant for absorption for the two different types of radicals. Casey et al.(1989) claimed that a desorbed monomeric radical in the aqueous phase is either being reabsorbed or terminates with other radicals, while propagation of a monomeric radical in the water phase is negligible. Though Casey et al.(1994) gave a detailed discussion on the justification of the assumptions used in their model, their expression for the rate constant for desorption is exactly the

same as that given by Ugelstad and Hansen (1976) and Nomura and Harada (1981). Morrison et al.(1994) applied Casey's et al.(1994) theory to styrene, where the rate constant for desorption was estimated at various particle sizes and monomer concentrations. It was found that the rate constant for desorption was mostly affected by particle size. However, Morrison's et al.(1994) estimation must be treated with caution because their experimental (measuring) error is quite large (50%).

15.5 Average Number of Radicals per Particle

To calculate the average number of radicals per particle, $\bar{n}$, a population balance must be written for the number of particles with zero, one, two and more radicals per particle. The solution of these population balance equations can be obtained under two steady-state hypotheses:

(1): The rate of radical flow into the water phase (radical desorption from polymer particles plus initiation) equals the rate of radical flow out of the water phase (radical absorption and termination).

(2): The rate of formation of particles with n free radicals is equal to the rate of disappearance of particles with n free radicals.

The first hypothesis can be expressed as,

$$k_{des}N\bar{p}\bar{n}/(N_A V_w) + R_I = k_{cp}[R\cdot]_w Np/(N_A V_w) + k_{cm}[R\cdot]_w Np/(N_A V_w) + k_{tw}[R\cdot]_w^2 + k_z[R\cdot]_w[Z]_w \quad (15.68)$$

The second hypothesis is expressed as $dN_n/dt = 0$, i.e., the formation and disappearance rates of particles containing n radicals are the same. N_n is the number of particles containing n radicals. There are four sources that affect N_n:

(1) When a radical enters a particle that has n-1 radicals, the rate of formation is :

$$k_{cp}[R\cdot]_w[N_{n-1}]$$

(2) When a radical desorbs from a particle that has n+1 radicals, the rate of desorption is:

$$k_{des}(n+1)[N_{n+1}]$$

(3) When two radicals terminate inside a particle that has n+2 radicals, the rate is:

$$k_t (n+2)(n+1)[N_{n+2}]/v_p$$

where v_p is the average volume of a single polymer particle in dm^3.

(4) When a radical reacts with inhibitors/impurities in a particle that has n+1 radicals, the rate is:

$$k_z[Z]_p n[N_{n+1}]$$

The disappearance of N_n can be expressed in a similar fashion. A recurrence formula can be set up to express the second hypothesis, which is:

$$k_{cp}[R\cdot]_w[N_n]+k_{des}(n)[N_n]+k_t[(n)(n-1)/v_p][N_n]+k_z[Z]_p(n)[N_n]$$
$$=k_{cp}[R\cdot]_w[N_{n-1}]+k_{des}(n+1)[N_{n+1}]+k_t[(n+1)(n+2)/v_p][N_{n+2}]+k_z[Z]_p(n+1)[N_{n+1}] \quad (15.69)$$

Applying the steady state hypotheses to the particle balances gives a series of simultaneous algebraic equations for particles with zero, one, two or more radicals. Assuming a monodisperse particle size distribution, O'Toole (1965) solved the series of algebraic equations. The solution of the above recursive equation was proposed as a modified Bessel function to give an expression for $\bar{n}$. Ugelstad et al.(1967) proposed the following expression as an approximate numerical solution:

$$\bar{n}=\cfrac{\alpha}{m+\cfrac{2\alpha}{m+1+\cfrac{2\alpha}{m+2+\cfrac{2\alpha}{m+3+\ldots}}}} \quad (15.70)$$

with

$$\alpha = \frac{k_{cp}[R\cdot]_w V_p N_A}{N_p k_t} \quad (15.71)$$

and

$$m = \frac{(k_{des}+k_f[Z]_p)V_p N_A}{k_t N_p} \quad (15.72)$$

The above solution given by equation 15.70 has been confirmed with experimental data in Friis and Hamielec (1982). Nomura et al.(1983) summarized the results of a number of experimental investigations from the literature, compared them to the predictions of the Bessel function solution and concluded that this solution is valid.

Several authors have also attempted to obtain an exact solution for the particle population balance equations without using the stead-state hypothesis. Ugelstad et al.(1976) claimed that their solution is not significantly different from O'Toole's solution for the same problem under the state-state hypothesis. Ballard et al.(1981) made similar statements in their studies. More recently, Li and Brooks (1993) gave an explicit analytical solution to the population balance equations for the particles, and the authors claimed that their solution represents an improvement over equation 15.70.

Another approach for obtaining $\bar{n}$ is to develop partial differential equations representing the number of particles containing zero, one, two or more radicals as functions of both time and volume. This will give a distribution of particles with different numbers of radicals. The average number of radicals per particle in this case can be obtained by summing the elements of all particle size distributions using the following formula:

$$\bar{n} = \frac{\sum_{i=0}^{\infty} iN_i(V)}{\sum_{i=0}^{\infty} N_i(V)} \tag{15.73}$$

This approach has been applied successfully by Min and Ray (1978), Lichti et al.(1983), Lin et al.(1981) and Chen and Wu (1990). Nevertheless, equation 15.73 does not have apparent advantages over equation 15.70. Additionally, equation 15.73 is more computationally expensive, therefore equation 15.70 was adopted in our emulsion model.

15.6 Overall Mass Balances and Molecular Weight Development

The emulsion polymerization model developed in this project is based on mass balances for each reacting species. All these mass balance equations are in the form of ordinary differential equations (ODE) and are solved simultaneously by an ODE solver. This section lists all the reactions involved in a homopolymerization in emulsion. Mass balances for each reactant, energy balances and molecular weight development equations for both linear and branched systems are also presented. The reactions that follow take place inside polymer particles.

Propagation:

$$R_r^{\cdot} + M \xrightarrow{k_p} R_{r+1}^{\cdot} \tag{15.74}$$

Termination by combination:

$$R_n^{\cdot} + R_m^{\cdot} \xrightarrow{k_{tc}} P_{n+m} \tag{15.75}$$

Termination by disproportionation:

$$R_n^{\cdot} + R_m^{\cdot} \xrightarrow{k_{td}} P_n + P_m \tag{15.76}$$

Chain transfer to monomer:

$$R_r^{\cdot} + M \xrightarrow{k_{fm}} P_r + R_1^{\cdot} \tag{15.77}$$

Chain transfer to polymer:

$$R_r^{\cdot} + P_s \xrightarrow{k_{fp}} P_r + R_s^{\cdot} \tag{15.78}$$

Chain transfer to chain transfer agent(CTA):

$$R_r^{\cdot} + CTA \xrightarrow{k_{fcta}} P_r + CTA^{\cdot} \tag{15.79}$$

Chain transfer to inhibitor/impurities:

$$R_r^{\cdot} + Z \xrightarrow{k_z} P_r - Z^{\cdot} \tag{15.80}$$

Terminal double bond polymerization:

$$R_n^{\cdot} + P_s \xrightarrow{k_p^{\bullet}} R_{n+s}^{\cdot} \tag{15.81}$$

Internal double bond polymerization:

$$R_n^{\cdot} + P_s \xrightarrow{k_p^{\bullet\bullet}} R_{n+s}^{\cdot} \tag{15.82}$$

The quantity of each species in the reaction mixture can be calculated through a differential equation

based on the species mass balance. Since this package also simulates homopolymerization in CSTR or semi-batch reactors, input and output flow rates of any reactant species are taken into account in all the kinetic, molecular weight development and energy balance differential equations. The following is a list of all these equations. In these equations, N_j is the number of moles of species *j*, F_j^{in} is the inlet molar flowrate of species *j*, F_j^{out} is the outlet molar flowrate of species *j*, V_p is the total volume of polymer particles, and V_w is the total volume of the aqueous phase.

Mass Balance Equations for Each Species:

monomer:

Ahough it is considered that the polymer particle phase is the main locus of polymerization, to make the model complete, monomer consumption in the aqueous phase is also included.

$$\frac{dN_M}{dt}=F_M^{in}-\frac{k_p[M]_p N p\bar{n}}{N_A V_p}-kp_w[M]_w[R\cdot]_w-F_M^{out} \tag{15.83}$$

initiator:

$$\frac{dN_I}{dt}=F_I^{in}-K_d[I]_w V_w-F_I^{out} \tag{15.84}$$

polymer:

Polymer produced in both polymer particle and aqueous phases is included.

$$\frac{dN_{Polymer}}{dt}=F_M^{in}+\frac{k_p[M]_p N p\bar{n}}{N_A V_p}+kp_w[M]_w[R\cdot]_w-F_M^{out} \tag{15.85}$$

inhibitor:

The mass balance below is the total consumption of inhibitor in both polymer particle and aqueous phases. It has been noted that oil soluble and water soluble inhibitors affect the reaction kinetics in a very different way. More details on this subject are given in Appendix 2.

$$\frac{dN_Z}{dt}=F_z^{in}-k_z[Z]_p\frac{N_p\bar{n}}{N_A V_p}-k_z[Z]_w[R\cdot]_w-F_z^{out} \tag{15.86}$$

CTA:

Like other small molecules in emulsion polymerization, CTA may partition itself between the polymer particle phase and the water phase depending on its solubility. The mass balance below is the overall

consumption rate of CTA in both phases:

$$\frac{dN_{CTA}}{dt} = F_{CTA}^{in} - \frac{k_{f_{CTA}}[CTA]_p N_p \bar{n}}{N_A V_p} - k_{f_{CTA}}[CTA]_w [R\cdot]_w - F_{CTA}^{out} \tag{15.87}$$

Finally, the change of the total volume of all polymer particles must be followed in order to calculate concentrations of reaction species. Note that polymer particles grow continuously in stages I and II, when there is constant monomer supply from monomer droplets, while in stage III, polymer particles shrink due to the density difference between polymer and monomer. Two separate equations are given below, during stages I and II:

$$\frac{dV_p}{dt} = \frac{MW_M k_p [M]_p N p\bar{n}/N_A + MW_M k_{pw}[M]_w [R\cdot]_w}{\phi_p \rho_p} \tag{15.88}$$

whereas in stage III:

$$\frac{dV_p}{dt} = \frac{MW_M k_{pw}[M]_w [R\cdot]_w}{\rho_p} - \frac{MW_M k_p [M]_p N p\bar{n}}{V_p N_A}\left(\frac{1}{\rho_m} - \frac{1}{\rho_p}\right) \tag{15.89}$$

energy balance:

$$\frac{d(V_{latex}\Delta H)}{dt} = F_H^{in} + \frac{k_p [M]_p N_p \bar{n}}{N_A V_p}(-\Delta H_p) + k_p [M]_w [R\cdot]_w (-\Delta H_p) - UA(T_R - T_{jacket}) - F_H^{out} \tag{15.90}$$

isothermal case:

$$\frac{d(V_{latex}\Delta H)}{dt} = 0 \tag{15.91}$$

enthalpy:

$$H = H_o + C_P (T_R - T_o) \tag{15.92}$$

Molecular Weight Development:

The average radical concentration inside polymer particles is defined as:

$$[R\cdot]_p = \frac{N_p \bar{n}}{N_A V_p} \tag{15.93}$$

instantaneous number average molecular weight:

$$M_n = \frac{MW_M}{(\tau + \beta/2)} \tag{15.94}$$

instantaneous weight average molecular weight:

$$M_w = \frac{MW_M(2\tau + 3\beta)}{(\tau + \beta)^2} \tag{15.95}$$

where

$$\tau = \frac{k_{td}(k_p[M]_p[R\cdot]_p)}{(k_p[M]_p)^2} + \frac{k_{fm}}{k_p} + \frac{k_{fcta}[CTA]_p}{k_p[M]_p} + \frac{k_z[Z]_p}{k_p[M]_p} \tag{15.96}$$

$$\beta = \frac{k_{tc}(k_p[M]_p[R\cdot]_p)}{(k_p[M]_p)^2} \tag{15.97}$$

To calculate the accumulated molecular weight averages for both linear and branched systems, the method of moments is used. From the definition of moments, the i^{th} moment of the polymer molecule distribution is:

$$\mu_i = \sum_{r=1}^{\infty} r^i [P_r] \tag{15.98}$$

When i=0, μ_o=[P], which is the total concentration of polymer molecules.

The accumulated number average and weight average molecular weights are defined by the following two equations:

$$\bar{M}_n = MW_M \frac{\mu_1}{\mu_o} \tag{15.99}$$

$$\bar{M}_w = MW_M \frac{\mu_2}{\mu_1} \tag{15.100}$$

0th moment:

$$\frac{1}{V_p}\frac{d(V_p\mu_o)}{dt} = \left(\tau+\frac{\beta}{2}-\frac{k_p^{\bullet\bullet}\mu_1}{k_p[M]_p}-\frac{k_p^{\bullet}\mu_o}{k_p[M]_p}\right) k_p[M]_p[R\cdot]_p-\mu_o V_{out} \tag{15.101}$$

1st moment:

$$\frac{1}{V_p}\frac{d(V_p\mu_1)}{dt}=k_p[M]_p[R\cdot]_p\left(\tau-\frac{k_{td}[R\cdot]_p}{k_p[M]_p}\right)-\mu_1 V_{out} \tag{15.102}$$

2nd moment:

$$\frac{1}{V_p}\frac{d(V_p\mu_2)}{dt} = \left\{\gamma+2\left(1+\frac{k_p^{\bullet}\mu_1+k_p^{\bullet\bullet}\mu_2}{k_p[M]_p}\right)\frac{\xi}{\lambda}+\frac{k_{tc}[R\cdot]_p}{k_p[M]_p}\frac{\xi^2}{\lambda^2}\right\}k_p[M]_p[R\cdot]_p-\mu_2 V_{out} \tag{15.103}$$

with

$$\gamma = 1+\frac{R_I}{k_p[M]_p[R\cdot]_p}+\frac{k_{fm}}{k_p}+\frac{k_{fcta}[CTA]_p}{k_p[M]_p}+\frac{k_z[Z]_p}{k_p[M]_p} \tag{15.104}$$

$$\lambda = \frac{k_t[R\cdot]_p}{k_p[M]_p}+\frac{k_{fm}}{k_p}+\frac{k_{fcta}[CTA]_p}{k_p[M]_p}+\frac{k_z[Z]_p}{k_p[M]_p}+\frac{k_{fp}\mu_1}{k_p[M]_p} \tag{15.105}$$

$$\xi = 1+\frac{k_{fm}}{k_p}+\frac{k_{fcta}[CTA]_p}{k_p[M]_p}+\frac{k_z[Z]_p}{k_p[M]_p}+\frac{k_p^{\bullet}\mu_1}{k_p[M]_p}+\frac{R_I}{k_p[M]_p[R\cdot]_p}+\left(\frac{k_{fp}}{k_p}+\frac{k_p^{\bullet\bullet}}{k_p}\right)\frac{\mu_2}{[M]_p} \tag{15.106}$$

The branching frequencies for both trifunctional and tetrafunctional branching averages are calculated as follows:

$$\frac{dV_p\mu_o\bar{B}_{n3}}{dt} = kp[R\cdot]_pV_p\left(\frac{k_{fp}}{kp}\mu_1+\frac{k_p^{\bullet}}{kp}\mu_0\right) \tag{15.107}$$

$$\frac{dV_p\mu_0\bar{B}_{n4}}{dt} = kp[R\cdot]_pV_p\frac{kp^{\bullet\bullet}}{kp}\mu_1 \tag{15.108}$$

15.7 Reaction Kinetics at High Conversion Levels

It is known that reaction kinetics in emulsion polymerization has its own unique characteristics compared to bulk/solution polymerization. Friis and Hamielec (1973) was the first group that studied the gel effect on the kinetics of styrene homopolymerization in emulsion. The existence of diffusion controlled termination was suggested by the observation that $\bar{n}$ starts to increase rapidly beyond 30% conversion (the conversion level at which monomer droplets start to disappear). This is due to the rapid decrease of k_t. The same group observed similar characteristics in MMA (Friis and Hamielec, 1974) and VAc homopolymerization (Friis and Hamielec, 1975a). In all cases, they used an empirical expression for the diffusion controlled k_t. In their expression, the diffusion controlled k_t was fitted with a polynomial expression shown below,

$$k_t = k_{t_o} \exp(-A_1 x + A_2 x^2 + A_3 x^3) \tag{15.109}$$

where k_{to} is the chemically controlled rate constant for termination. Gel effect in emulsion polymerization was also observed and treated in a quantitative way by Harris et al.(1981). They conducted seeded emulsion polymerization experiments of styrene. By assuming $\bar{n}$ equal to ½, the rate constant for propagation k_p was backcalculated. It was found that k_p decreased sharply after 85% conversion, and that the diffusion controlled k_p could be adequately described by free volume theory. Sundberg et al.(1981) used the approach to describe the diffusion controlled termination and propagation in styrene and MMA homopolymerization in emulsion. Sundberg et al.(1981) did an extensive study on gel effect phenomena in emulsion polymerization of styrene and MMA. The effects of particle size, number of particles, initiator concentration as well as temperature on k_t and k_p were studied in detail. It was concluded that gel effect phenomena do exist in emulsion polymerization of some monomer systems, having a profound effect on reaction kinetics. Both Harris et al.(1981) and Sundberg et al.(1981) used the same approach based on free volume theory and successfully described the gel effect observed in their experiments. Other authors that used the same approach include Hamielec and MacGregor (1982), and Dube et al.(1996). In this thesis, the free volume was used to describe diffusion controlled kinetic phenomena. Detailed implementation was already discussed in section 3.3.

It has been known that the interior of polymer particles is very viscous. For many monomer systems, there is usually at least 60~70% polymer in the particles at the very start of the reaction. During stages I and II, the viscosity of particles remains relatively constant due to the constant supply of monomers from monomer droplets. Inside polymer particles, the termination reaction becomes diffusion controlled once polymerization starts. The initial value of the rate constant for termination is low but relatively constant in stages I and II. Such postulation was confirmed by other groups. Harris et al.(1981) and Sundberg et al.(1981) claimed that molecular masses are typically controlled by transfer reactions at low conversion range and are relatively constant over much of the conversion history. Once all monomer droplets are depleted, more and more monomers are turning into polymer inside polymer particles and the interior of particles becomes more viscous. Under such circumstances, the rate constant for termination will begin to drop until it reaches its lower limit (the reaction diffusion controlled k_t). As polymerization proceeds, latex particles may turn glassy if the reaction is conducted below the polymer mixture glass transition temperature, and consequently, propagation becomes diffusion controlled. For some monomer systems, like EA and MA, it has already been demonstrated in Gao and Penlidis (1996) that the reaction kinetics in bulk polymerization is greatly affected by reaction diffusion control. In emulsion polymerization of these monomers, the dominance of reaction diffusion control phenomenon will be enhanced further. This is because at the beginning of the reaction, a polymer particle already has 60~70% polymer in it. The reader should bear in mind that the reaction diffusion control mechanism will play a bigger role under such circumstances.

Though the gel effect is significant in some cases, not every monomer system exhibits the same characteristics. The gel effect is not usually observed in polymerizations of monomers with high desorption rate, like vinyl acetate or vinyl chloride. Molecular weight in this case will be controlled by chain transfer reactions rather than termination. The gel effect phenomenon is more dominant when $\bar{n}$ becomes higher than 1, i.e., when there are more than one radicals in one particle. In this case, the rate of polymerization is independent of the overall particle number, and emulsion polymerization can be considered as "pseudo-bulk" polymerization.

Chapter 16. Emulsion Simulation Package/Database Overview

16.1 General Description

As the bulk and solution package, the emulsion simulation package consists of two major programs: **MASTER** and **DATABASE**. The user-interface and program structure of the two models are very similar to each other. A detailed description of the bulk/solution package was given in chapter 4. This chapter intends to give a very brief description of the emulsion model with emphasis on the characteristics that are unique to emulsion polymerization. Figure 16.1 displays the recipe design screen for emulsion polymerization. It will ask the user to define the reaction formulation, i.e., select the type and amount of monomer, initiator, emulsifier, etc. along with their own units. There is a prompt at the bottom center of the screen that will lead the user to other input/output screens of the program.

```
Dept. of Chemical Engineering - UW - Watpoly Simulator - Version 1.0

Reaction Formulation

Monomer 1     : Methyl Methacrylate        Amount   :   1.0000  L
Monomer 2     : Styrene                    Amount   :   0.3000  L

Initiator 1   : KPS                        Amount   :   0.0100  mol/L

Emulsifier1   : SDS                        Amount   :   0.0000  mol/L
Emulsifier2   : SDS                        Amount   :   0.0000  mol/L

Media         : Water                      Amount   :   0.0000  L

Inhibitor     : Hydroquinone               Amount   : 0.000D+00 mol/L

CT Agent      : Carbon Tetrachloride       Amount   : 0.000D+00 mol/L
              :

                          <Space> selects Units.

<Arrows>-Cursor      <F1>-Go      <F2>-<F4>-Other Screens      <F10>-Exit
```

Figure 16.1 Reaction Formulation Screen

Computational Options Screen

Figure 16.2 displays the computational options screen. On this screen, users can set up the initial reactor temperature, select reactor temperature profile options (isothermal, adiabatic, and user-defined temperature profile) and input the heat transfer parameter (UA is in cal/K·min, U is the overall

heat transfer coefficient, A is the heat transfer area). Maximum simulation time and conversion level will stop the simulation at the specified point. Numerical spacing and tolerance parameter determine the computation speed and accuracy. Polymerization induction time is another option. It is a useful option when water-soluble inhibitor is present in the emulsion polymerization system.

At the bottom half of this screen, different model options are listed. Each model option can be activated or deactivated in a toggled mode. At present, diffusion controlled propagation and termination according to Marten and Hamielec (1979,1982), and "reaction diffusion" according to Russel et al.(1988), Stickler et al.(1984) and Allen and Patrick (1974) are options available. Monomer partitioning can be solved either empirically (partition coefficients) or theoretically (via thermodynamic equations, see section 15.3). "**SSH**" stands for steady-state hypothesis for radicals. Other options include variable initiator efficiency, monomer soluble/water soluble inhibitors, seeded polymerization, emulsifier-free cases, etc. It should be stated here that there is no universal rule to determine what options must be selected for a specific polymerization system. It is up to the user to decide. The basic principle behind this is that a combination of options should be tried to achieve the best simulation performance and results. As always, experience and the process data/understanding are the guidelines.

```
Dept. of Chemical Engineering - UW - Watpoly Simulator - Version 1.0

Computational Options

Initial Temperature          328.15    K                    Case    Isothermal
Heat Transfer Parameter (UA)   1.00000 cal/K·min

Simulation End Time          250.00    min    Conversion Limit        0.9950
Numerical Solution Spacing     1.0     min    Tolerance Parameter     4
Induction Time                 0.00    min

Diffusion Controlled Propagation          [√]    Emulsifier-Free Reaction [ ]
Segmental Diffusion Termination           [√]    Seeded Emulsion Reaction [ ]
Diffusion Controlled Termination          [√]
Reaction Diffusion Termination          [ RNG ]
Variable Initiator Efficiency             [√]
Thermodynamic Monomer Partitioning        [ ]
SSH for Radicals                          [√]

                    <Space> toggles On [√] and Off [ ].

<Arrows>-Move Cursor              <F3>-Go Back              <F10>-Exit
```

Figure 16.2 Computational Options Screen

Output Files Screen

Figure 16.3 displays the list of all output files. This table is also an indication of what prediction capability this model has. In this screen, users can choose the output files to be generated in order to graphically view how a specific variable changes with either conversion or time. Each output file can be viewed by using the **SHOW** utility program supplied with the package. Users can also import output files to other graphics software, like Excel, Quattro, Lotus, Grapher etc. to view and plot the simulation results.

Dept. of Chemical Engineering - UW - Watpoly Simulator - Version 1.0

Output Files	Time	Conv.		Time	Conv.
Conversion	[√]	-	Trifunctional Branching	[ ]	[ ]
Instantaneous Mn	[ ]	[ ]	Tetrafunctional Branching	[ ]	[ ]
Instantaneous Mw	[ ]	[ ]	Inst. Copolymer Comp.	[ ]	[ ]
Instantaneous PDI	[ ]	[ ]	Acc. Copolymer Comp.	[ ]	[ ]
Accumulated Mn	[ ]	[ ]	Residual Monomer wt%	[ ]	[ ]
Accumulated Mw	[ ]	[ ]	Sequence Length Dist.	[ ]	[ ]
Accumulated PDI	[ ]	[ ]	Number of Particles	[ ]	[ ]
Instantaneous MWD	[ ]	[ ]	Particle Diameter(swollen)	[ ]	[ ]
Accumulated MWD	[ ]	[ ]	Particle Diameter	[ ]	[ ]
Polymerization Rate	[ ]	[ ]	n	[ ]	[ ]
Heat Generation	[ ]	[ ]	kp	[ ]	[ ]
Reactor Temperature	[ ]	[ ]	kt	[ ]	[ ]
Jacket Temperature	[ ]	[ ]	k_{des}	[ ]	[ ]
$[R\cdot]_w$	[ ]	[ ]			
$[R\cdot]_p$	[ ]	[ ]			

<Space> toggles On [√] and Off [ ].

<Arrows>-Move Cursor <F2>-Go Back <F10>-Exit

Figure 16.3 Output Files Screen

Flow Options Screen

Figure 16.4 displays the flow options screen. If the polymerization is carried out in the semi-batch mode, the flow options screen will let users input the specific inflow and outflow rates as well as their starting and ending flow time. For both CSTR and semi-batch cases, and for each reactant in the system, flow rate, and starting and ending times must be specified. Users again have the option to choose different units to meet simulation needs.

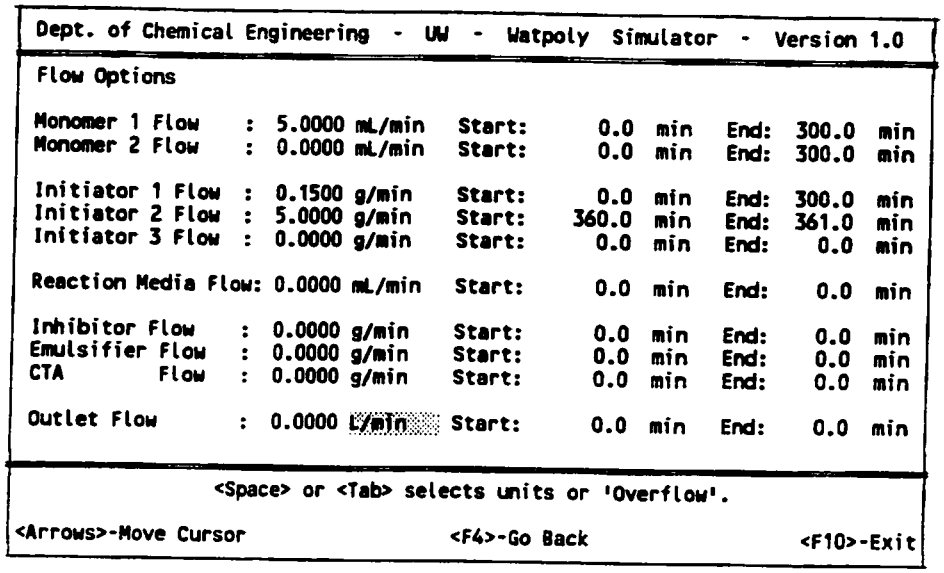

Figure 16.4 Flow Options Screen

16.2. Package Database Overview

The **DATABASE** program organizes and updates all the information for each species in the package database, such as physical properties, kinetic rate constants and other parameters. The database provides all the necessary information the **Master** program needs to perform a simulation. The following subsections will give a brief description for each reacting species.

16.2.1 Monomer Systems

The database includes five monomer systems as well as other reaction components such as initiators, emulsifiers, chain transfer agents (CTAs), etc. All monomers are listed in Table 16.1.

Table 16.1 Monomer List

Symbol	Chemical Name
EA	ethyl acrylate
MMA	methyl methacrylate
Sty	styrene
VAc	vinyl acetate
BA	butyl acrylate

16.2.2 Other Components

An emulsion polymerization typically involves monomer, initiator, emulsifier, water, and CTA added to produce polymer with desired molecular weight. Inhibitors are commonly used for monomer storage and transportation to prevent self-polymerization. If a monomer is not purified before use or the reactor is not properly deaerated before a run, the residual inhibitor or oxygen present in the reaction will kill radicals. Thus, an induction period is often observed. Table 16.2 lists the initiators, emulsifiers, CTAs and inhibitors currently available.

Table 16.2. Other Database Components

Initiator	Emulsifier	CTAs	Inhibitors
lauroyl peroxide	Fenopon Co436M	Carbon tetrachloride	oxygen
potassium persulphate	sodium dodecyl sulphate (SDS)	n-dodecyl mercaptan	hydroquinone
hydroxy peroxide	Aerosol MA/AMA	t-dodecyl mercaptan	DPPH
ammoniun persulphate	Aerosol OT/AOT	p-octyl mercaptan	methyl ethyl hydroquinone
sodium persulphate		GDMA	

DPPH* 2,2-diphenyl-1-picrylhydrazyl hydrate

GDMA* glycol dimercapto acetate

16.3 Description of Database Items

The main body of the database set for each monomer system consists of its physical and chemical properties. Physical properties for a monomer and its polymer are molecular weight, density, glass transition temperature, heat capacity, etc. Rate constants for various events in emulsion, like desorption, absorption, chain transfer reactions, and propagation and termination in both water and polymer phases represent monomer chemical reactivities. All these properties can in principle be measured and some can be calculated based on the monomer chemical structure. However, for most monomers, their kinetic rate constant values reported in the literature vary over a wide range, despite the fact that monomers like MMA, Styrene and VAc have been the research focus for many years. The lack of understanding of the polymerization mechanism, inconsistent parameter estimation techniques, lack of design of experiments and different techniques employed in the measurements make it very difficult to reach a commonly accepted single value of one particular rate constant. The current database at least provides a set of starting values for monomer characteristics. A set of monomer characteristics for styrene is listed below as an example.

Physical and Chemical Properties of Styrene

Items	Value	Unit
MW_m	100.12	g/mol
k_p	$4.703 \cdot 10^{11} \cdot \exp(-9805/RT)$	L/mol·min
$-\Delta H$	19.27	kcal/mol
T_{gm}	167.1	K
V_{fcrit}	$3.5819 \cdot \exp(-2125.7/RT)$	
V_{fm}	$0.025 + 0.001 \cdot (T-T_{gm})$	
ρ_m	0.949 - 0.00128(T-273.15)	g/cm^3
C_{pm}	430	cal/kg·K
k_t	$1.04619 \cdot 10^{10} \exp(-2950.45/RT)$	L/mol·min
k_{tc}%	100%	
B	1.0	universal value
δ	0.001	L/g
a	6.2	Å
σ	5.85	Å
j_c	120	
k_{fm}	$1.48678 \cdot 10^{12} \cdot \exp(-17543/RT)$	L/mol·min
k_{fp}	0	L/mol·min
k_p^*	0	L/mol·min
k_p^{**}	0	L/mol·min
ρ_p	1.11	g/cm^3

C_{pp}	437.5	cal/kg·K
T_{gp}	378	K
V_{fp}	$0.025 + 0.00048\cdot(T-T_{gp})$	
k_3	$0.00153\cdot\exp(14805/RT)$	
m	0.5	universal value
n	1.75	universal value
A	1.552	
k_{pw}	$4.703\cdot10^{11}\cdot\exp(-9805/RT)$	L/mol·min
k_{tw}	$1.04619\cdot10^{10}\cdot\exp(-2950.45/RT)$	L/mol·min
D_w	$1.76\cdot10^{-9}$	dm^2/min
D_p	$1.76\cdot10^{-12}$	dm^2/min
j_{cr}	5	
k_{wp}	1400	
σ	4.5	dyne/cm
λ	0.4	
$[M]_w$	0.005	mole/Lw

It must be mentioned that in the list above the rate constants for propagation and termination in the water phase could be different from their corresponding values in the polymer phase. This is true especially for polar monomers whose reactivity is affected by reaction media considerably. In the example of the styrene database, these values are identical. However, to account for media effect on other monomers (like carboxylic acids, acrylonitrile, etc.), rate constants for propagation and termination should have their own separate values.

Other components, like initiators, emulsifiers, etc. have their own database. Tables 16.3 and 16.4 are examples of a set of database items for potassium persulfate and sodium dodecyl sulfate, respectively.

Table 16.3. Database Items for Potassium Sulphate

Items	Value	Unit
MWm	271.3	g/gmol
k_d	$1.524\cdot10^{18}\cdot\exp(-33320/RT)$	L/mol·min
f	0.5	

Table 16.4. Database Items for Sodium Dodecyl Sulphate

Items	Value	Unit
MWm	288.38	g/gmol
CMC	0.008	mole/L
S_a	3×10^{-17}	dm^2
micelle radius	25~50	Å

Chapter 17. Simulation of Styrene Emulsion Homopolymerization

An emulsion polymerization model has been developed according to the kinetic scheme described in chapter 15. The database associated with the model was also developed in parallel. The next step is to test the model with a list of monomers with different emulsion polymerization characteristics. In emulsion polymerization, monomers are usually classified into three categories, i.e.,

Case I: monomers with high water solubility and significant desorption, like vinyl acetate, vinyl chloride, etc.

Case II: monomers with low water solubility and negligible desorption, like styrene, butadiene, etc.

Case III: monomers that exhibit significant gel effect like MMA.

In the following chapters, monomers in each category are tested. Such tests will verify our model's validity. The same model testing principles described in chapter 5 are used in this testing as well.

Early studies on emulsion polymerization kinetics were all focused on styrene. Styrene has been long considered the most thoroughly studied monomer in emulsion polymerization because it fits into the Smith-Ewart Case II kinetic scheme very well. Gardon (1968a,b,c,d) in a series of papers distinguished three intervals in styrene emulsion homopolymerization in batch. According to the Smith-Ewart Case II postulation, the average number of radicals per particle remains constant at 0.5 throughout stages I and II of the reaction. However, this is not always true. Bataille et al.(1982) conducted a series of experiments of styrene homopolymerization and observed that $\bar{n}$ is greater than 0.5 throughout the reaction. They attributed this to the gel effect. Sudol et al.(1986a, b) noticed in their studies on making monodispersed polystyrene latex seeds that $\bar{n}$ is ½ at the beginning of the reaction but it increases to as high as 10 at about 87% conversion. This is clearly due to the gel effect. Styrene has very low water solubility and negligible desorption, and the gel effect is pronounced in styrene emulsion polymerization. The polymer phase is rather viscous at the beginning of the reaction due to the presence of a high percentage of polymer in the particles, and hence it is reasonable to

consider that the termination reaction is diffusion controlled from the very beginning. This gel effect leads to a much lower initial value for the rate constant for termination. Friis and Hamilec (1973, 1975a, 1982) were the first group that studied the gel effect in emulsion homopolymerization of several monomers including styrene. The gel effect phenomenon was modelled by using an empirical expression for the rate constant of termination. A similar approach was also adopted by Morbidelli et al.(1983) in their modelling effort. Friis and Hamielec (1973) showed that $\bar{n}$ starts to increase quite early in the reaction. The gel effect affects not only the rate of polymerization but also the molecular weight. James Jr. and Piirma (1975) gave molecular weight trends for styrene as well as MMA throughout the entire reaction. The trends show that molecular weight of styrene starts to increase at the end of stage II, and that is exactly when the gel effect starts to take off. Similar statement were also made by Piirma et al.(1975).

Many papers have been reviewed to study the kinetics of styrene emulsion homopolymerization and collect kinetic as well as experimental data. Table 17.1 lists useful papers that focus on styrene emulsion polymerization kinetics.

Table 17.1 Papers on Styrene Emulsion Polymerization Kinetics

Authors	Remarks
Asua and de la Cal (1991)	estimation of rate constants for radical absorption and desorption
Bataille et al.(1982, 1984, 1988)*	full conversion data, studies on redox system
Blackley and Sebastian (1987, 1989)*	experimental data, redox system
Canegallo et al.(1993)*	online densitometer measurements
Campbell (1985)	experimental data, modelling
de la Rosa et al.(1996)*	calorimetry measurements
Giannetti (1993)	particle size distribution, modelling, kinetic parameter information
Harada et al.(1972)*	full conversion range experimental data, modelling
Hawkett et al.(1981)	radical absorption efficiency
James Jr. and Piirma (1975)	molecular weight development, gel effect studies
Lichti et al.(1981)	particle size distribution
Mayer et al.(1996)*	particle nucleation
Miller et al.(1997)	molecular weights
Morton et al.(1952)	kinetic parameters
Morbidelli et al.(1983)	modelling, studies on gel effect and ionic strength
Nomura et al.(1971b)	CSTR operation
Penboss et al.(1983)	seeded emulsion polymerization, particle nucleation
Piirma et al.(1975)	molecular weight development and kinetic studies
Said (1991)	molecular weights
Salazar et al.(1998)*	molecular weight control policy studies
Sudol et al.(1986a, b)	seeded emulsion polymerization, monodispersed particle latex

* paper contains data that are used for model testing

17.1 Model Testing Results

Bataille et al.(1982, 1984)

Bataille et al.(1982) conducted emulsion homopolymerization of styrene in a wide range of reaction conditions at 60°C. A total of five runs were performed, and the reported experimental conditions and recipes are summarized in the Table 17.2.

Table 17.2 Reaction Recipes for Bataille et al.(1982) *(all numbers are in wt%, amount of water is fixed at 100%)*

Recipe	run 1	run 2	run 3	run 4	run 5
potassium persulfate	0.24	0.24	1.00	0.24	1.00
sodium dodecyl sulfate	0.67	0.67	0.67	2.00	2.00
styrene	40	30	30	30	30

All five runs were simulated using the recipes/conditions listed in the Table 17.2. Simulation results on conversion are displayed in figures 17.1~17.3. In all five runs there are large but consistent discrepancies between our model predictions and reported conversion data. An investigative check on all runs suggests there is a systematic trend that all experimental data lag behind the model predictions. To identify the culprit of the discrepancies, the reported experimental setup and procedure were closely examined. It was reported by Bataille et al.(1982) that all reactions were conducted in a 1 liter glass reactor and samples were taken periodically by using a pipet. Though monomer was washed prior to the reaction to remove inhibitor, glass reactors are known to have poor seals and oxygen leakage during the reaction is very likely. Furthermore, when samples were taken using a pipet, the reactor contents were exposed to the atmosphere, and large quantities of oxygen entered the reactor. Finally, in Bataille's et al.(1982) experiment setup, nitrogen was not pumped through the reactor to keep oxygen away. According to the above discussion on Bataille's et al.(1982) experiment setup and practice, it was very likely that there was severe oxygen leakage in the reaction. Since oxygen can partition itself in both water and oil phases, its effect on reaction kinetics is an induction time (as appeared in runs #3 and #5) as well as an hindered reaction rate (in all runs). A detailed discussion on inhibitor effects on emulsion polymerization kinetics is given in

Appendix 2. Oxygen has a much less pronounced effect on particle generation, therefore, a much better agreement between model predictions and experimentally measured total particle number per liter of water is obtained (see figure 17.4).

As mentioned before, the rate constant for termination in styrene emulsion polymerization has a much lower initial value compared to the same rate constant in bulk and solution polymerization. In Bataille's et al.(1982) experiments, they suggested the k_t in their five runs is between $2.11 \sim 10.43 \times 10^3$ L/mol·sec, which is almost four orders of magnitude lower than the k_t of styrene in bulk and solution polymerization (which is about 4.3×10^7 L/mol·sec). This model uses a value of 7×10^3 L/mol·sec for k_t, which is in the right range of what Bataille et al.(1982) have proposed in their work. As for the rate constant for propagation k_p, Bataille et al.(1982) used values between 69~135 L/mol·sec. The value of k_p this model uses is 175 L/mol·sec which is fairly close to what Bataille et al.(1982) suggested.

The same group continued their research on styrene emulsion homopolymerization with focus on the effect of various redox systems on reaction kinetics (Bataille et al., 1984, 1988). Nitrogen was pumped through the reaction mixture to avoid oxygen. Simulation results from the runs from Bataille et al.(1984) are displayed in figures 17.5 and 17.6. Predictions for conversion are now in good agreement with reported conversion data. The better agreement is largely due to the absence of oxygen in the vessel. Predictions for weight average molecular weight are also in good agreement with reported experimental data.

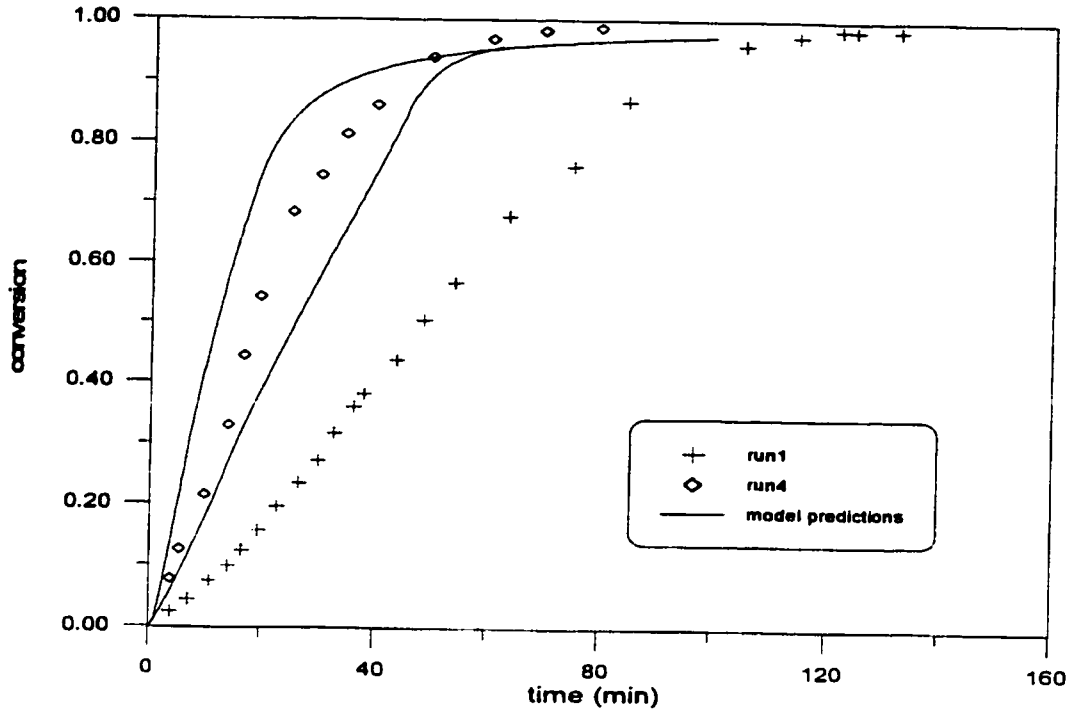

Figure 17.1 Simulation of Styrene Emulsion Homopolymerization at 60°C. (Runs #1 and #4)

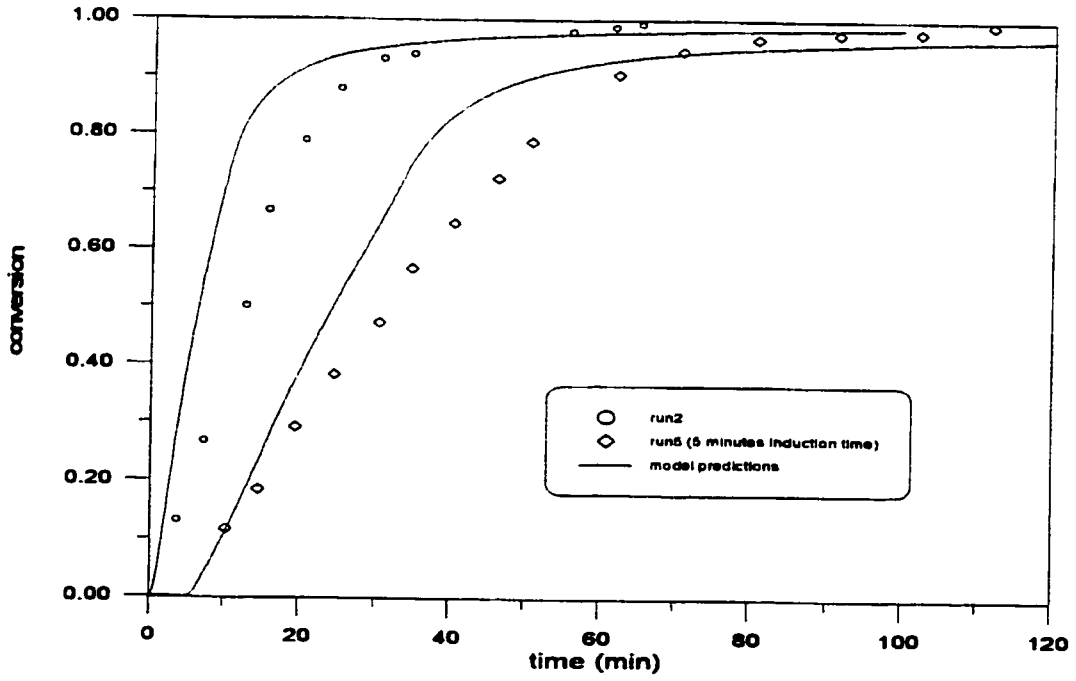

Figure 17.2 Simulation of Styrene Emulsion Homopolymerization at 60°C. (Runs #2 and #5)

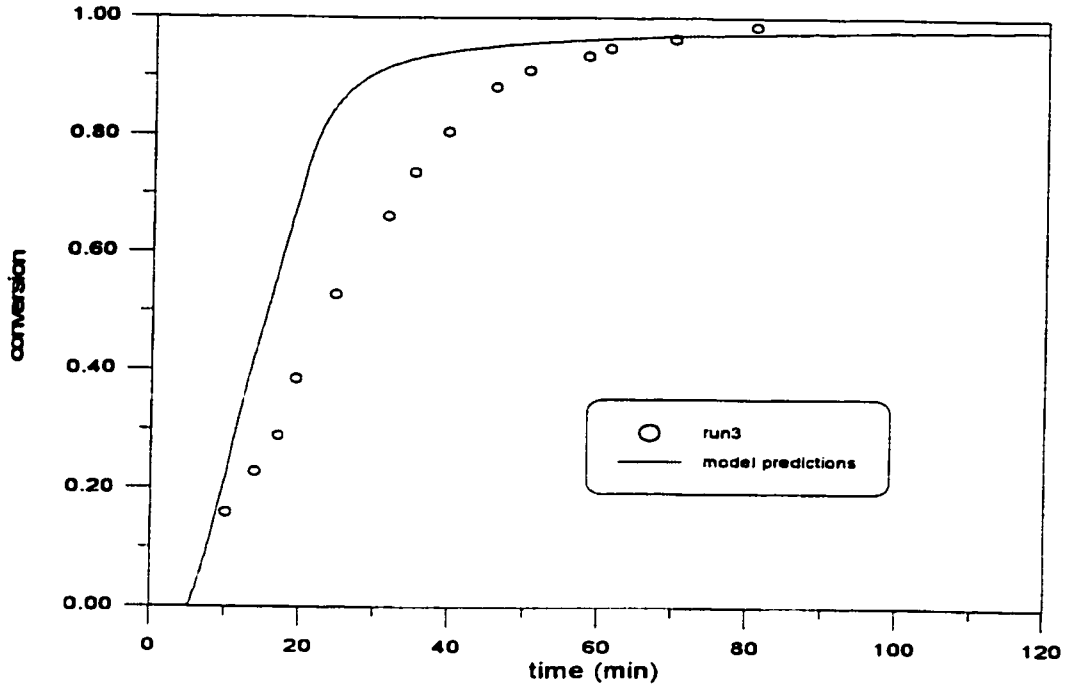

Figure 17.3 Simulation of Styrene Emulsion Homopolymerization at 60°C. (Run #3)

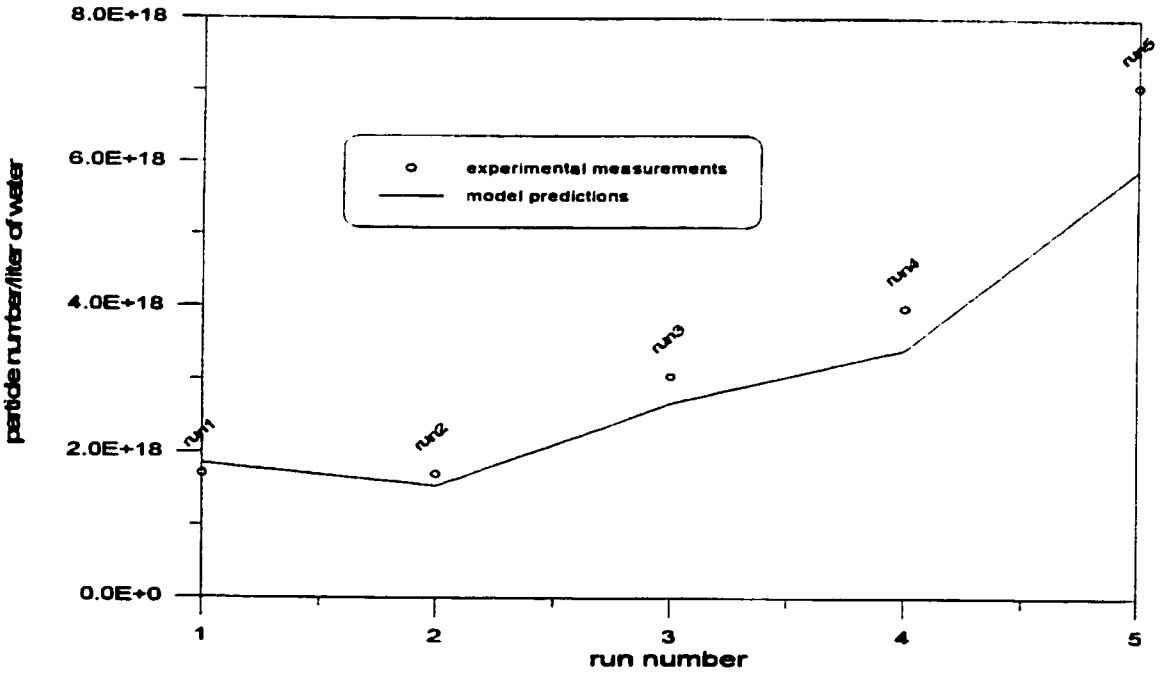

Figure 17.4 Simulation of Styrene Emulsion Homopolymerization at 60°C. (Model testing on particle generation)

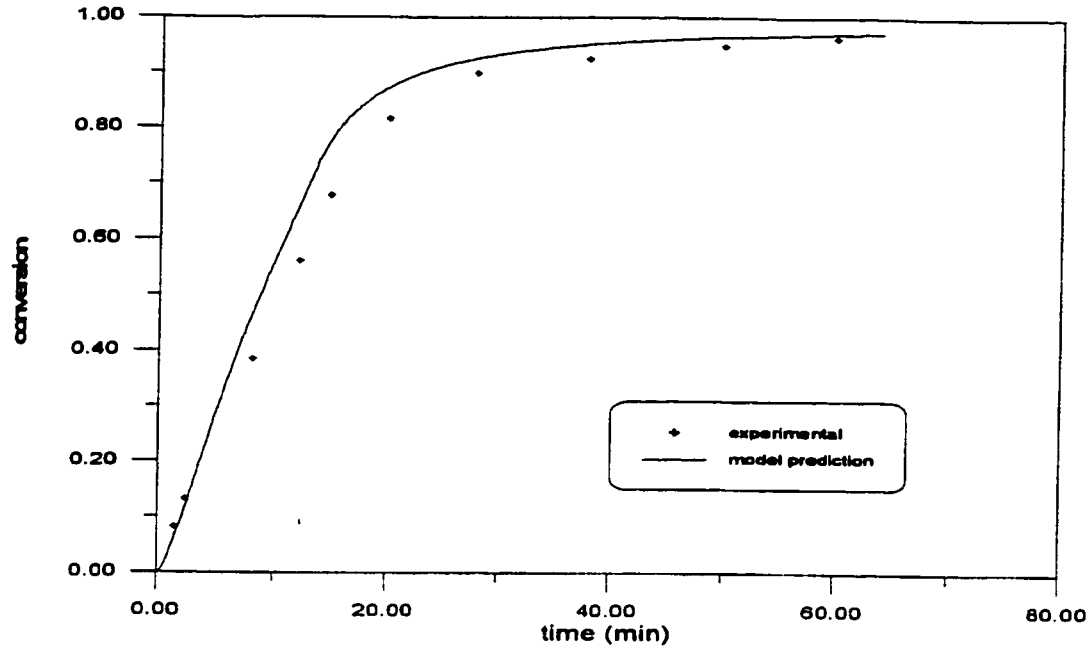

Figure 17.5 Simulation of Styrene Emulsion Homopolymerization at 60°C. (Water: 700g, Styrene: 300g, SDS: 14.28g, KPS: 7.07g)

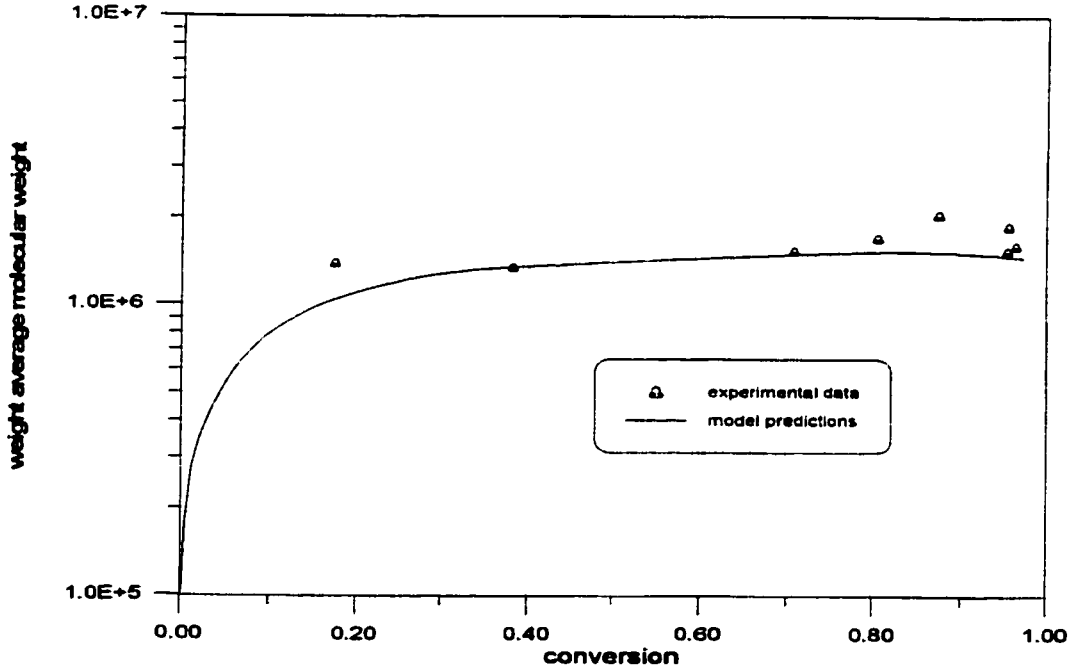

Figure 17.6 Simulation of Weight Average Molecular Weight in Styrene Emulsion Homopolymerization at 60°C.

Canegallo et al.(1993)

Online densitometer results in emulsion polymerization were reported by Canegallo et al.(1993). Problems associated with the online measurements such as thermal stability of samples, gas bubbles in the line, sample calibration, etc. were discussed in detail. Canegallo et al.(1993) used online densitometry try to follow the emulsion homopolymerization of styrene and MMA as well as the copolymerization of these two monomers. Their experimental data (online measurement of conversion) for styrene homopolymerization are presented in figure 17.7. Styrene homopolymerization was carried out with and without inhibitor removal. Apparently, the run without inhibitor removal is slower than the one with purified monomer. An initial induction time about 10~15 minutes was observed, this induction time was taken into account and the model delivered reliable predictions for both runs. The agreement is satisfactory.

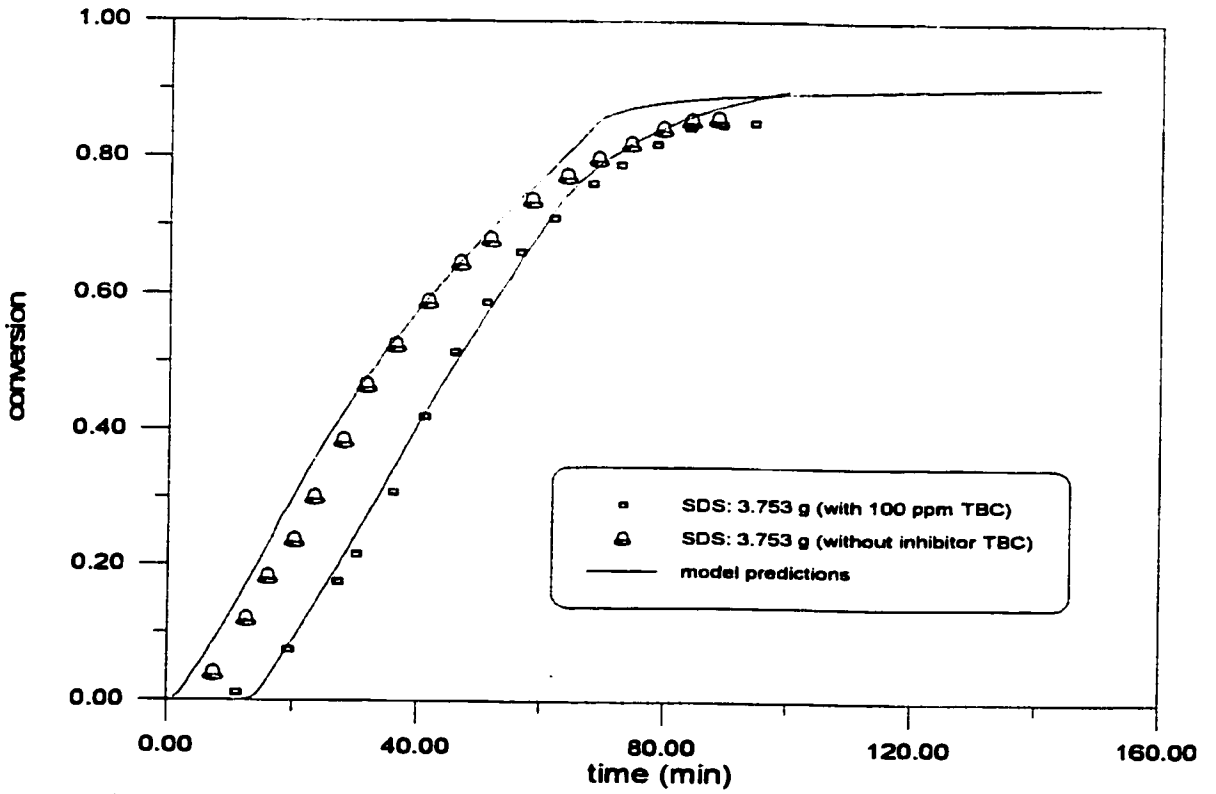

Figure 17.7 Simulation of Emulsion Homopolymerization of Styrene at 50°C. (Monomer: 90g, water: 603g, KPS: 1.05 wt%, SDS 3.753 g)

de la Rosa et al.(1996)

Recently, calorimetric techniques are used to obtain online measurements of conversion in emulsion polymerization. Since emulsion polymerization proceeds with a heat evolution, the measured heat release from the reaction can be translated into the rate of polymerization. de la Rosa et al.(1996) reviewed the use of calorimetry techniques and conducted a set of runs for styrene batch emulsion polymerization at 50°C at various levels of emulsifiers and initiators. In their first set of runs, the initiator concentration was set at 0.0046 mol/L with varying emulsifier levels between 0.05~0.07 mol/L. Model testing results on these three runs are displayed in figures 17.8~17.10. Very good agreement was obtained in all cases.

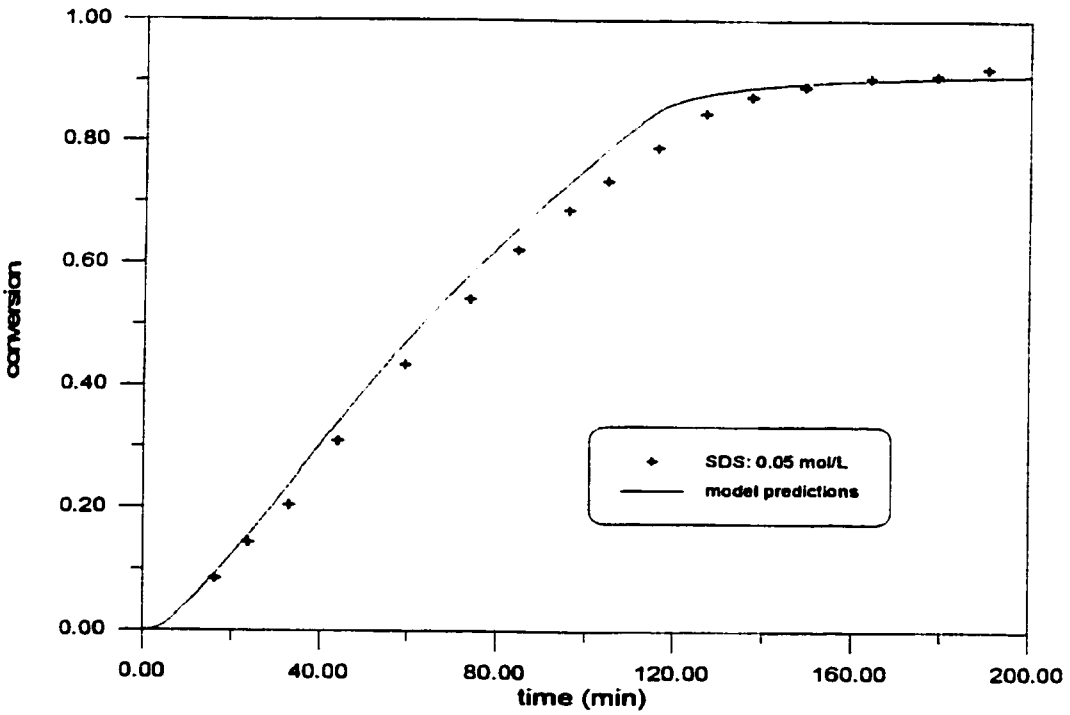

Figure 17.8 Simulation of Styrene Emulsion Homopolymerization at 50°C. (M: 196.53g, water: 393.06g, KPS: 0.0046 mol/L, SDS: 0.05 mol/L)

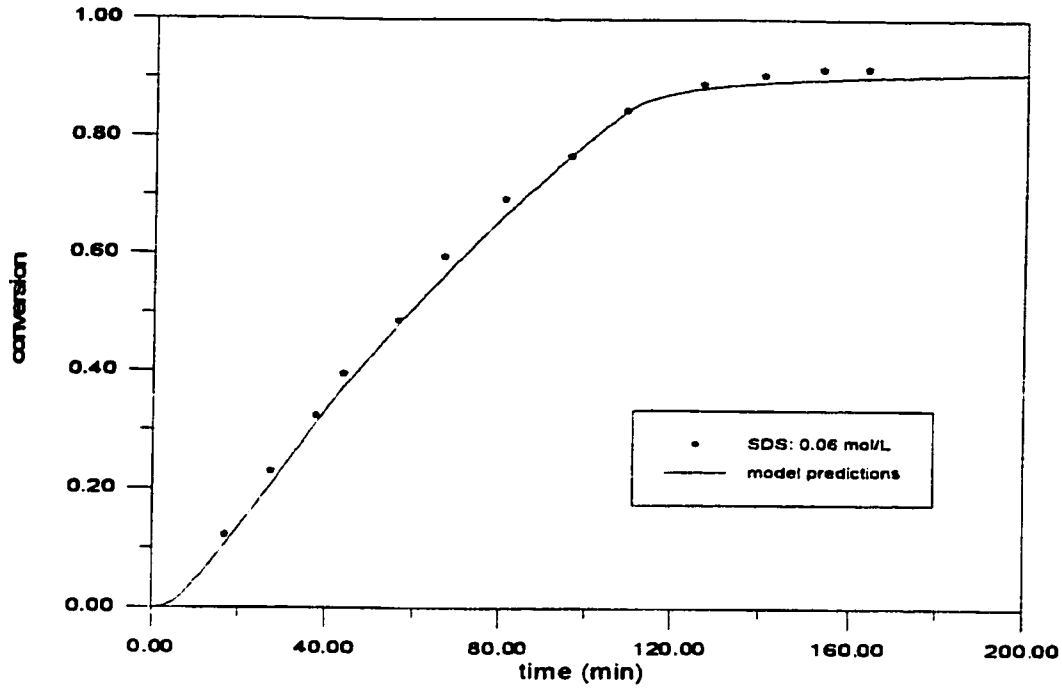

Figure 17.9 Simulation of Styrene Emulsion Homopolymerization at 50°C. (M: 196.53g, water: 393.06g, KPS: 0.0046 mol/L, SDS: 0.06 mol/L)

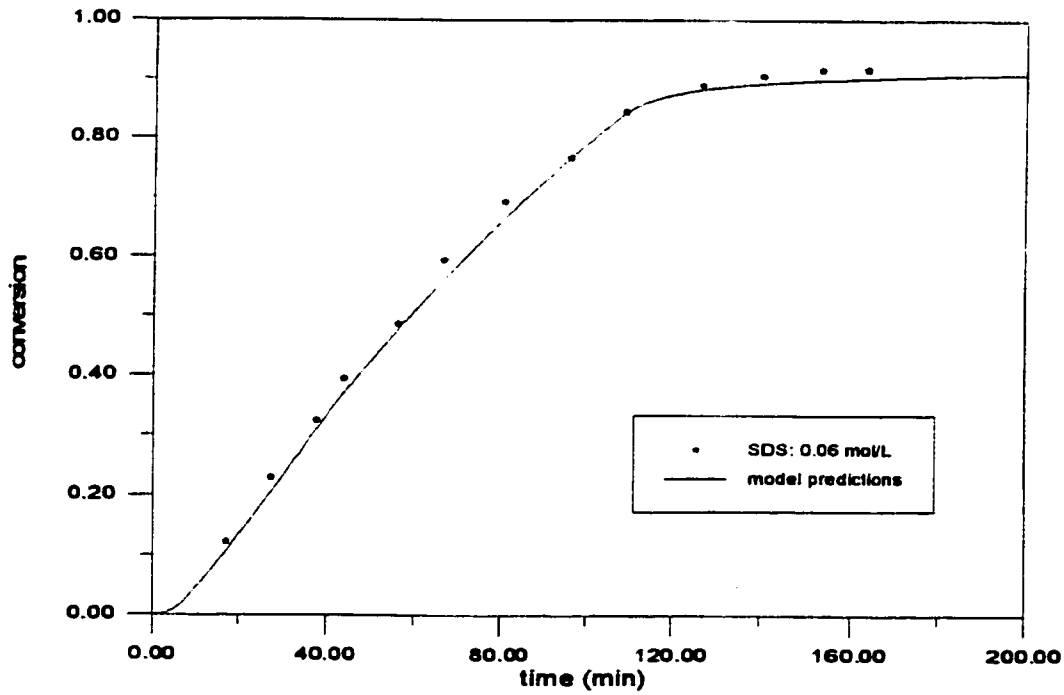

Figure 17.10 Simulation of Styrene Emulsion Homopolymerization at 50°C. (M: 196.53g, water: 393.06g, KPS: 0.0046 mol/L, SDS: 0.07 mol/L)

de la Rosa et al.(1996) plotted the measured heat of reaction versus conversion for the first set of experiments and found that in all cases the heat of reaction curves continue to increase and reach a maximum around 35~40% conversion. Since the rate of polymerization is directly proportional to the heat generation, they considered the peak at which Rp was at its maximum an indication that particles were continuously generated up to the maximum. de la Rosa (1996) further stated that in styrene emulsion homopolymerization there is no Stage II and Stage I lasts up to 40%. A typical heat of reaction curve is displayed in figure 17.11. Obviously, de la Rosa's et al.(1996) statement is in contradiction with the conventional emulsion kinetic scheme that the particle nucleation stage is short and usually ends within 5~10% of conversion. Before accepting de la Rosa's et al.(1996) statement that there is no stage II based on the heat generation profiles shown in figure 17.11, caution must be exercised. Indeed, the heat of reaction curves exhibit a maximum in all three runs, and this implies that the rate of polymerization reaches a maximum. However, this does not necessarily indicate that the continuous increase of heat generation (or rate of polymerization) is caused by more particles being generated. In fact, the heat generation is proportional to the product of rate of polymerization times the total volume of polymer particles. To put all this in mathematical form, the heat of reaction $\Delta H \propto Rp \cdot Vp$. At the end of stage I, Rp may stop increasing, however, the total polymer particle volume Vp keeps increasing, and thus the overall consumption rate of monomer is also increasing despite the fact that no new particles are generated. This trend will last up to the end of stage II which ends around 30~35% conversion for styrene. This coincides very well with the conversion levels at which the heat of reaction peaked. To summarize, it is likely that de la Rosa et al.(1996) misinterpreted their results displayed in figure 17.11. In fact, styrene emulsion homopolymerization conforms well with the Smith-Ewart case II kinetic scheme.

The second series of styrene emulsion polymerization experiments were conducted at fixed emulsifier concentration with varying initiator concentration, ranging from 0.0046 mol/L to 0.011 mol/L. de la Rosa et al.(1996) did not report conversion profiles but used capillary hydrodynamic fractionation (CHDF) to determine particle number. Reported total particle numbers per liter of water for four runs in the second set of experiments are displayed in figures 17.12~17.15. It should be noted that initiator concentration does not have a very drastic effect on particle nucleation. That's the reason why the

final Np values in figures 17.12~17.15 are relatively close to each other. Nevertheless, model predictions for all the experiments are in a very close range within experimental measurement error, considering the difficulty associated with particle number measurement determination, and hence model predictions should be considered satisfactory.

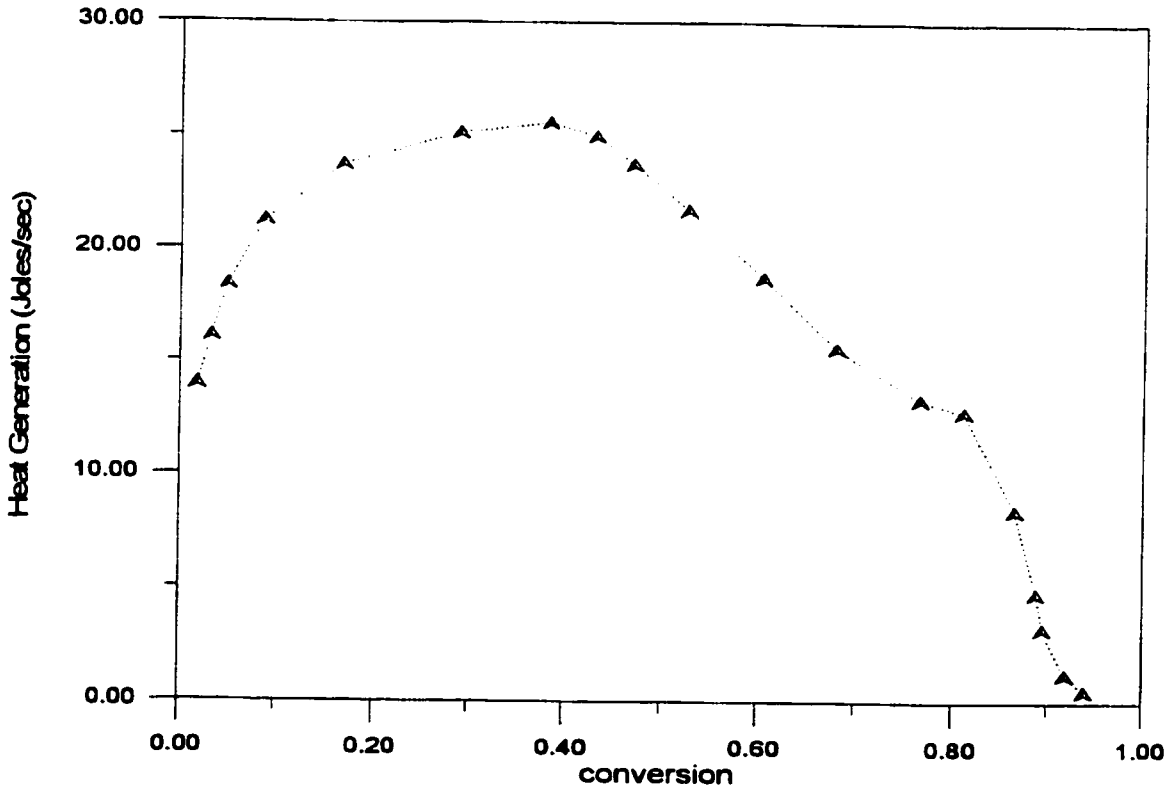

Figure 17.11 Heat of Reaction for Styrene Homopolymerization at 50°C.
(M: 196.53g, water:393.06g, KPS:0.0046 mol/L, SDS: 0.05 mol/L)

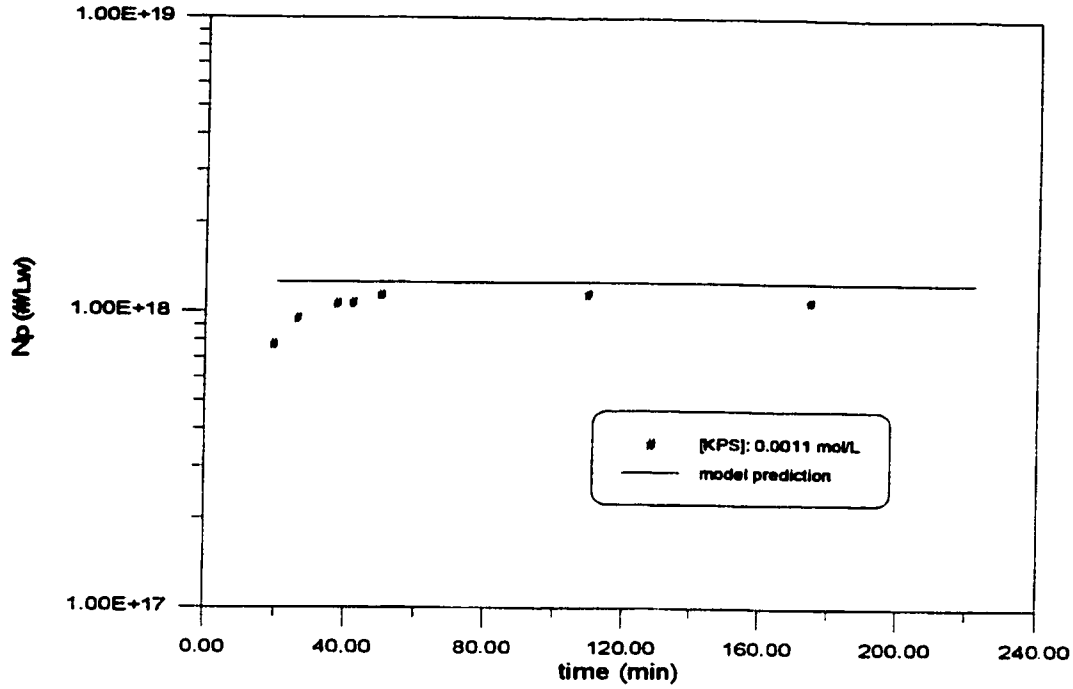

Figure 17.12 Simulation of Styrene Emulsion Homopolymerization at 50 °C. Prediction of Total Number of Particles.

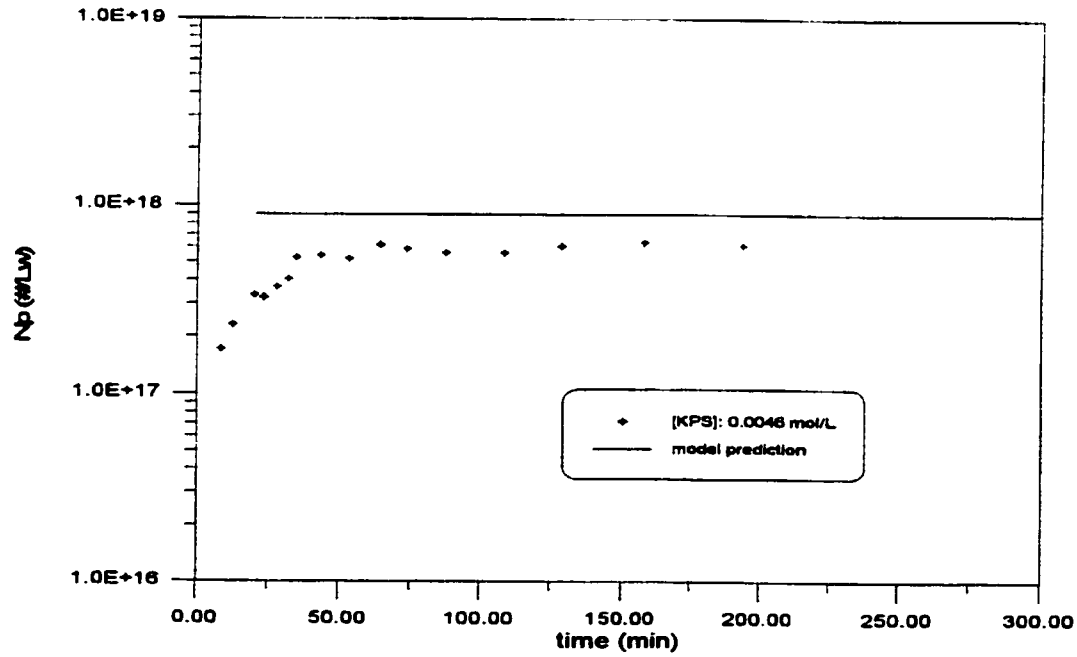

Figure 17.13 Simulation of Styrene Emulsion Homopolymerization at 50 °C. Prediction of Total Number of Particles

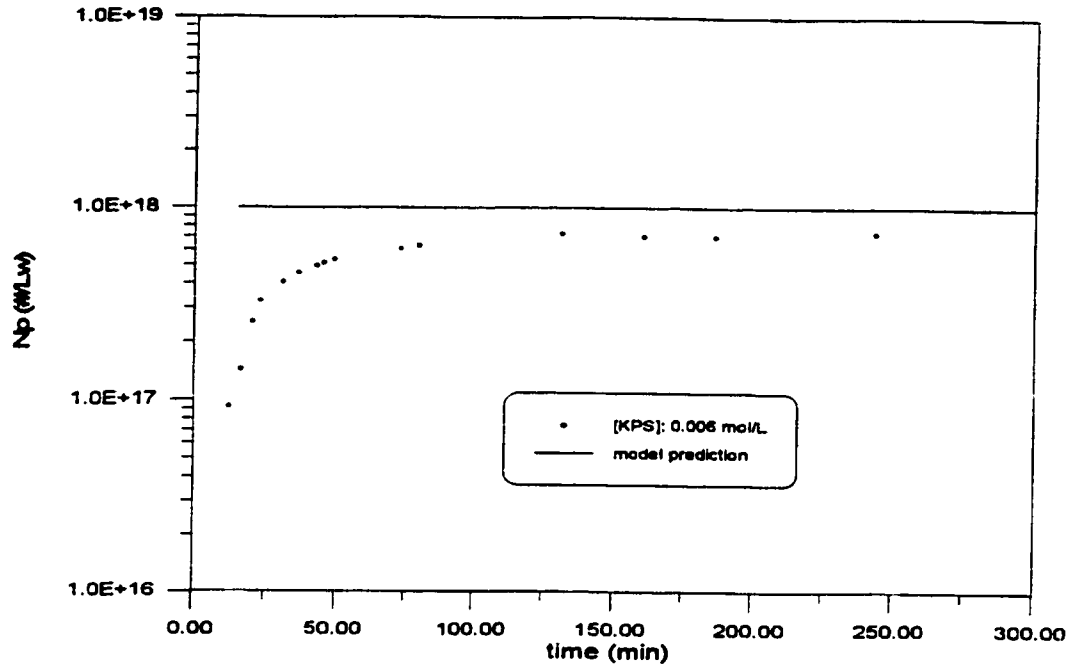

Figure 17.14 Simulation of Styrene Emulsion Homopolymerization at 50°C. Prediction of Total Number of Particles.

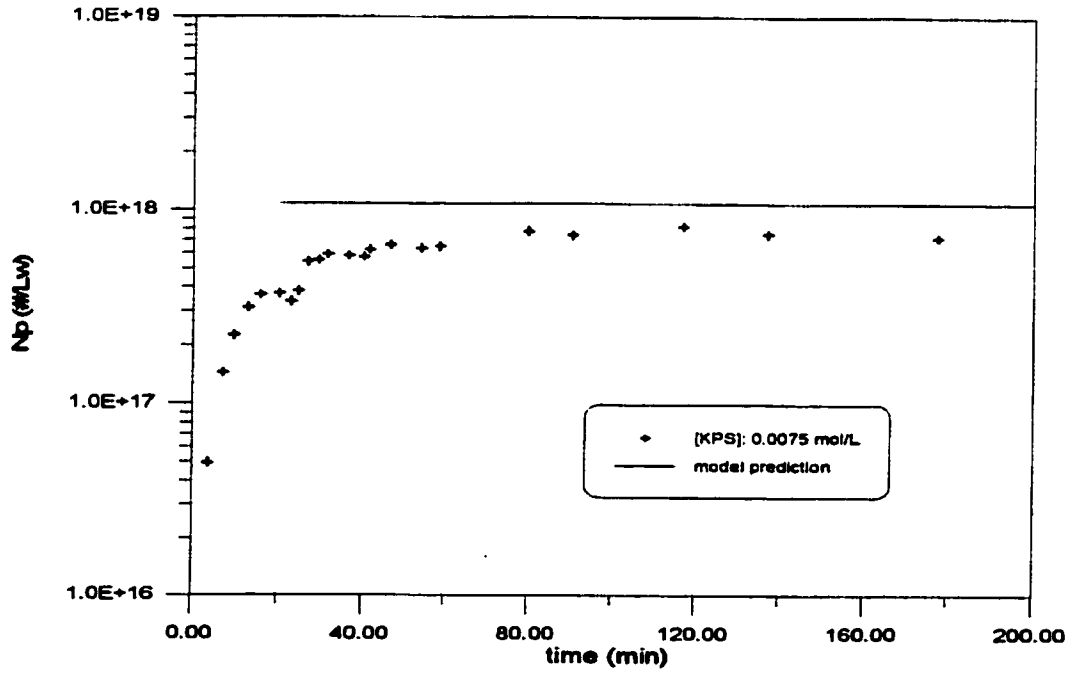

Figure 17.15 Simulation of Styrene Emulsion Homopolymerization at 50 °C. Prediction of Total Number of Particles.

Blackley and Sebastian (1987, 1989)

Blackley and Sebastian (1987, 1989) studied the influence of various emulsifiers and inorganic electrolytes on emulsion homopolymerization of styrene and copolymerization of styrene and acrylic acid. Two homopolymerization runs were carried out under identical reaction condition. Figure 17.16 displays their reported conversion profile including a replicated run along with model predictions. The experimental data reproducibility is good as can be seen in figure 17.16. The model successfully followed the conversion points throughout the entire run. Although the gel effect is present from the very beginning, the commonly observed S-shape conversion versus time curve in bulk/solution polymerization does not appear here. This is possibly due to the relative constant particle monomer-polymer composition during stages I and II.

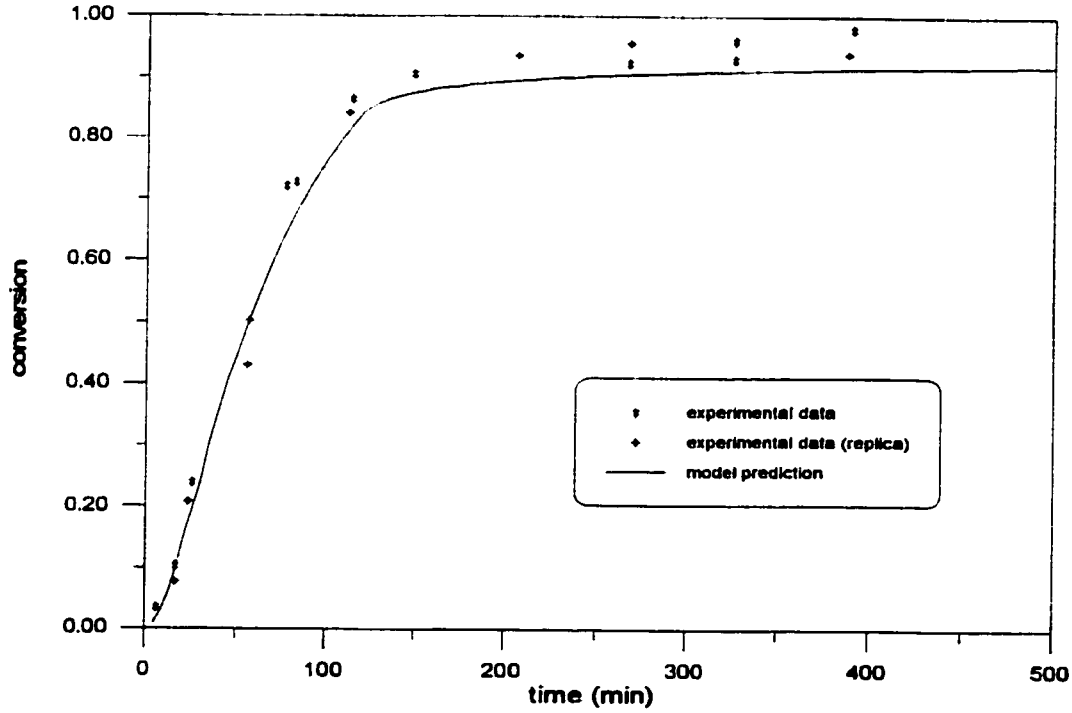

Figure 17.16 Simulation of Styrene Emulsion Homopolymerization at 45°C. (Sty: 100g, water: 200g, KPS: 0.5g, SDS: 5g)

Mayer et al.(1996)

Mayer et al.(1996) carried out styrene emulsion homopolymerization at changing temperatures. During the first 165 minutes of the reaction, the reactor temperature was kept at 50°C, whereas after this point, the temperature was raised to 75°C for about 80 minutes. The measured conversion is shown in figure 17.17. It can be seen that in the first temperature region, the reaction reached 90% conversion within one hour and a limiting conversion was present. In the next hour, polymerization was nearly halted due to the glassy state of the latex particles. When temperature was raised to 75°C, the elevated temperature brought the final conversion level higher up to 95%. In the model testing of this set of data, the programming temperature option was activated. This option enables the model to simulate the same reaction using the reported temperature profile. The final results are displayed in figure 17.17. The model gives good prediction of conversion in both the initial temperature region as well as in the elevated temperature region. The model also predicts the final particle diameter of 67.2 nm which agrees very well with the actual (transmission electron microscopy was used) measurement of 68 nm.

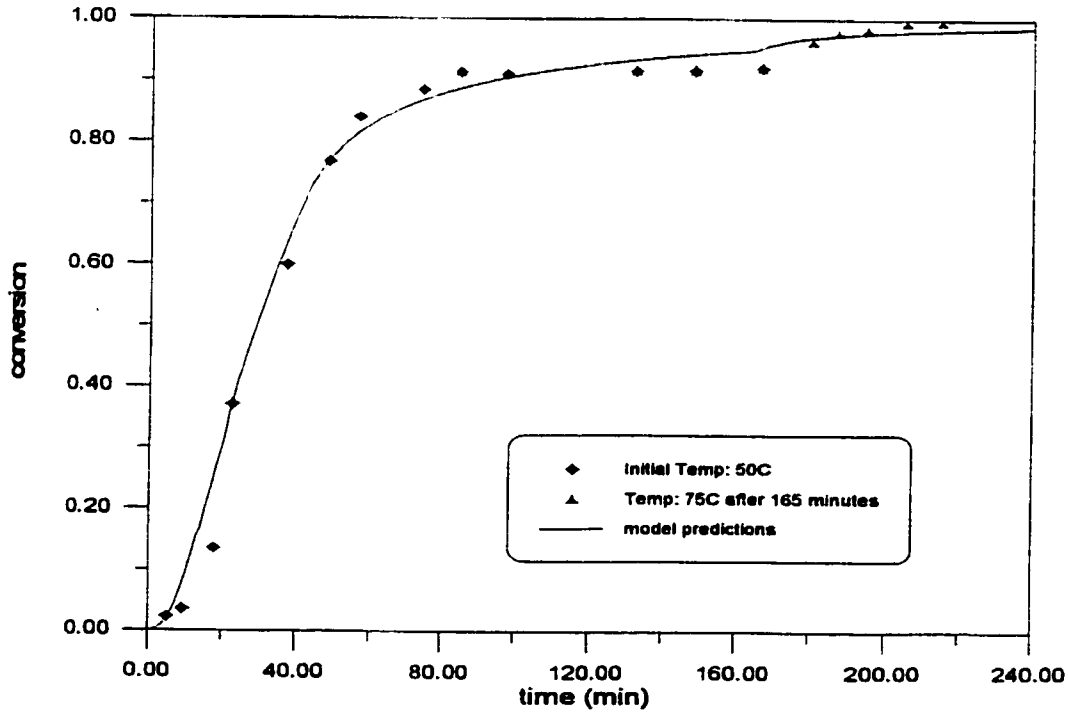

Figure 17.17 Simulation of Styrene Emulsion Homopolymerization.
Styrene: 4 mol/L, KPS: 0.0075 mol/L, SDS: 0.132 mol/L.

Harada et al.(1972)

Harada et al.(1972) performed detailed studies on styrene emulsion homopolymerization over a wide range of reaction conditions. They also developed a mathematical model to simulate all the experiments they conducted. Harada's et al.(1972) experiment results confirmed the fact that styrene is a typical case 2 monomer as Smith and Ewart's theory depicted. In all their runs, stage I ends at around 14% of conversion and stage II ends around 43%. This model predicts the end of stage II conversion level at 35%, which is close to what Harada et al.(1972) observed. Additionally, the monomer concentration inside polymer particles was measured as 5.45 mol/L. This measurement has confirmed that our model's prediction of 5.8 mol/L is very reasonable.

A set of five runs were simulated and the results are presented in figure 17.18. The effect of emulsifier concentration on reaction kinetics is clearly shown. Higher emulsifier concentration results in higher rate of polymerization. In all five runs, model predictions agree well with measured conversion data.

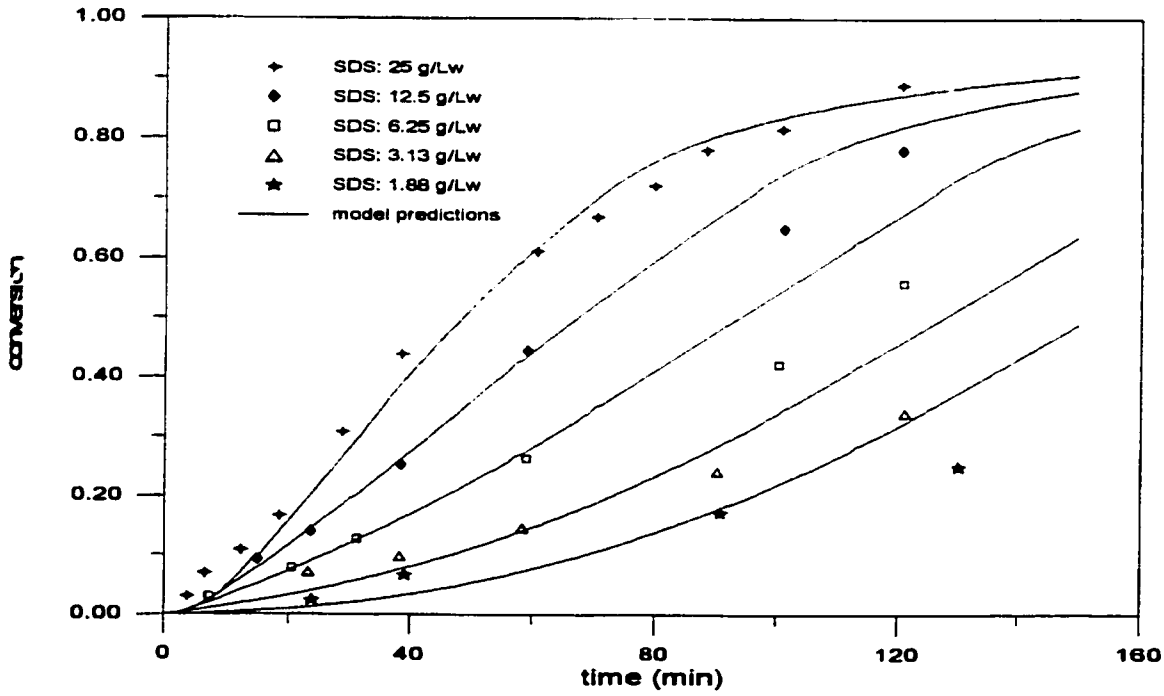

Figure 17.18 Simulation of Styrene Emulsion Homopolymerization at 50°C.
Water: 1 L, monomer: 572 ml, [KPS]: 0.0046 mol/Lw

Salazar et al.(1998)

It is known that polymer produced in emulsion polymerization has very high molecular weight compared to its bulk/solution counterpart. In order to control physical properties of the final product, CTAs are commonly used in emulsion polymerization. Salazar et al.(1998) performed some studies on molecular weight control in emulsion polymerization of styrene using various types of CTAs. It is known that in the mercaptan group, CTAs with more carbon units in the backbone have lower water solubility. A CTA with low water solubility resides predominantly in the monomer droplets at the beginning of the reaction. As the reaction proceeds, it must diffuse from the monomer droplets through the aqueous phase into the polymer particles. A CTA with lower water solubility usually encounters higher diffusion resistance, thus the effectiveness of a CTA depends not only on its chemical nature but also on its diffusivity. Salazar et al.(1998) listed the apparent chain transfer constant (defined as the ratio of the rate constant for chain transfer to CTA over propagation) for a number of CTAs with numbers of carbon atoms ranging from 9 to 13. It can be concluded that the higher the number of carbon atoms in a CTA's backbone (this implies that this CTA has a lower water solubility), the lower the chain transfer constant. Salazar et al.(1998) used t-nonyl mercaptan (with 9 carbon atoms) and n-dodecyl mercaptan (with 12 carbon atoms) in their experiments. The chain transfer constant for these two CTAs is 1.95 and 0.31, respectively. Though it is of theoretical advantage to use the 'true' chain transfer constant for the CTAs and then incorporate diffusion limitations for each CTA into the model, such practice is difficult due to the lack of information of certain parameters like diffusivity of CTAs in different phases. In contrast, the semi-empirical approach of using the "apparent" chain transfer coefficient provides an easy and effective way of modelling emulsion polymerization with CTAs, and its usefulness is confirmed in the simulation of experiments presented in Salazar et al.(1998)

Two homopolymerization runs of styrene were carried out by Salazar et al.(1998), with t-nonyl mercaptan and n-dodecyl mercaptan. These two runs were carried out under the same conditions and recipe, except for the use of different CTAs. Figures 17.19 and 17.20 display model predictions for conversion and unswollen polymer particle size ("dry" polymer particles without residual monomer) for the run with n-dodecyl mercaptan added, while figures 17.21 and 17.22 are the predictions for

the run with t-nonyl mercaptan added. The agreement between model predictions and measured conversion and particle size is very good. The results from both runs are very similar to each other, indicating the fact that the effect of both CTAs on the rate of polymerization and polymer particle size is very close to each other. Perhaps the biggest difference for these two CTAs is the way they affect the molecular weight profiles shown in figures 17.23 and 17.24. As mentioned before, t-nonyl mercaptan has higher water solubility and lower diffusion resistance, therefore its concentration in polymer particles is higher compared to n-dodecyl mercaptan. The more predominant presence of t-nonyl mercaptan in polymer particles results in a relatively lower molecular weight (both number and weight average) in the early stage of polymerization. As the reaction proceeds, more CTA is consumed and its concentration in the polymer particles gradually goes down, and subsequently polymer of higher molecular weight is produced. This trend is clearly shown in figures 17.23 and 17.24 for both number average and weight average molecular weights.

In contrast, n-dodecyl mercaptan has a very different way of affecting molecular weight of the polymer produced. Due to its low solubility and higher diffusion resistance, n-dodecyl mercaptan stays in the monomer droplets first and gradually diffuses into polymer particles. The result of such a characteristic is higher molecular weight averages in the beginning of the reaction, which gradually decrease as the reaction proceeds. It is very satisfactory to see that the unique trends of molecular weight averages influenced by two types of CTAs are followed very well by the model. This also proves that the use of an "apparent" chain transfer coefficient is very practical and reliable.

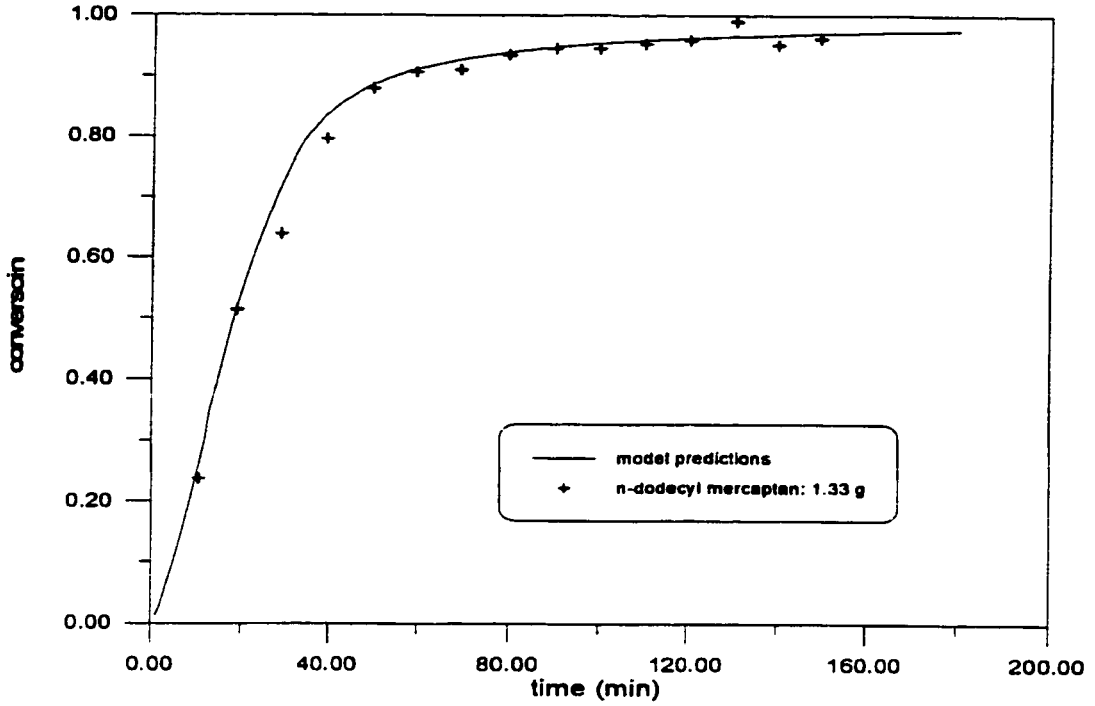

Figure 17.19 Simulation of Styrene Emulsion Homopolymerization at 70°C. (Styrene: 130.7g, water: 515.6, KPS: 0.233g, SDS: 2.62g)

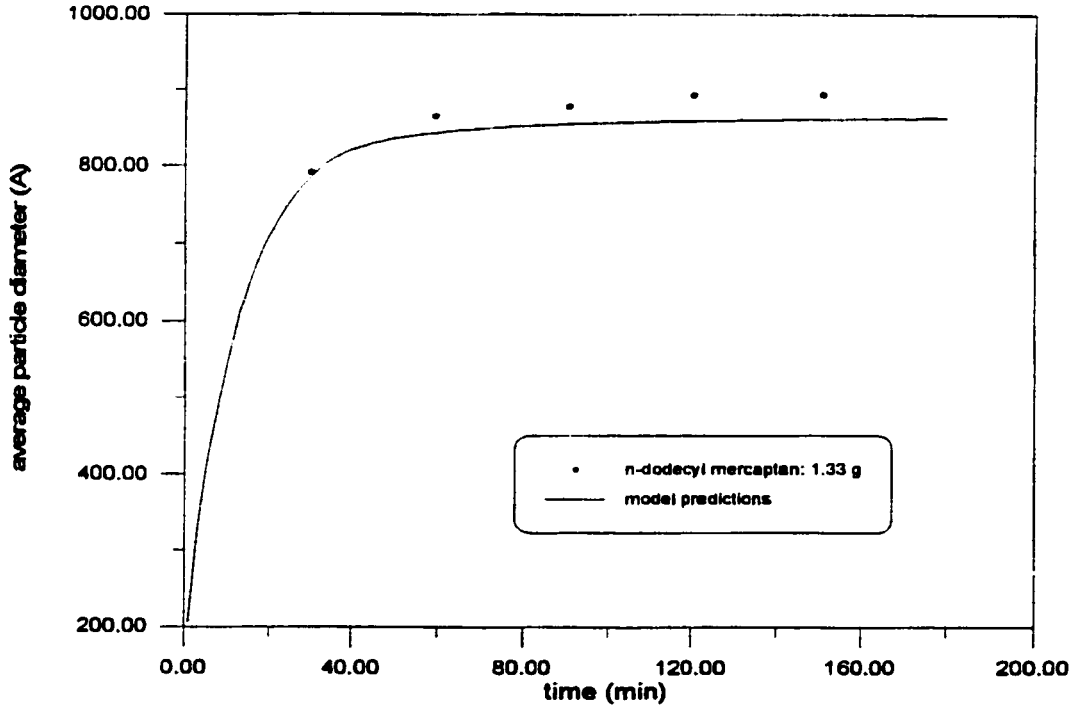

Figure 17.20 Simulation of Styrene Emulsion Homopolymerization at 70°C. Unswollen Particle Diameter. (Styrene: 130.7g, water: 515.6, KPS: 0.233g, SDS: 2.62g)

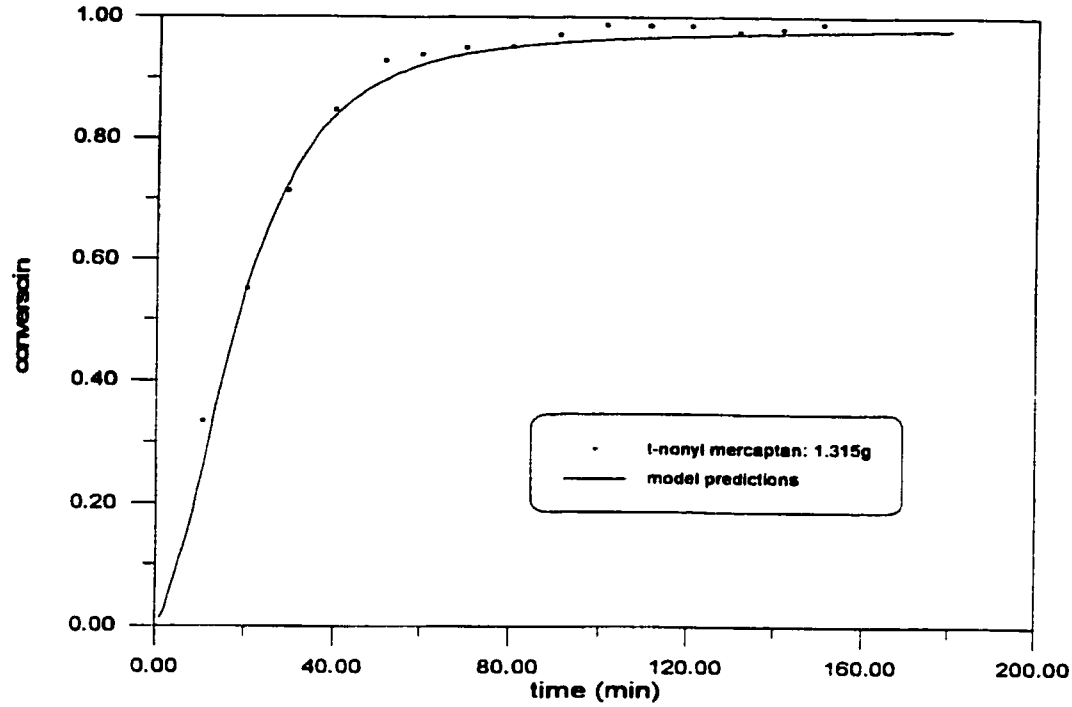

Figure 17.21 Simulation of Styrene Emulsion Homopolymerization at 70°C. (Styrene: 130.7g, water: 515.6, KPS: 0.233g, SDS: 2.62g)

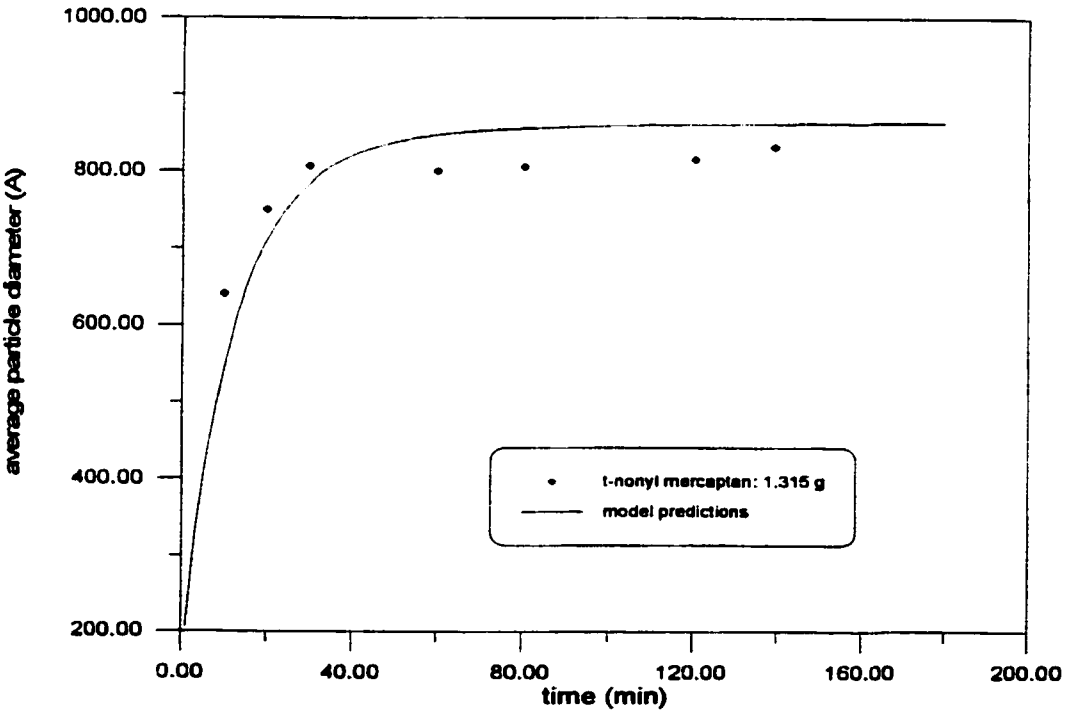

Figure 17.22 Simulation of Styrene Emulsion Homopolymerization at 70°C. Unswollen Particle Diameter (Styrene: 130.7g, water: 515.6, KPS: 0.233g, SDS: 2.62g)

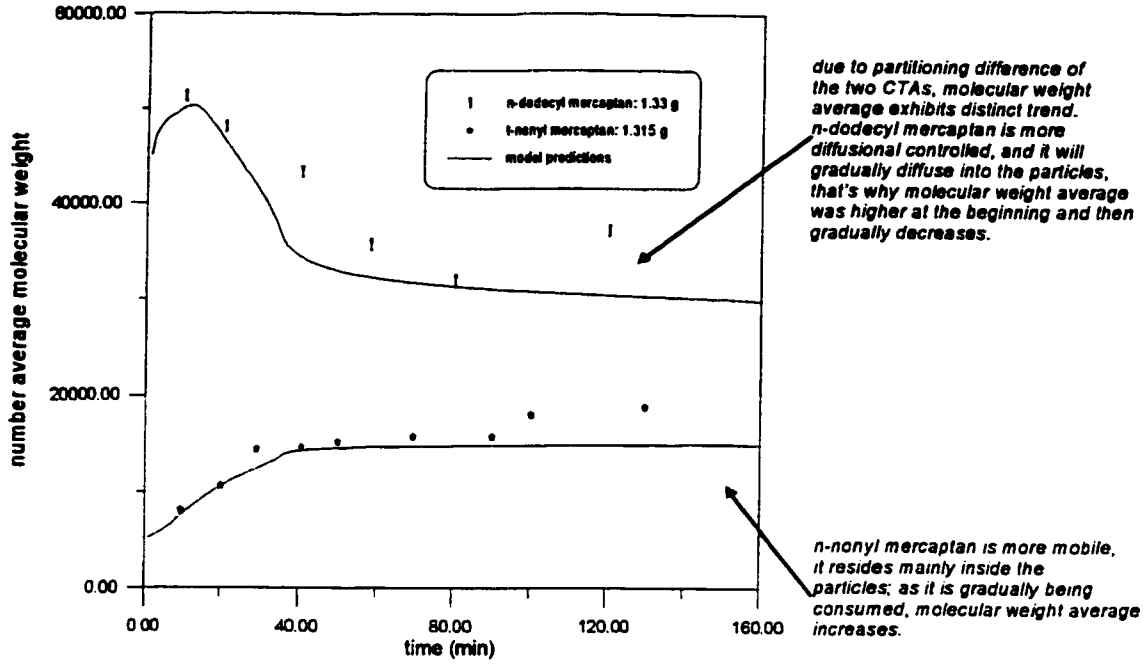

Figure 17.23 Simulation of Number Average Molecular Weight in Styrene Emulsion Homopolymerization at 70°C.
(Styrene: 130.7g, water: 515.6, KPS: 0.233g, SDS: 2.62g)

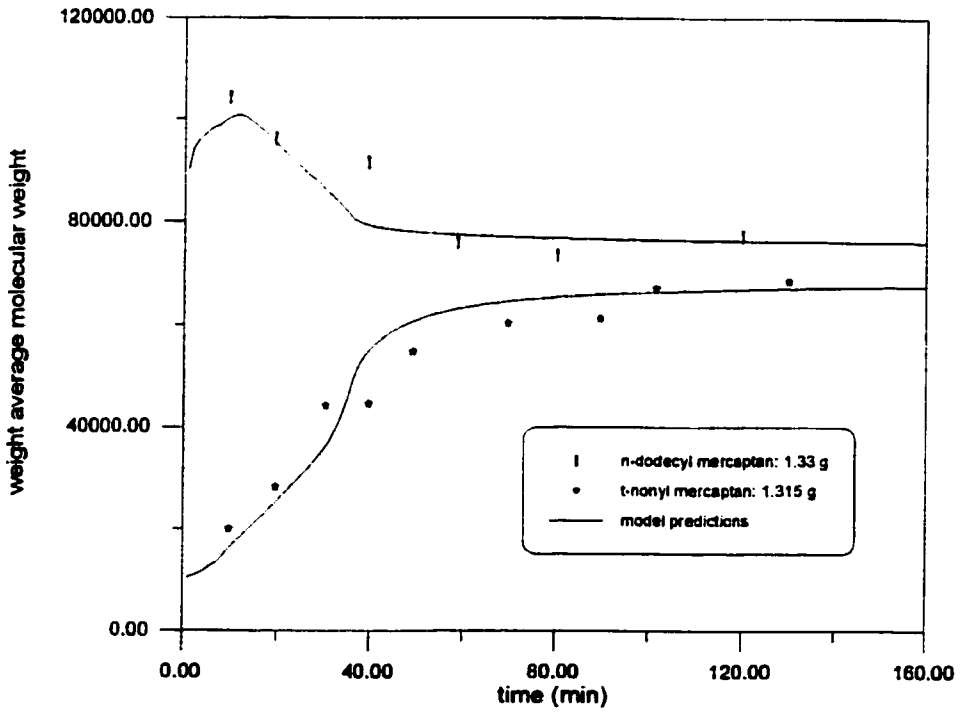

Figure 17.24 Simulation of Weight Average Molecular Wegith in Styrene Emulsion Homopolymerization at 70°C.
(Styrene: 130.7g, water: 515.6, KPS: 0.233g, SDS: 2.62g)

Chapter 18. Simulation of Emulsion Homopolymerization of Vinyl Acetate

Vinyl acetate bulk/solution polymerization is characterized as a system with high degree of branching. A detailed kinetic study and model testing of homo-/copolymerization for this monomer in bulk/solution are summarized in Gao and Penlidis (1996, 1998). In emulsion polymerization, vinyl acetate is a typical case I monomer with high water solubility and significant desorption. Kinetic studies on this monomer found in the literature are primarily focused on the desorption phenomenon. In addition to the difficulties in modelling branching in vinyl acetate polymerization, desorption makes modelling of vinyl acetate emulsion polymerization more complicated compared to other monomers with low water solubility like styrene or butadiene. The desorption process itself is very difficult to understand, despite the fact that it has been studied by a number of researchers for many years. A very good review on many aspects of vinyl acetate emulsion polymerization can be found in El-Aasser and Vanderhoff (1981). Chern and Poehlein (1987) also reviewed this subject and developed their own model to simulate vinyl acetate emulsion polymerization.

It is important to understand the characteristics associated with emulsion vinyl acetate before developing a mathematical model. These characteristics are:

(1): Emulsion polymerization kinetics of VAc does not fit the 0-1 Smith-Ewart kinetic scheme. Due to desorption, the average number of radicals per particle $\bar{n}$ is much lower than ½ (typically $\bar{n}$ is in the order of 10^{-2} ~10^{-3}) throughout the entire reaction in most cases.

(2): The rate of polymerization stays relatively constant throughout a large part of the reaction, and the gel effect is usually not observed. This is because desorption greatly reduces the probability of coexistence of multiple radicals inside one particle.

(3): Branching is important.

(4): Termination is not as important as it is in bulk reactions. Rate of propagation and molecular weight averages developed are less dependent on termination. In contrast, molecular weight is controlled by chain transfer reactions.

(5): Chain transfer to monomer reaction is the first step in the desorption process.

In the list above, desorption and chain transfer to monomer reaction are the most important features. It has been observed by a number of authors (Friis et al. 1974; Friis and Hamielec1975a, b; Friis and Nyhagen 1973) that the molecular weight of polymer produced in vinyl acetate emulsion polymerization is controlled by chain transfer reactions such as transfer to monomer/polymer/CTAs rather than termination reactions. Chain transfer to monomer is also the first step in the desorption process. Friis and Hamielec (1975a, b) pointed out that termination in vinyl acetate emulsion polymerization plays a minor role compared to emulsion polymerization of other monomers like styrene or MMA, and this is because it is unlikely that multiple radicals can coexist in one single particle due to the high rate of desorption. This conclusion was confirmed by the work of Friis et al.(1974). Friis et al.(1974) derived a model to calculate the leading moments of the molecular weight distribution as a function of conversion. It can be concluded from their work that molecular weight in vinyl acetate emulsion polymerization is controlled by chain transfer reactions and is independent of particle number and initiator concentration. Furthermore, branching is more significant in emulsion polymerization than observed in bulk/solution polymerization, and this can be attributed to the higher polymer content inside the particles even at the beginning of the reaction. The same method used by Friis et al.(1974) was also used by Friis and Hamielec (1975b) in their modelling effort on emulsion polymerization of vinyl acetate.

Friis and Nyhagen (1974) investigated vinyl acetate emulsion kinetics both experimentally and theoretically. They observed in their experiments that the conversion-versus-time curve was linear between 15~85% conversion levels. They explained this phenomenon is partly due to a decrease in the desorption rate of radicals from the polymer particles. To describe such a change mathematically, they derived an expression that relates the diffusivity in polymer particles to the free volume of the system as shown below:

$$D_p = D_{p_o} \exp \frac{-\beta x d_m (1-\alpha)}{(1-x)d_p + \alpha x d_m} \qquad (18.1)$$

where:

α: ratio of free volume for polymer over free volume for monomer, V_{fp}/V_{fm}

β: ratio of critical free volume V^* over free volume for monomer, V^*/V_{fm}

D_{po}: initial diffusivity in polymer particles

d_m: monomer density

d_p: polymer density

x: conversion

The critical free volume V^* defined in β in equation 18.1 is the free volume at which the system becomes diffusion controlled. The only other group that adopted a similar approach is Chern and Poehlein (1987).They proposed that the diffusivity of monomer D_m is:

$$D_m = D_{m_o}\exp[-V_m^*(1/V_f - 1/V_{f_o})] \tag{18.2}$$

where V_m^* is an adjustable parameter. Equations 18.1, 18.2 and 15.67 are all very similar to each other. They are all based on the same principle (free-volume theory). Friis and Nyhagen's equation directly links the diffusivity D_p with conversion level. A diffusivity that changes with conversion level is important in modelling vinyl acetate emulsion polymerization, since it reflects the influence of gel effect on the desorption process.

A detailed discussion on desorption has already been given in section 15.4. Many papers mentioned in section 15.4 are good references for this monomer system and they will no be cited here again. Selective papers are listed in Table 18.1, especially with respect to useful data sources for model testing.

Table 18.1 Selective Reference List for Vinyl Acetate Emulsion Polymerization

References	Remarks
Badran et al.(1990)	redox system initiation in VAc emulsion polymerization
Bataille et al.(1990)	agitation effect on reaction kinetics, experimental data
Chern and Poehlein (1987)	review on VAc emulsion polymerization, kinetic model
de la Cal et al.(1990)	kinetic parameters in VAc copolymerization
Dimitratos et al.(1990)	BA-VAc copolymerization
Dunn and Taylor (1965)	experimental data, effect of ionic strength
El-Aasser and Venderhoff (1981)	general review
Farber (1986)	CSTR operation of MMA-VAc
Friis and Nyhagen (1973)	general kinetic study of VAc polymerization, experimental data
Friis et al.(1974)	molecular weight and branching development
Friis and Hamielec (1975a,b)	kinetic studies and molecular weight development
Friis and Hamielec (1982)	studies on gel effect
Greene et al.(1982)	CSTR operation/stability of MMA, VAc polymerization
Hawkett et al.(1981)	radical absorption efficiency
Kiparissides et al.(1980a, b, c)	CSTR operation of VAc
Kiparissides et al.(1979)	oscillation studies on emulsion polymerization of VAc
Kong et al.(1988)	VAc-BA batch copolymerization
Kshirsagar and Poehlein (1994)	measurement of critical size of oligomer radicals before forming particles in VAc emulsion polymerization
Lange et al.(1991)	seeded emulsion polymerization of VAc
Lee and Mallinson (1990)	molecular weight development for VAc
Lee and Mallinson (1988)	surfactant effects on molecular weight and PDI
Lichti et al.(1977)	general kinetic studies
Lichti et al.(1981)	chain transfer mechanism in VAc
Litt et al.(1970)	seeded VAc homopolymerization experiments
Litt and Chang (1981)	chain transfer effect
Meuldijk et al.(1992)	polymerization of Vac in a pulsed packed column reactor

Misra et al.(1983)	batch and semibatch copolymerization of VAc-BA
Moustafa et al.(1997)	emulsifier-free emulsion polymerization of VAc
Noel et al.(1994)	VAc/MA copolymer, monomer partitioning
Nomura et al.(1971a)*	experimental data
Nomura et al.(1976)	experimental data and modelling
Nomura and Harada (1981)	rate constant for desorption
Omi et al.(1987)	general modelling
Penlidis et al.(1985a)*	experimental data, modelling
Sarkar et al.(1990)	thermal decomposition of KPS with VAc
Singh and Hamielec (1978)	full conversion experimental data, emulsifier-free reaction
Trivedi (1983)	experimental data, monomer partitioning
Urquiola et al.(1993)	emulsion polymerization of VAc using polymerizable surfactant
Zollars (1979)	experimental data, modelling

* experimental data tested

18.1 Model Testing Results

Nomura et al.(1971a)

Nomura et al.(1971a) performed a kinetic investigation on many aspects of vinyl acetate emulsion homopolymerization (effect of initiator levels, emulsifier levels, etc.). Their experimental runs were simulated and results are presented in figures 18.1~18.4. Figure 18.1 shows one run with 12.5 g/Lw SDS as emulsifier and 1.25 g/Lw KPS as initiator. It should be pointed out that in most of their runs there was oxygen present. The run shown in figure 18.1 is no exception. The prediction of the overall trend of conversion profile is good. The oxygen effect is more pronounced in runs with a lower initiator amount used. This can be seen in figure 18.2. A total of five runs were carried out with initiator concentration ranging from 0.156 g/Lw to 2.5 g/Lw. It is no surprise to see that the run with the lowest initiator concentration exhibits the longest induction time, while the run the with highest initiator concentration started almost immediately.

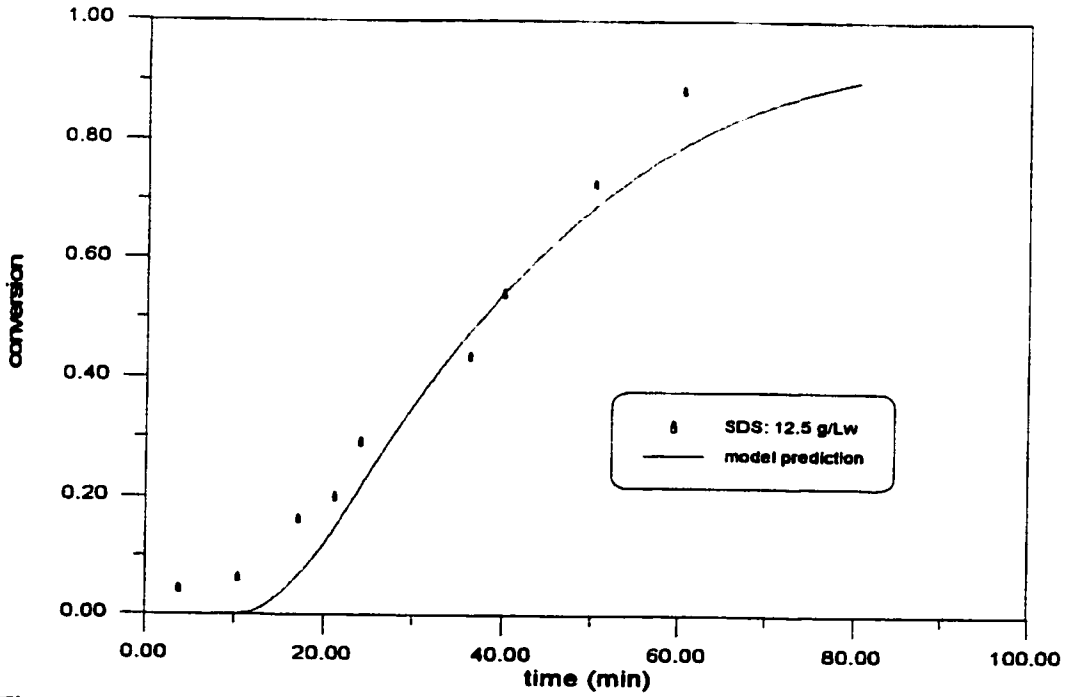

Figure 18.1 Simulation of Vinyl Acetate Emulsion Polymerization at 50°C. KPS: 1.25 g/Lw, M: 0.5 g/ml water.

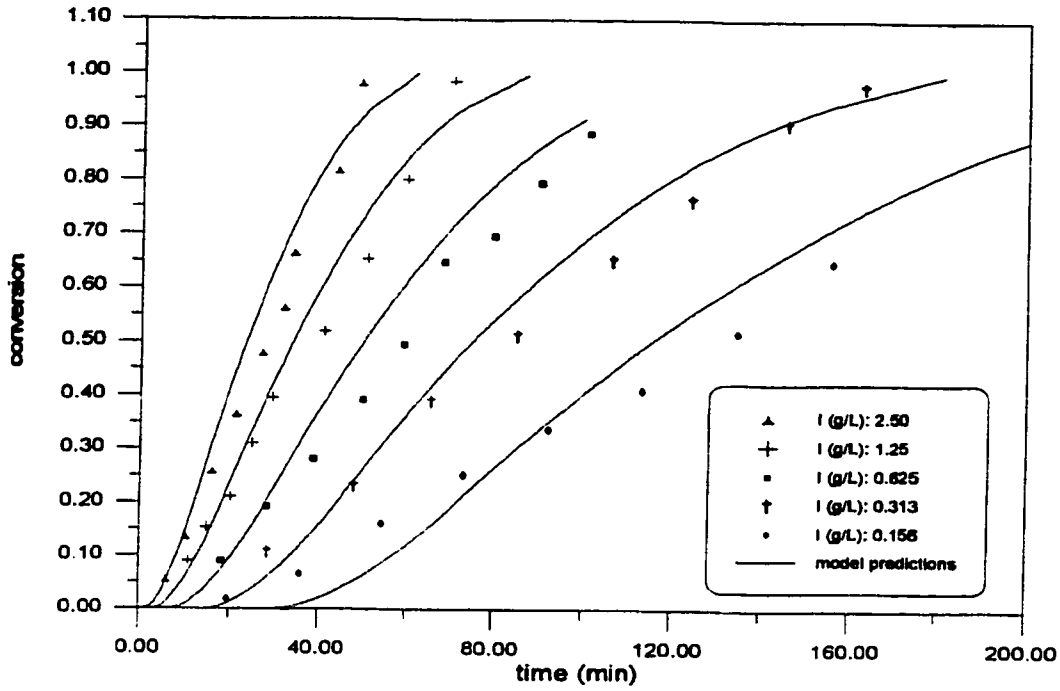

Figure 18.2 Simulation of Vinyl Acetate Emulsion Polymerization at 50°C. SDS: 6.25 g/Lw, M: 0.5 g/ml water.

Nomura et al.(1971a) stated that the conversion profile in most of their experiments exhibits linearity, therefore by assuming a constant Rp throughout the reaction, the average number of radicals per particle can be backcalculated if the total number of particles in the latex is known. It should be realized that the rate of polymerization may not be strictly constant, therefore $\bar{n}$ derived from this backcalculation method is only approximate. Nevertheless, it at least demonstrates the trend of how $\bar{n}$ changes during the reaction. Nomura et al.(1971a) reported $\bar{n}$ for some runs using the backcalculation method, and the reported $\bar{n}$ for one of their runs is compared with model predictions in figure 18.3. It is evident in figure 18.3 that at the beginning of the reaction, $\bar{n}$ is rather small and in the range of 10^{-3}. It gradually increases into the range of 10^{-2}, and at the end of the reaction, $\bar{n}$ increases considerably due to the decreased rate of desorption. The model follows the correct trend of $\bar{n}$ well as can be seen from figure 18.3.

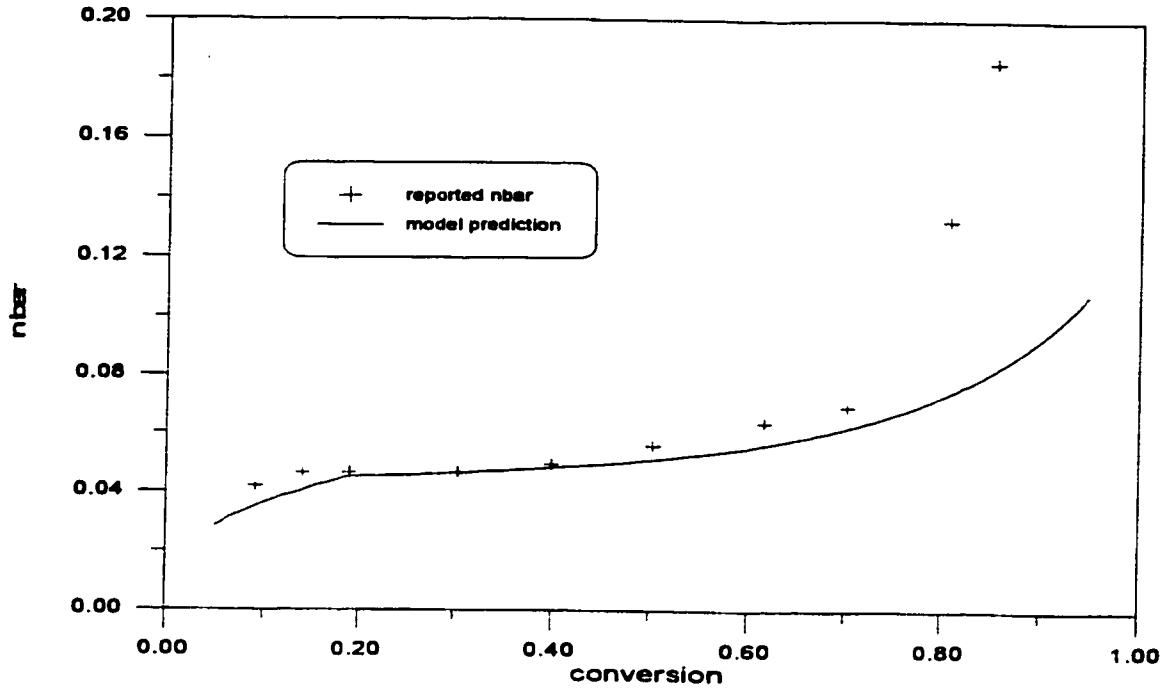

Figure 18.3 Comparison of Model Predicted and Reported $\bar{n}$.
SDS: 6.25 g/Lw, KPS: 1.25 g/Lw, M: 0.5 g/ml water.

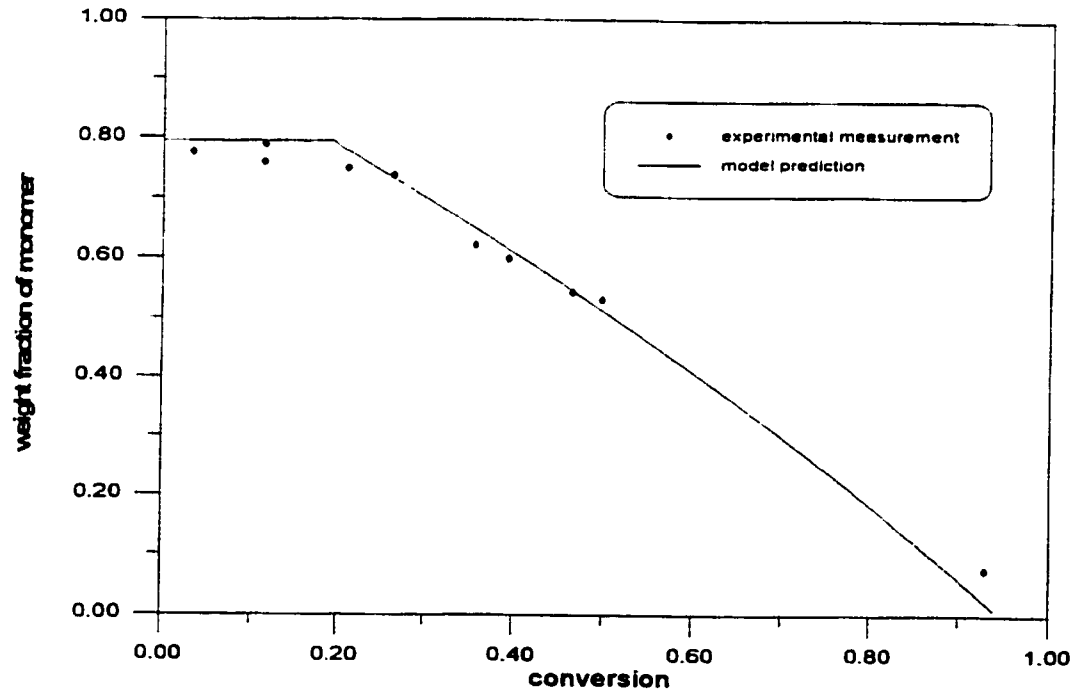

Figure 18.4 Monomer Partitioning in Vinyl Acetate Emulsion Homopolymerization at 50°C.
M: 0.5 g/ml water, SDS: 1.88 g/Lw, KPS: 1.25 g/Lw

Monomer partitioning plays an important role in emulsion polymerization. Nomura et al.(1971a) measured weight fraction of monomer in polymer particles for several runs with various amounts of initiator and emulsifier. It was found that variation of these conditions has little effect on monomer partitioning. Figure 18.4 demonstrates how vinyl acetate partitions itself among different phases. In stages I and II, the weight fraction of monomer remains nearly constant up to 20~25% conversion which marks the end of stage II, then it decreases steadily. The model prediction in figure 18.4 is given by using monomer partitioning coefficients, and the agreement is obviously very good.

Penlidis et al.(1985a)

Penlidis et al.(1985a) also investigated vinyl acetate emulsion homopolymerization and they developed a mathematical model for this monomer system. Many runs were performed under a variety of reaction conditions and recipes. Conversion was measured by either off-line gravimetry or on-line densitometry. Figures 18.5 and 18.6 show two runs performed at two levels of initiator. It is obvious that the reported conversion measurement are reliable because off-line gravimetry agrees with on-line densitometry well. In all the runs performed by Penlidis et al.(1985a), some inhibitors were left in the monomer solution in order to mimic real industrial practice. With various lengths of induction time, the model is able to deliver reliable predictions on conversion data.

Data reproducibility was very good in Penlidis' et al.(1985a) runs. This is demonstrated in figure 18.7. There are three runs conducted under the same reaction conditions, and the measured conversion points for all three runs agree with each other very well, and so does the model prediction. Figure 18.8 illustrates the temperature effect on the reaction. Three runs were carried out at similar reaction conditions but under three different temperatures. Apparently, a higher temperature results in a faster reaction rate. Furthermore, a higher temperature results in a shorter induction time. This is probably because impurities are consumed at a faster rate while more radicals are generated in the same period of time.

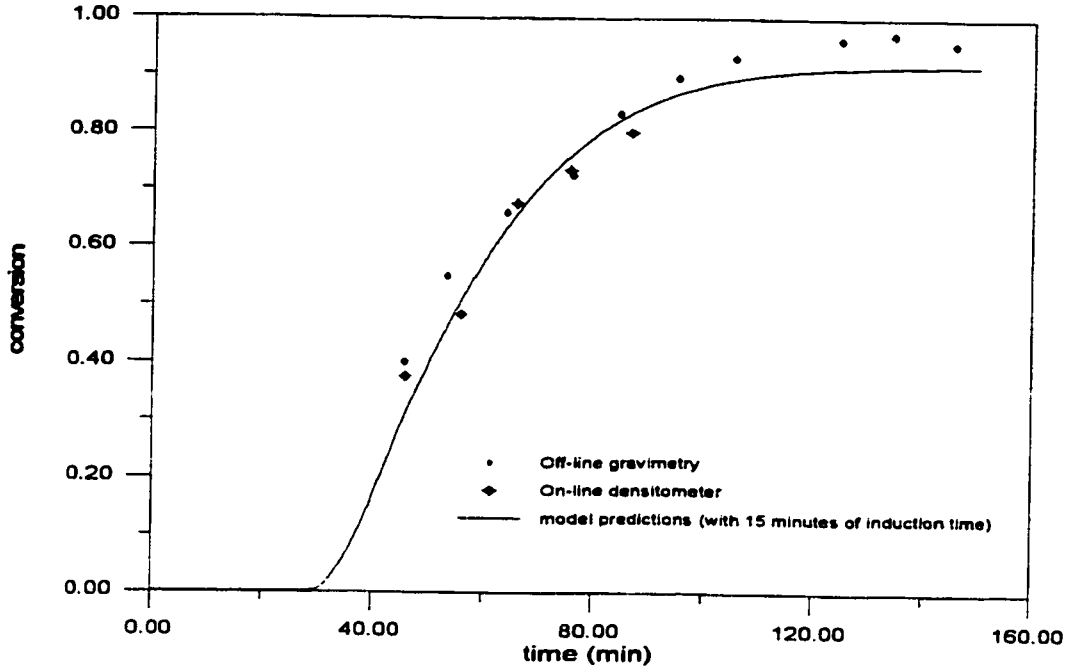

Figure 18.5 Simulation of Vinyl Acetate Emulsion Homopolymerization at 50°C. (VAc: 1.1 L, Water: 3 L, SDS: 33.6 g, KPS: 2.5 g)

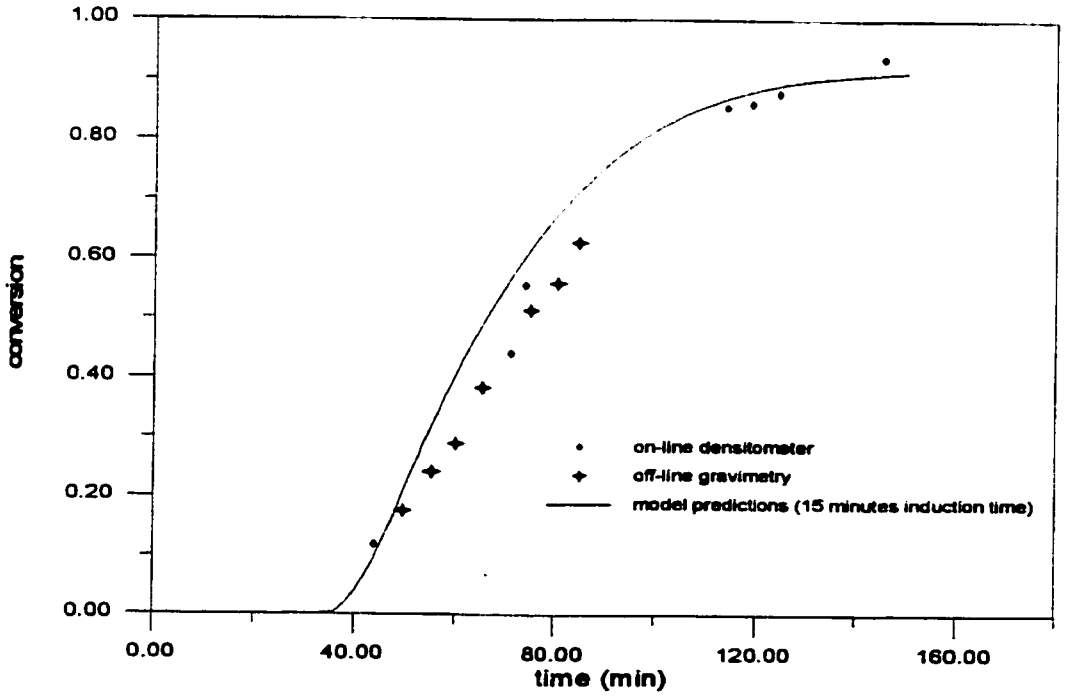

Figure 18.6 Simulation of Vinyl Acetate Emulsion Homopolymerization at 50°C. (VAc: 1.1 L, Water: 2.8 L, SDS: 33.6 g, KPS: 1.8 g)

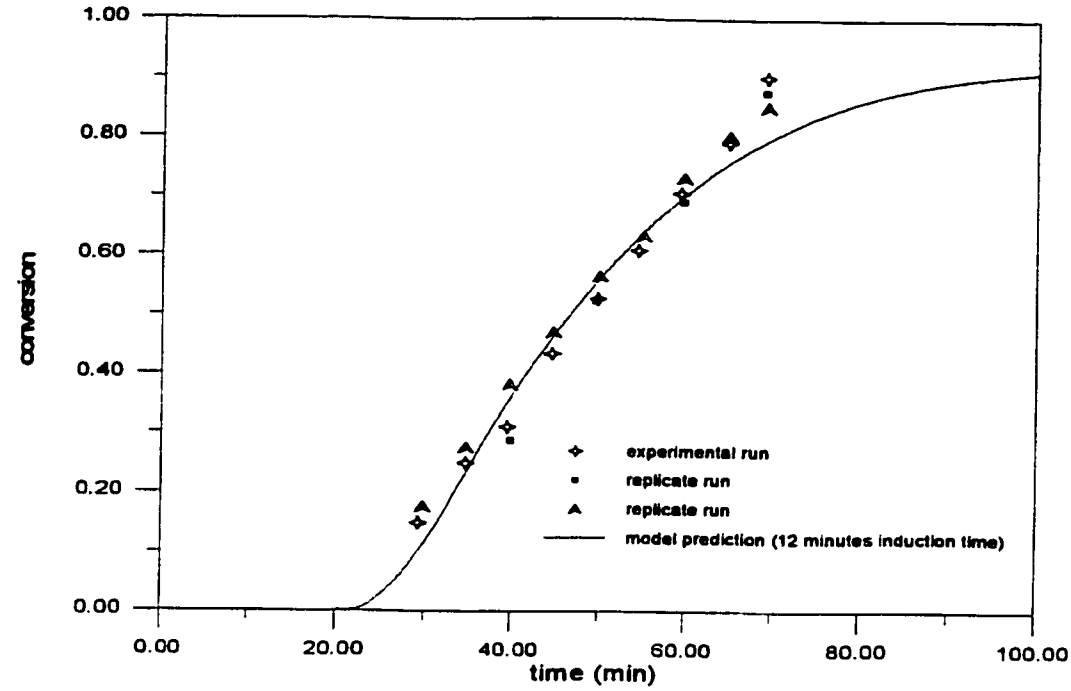

Figure 18.7 Simulation of Vinyl Acetate Emulsion Homopolymerization at 50°C. (VAc: 1.15 L, Water: 2.86 L, SDS: 28.8 g, KPS: 3 g)

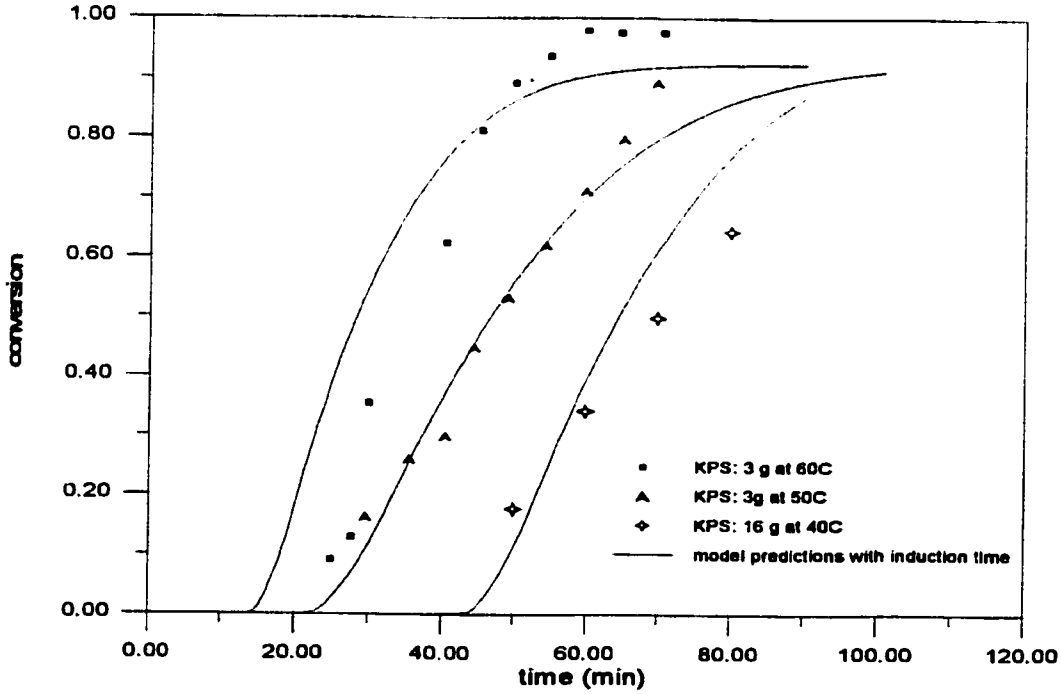

Figure 18.8 Simulation of Vinyl Acetate Emulsion Homopolymerization at Various Temperatures.
M: 1150 ml, water: 2860 ml, SDS: 28.8 g.

Penlidis et al.(1985a) also measured molecular weight data as well as particle size in their experiments. The average diameter of unswollen particles in several of their run was measured by off-line turbidity spectra and size exclusion chromatography. Results are plotted in figure 18.9. The two runs differ from each other in terms of level of emulsifier. As expected, the run with the higher amount of emulsifier generated smaller particles because the same amount of monomer is distributed among more particles, and as a consequence, the average particle size is smaller. The model prediction is in the right range with some discrepancies. The simulation results are nevertheless acceptable considering the uncertainties involved in the particle size measurement. There is usually approximately a 200 Å error involved in the measurement, therefore model predictions are within the correct range. Overall, model predictions on the trend of particle size profile are good.

Weight average molecular weights for runs at different temperatures were measured by using off-line low angle laser light scattering (LALLS) in figures 18.10 and 18.12, or LALLS-GPC in figure 18.11. All three figures reveal a trend that weight average molecular weight gradually increases as reaction proceeds. This is because at the later stages of the reaction, the desorption rate decreases and therefore $\bar{n}$ becomes larger. Clearly, the model follows such a trend well and the predictions for the weight average molecular weight are is quite satisfactory. The temperature effect on molecular weight is also evident. This is best seen in figure 18.12, whereas the weight average molecular weight for the 70°C run is lower than that of the 40°C run.

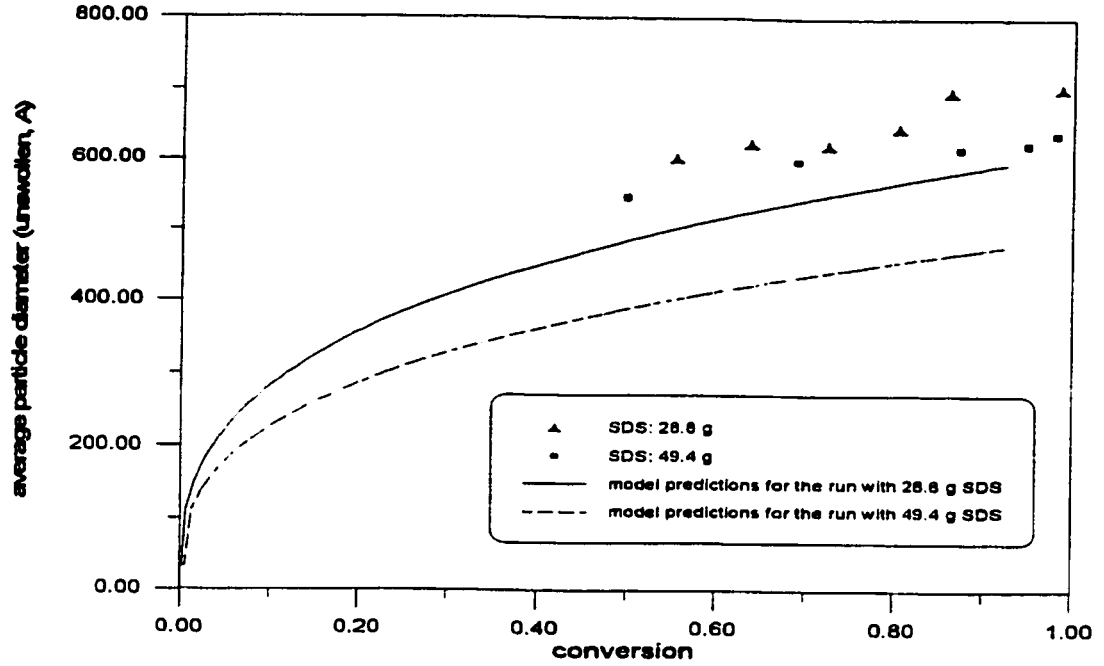

Figure 18.9 Average Unswollen Particle Diameter in Vinyl Acetate Emulsion Homopolymerization at 50°C.
M: 1150 ml, water: 2860 ml, KPS: 3 g.

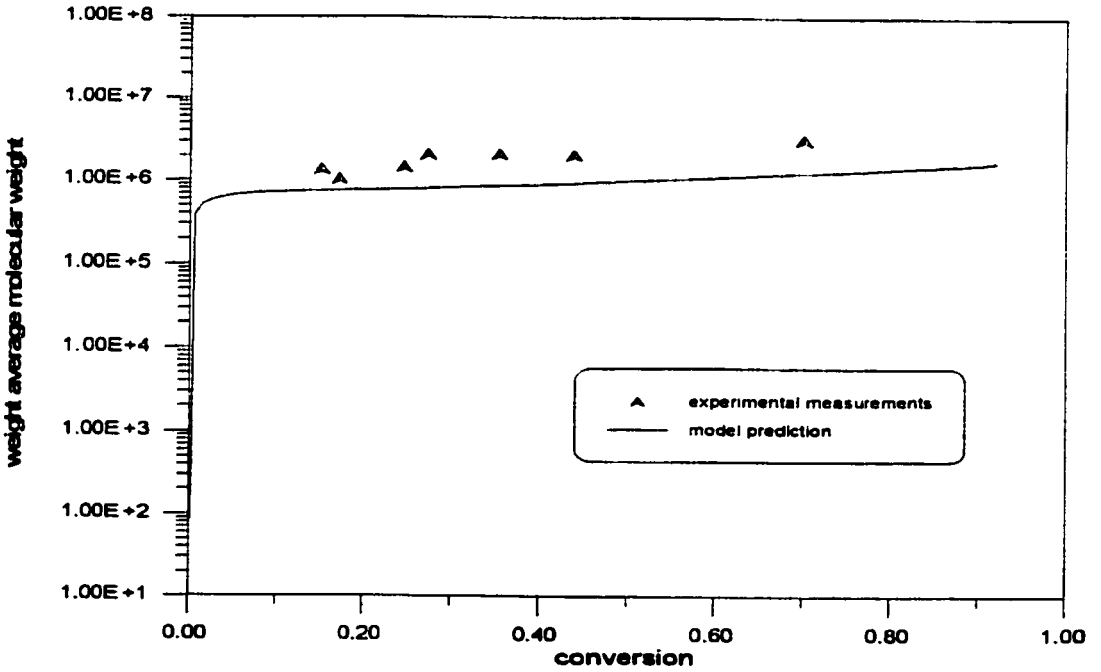

Figure 18.10 Weight Average Molecular Weight Data in Vinyl Acetate Emulsion Homopolymerization at 50°C.
M: 1150 ml, water: 2860 ml, KPS: 3g, SDS: 28.8 g

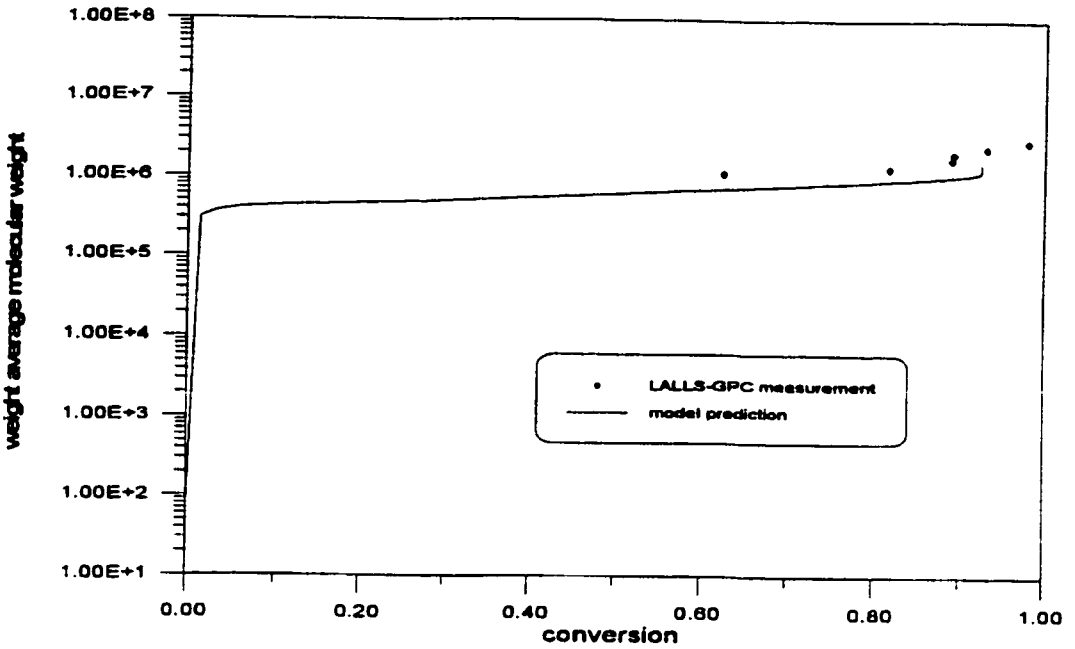

Figure 18.11 Weight Average Molecular Weight Data in Vinyl Acetate Emulsion Homopolymerization at 60°C.
M: 1150 ml, water: 2860 ml, KPS: 3 g, SDS: 28.8g.

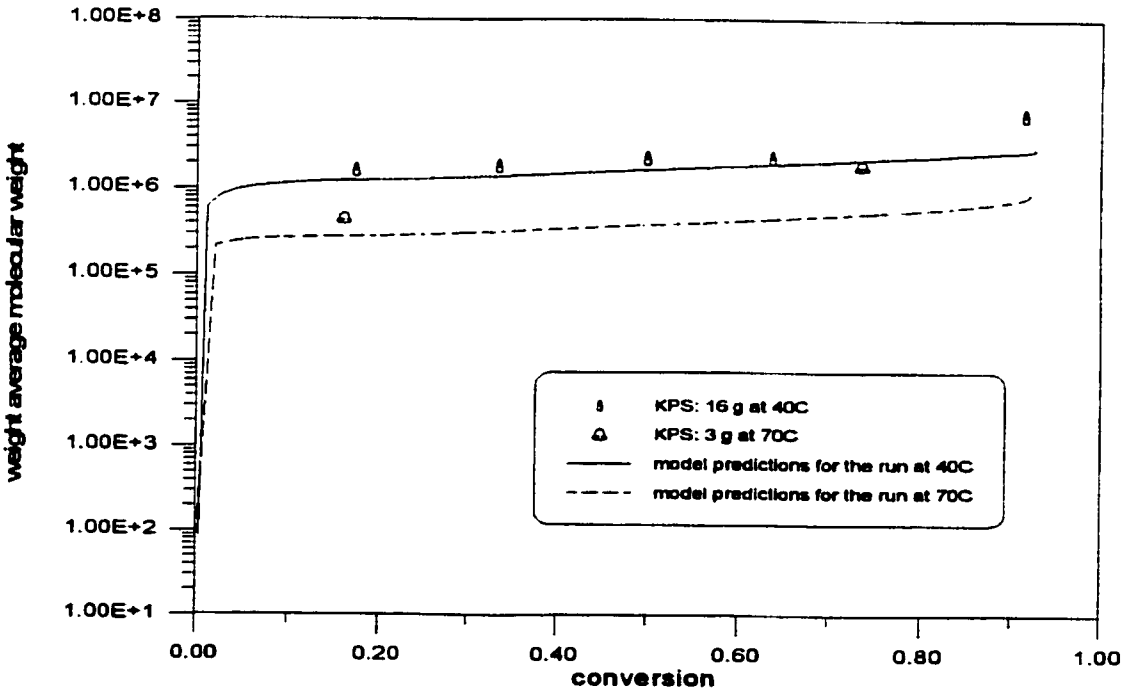

Figure 18.12 Weight Average Molecular Weight Data in Vinyl Acetate Emulsion Homopolymerization at 40 and 70°C.
M: 1150 ml, water: 2860ml, SDS: 28.8 g

Chapter 19. Simulation of Homopolymerization of Acrylic Monomers: Methyl Methacrylate, Butyl Acrylate and Ethyl Acrylate

19.1 Simulation of Methyl Methacrylate Emulsion Homopolymerization

Methyl methacrylate is characterized as a monomer with moderate water solubility, and the average number of radicals per particle is higher than 1/2. Methyl methacrylate is a classic Case III monomer. The gel effect is more pronounced in methyl methacrylate emulsion polymerization than styrene or vinyl acetate. This phenomenon was observed by a number of research groups. Zimmt (1959) performed emulsion polymerization of both styrene and methyl methacrylate. He noticed that in methyl methacrylate emulsion polymerization there was a strong acceleration in the rate of polymerization, while the same behaviour was not observed in styrene emulsion polymerization. The same characteristics were also confirmed by Friis and Hamielec (1974) and Sundberg et al.(1981). Additional evidence of the presence of strong gel effect was presented by Change et al.(1992). This group used ESR to measure the radical concentration inside the particles in both seeded and unseeded polymerizations of methyl methacrylate. In both cases, it was observed that there was a sharp increase in radical concentration at the late stages of the reaction. The average number of radicals per particle was backcalculated to be as high as 76 ~250. The shape of the radical concentration profile is nearly the same as that in bulk/solution polymerization. A strong gel effect also affects the molecular weight of polymethyl methacrylate. James Jr. and Piirma (1975) stated that weight average molecular weights increased in stage III and they attributed such an increase to autoacceleration. Though there is adequate evidence to state that methyl methacrylate emulsion polymerization exhibits a strong gel effect, the kinetic treatment of this phenomenon still needs much improvement. In the early studies, Friis and Hamielec (1974, 1976) used an empirical expression for the rate constant for termination to describe the conversion data collected in their experiments. Ballard et al.(1984, 1986a) also used an empirical expression for k_t in their studies. Nomura and Fujita (1994) stated that k_t was constant through stages I and II, and then it started to decrease. Sundberg et al.(1981) was the group that attempted to model the rate constant for termination from a theoretical basis. The free-volume theory was used to interpret the change of k_t in their experiments.

It is important to know that the starting value of k_t is many orders of magnitude smaller than its value in bulk/solution polymerization due to highly viscous particle media. This characteristic has been verified by a number of groups (Zimmt 1959; Gardon 1968d; Ballard et al. 1984, 1986a; Nomura and Fujita 1994). Many authors also used various methods to estimate values of k_t as well as the rate constant for propagation k_p, and their estimates are summarized in Table 19.1.

Table 19.1 Rate Constant for Termination and Propagation (MMA)

Temperature	40 °C	50 °C	60 °C
k_t (L/mol·s)		6000[a]	
		19000[b]	
		90000[c]	
		7000[f]	
k_p	171[c]	340[c]	500[c]
		790[c]	
		441[a]	650[d]
	450[f]	560[f]	684[f]

a: Ley et al.(1969)

b: Sundberg et al.(1981)

c: Soh (1980)

d: Nomura and Fujita (1994)

e: Ballard et al.(1986a, b)

f: value used by this model

Among the groups listed, work from Ballard et al.(1984, 1986a, b) is worth mentioning. The k_t value they estimated is much higher than most other groups. What they estimated was the "apparent" k_t which also includes the contribution from reaction diffusion controlled termination (approximately, 0.3×10^5). It must be stated here that reaction diffusion controlled termination plays an even more important role in emulsion polymerization than in bulk/solution polymerization. The reason for this

is simply that reaction mixture in polymer particles is very viscous even at the beginning of the reaction. This group also gave an empirical expression for k_p which is:

$$k_p = k_p^o \exp[-29.8(w_p - 0.84)] \tag{19.1}$$

Expression 19.1 is used when the weight fraction of polymer w_p exceeds 84%. In a very similar fashion, Nomura and Fujita (1994) presented the following two expression for k_t and k_p:

$$k_t = 8.5\times10^{-15}\exp(-12.3w_p) \tag{19.2}$$

$$k_p = 1.33\times10^{7}\exp(-13.6w_p) \tag{19.3}$$

w_p in the above expression is the weight fraction of polymer in the particles. Expression 19.3 is used only when $w_p > 73\%$. Before 73% conversion, k_p is set to be 650 L/mol·s.

Additional literature papers with regard to methyl methacrylate emulsion polymerization are also collected to gather kinetic information. Table 19.2 gives a list of papers that provide useful kinetic information or experimental data for model testing.

Table 19.2 Literature References on MMA Emulsion Polymerization

Authors	Remarks
Barton et al.(1992)*	seeded emulsion polymerization of methyl methacrylate
Ballard et al.(1984)	review on MMA emulsion polymerization, modelling
Ballard et al.(1986a)	measurement of rate constant for termination
Ballard et al.(1986b)	measurement of rate constant for propagation
Barton (1990)	MMA emulsion polymerization with oil soluble initiator: AIBN
Canegallo et al.(1993)*	online measurement of conversion using densitometry
Chang et al.(1992)	measurement of radical concentration in MMA emulsion seeded polymerization
Dube (1994)*	MMA emulsion homopolymerization
Fontenot and Schork (1993)*	MMA batch polymerization in mini/macroemulsions
Fontenot and Schork (1992/93a, b)*	MMA batch polymerization in mini/macroemulsions, mathematical modelling
Friis and Hamielec (1974)	studies on termination in MMA emulsion polymerization
Gardon (1968d)*	experimental data
James Jr. and Piirma (1975)	molecular weight development
Ley et al.(1969)	half life of propagating radicals in MMA emulsion polymerization
Louie et al.(1985)	effect of oxygen in MMA emulsion polymerization, modelling
Nomura and Fujita (1994)*	many experiments for MMA emulsion polymerization under a wide range of reaction conditions, simplified model developed
Schork and Ray (1987)	multiple steady-state studies in MMA continuous emulsion polymerization
Schork and Ray (1981)*	online densitometry in MMA emulsion polymerization
Soh (1980)	measurement of rate constant for propagation
Sundberg et al.(1981)	studies on diffusion controlled kinetics, experimental data
Tanrisever et al.(1996)	emulsifier-free MMA emulsion polymerization
Wang and Chu (1990)	reaction with mixed emulsifiers
Zimmt (1959)	experimental data on conversion and particle size

* Data used for model testing

19.1.1 Model Testing Results

Barton et al.(1992)

Barton et al.(1992) conducted experiments of seeded emulsion polymerization of methyl methacrylate. Polybutyl acrylate latex seed was prepared in batch emulsion polymerization at 60°C. The final conversion was measured as 95.6%. The average hydrodynamic diameter of the seed particles was measured as 170 nm, and the number of particle seeds was thus backcalculated as $1.09 \cdot 10^{17}$ per liter of polymer latex. Four polymerization runs were performed using various recipes. In two runs, retarder 2,2,6,6,-tetramethyl-4-octadecanoyloxypiperidinyl-1-oxyl (STMPO) was added to investigate its effect on reaction kinetics. It was observed that the presence of STMPO significantly suppressed the reaction. Table 19.3 gives the recipes used for all their runs.

Table 19.3 Recipes of seeded emulsion polymerization of MMA

Run No.	PBA latex (ml)	MMA (ml)	water (ml)	STMPO
1	50	10	20	not added
2	20	20	40	not added
3	50	10	20	yes
4	20	20	40	yes

Run 2 was simulated using the reported reaction conditions and recipe. Figure 19.1 displays the simulated conversion profile. It is noted that in run 2, the ratio of MMA to PBA solid in the initial charge is 3.16, and this implies an initial conversion of 25%. However, this is in contradiction to what is shown in figure 19.1, where the two conversion measurements at the early stages of the run are well below 20%. No reasonable explanation was given by Barton et al.(1992). Model predictions at higher conversion levels agree reasonable well with reported data. Figure 19.2 displays the change of the size of polymer particles. The model predicted that the initial particle diameter was at 160 nm and it gradually increased to the 230 nm level at which the limiting conversion occurred. Model predictions are in a very close range to what was reported by Barton et al.(1992).

Runs 3 and 4 are not simulated due to the lack of kinetic information of STMPO. Simulation of run

1 was impossible due to several factors. First, the initial MMA/PBA ratio in the charge is 0.632 which corresponds to an initial conversion level of about 62%. Apparently this not what was reported by Barton et al.(1992). Secondly, there was very little monomer added in this run and it was reported there were no monomer droplets formed. Such low level of monomer charge and the absence of monomer droplets may ultimately change MMA partitioning characteristics.

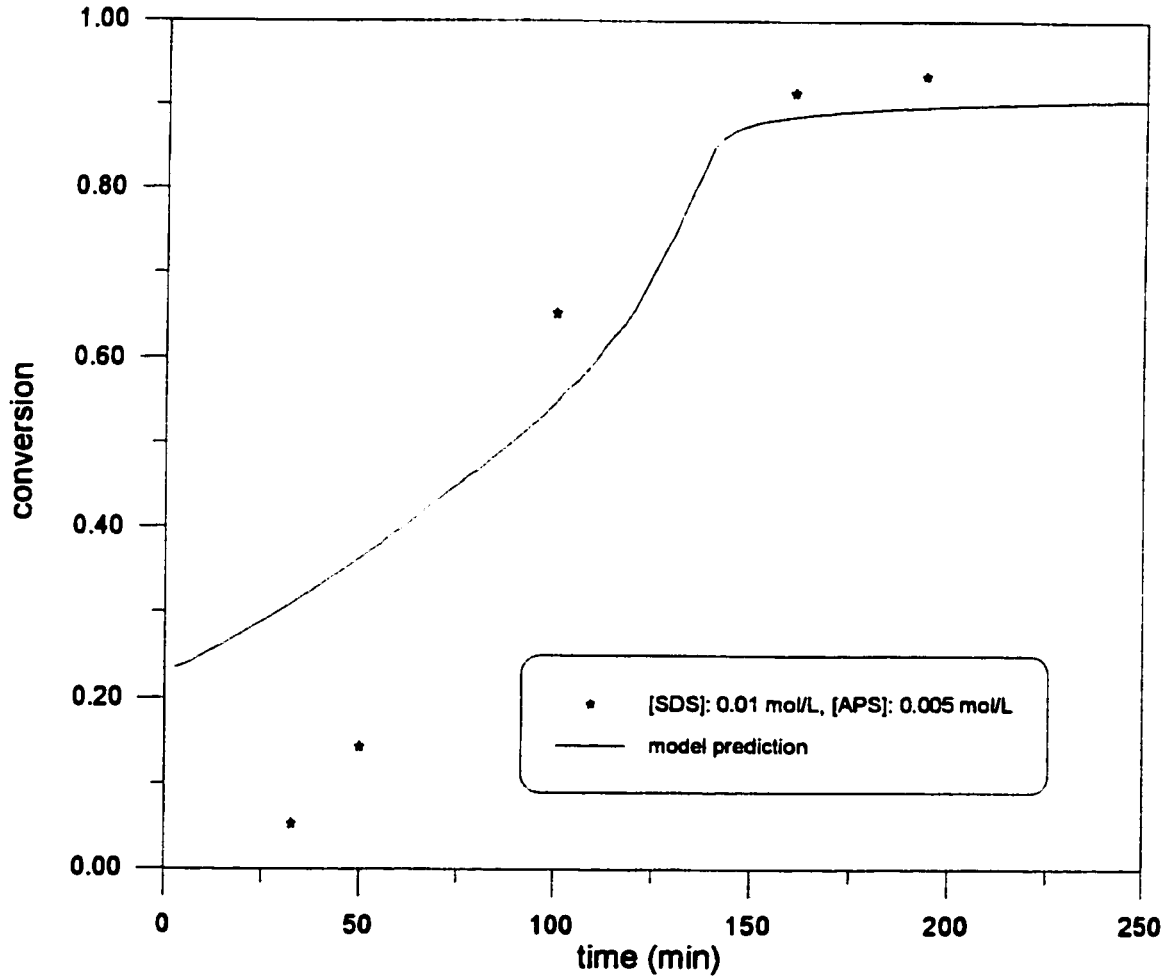

Figure 19.1 Simulation of Seeded Methyl Methacrylate Homopolymerization in Emulsion at 60C.
(0.294 gr polybutyl acrylate seed per ml latex, Np: 1.09E17 /L latex, initial seed diameter 170nm, final conversion in the seed: 95.6%, seed: 20 ml, MMA: 20 ml, water: 40 ml)

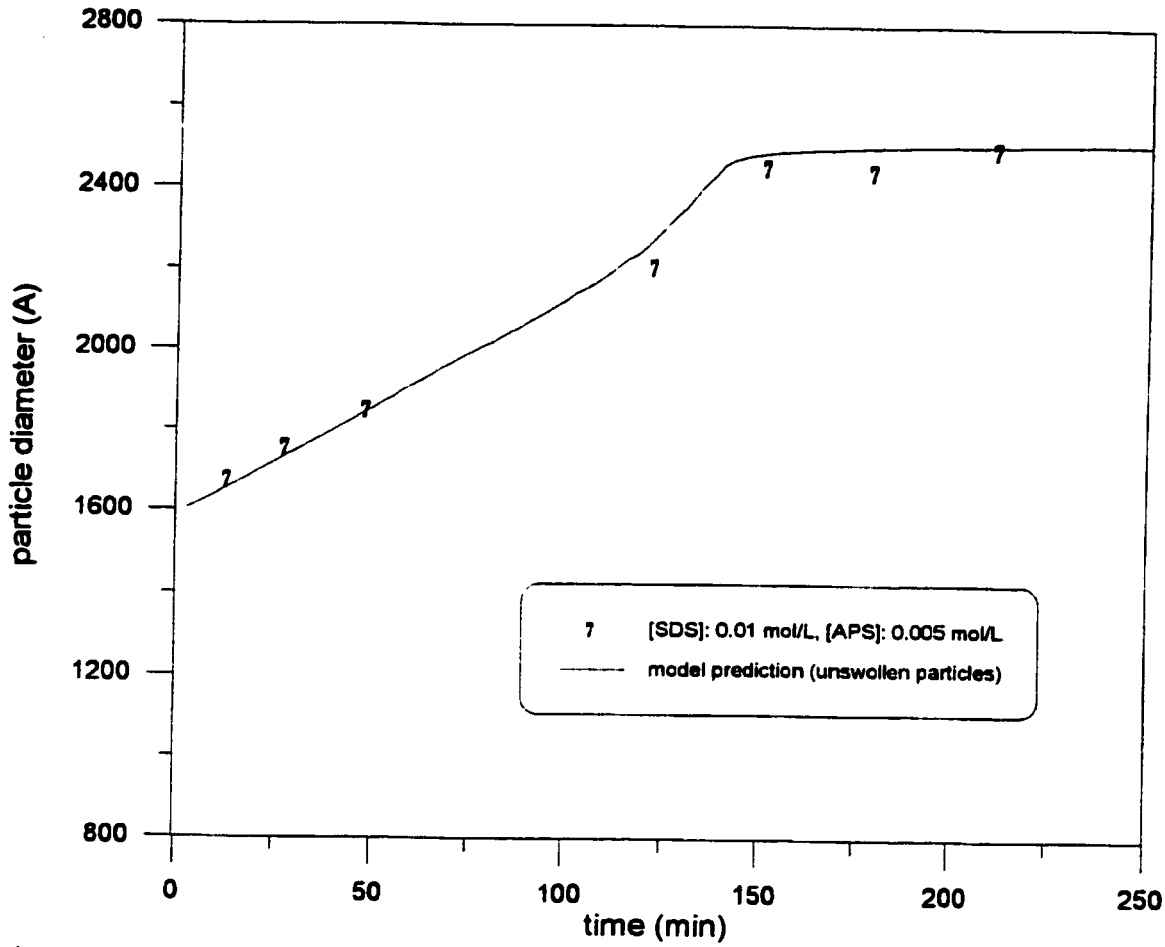

Figure 19.2 Simulation of Particle Size in Seeded Methyl Methacrylate Homopolymerization in Emulsion at 60C.
(0.294 gr polybutyl acrylate seed per ml latex, Np: 1.09E17 /L latex, initial seed diameter 170nm, final conversion in the seeds: 95.6%, seed: 20 ml, MMA: 20 ml, water: 40 ml)

Canegallo et al.(1993)

Canegallo et al.(1993) used calorimetry to measure online conversion data for several runs of methyl methacrylate at 50°C. The reported conversion profiles as well as model predictions are presented in figure 19.3. The shapes of the conversion curves resemble those observed in bulk/solution runs of the same monomer. Autoacceleration is present in all three runs and so is the limiting conversion. The current model describes all these kinetic characteristics very well.

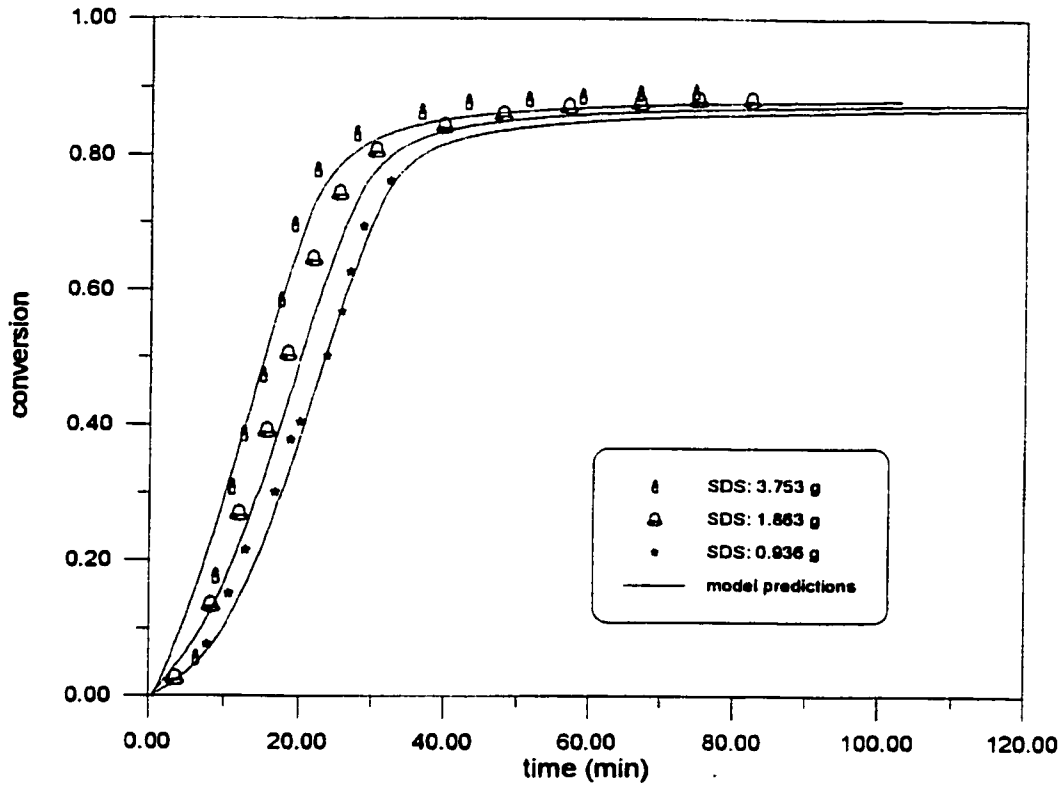

Figure 19.3 Simulation of Methyl Methacrylate Emulsion Homopolymerization at 50 °C Using Calorimetry.

Dube (1994)

Dube (1994) conducted one experiment of methyl methacrylate emulsion homopolymerization at 60 °C using mixed emulsifiers of AMA-80 and AOT-75. Conversion was determined by gravimetry. He also measured particle size as well as molecular weight. The simulation of conversion data is shown in figure 19.4. Model predictions can follow the conversion data very well up to 40%, at which point model predictions gradually lag behind the actual conversion measurements. Disagreement also exists in the final conversion. The model predicts a limiting conversion of about 90% while almost full conversion was determined in Dube's run. The observed discrepancies are suspected to be caused by nonisothermality. As emphasized before, this monomer system is characterized by a strong gel effect, and the polymerization is highly exothermic. It is still possible that at the peak of the reaction, there might be some heat accumulation. The possible nonisothermal polymerization may also be used to explain the observed full conversion. Theoretically speaking, there should be a limiting conversion in this experiment as the model predicts, because the reaction temperature is below the Tg of polymethacrylate methacrylate. Higher temperatures at the end of the reaction would surely result in a higher final conversion level. Another possible cause of the discrepancies at higher conversion levels is of course experimental anomalies during gravimetry, which was suspected in Dube (1994) for this specific run.

Figure 19.5 is the unswollen particle size for the run simulated. Figures 19.6 and 19.7 show experimental as well as simulation results for the number of particles and molecular weight averages. In all cases, the model gives satisfactory predictions. It can be said that all the important features for methyl methacrylate emulsion homopolymerization are adequately described by this model.

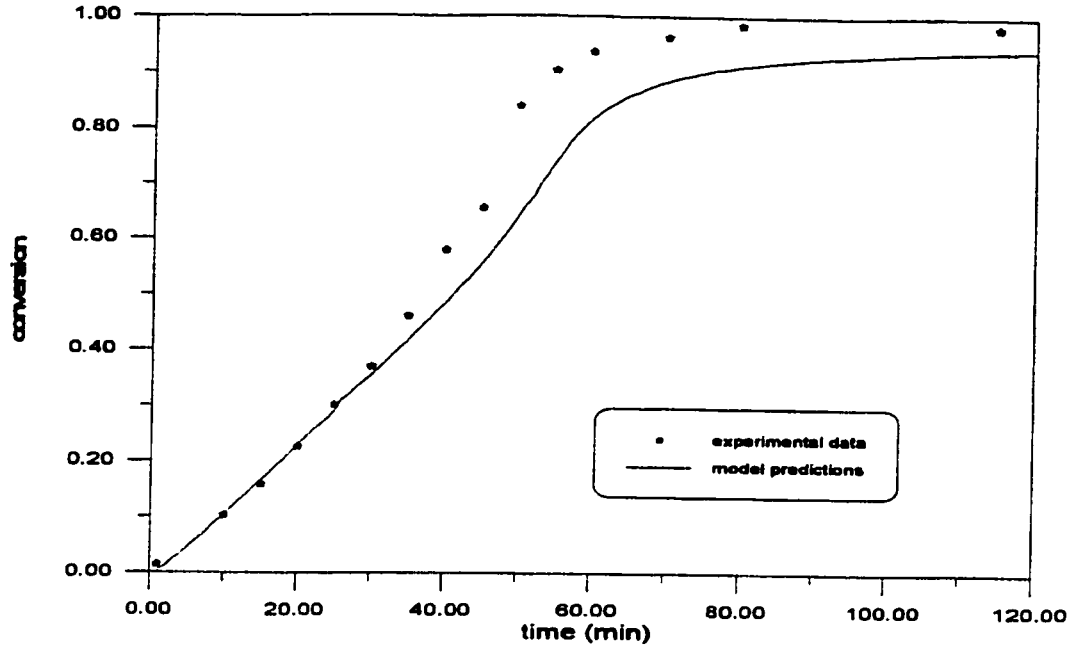

Figure 19.4 Simulation of Methyl Methacrylate Emulsion Homopolymerization at 60 °C.
(MMA: 1.5 kg, Water: 2.401 kg, APS: 1.0506g, AMA-80: 7.496g, AOT-75: 8.325g)

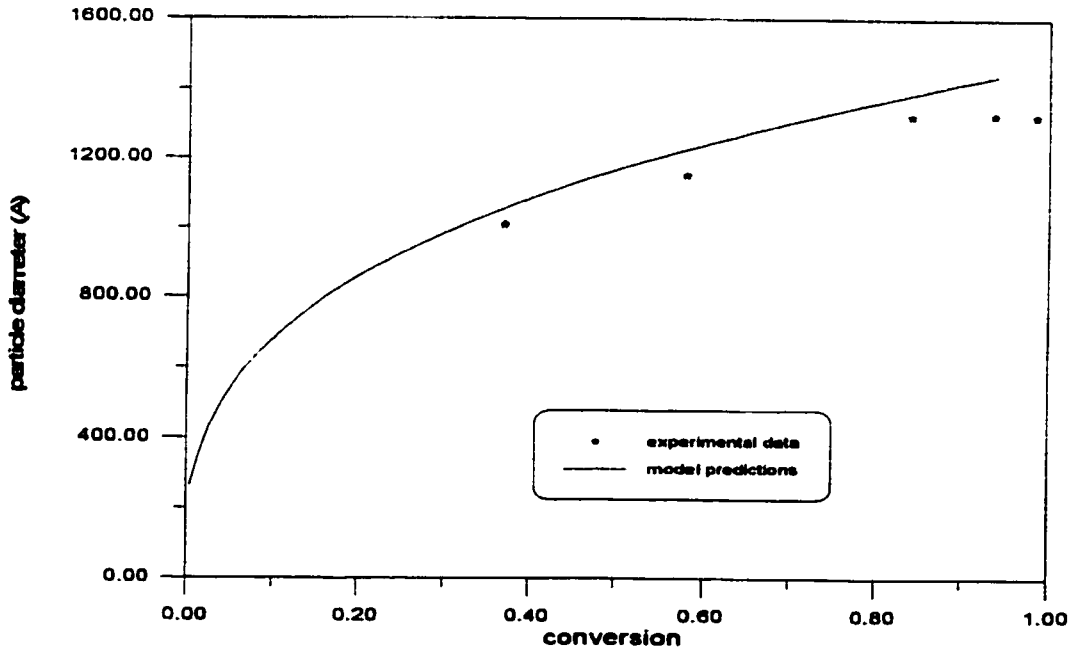

Figure 19.5 Simulation of Particle Size for Methyl Methacrylate Emulsion Homopolymerization at 60 °C.
(MMA: 1.5 kg, Water: 2.401 kg, APS: 1.0506g, AMA-80: 7.496g, AOT-75: 8.325g)

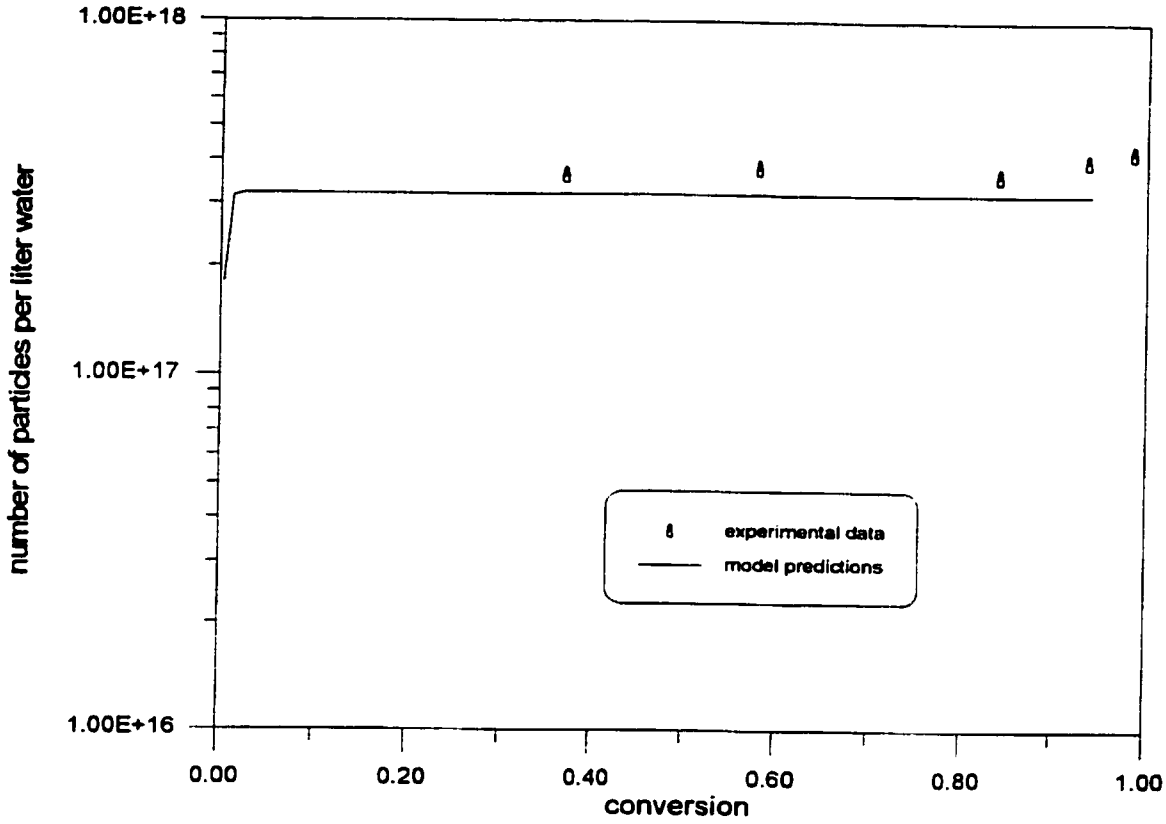

Figure 19.6 Simulation of Number of Particles in Methyl Methacrylate Emulsion Homopolymerization at 60°C.
(MMA: 1.5 kg, water:2.401 kg, APS: 1.0506 g, AMA-80: 7.496 g, AOT-75: 8.325)

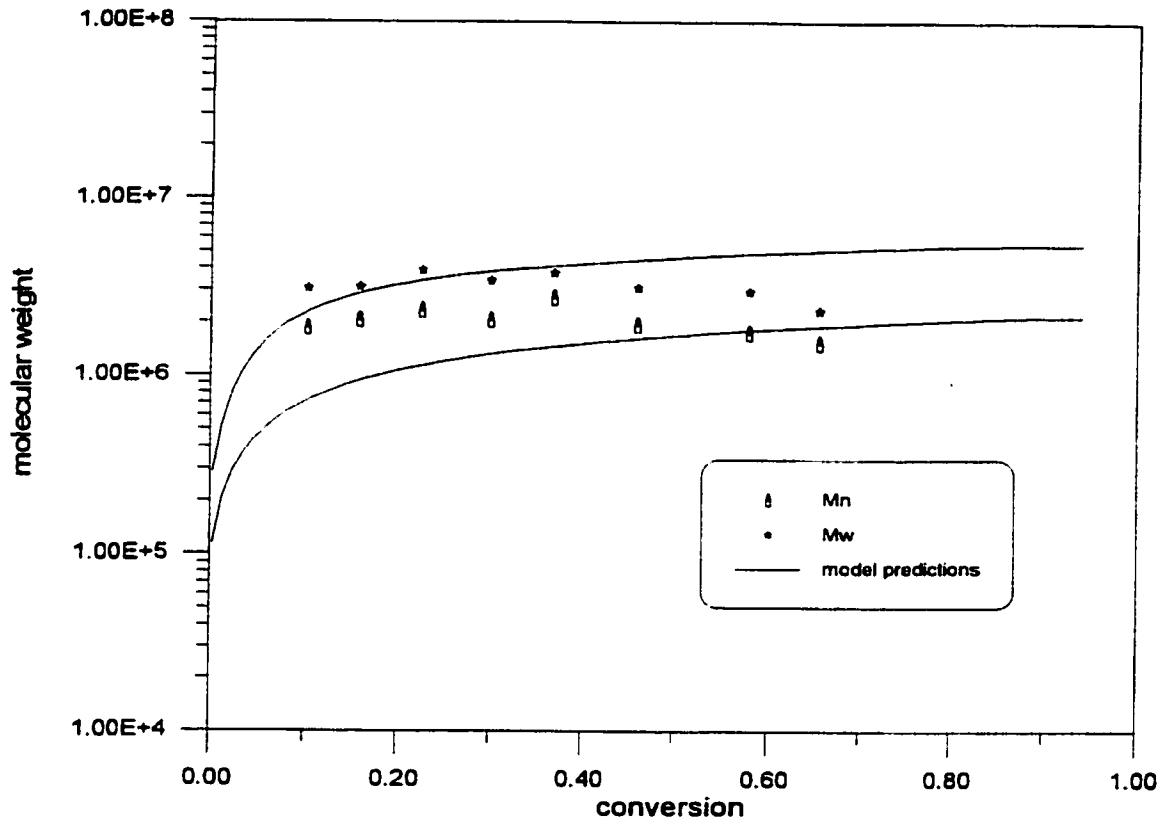

Figure 19.7 Simulation of Molecular Weight in Methyl Methacrylate Emulsion Homopolymerization at 60 °C.
(MMA: 1.5 kg, Water: 2.401 kg, APS: 1.0506g, AMA-80: 7.496g, AOT-75: 8.325g)

Fontenot and Schork (1992/1993a,b)

Fontenot and Schork (1992/1993a, b) is the first group that presented a mathematical model that can simulate both conventional emulsion as well as miniemulsion polymerization. In miniemulsion, monomer droplets are stabilized through the use of cosurfactants or stabilizers like long chain fatty alcohols or alkanes. Monomer droplets are typically much smaller than those in conventional emulsion polymerization. Fontenot and Schork (1992/1993a, b) conducted several conventional and miniemulsion polymerizations to study the effect of initiator and emulsifier on the reaction kinetics. Their work provides a good source of data for model testing. Figures 19.8~19.14 summarize model testing results using this group's data.

Figure 19.8 shows the effect of initiator on the rate of polymerization. In these three runs, the concentration of KPS ranges from 0.002~0.02 mol/Lw. Figures 19.9~19.12 show the effect of emulsifier on the rate of polymerization. A number of runs were carried out with a fixed amount of KPS at various emulsifier levels ranging from 0.0093 to 0.1 mol/Lw. For the run with 0.02 mol/Lw of SDS, Fontenot and Schork (1992/1993a) also measured the final particle diameter. Their reported diameter was in the range of 1000-1200 Å, which is very close to what our model predicted (see figure 19.13). For all the experiments tested, simulation results are in good agreement with actual experimental measurements regardless of the concentration level of emulsifier or initiator used in the recipe. This verifies our model's reliability once more.

The temperature effect on the rate of polymerization is best seen in figure 19.14. Three experiments were conducted at 40, 60 and 70°C. Model predictions are good for the 60 and 70 °C runs, but discrepancies exist for the 40 °C. As often observed in many other examples, impurity effects are suspected at low temperature levels. An additional 25 minutes of induction was used in the simulation. However, the measured conversion data still lag behind model predictions, which indicates the retardation effect of impurities.

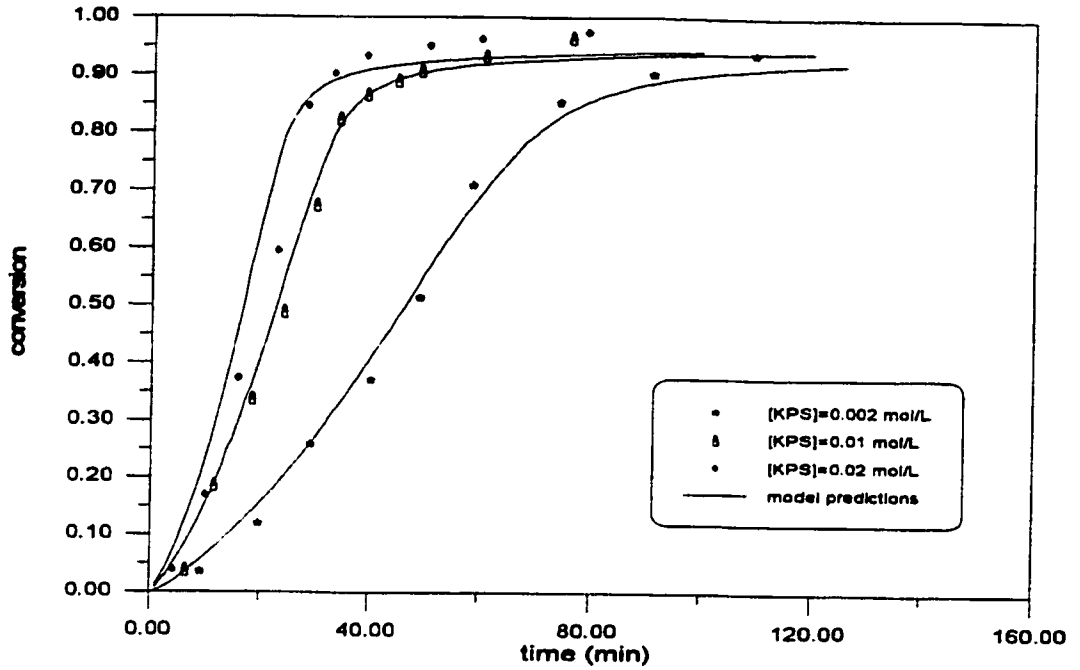

Figure 19.8 Simulation of Conversion in Methyl Methacrylate Emulsion Homopolymerization at 50 °C.
(MMA: 300 g, Water: 700 g, SDS: 0.02 mol/Lw)

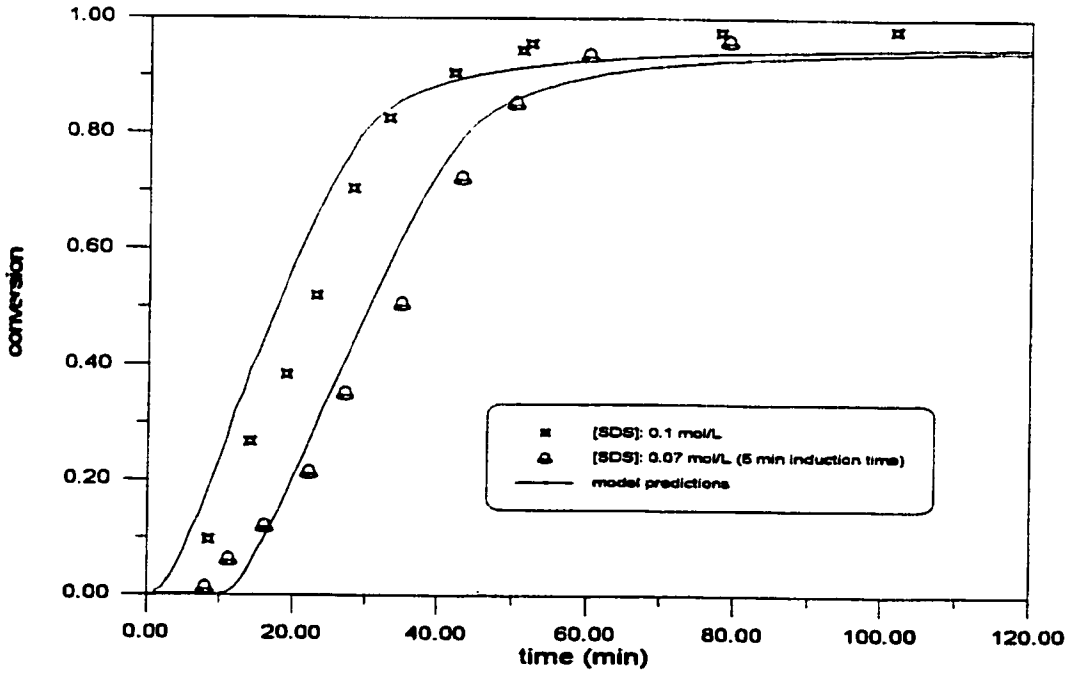

Figure 19.9 Simulation of Conversion in Methyl Methacrylate Emulsion Homopolymerization at 50 °C.
(MMA: 300 g, Water: 700 g, KPS: 0.005 mol/Lw)

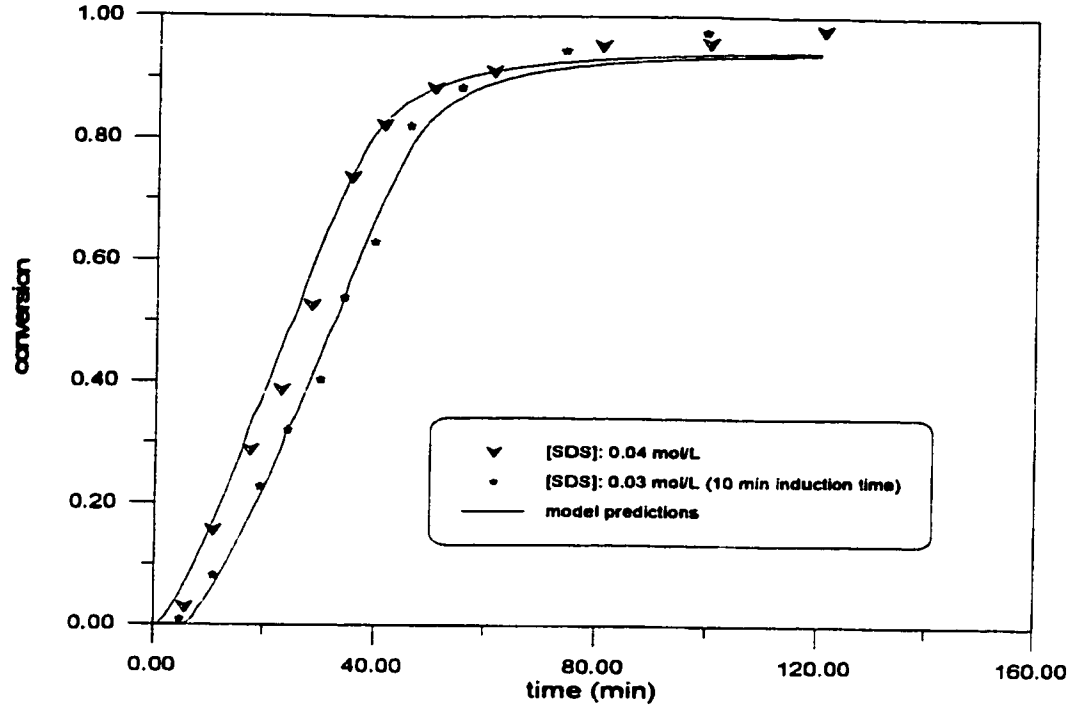

Figure 19.10 Simulation of Conversion in Methyl Methacrylate Emulsion Homopolymerization at 50 °C.
(MMA: 300 g, Water: 700 g, KPS: 0.005 mol/Lw)

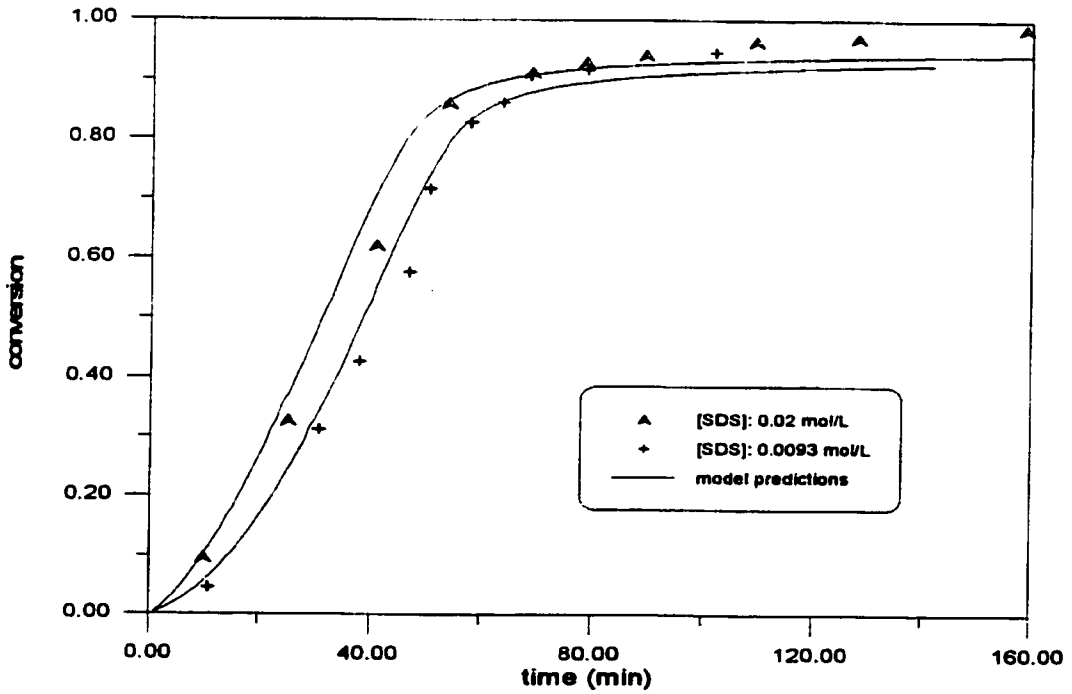

Figure 19.11 Simulation of Conversion in Methyl Methacrylate Emulsion Homopolymerization at 50 °C.
(MMA: 300 g, Water: 700 g, KPS: 0.005 mol/Lw)

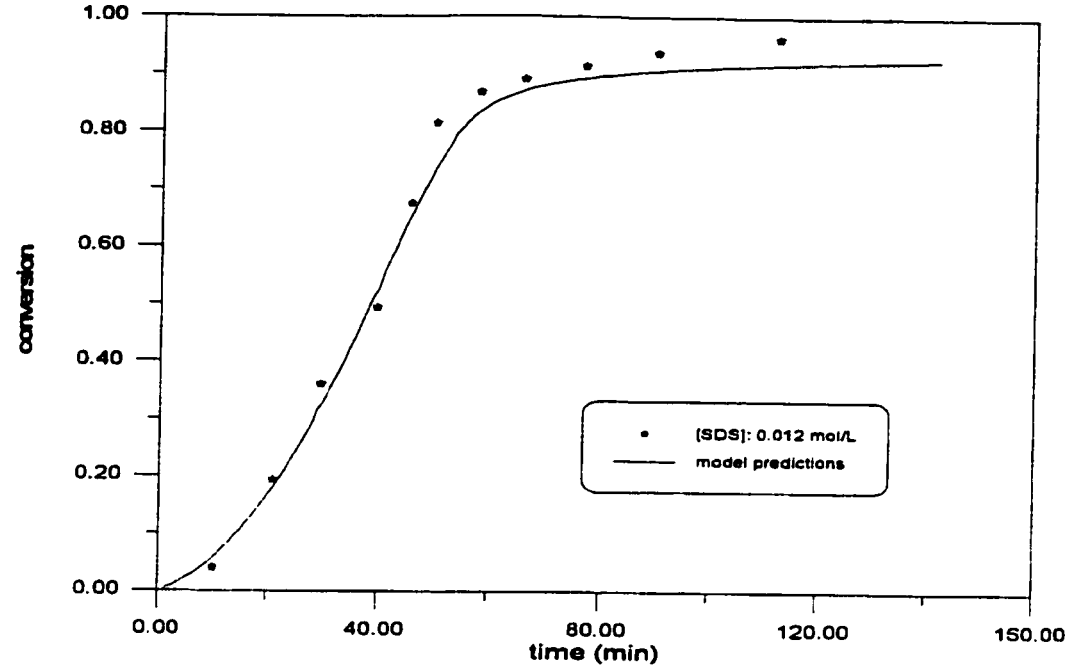

Figure 19.12 Simulation of Conversion in Methyl Methacrylate Emulsion Homopolymerization at 50 °C.
(MMA: 300 g, Water: 700 g, KPS: 0.005 mol/Lw)

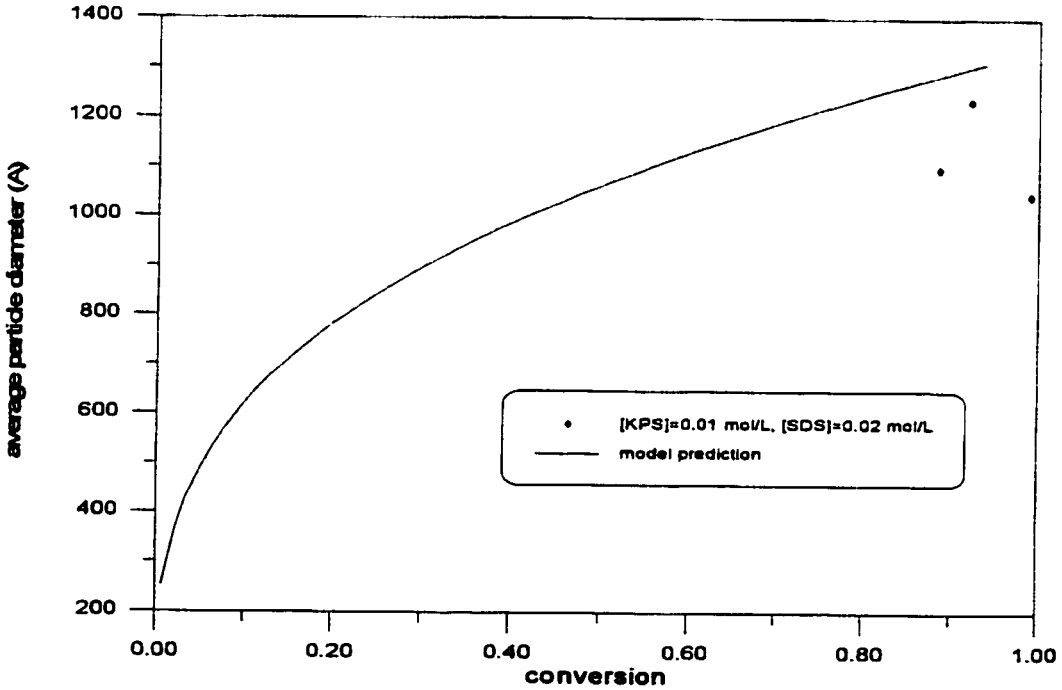

Figure 19.13 Simulation of Particle Size in Methyl Methacrylate Emulsion Homopolymerization at 50 °C. (MMA: 300 g, Water: 700 g)

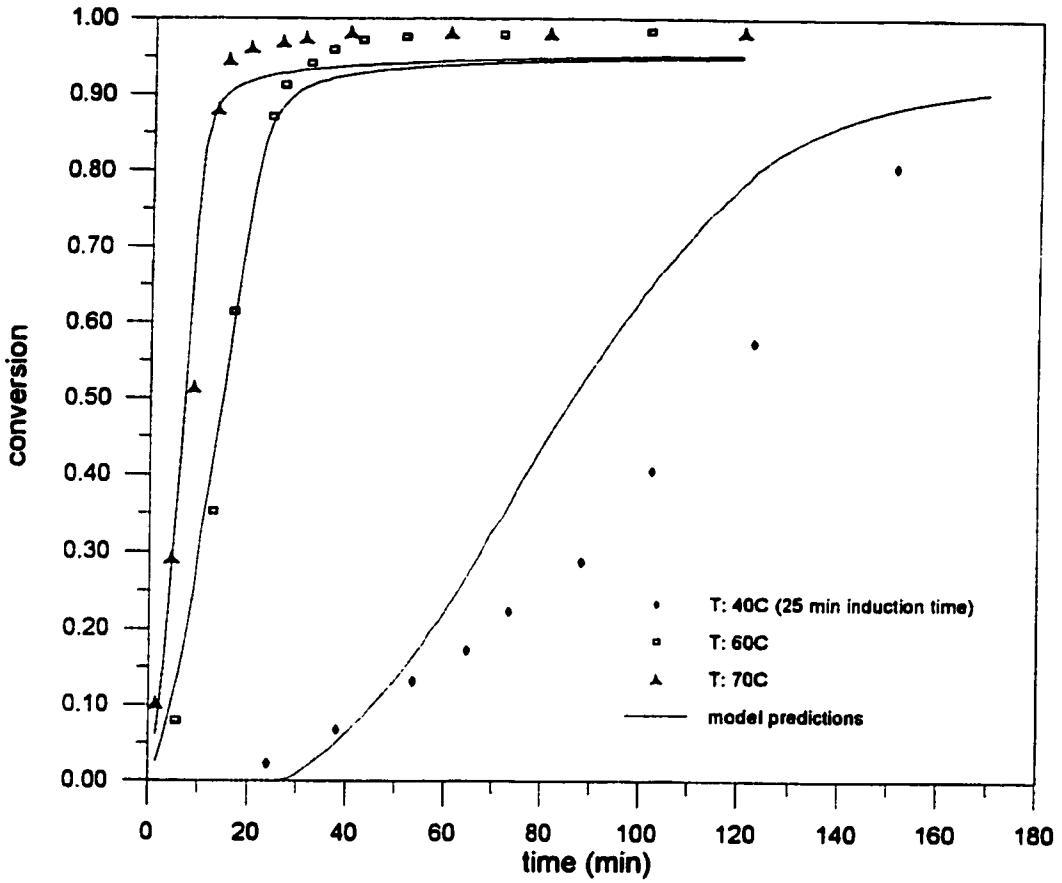

Figure 19.14 Simulation of Conversion in Methyl Methacrylate Emulsion Homopolymerization.
(MMA: 300 g, Water: 700 g, KPS: 0.005 mol/Lw: SDS: 0.02 mol/Lw)

Fontenot and Schork (1993)

Fontenot and Schork (1993) later conducted more experiments under a slightly modified recipe (different monomer to water ratio). Measured conversion data are presented in figures 19.15 and 19.16. The conversion curves displayed in figures 19.15 and 19.16 have the same shape as those experiments shown in figures 19.9~19.12 and 19.14. This implies that the amount of monomer does not affect the kinetics of polymerization.

They authors also reported published the number of particles for their runs. Instead of directly measuring the number of particles, they backcalculated the number of particle per liter of water using measured particle diameter results. Particle diameter was measured by using transmission electron microscopy. Model predicted numbers of particles for the three runs are plotted in figure 19.17 along with the values from Fontenot and Schork (1993). The agreement is satisfactory.

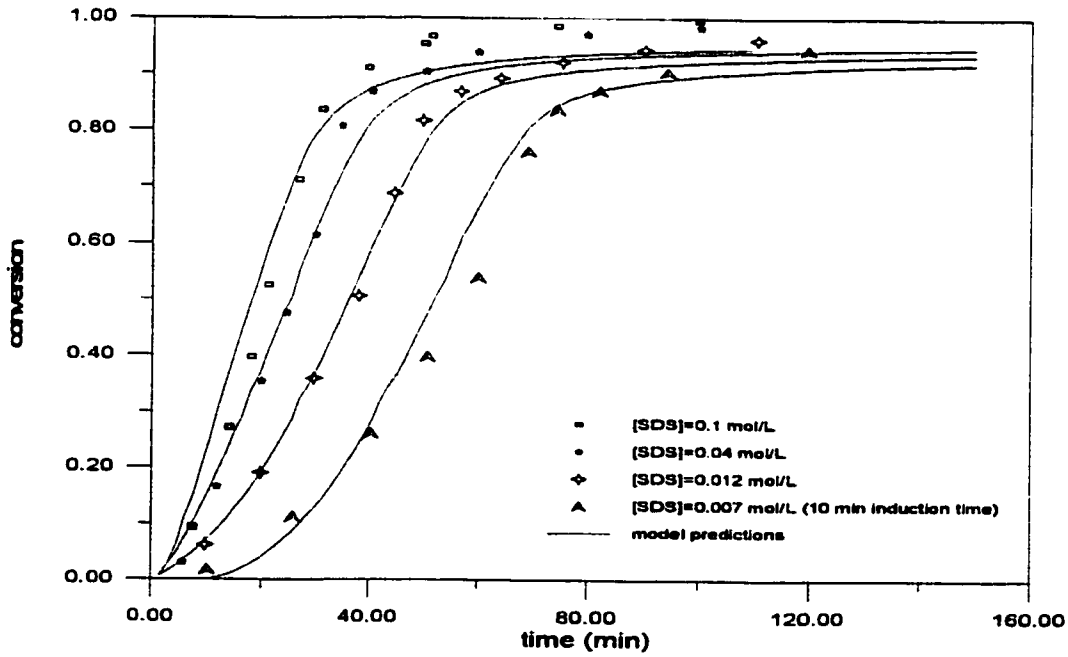

Figure 19.15 Simulation of Conversion in Methyl Methacrylate Emulsion Homopolymerization at 50 °C.
MMA: 220 g, water: 510 g, KPS: 0.005 mol/L.

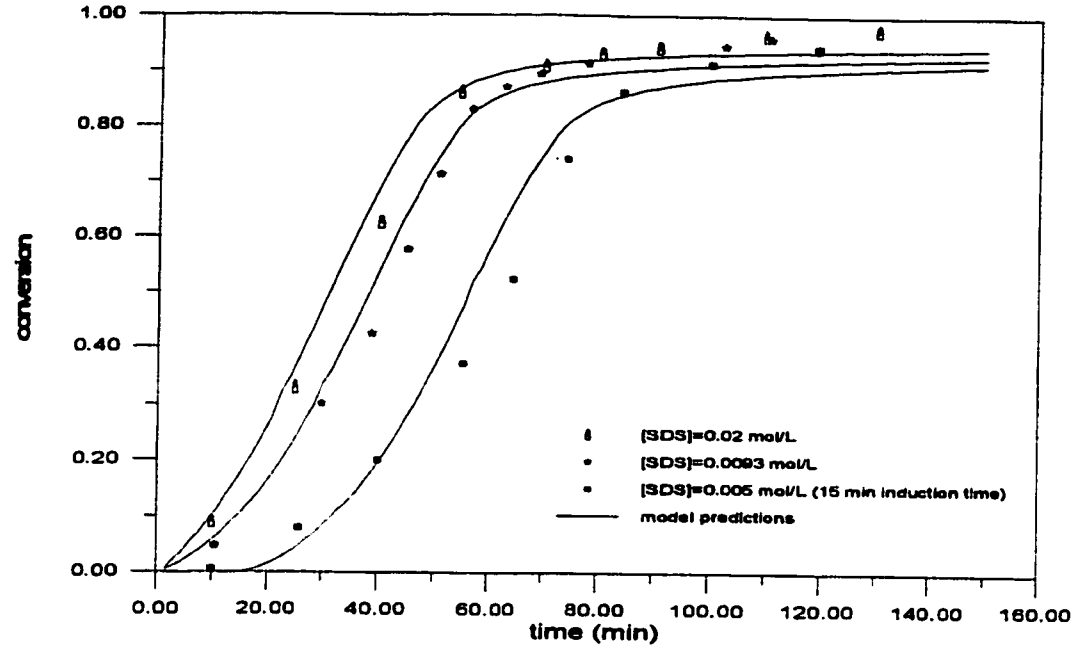

Figure 19.16 Simulation of Conversion in Methyl Methacrylate Emulsion Homopolymerization at 50 °C.
MMA: 220 g, water: 510 g, KPS: 0.005 mol/L.

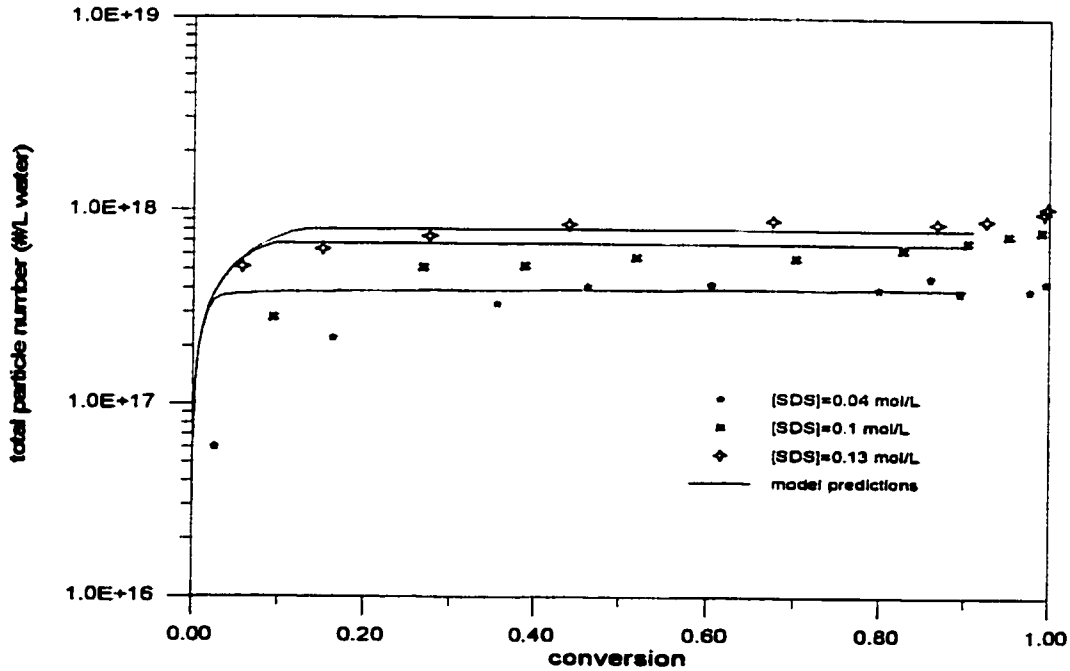

Figure 19.17 Number of Particles in Methyl Methacrylate Emulsion Homopolymerization at 50 °C.
MMA: 220 g, water: 510 g, KPS: 0.005 mol/L.

Gardon (1968d)

Gardon (1968d) carried out full conversion range experiments for a number of monomers including methyl methacrylate. He noticed that the ratio of k_t/k_p was low, and he stated that this would be the result of high viscosity within the particles. Gardon (1968d) performed one run of methyl methacrylate emulsion polymerization at 55°C. Model testing results for this run are displayed in figure 19.18.

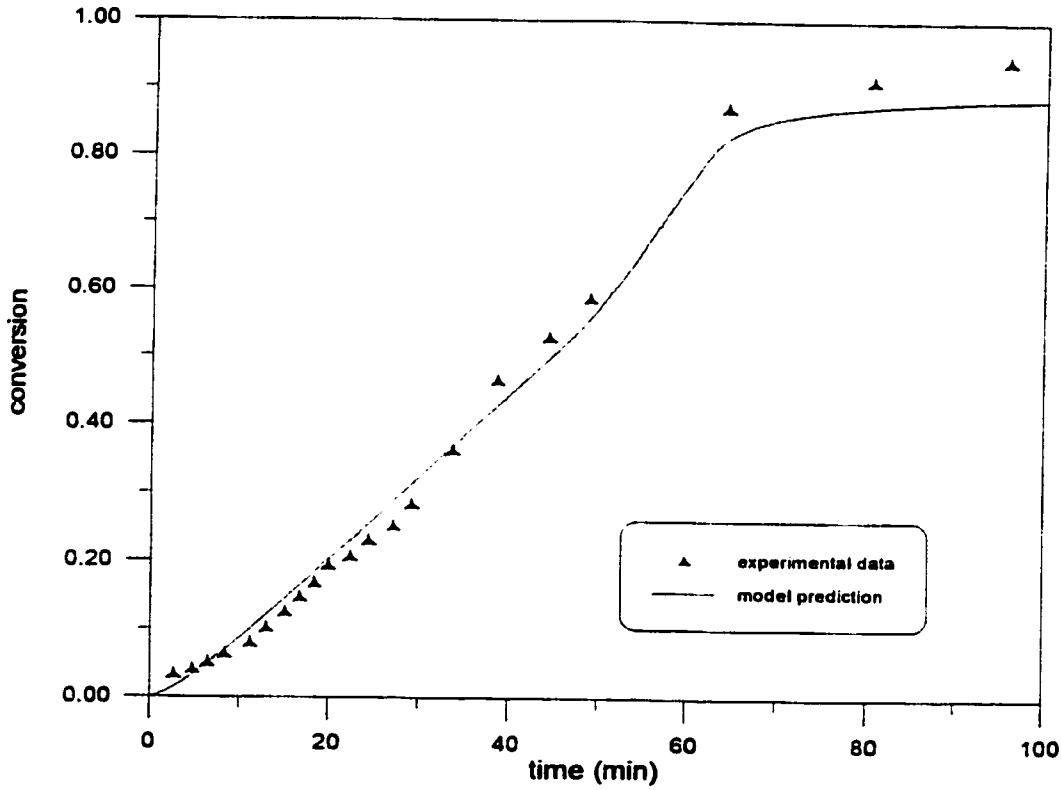

Figure 19.18 Simulation of Conversion in Methyl Methacrylate Emulsion Homopolymerization at 55 °C.
M/W: 40/60, SDS: 0.244 wt%, KPS: 0.165 wt%.

Schork and Ray (1981)

Schork and Ray (1981) conducted methyl methacrylate emulsion polymerization at 40 °C. Reaction conversion was monitored by an online densitometer. To verify their online measurements, they also used gravimetry to determine conversion offline. Both results are displayed in figure 19.19. It is, however, noticed that in the mid-range of conversion in their experiment, their online measurement gave lower conversion than that from offline samples. Since at the time there were more uncertainties associated with the online measurement, data obtained from their offline samples are more trustworthy. It is good to see that the model gives predictions that are closer to their offline measurements, which again indicates good reliability of our model's predictive powers.

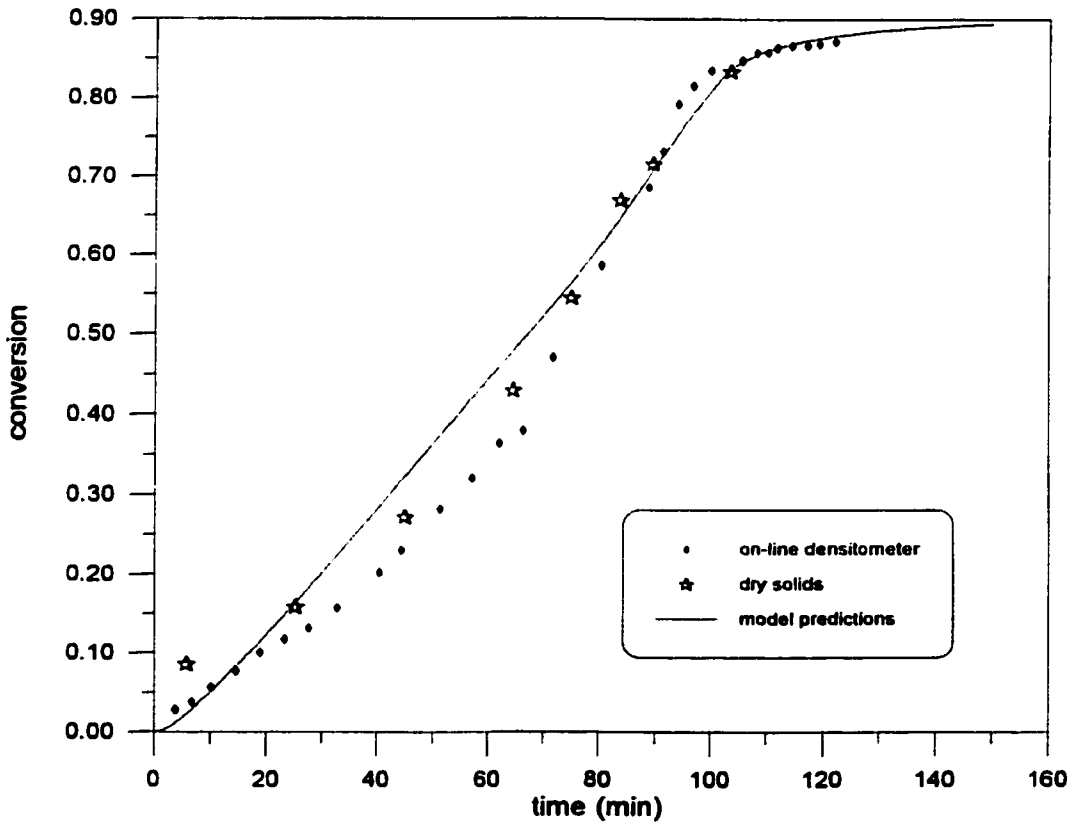

Figure 19.19 Simulation of Conversion in Methyl Methacrylate Emulsion Homopolymerization Using Online Densitometry.
(M/W: 43%, [SDS]: 0.02 mol/Lw, [APS]: 0.01 mol/Lw)

19.2 Simulation of Butyl Acrylate Emulsion Homopolymerization

Unlike monomers tested previously, butyl acrylate emulsion polymerization received little attention though it is an important ingredient in latex paints and adhesives. There has been no effort in the literature to cover detailed kinetic aspects of this monomer system. Maxwell et al.(1987) found butyl acrylate has moderate water solubility (0.006 mol/Lw) which is between styrene and methyl methacrylate. Maxwell et al.(1987) also measured monomer concentration in polymer latex particles, which was about 3.2 mol/L, and this leads to a partitioning coefficient between oil and water phases of about 533. The rate constant for termination determined by this group is 750 L/mol·sec (at about 85% conversion), which is very low. The low value of k_t is probably due to the gel effect. Maxwell et al.(1987) suggested that at the late stages of the reaction, termination is dominated by reaction diffusion control. Maxwell et al.(1987) estimated that the rate constant for desorption is 0.004 s^{-1}, and this indicates that desorption of this monomer is not very significant.

Capek and Fouassier (1997) found that monomer concentration in polymer particles is 4.4 mol/L, and estimated the rate constant for propagation at 1360 mol/L·sec at 60°C. This is very close to the current emulsion model's estimate of 1325 mol/L·sec. More information about k_p and k_t can be found in Barandiaran et al.(1992). Their estimation is 170 L/mol·sec for k_p and 3400 for k_t at no specified temperature.

Mallya and Plamthottan (1989) investigated several aspects of butyl acrylate emulsion polymerization kinetics. They found that monomer concentration in polymer latex particles is in the range of 3.1~3.25 mol/L, which is very close to Maxwell's et al.(1987) estimation. This group also claimed that k_t is in the range of 10^3~10^4 L/mol·s at 50°C. The low value of k_t leads to a high value for $\bar{n}$, which was estimated in the range of 5~30 at mid- to high conversion range. This group also estimated the rate constant for desorption as 0.0027 s^{-1}, which is similar to what Maxwell et al.(1987) estimated. The low desorption rate constant once again implies that desorption is not very significant in BA emulsion polymerization.

There have been no studies on molecular weight development for this monomer system. Lovell et

al.(1991) studied chain transfer to polymer in butyl acrylate emulsion polymerization. They presented direct evidence of chain transfer to polymer and formation of branched chains. The chain transfer to polymer proceeds via abstraction of a hydrogen atom from a tertiary C-H bond in a butyl acrylate repeating unit. Lovell et al.(1991) however did not estimate the rate constant for chain transfer to polymer.

From all the kinetic information gathered from the literature with regards to butyl acrylate emulsion polymerization, it can be summarized that butyl acrylate has the following reaction characteristics:

(1) moderate water solubility

(2) insignificant desorption, high $\bar{n}$

(3) strong gel effect; reaction diffusion control mechanism dominates in late stages of reaction

(4) presence of chain transfer to polymer, branching

Additional papers that might be useful for kinetic studies or modelling for this monomer are listed in Table 19.4.

Table 19.4 Literature Review on Butyl Acrylate Emulsion Homopolymerization.

References	Remarks
Barandiaran et al.(1992)	estimation of rate constant for desorption and absorption
Capek et al.(1987)	initiation of oil soluble initiator (AIBN)
Capek (1994)	effect of initiator type and concentration
Capek (1996)	use of mixed emulsifiers
Capek and Potisk (1992)*	copolymerization of BA/AN
Capek and Fouassier (1997)	photopolymerization of butyl acrylate
Chern and Chen (1996)	effect of carboxylic acid on particle nucleation in butyl acrylate emulsion polymerization
Chu and Lin (1992)	stabilization with mixed surfactants
Cruz et al.(1985)*	full conversion butyl acrylate homopolymerization
Dube (1994)*	batch emulsion polymerization of butyl acrylate
El-Aasser et al.(1983)	copolymerization of BA/VAc
Kong et al.(1988)*	full conversion range data
Kukulj et al.(1997)	catalytic chain transfer
Lovell et al.(1991)	chain transfer to polymer
Mallya and Plamthottam (1989)	rate constant for termination
Maxwell et al.(1987)	general kinetics
Maxwell et al.(1992c,d)	reaction kinetics at high conversion
Mcbain and Piirma (1989)	effect of steric length on reaction kinetics
O'Neill and Hoign (1972)	effect of emulsifier on reaction kinetics

* reported experimental data used for model testing

19.2.1 Model Testing Results

Capek and Potis (1992)

Capek and Potis (1992) performed one experiment of butyl acrylate emulsion homopolymerization at 60°C in their studies of crosslinking polymerization involving divinyl benzene. Measured conversion data are displayed in figure 19.20. It can be seen that conversion goes to completion due to the very low Tg (-45°C) of polybutyl acrylate. Despite the presence of some induction time, the model follows the conversion versus time curve very well.

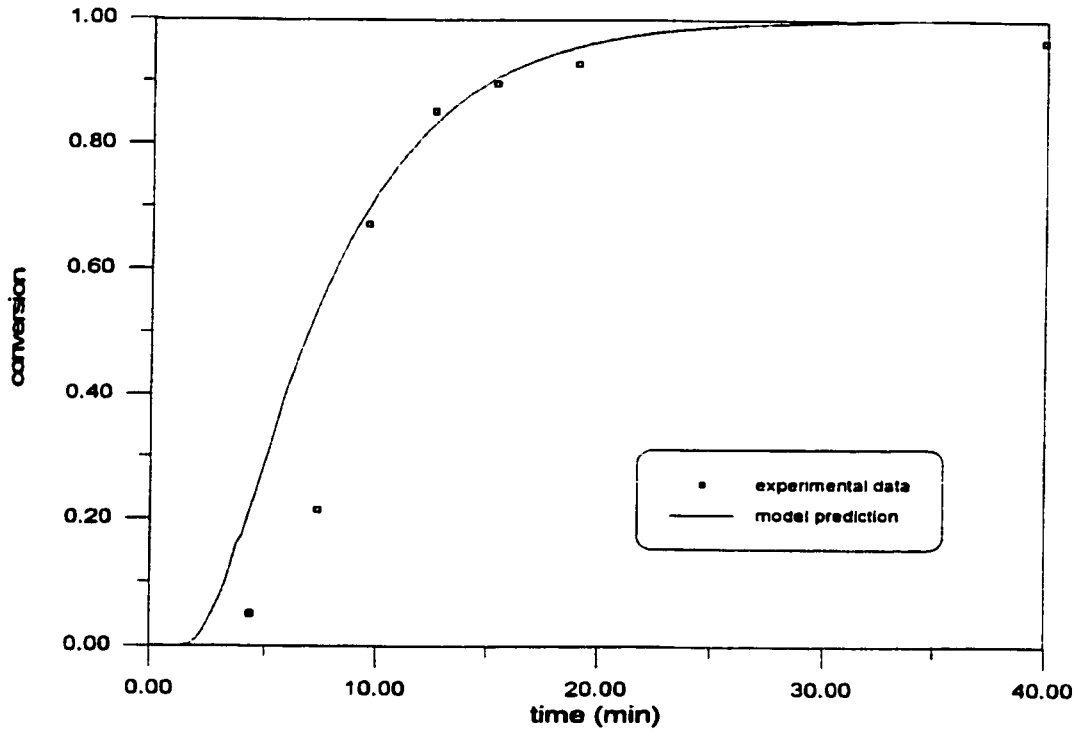

Figure 19.20 Simulation of Conversion in Butyl Acrylate Homopolymerization in Emulsion at 60C.
(Water: 100g, BA: 6.66g, SDS: 2g, APS: 0.2g)

Cruz et al.(1985)

This group performed studies on butyl acrylate/styrene copolymerization in emulsion. One homopolymerization run with butyl acrylate was carried out and is used for model testing. Apparently, the reported experimental data are problematic, as displayed in figure 19.21. The conversion curve reached a plateau after 80% conversion, indicating a reduced rate of polymerization. Full conversion was never reached as theory predicts, and an oxygen leak was suspected. Prediction on conversion at the early stages is in the right range.

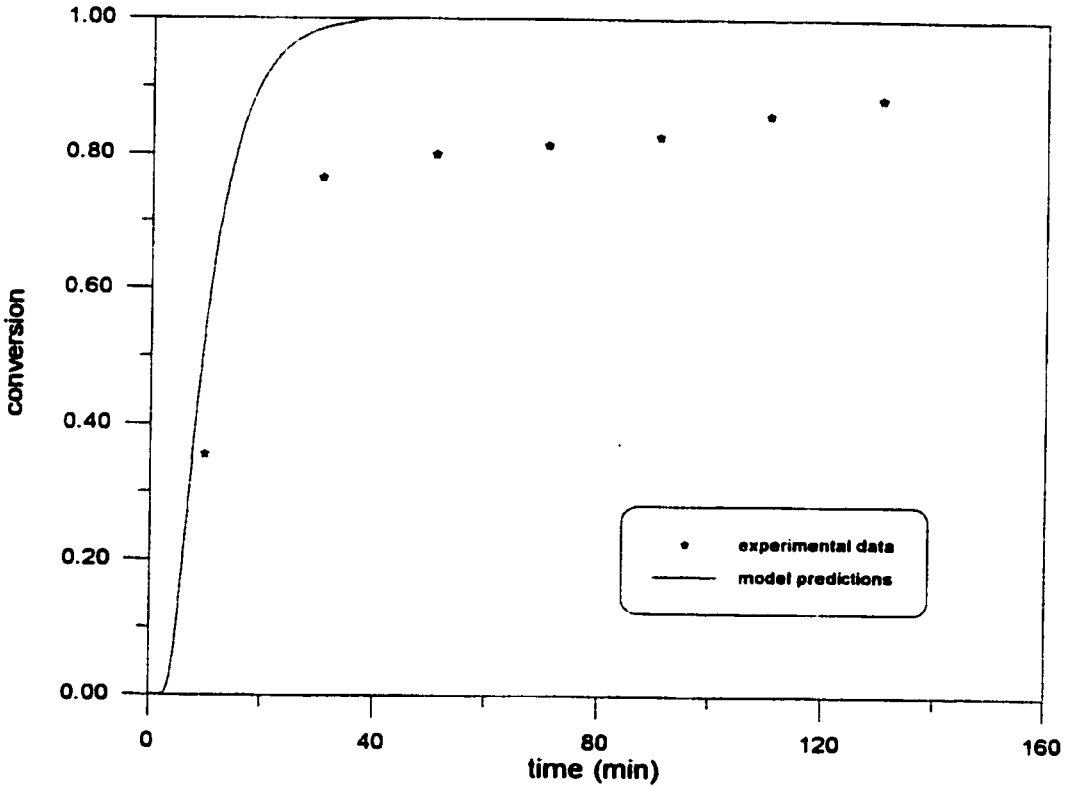

Figure 19.21 Simulation of Conversion in Butyl Acrylate Homopolymerization in Emulsion at 60C.
(BA: 100g, KPS: 4g, water: 600g, SDS: 0.1g)

Dube (1994)

Dube (1994) conducted two experimental runs of butyl acrylate emulsion homopolymerization using mixed emulsifiers of AMA–80 and AOT-75. The reaction was performed in a 5-liter stainless steel reactor. The initial reaction temperature was 60°C. Conversion results of the first run are displayed in figure 19.22. It is easy to see that there is a large discrepancy in the mid-range of the reaction. The disagreement is caused by nonisothermality in this run. Based on Dube'e own observations, severe temperature excursions (as much as 30°C) were observed in the beginning of the reaction. Such nonisothermality lasted for 30 minutes. This explains why between 10 to 40 minutes the reported conversion data points are much higher than the model predictions. It is clear that a reactor jacket alone is inadequate to remove the heat of reaction fast enough. To avoid heat accumulation, a cooling coil was installed in the same reactor in the second run, and the initiator amount was reduced by half to slow down the rate of polymerization. The reaction was then carried out at the same temperature. Better agreement is reached between model predictions and experimental results in the second run as shown in figure 19.25, though nonisothermality was not entirely eliminated.

Model predictions on particle diameter and number of particles for both runs are good. Simulation results for diameter for both runs are presented in figures 19.23 and 19.27, while results for total particle number are displayed in figures 19.24 and 19.26. The agreement indicates that temperature excursions have less of an effect on particle size as well as on the total number of particles.

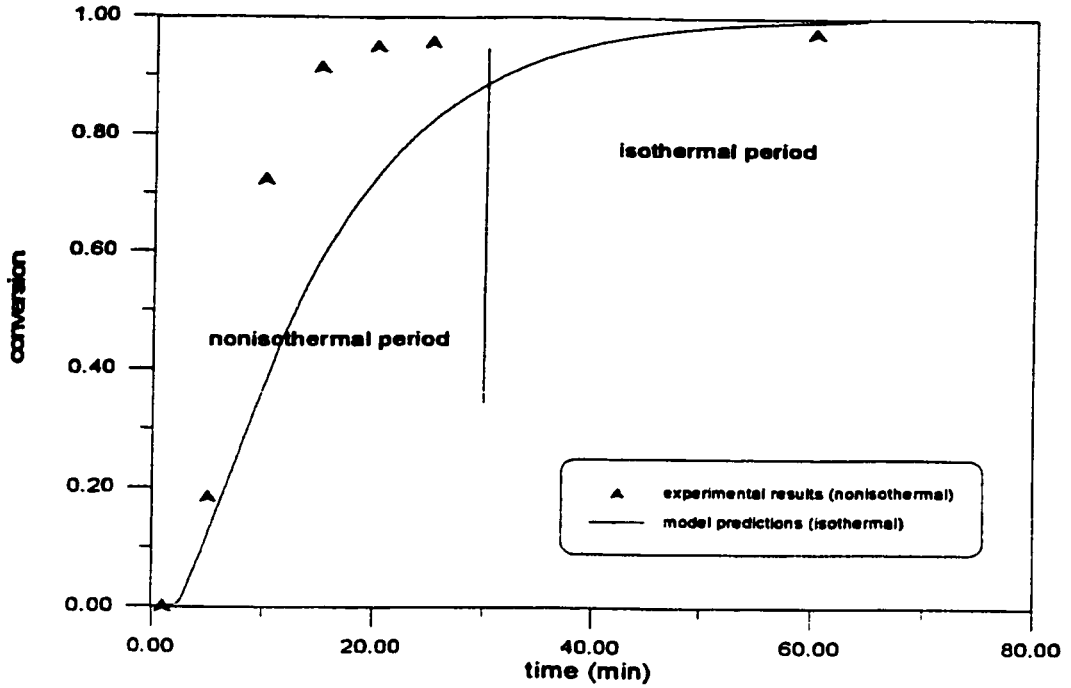

Figure 19.22 Simulation of Conversion in Butyl Acrylate Emulsion Homopolymerization under Nonisothermal Conditions. (initial temperature: 60°C, BA: 1436g, water: 2419 g, APS: 1.45 g AMA-80: 14.472 g, AOT-75: 14.325 g)

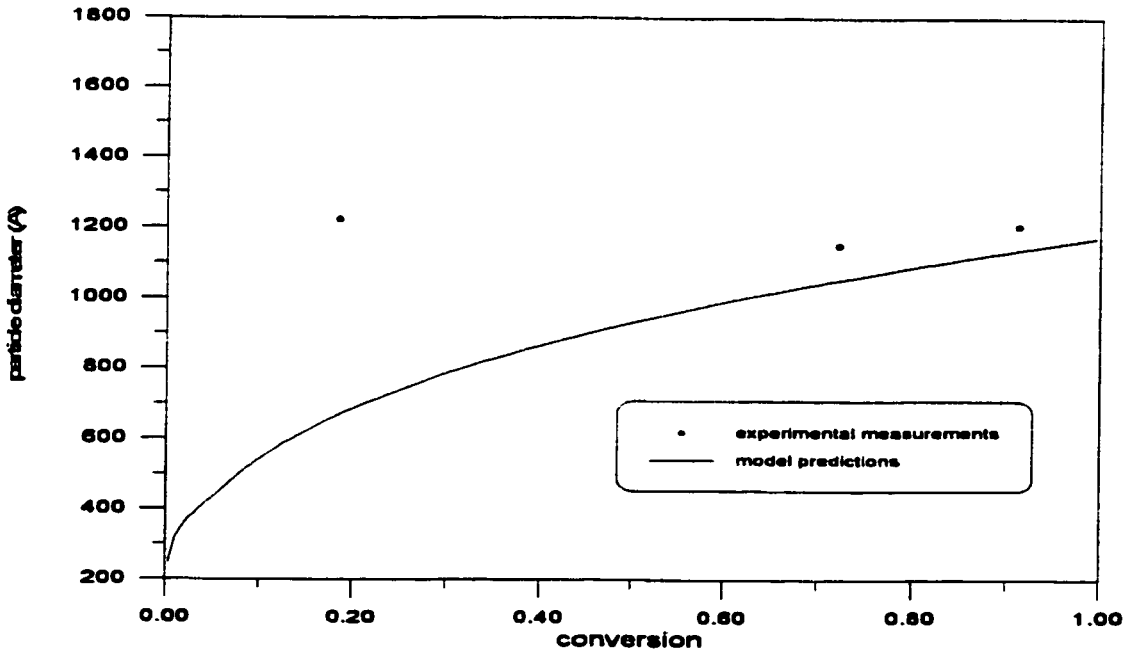

Figure 19.23 Simulation of Particle Size in Butyl Acrylate Emulsion Homopolymerization under Nonisothermal Conditions. (Initial temperature: 60 °C, BA: 1436 g, water: 2419 g, APS: 145 g, AMA-80: 14.472g, AOT-75: 14.325)

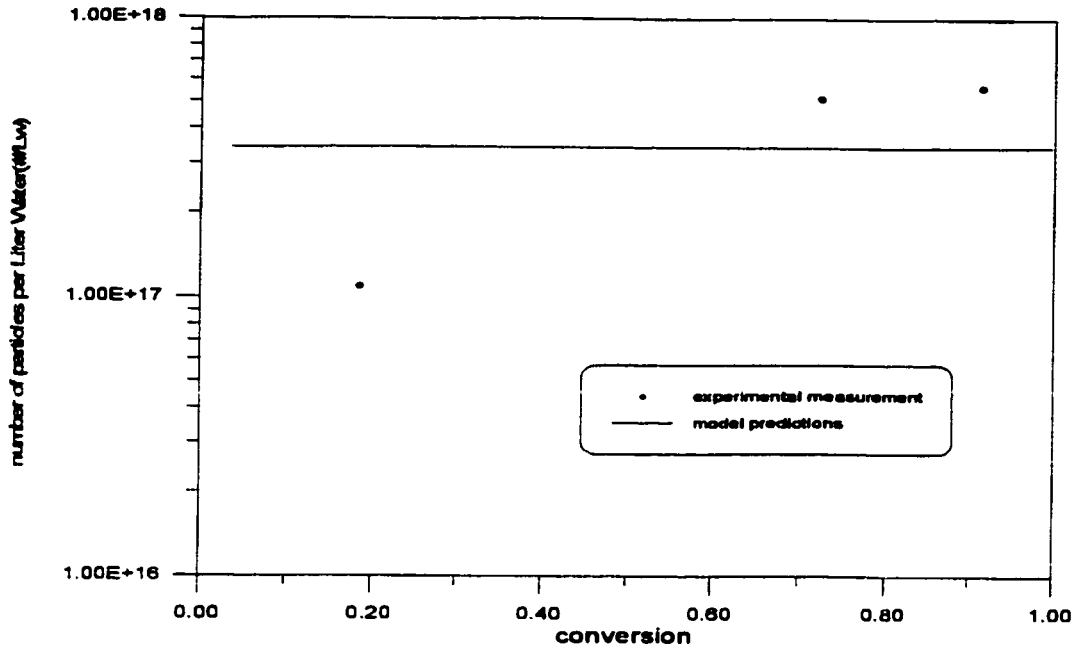

Figure 19.24 Simulation of Number of Particles in Butyl Acrylate Emulsion Homopolymerization under Nonisothermal Conditions.
(initial temperature: 60°C, BA: 1436g, water: 2419 g, APS: 1.45 g AMA-80: 14.472 g, AOT-75: 14.325 g)

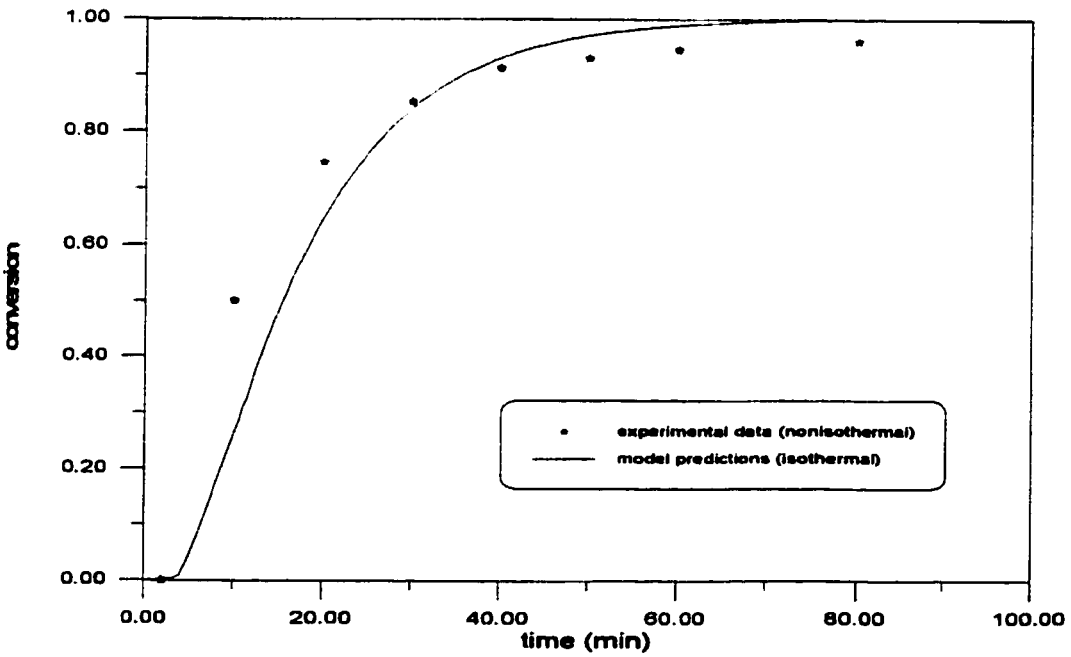

Figure 19.25 Simulation of Conversion in Butyl Acrylate Emulsion Homopolymerization at 60°C.
(BA: 1436g, water: 2419 g, APS: 1.45 g, AMA-80: 14.472 g, AOT-75: 14.325 g)

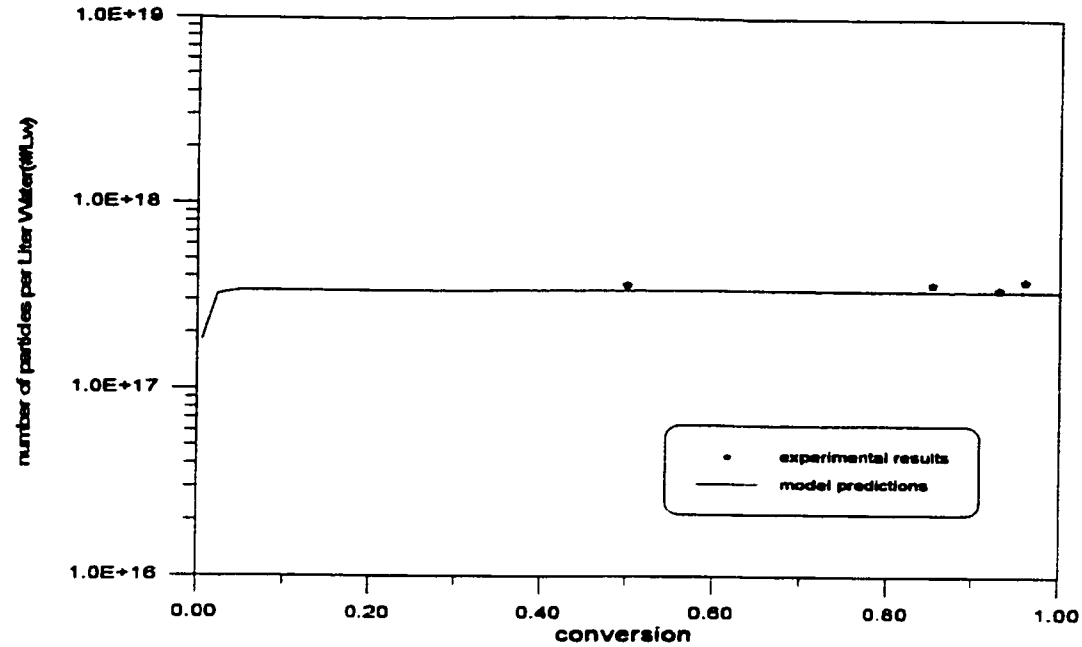

Figure 19.26 Simulation of Number of Particles in Butyl Acrylate Emulsion Homopolymerization at 60°C.
(BA: 1436g, water: 2419 g, APS: 1.45 g, AMA-80: 14.472 g, AOT-75: 14.325 g)

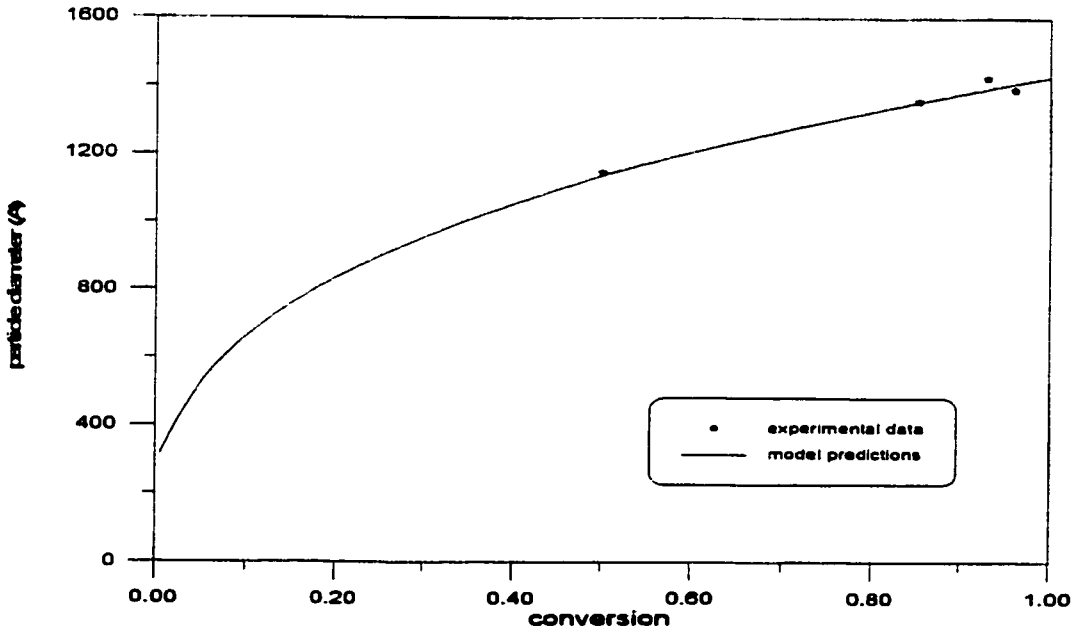

Figure 19.27 Simulation of Particle Size in Butyl Acrylate Emulsion Homopolymerization at 60°C.
(BA: 1436g, water: 2419 g, APS: 1.45 g, AMA-80: 14.472 g, AOT-75: 14.325 g)

Kong et al.(1988)

This group conducted copolymerization of BA/VAc in emulsion. One homopolymerization run can be used for model testing. The reaction temperature is 60°C, far above PBA's Tg, and no limiting conversion is expected. This is confirmed by the reported conversion measurements. The final conversion for the reaction is in the range of 95%. Overall model predictions are good.

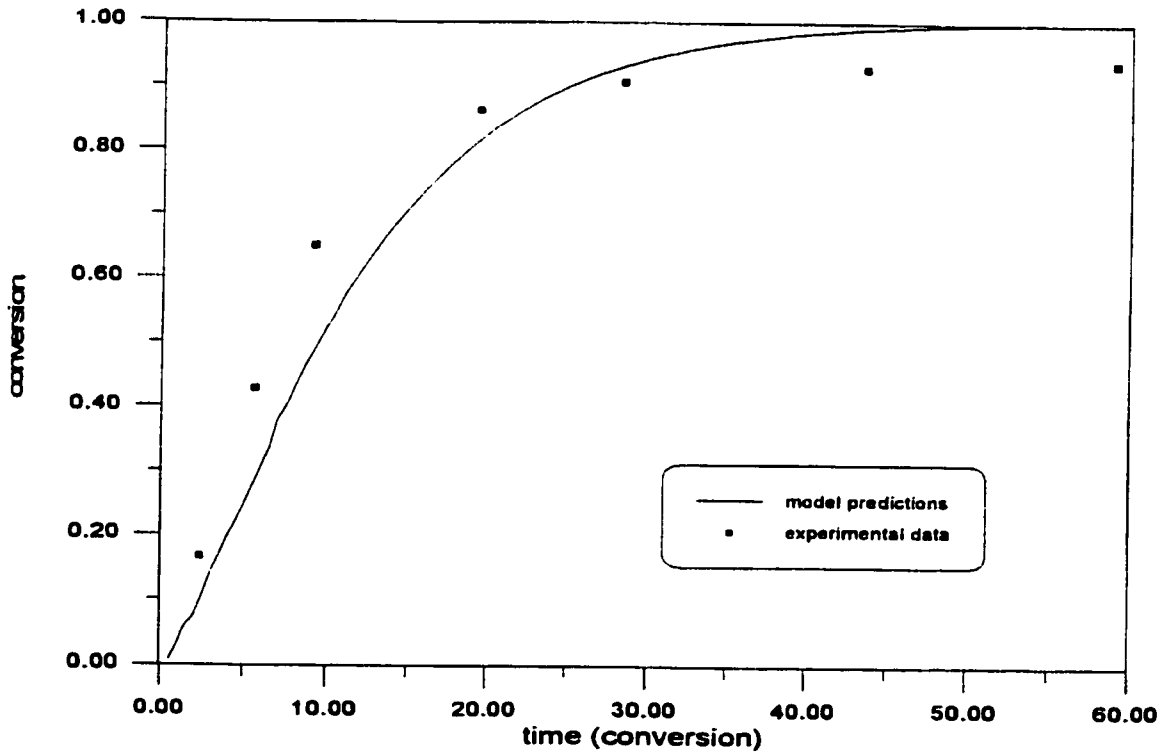

Figure 19.28 Simulation of Conversion in Butyl Acrylate Emulsion Homopolymerization at 60 °C.
(water: 400 g, AOT: 3 g, AMA: 3 g, BA: 200 g, APS: 0.6 g)

19.3 Simulation of Ethyl Acrylate Emulsion Homopolymerization

Ethyl acrylate is an important component in latex paints and adhesives due to its low polymer Tg. However, it has been rarely studied and is not well understood, because it is a very toxic monomer. Kinetic information with regards to this monomer has been collected and listed in Table 19.5.

Table 19.5 Literature Summary on Ethyl Acrylate Emulsion Homopolymerization

References	Remarks
Adhikari et al.(1987)	thermal decomposition of KPS in ethyl acrylate emulsion polymerization at 50°C
Arzamendi et al.(1991)	ethyl acrylate and methyl methacrylate copolymerization
Capek et al.(1990)*	copolymerization of ethyl acrylate with crosslinker
Capek (1992)	copolymerization of methyl methacrylate and ethyl acrylate
Fitch et al.(1985)	kinetics of particle nucleation
Maw and Piirma (1983)	use of nonionic emulsifier
McCurdy and Laidler (1964)	kinetic studies of acrylates and methacrylates
Shoaf and Pochlein (1989)	copolymerization of methacrylic acid and ethyl acrylate
Snuparek (1980)	emulsifier effect on ethyl acrylate emulsion homopolymerization
Yeliseyeva and Zuikov (1982)	emulsion polymerization of acrylic monomers

* experimental data used for model testing

Clearly, only very limited kinetic information or experimental data are available in the literature. Among the papers listed above, Adhikari et al.(1987) provided useful information on the thermal decomposition of KPS in ethyl acrylate emulsion polymerization. The rate constant for decomposition was measured as 1.4×10^{-6} s^{-1}. This value is nearly twice as high as what our emulsion model uses. The reason for this is obviously that Adhikari et al.(1987) measured an "apparent" rate constant for

decomposition which also includes initiator efficiency. Another useful piece of information from this group is the measured monomer partitioning coefficient between oil and water phases, which is about 16.

McCurdy and Laidler (1964) investigated the emulsion polymerization of a number of acrylates and methacrylates. They found that the rate of acrylates was consistently higher than methacrylates. They contributed this behavior to steric and inductive effects. Shoaf and Poehlein (1989) conducted copolymerization of ethyl acrylate and methacrylic acid. The water solubility of ethyl acrylate was 2.5 wt%. Perhaps the most useful work is from Capek et al.(1990). This group attempted to study copolymerization of ethyl acrylate with a number of divinyl monomers (used as crosslinkers). A set of experiments of emulsion homopolymerization of ethyl acrylate were carried out. Reported conversion, particle number and size were the only full conversion experimental data for model testing. Simulation results are presented in the section below.

19.3.1 Model Testing Results

Experiments from Capek et al.(1990) are the only available data for model testing. A set of runs were carried out at various emulsifier concentrations. Model testing results are displayed in figures 19.29~19.31. The most noticeable feature in these three runs was the fast rate of polymerization ethyl acrylate exhibited. Polymerization was completed within 15 minutes. The fast reaction observed in ethyl acrylate emulsion polymerization is not surprising, since its bulk/solution polymerization exhibits the same characteristics. Comparatively, the gel effect in emulsion polymerization is even more pronounced than it is in bulk. Figure 19.29 shows the run with the highest emulsifier concentration. There is clearly a very large discrepancy between model predictions and measured conversion. The possible reason for such a arge disagreement could be attributed to temperature excursions. In figure 19.29, the entire reaction was completed within 7-10 minutes. With such a high rate of polymerization, heat accumulation was very likely, especially since the reaction was conducted in a glass reactor without a cooling coil. As emulsifier levels were gradually reduced, the temperature excursions in the next two runs (figures 19.30 and 19.31) were not as severe as for the run in figure 19.29, and hence the data are closer to the model predictions.

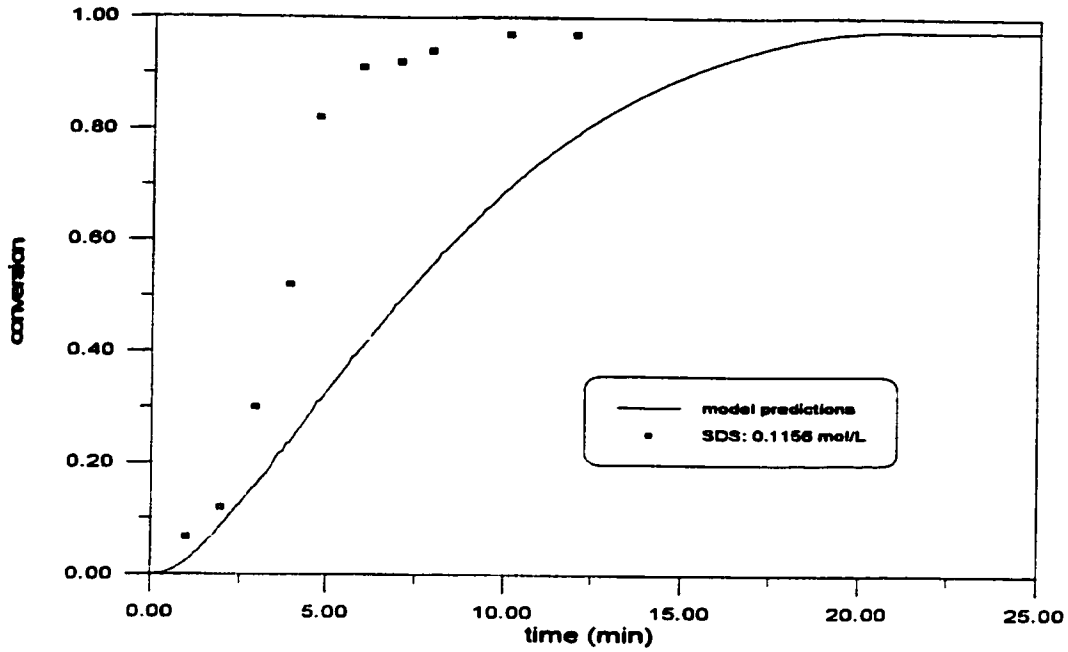

Figure 19.29 Simulation of Conversion in Ethyl Acrylate Emulsion Homopolymerization at 60°C.
(EA: 92.4g, water: 150 g, KPS: 0.1 g)

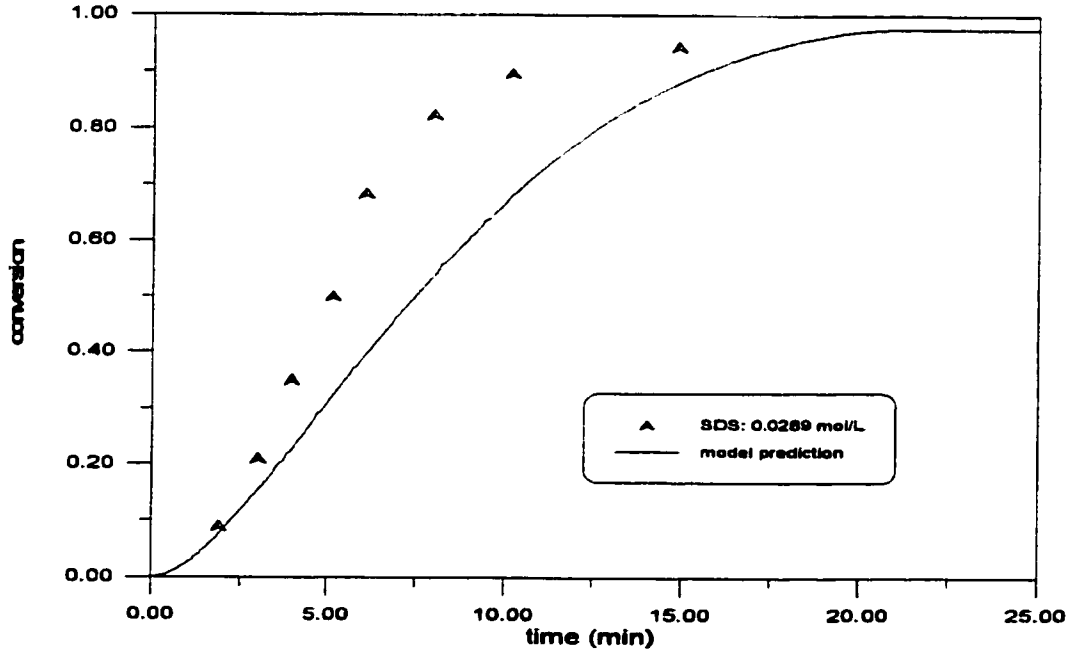

Figure 19.30 Simulation of Conversion in Ethyl Acrylate Emulsion Homopolymerization at 60°C.
(EA: 92.4g, water: 150 g, KPS: 0.1 g)

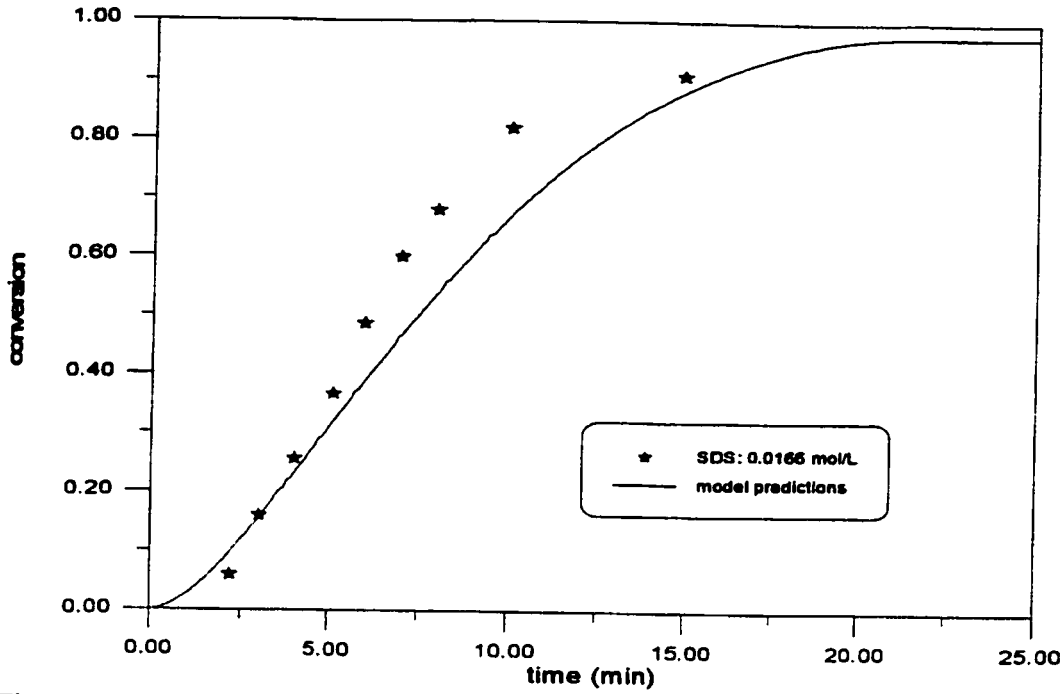

Figure 19.31 Simulation of Conversion in Ethyl Acrylate Emulsion Homopolymerization at 60°C.
(EA: 92.4g, water: 150 g, KPS: 0.1 g)

The model predictions for the run with the lowest emulsifier level (figure 19.31) agrees with the experimental data quite well, though temperature excursions may still not be entirely eliminated.

In summary, ethyl acrylate emulsion polymerization has the following characteristics:

(1): modest water solubility (close to that of methyl methacrylate)

(2): high rate of polymerization, pronounced gel effect

(3): insignificant desorption

Chapter 20. Extensions to Emulsion Copolymerization

20.1 Brief Literature Summary

After having developed a mathematical model for emulsion homopolymerization and achieved good model testing results, the next natural step is to extend it to simulate copolymerization systems. As has been demonstrated in the extensions of the bulk/solution model (from homopolymerization to copolymerization and eventually to terpolymerization) in the first volume of this thesis, the same methodology is used for the extension of the emulsion model.

If emulsion homopolymerization is considered as a very complex system, modelling of emulsion copolymerization is an even more challenging task. There has been little effort in modelling of emulsion polymerization before the 1980's. As already discussed in section 14.2, most literature models are limited to specific reaction conditions, and are far from being general in nature. A summary of models for emulsion polymerization is given in Table 14.1. In this chapter, only papers that presented a comprehensive and general model are discussed.

Despite recent progress on mathematical modelling of emulsion polymerization highlighted in section 14.2, there are relatively very few *general* models designed to simulate emulsion copolymerization of various systems.

Gilbert's group (Ballard et al., 1981; Richards et al., 1989; Congalidis et al.,1989) described their extension of homopolymerization to a copolymerization model using the pseudohomopolymerization approach. Their model neglected micellar nucleation, because micelles were considered merely a reservoir of emulsifier despite the fact that there is a large body of evidence of micellar nucleation. Monomer partitioning was solved empirically. Though many rate constants in their model are expressed as a mathematical average of individual rate constants of homopolymers, the authors used one single value in their implementation as a simplification.

Another copolymerization model available in the literature is the work of Dougherty (1986a, b). In

his model, monomer partitioning was solved using the knowledge of x_c. Though Dougherty's (1986a,b) model is comprehensive from a theoretical point of view, many simplifications were used when the model was implemented. Dougherty (1986a,b) used apparent rate constants and the rate constants for termination were expressed empirically as a function of conversion to reflect gel effect. The model was then tested to simulate copolymer system of Sty/MMA.

Hamielec and coworkers (Broadhead et al., 1985; Hamielec et al.,1987; Penlidis et al.,1986) gave a comprehensive review of modelling of emulsion polymerization. They also presented an emulsion copolymerization model based on a population balance approach. The pseudo-kinetic rate constant method was extensively used in their model. The gel effect was treated using free-volume theory instead of an empirical expression of rate constants for termination. Particle size distribution was modelled by using the particle birth time as an internal coordinate in their work.

The most recent advance is the effort from Saldivar et al.(1998). Their model for emulsion copolymerization is the continuation of previous work by Min and Ray's (1974) and is very sophisticated and comprehensive. An extensive review on modelling of emulsion copolymerization including particle size and molecular weights is given in Saldivar et al.(1998). In the model presented by Saldivar et al.(1998), the pseudo kinetic rate constant method was extensively used in describing almost all important phenomena (this includes chemical reactions in both oil and aqueous phases, desorption, absorption, particle nucleation, etc.) in copolymerization. Saldivar et al.(1998) stated that monomer partitioning in copolymerization can be solved either empirically through the use of partition coefficients or theoretically by using thermodynamic equilibrium, however they did not describe the actual implementation of either method. Their model was tested with three copolymer systems (Sty/MMA, Sty/α-methyl Sty, Sty/BD) with success.

It is worth noting that the use of the pseudo-kinetic rate constant method reduces a copolymerization kinetic scheme to that of a homopolymerization. The mathematical model structure of the copolymerization model is similar to that of the homopolymerization model. However, in emulsion copolymerization, certain phenomena, e.g., monomer partitioning and radical desorption, require

additional treatment. Model modifications with regards to these aspects are detailed in the following two sections.

20.2 Monomer Partitioning in Copolymerization

20.2.1 Literature Review

Solving monomer partitioning in emulsion homopolymerization has already been discussed in section 15.3. Monomer partitioning in copolymerization is of critical importance, since it is directly related to the calculation of the rate of polymerization as well as of copolymer composition. However, this is a very difficult subject. Monomer partitioning in copolymerization is much more complicated than in homopolymerization because it involves two monomers and their copolymer. Monomer partitioning in copolymerization can certainly be solved for by using empirical partition coefficients, however, these coefficients must be measured for every copolymer system investigated. A model for a copolymer system, when such partition coefficients are not available, will be unable to deliver adequate predictions. Under such circumstances, monomer partitioning can only be solved for through thermodynamic equilibrium. The use of partitioning coefficients in copolymerization is relatively easy, and is very similar to what has been described in section 15.3. In this chapter, emphasis will be focused on how to solve for partitioning through more general thermodynamic equilibrium equations.

In multicomponent emulsion polymerization, the number of thermodynamic equations needed to fully describe monomer partitioning increases drastically. In stages I and II when there is still monomer droplets present, there is total of three phases, namely, the polymer particle phase, the aqueous phase and the monomer droplet phase. For polymerization involving n monomers, a total of $3\times n$ nonlinear equations are needed. These $3\times n$ nonlinear equations must be solved for at each iteration simultaneously. In case of copolymerization, a total of six equations must be solved compared to only one (equation 15.51) that has to be solved for in homopolymerization. The thermodynamic equations for the chemical potential for monomers A and B in all three phases are listed below:

$$\Delta G_{A,particle}/RT = Ln\phi_A^P + (1-m_{AB})\phi_B^P + \phi_P^P + \chi_{AB}(\phi_B^P)^2 + \chi_{AP}(\phi_P^P)^2 + \phi_B^P\phi_p^P(\chi_{AB}+\chi_{AP}-\chi_{BP}m_{AB}) + \frac{2\sigma\bar{V}_{A,m}}{RTr_p} \quad (20.1)$$

$$\Delta G_{B,particle}/RT = Ln\phi_B^P + (1-m_{AB})\phi_A^P + \phi_P^P + \chi_{AB}(\phi_A^P)^2 + \chi_{BP}(\phi_P^P)^2 + \phi_A^P\phi_p^P(\chi_{AB}+\chi_{BP}-\chi_{AP}m_{AB}) + \frac{2\sigma\bar{V}_{B,m}}{RTr_p} \quad (20.2)$$

$$\Delta G_{A,droplet}/RT = Ln\phi_A^d + (1-m_{AB})\phi_B^d + \chi_{AB}(\phi_B^d)^2 + \frac{2\sigma\bar{V}_{A,m}}{RTr_d} \quad (20.3)$$

$$\Delta G_{B,droplet}/RT = Ln\phi_B^d + (1-m_{AB})\phi_A^d + \chi_{AB}(\phi_A^d)^2 + \frac{2\sigma\bar{V}_{B,m}}{RTr_d} \quad (20.4)$$

$$\Delta G_{A,aqueous}/RT = Ln\frac{\phi_A^w}{\phi_{A,S}^w} \quad (20.5)$$

$$\Delta G_{B,aqueous}/RT = Ln\frac{\phi_B^w}{\phi_{B,S}^w} \quad (20.6)$$

where:

χ_{AB}: interaction parameter between monomer A and B

χ_{iP}: interaction parameter between monomer i and polymer (i=A, B)

m_{AB}: ratio of molar volume of monomer A and B, i.e., $m_{AB}=V_{A,m}/V_{B,m}$

ϕ_i^p: volume fraction of monomer i in the polymer particle phase (i=A, B)

ϕ_p^p: volume fraction of polymer in the polymer particle phase

ϕ_i^d: volume fraction of monomer i in monomer droplet (i=A, B)

ϕ_i^w: volume fraction of monomer i in aqueous phase (i=A, B)

$\phi_{i,s}^w$: volume fraction of monomer i in aqueous phase at saturation level in homopolymerization of monomer i (i=A, B)

r_d, r_p: radius of monomer droplets and polymer particles

σ: surface tension of polymer particles or monomer droplets

Expressions for the chemical potential of monomers A/ B in the polymer particle phase, monomer droplets and aqueous phase are expressed by equations 20.1/20.2, 20.3/20.4 and 20.5/20.6, respectively. The equilibrium equations in stages I and II are constructed as following;

$$\Delta G_{A,particle}/RT = \Delta G_{A,droplet}/RT \quad (20.7)$$

$$\Delta G_{A,particle}/RT = \Delta G_{A,aqueous}/RT \quad (20.8)$$

$$\Delta G_{A,aqueous}/RT = \Delta G_{A,droplet}/RT \quad (20.9)$$

$$\Delta G_{B,particle}/RT = \Delta G_{B,droplet}/RT \quad (20.10)$$

$$\Delta G_{B,particle}/RT = \Delta G_{B,aqueous}/RT \quad (20.11)$$

$$\Delta G_{B,aqueous}/RT = \Delta G_{B,droplet}/RT \quad (20.12)$$

Equations 20.7~20.12 are solved simultaneously for seven unknowns, i.e., the volume fraction of both monomers in all three phases plus the volume fraction of the polymer in polymer particle phase. Compared to equation 15.47, equations 20.1 and 20.2 involve three more interaction parameters, i.e., χ_{AB}, χ_{AP} and χ_{BP}. These three parameters are usually difficult to obtain. Liu et al.(1997) stated that it was very difficult or nearly impossible to measure the interaction parameter of acrylonitrile and polyacrylonitrile in their studies on swelling in styrene/acrylonitrile emulsion copolymerization, so they instead used solubility information to estimate the interaction parameters.

In equations 20.3 and 20.4, the last term on the right hand side represents the enthalpy contribution from surface tension, and since monomer droplets are very large compared to polymer particles, this term can be safely dropped. When in stage III, monomer droplets disappear, and the thermodynamic equilibrium equations reduce to equations 20.8 and 20.11.

A number of research groups stated that they solved monomer partitioning using the thermodynamic approach. Guillot (1985, 1986) listed thermodynamic equilibrium equations for styrene/acrylonitrile copolymerization. His model can predict monomer concentration in particles and copolymer composition, however, his group has never described how the equations were actually solved. Mead

and Poehlein (1988, 1989) developed a model to simulate styrene/methyl acrylate emulsion copolymerization in a CSTR. Equilibrium equations similar to equations 20.1~20.12 were listed. Delgado et al.(1988) applied the same method to butyl acrylate/vinyl acetate copolymerization. Guo et al.(1992) studied styrene microemulsion polymerization and treated monomer partitioning in a similar way. Other groups that used the thermodynamic approach but did not discuss the actual implementation include Saldivar et al.(1998), Liu et al.(1997) and Rawling and Ray (1988a, b).

German's group performed detailed studies on monomer partitioning in both homopolymerization and copolymerization. Solving the thermodynamic equilibrium equations in all three stages in homopolymerization was first discussed in Maxwell et al.(1992a). This group also studied the effect of particle size, temperature and molecular weight on monomer partitioning. Monomer-polymer interaction parameters for several monomers (styrene, methyl acrylate, methyl methacrylate and vinyl acetate) were estimated. Maxwell et al.(1992b) later extended their work to copolymerization of styrene/methyl acrylate, and the thermodynamic equilibrium equations were simplified under several assumptions: (1): interaction parameters χ_{AP}, χ_{BP} were assumed to be the same; (2): molar volumes for each monomer are close to each other so $m_{AB} \approx 1$; (3): contributions of mixing of the two monomers in monomer droplets are small compared to the other terms in equations 20.3 and 20.4. By using these assumptions, equations 20.1~20.6 are greatly simplified and can be easily solved. Maxwell et al.(1992b) investigated several copolymer systems (styrene/butyl acrylate, styrene/methyl acrylate, methyl acrylate/butyl acrylate) and experimentally determined the concentration of monomers in each phase. They concluded that the ratio of volume fractions of the two monomers in polymer particles is very close to that in monomer droplets. Additionally, the relationship between the concentration of monomer in the aqueous phase and in the monomer droplet phase obeys Henry's law. Maxwell et al.(1993) and Schoonbrood and German (1994) later gave more justification to the assumptions they used through parameter sensitivity work. Noel et al.(1994) used the same assumption and studied monomer partitioning in styrene/methyl acrylate copolymerization. Schoonbrood (1994) extended the work to the terpolymer system of styrene/methyl methacrylate/methyl acrylate using the same method. Though this simplified method from German's group has been adequate in describing the specific copolymer system, its validity for other copolymer

systems has not been tested. It is still desirable that the full equilibrium equations 20.1~20.6 be solved numerically without being limited to certain systems. The section below will present the implementation of a general method that can solve monomer partitioning in emulsion copolymerization.

20.2.2 Model Implementation

The subject of the actual implementation of solving monomer partitioning in copolymerization is hardly ever discussed. Most groups just present the thermodynamic equilibrium equations without describing how these equations are actually solved. Solving equations 20.1~20.6 is not an easy task. Conventional numerical methods for solving sets of nonlinear equations like Gauss Elimination or LU decomposition are time consuming and they greatly reduce the overall computation speed. Certainly an easy yet efficient method is still needed. Such a method can be found in Armitage et al.(1994). Armitage's et al.(1994) method has several major advantages which are easy implementation, quick convergence, and applicability to all three stages. A detailed implementation is highlighted below. By definition, the volume fraction of monomer j in monomer droplets, polymer particles and aqueous phase can be expressed as $\phi_j^d=V_j^d/V_d$, $\phi_j^p=V_j^p/V_p$ and $\phi_j^w=V_j^w/V_{wt}$, respectively. Now, rewriting the thermodynamic equilibrium equations 20.9 and 20.12 by substituting equations 20.3(20.4) and 20.5 (20.6) into equation 20.9 (20.12) yields:

$$V_j^d = \frac{\phi_j^w V_d}{\phi_{j,s}^w D_j} = \frac{V_j^w V_d}{V_{wt}\phi_{j,s}^w D_j} \tag{20.13}$$

Similarly, substituting equations 20.1 (20.2) and 20.5 (20.6) into equations 20.8 (20.11) leads to:

$$\phi_j^p = \frac{\phi_j^w}{\phi_{j,s}^w P_j} = \frac{V_j^w}{V_{wt}\phi_{j,s}^w P_j} \tag{20.14}$$

where:

$$D_j = \exp[(1-m_{AB})\phi_i^d + \chi_{ji}(\phi_i^d)^2] \tag{20.15}$$

$$P_j = \exp[(1-m_{ji})\phi_i^p + \phi_p^p + \chi_{ji}(\phi_i^p)^2 + \chi_{jp}(\phi_p^p)^2 + \phi_i^p\phi_p^p(\chi_{ji} + \chi_{jp} - \chi_{ip}m_{ji}) + \frac{2\sigma\bar{V}_{j,m}}{r_p RT}] \quad (20.16)$$

In the above equations, subscripts i or j stand for monomers A or B, and superscripts w, d and p stand for aqueous, monomer droplet and polymer particle phases, respectively. Other symbols in equations 20.13~20.16 are explained below:

V_j^d: volume of monomer i in monomer droplets, j=A or B

V_j^p: volume of monomer i in polymer particles, j=A or B

V_j^w: volume of monomer i in aqueous droplets, j=A or B

V_j: total volume of monomer i in all phases

V_{wt}: total volume of the aqueous phase including dissolved monomers

V_d: total volume of all monomer droplets

The overall material mass balance is as follows:

$$V_j = V_j^d + V_j^w + V_j^p \quad where \quad j=A,B \quad (20.17)$$

$$V_{wt} = V_w + V_A^w + V_B^w \quad (20.18)$$

$$V_d = V_A^d + V_B^d \quad (20.19)$$

$$V_p = V_A^p + V_B^p + V_{pol} \quad (20.20)$$

V_{pol} in equation 20.20 is the volume of polymer in all polymer particles. Since $V_j^p/V_{pol} = \phi_j^p/\phi_p^p$, substituting ϕ_j^p with equation 20.14 yields:

$$V_j^p = \frac{\phi_j^p V_{pol}}{\phi_p^p} = \frac{V_j^w V_{pol}}{V_{wt}\phi_{j,s}^w P_j \phi_p^p} \quad (20.21)$$

Substitution of equations 20.13 and 20.21 into equation 20.17 leads to:

$$V_j = V_j^w \left[\frac{V_d}{V_{wt}\phi_{j,s}^w D_j} + 1 + \frac{V_{pol}}{V_{wt}\phi_{j,s}^w P_j \phi_p^p} \right] \qquad (20.22)$$

The original algorithm proposed by Armitage et al.(1994) was implemented using different classes of particles, whereas in this thesis we modified it and applied it to a monomdispersed particles population. The detailed algorithm is as follows:

(1): estimate the initial values for V_{pol}, V_p, V_d and V_w

(2): $\phi_p^p = V_{pol}/V_p$

(3): assume $\phi_A^p = (1-\phi_p^p)V_A/(V_A+V_B)$

(4): $\phi_B^p = 1-\phi_A^p-\phi_p^p$

(5): assume $\phi_A^d = V_A/(V_A+V_B)$

(6): $\phi_B^d = 1-\phi_A^d$

(7): calculate V_A^w and V_B^w using equation 20.22

(8): calculate V_A^d and V_B^d using equation 20.13, then obtain $\phi_A^d = V_A^d/(V_A^d+V_B^d)$; $\phi_B^d = 1-\phi_A^d$

(9): calculate ϕ_A^p, ϕ_B^p using equation 20.14, and ϕ_P^p

(10): V_A^p and V_B^p can be calculated using equation 20.21

(11): obtain new V_p, V_{wt}, V_d using equations (20.18), (20.19), (20.20)

(12): repeat steps 7~11 until convergence in V_p is reached

It is important to realize that steps 3 and 5 represent a crucial assumption used in this algorithm which is that the volume fraction of monomer A in polymer particles and monomer droplets can be approximated as the overall volume fraction of monomer A in the feed at the beginning of the reaction. The assumption in step 3 is justified for two reasons (1): there is no polymer in the polymer particles at the beginning of the reaction and ϕ_A^p calculated in step 3 is an initial guess; (2): ϕ_A^p is recalculated in step 9. The assumption in step 5 is justified by the work of Maxwell et al.(1992b, 1993) and ϕ_A^d is recalculated in step 8.

After implementing Armitage's algorithm, the model was tested for the validity of the algorithm. In the model testing phase, a copolymerization of styrene/methyl methacrylate was employed using a

conventional recipe (Sty: 50g, MMA: 50g, SDS: 6.25g, KPS: 1.25g, water: 1L, Temperature: 50 °C). Testing results are presented in figures 20.1~20.3. Figure 20.1 shows the change of monomer concentration in the polymer particles. It is clear that in stages I and II, monomer concentration in the polymer particles increases as convention and particle size increases. After 30% conversion, the concentration for both monomers in polymer particles starts to decrease due to the depletion of monomer droplets. Figure 20.2 displays the change of total volume of all three phases. The total volume of monomer droplets decreases from the very start of the reaction and it gradually goes to zero around 30%, which marks the end of stage II. The total volume of polymer particles increases before 30% due to particle growth in stages I and II. It then decreases after 30% (in stage III) due to the density difference between monomer and polymer. The total volume of the aqueous phase remains nearly constant throughout the entire reaction. Figure 20.3 shows the changes of the volume of each individual monomer in all three phases. It is satisfactory to observe that both monomers disappear in monomer droplets at about the same time (around 30%). Finally, figure 20.4 verifies one important monomer partitioning characteristic in emulsion copolymerization, i.e., the ratio of monomer volume (V_A^p/V_B^p) in polymer particles is nearly identical to the ratio of V_A^d/V_B^d in monomer droplets. It is satisfactory to see that the current model is able to describe all important monomer partitioning characteristics in emulsion copolymerization correctly.

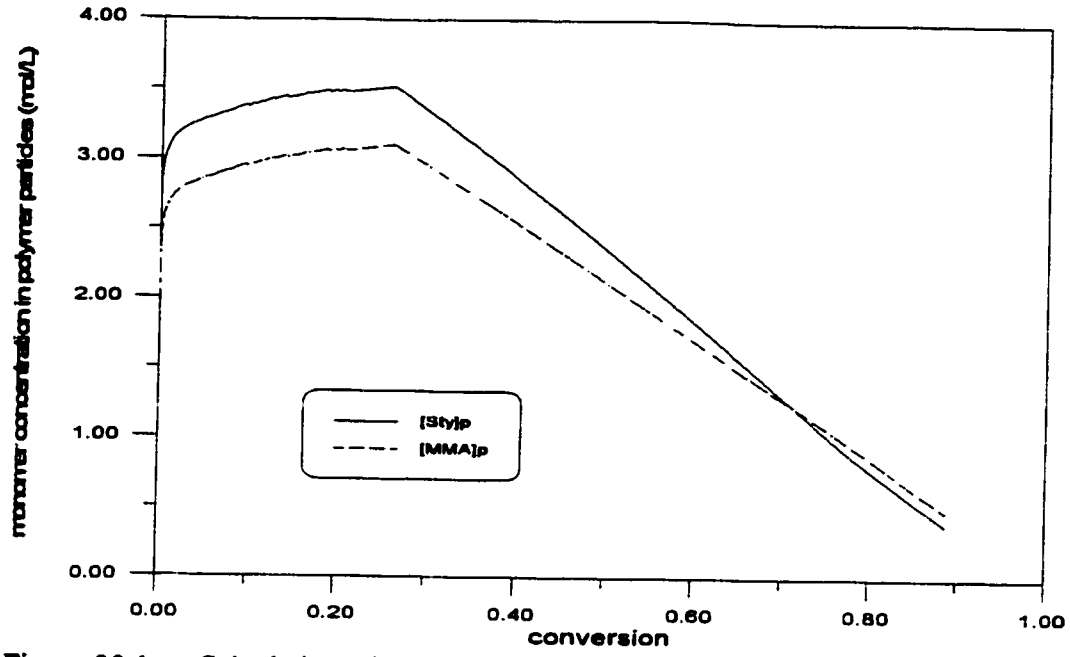

Figure 20.1 Calculation of Monomer Concentration in Polymer Particles in Styrene and Methyl Methacrylate Emulsion Copolymerization

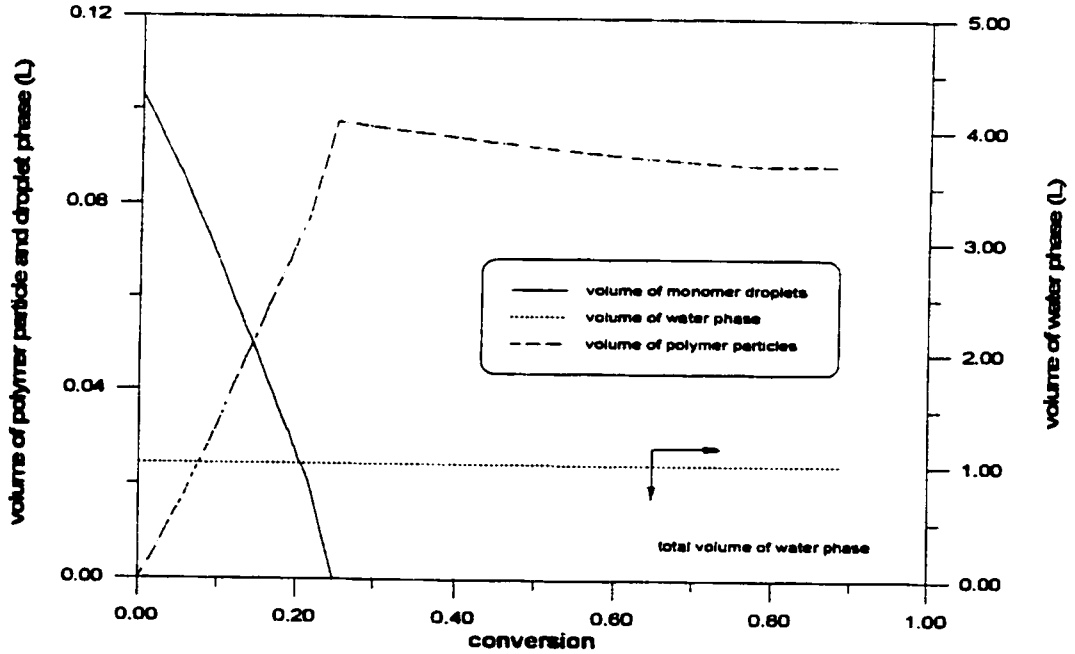

Figure 20.2 Total Volume of All Three Phases in Styrene and Methyl Methacrylate Emulsion Copolymerization

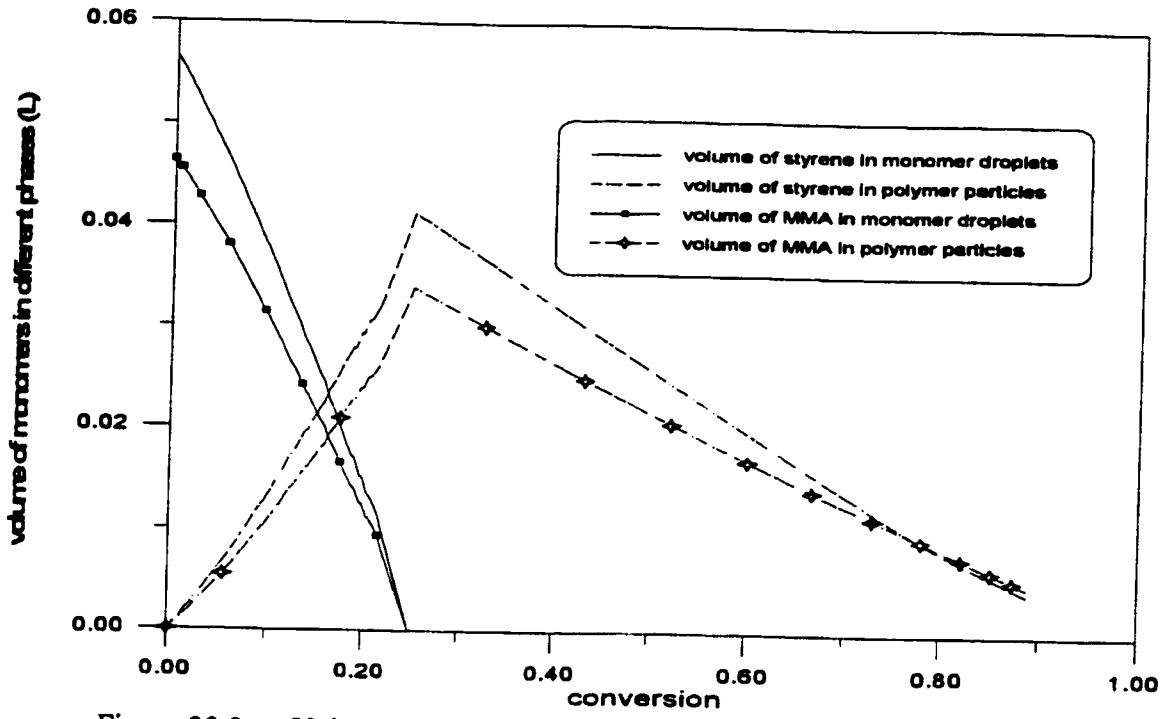

Figure 20.3 Volume of Individual Monomers in Different Phases.

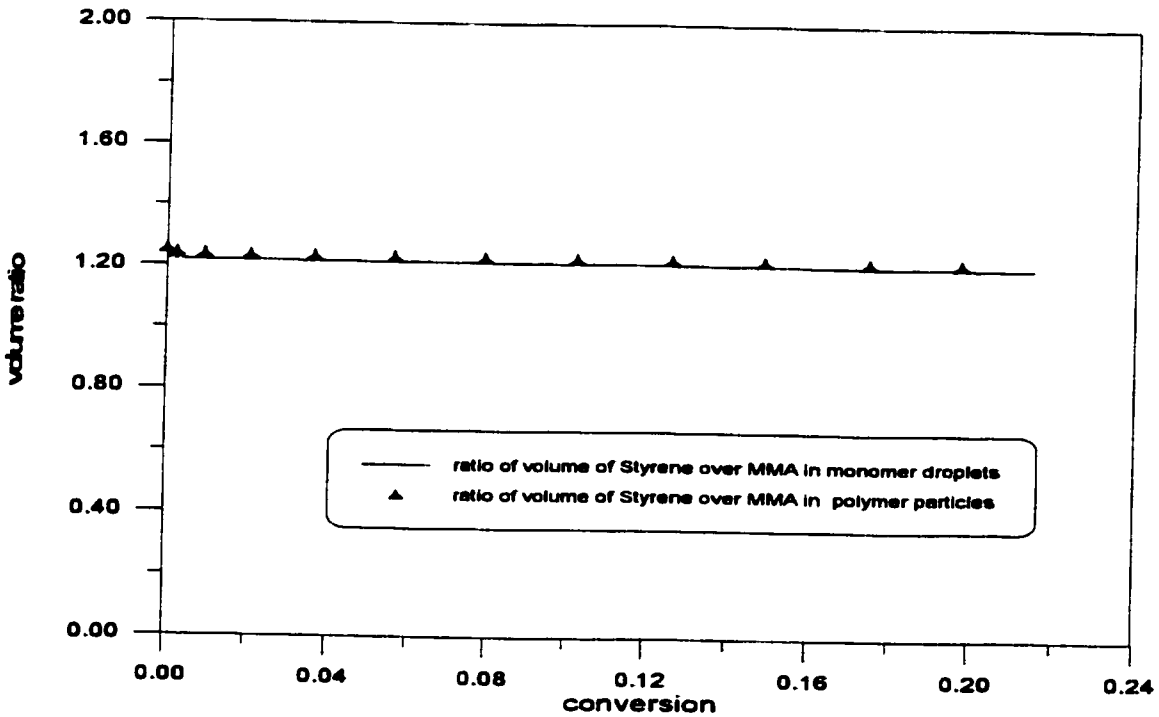

Figure 20.4 Comparison of Ratio of Volume of Styrene over Methyl Methacrylate in Monomer Droplets and Polymer Particles.

20.3 Desorption in Copolymerization

Desorption for emulsion homopolymerization has already been discussed in section 15.4. Expressions for rate constant for desorption proposed by Asua et al.(1989) and Nomura and Harada (1981) have been closely examined and compared. Asua's expression is chosen and implemented into the current model for its advantages and generality. It must be stated that Asua's expression (equation 15.62) is only applicable for emulsion homopolymerization. It must be modified when applied to emulsion copolymerization. Forcada and Asua (1990) derived a new expression for the overall rate constant for desorption in emulsion copolymerization as follows:

$$\bar{k}_{des} = k_{des,A} + k_{des,B} \tag{20.23}$$

$k_{des,A}$ and $k_{des,B}$ in equation 20.23 are the rate constants for desorption of monomeric radicals of type A and B, respectively. They can be calculated as follows:

$$k_{des,i} = (k_{fm,A}P_A + k_{fm,B}P_B)[M_i]_p \frac{K_{o,i}}{\beta_i K_{o,i} + k_{p,A}[M_A]_p + k_{p,B}[M_B]_p} \tag{20.24}$$

where (i=A *or* B):

$$P_A = \frac{k_{p,BA}[M_A]_p}{(k_{p,BA}[M_A]_p + k_{p,AB}[M_B]_p)} \tag{20.25}$$

$$P_B = 1 - P_A \tag{20.26}$$

$$\beta_i = \frac{k_{pw,iB}[M_B]_w + k_{tw,iB}[R\cdot]_w}{k_{pw,iB}[M_B]_w + k_{tw,iB}[R\cdot]_w + k_{cp,i}[N_p] + k_{cm,i}[MIC] + k_{z,i}[Z]_w} \tag{20.27}$$

$k_{cp,i}$: rate constant for radical absorption by polymer particles for monomer i

$k_{cm,i}$: rate constant for radical absorption by micelles for monomer i

$k_{z,i}$: rate constant for chain transfer to inhibitor for monomer i

$k_{fm,i}$: rate constant for chain transfer to monomer for monomer i

$K_{o,i}$ in equation 20.24 can be calculated using equation 15.63. It has been verified by Asua et al.(1989) and Forcada and Asua (1990) that expression 20.23 can adequately calculate the overall rate constant

for desorption in emulsion copolymerization. This expression has been implemented into the current model.

20.4 Simulation of Copolymerization of Styrene/MMA in Emulsion

A number of groups have studied this copolymer system in their kinetic studies of emulsion copolymerization. Among them, Nomura's group has performed many experiments. This group also developed a model to simulate styrene/MMA emulsion copolymerization. Nomura et al.(1982) first quantified desorption in emulsion copolymerization of this system due to the presence of MMA. Nomura et al.(1982) also investigated monomer partitioning in this copolymer system. Monomer concentration for both monomers in polymer particles was expressed as a function of weight fraction of MMA (w_{md}) in monomer droplets as shown below:

$$[M_{Sty}]_p = 22.4 \frac{1-w_{md}}{4-w_{md}} \tag{20.28}$$

$$[M_{MMA}]_p = 27.6 \frac{w_{md}}{5-w_{md}} \tag{20.29}$$

Nomura et al.(1988) further studied monomer partitioning of this copolymer system when concentration of emulsifier was in the vicinity of CMC. The same group (Nomura et al., 1983) later proposed a method of solving for $\bar{n}$. Nomura et al.(1985, 1989) presented detailed model development and tested their model with experimental data for conversion, copolymer composition and monomer concentration in polymer particles. Research work from Nomura's group provides both kinetic information for model development and experimental data for model testing.

Asua's group also developed a model to simulate emulsion copolymerization of styrene/MMA. They carried out experiments to collect data for their model testing. Forcada and Asua (1990) presented their model development in detail. An expression for the overall rate constant for desorption was derived (equation 20.23). The same group (Forcada and Asua, 1991) presented a method to calculate molecular weight averages for this copolymer system. Experimental work from Asua's group is a

good data source for model testing. Model testing results using their reported data are presented in section 20.5.

Other research groups also investigated the kinetics of emulsion copolymerization of this copolymer system. Goldwasser and Rudin (1982) provided some kinetic information for the rate constant of cross chain transfer to monomer. They also presented their estimates of reactivity ratios. Rio et al.(1985) focused their work on how physical properties of this copolymer are affected by polymer composition. Models that can simulate this copolymer system were also developed by Richards et al.(1989) and Dougherty (1986a, b). Both groups tested their models with experimental data from Nomura's group. Their research provides a lot of kinetic information for many key parameters.

20.5 Model Testing Results

Nomura et al.(1982)

Nomura et al.(1982) performed a number of experiments under various reaction conditions. Figure 20.5 presents four runs with various amounts of initiator (KPS). The agreement between model predictions and reported conversion data is very good. Limiting conversion was observed in all four runs, and this is expected since the reaction temperature is well below the Tg of copolymer. The effect of emulsifier on the rate of polymerization is shown in figure 20.6. It is satisfactory to see that the current model delivers reliable predictions on conversion versus time profiles under a wide range of reaction conditions. Nomura et al.(1982) reported the total number of particles per liter of water for the runs shown in figure 20.6. Comparison of predictions from the current model and the experimental data is shown in figure 20.7. It is obvious that particle nucleation was completed within 5~10% conversion, and the total number of particles in all four runs remained very stable in the subsequent course of the reaction. This important particle nucleation characteristic is adequately described by the model.

The effect of monomer feed composition on the rate of reaction was studied by Nomura et al.(1982) in a number of runs. Simulation results are presented in figure 20.8. Copolymerizations with higher

styrene content exhibit lower rate of polymerization, as expected.

Copolymer composition is simulated by our model in figure 20.9. The good agreement between our model predictions and reported measurements shown in figure 20.9 indicates the important fact that the estimation of reactivity ratios from bulk/solution copolymerization can be used for the same copolymer system in emulsion copolymerization provided monomer partitioning is solved for satisfactorily. Model testing results for monomer partitioning for this copolymer system are given in figures 20.10 and 20.11. Nomura et al.(1982) reported monomer concentration of styrene and MMA in polymer particles throughout the entire course of the reaction. The solid lines in figures 20.10 and 20.11 are model's predictions by solving for thermodynamic equilibrium equations using Armitage's algorithm (described in section 20.2). It is very satisfactory to see that the model can adequately describe the monomer concentration changes at all five different monomer feed ratios. The good agreement also further confirms the validity of Armitage's algorithm.

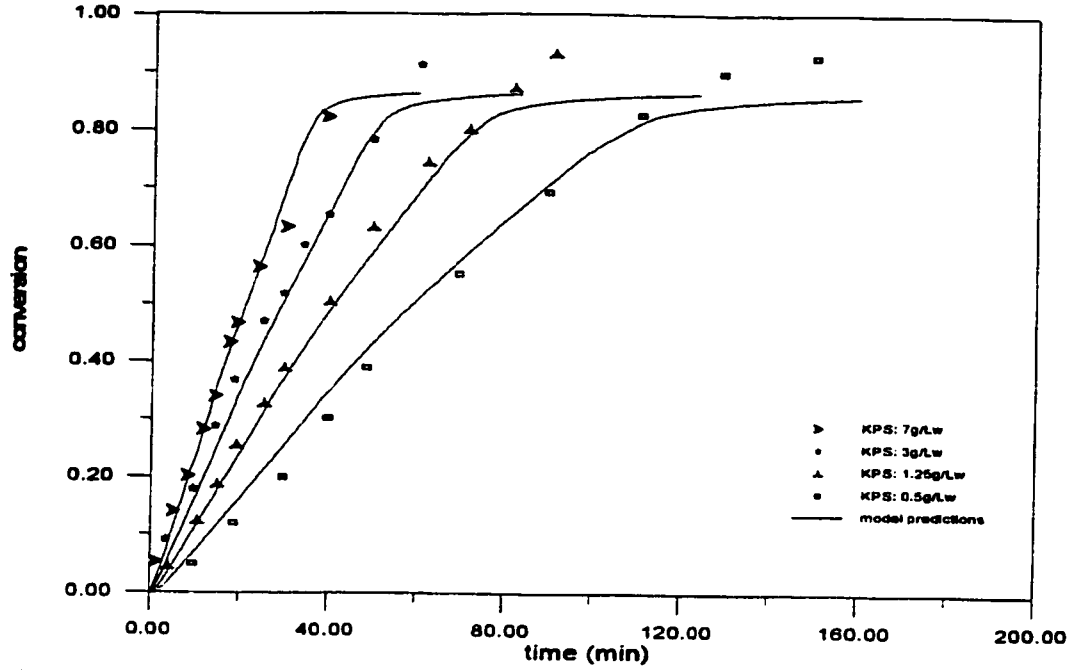

Figure 20.5 Simulation of Styrene/Methyl Methacrylate Emulsion Copolymerization at 50°C.
Styrene: 100 g/Lw, MMA: 100 g/Lw, SDS: 6.25 g/Lw

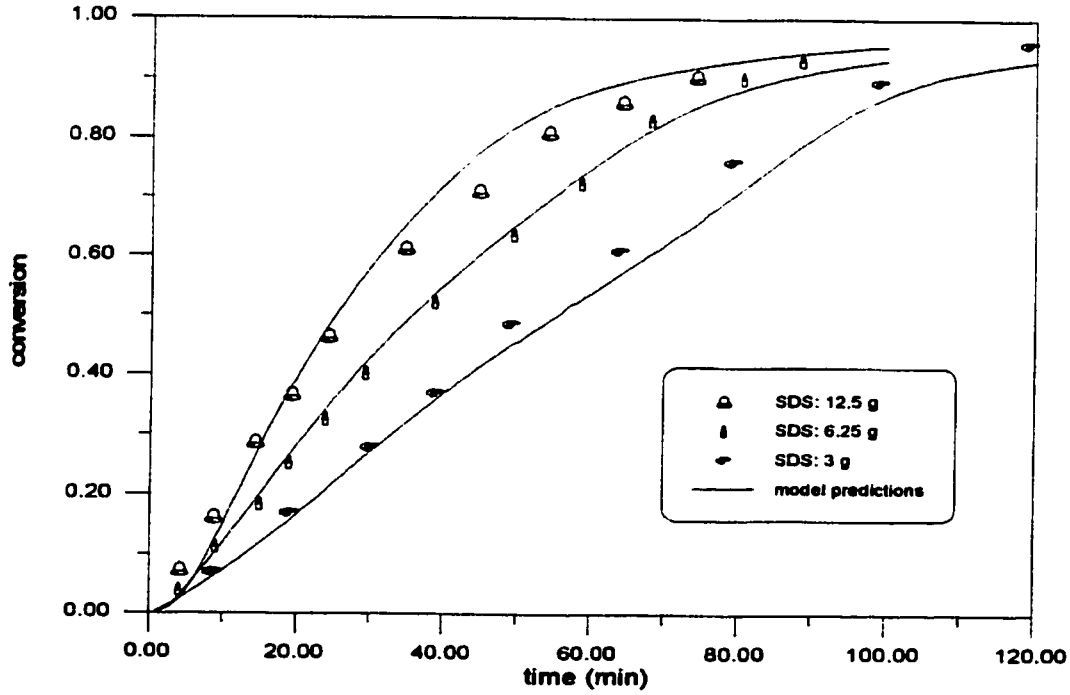

Figure 20.6 Simulation of Styrene/Methyl Methacrylate Emulsion Copolymerization at 50°C.
Styrene: 100 g/Lw, MMA: 100 g/Lw, KPS 1.25 g/Lw.

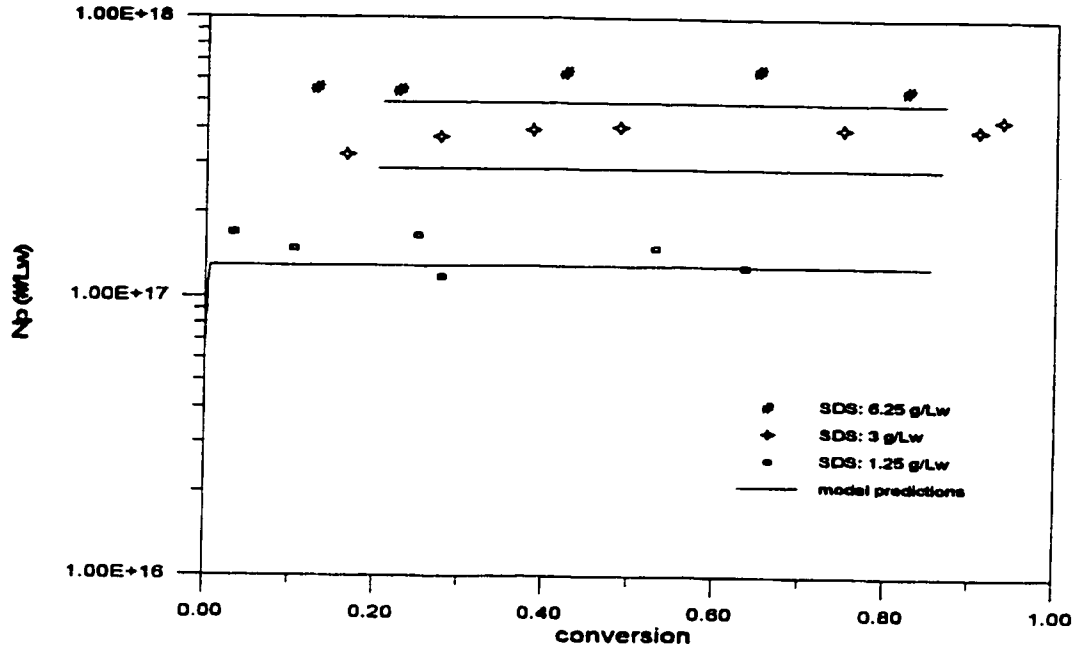

Figure 20.7 Prediction of Number of Particles in Styrene/Methyl Methacrylate Emulsion Copolymerization at 50°C.
Styrene: 100 g/Lw, MMA: 100 g/Lw, KPS 1.25 g/Lw.

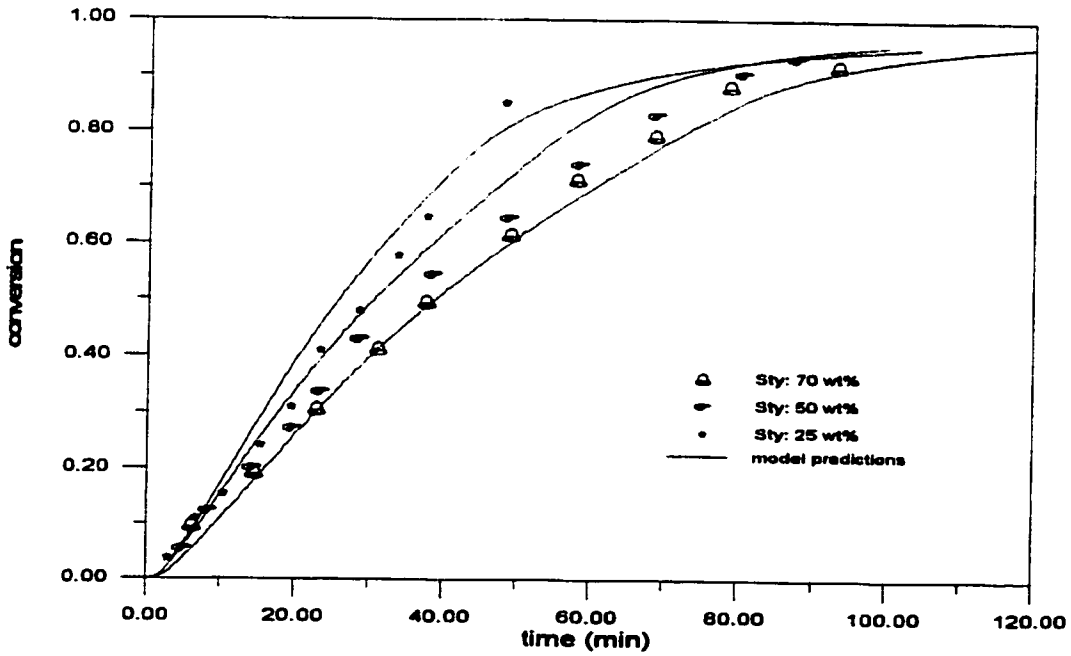

Figure 20.8 Simulation of Styrene/Methyl Methacrylate Emulsion Copolymerization at Various Monomer Feeds.
Styrene: 100 g/Lw, MMA: 100 g/Lw, SDS 6.25 g/Lw, KPS: 1.25 g/Lw.

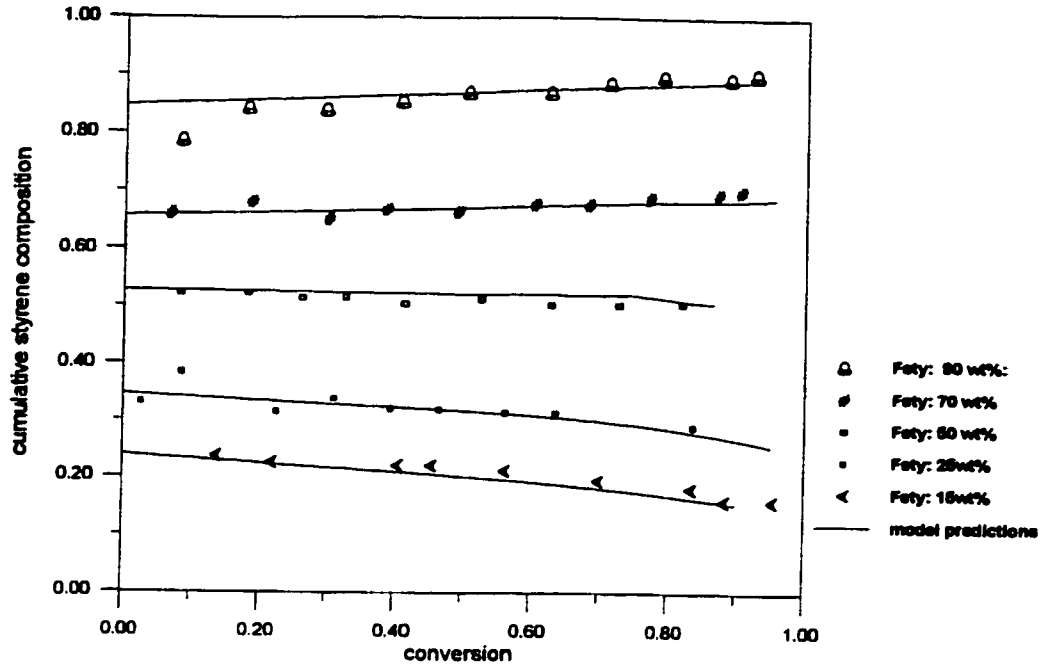

Figure 20.9 Calculation of Copolymer Composition in Styrene and Methyl Methacrylate Emulsion Copolymerization at 50°C.

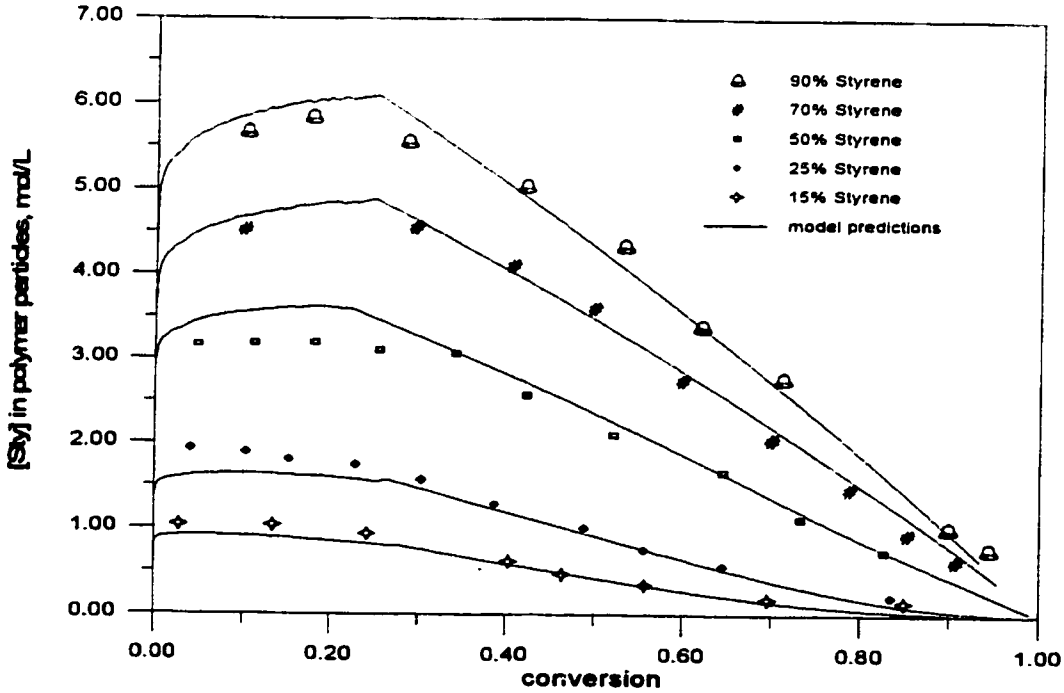

Figure 20.10 Prediction of Styrene Concentration in Polymer Particles by Solving Thermodynamic Equilibrium Equations.

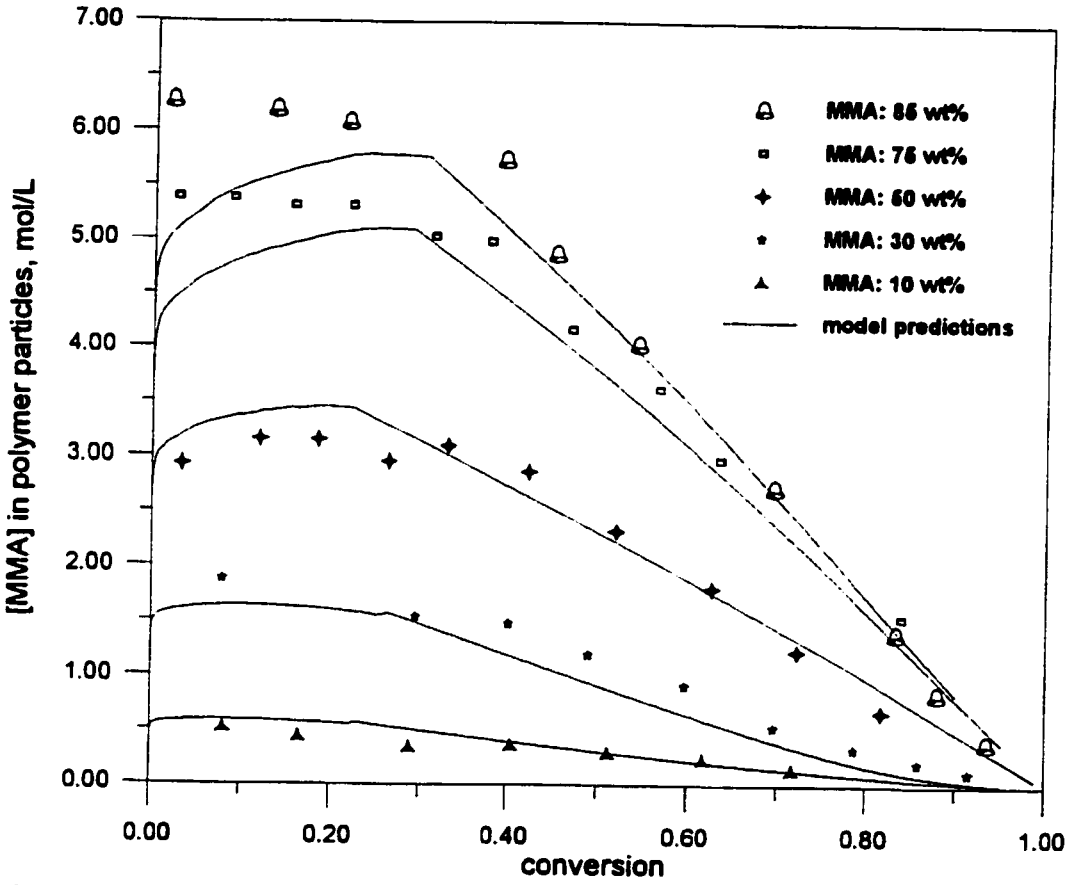

Figure 20.11 Prediction of Methyl Methacrylate Concentration in Polymer Particles by Solving Thermodynamic Equilibrium Equations.

Forcada and Asua (1990, 1991)

Another good data source for model testing is the work from Forcada and Asua (1990). This group performed a set of five runs at various monomer feed compositions. The molar ratio of styrene in the monomer feed ranged from 10 to 90%. Comparison of our model's predictions and reported conversion profiles are presented in figures 20.12~20.15. In some of their runs (figures 20.13~20.15), noticeable induction time was observed at the beginning of the reaction. The model predictions for copolymer composition for all five runs are displayed in figure 20.16 along with reported data. The agreement is good. Based on the model testing results in figures 20.9 and 20.16, it can be stated that the Mayo-Lewis equation derived for bulk/solution polymerization can still be used in copolymerization as long as monomer partitioning is adequately solved for.

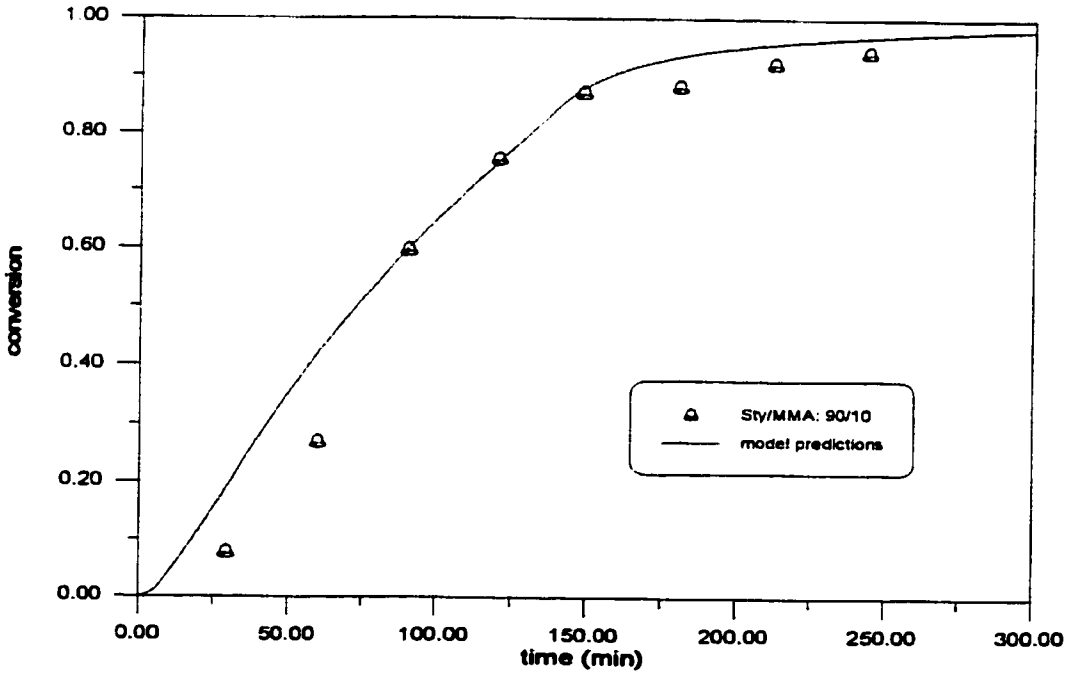

Figure 20.12 Simulation of Styrene and Methyl Methacrylate Emulsion Copolymerization at 50 °C.
Sty+MMA: 90 g, KPS: 0.18 g, SDS: 2.25 g, water: 270 g.

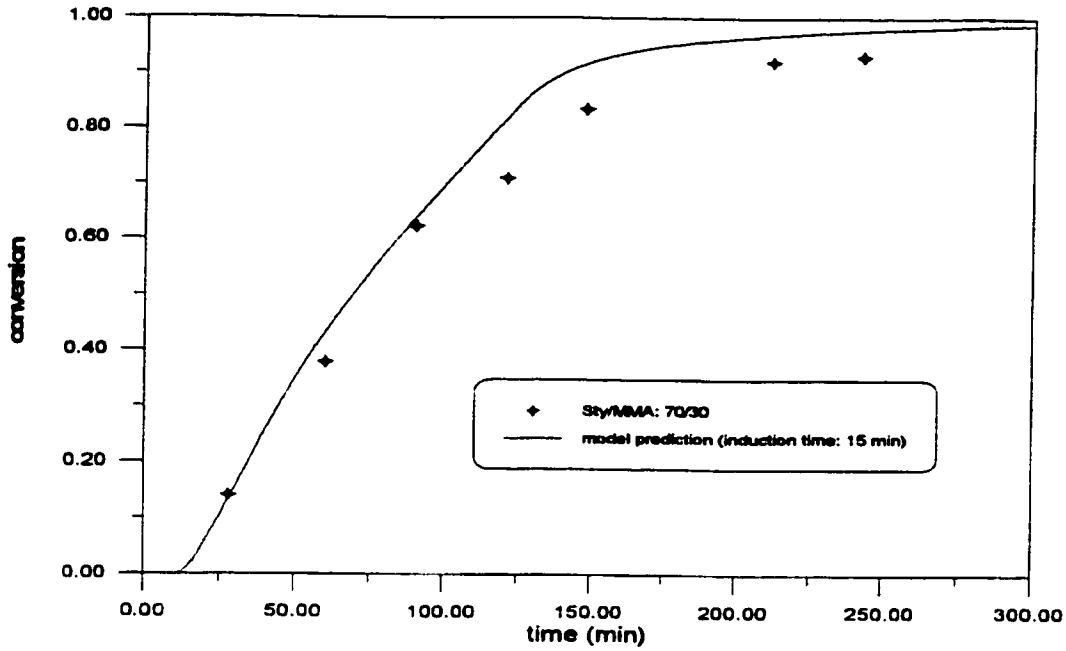

Figure 20.13 Simulation of Styrene and Methyl Methacrylate Emulsion Copolymerization at 50 °C.
Sty+MMA: 90 g, KPS: 0.18 g, SDS: 2.25 g, water: 270 g.

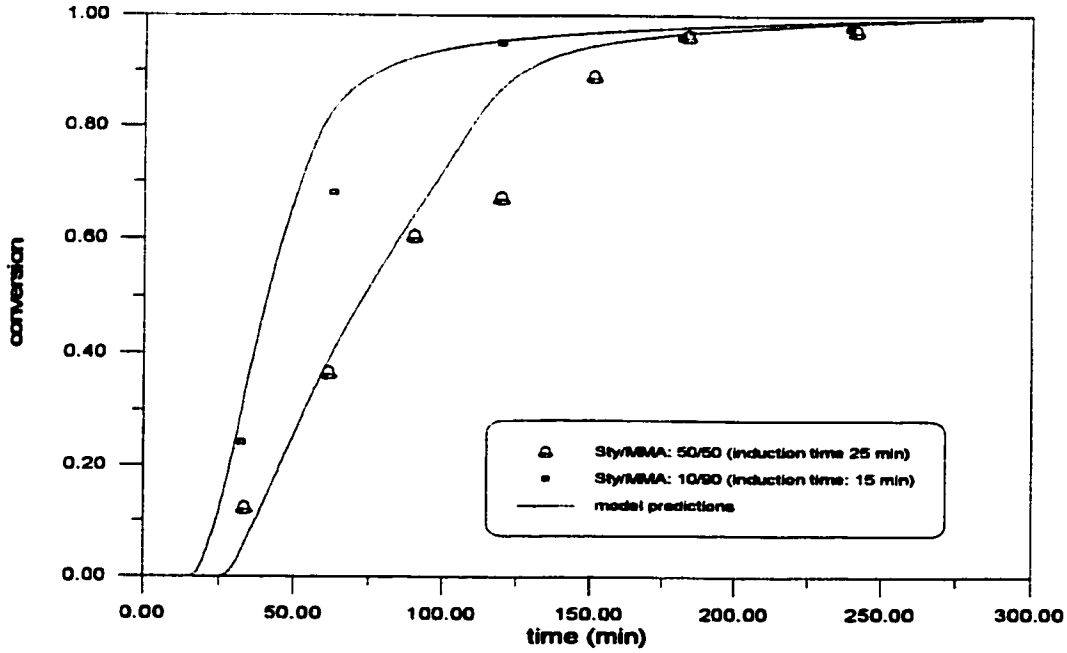

Figure 20.14 Simulation of Styrene and Methyl Methacrylate Emulsion Copolymerization at 50°C.
Sty+MMA: 90 g, KPS: 0.18 g, SDS: 2.25 g, water: 270 g.

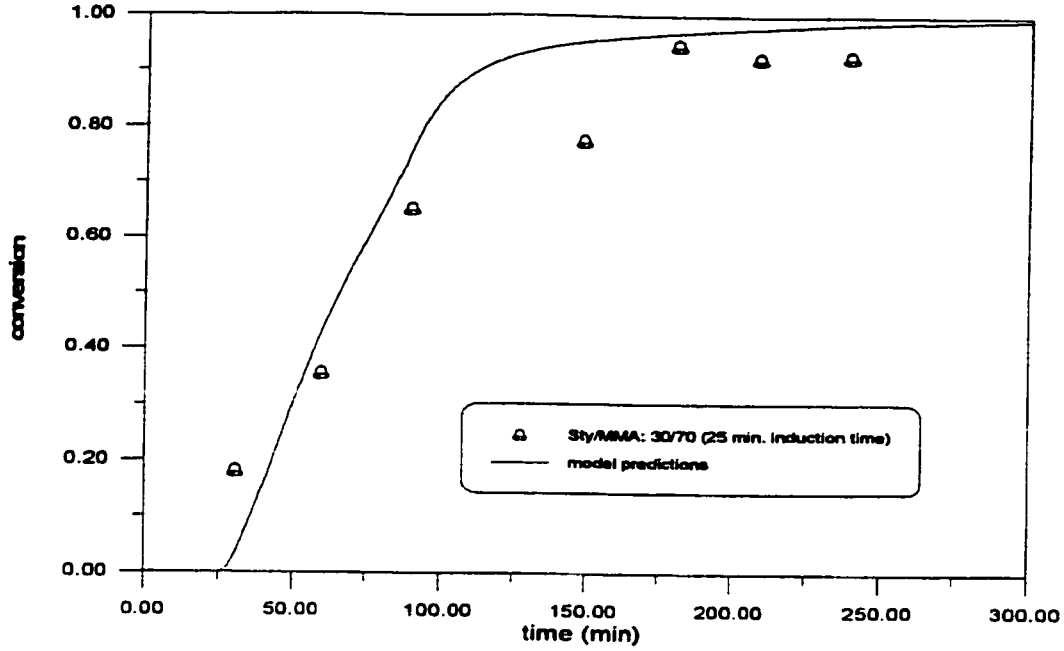

Figure 20.15 Simulation of Styrene and Methyl Methacrylate Emulsion Copolymerization at 50°C.
Sty+MMA: 90 g, KPS: 0.18 g, SDS: 2.25 g, water: 270 g.

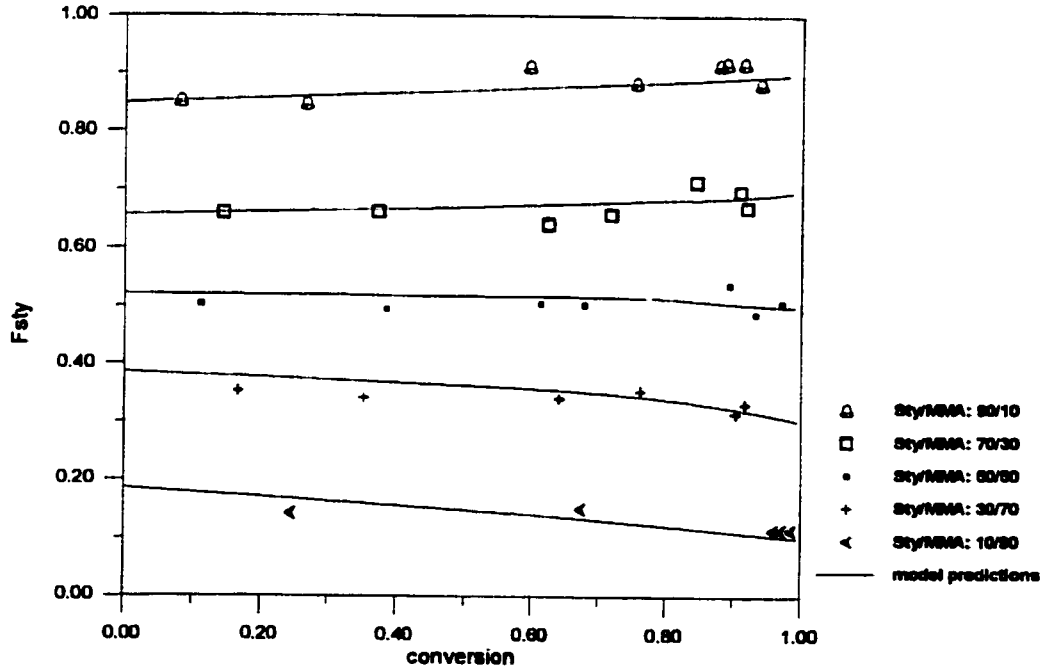

Figure 20.16 Simulation of Styrene and Methyl Methacrylate Emulsion Copolymerization at 50°C.
Sty+MMA: 90 g, KPS: 0.18 g, SDS: 2.25 g, water: 270 g

Chapter 21. Concluding Remarks and Future Work

21.1 Concluding Remarks

The deliverable from this project is a comprehensive simulation package for multicomponent free-radical polymerization in bulk, solution and emulsion. The extensive research effort provides better understanding of the kinetics of homo-/co-/terpolymerization of many monomer systems. The literature review and model testing presented in this thesis are believed to be the most extensive so far in the literature. Important aspects of bulk/solution and emulsion polymerization have been discussed. The simulation package has been tested extensively for many monomer systems with experimental data. In most cases, model predictions are satisfactory and this confirms the reliability of this simulation package.

In the testing of bulk/solution copolymerization, Sty/2-HEA is found to be a problematic system, mainly due to difficulties in monomer purification and polymer characterization. A better understanding of the kinetics of this copolymer system could be obtained if more experiments are carried out with extra care.

The kinetic investigation and simulation of terpolymerization of BA/MMA/VAc over the entire conversion range has been conducted for the first time. The satisfactory simulation results mark the successful accomplishment of the long-term project of developing a general and flexible simulation package for multicomponent polymerization. Bulk BA/MMA/VAc terpolymerization exhibited a similar "double-rate phenomenon" observed in BA/VAc and MMA/VAc copolymerizations. Solution terpolymerization of BA/MMA/VAc revealed that toluene has a significant effect on reaction kinetics, and all these aspects are adequately described by the model. Due to the scarcity of available experimental data, the model was not tested extensively for terpolymerization. More experiments on other terpolymer systems will provide valuable model testing material. The solvent effect of toluene on reaction kinetics is also worthy of future investigation.

The emulsion model is one of the very few that can simulate emulsion homo-/copolymerization under

a very wide range of reaction and operation conditions (batch, semibatch, seeded or unseeded, etc.). Important physicochemical phenomena (particle nucleation, absorption and desorption of radicals, monomer partitioning and gel effect) occurring in emulsion polymerization have all been addressed. Monomer partitioning in both homo- and copolymerization is solved either empirically (using partitioning coefficients) or via thermodynamic equilibrium equations . Great effort has been made to keep the model structure simple yet still rigorous.

The extensiveness of the database of this simulation package is the most important feature that makes this package distinct from other models presented in the literature. It utilizes the database from the homopolymerization package of Gao and Penlidis (1996) with additional information for co-/terpolymerization. The database contains physical/chemical information for many monomers, initiators, emulsifiers, solvents and other polymerization ingredients. The richness of the database and its structure provide both the bulk/solution model and the emulsion model with great flexibility to simulate homo-/co-/terpolymerization for different recipes under a wide range of conditions.

21.2 Future Work

The last objective in the long term goals concerning bulk and solution polymerizations is to extend this model to simulate multicomponent polymerization, an area of very limited understanding and experimental information.

As for the emulsion model, after the mathematical model frame is established, it should be further tested for many homo-/copolymer systems. It will also be extended to simulate terpolymerization emulsion polymerization. A systematic approach involving careful experimental design and polymer property measurements would definitely provide valuable information for model development, parameter estimation and model testing.

It is believed that after this effort of developing and testing this simulation package, it will prove to be a very useful tool for various industrial and research applications as it was demonstrated in

previous publications (Gao and Penlidis, 1996, 1998). As an epilogue with respect to the philosophy behind modelling of free-radical polymerization in general (admittedly, a largely unstudied and controversial subject), we ought to agree with the following comment: "... It is the mark of an instructed mind to rest satisfied with the degree of precision which the nature of the subject permits and not to seek an exactness where only an approximation of the truth is possible" (Aristotle, many centuries ago).

Nomenclature

a	partition coefficient for monomer radicals between aqueous and polymer phases, defined in equation 15.61
a	root-mean-square end-to-end distance per square root of the number of monomer units
A	parameter in free volume model
A_{mic}	total surface area of free micelles , dm^2
A_{md}	total surface area of monomer droplets, dm^2
A_p	total surface area of polymer particles, dm^2
B	parameter in free volume model
B_{n3}	number of trifunctional branch points per polymer chain
B_{n4}	number of tetrafunctional branch points per polymer chain
Cp	heat capacity, cal/mol·K
CTA	chain transfer agent
[CTA]	concentration of chain transfer agent, mol/L
$[CTA]_w$	concentration of chain transfer agent dissolved in water, mol/L
d_p	diameter of polymer particle, dm
D_{po}	initial diffusivity of monomer radicals in polymer phase, dm^2/s
D_p	diffusivity of monomer radicals in polymer phase, dm^2/s
D_w	diffusivity of monomer radicals in water phase, dm^2/s
f	initiator efficiency
F	radical capture efficiency
F_j^{in}	inlet flow rate of species i, mol/min
F_j^{out}	outlet flow rate of species i, mol/min
f_i	mole fraction of monomer type i in the monomer feed
F_i	mole fraction of monomer type i in the polymer chain
ΔH	reaction enthalpy, cal/mol
H	enthalpy, cal/mol

H_o	enthalpy at reference temperature of T_o, cal/mol
I	initiator
[I]	concentration of initiator, mol/L
$[I]_w$	concentration of initiator dissolved in water, mol/L
j_c	monomer units per segment
j_{cr}	critical chain length at which water phase radical can be absorbed
ΔG_i	Gibbs free energy for species i
k_{cp}	rate constant of radicals captured by polymer particles, L/min,
k_{cm}	rate constant of aqueous phase radicals captured by micelles, L/min
k_d	rate constant of initiator decomposition, 1/min
k_{des}	rate constant of desorption, 1/min
k1	rate constant of reaction 15.4, L/mol·min
k2	rate constant of reaction 15.5, L/mol·min
k_{fcta}	rate constant of transfer to chain transfer agent, L/mol·min
k_{fm}	rate constant of chain transfer to monomer, L/mol·min
k_{ft}	rate constant of chain transfer to small molecules, L/mol·min
k_p	rate constant for propagation, L/mol·min
k_p^*	rate constant for chain transfer to terminal double bond, L/mol·min
k_p^{**}	rate constant for chain transfer to internal double bond, L/mol·min
k_{pw}	rate constant for propagation in aqueous phase, L/mol·min
k_t	overall rate constant for termination, L/mol·min
k_3	free volume parameter
$k_t\%$	percentage of termination reaction by combination
k_{t12}	rate constant for cross termination, L/mol·min
k_{tw}	rate constant for termination in water phase, L/mol·min
k_{wp}	partition coefficient defined in equation 15.46
k_z	rate constant of chain transfer to inhibitor, L/mol·min
m_d	partition coefficient for monomer radicals between aqueous phase and polymer phase

M	monomer
$[M]$	monomer concentration, mol/L
$[M]_p$	monomer concentration in polymer particles, mol/L
$[M]_w$	monomer concentration in water phase, mol/L
$[M]_{w,sat}$	saturated concentration in aqueous phase at saturation level in homopolymerization of the monomer, mol/L
MIC	micelles
[MIC]	micelle concentration in water phase, mol/L
M_n	instantaneous number average molecular weight, Daltons
M_w	instantaneous weight average molecular weight, Daltons
$\bar{M}_n$	accumulated number average molecular weight, Daltons
$\bar{M}_w$	accumulated weight average molecular weight, Daltons
MW_M	molecular weight of monomer
n	number of radicals
$\bar{n}$	average number of radicals per particle
N_A	Avogadro's number, 6.02×10^{23} molecules/mol
N_{Fe}^{2+}	number of moles of Fe^{2+} ions
N_{Fe}^{3+}	number of moles of Fe^{3+} ions
$N_i(V)$	number of particles containing i number of radical of volume V
N_j	number of moles of species j
$N_{p\,homo}$	number of particles generated by homogeneous nucleation
$N_{p\,mic}$	number of particles generated by micellar nucleation
N_p	total number of polymer particles
N_n	number of polymer particles contain n radicals
N_{seed}	total number of seeds
P	polymer
P_r	polymer of chain length r
r_1, r_2	reactivity ratios

r_{mic}	radius of micelle, dm
r_p	radius of particle, dm
R	gas constant, 1.987 cal/mol·K
$R_1\cdot$	radicals of monomer type 1
$R_2\cdot$	radicals of monomer type 2
RA	reducing agent
[RA]	concentration of reducing agent, mol/L
R_c	rate of radical capture
R_I	rate of initiation, mol/L·min
R_{It}	rate of thermal initiation, mol/L·min
$R_j\cdot$	radical with j monomer units
$[R_r\cdot]$	concentration of free radical of chain length r, mol/L
$[R\cdot_1]_w$	concentration of free radicals of chain length 1 in the water phase, mol/L
$[R\cdot_j]_w$	concentration of free radicals of chain length j in the water phase, mol/L
$[R\cdot_o]_w$	concentration of primary free radicals in the water phase, mol/L
$[R\cdot]$	free radical concentration, mol/L
$[R\cdot]_w$	total free radical concentration in the water phase, mol/L
$R_o\cdot$	primary radical without monomer fragment
R_p	rate of polymerization
$R_r\cdot$	radical of chain length r
R_t	rate of termination
S_a	area covered by one molecule of emulsifier, dm^2/molecule
S	solvent
[S]	solvent concentration, mol/L
$[S]_{cmc}$	critical micellar concentration, mol/L
$[S]_t$	total concentration of surfactant, mol/L
T	temperature, K
T	a small molecule
T_o	reference temperature, K

Tg_j	glass transition temperature of component j, K
T_{jacket}	temperature of reactor jacket, K
T_r	temperature of reactor
UA	product total heat transfer coefficient and area, cal/K
V_d	total volume of monomer droplets, L
V_f	free volume of the system, L
V_{fcri}	critical free volume at which propagation become diffusion controlled, L
V_{fj}^o	free volume of component j at its glass transition temperature, L
V_j	volume of component j, L
V_j	volume of component j in all phases, L
V_j^w	volume of component j aqueous phase, L
V_j^p	volume of component j in polymer particles, L
V_j^d	volume of component j in monomer droplets, L
V_m	molar volume of monomer, L
V_{mseed}	molar volume of monomer in the seed, L
V_{latex}	total volume of latex, L
v_p	average volume of a polymer particle, L
V_p	total volume of polymer particles, L
V_{pseed}	volume of polymer in the seed, L
V_R	active reactor volume, L
V_{seed}	total volume of seeds, L
V_w	total volume of water, L
V_{wt}	total volume of aqueous phase, L
W_j	weight fraction of component j in the copolymer chain
w_p	weight fraction of polymer
x	monomer conversion level
x_c	conversion level at the end of interval II in emulsion polymerization
x_{seed}	final conversion in seeds
z	critical chain length at which water phase radicals can be irreversibly absorbed

Z	inhibitor
$[Z]$	concentration of inhibitor, mol/L
$[Z]_w$	concentration of inhibitor dissolved in water, mol/L

Greek Letters

α_j	free volume expansion coefficient of species j
τ	parameter used to calculate molecular weights
β	parameter used to calculate molecular weights
ϵ	ratio of radical absorption between micelles and particles, used in equation
σ	surface tension, dyn/cm
σ	Lennard-Jones parameter
ρ_m	density of monomer, g/cm^3
ρ_p	density of polymer, g/cm^3
ρ_{des}	rate of desorption, mol/L·min
ϕ	cross termination factor
ϕ_j^p	volume fraction of species j in polymer particles
ϕ_j^d	volume fraction of species j in monomer droplets
ϕ_j^w	volume fraction of species j in aqueous phase
ϕ_j	volume fraction of species j
ϕ_p^p	volume fraction of polymer in polymer particles
$\chi_{i,j}$	interaction coefficient between species i and j

Subscripts

j	reacting species
i, j	monomer type
m	monomer
p	polymer

p	polymer particles
d	monomer droplets
w	aqueous phase

Superscripts

p	polymer particles
d	monomer droplets
w	aqueous phase

References on Emulsion (Volume 2)

Adams, M.E., Napper D.H., Gilbert R.G. and Sangster D.F.(1986) *J. Chem. Soc. Faraday Trans.* **82**, 1979

Adhikari, M.S., Sarkar, S., Banerjee, M., and Knoar, R.S.(1987). Thermal Decomposition of Potassium Persulfate in Aqueous Solution at 50°C in the Presence of Ethyl Acrylate. *J.Appl.Polym.Sci.* **34**, 109-125.

Alexander, A.E. and D.H. Napper (1971) Emulsion Polymerization, in: D.P. Jensen (Ed.), Progress in Polymer Science, Pergamon Press, Oxford, New York, 145-197.

Allen P. E. M. and Patrick C. R. (1974) *Kinetics and Mechanisms of Polymerization Reactions.* John Wiley&Sons, New York, London, Syndey, Toronto.

Anderson H.M. and Proctor S.I.(1965) Redox Kinetics of the Peroxydisulfate-iron-sulfoxylate System. *J. Polym. Sci.* **A3**, 2343

Armitage, P.D., De La Cal, J.C., and Asua, J.M.(1994). Improved Methods for Solving Monomer Partitioning in Emulsion Copolymer Systems. *J.Appl.Polym.Sci.* **51**, 1985-1990.

Arzamendi, G., Leiza, J.R., and Asua, J.M.(1991). Semicontinuous Emulsion Copolymerization of Methyl Methacrylate and Ethyl Acrylate. *J.Polym.Sci.Chem.* **29**, 1549-1559.

Arzamendi, G., Leiza, J.R., and Asua, J.M.(1991). Semicontinuous Emulsion Copolymerization of Methyl Methacrylate and Ethyl Acrylate. *J.Polym.Sci.Chem.* **29**, 1549-1559.

Asua J.M., Adams M.E. and Sudol E.D.(1990) A New Approach for the Estimation of Kinetic Parameters in Emulsion Polymerization Systems. I. Homopolymerization under Zero-One Conditions. *J.Appl.Polym.Sci.* **39**, 1183-1213

Asua J.M., Sudol E.D., and El-Aasser M.S.(1989). Radical Desorption in Emulsion Polymerization. *J.Polym.Sci.Chem.* **27**, 3903-3913.

Asua J.M. and De La Cal J.C.(1991). Entry and Exit Rate Coefficients in Emulsion Polymerization of Styrene. *J.Appl.Polym.Sci.* **42**, 1869-1877.

Badran A.S., Moustafa A.B., Yehia A.A., and Shendy S.M.M.(1990). Emulsion Polymerization of Vinyl Acetate Initiated by Potassium Persulfate-Cyclohexanone Sodium Bisulfite Redox Pair System. *J.Polym.Sci.Chem.* **28**, 411-424.

Ballard M.J., Gilbert R.G., and Napper D.H.(1981). Improved Methods for Solving the Smith-Ewart Equations in the Steady State. *J.Polym.Sci.Lett.* **19**, 533-537.

Ballard M.J., Napper D.H., and Gilbert R.G.(1984). Kinetics of Emulsion Polymerization of Methyl Methacrylate. *J.Polym.Sci.Chem.* **22**, 3225-3253.

Ballard M.J., Napper D.H., Gilbert R.G., and Sangster D.F.(1986a). Termination-Rate Coefficients in Methyl Methacrylate Polymerizations. *J.Polym.Sci.Chem.* **24**, 1027-1041.

Ballard M.J., Gilbert R.G., Napper D.H., Pomery P.J., O'Sullivan P.W., and O'Donnel J.H.(1986b). Propagation Rate Coefficients from Electron Spin Resonance Studies of the Emulsion Polymerization of Methyl Methacrylate. *Macromol.* **19**, 1303-1308.

Barandiaran M.J., Adams M.E., De La Cal J.C., Sudol E.D., and Asua J.M.(1992). New Approach for the Estimation of Kinetic Parameters in Emulsion Polymerization Systems. II. Homopolymerization Under Conditions Where n > 0.5. *J.Appl.Polym.Sci.* **45**, 2187-2197.

Barette K.E.J. (1975) Dispersion Polymerization in Organic Medi. Wiley, New York

Barton J.(1990). On the Initiation Mechanism in Emulsion Polymerization Systems. *Makromol.Chem.Macro.Symp.* **31**, 11-23.

Barton J., Hlouskova, Z., and Juranicova V.(1992). Partitioned Polymerization, 4. Seeded Emulsion Polymerization of Methyl Methacrylate. *Makromol.Chem.* **193**, 167-177.

Bataille P., Van, B.T., and Pham Q.B.(1982). Emulsion Polymerization of Styrene. I. Review of Experimental Data and Digital Simulation. *J.Polym.Sci.Chem.* **20**, 795-810.

Bataille F., Bataille P., and Fortin R.(1988). Emulsion Polymerization of Styrene IV: Effect of Co(II), Ni(II), and Pb(II) on the Polymerization of Styrene Initiated by Potassium Persulfate. *J.Polym.Sci.Chem.* **26**, 1471-1477.

Bataille P. and Gonzalez A.(1984). Emulsion Polymerization of Styrene. III. Effect of Ti(III) and Cl(1) on the Polymerization of Styrene Initiated by Potassium Persulfate. *J.Polym.Sci.Chem.* **22**, 1409-1417.

Bataille F., Dalpe, J.F., Dubuc F., and Lamoureux L.(1990). The Effect of Agitation on the Conversion of Vinyl Acetate Emulsion Polymerization. *J.Appl.Polym.Sci.* **39**, 1815-1820.

Blackley D.C. and Sebastian S.A.R.D.(1987). Influence of Surfactant Type and Purity upon Emulsion Copolymerization of Styrene and Acrylic Acid. *Bri.Polym.J.* **19**, 25-30.

Blackley D.C. and Sebastian S.A.R.D.(1989). Effects of Inorganic Electrolytes upon Emulsion Polymerisation Reactions. I. Effects upon Kinetics of Styrene Emulsion

Broadhead T.O., A.E. Hamielec and J.F. MacGregor (1985) Dynamic Modelling of the Batch, Semi-Batch and Continuous Production of Styrene/Butadiene Copolymers by Emulsion Polymerization. *Makromol.Chem.Suppl.* **10/11**, 105-128.

Campbell J.D.(1985) M.A.Sc. Thesis, Chemical Engineering, McMaster Univeristy

Canegallo S., Storti G., Morbidelli M., and Carra S.(1993). Densimetry for On-Line Conversion Monitoring in Emulsion Homo- and Copolymerization. *J.Appl.Polym.Sci.* **47**, 961-979.

Capek I.(1992). On the Kinetics of Emulsion Copolymerization of Methyl Methacrylate and Ethyl Acrylate in the Presence of Hydrocarbons. *Makromol.Chem.* **193**, 1423-1438.

Capek I., Kostrubova J., and Barton J.(1990). Effect of a Bi-Unsaturated Monomer on the Emulsion Polymerization of Ethyl Acrylate. *Makromol.Chem.Macro.Symp.* **31**, 213-226.

Capek I., Barton J., and Karpatyova A.(1987). Emulsion Polymerization of Butyl Methacrylate Initiated by 2,2'- Azoisobutyronitrile, 3. On the Applicability of the Modified Smith-Ewart Model. *Makromol.Chem.* **188**, 703-710.

Capek I. and Potisk P.(1992). Radical Emulsion Polymerization of n-Butyl Acrylate and Its Copolymerization with Acrylonitrile in the Presence of Crosslinker. *Polym.J.* **24**, 1037-1048.

Capek I.(1994). Emulsion Polymerization of Butyl Acrylate, 2[a)] Effect of the Initiator Type and Concentration. *Macromol.Chem.Phys.* **195**, 1137-1146.

Capek I.(1996). Photopolymerization of Butyl Acrylate in Direct Emulsifier-Mixed Micelles. *Makromol.Rep.* **33**, 209-217.

Capek I. and Fouassier J.P.(1997). Kinetics of Photopolymerization of Butyl Acrylate in Direct Micelles. *Eur.Polym.J.* **33**, 173-181.

Casey B.S., Morrison B.R., Maxwell I.A., Gilbert R.G., and Napper D.H.(1994). Free Radical Exit in Emulsion Polymerization. I. Theoretical Model. *J.Polym.Sci.Chem.* **32**, 605-630.

Chang H.-R., Parker H.-Y., and Westmoreland D.G.(1992). Continuous ESR Measurement of Propagating Free-Radical Concentrations for Batch Emulsion Polymerization of Methyl Methacrylate. *Macromol.* **25**, 5557-5558.

Chen S.A. and Wu K.-W.(1990). Emulsion Polymerization: Determination of the Average Number of Free Radicals per Particle by Use of the Number Average Volume of the Particles. *J.Polym.Sci.Chem.* **28**, 2857-2866.

Chern C.S. and Chen Y.C.(1996). Semibatch Emulsioin Polymerization of Butyl Acrylate

Stabilized by a Polymerizable Surfactant. *Prog.Polym.Sci.* **28**, 627-632.

Chern C.S. and Poehlein G.W.(1987). Reaction Kinetics of Vinyl Acetate Emulsion Polymerization. *J.Appl.Polym.Sci.* **33**, 2117-2136.

Chu H.-H. and Lin C.C.(1992). The Stabilization Effect of Mixed-Surfactants in the Emulsion Polymerization of n-Butyl Acrylate. *Polym.Bull.* **28**, 419-426.

Congalidis J.P., J.R. Richards and R.G. Bilbert (1989) Mathematical Modeling of Emulsion Copolymerization Reactors, in: International Symposium on Computer Applications in Applied Polymer Science. ACS ser. 195 360-378.

Cruz M.A., Palacios J., Garcia-Rejon A., Ruiz L.M., and Rios Guerrero L.(1985). Copolymerisation en Emulsion Styrene-Acrylate de Butyl en Reacteur Ferme. *Makromol.Chem.Suppl.* **10/11**, 87-103.

de la Cal J.C., Adams M.E., and Asua J.M.(1990). Parameter Estimation in Emulsion Copolymerization. *Makromol.Chem.Macromol.Symp.* **35/36**, 23-40.

de Arbina L.L., Barandiaran M.J., Gugliotta L.M. and Asua J.M.(1996) Emulsion Polymerization: Particle Growth Kinetics. *Polymer* **37**, 5907-5916

de La Rosa L.V., Sudol E.D., El-Aasser M.S., and Klein A.(1996). Details of the Emulsion Polymerization of Styrene Using a Reaction Calorimeter. *J.Polym.Sci.Chem.* **34**, 461-473.

Delgado J., El-Aasser M.S., Silebi C.A., Vanderhoff J.W., and Guillot J.(1988). Miniemulsion Copolymerization of Vinyl Acetate and Butyl Acrylate. II. Mathematical Model for the Monomer Transport. *J.Polym.Sci.Phys.* **26**, 1495-1517.

Dickinson R.G.(1976) *PhD Thesis*, Chemical Engineering, University of Waterloo

Dimitrados Y.N.(1989) *PhD Thesis*, Chemical Engineering, Lehigh University

Dimitratos J., El-Aasser M.S., Georgakis C., and Klein A.(1990). Pseudosteady States in Semicontinuous Emulsion Copolymerization. *J.Appl.Polym.Sci.* **40**, 1005-1021.

Dougherty E.P. (1986b) The SCOPE Dynamic Model for Emulsion Polymerization II. Comparison with Experiment and Applications. *J. Appl. Polym. Sci.* **32**, 3079-3095.

Dougherty E.P. (1986a) The SCOPE Dynamic Model for Emulsion Polymerization I. Theory. *J. Appl. Polym. Sci.* **32**, 3051-3078.

Dube A.M.(1994) Ph.D Thesis, Department of Chemical Engineering, University of Waterloo

Dubé M.A., A. Penlidis R.K. Mutha and Cluett W.R.(1996). Mathematical Modelling of Emulsion Copolymerization of Acrylonitrile/Butadiene. *Ind. Eng. Chem. Res.* **35**, 4434-4448

Dunn A.S. and Taylor P.A.(1965). The Polymerization of Vinyl Acetate in Aqueous Solution Initiated by Potassium Persulfate at 60°C. *Makromol.Chem.* **83**, 207-219.

El-Aasser M.S., Makgawinata T., and Vanderhoff J.W.(1983). Batch and Semicontinuous Emulsion Copolymerization of Vinyl Acetate---Butyl Acrylate. I. Bulk, Surface, and Colloidal Properties of Copolymer Latexes. *J.Polym.Sci.Chem.* **21**, 2363-2382.

El-Aasser M.S. and Vanderhoff J.W.(1981). *Emulsion Polymerization of Vinyl Acetate*, Applied Science Publishers, London.

Farber J.N.(1986). Steady State Multiobjective Optimization of Continuous Copolymerization Reactors. *Polym.Eng.Sci.* **26**, 499-507.

Fitch R.M. and Tsai C.H.(1971b) Homogeneous Nucleation of Polymer Colloids, IV: The Role of Soluble Oligomeric Radicals. In: Fitch RM (ed)Polymer Colloids. pp 103-116

Fitch R.M. and Tsai C.H.(1971a) Particle Formation in Polymer Collids, III. Prediction of the Number of Particles by a Homogeneous Nucleation Theory. Polymer Colloids Fitch R.M. (Ed), Plenum Press, New York 73-102

Fitch R.M., Palmgren T.H., Aoyagi T., and Zuikov A.(1985). Kinetics of Particle Nucleation and Growth in the Emulsion Polymerization of Acrylic Monomers. *J.Poly.Sci.Poly.Sym.* **72**, 221-224.

Fitch RM (1981) Latex Particle Nucleation and Growth. In: Basset DR, Hamielec AE (eds)Emulsion Polymers and Emulsion Polymerization. pp 1-29

Fitch R.M., Palmgren T.H., Aoyagi T., and Zuikov A.(1985). Kinetics of Particle Nucleation and Growth in the Emulsion Polymerization of Acrylic Monomers. *J.Poly.Sci.Poly.Sym.* **72**, 221-224.

Fitch R.M. and Shih L.B.(1975) Emulsion Polymerization: Kinetics of Radical Capture by the Particle. *Prog. Colloid Polym. Sci.* **56**, 1-11

Flory P.J.(1953) Principles of Polymer Chemistry. New York, Cornell University Press

Fontenot K. and Schork F.J.(1993). Batch Polymerization of Methyl Methacrylate in Mini/Macroemulsions. *J.Appl.Polym.Sci.* **49**, 633-655.

Fontenot K. and Schork F.J.(1992/1993a). Simulation of Mini/Macro Emulsion Polymerizations. I. Development of the Model. *Polym.React.Eng.* **1**, 75-109.

Fontenot K. and Schork F.J.(1992/1993b). Simulation of Mini/Macro Emulsion Polymerization II. Sensitivities and Experimental Comparison. *Polym.React.Eng.* **1**, 289-342.

Forcada J. and Asua J.M.(1990). Modeling of Unseeded Emulsion Copolymerization of Styrene and Methyl Methacrylate. *J.Polym.Sci.Chem.* **28**, 987-1009.

Forcada J. and Asua J.M.(1991). Emulsion Copolymerization of Styrene and Methyl Methacrylate. II. Molecular Weights. *J.Polym.Sci.Chem.* **29**, 1231-1242.

Friis N. and Hamielec A.E.(1973). Kinetics of Styrene Emulsion Polymerization. *J.Polym.Sci.* **11**, 3321-3325.

Friis N. and Hamielec A.E.(1974). Note on Kinetics of Methyl Methacrylate Emulsion Polymerization. *J.Polym.Sci.Chem.* **12**, 251-254.

Friis N., Goosney D., Wright J.D., and Hamielec A.E.(1974). Molecular Weight and Branching Development in Vinyl Acetate Emulsion Polymerization. *J.Appl.Polym.Sci.* **18**, 1247-1259.

Friis N. and Hamielec A.E.(1975a) Gel-Effect in Emulsion Polymerization of Vinyl Monomers. *Polymer Prep.* **16(1)**, 192-197

Friis N. and Hamielec A.E.(1975b). Kinetics of Vinyl Chloride and Vinyl Acetate Emulsion Polymerization. *J.Appl.Polym.Sci.* **19**, 97-113.

Friis N. and Hamielec A.E.(1982). Gel Effect in Emulsion of Vinyl Monomers. In *Emulsion Polymerization* (Piirma, I., Ed.) 82-91.

Friis N. and Nyhagen L.(1973). A Kinetic Study of the Emulsion Polymerization of Vinyl Acetate. *J.Appl.Polym.Sci.* **17**, 2311-2327.

Gao J. and Penlidis A.(1996) A Comprehensive Simulator/Database Package for Reviewing Free-Radical Homopolymerization. *J. Macromol. Sci. Revs.* **36(2)**, 199-404

Gao J. and Penlidis A.(1998) A Comprehensive Simulator/Database Package for Reviewing Free-Radical Homopolymerization. *J. Macromol. Sci. Revs.* **38(4)**, 199-404

Gardon J.L. (1968a) Emulsion Polymerization. I. Recalculation and Extension of the Smith-Ewart Theory. *J.Polym.Sci.Chem.* **6**, 623-641

Gardon J.L. (1968b) Emulsion Polymerization. II. Review of Experimental Data in the Context of the Revised Smith-Ewart Theory. *J.Polym.Sci.A-1* **6**, 643-664.

Gardon J.L. (1968c) Emulsion Polymerization. III. Theoretical Prediction of the Effects of Slow

Termination Rate within Latex Particles. *J.Polym.Sci.Chem.* **6**, 623-641

Gardon J.L. (1968d) Emulsion Polymerization. IV. Experimental Verification of the Theory Based on Slow Termination Rate within Latex Particles. *J.Polym.Sci.A-1.* **6**, 687-710

Gardon J.L. (1968e) Emulsion Polymerization. V. Lowest Theoretical Limits of the Ratio kt/kp. *J.Polym.Sci.A-1.* **6**, 2853-2857

Gardon J.L. (1968f) Emulsion Polymerization. VI. Concentration of Monomers in Latex Particles. *J.Polym.Sci.A-1.* **6**, 2859-2879

Giannetti E., G. Storti and M. Morbidelli (1988) Emulsion Polymerizations. II Kinetics, Molecular Weight Distributions, and Polymer Microstructure of Emulsion Copolymers. *J.Polym.Sci.Chem.* **26**, 2307-2343.

Giannetti E. (1989) Emulsion Polymerizations. 3. Theory of Emulsion Copolymerization Kinetics. *Macromolecules.* 22, 2094-2102.

Giannetti E.(1993). Nucleation Mechanisms and Particle Size Distributions of Polymer Colloids. *AIChE J.* **39**, 1210-1227.

Gilbert R.G. (1995) Emulsion Polymerization: A Mechanistic Approach. Academic Press, New York

Gilbert R.G. and D.H. Napper (1983) The Direct Determination of Kinetic Parameters in Emulsion Polymerization Systems. *J. Macromol. Sci.-Rev. Macromol. Chem. Phys.* **C23**, 127-186

Goldwasser J.M. and Rudin A.(1982). Emulsion Copolymerization of Styrene and Methyl Methacrylate. *J.Polym.Sci.Chem.* **20**, 1993-2006. Greene, R.K., Gonzalez, R.A., and Poehlein, G.W.(1982). *Emulsion Polymerization* (Piirma, I., Ed.) 341-358.

Greene R.K., Gonzalez R.A., and Poehlein G.W.(1982). *Emulsion Polymerization* (Piirma, I., Ed.) 341-358.

Guillot J.(1985). Some Thermodynamic Aspects in Emulsion Copolymerization. *Makromol.Chem.Suppl.* **10/11** , 235-264.

Guillot J.(1986). Emulsion Polymerization High Conversion Polymerization Polycondensation. (Reichert, K.H. and Geiseler, W., Eds.) *Huthig&Wepf Verlag Basel, New York.* 147-164.

Guo J.S., Sudol E.D., Vanderhoff J.W., and El-Aasser M.S.(1992). Modelling of the Styrene Microemulsion Polymerization. *J.Polym.Sci.Chem.* **30**, 703-712.

Hamielec A.E., J.F. MacGregor and A. Penlidis (1983) Modelling Copolymerizations-Control of Composition, Chain Microstructure, Molecular Weight Distribution, Long Chain Branching and Crosslinking in: K.H. Reichert and W. Geiseler (Eds.) *Polymer Reaction Engineering. Hanser Publishers, New York.* 21-27.

Hamielec A.E. and J.F. MacGregor (1982) Latex Reactor Principles: Design, Operation, and Control, in: I. Piirma (Ed.), Emulsion Polymerization, Academic Press. NY. London, pp. 319-355.

Hamielec A.E., MacGregor J.F., and Penlidis, A.(1987). Multicomponent Free-Radical Polymerization in Batch, Semi-Batch and Continuous Reactors. *Makromol.Chem.Macromol.Symp.* **10/11**, 521-570.

Hansen F.K. and Ugelstad J.(1978) Particle Nucleation in Emulsion Polymerization. I. A Theory for Homogeneous Nucleation. *J. Polym. Sci. Polym. Chem.* **16**, 1953-1979

Hansen F.K. and Ugelstad J.(1982) Particle Formation Mechanism. in: Emulsion Polymerization. Editor I. Piirma. Academic Press, New York. Pg. 51-92

Harada M., Nomura, M., Kojima, H., Eguchi, W., and Nagata, S.(1972). Rate of Emulsion Polymerization of Styrene. *J.Appl.Polym.Sci.* **16**, 811-833.

Harada M., M. Nomura W. Eguchi and S. Nagata (1971) Studies of the Effect of Polymer Particles on Emulsion Polymerization. *J.Chem.Eng.Jap.* **4**, 54-60

Harkins W.D.(1947) *J. Am. Chem. Soc.* **69**, 1428

Harris B., Hamielec A.E. and Marten L.(1981). *Emulsion Polymers and Emulsion Polymerization* (Basset, D.R. and Hamielec A.E., Eds.) 2 edition. Washington, D.C. 315-326.

Harvey and Leonard (1972) Thermodynamics of Equilibrium Copolymerization in Solution Bulk Copolymerization. *Macromolecules* **5**, 698

Hawkett B.S., Napper D.H. and Gilbert R.G. (1981) Radical Capture Efficiencies in Emulsion Polymerization. *J.Polym.Sci.Chem.* **19**, 3173-3179

Huggins M.L.(1958) Physical Chemistry of High Polymers. New York, John Wiley & Sons

Huo B.P., Campbell J.D. and Penlidis A., MacGregor J.F. and Hamielec A.E.(1988) Effect of Impurities on Emulsion Polymerization : Case II Kinetics. *J. Appl. Polym. Sci.* **35**, 2009-2021

James Jr., H.L. and Piirma, I.(1975). Molecular Weigth Development in Styrene and Methyl

Methacrylate Emulsion Polymerization. *Polym.Prepr.* **16**, 198-204.

Kiparissides C. and Ponnuswamy, S.R.(1981) Application of Population Balance Equations to Latex Reactors. *Chem. Eng. Commun.* **10**, 283-291

Kiparissides C.(1978) *PhD Thesis*, Chemical Engineering, McMaster University

Kiparissides C., MacGregor J.F., and Hamielec A.E.(1980c). Continuous Emulsion Polymerization of Vinyl Acetate. Part III: Detection of Reactor Performance by Turbudity-Spectra and Liquid Exclusion Chromatography. *Cnd.J.Chem.Eng.* **56**, 65-71.

Kiparissides C., MacGregor J.F., and Hamielec A.E.(1979). Continuous Emulsion Polymerization. Modeling Oscillations in Vinyl Acetate Polymerization. *J.Appl.Polym.Sci.* **23**, 401-418.

Kiparissides C., MacGregor J.F., and Hamielec A.E.(1980a). Continuous Emulsion Polymerization of Vinyl Acetate. Part I. Experimental Studies. *Cnd.J.Chem.Eng.* **58**, 48-55.

Kiparissides C., MacGregor J.F., and Hamielec A.E.(1980b). Continuous Emulsion Polymerization of Vinyl Acetate. Part II: Parameter Estimation and Simulation. *Cnd.J.Chem.Eng.* **58**, 56-64.

Kong X.Z., Pichot C., and Guillot J.(1988). Kinetics of Emulsion Copolymerization of Vinyl Acetate with Butyl Acrylate. *Eur.Polym.J.* **24**, 485-492.

Kshirsagar R.S. and Poehlein G.W.(1994) Radical Entry into Particles During Emulsion Polymerization of Vinyl Acetate. *J. Appl. Polym. Sci.* **54**, 909-921

Kukulj D., Davis T.P., Suddaby, K.G., Haddleton D.M., and Gilbert R.G.(1997). Catalytic Chain Transfer for Molecular Weight Control in the Emulsion Homo- and Copolymerizations of Methyl Methacrylate and Butyl Methacrylate. *J.Polym.Sci.Chem.* **35**, 859-878.

Lange D.M., Poehlein G.W., Hayashi S., Komatsu A., and Hirai T.(1991). Kinetic Analysis of Seeded Emulsion Polymerization of Vinyl Acetate. *J.Polym.Sci.Chem.* **29**, 785-792.

Lee C.H. and Mallinson R.G.(1990). Surfactant Effects in the Emulsion Polymerization of Vinyl Acetate. *J.Appl.Polym.Sci.* **39**, 2205-2218.

Lee C.H. and Mallinson R.G.(1988). A Model for Molecular Weights in Vinyl Acetate Emulsion Polymerization. *AIChE J.* **34**, 840-848.

Ley G.J.M., Schneider C., and Hummel D.O.(1969). Half-Life Measurements in Emulsion Polymerization. *J.Polym.Sci.C* **27**, 119-137.

Li B.G. and Brooks B.W.(1993). Prediction of Average Number of Radicals per Particle for Emulsion Polymerization. *J.Polym.Sci.Chem.* **31**, 2397-2402.

Lichti G., R.G. Gilbert and D.H. Napper (1982) Theoretical Predictions of the Particle Size and Molecular Weight Distributions in Emulsion Polymerization. in: I. Piirma (Ed.), Emulsion Polymerization. Academic Press, New York, pp. 94-144.

Lichti G., Gilbert R.G., and Napper D.H.(1983). The Mechanism of Latex Particle Formation and Growth in the Emulsion Polymerization of Styrene Using the Surfactant Sodium Dodecyl Sulfate. *J.Polym.Sci.Chem.* **21**, 269-291.

Lichti G., Gilbert R.G., and Napper D.H.(1977). The Growth of Polymer Colloids. *J.Polym.Sci.Chem.* **15**, 1957-1971.

Lichti G., B.S. Hawkett R.G. Gilbert D.H. Napper and D.F. Sangster (1981) Styrene Emulsion Polymerization: Particle-Size Distributions. *J.Polym.Sci.Chem.* **19**, 925-938.

Lin C., Ku H.c. Chiu W.Y.(1981) Simulation Model for the Emulsion Copolymerization of Acrylonitrile and Styrene in Azeotropic Composition. *J. Appl. Polym. Sci.* **26**, 1327

Litt M.H. and Stannett V.(1970). Emulsion Polymerization of Vinyl Acetate. II. *J.Polym.Sci.A-1* **8**, 3607-3649.

Litt M.H. and Chang K.H.S.(1981). *Emulsion Polymers and Emulsion Polymerization* (Basset, D.R. and Hamielec, A.E., Eds.) 455-470.

Liu X., Nomura M., and Fujita K.(1997). Thermodynamic Correlation of Partial and Saturation Swelling of Styrene-Acrylonitrile Copolymer Particles by Styrene and Acrylonitrile Monomers. *J. Appl. Polym. Sci.* **64**, 931-939

Louie B.M., Chiu W.Y., and Soong D.S.(1985). Control of Free-Radical Emulsion Polymerization of Methyl Methacrylate by Oxygen Injection. I. Modeling Study. *J.Appl.Polym.Sci.* **30**, 3189-3223.

Lovell P.A., Shah T.H., and Heatley F.(1991). Chain Transfer to Polymer in Emulsion Polymerization of n-butyl acrylate Studied by ^{13}C NMR Spectroscopy and GPC. *Polym.Comm.* **32**, 98-103.

Mallya P. and Plamthottam S.S.(1989). Termination Rate Constant in Butyl Acrylate Batch Emulsion Polymerization. *Polym.Bull.* **21**, 497-504.

Marten F. L. and Hamielec A. E. (1979) High Conversion Diffusion-Controlled Polymerization. In *Polymer Reactors and Processes. ACS Symposium Series, 104* (Edited by Henderson J. N. and

Marten F. L. and Hamielec A. E. (1982) High-Conversion Diffusion-Controlled Polymerization of Styrene. I. *J. Appl. Polym. Sci.* **27**, 489-505.

Maw T. and Piirma I.(1983). Emulsion Polymerizatio in the Presence of Nonionic Surfactant. *Polym.Prepr.* **24**, 71-72.

Maxwell I.A., Napper D.H., and Gilbert R.G.(1987). Emulsion Polymerization of Butyl Acrylate. Kinetics of Particle Growth. *J.Chem.Soc.Faraday Trans.* **83**, 1449-1467.

Maxwell I.A., Morrisson B.R. and Napper D.H. and Gilber R.G.(1991) Entry of Free Radicals into Latex Particles in Emulsion Polymerization. *Macromol.* **24,** 1629

Maxwell I.A., Kurja, J., Van Doremaele G.H.J.V., German A.L., and Morrison B.R. (1992a). Partial Swelling of Latex Particles with Monomers. *Makromol.Chem.* **193**, 2049-2063.

Maxwell I.A., Kurja J., Van Doremaele G.H.J., and German A.L.(1992b). Thermodynamics of Swelling of Latex Particles with Two Monomers. *Makromol.Chem.* **193**, 2065-2080.

Maxwell I.A., Morrisson B.R. and Napper D.H. and Gilber R.G.(1992c) The Effect of Chain Transfer Agent on the Entry of Free Radicals in Emulsion Polymerization. *Makromol. Chem.* **193,** 303

Maxwell I.A., Verdurmen E.M.F.J., and German, A.L.(1992d). High-Conversion Emulsion Polymerization. *Makromol.Chem.* **193**, 2677-2695.

Maxwell I.A., Noel L.F.J., schroonbrood H.A.S., and German A.L.(1993). Thermodynamics of Swelling of Latex Particles with Two Monomers: A Sensitivity Analysis. *Makromol.Chem., Theory Simul.* **2**, 269-274.

Mayer M.J.J., van den Boomen F.H.A.M., Paquet D.A., Meuldijk J., and Thoenes D.(1996). The Polymerization Rate of Freshly Nucleated Particles during Emulsion Polymerization with Micellar Nucleation. *J.Polym.Sci.Chem.* **34**, 1747-1751.

McBain C.B.D. and Piirma I.(1989). Influence of Steric Length in Electrosteric Surfactants on Emulsion Polymerization. *J.Appl.Polym.Sci.* **37**, 1415-1422.

McCarthy S.J., Elbing E.E., Wilson I.R., Gilbert R.G., Napper D.H., and Sangster D.F.(1986). Seeded Heterogeneous Polymerization of Acrylonitrile. *Macromol.* **19**, 2440-2448.

McCurdy K.G. and Laidler K.(1964). Rates of Polymerization of Acrylates and Methacrylates in Emulsion Systems. *Cnd.J.Chem.Eng.* **42**, 825-828.

Mead R.N. and Poehlein G.W.(1988) Emulsion Copolymerization of Styrene-Methyl Acrylate and Styrene-Acrylonitrile in Continuous Stirred Reactor Tanks. 1. *Int. Eng. Chem. Res.* **28,** 51

Mead R.N. and Poehlein G.W.(1989) Free-Radical Transport from Latex Particles. *J. Appl. Polym. Sci.* **38,** 105-122

Meuldijk J., van Strien C.J.G., van Doormalen F.A.H.C., and Thoenes, D.(1992). A Novel Reactor for Continuous Emulsion Polymerization. *Chem.Eng.Sci.* **47**, 2603-2608.

Miller C.M., Clay, P.A., Gilbert R.G., and El-Aasser M.S.(1997). An Experimental Investigation on the Evolution of the Molecular Weight Distribution in Styrene Emulsion Polymerization. *journal unknown* 989-1006.

Min K.W. and Ray W.H.(1974) On the Mathematical Modelling of Emulsion Polymerization Reactor. *J. Macromol. Sci., Revs. Macromol. Chem.* **C11**, 177-255

Min K.W. and Ray W.H.(1976) Structure Framework for Modelling Emulsion Polymerization Reactor. *ACS Symposium Ser.* **24**, 359-366

Min K.W. and Ray W.H.(1978) The Computer Simulation of Batch Emulsion Polymerization Reactors Through a Detailed Mathematical Model. *J. Appl. Polym. Sci.* **22**, 89-112

Misra S.C., Pichot C., El-Aasser M.S., and Vanderhoff, J.W.(1983). Batch and Semicontinuous Emulsion Copolymerization of Vinyl Acetate-Butyl Acrylate. II. Morphological and Mechanical Properties of Copolymer Latex Films. *J.Polym.Sci.Chem.* **21**, 2383-2396.

Morbidelli M., Storti G., and Carra S.(1983). Role of Micellar Equilibria on Modelling of Batch Emulsion Polymerization Reactors. *J.Appl.Polym.Sci.* **28**, 901-919.

Morrison B.R., Casey B.S. Lacik, I., Leslie G.L., Sangster, D.F., Gilbert, R.G., and Napper, D.H.(1994). Free Radical Exit in Emulsion Polymerization. II. Model Discrimination via Experiment. *J.Polym.Sci.Chem.* **32**, 631-649.

Morton M., Salatiello P.P., and Landfield H.(1952). Absolute Propagation Rates in Emulsion Polymerization. III. Styrene and Isoprene. *J.Polym.Sci.* **VIII**, 279-287.

Morton M., Kaizerman S., and Altier M.W.(1954). Swelling of Latex Particles. *J.Colloid Sci.* **9**, 300-312.

Moustafa A.B., Abd El-Hakim A.A., and Mohamed G.A.(1997). Some Parameters Affecting the Emulsifier-Free Emulsion Polymerization of Vinyl Acetate. *J.Appl.Polym.Sci.* **63**, 239-246.

Napper D.H. and Alexander A.E.(1962) Polymerization of Vinyl Acetate in Aqueous Media, Part II. The Kinetic Behavior in the Presence of Low Concentration of Added Soaps. *J. Polym. Sci.* **61**, 127

Napper D.H., Netschey A. and Alexander A.E.(1971) Effects of Nonionic Surfactants on Seeded Polymerization. *J. Polym. Sci. A-1.* **9**, 81-89

Noel L.F.J., Van Zon J.M.A.M., Maxwell I.A., and German A.L.(1994). Prediction of Polymer Composition in Batch Emulsion Copolymerization. *J.Polym.Sci.Chem.* **32**, 1009-1026.

Nomura M., Harada, M., Nakagawara K., Eguchi, W., and Nagata S.(1971a). The Role of Polymer Particles in the Emulsion Polymerization of Vinyl Acetate. *J.Chem.Eng.Jap.* **4**, 160-166.

Nomura M., Kojima, H., Harada M., Eguchi, W., and Nagata S.(1971b). Continuous Flow Operation in Emulsion Polymerization of Styrene. *J.Appl.Polym.Sci.* **15**, 675-691.

Nomura M., Harada M., Eguchi W., and Nagata S.(1976). *Emulsion Polymerization* (Piirma, I. and Gardon, J.L., Eds.) 102-121.

Nomura M. and Harada M.(1981). Rate Coefficient for Radical Desorption in Emulsion Polymerization. *J.Appl.Polym.Sci.* **27**, 17-26.

Nomura M., Yamamoto K., Horie I., and Fujita K.(1982). Kinetics of Emulsion Copolymerization. II. Effect of Free Radical Desorption on the Rate of Emulsion Copolymerization of Styrene and Methyl Methyacrylate. *J.Appl.Polym.Sci.* **27**, 2483-2501.

Nomura M., Kubo M., and Fujita K.(1983). Kinetics of Emulsion Copolymerization. III. Prediction of the Average Number of Radical per Particle in an Emulsion Copolymerization System. *J.Appl.Polym.Sci.* **28**, 2767-2776.

Nomura M. and Fujita K.(1985). On the Prediction of the Rate of Emulsion Copolymerization and Copolymer Composition. *Makromol.Chem.Suppl.* **10/11**, 25-42.

Nomura M., Fujita K., Kouno Y., and Satpathy U.S.(1988). Investigation on the Locus of Particle Formation in Emulsion Polymerization Containing Partially Water-Soluble Monomers. *J.Polym.Sci.C* **26**, 385-390.

Nomura M., Horie I., and Kubo M.(1989). Kinetics and Mechanism of Emulsion Copolymerization. IV. Kinetic Modelling of Emulsion Copolymerization of Styrene and Methyl Methacrylate. *J.Appl.Polym.Sci.* **37**, 1029-1050.

Nomura M. and Fujita K.(1994b). Kinetics and Mechanisms of Unseeded Emulsion

Polymerization of Methyl Methacrylate. *Polym.React.Eng.* **2**, 317-345.

O'Neill T. and Hoigne J.(1972). γ–Radiation-Initiated Emulsion Polymerization of *n*-Butyl Acrylate and of Methyl Methacrylate. *J.Polym.Sci.A-1* **10**, 581-593.

Omi S., Kushibiki K., and Iso M.(1987). The Computer Modelling of Multicomponent, Semibatch Emulsion Copolymerization. *Polym.Eng.Sci.* **27**, 470-482.

O'Toole J.T.(1965). Kinetics of Emulsion Polymerization. *J.Appl.Polym.Sci.* **9**, 1291-1297.

Penboss I.A., Napper D.H., Gilbert RG (1983) Styrene Emulsion Polymerization. J. Chem. Soc. Faraday Trans. **79**, 1257-1271

Penlidis A., MacGregor J.F. and Hamielec A.E.(1988) Effect of Impurities on Emulsion Polymerization: Case I Kinetics. *J. Appl. Polym. Sci.* **35**, 2023

Penlidis A., MacGregor J.F. and Hamielec A.E.(1985a) A Theoretical and Experimental Investigation of the Batch Emulsion Polymerization of Vinyl Acetate. *Polym.Proc.Eng.* **3**, 185-218.

Penlidis A., MacGregor, J.F. and Hamielec, A.E.(1986) Mathematical Modelling of Emulsion Polymerization Reactors: A Population Balance Approach and Its Applications. *ACS Vol. 313*, 219-240. (Editor: Prorder T.)

Penlidis A., MacGregor J.F. and Hamielec A.E. (1985b) Dynamic Modeling of Emulsion Polymerization Reactors. *AIChE J.* **31**, 881-889.

Penlidis A., Hamielec A.E and MacGregor A.E.(1984) Dynamic Modelling of the Continuous Emulsion Polymerization of Vinyl Chloride. *J.Vinyl Tech.* **6**, 134-142.

Piirma I., Kamath, V.R., and Morton, M.(1975). The Kinetics of Styrene Emulsion Polymerization. *Polym.Prep.* **16**, 187-191.

Pollock M.J., MacGregor J.F. and Hamielec A.E.(1981) In "Computer Applications in Applied Polymer Science." ACS Symposium Series 197, Washington, D.C.

Priest W.J.(1952) Particle Growth in the Aqueous Polymerization of Vinyl Acetate. *J. Phys. Chem.* **56**, 1077-1083

Rawlings J.B.(1985) *PhD Thesis* , Chemical Engineering, University of Wisconson

Rawlings J.B. and W.H. Ray (1988b) The Modelling of Batch and Continuous Emulsion Polymerization Reactors. Part II: Comparison with Experimental Data from Continuous Stirred

Tank Reactors. *Polym.Eng.Sci.* **28**, 257-274.

Rawlings J.B. and Ray W.H.(1988a) The Modelling of Batch and Continuous Emulsion Polymerization Reactors. Part I: Model Formulation and Sensitivity to Parameters. *Polym. Eng. Sci.* **28**, 237-256.

Richards J.R., J.P. Congalidis and R.G. Gilbert (1989) Mathematical Modelling of Emulsion Copolymerization Reactors. *J.Appl.Polym.Sci.* **37**, 2727-2756.

Rios L., Garcia-Rejon A., Cruz M.A., Palacios J., and Ruiz L.M.(1985). Batch and Semicontinuous Emulsion Copolymerization Styrene/Methyl Methacrylate: Kinetics and Viscoelastic Properties. *Makromol.Chem.Suppl.* **10/11**, 477-488.

Russell G.T., Napper D.H., and Gilbert R.G.(1988) Termination in Free-Radical Polymerizing Systems at High Conversion. *Macromol.*, **21**, 2133-2140

Said Z.F.M.(1991). Molecular-weight Distributions in the Thermally Initiated Emulsion Polymerization of Styrene. *Makromol.Chem.* **192**, 405-414.

Salazar A., Gugliotta L.M., Vega J.R., and Meira G.R.(1998). Molecular Weight Control in a Starved Emulsion Polymerization of Styrene. *Ind. Eng. Chem. Res.*, **37**, 3582-3591

Saldivar E., P. Dafniotis and W.H. Ray (1998) Mathematical Modeling of Emulsion Copolymerization reactors. I. Model Formulation and Application to Reactors Operating with Micellar Nucleation. *J.Macromol.Sci.-Revs.Macromol.Chem.* **38**, 207-325.

Sarkar S., Adhikari, M.S., Banerjee, M., and Knoar, R.S.(1990). Mechanism of Persulfate Decomposition in Aqueous solution at 50C in the Presence of Vinyl Acetate and Nitrogen. *J.Appl.Polym.Sci.* **39**, 1061-1077.

Schroonbrood H.A.S.(1994) PhD Thesis, University of Eindhoven

Schroonbrood H.A.S. and German, A.L.(1994). Thermodynamics of Monomer partitioning in Polymer Latices: Effect of Molar Volume of the Monomers. *Macromol.Rapid Commun.* **15**, 259-264.

Schork F.J. and Ray W.H.(1987). The Dynamics of the Continuous Emulsion Polymerization of Methylmethacrylate. *J.Appl.Polym.Sci.* **34**, 1259-1276.

Schork F.J. and Ray W.H.(1981). On-line Monitoring of Emulsion Polymerization Reactor Dynamics. In: Emulsion Polymers and Emulsion Polymerization. ACS Ser. 165. Ed. Bassett D.R. and Hamielec A.E. Pg. 505-514

Shoaf G.L. and Poehlein G.W.(1989). Batch and Continuous Emulsion Copolymerization of Ethyl Acrylate and Methacrylic Acid. *Polym.Plast.Technol.Eng.* **28**, 289-317.

Singh S. and Hamielec A.E.(1978). Liquid Exclusion Chromotography. A Technique for Monitoring the Growth of Polymer Particles in Emulsion Polymerization. *J.Appl.Polym.Sci.* **22**, 577-584.

Smith W.V. and Ewart R.H.(1948) J. Chem. Phys. **16**, 592

Snuparek Jr., J.(1980). The Effectiveness of Some Commercial Emulsifiers in Emulsion Polymerization I. *Die Angewandte Makromol.Chem.* **88**, 61-68.

Soh S.K.(1980). Measurements of Propagation Rate Constant from Emulsion Polymerization. *J.Appl.Polym.Sci.* **25**, 2993-2998.

Song Z.G. and Poehlein G.W.(1988a) Particle Formation in Emulsion Polymerization: Transient Particle Concentration. *J. Macromol. Sci. Chem.* **A25**, 403-443

Song and Poehlein (1988b) Particle Formation in Emulsion Polymerization: Particle Number at Steady-State. *J. Macromol. Sci. Chem.* **A25**, 1587-1632

Stickler M., Panke., D., and Hamielec, A.E.(1984) Polymerization of Methyl Methacrylate up to High Degrees of Conversion: Experimental Investigation of the Diffusion-Controlled Polymerization. *J. Polym. Sci. Polym. Chem.* **22**, 2243-2253

Storti G., Morbidelli M., and Carra S.(1989). *Computer Applications in Applied Polymer Science II* 79-402.

Sudol E.D., El-Aasser, M.S., and Vanderhoff, J.W.(1986a). Kinetics of Successive Seeding of Monodisperse Polystyrene Latexes. I. Initiation via Potassium Persulfate. *J.Polym.Sci.Chem.* **24**, 3499-3513.

Sudol E.D., El-Aasser, M.S., and Vanderhoff, J.W.(1986b). Kinetics of Successive Seeding of Monodisperse Polystyrene Latexes. II. Azo Initiators with and without Inhibitors. *J.Polym.Sci.Chem.* **24**, 3515-3527.

Sundberg D.C., Hsieh, J.Y., Soh, S.K., and Baldus, R.F.(1981). *Emulsion Polymers and Emulsion Polymerization* (Basset, D.R. and Hamielec, A.E., Eds.) 327-343.

Tanrisever T., Okay, O., and Sonmezoglu, C.(1996). Kinetics of Emulsifier-Free Emulsion Polymerization of Methyl Methacrylate. *J.Appl.Polym.Sci.* **61**, 485-493.

Trivedi M.K., Rajagopal, K.R., and Joshi, S.N.(1983). Emulsion Polymerization of Vinyl Acetate.

J.Polym.Sci.Chem. **21**, 2011-2016.

Ugelstad J. and Hansen F.K.(1976). Kinetics and Mechanism of Emulsion Polymerization. *Rubber Chem. Tech.* **49**, 536-609

Ugelstad J., Mork P.c. and Aasen J.O.(1967) Kinetics of Emulsion Polymerization. *J. Polym. Sci. A-1* **5**, 2281-2288

Ugelstad J., Mork, P.C., Dahl, P., and Rangnes, P.(1969). A Kinetic Investigation of the Emulsion Polymerization of Vinyl Chloride. *J.Polym.Sci.C* **27**, 49-68.

Urretabizkaia A. and Asua J.M.(1994a). High Solids Content Emulsion Terpolymerization of Vinyl Acetate, Methyl Methacrylate, and Butyl Acrylate. I. Kinetics. *J.Polym.Sci.Chem.* **32**, 1761-1778.

Urretabizkaia A., Arzamendi G., Unzue M.J., and Asua J.M.(1994b). High Solids Content Emulsion Terpolymerization of Vinyl Acetate, Methyl Methacrylate, and Butyl Acrylate. II. Open Loop Composition Control. *J.Polym.Sci.Chem.* **32**, 1779-1788.

Urquiola M.B., Sudol E.D., Dimonie V., and El-Aasser M.S.(1993). Emulsion Polymerization of Vinyl Acetate Using a Polymerizable Surfactant. III. Mathematical Model. *J.Polym.Sci.Chem.* **31**, 1403-1415.

Wang H.H. and Chu, H.-H.(1990). The Stabilization Effect of Mixed-Surfactants in the Emulsion Polymerization of Methyl Methacrylate. *Polym.Bull.* **24**, 207-214.

Yeliseyeva V.I. and Zuikov A.V. (1982) Interfacial Phenomena in Emulsion Polymerization of Polar Monomers. In: Piirma I, Gardon J.L. (eds) Emulsion Polymerization. pp 62-81

Zimmt W.S.(1959). The Emulsion Polymerization of Methyl Methacrylate. *J.Appl.Polym.Sci.* **1**, 323-328.

Zollars R.L., Chen C.T. and Jones D.A.(1979) Kinetics of the Emulsion Polymerization of Vinyl Acetate. *J. Appl. Polym. Sci.* **34**, 733-742

Appendix 1. Seeded Emulsion Polymerization

Seeded emulsion polymerization is a process widely used in both industry and research. In seeded polymerization, polymer particles are preformed in a separate reaction and a subsequent polymerization is then carried out. Major advantages of seeded emulsion polymerization are: (1) further complication of reaction kinetics is avoided due to the absence of particle nucleation; (2) physical properties (particle size, number of particles) of the preformed particles can be determined in advance. The kinetics of seeded polymerization were studied by Napper et al. (1971) and Ugelstad and Hansen (1976). In the recent literature, almost 75% of the publications deal with seeded systems. Simulation of seeded emulsion polymerization has been implemented in the emulsion model as an user option. When this option is activated, the model will automatically initialize the mass balance equations for monomer, polymer and particle number. This is described in the equations below.

The volume of the seeds can be calculated by the following:

$$V_{seed} = V_{m_{seed}} + V_{p_{seed}} = \frac{N_{seed}\pi dp^3_{seed}}{6} \qquad \text{(A1.1)}$$

where:

dp_{seed}: diameter of the seeds

V_{mseed}: volume of monomer in the seeds

V_{pseed}: volume of polymer in the seeds

N_{seed}: total number of seeds

When seeds are preformed, if there is still some monomer left in the seeds, the final conversion level in the seeds can be calculated as :

$$x_{seed}\% = \frac{V_{p_{seed}}\rho_p}{V_{p_{seed}}\rho_p + V_{p_{seed}}\rho_p} \qquad \text{(A1.2)}$$

Where: $x_{seed}\%$: final conversion level in the seeds

Combining equations A1.1 and A1.2 leads to the total volume of initial polymer in the seeds as:

$$V_{p_{seed}} = \frac{N_{seed}\pi\, dp_{seed}^3/6}{1+\left(\frac{1-x_{seed}}{x_{seed}}\right)\frac{\rho_p}{\rho_m}} \qquad \text{(A1.3)}$$

The initial volume of monomer in the seeds is:

$$V_{m_{seed}} = V_{seed} - V_{p_{seed}} \qquad \text{(A1.4)}$$

The total number of seeds (particles) N_{seed}, average seed diameter dp_{seed} and the total volume of seeds V_{seed} are usually reported, thus the volume of polymer and monomer in the seeds can be calculated by using equations A1.3 and A1.4. These two values are needed for initialization of the overall mass balances for monomer and polymer in the subsequent polymerization.

Appendix 2. Impurity Effects on Emulsion Kinetics

Impurity or inhibitor plays an important role in emulsion polymerization, yet how it affects the reaction kinetics has been rarely studied. Louie et al.(1985) found that oxygen acts as inhibitor in methyl methacrylate emulsion polymerization, however their work was limited to theory without experimental verification. Perhaps Huo et al.(1988) and Penlidis et al.(1988) are one of the very few groups that investigated impurity effects in emulsion polymerization more systematically both experimentally and theoretically. Based on partitioning, different types of impurities can be classified as water-soluble or oil-soluble. It has been demonstrated by Huo et al.(1988) and Penlidis et al.(1988) that these two types of impurities affect reaction kinetics in a very different way.

Oxygen is considered as a water-soluble impurity. Huo et al.(1988) discovered that oxygen acts mainly by scavenging free radicals in the aqueous phase. This effect directly leads to induction times. After all oxygen is consumed in the aqueous phase, polymerization starts and proceeds normally. It is expected that other types of water soluble impurities will behave in the same fashion. In the experiments carried out by Huo et al.(1988), various amounts of water soluble inhibitor of hydroquinone were injected in the batch emulsion polymerization of styrene. Different lengths of induction time were observed in their runs. The conversion results from Huo et al.(1988) are plotted in figure A2.1. The amount of hydroquinone was between 20 ppm and 100 ppm. Induction times of 20 to 40 minutes were observed. It is important to notice that the conversion curves for all four runs were nearly parallel to each other. This indicates that the rate of polymerization for the these runs is not affected by the presence of hydroquinone. All four runs reached a final conversion level of about 90%. The current model predicts the conversion profile for all four runs very well.

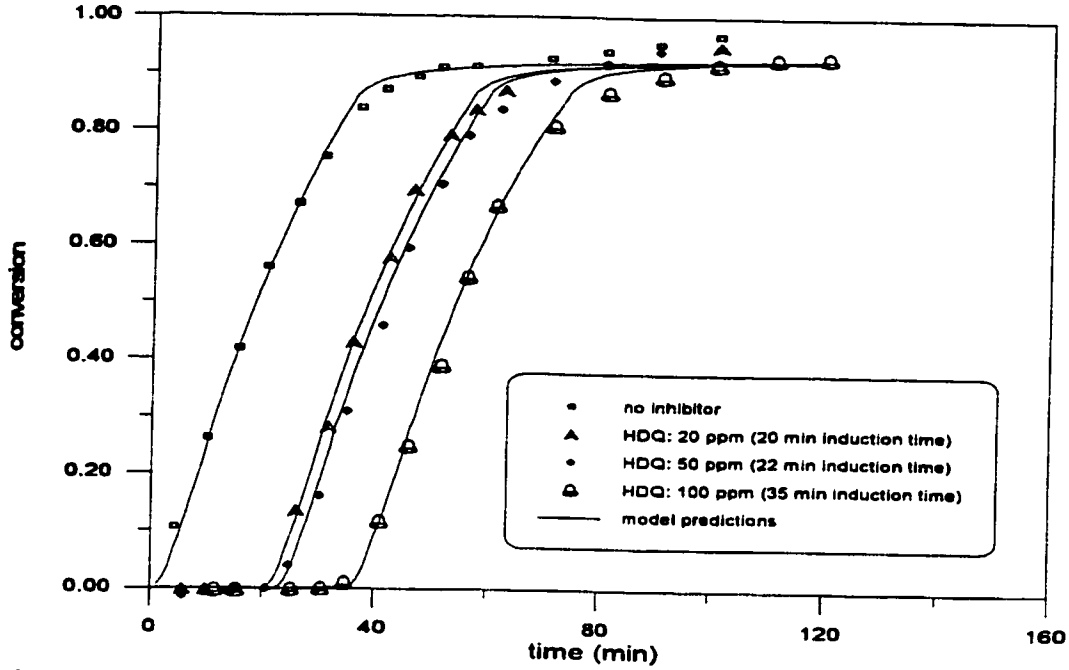

Figure A2.1 Effect of Water Soluble Inhibitor in Styrene Homopolymerization at 60°C.
Styrene: 1053 g, water: 2L, SDS: 63.18g, KPS: 3.263g

Monomer soluble impurity behaves in a much different way. Monomer soluble impurity hinders the polymerization inside the particles, and this leads to a suppressed rate of polymerization. Furthermore, since particles grow at a much slower rate, micelles disappear at a slower rate. The direct result of this is a prolonged nucleation stage, which subsequently results in more particles generated. After the impurity is consumed, the rate of polymerization can be higher than those reactions with less or no impurity due to the higher number of particles generated. Huo et al.(1988) investigated styrene emulsion homopolymerization with t-butyl catechol as the monomer soluble inhibitor. Similar to their studies on water soluble impurities, a set of experiments were performed with different levels of t-butyl catechol. Measured conversion data are plotted in figures A2.2~A2.4. A small amount of t-butyl catechol will also dissolve in the water phase and result in some induction time. The effect of t-butyl catechol on particle size is demonstrated in figure A2.5. As expected, the average particle diameter for the run with 200 ppm t-butyl catechol is smaller than that with 50 ppm t-butyl catechol due to a slower particle growth rate.

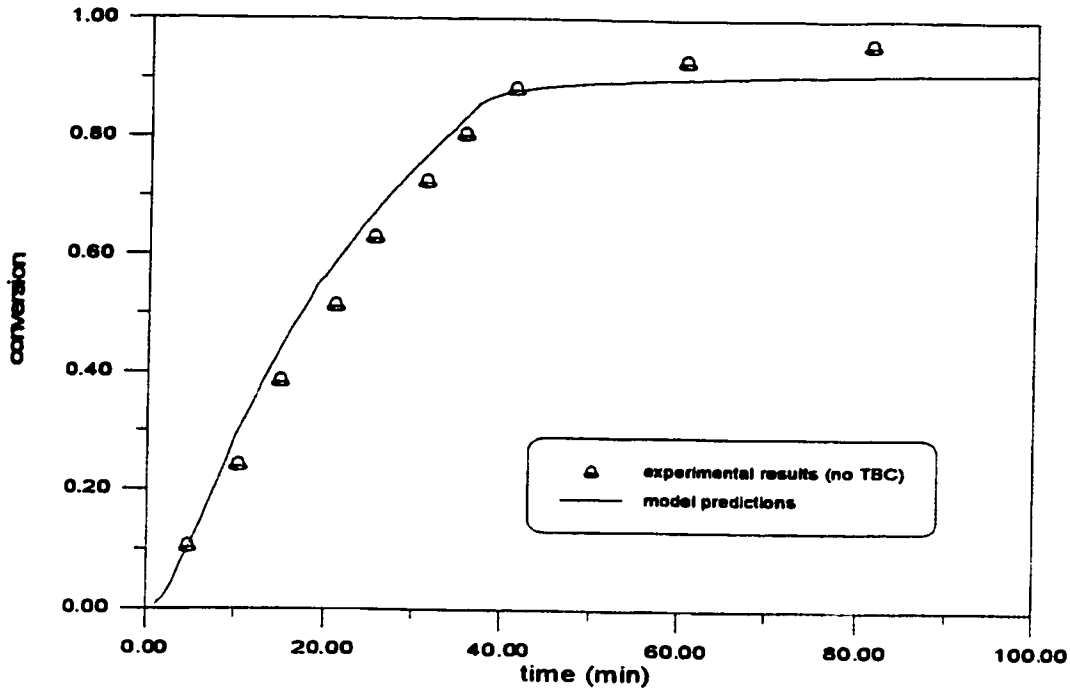

Figure A2.2 Styrene Emulsion Homopolymerization without Impurities at 55°C. Styrene: 100 g, water: 200 g, SDS: 6 g, KPS: 0.31 g.

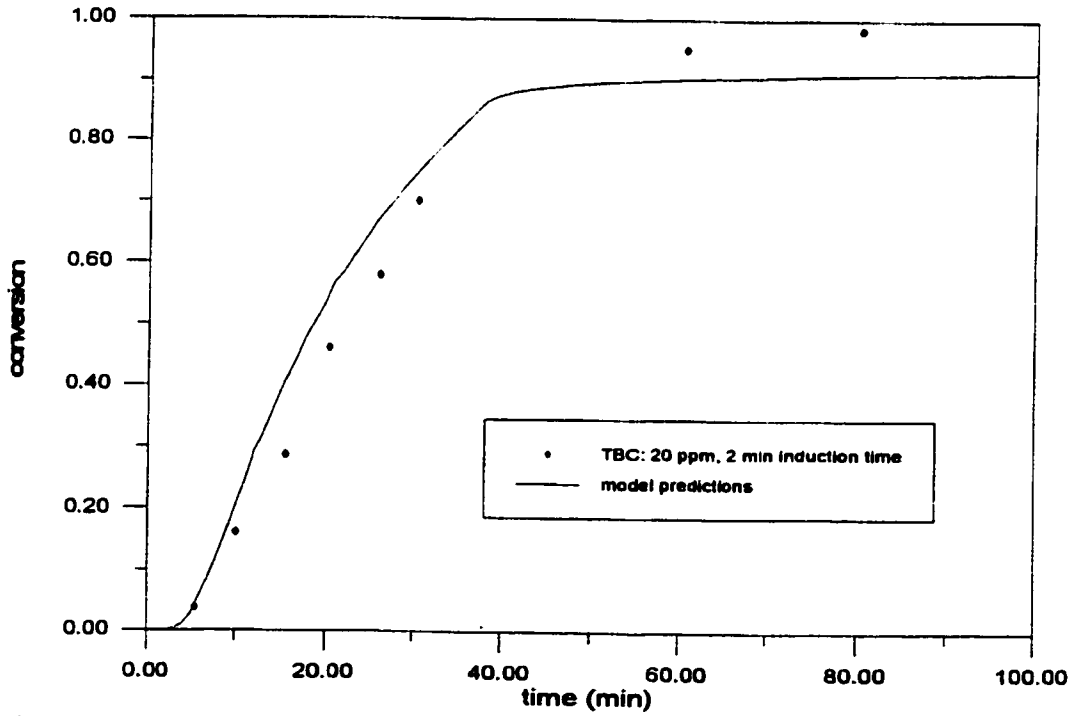

Figure A2.3 Styrene Emulsion Homopolymerization with Monomer Soluble Impurities at 55°C.
Styrene: 100 g, water: 200 g, SDS: 6 g, KPS: 0.31 g.

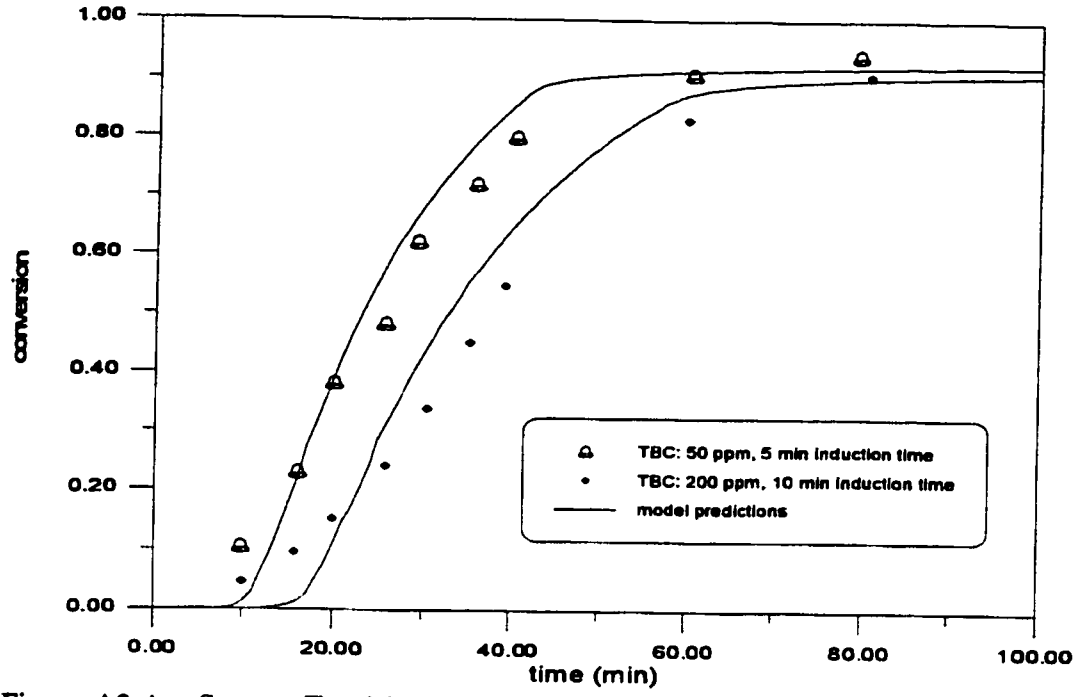

Figure A2.4 Styrene Emulsion Homopolymerization with Monomer Soluble Impurities at 55°C.
Styrene: 100 g, water: 200 g, SDS: 6 g, KPS: 0.31 g.

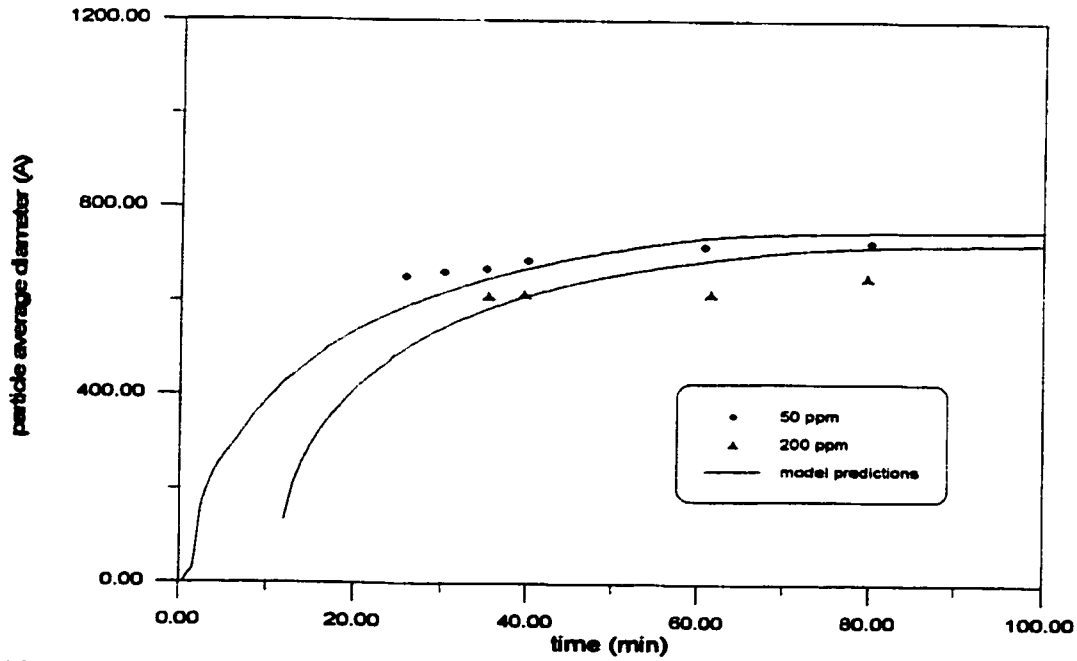

Figure A2.5 Particle Size in Styrene Emulsion Homopolymerization with t-Butyl Catechol at 55°C.
Styrene: 100 g, water: 200 g, SDS: 6 g, KPS: 0.31 g.

Penlidis et al.(1988) further extended Huo's et al.(1988) studies on impurities to vinyl acetate emulsion polymerization. A total of five runs were performed with various levels of t-butyl catechol. Figure A2.6 shows the experiment without any t-butyl catechol added. Induction time was observed in this run due to traces of oxygen in the aqueous phase. Penlidis et al.(1988) added t-butyl catechol in the other four runs. Figures A2.7~A2.8 compare our model predictions with reported conversion data. It is obvious that a higher inhibitor level leads to a lower rate of polymerization. Oxygen was present in all runs and it resulted in induction times of various lengths. The inhibitor effect on particle size is more pronounced in the runs with 100 ppm and 200 ppm t-butyl catechol. Simulation results for particle diameter for three runs without inhibitor and with 100 ppm and 200 ppm inhibitor are presented in figures A2.9~A2.11. The final particle diameter for the runs with inhibitor is about 800 Å, compared to the particle diameter for the run without inhibitor (1200Å). The smaller particle size is the direct result of the inhibitor effect on particle growth. It is satisfactory that the model is able to describe the effect of t-butyl catechol on both particle growth rate and the final particle size well.

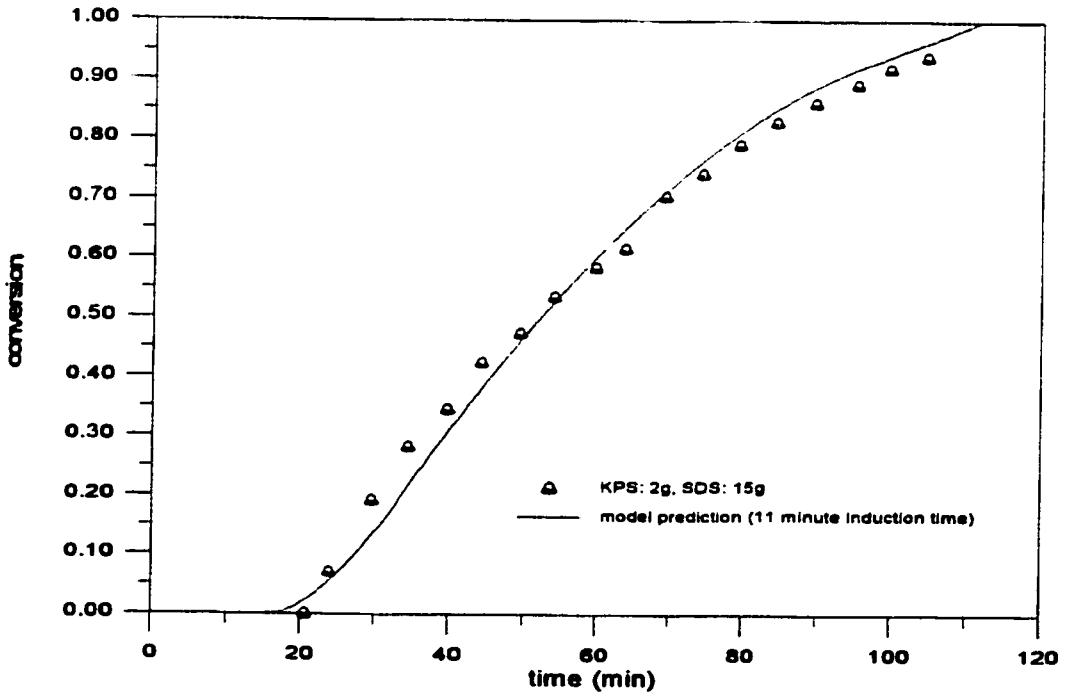

Figure A2.6 Emulsion Homopolymerization of Vinyl Acetate without Monomer Soluble Inhibitor. (VAc: 1.15 L, water: 2.86 L)

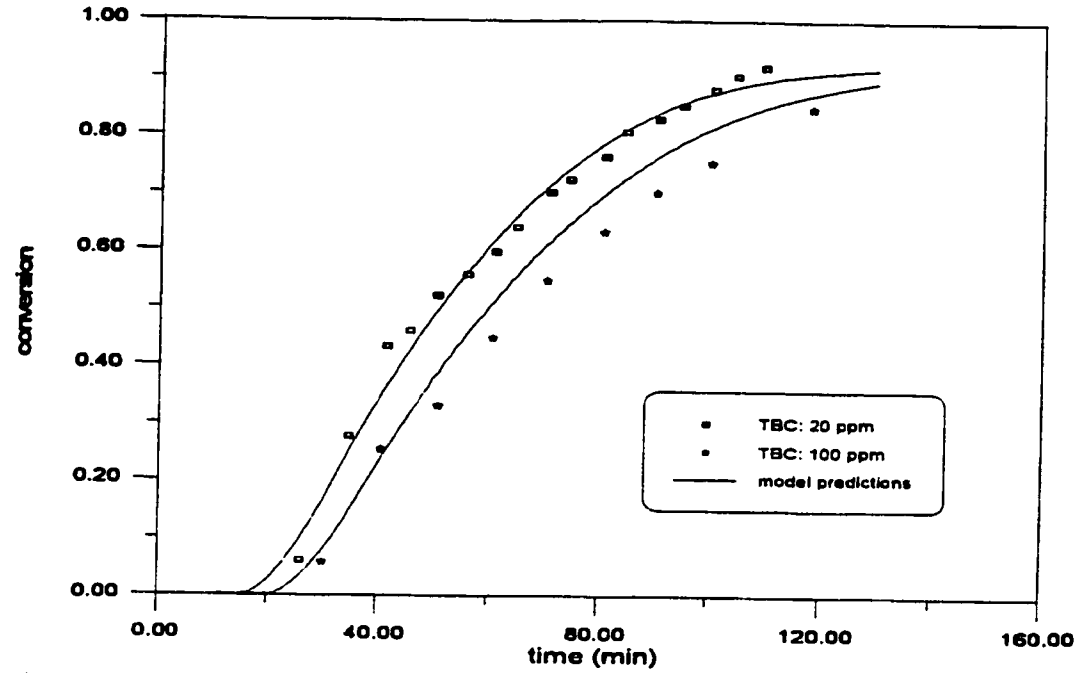

Figure A2.7 Emulsion Homopolymerization of Vinyl Acetate with Monomer Soluble Inhibitor. (VAc: 1.15 L, water: 2.86 L)

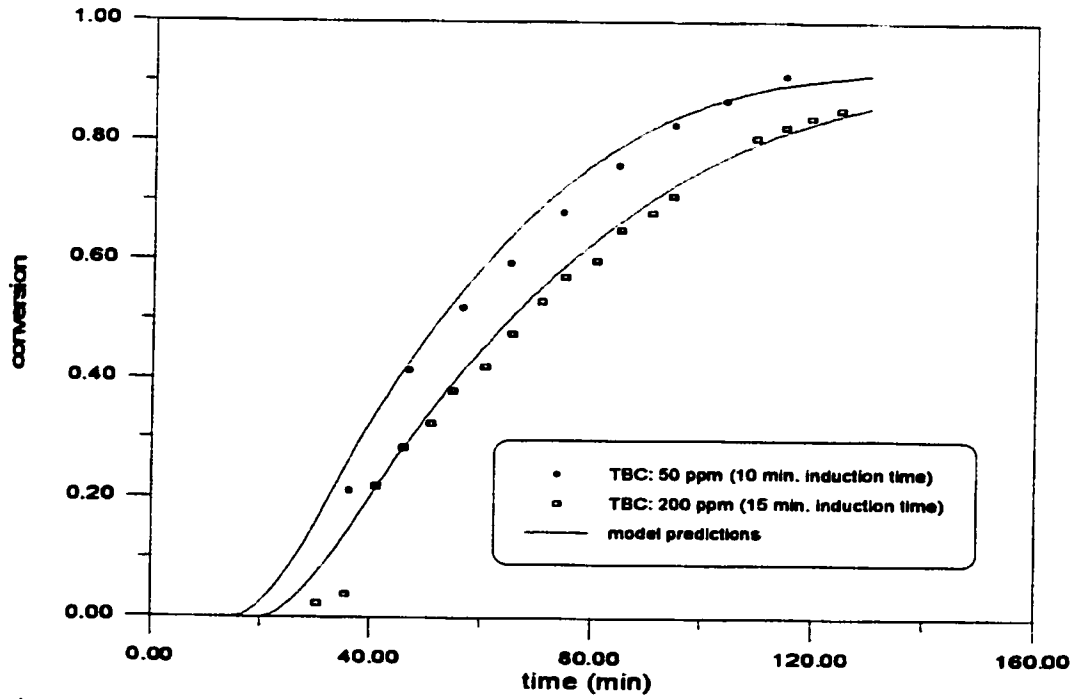

Figure A2.8 Emulsion Homopolymerization of Vinyl Acetate with Monomer Soluble Inhibitor. (VAc: 1.15 L, water: 2.86 L)

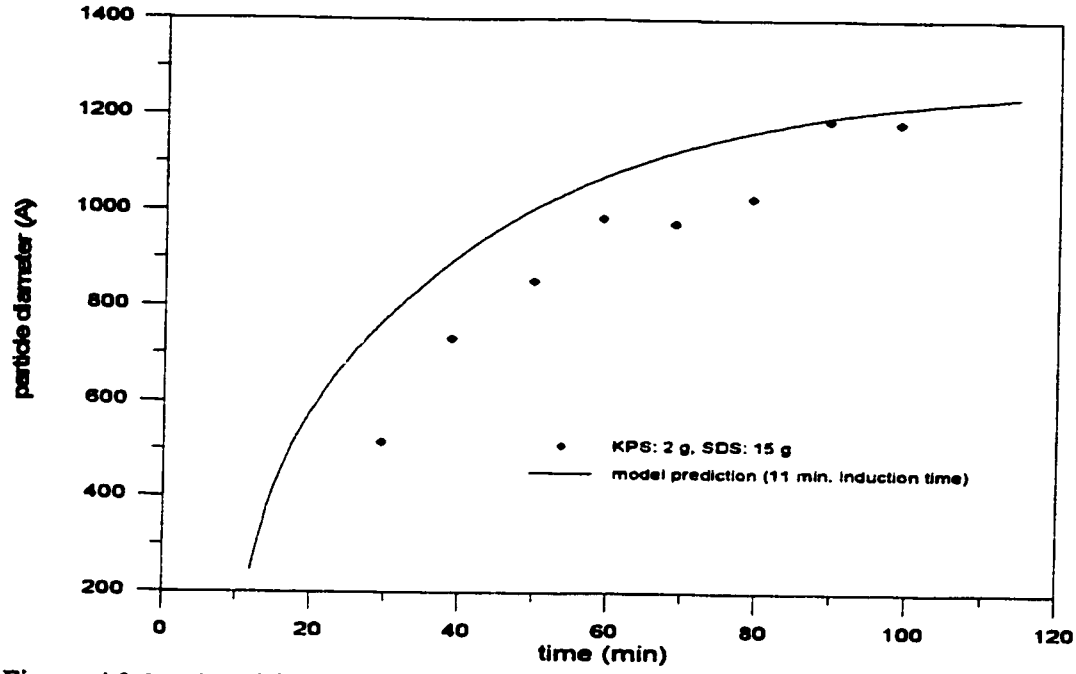

Figure A2.9 Emulsion Homopolymerization of Vinyl Acetate without Monomer Soluble Inhibitor. (VAc: 1.15 L, water: 2.86 L)

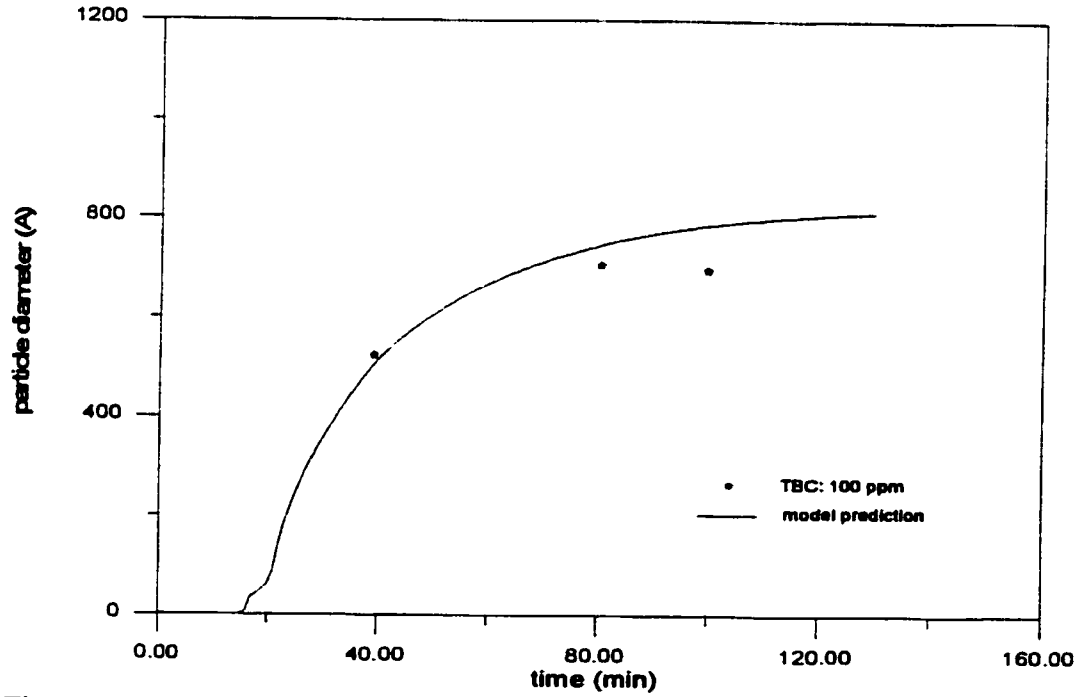

Figure A2.10 Emulsion Homopolymerization of Vinyl Acetate with Monomer Soluble Inhibitor. (VAc: 1.15 L, water: 2.86 L)

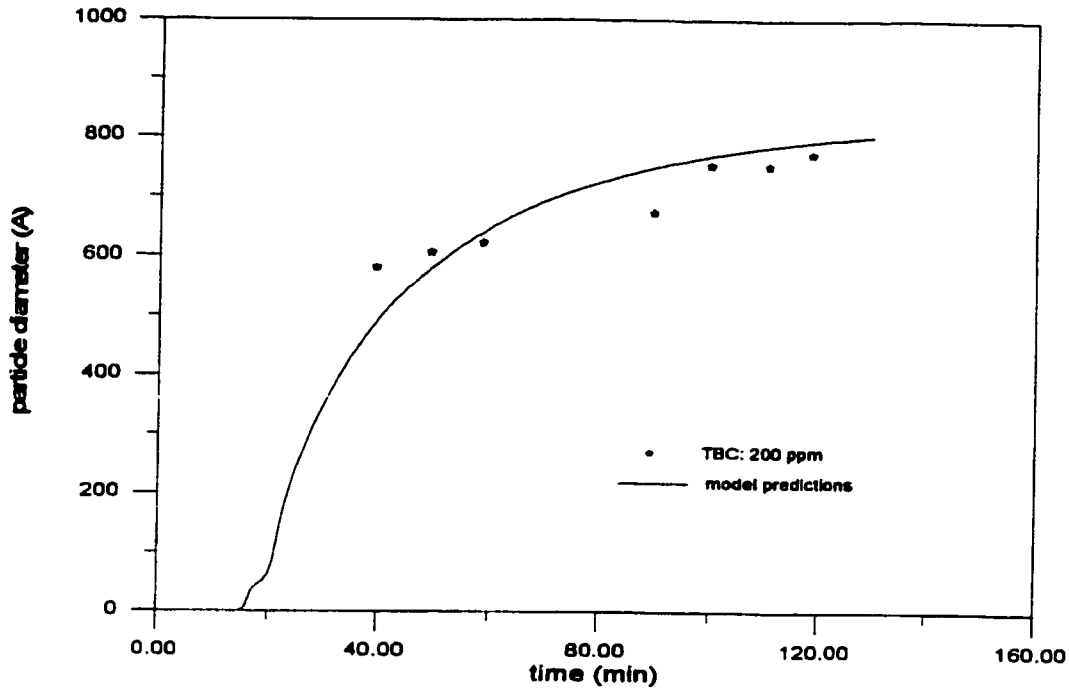

Figure A2.11 Emulsion Homopolymerization of Vinyl Acetate with Monomer Soluble Inhibitor. (VAc: 1.15 L, water: 2.86 L)